Secrets of Field-Space-Mechanics

Insights into a higher-dimensional Space-Time

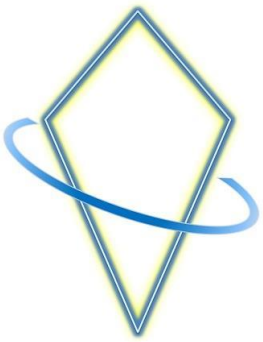

Patrick Hofmann

Preface

Field-Space-Mechanics is an extension of the theory of relativity that unifies the macrocosm and microcosm through a 7-dimensional space-time framework. The model integrates geometric fields to describe gravity, electromagnetism and quantum effects. This theory is based on the idea that matter is a geometric effect of relativistic fields, scalable across all orders of magnitude. Point particles from classical models are replaced by hollow body vibrations that generate relativistic fields in the wave-field. This treatise aims to provide a profound understanding of the overarching connections to the possible unification of all four fundamental forces. The content is aimed at all readers interested in science who want to learn about a new perspective on theoretical physics.

New fundamental model of physics

This model supports the two-world view from epistemology by expanding the visible perspective with visible space and additionally incorporating invisible space, which explains dark energy, for example. This paper answers the following questions. Where does the electron's charge come from? What is dark energy or dark matter? What mechanical circumstance causes the universe to expand? Can wave-particle duality be resolved? How can gravitational waves be modelled and calculated? Is a mouldable field propagation velocity possible? Standard scientific models leave some essential phenomena of physics unresolved. With the help of 7-dimensional Field-Space-Mechanics, it is possible to find a new approach to the causes of the effect of matter in space-time.

The essential innovation

The striking innovation of Field-Space-Mechanics lies in the design of a new particle model that can predict arbitrary particle masses with their coupling frequencies. The quantitative results agree almost completely with experimental measurements and can therefore be used as a significant verification argument for this qualitative model. This makes the characteristic coupling frequencies for elementary particles and complex particles with their variations accessible. The basis for all these mass calculations is the electron mass, which is, it should be noted, a natural constant. The present model also claims to map the internal structure of elementary particles and to predict the conditions under which a particular interaction occurs. The required field-space structure in space-time is the result of a relativistic view of the cosmos, which arises from the Field-Space-Mechanics model.

Due to its complexity, the ontology of Field-Space-Mechanics is explained step by step in the course of the treatise on the respective topics and substantiated with

formulas and examples. The overall metaphysical context is summarized at the end. The essential variables are the object frequency, the object mass, the so-called circular frequency, and the field radius. The angular frequency and the field radius are redefined within the framework of this field-space-mechanical model.

According to the description of Field-Space-Mechanics, it appears to be the case that our view of three-dimensional space is fundamentally limited when it comes to making physical predictions in the relativistic and microscopic realm. The reader is led from visible three-dimensional space into an invisible space, from which the cause and effect of matter are explored from a new perspective.

Basic approach

The derivation of Field-Space-Mechanics is a top-down approach. This involves making assumptions that enable the explanation of overarching relationships. For example, visible and invisible matter are recorded and formulated in a consistent manner. The formulas and results stand on their own, but due to their degree of abstraction, they require a sustained bottom-up approach and further in-depth analysis in order to explain specific phenomena.

"Where there is a will, there is a way." – Dalai Lama

Acknowledgements

This work could not have been completed without any support. I would like to express my particular gratitude to Dipl.-Ing. Robert Gansler for his careful proofreading and critical review. I would also like to thank my wife, Jennifer, without her support I would not have found the time to write this manuscript.

The author is aware that the model presented here is challenging for the reader, especially where physics and metaphysics mix and sometimes even collide. To distinguish it from the standard model of physics, it was necessary to introduce new terms. The author hopes that the compromise is successful and that it will motivate readers to pursue Field-Space-Mechanics further.

Motivation – possible achievements

a) Expanded understanding of **life**

b) **Calculation** of **mass** and **frequency** for already known **particles** and **particles** that can be predicted using Field-Space-Mechanics

c) **Unification of all four fundamental forces** into one model

d) A model for the **wave-particle duality**

e) New understanding of **visible** and **hidden particles**

f) **Expanded understanding** of **the theory of relativity** and **particle physics**

g) **Calculation** of **event horizons** for all **particle sizes**

h) Alternative description **of black holes**

i) **New forms of propulsion** in aviation/aerospace technology/the automotive industry

j) Optimised **hot fusion**

k) Alternative concept for **cold fusion**

l) **New computer technologies** in terms of storage capacity and performance by using the relativistic oscillation properties of photons during their periodic inertial motion in space-time

m) **Teleportation technology** through the mathematical describability of the organism

Table of contents

Chapter

1 Introduction to Field-Space-Mechanics

"The basis of knowledge is doubt about all knowledge" - René Descartes

1.1 Observable Theory of Relativity - The extension of the reference system

The aim of this chapter is to recognise that the existing model of the general theory of relativity (GTR) must be extended in order to gain further information about the previously hidden causes of various space-time mechanical effects and to make these relativistically calculable. The elaboration of the special theory of relativity (STR) for 3-dimensional space, which will be generalised in the course of the following chapters, will serve as a starting point. Einstein's core statement is that an object of mass or energy bends space-time. Objects take the courses of a space-time curvature, which leads to the formulation of the law of gravity. GTR assumes that a perfectly self-contained inertial system can only change its direction or speed due to its inertia if an external force acts on it. A body with a mass M is therefore accelerated within the sphere of influence of a gravitational field. Furthermore, the theory assumes that the **maximum velocity V_{max}** in a vacuum has the same value of

$$V_{max} = 299792458 \frac{\text{m}}{\text{s}} = c.$$

As a result, space and time can change dynamically in relation to the maximum speed $V_{max} = c$ and an object can only reach this speed asymptotically. Light propagates in a gravitational field along a curved path. This is dependent on the observer relative to moving objects.

The assumptions from GTR are:

Equivalence principle: The force of gravity is identical to the force of inertia in an accelerated reference system.

Gravitational red shift: The wavelength of light propagating against a gravitational field increases.

Gravitational blue shift: The wavelength of light travelling towards a gravitational field decreases.

Reference system: The spatiotemporal behaviour of an object can be clearly described using a reference system, such as the Cartesian coordinate system, with its location-dependent variables.

Inertial system: A reference system is an inertial system if a body remains at rest or moves uniformly relative to the reference frame. To achieve this state, an object must be free of other forces.

Mach's principle: Mach's principle: States that the universe does not generate any additional space-time deformation for local objects. Taking Mach's principle into account, this means that there is no global dilation effect on the speed of light. As observed in countless experiments, the speed of light is equated with the maximum speed $V_{max} = c$.

Measuring principle of light via resonator mirrors: A light wave has a certain distance between two mirrors for a travelling and returning wavelength, which fulfils a resonance condition *with* $n \frac{\lambda}{2} = l$. n stands for an integer multiple of the wavelength of the light. The distance between the resonator mirrors is the distance l. The area between two resonance areas contains the entire spectrum of the light and is defined as *FSR* - free spectral range. With constant repetition of the wave movement per second, a frequency f is created. The speed of light can be represented by the product of the free spectral range and the distance between the resonators:

$$c = FSR \cdot 2l \tag{1.01}$$

In order to carry out a measurement, a setup is realised in a vacuum environment using a light-emitting diode as a transmitter and a photodiode as a receiver. The path of a light wave is adjusted by several mirrors and distances from each other. If an emitted wavelength hits the photodiode at a certain distance s, an alternating voltage is recorded. The phase position for two received wavelengths can be determined between two differently set distances. Two different propagation times with the same frequency are recorded using an oscilloscope. The path length s between two wavelengths is shifted with an adjustment of Δl so that a phase position of π is measured. The transit time difference must be calculated as

$$\Delta t = \frac{1}{2}\frac{1}{f}. \tag{1.02}$$

The speed of light c is finally calculated as

$$c = \frac{\Delta l}{\Delta t}. \tag{1.03}$$

The Technical University of Munich uses this principle to carry out its light measurements as part of its experimental physics programme.

To begin with, the deformation of space-time will be described in terms of velocity states, which corresponds to the special case. These velocities are a snapshot of the state of motion that occurs in an accelerated space-time under gravity. With the dynamic temporal change of the velocities to a relativistic acceleration-behaviour, the special consideration is raised to the general theory of relativity.

The **Minkowski metric** of the four-digit tensor in 3-dimensional space from the STR is as follows:

$$-\frac{dx^2}{dt^2} - \frac{dy^2}{dt^2} - \frac{dz^2}{dt^2} + c^2 = \frac{ds^2}{dt^2} \tag{1.04}$$

The term $\left[-\frac{dx^2}{dt^2} - \frac{dy^2}{dt^2} - \frac{dz^2}{dt^2} \right]$ corresponds to a vectorial quadratic object velocity in 3-dimensional space in the form of a differential geometry.

$[c^2]$ is the maximum square velocity V_{max}^2 for objects and is also the reference value for a non-deformed space at rest.

The term $\left[\frac{ds^2}{dt^2} \right]$ describes the behaviour of light within a deformed space, which is registered by an external observer.

With this metric, STR is able to calculate a space-time curvature caused by a gravitational field that exerts a force on an object. In other words, a moving object mass additionally curves space-time at its location in addition to its rest mass. The reasons why a moving object in a vacuum additionally curves space or how a gravitational field arises are not initially answered by the classical approach.

The following three phenomena from STR go back to the transformations by H. A. Lorentz:

1) Time runs slower for objects under the influence of speed. This phenomenon is known as time dilation.

$$t_{obj} = t \frac{c}{\sqrt{c^2 - V_{obj}^2}} \tag{1.05}$$

t - time elapsing for a non-deformed space-time

t_{obj} - object time in a deformed space-time

c - maximum speed $V_{max} = c$

V_{obj} - resulting velocity vector in the 3-dimensional space

2) Objects shrink under the influence of speed in the direction of movement. This phenomenon is known as length contraction .

$$x' = x \frac{\sqrt{c^2 - V_{obj}^2}}{c} \tag{1.06}$$

x - space segment without deformation
x' - deformed space segment

3) Objects become heavier when energy is added. This effect is known as relativistic mass increase.

$$E = m\,c^2 \frac{c}{\sqrt{c^2 - V_{obj}^2}} \tag{1.07}$$

E - energy
m - object mass

Point 3) states that an energy-mass equivalence applies to a moving object. Objects, that are already accelerating or under the influence of gravity, are only further accelerated by the addition of kinetic energy. The Field-Space Mechanics (FSM) model will demonstrate that a deformation of space-time also occurs as a result of potential energy.

If the term "velocity" is replaced by "acceleration and increasing gravity", then these relationships are formulated in general relativistic terms.

The strength of general relativity lies in the fact that this model describes the gravitational interaction between objects via its geometry, independently of any inertial frame of reference. This stems from the fundamental approach of focusing on the relativistic relationship between objects, which renders other influences on an observation irrelevant. The predictions match observations in the cosmological context with great precision. In the GTR model, the speed of light can safely be equated with the invariant quantity c as the maximum speed $V_{max} = c$. However, this involves measuring photons, which presuppose an undeformed surrounding space. During the experiment to measure light, it is not guaranteed that the measuring apparatus has also been compressed. It stands to reason that, if this fact is disregarded, the speed of light corresponds to the maximum speed. This refers to a measurement that is situated within the influence of a gravitational field such as that of the Earth, or which takes into account the inertial motion of the solar system, the galaxy and the universe. The measuring apparatus is therefore subjected to an external force that is not recorded, but which ought to affect a light measurement. This information is lost as long as only the gravitational relationship between objects is considered.

The doubt here does not lie in the concept of maximum speed. It is not plausible that the measured speed of light corresponds to the maximum speed as an inertial reference value if the Earth is not at rest, the galaxy is moving, and the surrounding

universe generates a space-time deformation of its own. General Relativity yields more realistic results when the reference frame includes all objects and the mass of the universe. The introduction of a global inertial system could resolve this doubt and lead to further insights. The approach to potentially resolving the doubt once again starts from the Lorentz transformation.

The term $\frac{\sqrt{c^2 - V_{obj}^2}}{c}$ from the length contraction can also be reformulated mathematically as follows:

$$x' = x \sqrt{1 - \left(\frac{V_{obj}}{c}\right)^2} \qquad (1.08)$$

→ The proportion $\frac{V_{obj}}{c}$ corresponds to the solution of a sine or cosine function for the angle 0° ... 90° or the radian measure between 0 ... $\frac{\pi}{2}$.

Thesis:

A field propagation velocity V_{Field} (the speed of light) follows its own reference frame relative to the maximum velocity V_{max} = c. It is only at the location of the relativistic inertial system that the field propagation velocity V_{Field} reaches the maximum velocity V_{max}, as the space-time-mechanical effects of the Lorentz transformation prevail with a factor of 1. All relativistic systems can alternatively be represented and stabilised trigonometrically. In this context, the state with an angle of 0° or 90° would be the point where a spatial segment experiences either the minimum Lorentz contraction with a factor of 1 or – as a fictitious maximum – infinity for a singularity. For this thesis, the Mach principle is disregarded. The result is formulated at the conclusion of **Chapter 2.4**.

In principle, the trigonometric representation of the Lorentz transformation results in two reference frames that could be considered as inertial frames for the theory of relativity:

$$\sqrt{c^2 - v_{obj}^2} = \sqrt{c^2 - c^2 \cos^2(kt)} \qquad \text{to: } = c \sin(kt) \qquad \text{or:} \qquad (1.09)$$

$$\sqrt{c^2 - v_{obj}^2} = \sqrt{c^2 - c^2 \sin^2(kt)} \qquad \text{to: } = c \cos(kt) \qquad (1.10)$$

The matter is therefore given a sin(*kt*) or cos(*kt*) dependent proper time. *k* is a characteristic constant that describes how often a period is repeated per second. The nominal time *t* describes the time interval that elapses between the start and end of a period *T*. The time *t* also describes the temporal sequence in Minkowski's metric. The time *t* thus refers to an inertial location without a deformed space-time. An object time

t_{obj} is relative to the time t that results from a space-time deformation and corresponds to the proper time of the object.

Note: The sine or cosine function maps the exact course of a spatially distorted spatial segment relative to the inertial system. Beyond 90°, the changing slopes must be taken into account for the remaining quadrants.

H. A. Lorentz's preliminary work therefore results in two possible reference systems that indicate the location of the inertial system. Both reference systems with their sine and cosine functions have a phase of 90° to each other. Both reference systems are therefore trigonometrically orthogonal to each other with regard to the maximum velocity $V_{max} = c$ and can be related to each other as velocity components using the Pythagorean theorem. That results in the square maximum velocity $V_{max}^2 = c^2$:

$$V_{max}^2 = c^2 = (c \sin(kt))^2 + (c \cos(kt))^2 = V_{obj}^2 + V_{field}^2 \quad (1.11)$$

V_{obj} – object velocity relative to the maximum velocity $V_{max} = c$, it trigonometrically represents a cathetus of the Pythagorean triangle

V_{field} – field propagation velocity relative to the maximum velocity $V_{max} = c$, it trigonometrically maps the second cathetus

V_{max} – maximum velocity for objects, it trigonometrically maps the hypotenuse between the two cathets for V_{obj} and V_{field}

Which reference system belongs to the object velocity V_{obj} or the field velocity V_{field} is still open up to this point.

Insert into the Minkowski metric: $-\frac{dx^2}{dt^2} - \frac{dy^2}{dt^2} - \frac{dz^2}{dt^2} + V_{obj}^2 + V_{field}^2 = \frac{ds^2}{dt^2}$

The term $-\frac{dx^2}{dt^2} - \frac{dy^2}{dt^2} - \frac{dz^2}{dt^2}$ describes the quadratic vectorial observed object velocity in space and is therefore equal to the quadratic velocity component V_{obj}^2, which represents the cathetus relative to the quadratic maximum velocity $V_{max}^2 = c^2$.

with: $-\frac{dx^2}{dt^2} - \frac{dy^2}{dt^2} - \frac{dz^2}{dt^2} + V_{obj}^2 = 0$ → this results in: $V_{field}^2 = \frac{ds^2}{dt^2}$ (1.12)

Findings:

- ➔ A space-time deformation is characterised by a reduced field propagation velocity V_{field} and an increased object velocity $V_{obj.}$
- ➔ Photons propagate along a field propagation velocity V_{field}. A speed of light V_{field} is measured instead of the maximum speed $V_{max} = c$ in a resonator!
- ➔ Light has its own object time.
- ➔ The proper time of objects can therefore only be represented completely with these two reference systems or by a superordinate inertial system.

The obviously invisible or immeasurable processes of a reduced field propagation velocity V_{field} describe the effect of a field deformation during the space-time deformation. The description of such field deformations is the next step towards a 7-dimensional relativity theory of Field-Space-Mechanics (FSM-STR). The inertial system for this theory of relativity could provide information on how a space-time deformation is to be formulated via its field attributes.

The required inertial system for both reference systems $c \sin(kt)$ and $c \cos(kt)$ exists by definition at the location of the minimum length contraction, with the factor 1 for the formula (1.08). The maximum velocity $V_{max} = c$ can only be measured with the aid of light waves for the inertial case if the reference system for the field propagation velocity V_{field}, which represents the velocity of the photons, corresponds to the state of the inertial system. A perfect inertial frame would be found at this location. In order to finally answer the question of the inertial system, the two reference systems must be assigned to the velocities V_{obj} and V_{field}. This will be analysed in more detail in the next chapter.

The need to expand the 3D visible space into a 6D field-space:

Both reference systems have an influence on the state and effect of photons and must therefore be represented. Since the field propagation velocity V_{field} is not captured in the three-dimensional space of the *c*-metric system, a further 3-dimensional space is required to describe the processes governing the field propagation velocity V_{field} and to project the effect into visible space. In this way, the 3-dimensional space of the *c*-metric system is extended to six spatial dimensions. Therefore, both reference systems exist simultaneously for the object velocity V_{obj} as well as for the field propagation velocity V_{field} *c*-metrically and can thus be represented trigonometrically in relation to each other. Thus, both velocity parameters no longer evolve independently in a 4-dimensional relativistic manner, but are interdependent within a mathematically 7-dimensional, periodically repeating inertial motion. Trigonometrically, the resulting velocity is always the maximum velocity $V_{max} = c$, which, upon reduction of the metric, leads back to GTR. The metric is defined in **Chapter 2.2**.

<u>In other words, the context up to this point is as follows:</u>

In two reference systems moving uniformly in relation to each other, a flash of light emitted by a moving object with the speed V_{obj} in 3-dimensional space with a speed V_{field} always propagates as a spherical wave with the same speed *c* in a 6-dimensional space.

Figure 1.1 shows the previously derived relationship between the object velocity V_{obj} and the field propagation velocity V_{field}, relative to the maximum velocity $V_{max} = c$. The figure shows a 5-dimensional section of a 6-dimensional space. A 6-dimensional representation would ultimately run back into itself along its entire surface.

The object velocity V_{obj} marked in blue is the velocity that takes place vectorially in the particle-field $F_{1\text{-}3}$. This object velocity is represented in the wave-field $F_{4\text{-}6}$ orthogonally to the dimensional plane D_{56} as a yellow vector and has the same pointer length in the representation. The field velocity F_{field} is represented in the wave-field parallel to the dimensional plane $D_{56.}$ In this way, a vectorial object velocity and a contracted field propagation velocity act simultaneously in the particle-field.

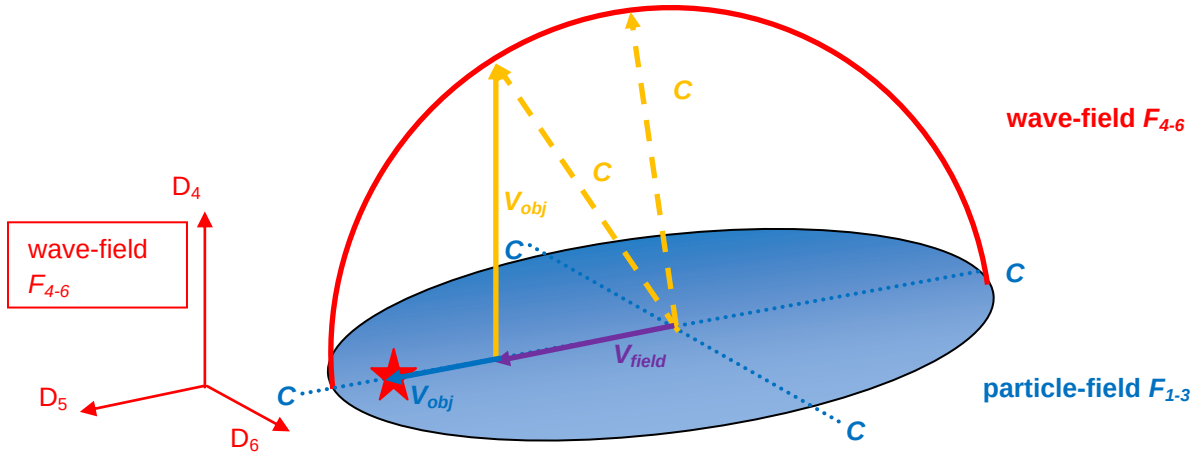

Figure 1.1: 5-dimensional representation of a field deformation for a moving object in field-space

Formula (1.11) for comparison:

$$c^2 = (c \sin(kt))^2 + (c \cos(kt))^2 = V_{obj}^2 + V_{field}^2$$

Up to this point, the answer is still pending as to which reference system according to formula (1.09) or (1.10) corresponds to the object velocity or the field propagation velocity and where the relativistic inertial system for both reference systems is located.

The next chapter first categorises both reference systems in a 6-dimensional field-space and describes some assumptions that must be made with the previous connections of space-time.

1.2 Definitions for Field-Space-Mechanics

Field-Space-Mechanics (FSM) is based on the realisation that 3-dimensional space R^3 must be extended to a 6-dimensional space R^6 in the *c*-metric system in order to represent and model field deformations. This chapter describes the terms associated with FSM and defines them via axioms.

Axiom 1a: The dimensions of space-time

Physical **space-time** is a 7-dimensional pseudo-Riemannian manifold, with one time dimension and six space dimensions of the so-called **field-space**, whereby three space dimensions represent the visible space in the particle-field $F_{1\text{-}3}$ and three represent the invisible space in the wave-field $F_{4\text{-}6}$.

Effect:

This axiom defines the basic structure of the FSM and enables the separation of visible and invisible matter.

Number of dimensions in Field-Space-Mechanics:

In addition to the dimension of time, the FSM model has six spatial dimensions:

- three spatial axes D_1, D_2, D_3 in index form as $D_{1\text{-}3}$ in the particle-field $F_{1\text{-}3}$

The following applies to the unit vectors :

$$\vec{e_2} \times \vec{e_3} = \vec{e_1} \quad (1.13)$$

$$\vec{e_3} \times \vec{e_1} = \vec{e_2} \quad (1.14)$$

$$\vec{e_1} \times \vec{e_2} = \vec{e_3} \quad (1.15)$$

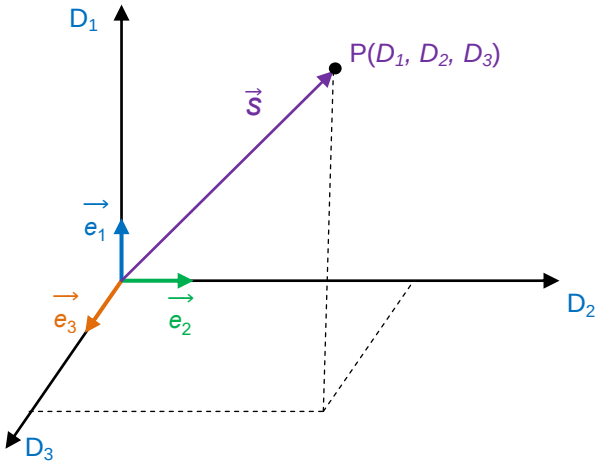

Figure 1.2: 3-dimensional representation of the particle-field $F_{1\text{-}3}$

- three spatial axes D_4, D_5, D_6 in index form as $D_{4\text{-}6}$ in the wave-field $F_{4\text{-}6}$

The following applies to the unit vectors:

$$\vec{e_5} \times \vec{e_6} = \vec{e_4} \quad (1.16)$$
$$\vec{e_4} \times \vec{e_6} = \vec{e_5} \quad (1.17)$$
$$\vec{e_4} \times \vec{e_5} = \vec{e_6} \quad (1.18)$$

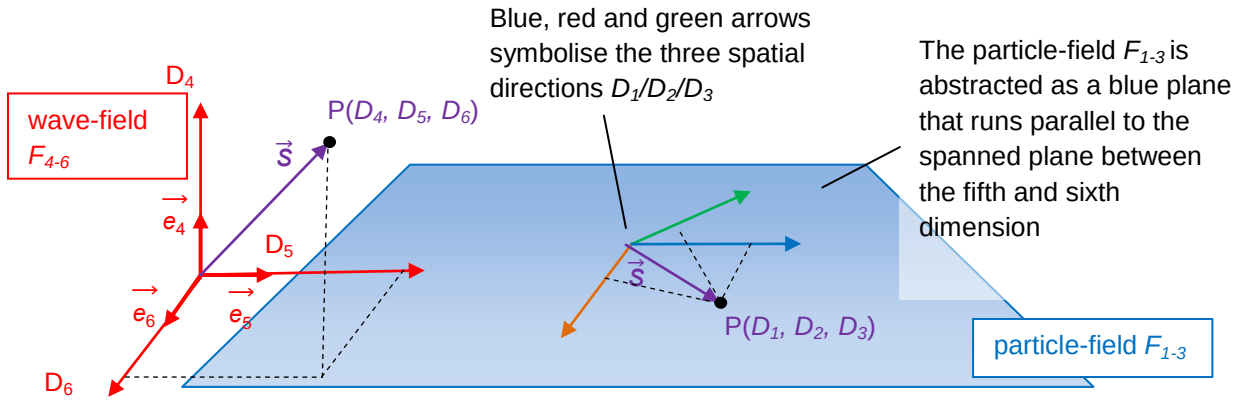

Figure 1.3: 6-dimensional representation of the field-space from the perspective of the wave-field $F_{4\text{-}6}$

Axiom 1b: The dimensions of space-time

By definition, **space-time is matter** and therefore forms an energy equivalent. This energy equivalent is proportional to the geometric expansion of space-time.

Effect:

An uneven distribution of energy within the space-time geometry deforms space-time, whereby the resulting space-time tension is directly proportional to the local energy gradient.

Axiom 1c: The dimensions of space-time

Space-time opposes the propagation of an electromagnetic wave, causing its propagation speed and thus its kinetic energy to be modelled relativistically.

Effect:

The effective inertial force of space-time thus determines the dynamics of spatial expansion. Consequently, the propagation behaviour of an electromagnetic wave is proportional to the expansion of space.

Axiom 2: The division of field-space into particle-field and wave-field

The six spatial dimensions of the field-space are divided into two orthogonal, 3-dimensional fields. The **particle-field** $F_{1\text{-}3}$ produces discrete matter as field compressions and the **wave-field** $F_{4\text{-}6}$ models waveforms as the cause of the effect in the particle-field. The particle-field is the effect, the wave-field is the cause, and they **exchange** their **fields** parallel to the **dimensional plane** D_{56}.

Effect:

This axiom enables the unification of macrocosm and microcosm by describing discrete arbitrary particles as the effect of invisible waves.

The particle-field *F* with index $F_{1\text{-}3}$ is the reference field that models visible matter as discrete objects. The particles in it are field compressions that act discretely and can be localised. The particle-field $F_{1\text{-}3}$ exchanges its field with the wave-field $F_{4\text{-}6}$ and vice versa. The total mass of the universe is distributed over both reference fields. The particle-field $F_{1\text{-}3}$ is linked to the wave-field $F_{4\text{-}6}$ by running parallel to the dimensional plane spanned between the so-called fifth and sixth dimensions. This area is shown as a blue area in **Figure 1.3.** A 6-dimensional space R^6 cannot be visualised in 3 dimensions. From the point of view of the wave-field $F_{4\text{-}6}$, the particle-field $F_{1\text{-}3}$ is therefore abstracted as a flat plane that runs back into itself as a band.

This perspective would be comparable to a hologram, which appears to the observer as a 3-dimensional image, but is actually 2-dimensional. Not all phenomena of a hologram (observer) can be predicted by a holographic measurement. The causes of localities lie in the processes of the wave-field $F_{4\text{-}6}$.

The wave-field *F* with index $F_{4\text{-}6}$ is the reference field that produces fields in wave form. This reference field makes it possible to describe the quantum mechanical processes as the cause of the effect in the particle-field $F_{1\text{-}3.}$ The effects of space-time are also modelled as a cause in the wave-field $F_{4\text{-}6.}$ The pictorial difference between the particle-field $F_{1\text{-}3}$ and wave-field $F_{4\text{-}6}$ is that the wave-field $F_{4\text{-}6}$ resembles an ocean in which matter is not measurable. In contrast, the particle-field $F_{1\text{-}3}$ represents the water surface, which makes it possible to measure emitted fields as vibrating, evaporated water droplets and moving bodies in a velocity diagram.

Axiom 3: The dimensional planes

The **dimensional planes** D_{45}, D_{46}, D_{56} are the surfaces spanned between the compact wave-field dimensions D_4, D_5, D_6, on which photons move and interact. The unit vectors follow the cross product rules.

Here, $\overrightarrow{\mathbf{dA}}$ stands for the vectorial area those results from two spanned dimensions.

$$\overrightarrow{e_6}\, dD_4 dD_5 = \overrightarrow{dA} = D_{45} \quad (1.19)$$

$$\overrightarrow{e_5}\, dD_4 dD_6 = \overrightarrow{dA} = D_{46} \quad (1.20)$$

$$\overrightarrow{e_4}\, dD_5 dD_6 = \overrightarrow{dA} = D_{56} \quad (1.21)$$

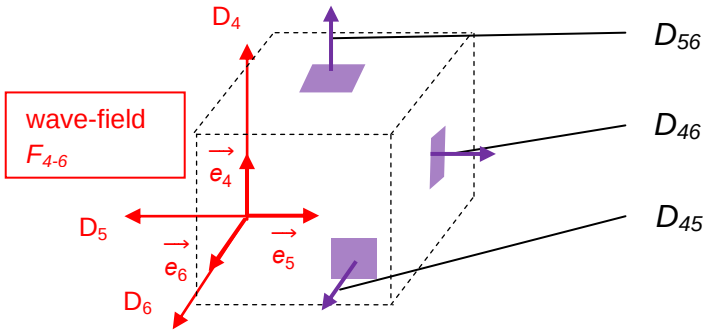

Figure 1.4: Representation of dimensional areas in the wave-field $F_{4\text{-}6}$

Effect:

This axiom ensures the geometric structure of the compact dimensions and enables mathematical representation during field exchange.

Axiom 4: The field-space dimensions

The **dimensions** of the **field-space** are antisymmetric and isotropic. The unit vectors follow the cross-product rules.

Effect:

This axiom ensures the antisymmetric geometry.

Axiom 5: The field propagation speed and object speed

The **speed parameters** V_4 and V_5 are orthogonal speed vectors that form the cathets of a Pythagorean triangle. In this triangle, the **maximum speed** $V_{max} = c$ forms the hypotenuse. The velocities are sinusoidal or cosinusoidal relative to the maximum velocities:

$$c^2 = (c \sin(kt))^2 + (c \cos(kt))^2 = V_4^2 + V_5^2 \quad (1.22)$$

The assignment is derived in **Chapter 2.1**.

Effect:

This axiom shifts the modelling of a space-time deformation into the wave-field.It enables the description of relativistic fields as the vibrational behaviour of matter using rotation matrices in the dimensional planes, e.g. D_{45} with $\overrightarrow{e_6}\, dD_4 dD_5 = \overrightarrow{dA} = D_{45}$.

The **object velocity V_3** is the velocity in the particle-field at which an object travels a certain measurable distance *s.* The index "3" denotes the three spatial directions $D_{1\text{-}3}$ of the visible part of the field-space.

The **field propagation velocity V_4** (corresponds to: V_{obj}) denotes the velocity of a field that runs through the fourth dimension of the field-space and acts parallel to an object velocity V_3.

The **field propagation velocity V_5** (corresponds to: V_{field}) denotes the velocity of a field that runs through the fifth dimension of the field-space and reflects the propagation velocity of fields in the particle-field.

Axiom 6: The field angle α

The **field angle α** describes the angle between the field propagation velocity V_5 in the fifth dimension or the field propagation velocity V_4 in the fourth dimension in relation to the maximum velocity V_{max}. This angle measurement takes a snapshot of all relativistic quantities as a phase from a rotation that occurs within a space-time deformation relative to the inertial system. The field angle [α] is in angles °.

Effect:

This axiom relates gravitational states to geometry depending on their oscillatory contributions.

Axiom 7: Field deformation

A **field deformation** in particle-field $F_{1\text{-}3}$ represents the proportional effect of a space-time deformation on arbitrary fields and their velocity vectors in wave-field $F_{4\text{-}6}$. The cause of a field deformation is modelled by the relativistic ratio of the two vectors for field propagation velocities V_4 and V_5, which act in their respective reference systems according to formulas (1.09) and (1.10) in the wave-field $F_{4\text{-}6}$. Both velocity vectors are subsequently defined by the indices, which in turn mark the action space in which they clearly develop their respective share of the effect on angular momentum. For simplicity, the velocity vectors are further represented in magnitude form with their indices.

Effect:

This axiom enables matter to be described as a geometric effect.

Figure 1.5 shows the previous result for a field deformation under the above defined designations for the field-space. There is no field deformation if the field propagation velocity V_5 corresponds to the maximum velocity with $V_{max} = c$. A field deformation occurs as soon as the field propagation velocity V_5 with $V_5 < c$ is present. The calculable speed of light corresponds to the velocity vector V_5.

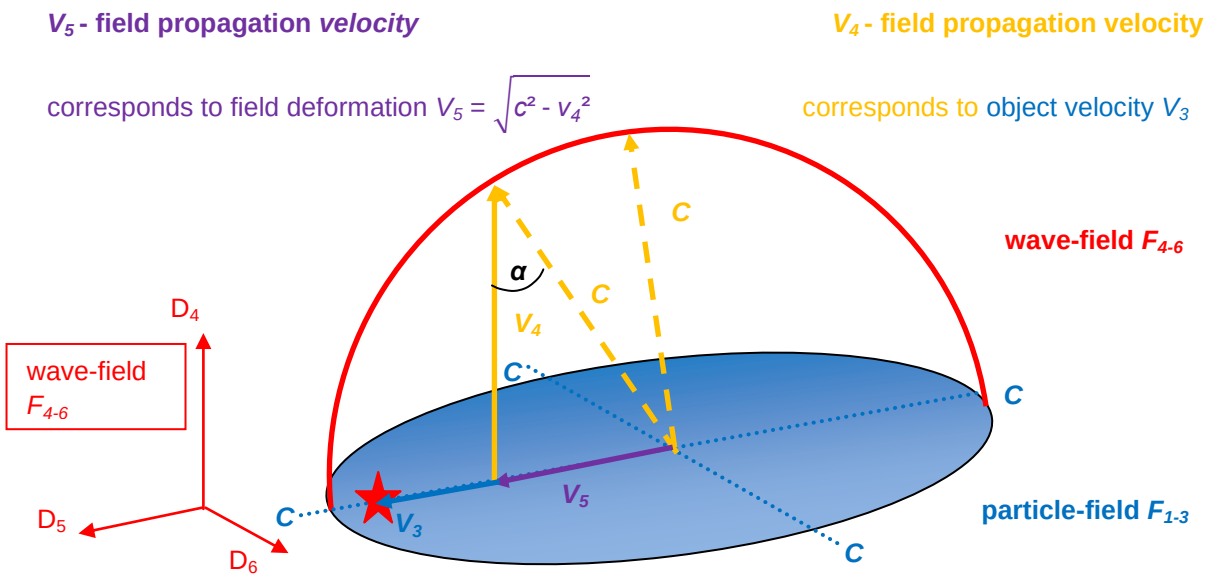

Figure 1.5: Adjusted indices for a field deformation in field-space

The field angle *α* shown in **Figure 1.5** corresponds to the general factor (*kt*) in the formulae (1.09) and (1.10) and thus describes the dynamics of the expansion of a photon and of the universe as a whole of all photons. Gravity and electrodynamics are described in the same geometric structure in a freely scalable manner.

Axiom 8: The principle of action in FSM

The dynamics of the universe are determined by the principle of **least action** in 7-dimensional space-time, whereby action combines geometric fields and hollow body vibrations.

Effect:

This axiom explains why field bodies, from photons to the size of a universe, periodically expand and contract.

Axiom 9: Scalability across all orders of magnitude

FSM is scalable across all physical orders of magnitude, from subatomic structures to the cosmos. **Matter and energy are geometric effects that operate through relativistic fields at all scales.**

Effect:

This axiom connects the microcosm with the macrocosm.

Axiom 10: The photon field of the universe is the fundamental field

The entire matter of the universe is realised as a **photon field** which is subject to space-time mechanical processes. The photon field is the basic electromagnetic field that fills the entire cosmic field-space and provides the matter for the two reference

fields, namely particle-field F_{1-3} and wave-field F_{4-6}. Depending on the cosmic space-time deformation, this photon field manifests itself relativistically with a higher field density as wave-field F_{4-6} and a lower field density as particle-field F_{1-3}.

Effect:

This axiom explains the source of matter within the universe.

Axiom 11: The global, electrical potential of the universe

Matter is formed orthogonally above and below the dimensional plane D_{56}. These formations parallel to the fourth spatial dimension act like **two electrical voltage potentials**, separated by the dimensional plane D_{56}. With the dynamic expansion of space in the universe, these two voltage potentials continue to act as a displacement current between two charged capacitor plates. The minimum of the voltage potentials can therefore be found at the location of the minimum length contraction for a space segment.

Effect:

This axiom explains how matter generates an electric potential. It makes it possible to explain and calculate particles of varying complexity.

Axiom 12: The particle model and coupling frequencies

The **particle model** replaces point particles with hollow body vibrations in the wave-field, which generate relativistic fields. The **coupling frequencies** are derived from the electron frequency, and **object masses** are derived from the electron mass as the base quantity for the minimum excitation.

Effect:

This axiom enables the unification of fundamental forces.

Axiom 13: The minimum coupling frequency for fine structures

From the **minimum coupling frequency** onwards, photons are able to interact electrically with their environment. From this frequency onwards, invisible photons from the dark energy pool enter into an electrical interaction within the photon field.

Effect:

This axiom enables the separation and description of uncoupled (dark) energy and coupled energy.

Axiom 14a: Photons in a bundle

Photons from a bundle of several photons are able to approach each other at a recurring point of contact in the wave-field $F_{4\text{-}6}$ to a **minimum distance** of their wavelength **($\lambda \sim 0$)**.

Effect:

There is no collapse upon approach, but rather a field exchange at the point of greatest deflection.

Axiom 14b: Photons in a bundle

The frequency of individual photons from a bundle of several photons reaches its **maximum deflection** when they oscillate at an integer multiple of the frequency of the bundle. The field strength is therefore strongest when the photons are at their common **point of contact**.

Effect:

The interaction from the wave-field $F_{4\text{-}6}$ into the particle-field $F_{1\text{-}3}$ occurs with its amplitude. A measurement in the wave-field registers a sinusoidal deviation or disturbance relative to the amplitude during the ongoing period.

Axiom 14c: Photons in a bundle

A **field exchange** between particles takes place at a distance equal to half their wavelength $\frac{\lambda}{2}$.

Effect:

The distances between two objects involved in an interaction can be predicted on the basis of their particle structure.

Chapter

2 Relativistic Consideration of Field-Space-Mechanics

2.1 Special Theory of Relativity of Field-Space-Mechanics

Creating the inertial system:

Both velocity parameters V_4 and V_5 each form a reference system in relation to the maximum velocity $V_{max} = c$. Due to the orthogonal alignment of the dimensional plane D_{45} to D_{56}, the following applies to each other: $V_4^2 + V_5^2 = c^2$.

Extreme cases:

An object moves in the particle-field with $V_3 = V_4 = c$, then $V_5 = 0$ applies.

An object moves in the particle-field with $V_3 = V_4 = 0$, then $V_5 = c$ applies.

Special case for the measurable photon in the particle-field: $V_3 = V_5 = c$, then $V_4 = 0$ applies

Figure 2.1 supplements **Figure 1.5** with two possible observation points for the detection of a field deformation within a 6-dimensional field-space, which could be observed outside a space-time deformation.

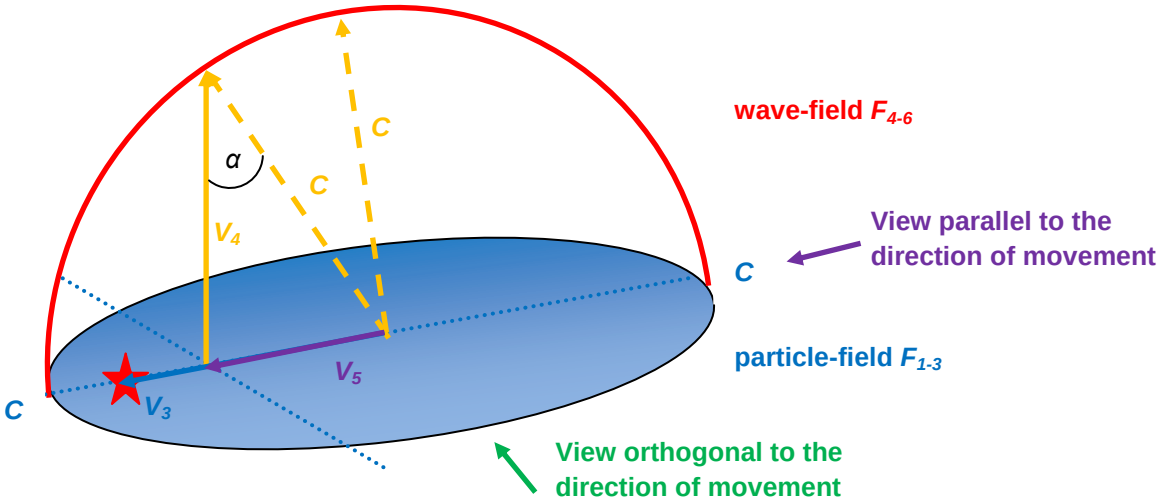

Figure 2.1: 5-dimensional representation of the field deformation supplemented with the labelling of a parallel and orthogonal observer perspective

The blue arrow describes the speed of an object within an imaginary light resonator. The reflection of emitted photons occurs at the edge. From the object's point of view, the light emitted in the opposite direction with the maximum speed $V_{max} = c$ appears to move away relatively with $c + V_3$ and catches up again with $c - V_3$ after hitting the resonator. The light emitted in the direction of movement initially moves away from the object relatively with $c - V_3$ and appears to return with $c + V_3$. As all photons in a resonator must meet again simultaneously at one point by definition of the maximum speed, a field deformation effect in the direction of movement with $\sqrt{c^2 - v_3^2}$ applies to the object due to its object speed V_3. The path component for the propagation of light in the direction $c - V_3$ and $c + V_3$ can be represented with the same total value at the location of the inertial system. For the field propagation velocity V_4 shown in **Figure 2.2**, the definition applies that the magnitude is equal to the object velocity V_3.

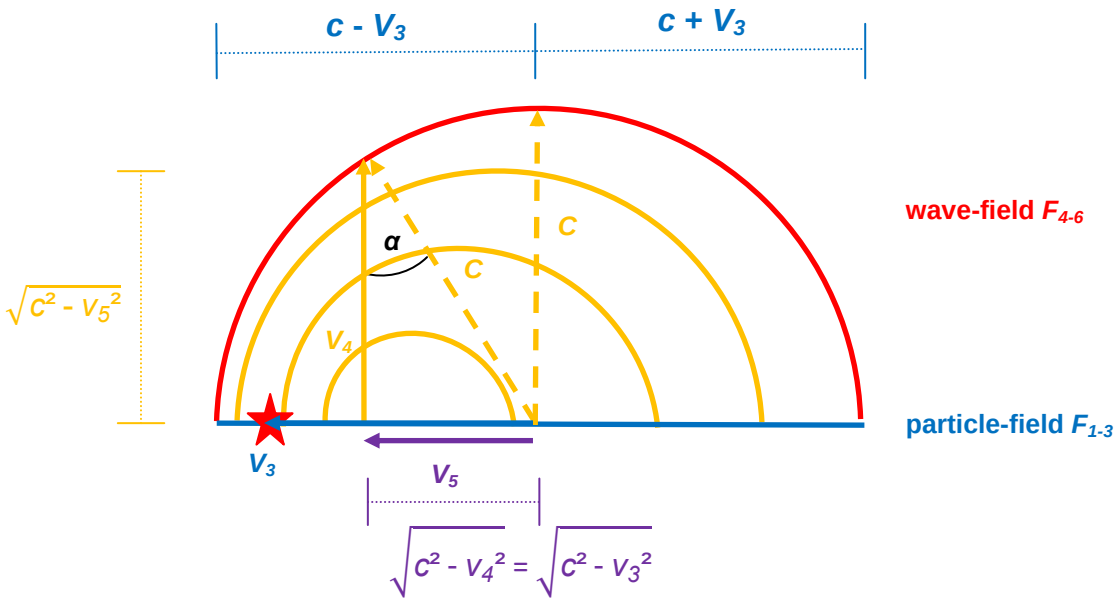

Figure 2.2: Field deformation orthogonal to the direction of movement, 4-dimensional representation

At maximum speed $V_{max} = c$ in the direction of movement towards the object:

$$V_a = \frac{\text{Raum}}{\text{Zeit}} = c\,\frac{(c - V_3)}{\sqrt{c^2 - V_3^2}} = c\,\sqrt{\frac{c - V_3}{c + V_3}} \qquad (2.01)$$

With maximum speed $V_{max} = c$ against the direction of movement of the object:

$$V_b = \frac{\text{Raum}}{\text{Zeit}} = c\,\frac{(c + V_3)}{\sqrt{c^2 - V_3^2}} = c\,\sqrt{\frac{c + V_3}{c - V_3}} \qquad (2.02)$$

Temporally resulting clocking t_{res} for an imaginary resonator over an equal path s:

$$t_{res} = t_{hin} + t_{her} = \frac{s}{V_a} + \frac{s}{V_b} = \frac{2s}{\sqrt{c^2 - V_3^2}} \tag{2.03}$$

This speed of light is measured in a light resonator over a distance s if the observer is orthogonal to the direction of movement:

$$V_{res} = V_5 = \sqrt{c^2 - v_3^2} \tag{2.04}$$

A **space-time deformation** caused by a moving object in the particle-field $F_{1\text{-}3}$ with an object velocity V_3 acts in the wave-field $F_{4\text{-}6}$ with the field propagation velocity V_4 **orthogonally** to a **field deformation**, which in turn is expressed by the field propagation velocity V_5. The speed of light is reduced to the field propagation velocity V_5 with the term $\sqrt{c^2 - v_3^2}$. Lorentz contraction and gravitational redshift are perceived as real space-time mechanical effects for the 5-dimensional view of space.

→ The trigonometric solution for the space-time deformation is:

$$V_4 = V_3 = c \cos(\alpha) \tag{2.05}$$

→ The trigonometric solution for the field deformation is:

$$V_5 = c \sin(\alpha) \tag{2.06}$$

→ For length contraction: $x' = x \sin(\alpha) = x \frac{V_5}{c}$ (2.07)

The object time of the moving object must be slower by a factor of $\frac{c}{\sqrt{c^2 - V_3^2}}$ than in a reference system that is at rest with respect to the surrounding field-space.

→ The trigonometric solution for the object time is:

$$t_{obj} = \frac{c}{V_5} t = \frac{t}{\sin(\alpha)} \tag{2.08}$$

The greater the field propagation velocity V_4 is effected, the longer the periodic inertial movements in the wave-field $F_{4\text{-}6}$, which extends the object time.

An inertial frame can be determined by assigning both velocity parameters $V_4(t) = c \cos(\alpha)$ and $V_5(t) = c \sin(\alpha)$. At the end of the spatial expansion of the universe with the maximum volume radius $r(t) = r$, the space-time mechanical effect with the Lorentz factor 1 for $V_5(t) = c \sin(\alpha)$ is present. This corresponds to the minimum length contraction of a spatial segment. The field angle α is 90° in this case. In the FSM model, the space-time mechanical effects are considered relative to the minimum Lorentz contraction at the point of maximum expansion of the universe. These results provide a reference point for space-time and its space-time mechanical equalising forces during the expansion of the universe, which gives it a beginning and an end according to the extreme cases mentioned above. If there were an imaginary observer outside the universe, then this observer could register the field propagation velocity V_5 depending on space-time mechanical influences in the universe. The imaginary observer recognises the electromagnetic photon field and the accelerated movement of the space expansion of the universe with $r''(t)$ from outside. The length of a space segment is now registered as dynamic. From the point of view of the inertial system, electromagnetic waves such as those of a visible photon are always detected as a gravitational redshift in the area of influence of a space-time deformation.

The observer should now stand parallel to the direction of movement in the universe and recognise the space-time mechanical effects:

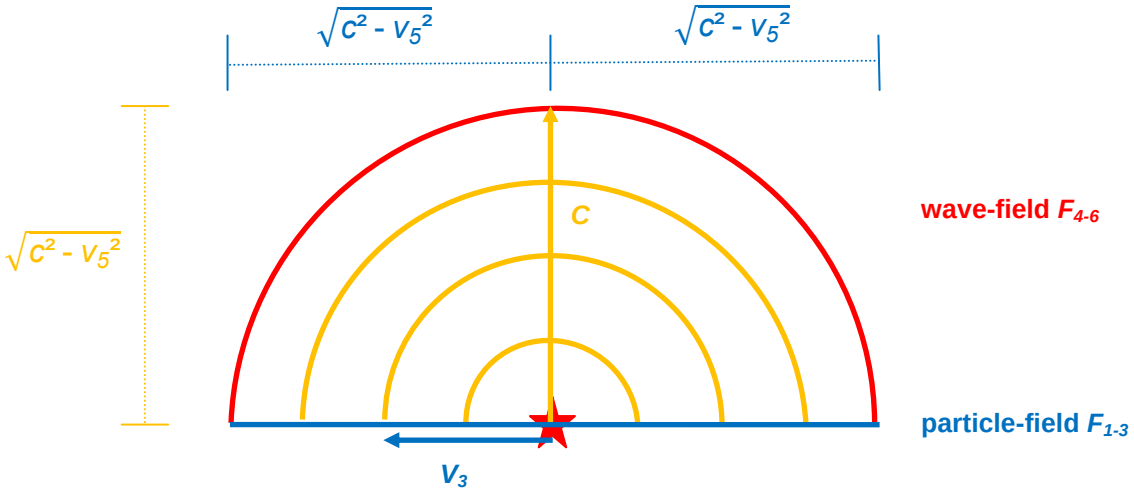

Figure 2.3: Field deformation parallel to the direction of movement

Lorentz transformation of time: The time dilation resulting from the Lorentz transformation and the gravitational redshift is also recognised.

Lorentz transformation of space: Parallel to the direction of movement, no contraction can be detected because the observer does not detect any change in the maximum velocity $V_{max} = c$.

The speed of light from a parallel perspective:

$$V_{res} = c \frac{\sqrt{c^2 - V_5^2}}{\sqrt{c^2 - V_5^2}} = c \qquad (2.09)$$

The light resonator determines the field propagation velocity with the maximum velocity $V_{max} = c$ instead of with a shortened V_5, with and without the influence of the moving reference system. Even if the resonator were located in a non-moving reference system with $V_3 = 0$, the speed of the light could also only be determined with this value *c.* The observer is therefore unable to determine the magnitude of his own length contraction if the direction of motion is parallel. All other spatial directions result in the same solution from this perspective.

A field deformation between the current field propagation velocity V_5 and the maximum velocity $V_{max} = c$ is only registered if the observer is outside the influence of the space-time deformation and observes a movement orthogonal to the direction of movement.

Findings from FSM-STR for 7-dimensional field-space with time:

1) The field propagation velocity V_4 is proportional to the space-time mechanical effects of a space-time deformation.
2) The field propagation velocity V_5 is proportional to the space-time mechanical effects of a field deformation.
3) The field propagation velocity V_5 corresponds to the speed of light of photons.
4) An object with an object velocity V_3 in the particle-field $F_{1\text{-}3}$ can move through the connection in the wave-field $F_{4\text{-}6}$ by reducing its field propagation velocity V_5 in favour of V_4:
   → an object moves in the particle-field with $V_3 = V_4 \rightarrow c$, then $V_5 \rightarrow 0$
   → an object moves in the particle-field with $V_3 = V_4 \rightarrow 0$, then $V_5 \rightarrow c$
5) A measurable photon propagates faster and faster with $V_5 = c \sin(\alpha)$ as the universe expands and the space-time mechanical effects diminish.

Interpretation of the Lorentz factor for FSM:

Case a. Lorentz factor = 1:

The space-time deformation is minimal. Space-time slows down the field propagation velocity V_5 to the maximum velocity $V_{max} = c = V_5$.

Case b. Lorentz factor > 1:

There is an increased space-time deformation, which requires additional energy for the contraction work. The field propagation velocity V_5 is contracted relative to the maximum velocity $V_{max} = c$. In **Chapter 7**, the cosmic processes are calculated for cases with a Lorentz factor > 1.

Case c. Lorentz factor < 1:

As soon as the Lorentz factor falls below 1, an electromagnetic wave expands further in space-time. Consequently, a wave period with its field propagation speed V_5 travels a greater distance relative to the nominal case with the maximum speed V_{max}. This case has not yet been observed.

2.2 General Theory of Relativity of Field-Space-Mechanics

- Draft version -

The purpose of this chapter is to define the field equations based on the geometric foundations of the FSM model. The predicted and heuristically derived relationships presented in the following chapters are thus scientifically valid. Simulation models can be developed on this basis. For specific applications, the general formulas and relationships must be further refined and defined. These elaborated mathematical foundations form the basis for establishing further relationships. For the sake of clarity, we intend to remain within these foundations for the purposes of this paper.

1. Precise diagonal metric
2. Derivation of the geodesic equation
3. Christoffel symbols
4. Riemann tensor
5. Ricci tensor
6. Einstein tensor
7. Impulse energy tensor
8. Gauge potential
9. 7-dimensional field equations
10. Compactification from 7D to 4D with its principle of action
11. Wave equation for gravitational waves
12. Field radius r
13. Circular frequency k
14. Photon Subspace Theory
15. Group Theory
16. Chern classes
17. Fine structure constant
18. Spin-0-Pair Theory – Entanglement
19. Scalability
20. Comparison

1. Precise diagonal metric

The FSM predicts a dynamic 7-dimensional field-space with time ($D_{1\text{-}3}$ as visible dimensions in the particle-field $F_{1\text{-}3}$; $D_{4\text{-}6}$ as compact dimensions in the wave-field $F_{4\text{-}6}$, time t). The observable space in the particle-field $F_{1\text{-}3}$ is understood as a projection of the wave-field $F_{4\text{-}6}$ or as a hologram. The metric must be able to quantify the relationships described in the axioms (**Chapter 1.2**). It is diagonal to ensure the orthogonality of the dimensional planes D_{45}, D_{46}, D_{56}, and contains scaling factors for possible photon subspaces.

Definition of dimensions and indices:

- 7-dimensional (7D) space-time indices with field-space and time; Lorentz indices, covariant at the bottom, contravariant at the top with metric
- M, N = 0, 1, 2, 3, 4, 5, 6
- 0 – time coordinate (t), unit : m, normalised by the product (ct)
- 1, 2, 3 – visible space-time dimensions of the 'particle-field'; x, y, z; unit: m
- 4, 5, 6 – compact dimensions of the 'wave-field'; y^4, y^5, y^6; unit: m; this is the space for internal degrees of freedom that generate wave fields
- μ, ν = 0, 1, 2, 3 – only the visible 4D space-time indices in the particle-field
- m, n = 4, 5, 6 – only the compact 3D wave-field dimensions

Global and local gravitational effects dominate in visible 4D space. Compact space generates massive fields through reduction.

Starting point – Minkowski metric with the STR metric in 4D:

$$-\frac{dx^2}{dt^2} - \frac{dy^2}{dt^2} - \frac{dz^2}{dt^2} + c^2 = \frac{ds^2}{dt^2}$$

$$ds^2 = -c^2\,dt^2 + dx^2 + dy^2 + dz^2 = \eta_{\mu\nu}\,dx^\mu\,dx^\nu \qquad (2.10)$$

- ds^2 – the invariant length square (interval); unit: m²; measures the space-time distance
- $\eta_{\mu\nu}$ – diag(-1,1,1,1) the metric tensor (flat, Lorentz-signed); dimensionless
- c – maximum speed $V_{max} = c = 299792458\ \frac{m}{s}$

Extension to 7D – Minkowski metric with the STR metric in 7D::

Physical space-time is a smooth, orientable, pseudo-Riemannian manifold. The FSM predicts that the wave-field $F_{4\text{-}6}$ is linked to the visible particle-field $F_{1\text{-}3}$ via its compact dimensions.

$$7D = 4D_x \times 3D_y$$

$$ds^2 = -c^2\,dt^2 + dx^2 + dy^2 + dz^2 + dy_4^2 + dy_5^2 + dy_6^2 = \eta_{MN}\,dx^M\,dx^N \qquad (2.11)$$

- η_{MN} – Diagonal metric; signature (-, +, +, +, +, +, +)

The diagonal metric describes an empty, flat 7-dimensional space-time without gravity or oscillations.

Introduction of a local metrical disturbance h_{MN}:

To take into account gravity, vector and scalar fields, the perturbation h_{MN} is added:

$$g_{MN} = \eta_{MN} + h_{MN} \tag{2.12}$$

- h_{MN} – perturbative disturbance; dimensionless

Block structure for h_{MN}:

$$h_{MN} = \begin{pmatrix} h_{\mu\nu} & h_{\mu m} \\ h_{m\nu} & h_{mn} \end{pmatrix} \tag{2.13}$$

a) $h_{\mu\nu}$ – Gravity with an oscillating isotropic gravitational disturbance

The 4D-visible curvature must take into account the periodic cavity vibration in the form of a mathematical rotation. **Figures 2.11** and **2.12** show that the local electromagnetic oscillation, as a subspace within the universe, merely permits a periodic variation in its inertial force between $\cos(kt = 0) = 1$ for the maximum at the location of the D_{56} dimensional plane and $\cos(kt = 90°) = 0$.

$$g_{\mu\nu} = \eta_{\mu\nu} + h_{\mu\nu} \tag{2.14}$$

Static gravity generates the Schwarzschild metric:

$$h_{\mu\nu} = \frac{2\,G\,M}{c^2\,r_S}\,\delta_{\mu\nu}$$

A periodic disturbance term counteracting the static gravitational force is now taken into account. This results in an oscillating isotropic gravitational disturbance:

$$h_{\mu\nu} = \frac{G\,M}{c^2\,r}\,(1+\cos(kt+\beta))\,\delta_{\mu\nu} \tag{2.15}$$

$h_{00} = 2\,\frac{G\,M}{c^2\,r}$ → Reduction to a static solution according to Schwarzschild

In component notation:

$$h_{tt} = -\frac{G\,M}{c^2\,r}\,(1 + \cos(kt + \beta)); \; h_{xx} = h_{yy} = h_{zz} = \frac{G\,M}{c^2\,r}\,(1 + \cos(kt + \beta))$$

$h_{\mu\nu} = 0$ for $\mu \neq \nu$

- G – gravitational constant; $G = 6{,}674\ 10^{-11}\ \frac{m^3}{kg\ s^2}$
- M – mass; unit: kg
- c – maximum speed $V_{max} = c = 299792458\ \frac{m}{s}$
- r – field radius; unit: m
- k – angular frequency; unit: $\frac{1}{s}$
- (1+ cos(kt)) – oscillation of the local disturbance; describes the periodic evolution of inertia parallel to the fourth dimension; it takes into account the relationship: $c^2 = V_4^2 + V_5^2$
  a) cos(kt = 0) = 1 – point of contact parallel to the plane of dimensions D_{56}; maximum amplitude of the inertial motion
  b) cos(kt = 90°) = 0 means an orthogonal displacement of its inertial force relative to the dimension plane D_{56}, smallest amplitude of inertial motion
  c) For objects in a state of rotation, the intrinsic rotation that averages out the oscillation results in [1 + cos(kt) = 1] with $\frac{G\,M}{c^2\,r}$
  d) For the static case, this yields the fixed maximum, the Schwarzschild dynamics $\frac{2\,G\,M}{c^2\,r}$
- β – deviation angle as fixed phase shift; unit: rad, dimensionless; 0° < β < 90°; explains coordinate-dependent interaction effects
  a) At 0°, the field exchange with the particle field is maximally parallel to the dimensional plane D_{56}. → strong interaction dominates completely
  b) A possible deviation of β up to 90° results in a shift from strong interaction to weak interaction
  c) Although the interaction for β = 90° persists in the wave-field, it no longer acts in the particle-field
  d) Explains the possible interaction of dark matter with 4D
- $\delta_{\mu\nu}$ – Kronecker delta; 1 at $\mu = \nu$; 0 otherwise

b) $h_{\mu m}$ – perturbable vector fields

$h_{\mu m} = h_{m\mu} = (A^a_\mu + \delta A^a_\mu)\,\delta_{am}$

- Indices: a, m = 4, 5, 6; μ = 0, 1, 2, 3
- A^a_μ – Vector field in 7D; geometrically, it links the wave-field to the particle-field; following compactification to 4D, it behaves as a gauge potential.

- δA^a_μ – Possibility of deviation, e.g. due to an external disturbance via the particle-field; compensating forces counteract the disturbance.
- δ_{am} – dimensional planes

c) $h_{m\nu}$ – perturbable vector fields

$h_{m\nu} = h_{\nu m} = (A^a_\nu + \delta A^a_\nu)\ \delta_{am}$

- Indices: a, m = 4, 5, 6; ν = 0, 1, 2, 3

d) h_{mn} – Curvature in the wave-field

$h_{mn} = 0$

- In the wave-field, there is no curvature of space-time, but only vector fields which, within this Euclidean space ($3D_y$), model the deformation of space-time in particle-field ($4D_x$).
- Following compactification, scalar terms will appear at this point that stabilise a dynamic space-time deformation via feedback.

Incorporation of the global curvature of the universe:

The universe possesses its own inertial motion in space-time, which further influences the surrounding curvature of objects. The effect of global curvature is measured by the deviation from orthogonality to the D_{56} dimensional plane for all objects. This additional space-time curvature describes the influence of dark energy on massive objects. For g_{MN}, the term

$[1 + \cos(k_{Uni}\, t)]$

is introduced to account for the global influence of dark energy on local space-time curvature. This term decreases dynamically to a factor of $(1 + \cos(90°))$ as the universe expands to its maximum size.

$$g_{MN} = [1 + \cos(k_{Uni}\, t)]\ (\eta_{MN} + h_{MN}) \tag{2.16}$$

Explicit matrix: (2.17)

$$g_{MN} = \begin{pmatrix} g_{00} & 0 & 0 & 0 & A^4_0 + \delta A^4_0 & A^5_0 + \delta A^5_0 & A^6_0 + \delta A^6_0 \\ 0 & g_{11} & 0 & 0 & A^4_1 + \delta A^4_1 & A^5_1 + \delta A^5_1 & A^6_1 + \delta A^6_1 \\ 0 & 0 & g_{22} & 0 & A^4_2 + \delta A^4_2 & A^5_2 + \delta A^5_2 & A^6_2 + \delta A^6_2 \\ 0 & 0 & 0 & g_{33} & A^4_3 + \delta A^4_3 & A^5_3 + \delta A^5_3 & A^6_3 + \delta A^6_3 \\ A^4_0 + \delta A^4_0 & A^4_1 + \delta A^4_1 & A^4_2 + \delta A^4_2 & A^4_3 + \delta A^4_3 & g_{44} & 0 & 0 \\ A^5_0 + \delta A^5_0 & A^5_1 + \delta A^5_1 & A^5_2 + \delta A^5_2 & A^5_3 + \delta A^5_3 & 0 & g_{55} & 0 \\ A^6_0 + \delta A^6_0 & A^6_1 + \delta A^6_1 & A^6_2 + \delta A^6_2 & A^6_3 + \delta A^6_3 & 0 & 0 & g_{66} \end{pmatrix}$$

$$g_{00} = - c^2 [1 + \cos(k_{Uni}\, t)] \left(1 - \frac{G\, M}{c^2\, r} (1 + \cos(kt + \beta))\right)$$

$$g_{11} = g_{22} = g_{33} = [1 + \cos(k_{Uni}\, t)] \left(1 + \frac{G\, M}{c^2\, r} (1 + \cos(kt + \beta))\right)$$

$$g_{44} = g_{55} = g_{66} = [1 + \cos(k_{Uni}\, t)]$$

Line element ds^2:

$$ds^2 = g_{MN}\, dx^M\, dx^N$$

$ds^2 = [1 + \cos(k_{Uni}\, t)] \times$ [flat 7D Minkowski space + oscillating isotropic gravitational perturbation + vector coupling terms]

$$ds^2 = [1 + \cos(k_{Uni}\, t)] [- c^2\, dt^2 + dx^2 + dy^2 + dz^2 + dy_4^2 + dy_5^2 + dy_6^2 + \frac{G\, M}{c^2\, r} (1 + \cos(kt + \beta)) (c^2\, dt^2 + dx^2 + dy^2 + dz^2) + 2(A_\mu^a + \delta A_\mu^a)\, dy_a\, dx^\mu] \quad (2.18)$$

- $[1 + \cos(k_{Uni}\, t)]$ – dilatational cosmic oscillation; k_{Uni} – the angular frequency of the universe; a factor of 1 results in the observable relativity of space-time; the dynamics $\cos(k_{Uni}\, t)$ result in a global, non-observable relativity, explaining the ratio between dark energy and already coupled matter
- $[- c^2\, dt^2 + dx^2 + dy^2 + dz^2]$ – flat 4D space-time as a background; STR
- $[dy_4^2 + dy_5^2 + dy_6^2]$ – flat, compact wave-field dimensions; similar to Kalzua-Klein
- $[\frac{G\, M}{c^2\, r} (1 + \cos(kt + \beta)) (c^2\, dt^2 + dx^2 + dy^2 + dz^2)]$ – oscillating isotropic gravity; similar to Schwarzschild, but with oscillating inertial dynamics for arbitrarily scalable electromagnetic waves
  $(1 + \cos(kt + \beta))$ – focus on amplitude → factor 2 (Schwarzschild solution)
  $(1 + \cos(kt + \beta))$ – the dynamic case produces factor 1 (Kerr-like)
- β – for the D_{56} dimensional plane: maximum interaction at $\beta = 0$, dynamically weak interaction at $0 < \beta < 90°$
- $[2(A_\mu^a + \delta A_\mu^a)\, dy_a\, dx^\mu]$ – perturbable vector fields from wave-field dimensions; Kaluza–Klein-like
- A_μ^a – Vector field in 7D; dimensionless in the 7D context; with compactification, the effective 4D coupling is achieved through rescaling: $A_\mu^a \rightarrow A_\mu^a / R$

The metric implements the definition given in **Chapter 1.1**.

Reduction to STR/GTR and verification:

The first step is to eliminate the compact wave-field dimensions for the observable 4D space-time (t, x, y, z). Consequently, the movements:

$$dy_4^2 = dy_5^2 = dy_6^2 = 0$$

$ds^{2\,(4)} = [1 + \cos(k_{Uni}\, t)]\, [- c^2\, dt^2 + dx^2 + dy^2 + dz^2 + \frac{G\, M}{c^2\, r}\, (1 + \cos(kt + \beta))\, (c^2\, dt^2 + dx^2 + dy^2 + dz^2]$

$ds^{2\,(4)} = [1 + \cos(k_{Uni}\, t)]\, \eta_{\mu\nu}\, dx^{\mu}\, dx^{\nu} + h_{\mu\nu}\, dx^{\mu}\, dx^{\nu}$

GTR and STR ignore the global curvature $\cos(k_{Uni}\, t)$ in the universe:

$\cos(k_{Uni}\, t) = 0$

$ds^{2\,(4)} = \eta_{\mu\nu}\, dx^{\mu}\, dx^{\nu} + h_{\mu\nu}\, dx^{\mu}\, dx^{\nu}$

Borderline case STR:

$h_{\mu\nu} \rightarrow 0$

$ds^2 = - c^2\, dt^2 + dx^2 + dy^2 + dz^2$

Borderline case GTR:

a) Fixing the local oscillation at the point of maximum value using $kt = \beta = 0$:

$\cos(kt = 0°) = 1 \rightarrow 1 + \cos(kt = 0°) = 2$

The Schwarzschild solution for the perturbation is as follows::

$$h_{\mu\nu} = \frac{G\, M}{c^2\, r}\, 2\, \delta_{\mu\nu}$$

Using the static approximation, this leads to the Schwarzschild metric.

b) Oscillation about the time-averaged value:

$<\cos(kt) = 0> \rightarrow <1 + \cos(kt) = 1>$ for: $\beta = 0$

The following applies to the effective disturbance during oscillation:

$$h_{\mu\nu} = \frac{G\, M}{c^2\, r}\, \delta_{\mu\nu}$$

This results in half the Schwarzschild strength for models involving rotating objects, as is also the case in the Kerr metric.

<u>An example based on the gravitational lensing effect:</u>

The gravitational lensing effect is a phenomenon in which light rays are deflected by the curvature of space-time around a massive object, resulting in distortions, multiple images, or magnifications of distant sources. The critical impact parameter *b* is derived using both the Schwarzschild and Kerr metrics. To verify the FSM model, the critical impact parameter *b* should also be derived.

Derivation via FSM:

If ignoring the global component, photons are always null-geodesic with:

$ds^2 = 0$

It contains two conserved quantities that are not affected by any external forces:

a) Energy parameter E → internal energy increases with the addition of matter

b) Angular momentum parameter L → accumulates as a result of the absorption of matter the angular momentum

$$ds^2 = 0 = g_{00} (\frac{dt}{d\lambda})^2 + g_{rr} (\frac{dr}{d\lambda})^2 + g_{\varphi\varphi} (\frac{d\varphi}{d\lambda})^2$$

$$\frac{dt}{d\lambda} = - \frac{E}{g_{00}} \; ; \; \frac{d\varphi}{d\lambda} = \frac{L}{g_{\varphi\varphi}}$$

- φ – azimuth angle

Insert into $ds^2 = 0$:

$$0 = g_{00} (- \frac{E}{g_{00}})^2 + g_{rr} (\frac{dr}{d\lambda})^2 + g_{\varphi\varphi} (\frac{L}{g_{\varphi\varphi}})^2$$

With:

$$g_{\varphi\varphi} \approx r^2 \; ; \qquad g_{rr} \approx 1 \; ; \qquad g_{00} = - c^2 [1 + \cos(k_{Uni}\, t)] (1 - \frac{G\, M}{c^2\, r} (1 + \cos(kt + \beta)))$$

- $[1 + \cos(k_{Uni}\, t)]$ – omitted with $\cos(k_{Uni}\, t) = 0$ for local viewing
- $(1 + \cos(kt + \beta))$ – generated by g_{00} and simplified to $f = (1 + \cos(kt + \beta))$
- $\frac{1}{g_{00}} = \frac{1}{c^2} (1 + \frac{f\, G\, M}{c^2\, r})$

This leads to the radial equation derived from the null geodesic condition:

$$(\frac{dr}{d\lambda})^2 = E^2 \frac{1}{c^2} (1 + \frac{f\, G\, M}{c^2\, r}) - \frac{L^2}{r^2}$$

Conversion using $\frac{E^2\, r^2}{L^2} = 1$, with c as the natural unit according to convention:

$$(\frac{dr}{d\lambda})^2 = E^2 - [\frac{L^2}{r^2} (1 - \frac{f\, G\, M}{c^2\, r})] = E^2 - V_{eff}(r)$$

The effective potential $V_{eff}(r)$ is factored by the centrifugal term:

$$V_{eff}(r) = \frac{L^2}{r^2} (1 - \frac{f\, G\, M}{c^2\, r})$$

The following is the derivation of the impact parameter b_{crit} as the transition radius for photons that fall into the black hole or are merely deflected. At the photon sphere with radius r_{ph}, a circular orbit holds $\frac{dr_{ph}}{d\lambda} = 0$.

$E^2 - V_{eff}(r) = 0$

Possible instability occurs as a function of the field radius r_{ph} at $V_{eff}(r)$ auf. To this end, the extremum is determined:

$$\frac{dV_{eff}}{dr_{ph}} = \frac{1}{dr_{ph}} [L^2(-2r_{ph}^{-2} - \frac{f\,G\,M}{c^2} r_{ph}^{-3})] = 0$$

$$\frac{dV_{eff}}{dr_{ph}} = L^2 (-2r_{ph}^{-3} + 3\frac{f\,G\,M}{c^2} r_{ph}^{-4}) = 0$$

$$r_{ph} = 1{,}5\,\frac{f\,G\,M}{c^2} = 1{,}5\,r\,f \rightarrow \text{This is the unstable circular path of a photon.} \qquad (2.19)$$

Using r_{ph} with $r_{ph} = 1{,}5\,r\,f$:

$$E^2 = \frac{L^2}{r_{ph}^2} (1 - \frac{f\,G\,M}{c^2\,r_{ph}}) = \frac{L^2}{r_{ph}^2} (1 - \frac{f\,r}{r_{ph}})$$

$$\frac{L^2}{E^2} = 6{,}75\,r^2\,f^2$$

The critical impact parameter b_{crit} is defined as $\frac{L}{E}$:

$$\frac{L}{E} = b_{crit} = \sqrt{6{,}75}\,r\,f = 2{,}598\,r\,f \qquad (2.20)$$

- r – field radius
- $f = (1 + \cos(kt + \beta))$
- β – deviation angle; here, it describes the prograde/retrograde deviation from the orthogonal angle of incidence into the black hole

a) Borderline case:

$r_{ph} = 1{,}5\,r\,(1 + \cos(kt + \beta))$

A reference point must be defined as the initial position. This should be defined by an orthogonal angle of incidence at:

$kt + \beta = 0°$

$r_{ph} = 1{,}5\,r\,(1+ 1) = 3\,r$

$b_{crit} = 2{,}598\,r\,f = 2{,}598\,r\,(1+ 1) = 5{,}196\,r$ → as in the case of Schwarzschild and Kerr

- For $b_{crit} < 5{,}196\ r$ photons are captured by the black hole
- For $b_{crit} = 5{,}196\ r$ photons orbit in an unstable manner on the photosphere
- For $b_{crit} > 5{,}196\ r$ photons are deflected (**gravitational lensing effect**)

The natural limits of the extreme values for prograde and retrograde rotation reach certain maximum values that are multiples of the field radius r.

b) Case for the prograde (with the) rotation:

The minimum value for r_{ph} can only be the simple factor for the field radius r, because the photon can no longer be detected after that.

For: $r_{ph} = r$	For: $r_{ph} = 1{,}5\ r$
$r = 1{,}5\ r\ (1 + \cos(kt = 0° + \beta))$	$1{,}5\ r = 1{,}5\ r\ (1 + \cos(kt = 0° + \beta))$
$\frac{2}{3} = (1 + \cos(kt = 0° + \beta))$	$1 = (1 + \cos(kt = 0° + \beta))$

Deviation from the relative value $kt = 0°$:

$\cos(kt = 0° + \beta)) = \frac{2}{3} - 1 = -\frac{1}{3}$	$\cos(kt = 0° + \beta)) = 0$
$\beta = \arccos(-\frac{1}{3}) \approx 109{,}5°$	$\beta = \arccos(0) \approx 90°$
$b_{crit} = 2{,}598\ (1 + \cos(kt = 0° + \beta = 109{,}5°))$	$b_{crit} = 2{,}598\ (1 + \cos(kt = 0° + \beta = 90°))$
$b_{crit} = 1{,}73\ r$ (near Kerr)	$b_{crit} = 2{,}598\ r$

With an angle of incidence of < 90° in prograde rotation, a photon is captured by the black hole at a distance of $r_{ph} = 1{,}5\ r$ from the photon sphere. The angle of incidence of 109.5° at $r_{ph} = r$ means that a photon moves away from the black hole at an angle of 19.5°. This could apply to matter that, due to electrostatic repulsion, makes an additional negative contribution to the gravitational force.

Hypothetically, the term $(1 + \cos(kt = 0° + \beta))$ would allow for an amplification up to $r_{ph} = \frac{\lambda_{BH}}{2\pi}$ with β close to 180°. An angle of 180° would correspond to the direct direction out of the black hole.

- λ_{BH} – wavelength of the black hole within the event horizon r

c) Case of retrograde (opposite) rotation:

For: $r_{ph} = 4\ r$

The cosine function is restricted to values between 0 and 1. If the transition is to be considered relative to the critical boundary, then the orthogonal angle to the black

hole must be at cos(0) with respect to the opposite quadrant. Turning the quadrant 90° relative to the critical boundary for r_{ph} triggers the necessary reflection. This is accounted for by an additional factor of 1.

$4\,r = 1{,}5\,r\,(1 + 1 + \cos(kt = 0° + \beta))$

$\frac{8}{3} = (1 + 1 + \cos(kt = 0° + \beta)$

$\beta = \arccos(\frac{2}{3}) \approx 48{,}2°$

$b_{crit} = 2{,}598\,((1 + 1 + \cos(kt = 0° + \beta = 48{,}2°)) = 6{,}93\,r$ (near Kerr)

For: $r_{ph} = 4{,}5\,r$

$4{,}5\,r = 1{,}5\,r\,(1 + 1 + \cos(kt = 0° + \beta))$

$3 = (1 + 1 + \cos(kt = 0° + \beta))$

$\beta = \arccos(1) = 0°$ → trigonometric limit

$b_{crit} = 2{,}598\,((1 + 1 + \cos(kt = 0° + \beta = 0°)) = 7{,}794\,r$

At a retrograde angle of incidence of 48.2°, a photon is deflected by the photon sphere at $r_{ph} = 4\,r$. In the case of a 90° angle, deflection occurs already at a distance of $r_{ph} = 4{,}5\,r$.

2. Derivation of the geodesic equations

The geodesic equations define the trajectories of particles and fields in the 7-dimensional FSM geometry. Geodesics are the generalised ‘straight lines’ in curved spaces and explain in the FSM how mass arises from frequency multiples and charge from rotation in compact dimensions. Geodesics of the FSM are comparatively simple because they use the orthogonal dimensions to directly derive causal effects such as gravity as a counterforce to electromagnetism, thus representing the visible particle-field $F_{1\text{-}3}$ as a holographic projection.

Starting point – The invariant line length in the FSM metric:

$$ds^2 = g_{MN}\,dX^M\,dX^N \qquad (2.21)$$

- ds^2 – invariant line length square
- g_{MN} – 7-dimensional metric tensor (dimensionless) for curvature and rotations; M, N = 0,…, 6 (0 = time t, 1, 2, 3 = particle-field, 4, 5, 6 = wave-field)
- dX^M bzw. dX^N – infinitesimal coordinate shift; unit: m; to parameterise trajectories

Effect function for geodesists:

Geodesics are the paths that maximise the integral over the arc length (or, equivalently, the proper time τ).

Functional S for geodesists (shortest curves) in 7D:

$$S = \int ds = \int_{\lambda_1}^{\lambda_2} \sqrt{g_{MN} \frac{dx^M}{d\lambda} \frac{dx^N}{d\lambda}}\, d\lambda \tag{2.22}$$

Zero-geodetic curves or timelike curves:

$$S = -\int_{\lambda_1}^{\lambda_2} \sqrt{-g_{MN} \frac{dx^M}{d\lambda} \frac{dx^N}{d\lambda}}\, d\lambda \tag{2.23}$$

- S – effect/action; unit: m; line length is minimised; $\delta S = 0$ yields equations of motion
- λ – affine parameter; $\lambda = 0, 1, 2, 3, 4, 5, 6$; parameterised trajectory $x^M(\lambda)$; is orthogonal to the velocity; proportional to the proper time τ; unit normalised to: m
- τ – proper time; $\tau = t_{Obj}$; unit: s; causes for solid particles: $ds^2 = -c^2\, d\tau^2$
- $g_{MN}(M)$ – 7-dimensional metric tensor; dynamic with $\cos(kt)$; defines the 'length' in curved space-time
- $\frac{dX^M}{d\lambda}$ or $\frac{dX^N}{d\lambda}$ – speed along the trajectory (tangential vector); describes the direction and speed of movement; unit: $\frac{m}{m}$ becomes dimensionless

For massive particles, the additional condition $g_{MN} \dot{X}^M \dot{X}^N = -c^2$ as a normalised tangential vector also applies, but the direct variation of S already leads to the affine geodesic.

The Lagrange function (Lagrangian):

The integrand of the impact function is the Lagrange function $\mathcal{L}$:

$$\mathcal{L} = \frac{ds}{d\lambda}$$

For timelike:

$$\mathcal{L} = -\sqrt{-g_{MN} \frac{dx^M}{d\lambda} \frac{dx^N}{d\lambda}} = -\sqrt{-g_{MN} \dot{x}^M \dot{x}^N} \qquad \text{with: } \dot{x}^M = \frac{dx^M}{d\lambda}$$

Or, equivalently, for the extreme case:

$$\mathcal{L}(X, \dot{X}) = -\frac{1}{2} g_{MN}(X)\, \dot{x}^M \dot{x}^N \tag{2.24}$$

- $\mathcal{L}$ – is scalar density; is a kinetic energy-like function for geodesics; unit: $\frac{m^2}{m^2}$; becomes dimensionless

The Euler-Lagrange equations:

For a system with coordinates x^λ ($\lambda = 0,\ldots, 6$), the Euler-Lagrange equations are:

$$\frac{d}{d\lambda}\left(\frac{\partial \mathcal{L}}{\partial \dot{x}^\lambda}\right) - \frac{\partial \mathcal{L}}{\partial x^\lambda} = 0 \tag{2.25}$$

- $\frac{d}{d\lambda}\left(\frac{\partial \mathcal{L}}{\partial \dot{x}^\lambda}\right)$ – term minimises the action S and defines geodesics; unit: $\frac{1}{m}$
- $\frac{\partial \mathcal{L}}{\partial \dot{x}^\lambda}$ – canonical momentum (covariant) with respect to the coordinate x^λ; similar to the classic pulse $p = \frac{\partial \mathcal{L}}{\partial V}$; unit: $\frac{m}{m}$ becomes dimensionless
- $\frac{\partial \mathcal{L}}{\partial x^\lambda}$ – time derivation; explicit dependence on coordinates via $g_{MN}(x)$ generates ‘forces’ through curvature; unit: $\frac{1}{m}$

Calculation of the derivatives:

Impulse p_λ:

$$p_\lambda = \frac{\partial \mathcal{L}}{\partial \dot{x}^\lambda} = \frac{1}{2} \cdot 2\, g_{KN}\, \dot{x}^N = g_{KN}\, \dot{x}^N$$

Time derivative of the impulse:

$$\frac{d}{d\lambda}\left(\frac{\partial \mathcal{L}}{\partial \dot{x}^\lambda}\right) = \frac{d}{d\lambda}\left(g_{\lambda N}\, \dot{x}^N\right) = \partial_M g_{\lambda N}\, \dot{x}^M\, \dot{x}^N + g_{\lambda N}\, \ddot{x}^N$$

- $\partial_M g_{\lambda N}$ – spatio-temporal derivation of the metric; unit: $\frac{1}{m}$
- $\dot{x}^M$ or $\dot{x}^N$ – unit: $\frac{m}{m}$ becomes dimensionless
- $\ddot{x}^N = \frac{d^2 x^N}{d\lambda^2}$ – unit: $\frac{1}{m}$

Explicit derivation:

$$\frac{\partial \mathcal{L}}{\partial x^\lambda} = \frac{1}{2}\left(\partial_\lambda g_{MN}\right) \dot{x}^M\, \dot{x}^N$$

- $(\partial_\lambda g_{MN})$ – is the derivative of the metric with respect to x^λ; unit: $\frac{1}{m}$

Insert into the Euler-Lagrange equation:

$$\frac{d}{d\lambda}\left(\frac{\partial \mathcal{L}}{\partial \dot{x}^\lambda}\right) - \frac{\partial \mathcal{L}}{\partial x^\lambda} = 0 \rightarrow \partial_M g_{\lambda N}\, \dot{x}^M \dot{x}^N + g_{\lambda N}\, \ddot{x}^N - \frac{1}{2}\,(\partial_\lambda g_{MN})\, \dot{x}^M \dot{x}^N = 0$$

Multiplying by -1 and rearranging gives:

$$- g_{\lambda N}\, \ddot{x}^N - \partial_M g_{\lambda N}\, \dot{x}^M \dot{x}^N + \frac{1}{2}\,(\partial_\lambda g_{MN})\, \dot{x}^M \dot{x}^N = 0$$

$$\ddot{x}^\lambda = g^{\lambda P}\left(\partial_M g_{PN}\, \dot{x}^M \dot{x}^N - \frac{1}{2}\,(\partial_P g_{MN})\, \dot{x}^M \dot{x}^N\right) \qquad (2.26)$$

- $g^{\lambda P}$ – inverse metric; dimensionless
- Index: P = 0, 1, 2, 3, 4, 5, 6; contravariant

Transformation to the geodesic equation with Christoffel symbols:

The standard form of Christoffel symbols of the second kind is:

$$\Gamma^\lambda_{MN} = \frac{1}{2}\, g^{\lambda P}\,(\partial_M g_{NP} + \partial_N g_{MP} - \partial_P g_{MN})$$

- Γ^λ_{MN} – Christoffel's symbol; unit: $\frac{1}{m}$; describes the curvature/affine connection → shows the extent to which the curvature depends on time-deforming massive objects

By inserting and renaming the indices, it can be seen that the expression is exactly:

$$\ddot{x}^\lambda + \Gamma^\lambda_{MN}\, \dot{x}^M \dot{x}^N = 0 \qquad (2.27)$$

This is the geodesic equation in affine parameterisation.

Euler-Lagrange equations that generate geodesics:

The Euler-Lagrange equation for the FSM Lagrange function

$$\mathcal{L} = \frac{1}{2}\, g_{MN}\, \dot{x}^M \dot{x}^N$$

Is with $g_{MN} = [1 + \cos(k_{Uni}\, t)]\,(\eta_{MN} + h_{MN})$::

$$\ddot{x}^\lambda + \Gamma^\lambda_{MN}\, \dot{x}^M \dot{x}^N = 0$$

and is equivalent to the geodesic equation:

$$\frac{d^2x^\lambda}{d^2\lambda^2} + \Gamma^\lambda_{MN} \frac{dx^M}{d\lambda} \frac{dx^N}{d\lambda} = 0 \qquad (2.28)$$

- $\frac{d^2x^\lambda}{d^2\lambda^2}$ – acceleration, measures track curvature
- Γ^λ_{MN} – describes a geometric expression of how space-time itself directs the movement of objects; unity: $\frac{1}{m}$
- $\frac{dX^M}{d\lambda}$ bzw. $\frac{dX^N}{d\lambda}$ – tangential vector
- $\frac{dX^4}{d\tau}$ corresponds specifically to V_4 from **Kapitel 1.2**
- $\frac{dX^5}{d\tau}$ corresponds specifically to V_5 from **Kapitel 1.2**

In FSM, the time- and cosine-dependent terms in g_{MN} make the Christoffel symbols dynamic. This is the key to unifying the four fundamental forces and leads to new effects such as coupling frequencies.

Reduction to 4D and FSM-specific effects:

In the limiting cases (compact → 0) the compact wave-field dimensions (dy_4, dy_5, dy_6) are integrated and averaged. Following reduction to GTR, effective fields and scalars ϕ are obtained:

$$\frac{d^2X^\mu}{d^2\tau^2} + \Gamma^\mu_{\nu\rho} \frac{dX^\nu}{d\tau} \frac{dX^\rho}{d\tau} = 0 \qquad \text{with: } \Gamma \text{ from } g^{eff}_{\mu\nu} \text{ inclusive half } r_s \text{ due to } \cos(kt)$$

- $g^{eff}_{\mu\nu}$ – effective 4-dimensional metric provides observable physics
- ν, ρ – Counting variables for 4D space-time directions, they ‘count’ the possible velocity combinations. They are submitted to $\Gamma^\mu_{\nu\rho}$.

The additional terms of the FSM extension generate the quantum effects.

3. Christoffel symbols in FSM

Christoffel symbols are the central affine connection in space-time and describe how vectors change under parallel transport. In the FSM, they arise from the oscillating metric and couple global cosmic modulations, local gravitational disturbances and vector fields. They are time-dependent and form the basis for the geodesic equation. The metric is given by

$ds^2 = g_{MN}\, dx^M\, dx^N$

$ds^2 = [1 + \cos(k_{Uni}\, t)]\, [- c^2\, dt^2 + dx^2 + dy^2 + dz^2 + dy_4^2 + dy_5^2 + dy_6^2 + \frac{G\, M}{c^2\, r}\, (1 + \cos(kt + \beta))\, (c^2\, dt^2 + dx^2 + dy^2 + dz^2) + 2(A_\mu^a + \delta A_\mu^a)\, dy_a\, dx^\mu]$

General formula for Christoffel symbols Γ of the second kind and perturbation approach:

$$\Gamma^\lambda_{MN} = \frac{1}{2}\, g^{\lambda P}\, (\partial_M g_{NP} + \partial_N g_{MP} - \partial_P g_{MN}) \qquad (2.29)$$

- Γ^λ_{MN} – describes the change in vectors during parallel transport; unit: $\frac{1}{\mathrm{m}}$
- $\partial_M = \frac{\partial}{\partial x^M}$ – is the derivative; unit: $\frac{1}{\mathrm{m}}$
- $g^{\lambda P}$ – inverse metric; dimensionless
- Indices: λ, M, N, P = 0, 1, 2, 3, 4, 5, 6

The expression follows from the requirement that the covariant derivative of the metric tensor vanishes ($\nabla_P\, g_{MN} = 0$).

The metric is defined as

$g_{MN} = [1 + \cos(k_{Uni}\, t)]\, (\eta_{MN} + h_{MN})$

The disturbance involving h_{MN} is treated perturbatively. It is approximated by $\Gamma \approx \Gamma_0 + \delta\Gamma$, whereas Γ_0 is assumed to be flat:

$$\Gamma^\lambda_{MN} \approx \frac{1}{2}\, \eta^{\lambda P}\, (\partial_M\, h_{NP} + \partial_N\, h_{MP} - \partial_P\, h_{MN}) + \text{other terms}$$

- Γ^λ_{MN} – addition to the above: codified curvature; λ – guidance; M, N – initial direction
- $\frac{1}{2}$ – normalisation factor, results in symmetry of Γ
- $\eta^{\lambda P}$ – inverse Minkowski metric with (-1, 1, 1, 1, 1, 1, 1)
- $\partial_M\, h_{NP}$ – derivative; unit: $\frac{1}{\mathrm{m}}$; measures the change in metric in the M-direction
- $\partial_N\, h_{MP}$ – symmetric term, records changes in the metric in the N-direction
- $-\, \partial_P\, h_{MN}$ – subtraction corrects for the P-direction and ensures freedom from torsion

Inversion of the metric for further calculation:

From the diagonal metric (point 1), in a linear approximation, because $h_{MN} << 1$ is small:

$$g^{MN} \approx \frac{1}{1+\cos(k_{Uni}\, t)} (\eta^{MN} - h^{MN}) \tag{2.30}$$

Whereas:

$h^{MN} = \eta^{MP}\, \eta^{QN}\, h_{PQ}$

- η^{MN} – inverse of the full 7-dimensional Minkowski metric; dimensionless
- g^{MN} – inverse metric, perturbative; dimensionless
- Indices: M, N, P, Q = 0, 1, 2, 3, 4, 5, 6

Elements of the Christoffel symbols in the FSM:

$$\Gamma^{\lambda}_{MN} = \Gamma^{\lambda\,(\text{global})}_{MN} + \Gamma^{\lambda\,(\text{local})}_{MN} + \Gamma^{\lambda\,(\text{Vector})}_{MN} \tag{2.31}$$

- Global: cosmic oscillation with $[1 + \cos(k_{Uni}\, t)]$
- Local: local oscillation; GTR-like: classical gravitational curvature with: $(1 + \cos(kt + \beta))$
- Vector: Coupling via vector fields with $2(A^{a}_{\mu} + \delta A^{a}_{\mu})\, dy_a\, dx^{\mu}$

Calculation of Christoffel symbols for the global component $\Gamma^{\lambda\,(\text{global})}_{MN}$:

$$\Gamma^{\lambda\,(\text{global})}_{MN} = \frac{1}{2}\, \eta^{\lambda P} (\partial_M [\cos(k_{Uni}\, t)]\, \eta_{NP} + \partial_N [\cos(k_{Uni}\, t)]\, \eta_{MP} - \partial_P [\cos(k_{Uni}\, t)]\, \eta_{MN})$$

Given that the derivative ∂_M is non-zero only for the time coordinate M = 0 and

$\partial_0 [\cos(k_{Uni}\, t)] = - k_{Uni} \sin(k_{Uni}\, t)$,

the expression simplifies to:

$$\boldsymbol{\Gamma^{\lambda\,(\text{global})}_{MN} = -\frac{1}{2}\, k_{Uni} \sin(k_{Uni}\, t)\, (\eta^{\lambda}_{N}\, \delta^{0}_{M} + \eta^{\lambda}_{M}\, \delta^{0}_{N} - \eta_{MN}\, \eta^{\lambda 0})} \tag{2.32}$$

- $\eta^{\lambda}_{N}\, \delta^{0}_{M}$ or $\eta^{\lambda}_{M}\, \delta^{0}_{N}$ – terms generate a time-dependent acceleration in the time direction (global ‘acceleration’ and ‘deceleration’ of the entire space-time)
- $- \eta_{MN}\, \eta^{\lambda 0}$ – minusterm corrects the spatial components and ensures consistency with the metric inversion
- $\eta^{\lambda P}$ and η_{MN} – are the scalar Minkowski components; dimensionless
- k_{Uni} – cosmic angular frequency $k_{Uni} = \frac{c}{r_{Uni}}$
- Indices: M, N, P, λ = 0, 1, 2, 3, 4, 5, 6

This expression is substituted directly into the geodesic equation in the FSM, generating the global pulsating force that modulates the entire universe.

Calculation of Christoffel symbols for the local component $\Gamma^{\lambda\,(\text{local})}_{MN}$:

The local term arises solely from the derivative of the local gravitational perturbation with:

$h_{\mu\nu} = \frac{GM}{c^2\, r}\,(1 + \cos(kt + \beta))\,\delta_{\mu\nu}$ with: $h_{mn} = 0$; $h_{\mu m} = 0$ with a purely local component

Perturbative 7D:

$$\Gamma^{\lambda}_{MN} \approx \frac{1}{2}\,\eta^{\lambda P}\,(\partial_M h_{NP} + \partial_N h_{MP} - \partial_P h_{MN})$$

Given that $h_{\mu\nu}$ is non-zero only for μ, $\nu = 0, 1, 2, 3$ (visible 4D block), the expression reduces to the 4D components with:

$$\Gamma^{\sigma}_{\mu\nu} \approx \frac{1}{2}\,\eta^{\sigma\rho}\,(\partial_\mu h_{\nu\rho} + \partial_\nu h_{\mu\rho} - \partial_\rho h_{\mu\nu}) \qquad (2.33)$$

- $\eta^{\sigma\rho}$ – inverse Minkowski with diag(-1, 1, 1, 1); for a flat basis
- $h_{\mu\nu}$ – dynamic term, generates gravity with:
  $h_{\mu\nu} = \frac{GM}{c^2\, r}\,\delta_{\mu\nu}$

For the majority share Γ^{r}_{tt}, radial, weak field, $r >> \frac{GM}{c^2}$ with $-\partial_\rho h_{\mu\nu}$:

$$\Gamma^{r}_{tt} = -\frac{1}{2}\,\partial_r\,[\,\frac{GM}{c^2\, r}\,(1 + \cos(kt + \beta))\,]$$

$$\Gamma^{r}_{tt} = \frac{1}{2}\,\frac{GM}{c^2\, r^2}\,(1 + \cos(kt + \beta)) \qquad (2.34)$$

- ∂_r – radial discharge according to $(\frac{1}{r})$ results in a field strength ~ $(\frac{1}{r^2})$
- $\Gamma^{r}_{tt} = \frac{1}{2}\,\frac{GM}{c^2\, r^2}$ – GTR solution; produces purely static curvature
- $(1 + \cos(kt + \beta))$ – the mean reproduces Newtonian gravity, but dynamically within the FSM; see the approach in **Chapter 2.3**, 'Sine Periodicity'
- $\partial_r h_{tt}$ – provides the radial gradient of the local oscillation and generates the attractive curvature, which is modulated by the factor $(1 + \cos(kt + \beta))$
- Other derivatives, e.g. ∂t terms, give rise to additional time-dependent contributions which describe the oscillating force in the geodesic equation.

Calculation of Christoffel symbols for the vector component $\Gamma^{\lambda\,(\mathrm{Vector})}_{MN}$:

The vector coupling term arises from the mixed metric term of the FSM:

$2(A^a_P + \delta A^a_P)\, dy_a\, dx^\mu$

$\Gamma^\lambda_{MN} = \frac{1}{2}\, g^{\lambda P}\, (\partial_M g_{NP} + \partial_N g_{MP} - \partial_P g_{MN})$ with: $g^{\lambda P} \approx \eta^{\lambda P}$ in a linear approximation

$$\Gamma^\lambda_{MN} \approx \frac{1}{2}\, g^{\lambda P}\, \partial_M\, [2(A^a_P + \delta A^a_P)\, dy_a\, dx^\mu]\, \delta_{aN} \tag{2.35}$$

- $g^{\lambda P} \approx \eta^{\lambda P}$; flat inverse metric in linear order
- ∂_M – derivative with respect to a coordinate M; causes the field strength $F_{MP} = \partial_M A_P - \partial_P A_M$
- A^a_P – background vector field
- δA^a_P – small fluctuations/disturbances in the vector field
- δ_{aN} – Kronecker delta; projected onto the direction of the compact wave-field dimensions or the vector index a

Explicitly 7D for all components:

$$\boldsymbol{\Gamma^{\lambda\,(\mathrm{Vector})}_{MN} = \frac{1}{2}\, g^{\lambda P}\, [\partial_M\, (A^a_P + \delta A^a_P) + \partial_N\, (A^a_M + \delta A^a_M) - \partial_P\, (A^a_M + \delta A^a_N)]} \tag{2.36}$$

Explicitly 4D for the interaction/coupling between 4D-visible and 3D-compact:

$$\Gamma^{\lambda\,(\mathrm{Vector})}_{\mu a} = \frac{1}{2}\, g^{\lambda P}\, [\partial_\mu\, (A^a_P + \delta A^a_P) + \partial_a\, (A^a_\mu + \delta A^a_\mu) - \partial_P\, (A^a_\mu + \delta A^a_\mu)]$$

Predominant part:

$$\Gamma^{\lambda\,(\mathrm{Vector})}_{\mu a} = \frac{1}{2}\, \eta^{\lambda P}\, \partial_\mu\, (A^a_P + \delta A^a_P)$$

- This term describes the interaction of the vector fields between the visible 4D space-time (0, 1, 2, 3) and the compact wave-field dimensions (4, 5, 6).
- δA^a_P – disturbance term; provides local counteracting forces during deformation
- Indices: $\lambda, P = 0, 1, 2, 3, 4, 5, 6$; $\mu, \nu = 0, 1, 2, 3$; $a = 4, 5, 6$

Results for the Christoffel symbols in the FSM:

The Christoffel symbols in the FSM are time-dependent and contain both global and local oscillations.

$$\Gamma^\lambda_{MN} = \Gamma^{\lambda\,(\mathrm{global})}_{MN} + \Gamma^{\lambda\,(\mathrm{local})}_{MN} + \Gamma^{\lambda\,(\mathrm{Vector})}_{MN}$$

- $\Gamma^{\lambda\,(\text{global})}_{MN} = -\frac{1}{2}\, k_{Uni} \sin(k_{Uni}\, t)\, (\eta^{\lambda}_{N}\, \delta^{0}_{M} + \eta^{\lambda}_{M}\, \delta^{0}_{N} - \eta_{MN}\, \eta^{\lambda 0})$
- $\Gamma^{\lambda\,(\text{local})}_{MN} \approx \frac{1}{2}\, \eta^{\lambda P}\, (\partial_M\, h_{NP} + \partial_N\, h_{MP} - \partial_P\, h_{MN})$
- $\Gamma^{\lambda\,(\text{Vector})}_{MN} = \frac{1}{2}\, g^{\lambda P}\, [\partial_M\, (A^{a}_{P} + \delta A^{a}_{P}) + \partial_N\, (A^{a}_{M} + \delta A^{a}_{M}) - \partial_P\, (A^{a}_{M} + \delta A^{a}_{N})]$

The main components for 4D: (2.37)

$$\Gamma^{\lambda}_{MN} = \frac{1}{2}\frac{GM}{c^2\, r^2}\, [1 + \cos(kt + \beta)] + \frac{1}{2}\, \eta^{\lambda P}\, \partial_{\mu}\, (A^{a}_{P} + \delta A^{a}_{P}) - \frac{1}{2}\, k_{Uni} \sin(k_{Uni}\, t)\, (\eta^{\lambda}_{N}\, \delta^{0}_{M} + \eta^{\lambda}_{M}\, \delta^{0}_{N} - \eta_{MN}\, \eta^{\lambda 0})$$

4. The Riemann tensor in FSM

The Riemann tensor measures the intrinsic curvature of space-time by quantifying vectors that change when transported in parallel around a closed loop. It is a measure of whether a space is curved or flat. In flat spaces such as Minkowski space, the Riemann tensor disappears completely. For FSM, the Riemann tensor is extended to capture curvature not only in 4-dimensional observable space-time, but also in compact dimensions in the wave-field. This is essential for the field equations. In the FSM, it includes time-dependent contributions from global cosmic oscillations, local gravitational perturbations and vector coupling.

Parallel transport of a vector V^{σ}:

A vector V^{P} is transported parallel to a curve with tangent vector $u^{M} = \frac{dx^{M}}{d\lambda}$ if its covariant derivative vanishes:

$$\nabla_M\, V^{\rho} = \partial_M\, V^{\rho} + \Gamma^{P}_{MQ}\, V^{Q} = 0$$

If the same vector is transported along two different paths around an infinitesimally small loop (an area with sides of length δx^{M} and δx^{N}), a difference ΔV^{ρ} results. This difference defines the Riemann tensor:

$$\Delta V^{\rho} = -\, R^{P}_{QMN} V^{Q}\, \delta x^{M}\, \delta x^{N} \qquad (2.38)$$

- V^{ρ} – displacement vector; unit: m
- R^{P}_{QMN} – Riemann tensor; unit: $\frac{1}{m^2}$; quantifies curvature; indices: P up is the direction of the vector; Q is the vector index below; M, N are the grinding directions
- Indices: P, Q above – contravariant; P, Q = 0, …, 6; vector components
- Indices: M, N = 0, …, 6; directions of the loop

Definition – Riemann tensor from Christoffel symbols 7D:

$$R^{P}_{QMN} = \partial_M \Gamma^{P}_{NQ} - \partial_N \Gamma^{P}_{MQ} + \Gamma^{P}_{ML}\,\Gamma^{L}_{NQ} - \Gamma^{P}_{NL}\,\Gamma^{L}_{MQ} \tag{2.39}$$

- ∂_M – partial derivative with respect to x^M; unit: $\frac{1}{\mathrm{m}}$; measures the change in the Γ; index *M* below corresponds to the direction
- Γ^{P}_{NQ} – Christoffel symbol; unit: $\frac{1}{\mathrm{m}}$; joining term; indices: *P* on top is the goal; *N*, *Q* below correspond to the source
- $\Gamma^{P}_{ML}\,\Gamma^{L}_{NQ}$ – a square correction arising from the non-commutative nature of the connection; unity: $\frac{1}{\mathrm{m}^2}$; introduces non-linear terms that generate curvature via Γ-interactions; *L* is summed over the index 0,…, 6
- $-\Gamma^{P}_{NL}\,\Gamma^{L}_{MQ}$ – a square correction arising from the non-commutative nature of the connection; induces antisymmetry in *M, N* for curvature
- Indices of R^{P}_{QMN} – *P* vector is shown above; *Q* below is the vector index; *M*, *N* the subscripts indicate the directions; antisymmetric

Perturbative approximation in FSM:

In a linear approximation where $h_{MN} << 1$ and using the Christoffel symbols already derived, the Riemann tensor simplifies. In the first order with linear curvature, ΓΓ is neglected for weak fields:

$$R^{P}_{QMN} \approx \partial_M \Gamma^{P}_{NQ} - \partial_N \Gamma^{P}_{MQ} \tag{2.40}$$

The Christoffel symbols consist of:

$$\Gamma^{\lambda}_{MN} = = \Gamma^{\lambda\,(\mathrm{global})}_{MN} + \Gamma^{\lambda\,(\mathrm{local})}_{MN} + \Gamma^{\lambda\,(\mathrm{Vector})}_{MN}$$

Specific contributions from Γ^{λ}_{MN}:

Example: a radial term in a weak field, to be detected in the visible universe

Global contribution (cosmic oscillation):

$$R^{P\,(\mathrm{global})}_{QMN} \approx \partial_M \left(-\frac{1}{2}\, k_{Uni} \sin(k_{Uni}\, t)\, \eta^{P}_{Q}\, \delta^{N}_{0}\right) - \partial_N \left(-\frac{1}{2}\, k_{Uni} \sin(k_{Uni}\, t)\, \eta^{P}_{Q}\, \delta^{M}_{0}\right) \tag{2.41}$$

Local contribution (gravitational disturbance):

$$R^{r\,(\mathrm{local})}_{QMN} \approx \partial_r \left(\frac{1}{2}\frac{GM}{c^2\, r^2}\,(1 + \cos(kt + \beta))\right) = -\frac{2}{2}\frac{GM}{c^2\, r^3}\,(1 + \cos(kt + \beta))$$

$$R^{r\,(\text{local})}_{QMN} = -\frac{GM}{c^2\, r^3}\,(1 + \cos(kt + \beta)) \tag{2.42}$$

- $\partial_r h_{tt}$ → contributes to Γ^r_{tt}
- $\partial_r h_{rr} \approx 0$
- $\partial_r h_{tr} \approx 0$
- $\partial_r h_{rt} \approx 0$

Vector contribution (coupling):

$$R^{\lambda\,(\text{Vector})}_{\mu ab} \approx \partial_\mu \left(\frac{1}{2}\, \eta^{\lambda P}\, \partial_a\, (A^a_P + \delta A^a_P)\right) \tag{2.43}$$

- $\frac{G\,M}{c^2\, r^3}$ – spherically symmetric term; results in higher moments of curvature
- $R^{\lambda\,(\text{Vector})}_{\mu ab}$ – describes in detail the interaction between visible 4D space and the compact 3D wave-field dimensions
- Indices: λ – event component, $\lambda = 0, \ldots, 6$; μ below is a visible 4D index, $\mu = 0, 1, 2, 3$; a, b – first and second compact indices, a, $b = 4, 5, 6$; ρ – summary index, $\rho = 0,\ldots, 6$; a in A^a_P – indicates, which of the three vector fields A^4, A^5, A^6 originates from the compact dimensions

Reduction from 7D to 4D:

After integration over the compact dimensions y_4, y_5, y_6 and averaging, the effective 4D Riemann tensor is obtained:

$$R^{\rho}_{\sigma\mu\nu} = R^{\rho\,(\text{global})}_{\sigma\mu\nu} + R^{\rho\,(\text{local})}_{\sigma\mu\nu} + R^{\rho\,(\text{Vector})}_{\sigma\mu\nu}$$

5. The Ricci tensor in FSM

The Ricci tensor describes a contraction of the Riemann tensor from point 4 and reduces the local curvature from a 4-tensor form to a symmetric 2-tensor form. This tensor measures the average curvature in every direction and is crucial to the Einstein field equations, which relate the energy density and momentum of matter. In FSM, the Ricci tensor is time-dependent.

Contraction of the Riemann tensor:

The Ricci tensor is formed by contracting the first and third indices of the Riemann tensor, i.e. summing over a common index. In full form:

$$R_{MN} = \sum_P R^P_{MPN} \tag{2.44}$$

- R_{MN} – Ricci tensor, unit: $\frac{1}{m^2}$; causes combined curvature in directions M and N
- R^{P}_{MPN} – Riemann tensor; unit: $\frac{1}{m^2}$; causes complete curvature; indices here: P top/bottom is contracted, summed over $P = 0,\ldots, 6$
- $\sum\rho$ – summation over P; reduced 4-Index-Riemann-tensor to a 2-index tensor that measures the local energy density

Application of Riemann's formula:

$$R^{P}_{QMN} = \partial_M \Gamma^{P}_{NQ} - \partial_N \Gamma^{P}_{MQ} + \Gamma^{P}_{ML}\,\Gamma^{L}_{NQ} - \Gamma^{P}_{NL}\,\Gamma^{L}_{MQ}$$

Contraction over P (first and third index):

$$R_{MN} = \partial_P \Gamma^{P}_{NM} - \partial_N \Gamma^{P}_{PM} + \Gamma^{P}_{PL}\,\Gamma^{L}_{NM} - \Gamma^{P}_{NL}\,\Gamma^{L}_{PM} \tag{2.45}$$

- $\partial_P \Gamma^{P}_{NM}$ – derivative and sum, unit: $\frac{1}{m^2}$; measures the change in the connection in P-direction; P summed up $0,\ldots, 6$
- $-\partial_N \Gamma^{P}_{PM}$ – subtraction; causes antisymmetry; correction for the N-direction
- $\Gamma^{P}_{PL}\,\Gamma^{L}_{NM}$ – product; unit: $\frac{1}{m^2}$; causes non-linear interactions between Γ; P summed up
- $-\Gamma^{P}_{NL}\,\Gamma^{L}_{PM}$ – subtraction; causes antisymmetry in the nonlinear terms
- L – cumulative running index $\lambda = 0,\ldots, 6$; takes all directions into account in the products

Formula (2.45) is covariant and dynamic in the FSM due to the sine/cosine terms in Γ.

Perturbative approximation in the FSM:

Due to $\Gamma \sim \delta g$ (first order), the second-order Γ products $\sim (\delta g)^2$ are negligible in linear approximation for $h_{MN} << 1$:

$$R_{MN} \approx \partial_P \Gamma^{P}_{NM} - \partial_N \Gamma^{P}_{PM} \tag{2.46}$$

As the Christoffel symbols consist of three parts (global, local, vector), the Ricci tensor is given by:

$$R_{MN} = R^{(\text{global})}_{MN} + R^{(\text{local})}_{MN} + R^{(\text{Vector})}_{MN}$$

Each Christoffel component contributes its own Ricci component. The global oscillation modulates the overall curvature of space-time, the local component modulates the gravitational curvature around the mass, and the vector component modulates the coupling to the wave-field.

Contributions and explicit forms:

Global contribution:

$$R_{MN}^{(\text{global})} \approx \partial_P \left(-\frac{1}{2} k_{Uni} \sin(k_{Uni}\, t)\, \eta_N^P\, \delta_M^0\right) - \partial_N \left(-\frac{1}{2} k_{Uni} \sin(k_{Uni}\, t)\, \eta_P^P\, \delta_M^0\right) \tag{2.47}$$

Local contribution:

$$R_{MN}^{(\text{local})} = \partial_P \left(\frac{1}{2} \frac{GM}{c^2\, r^2} (1 + \cos(kt + \beta))\, \delta_N^r\, \delta_M^t\right) - \partial_N \Gamma_{PM}^P$$

$$R_{MN}^{(\text{local})} \approx \partial_P \left(\frac{1}{2} \frac{GM}{c^2\, r^2} (1 + \cos(kt + \beta))\, \delta_N^r\, \delta_M^t\right) \tag{2.48}$$

- $\partial_N \Gamma_{PM}^P \approx 0$ for low-field, radial, $M = N = t$

Vector contribution:

$$R_{MN}^{(\text{Vector})} = \partial_P \left(\frac{1}{2}\, \eta^{P\rho}\, \partial_M\, (A_\rho^a + \delta A_\rho^a)\, \delta_a^N\right) \tag{2.49}$$

- δ_a^N – Kronecker delta; isolates the components of the Riemann tensor with $N \in \{4, 5, 6$ that relate to the compact wave-field dimensions, and prevents this vectorial contribution from occurring directly in pure 4D (μ, $\nu = 0, 1, 2, 3$). This shifts the cause of the interaction/coupling into the wave-field.
- Sum index: $\rho = 0, \ldots, 6$; contracts the inverse metric using the inner derivative

Reduced to an effective 4D:

By reducing the indices M and N to μ and $\nu = 0, 1, 2, 3$, the 4D solution of Ricci is obtained:

$$R_{\mu\nu}^{(4)} = R_{\mu\nu}^{(\text{global})} + R_{\mu\nu}^{(\text{local})} + R_{\mu\nu}^{(\text{Vector})}$$

Ricci scalar R:

The Ricci scalar is the full contraction of the Riemann tensor with the inverse metric, and gives the local mean curvature of space-time as a scalar value.

$$R = g^{MN} R_{MN} = g^{MN} R_{MPN}^P \tag{2.50}$$

with: $g^{MN} \approx \frac{1}{1+\cos(k_{Uni}\, t)} (\eta^{MN} - h^{MN})$

- R – curvature scalar, unit: $\frac{1}{m^2}$; indicates local scalar curvature; positive for expanding systems, negative for bound systems; dynamic in FSM

- g^{MN} – inverse metric; increases the indices of the Ricci tensor; the indices M and N above are covariant; M, N = 0,…, 6; in 7D
- R_{MN} – Ricci tensor; unit: $\frac{1}{m^2}$; summarises curvature; indices M, N in the bottom are covariant
- Contraction with the implicit summation over M and N reduces the 2-index Ricci tensor to a scalar that measures the trace of the curvature

Perturbative approximation with $h_{MN} << 1$:

$$R \approx \eta^{MN} R_{MN}$$

$$R = R^{(\text{global})} + R^{(\text{local})} + R^{(\text{Vector})}$$

Global contribution:

$$R^{(\text{global})} \approx \eta^{MN} [\partial_P (-\frac{1}{2} k_{Uni} \sin(k_{Uni} t) \eta^P_N \delta^0_M) - \partial_N (-\frac{1}{2} k_{Uni} \sin(k_{Uni} t) \eta^P_P \delta^0_M)]$$

Local contribution:

$$R^{(\text{local})} \approx \eta^{MN} [\partial_P (\frac{1}{2} \frac{GM}{c^2 r^2} (1 + \cos(kt + \beta)) \delta^r_N \delta^t_M)] = - \frac{GM}{c^2 r^3} (1 + \cos(kt + \beta))$$

Vector contribution:

$$R^{(\text{Vector})} \approx \eta^{MN} [\partial_P (\frac{1}{2} \eta^{P\rho} \partial_M (A^a_\rho + \delta A^a_\rho) \delta^N_a)]$$

Reduction to 4D:

The compact wave-field dimensions y_4, y_5, y_6 are integrated and averaged.

$$R^{(4)} = R^{(\text{global})} + R^{(\text{local})} + R^{(\text{Vector})}$$

6. The Einstein tensor in FSM

The Einstein tensor links the curvature of geometry with the energy-momentum distribution and forms the basis of Einstein's field equations. This tensor combines the Ricci tensor (point 5.) and the scalar curvature term to create a divergence-free form that describes gravity as geometric effects. In FSM, this tensor explains how curvature leads to gravity and other forces.

Definition of the Einstein tensor from the Ricci tensor and scalar:

The Einstein tensor is a linear combination of the Ricci tensor, metric and scalar.

$$G_{MN} = R_{MN} - \frac{1}{2} g_{MN} R \qquad (2.51)$$

- G_{MN} – Einstein tensor; unit: $\frac{1}{m^2}$; links curvature with matter/energy; indices M, N below are covariant; M, N = 0,…, 6; in 7D (0 = time, 1, 2, 3 = visible, 4, 5, 6 = compact)
- R_{MN} – Ricci tensor; unit: $\frac{1}{m^2}$; causes local curvature; indices: M, N
- $\frac{1}{2}$ – normalisation factor; makes Einstein tensor G trace-free
- g_{MN} – metric tensor from point 1.; multiplied scalar to tensor form
- R – curvature scalar for the average curvature; unit: $\frac{1}{m^2}$

The purpose of this definition is to ensure that there is no divergence, thereby guaranteeing the conservation of energy:

$$\nabla^M G_{MN} = 0 \tag{2.52}$$

Inserting the Ricci tensor and scalar from point 5.:

$$G_{MN} = (R_{MN}^{(\text{global})} + R_{MN}^{(\text{local})} + R_{MN}^{(\text{Vector})}) - \frac{1}{2} g_{MN} (R^{(\text{global})} + R^{(\text{local})} + R^{(\text{Vector})}) \tag{2.53}$$

- $-\frac{1}{2} g_{MN}$ () – combination; makes G divergent free by distributing the scalar curvature isotropically in all directions

The tensor is covariant and time-dependent in FSM through sin(kt) or cos(kt) in the Γ.

Perturbative approximation in FSM:

In the linear approximation, ΓΓ ~ $(\delta g)^2$, $g \approx g_0$ is neglected and the following applies $h_{MN} << 1$:

$$G_{MN} \approx R_{MN} - \frac{1}{2} \eta_{MN} R \tag{2.54}$$

Specific contributions:

$$G_{MN} = G_{MN}^{(\text{global})} + G_{MN}^{(\text{local})} + G_{MN}^{(\text{Vector})}$$

Global contribution:

$$G_{MN}^{(\text{global})} = R_{MN}^{(\text{global})} - \frac{1}{2} \eta_{MN} R^{(\text{global})} \tag{2.55}$$

- $R_{MN}^{(\text{global})} \approx \partial_P (-\frac{1}{2} k_{Uni} \sin(k_{Uni}\, t)\, \eta_N^P\, \delta_M^0) - \partial_N (-\frac{1}{2} k_{Uni} \sin(k_{Uni}\, t)\, \eta_P^P\, \delta_M^0)$
- $R^{(\text{global})} \approx \eta^{MN} [\partial_P (-\frac{1}{2} k_{Uni} \sin(k_{Uni}\, t)\, \eta_N^P\, \delta_M^0) - \partial_N (-\frac{1}{2} k_{Uni} \sin(k_{Uni}\, t)\, \eta_P^P\, \delta_M^0)]$

Local contribution:

$$G_{MN}^{(\text{local})} = R_{MN}^{(\text{local})} - \frac{1}{2}\,\eta_{MN}\,R^{(\text{local})} \tag{2.56}$$

- $R_{MN}^{(\text{local})} = \partial_P \left(\frac{1}{2}\frac{GM}{c^2\,r^2}\,(1 + \cos(kt + \beta))\,\delta_N^r\,\delta_M^t\right) - \partial_N \Gamma_{PM}^P$
- $\partial_N \Gamma_{PM}^P \approx 0$ for low-field, radial, $M = N = t$
- $R^{(\text{local})} \approx \eta^{MN}\left[\partial_P \left(\frac{1}{2}\frac{GM}{c^2\,r^2}\,(1 + \cos(kt + \beta))\,\delta_N^r\,\delta_M^t\right)\right]$

Vector contribution:

$$G_{MN}^{(\text{Vector})} = R_{MN}^{(\text{Vector})} - \frac{1}{2}\,\eta_{MN}\,R^{(\text{Vector})} \tag{2.57}$$

- $R_{MN}^{(\text{Vector})} = \partial_P \left(\frac{1}{2}\,\eta^{P\rho}\,\partial_M\,(A_\rho^a + \delta A_\rho^a)\,\delta_a^N\right)$
- $R^{(\text{Vector})} \approx \eta^{MN}\left[\partial_P \left(\frac{1}{2}\,\eta^{P\rho}\,\partial_M\,(A_\rho^a + \delta A_\rho^a)\,\delta_a^N\right)\right]$

The absence of divergence, as shown by the Bianchi identities, ensures the conservation of energy:

The second Bianchi identities are geometric identities for the Riemann tensor in torsion-free spaces and are given by:

$$\nabla_R\,R_{QMN}^P + \nabla_M\,R_{QNR}^P + \nabla_N\,R_{QRM}^P = 0 \tag{2.58}$$

- ∇_R – covariate derivative with respect to R; unit: $\frac{1}{\text{m}}$; takes curvature into account; index R below is covariant; $R = 0,\ldots, 6$ in 7D
- R_{QMN}^P – Riemann tensor; unit: $\frac{1}{\text{m}^2}$; full curvature, indices: P above is Vector; Q below is the vector index; M, N directions are given below
- $\nabla_R\,R_{QMN}^P$ or $\nabla_M\,R_{QNR}^P$ or $\nabla_N\,R_{QRM}^P$ – cyclic permutation results in antisymmetry in R, M, N
- $\nabla_N\,R_{QRM}^P$ – closes the cycle; implies identity with zero, i.e. the curvature is consistent
- 0 – zero tensor; due to geometric necessity
- Indices: P upper free index, Q lower free index, M, N, R are loop directions; P, Q, M, N, $R = 0,\ldots, 6$

These identities always hold for any affine transformation (including in the FSM with oscillations and vector fields). They are a purely geometric property of the Christoffel symbols and state that the curvature is ‘cyclic’.

Contraction across the first and third index ($P = Q$):

$$\nabla_R R^P_{MPN} + \nabla_M R^P_{NPR} + \nabla_N R^P_{RPM} = 0$$

The contracted form is:

$$\nabla_R R^R_{MN} + \nabla_M R - \nabla_N R^R_{MR} = 0 \qquad \text{with: } R = R^P_P \text{ as the Ricci scalar}$$

Substituting into the Einstein tensor:

$$G_{MN} = R_{MN} - \frac{1}{2} g_{MN} R$$

The contracted Bianchi identity is multiplied by g^{MN}, and the metric compatibility condition $\nabla_g = 0$ is applied:

$$\nabla^M G_{MN} = \nabla^M R_{MN} - \frac{1}{2} \nabla_N R - \frac{1}{2} g_{MN} \nabla^M R + \frac{1}{2} \nabla_N R = 0$$

$$\boxed{\nabla^M G_{MN} = 0} \qquad (2.59)$$

- $\nabla^M G_{MN}$ – covariate divergence; unit: $\frac{1}{m^3}$; results in the maintenance rate

The absence of divergence ensures that the left-hand side of the field equation

$$G_{MN} = \frac{8\pi G_7}{c^4} T_{MN}$$

automatically enforces local momentum-energy conservation in the FSM for:

$$\nabla^M T_{MN} = 0$$

It is shown that the Einstein tensor G is divergence-free in FSM geometry and that conservation is guaranteed despite rotations.

Reduction for 4D with $\mu, \nu = 0, 1, 2, 3$:

After integration over the compact dimensions y_4, y_5, y_6 and averaging, the effective 4D reduction is obtained:

$$\nabla^\mu G^{(4)}_{\mu\nu} = 0$$

The oscillating terms and vector fields do not violate these identities, because the Bianchi identities are geometrically invariant.

7. Impulse energy tensor in the FSM

The momentum-energy tensor in FSM describes the distribution of energy, momentum, and tension in 7-dimensional field-space. It is symmetrical $T_{MN} = T_{NM}$ and divergence-free $\nabla^M T_{MN} = 0$ in order to ensure conservation laws. In FSM, the momentum-energy tensor arises from the electric/gravitational potential of the universe and photon fields. It links geometry with physical effects. This tensor is derived based on the method of the variation principle of GTR and extended to a 7-dimensional model.

Variation principle definition from matter action:

$$T_{MN} = -\frac{2}{\sqrt{-g}} \frac{\delta S_m}{\delta g^{MN}} \quad \text{; with: } S_m = \int \mathcal{L}_m \sqrt{-g}\, d^7x \text{ the matter action} \tag{2.60}$$

- T_{MN} – impulse energy tensor; normalized per volume segment of the wave-field with unit: $\frac{J}{m^3}\frac{1}{m^3} = \frac{J}{m^6} = \frac{kg}{m^4 s^2}$; source of curvature; indices: M, N below are covariant; M, N = 0,…, 6 in 7D (0 = time; 1, 2, 3 = visible; 4, 5, 6 = compact)
- - 2 – normalization factor; appropriate scaling for field equations
- $\sqrt{-g}$ – root of the metric determinant in 7D; produces an invariant volume element from the metric (point 1.); with $g = \det g_{MN}$
- $\frac{\delta S_m}{\delta g^{MN}}$ – functional normalized variation; unit: $\frac{kg}{m^4 s^2}$; measures the metric dependence of matter; δ corresponds to a small variation
- S_m – action, measure of dynamism; unit: Js; causes the integral over the Lagrangian of matter/fields
- g^{MN} – inverse metric causes variation in the indices above
- d^7x – integral over 7D volume element, including compact dimensions
- $\mathcal{L}_m$ – Lagrange density from fields, in FSM from photon field

The tensor T_{MN} is defined as the response of matter to a change in metric. In FSM, S_m contains geometric fields in the form of sinusoidal oscillations.

Phenomenological form for perfect fluidity, classic basis in FSM:

The perfect fluid is isotropic and viscosity-free:

$$T_{MN}^{(classical)} = \left(\rho + \frac{p}{c^2}\right) u_M u_N - p\, g_{MN} \tag{2.61}$$

This term models the rest energy density (ρ) and pressure (p) along the trajectory (u_M). In FSM, the energy density ρ arises from the electrically internal fion mass within a beam, and p arises from the field tension of the exchange fion in a vacuum. In the FSM, so-called fions (**Chapter 3.2**) take on the physical role of photons in a

beam. They are, in comparative terms, similar to an extension of the classical gluon. Furthermore, fions can actively generate a potential relative to the D_{56} dimensional plane, can split by producing an exchange particle and a passive (dark) fion, and can recombine following a field exchange.

- ρ – standardized energy density; unit: $\frac{\text{kg}}{\text{m}^4\text{s}^2}$; total energy per 6D volume (including resting mass)
- p – standardized pressure; unit: $\frac{\text{kg}}{\text{m}^4\text{s}^2}$; is isotropic force; $p = 0$ for dust; $p = \frac{\rho}{3}$ for radiation
- u_M – quadruple pulse; dimensionless without specific index assignment; causes the scalar direction of movement; e.g.: $u^M u_M = - c^2$ with index M below for covariant components (transformed like gradients ∂_M); M above for countervariant component (transformed as differentials dx^M);
- $(\rho + \frac{p}{c^2})$ – enthalpy density
- $(\rho + \frac{p}{c^2})\, u_M\, u_N$ – dynamic term; unit: $\frac{\text{kg}}{\text{m}^4\text{s}^2}$; pulse flow
- $- p\, g_{MN}$ – isotropic pressure in all directions
- g_{MN} – full metric from point 1.; causes projection

Relativistic fields correspond to photons as hollow-body oscillations, with angular momentum generating momentum density. This reproduces classical physics, whereby in FSM the energy density ρ emerges from the geometric mass as resistance to fields.

Extension through compact portion of the wave-field:

Metric:

$$g_{MN} = [1 + \cos(k_{Uni}\, t)]\, (\eta_{MN} + h_{MN})$$

The following applies to the global component with $h_{MN} = 0$:

$$g_{MN}^{\text{global}} = [1 + \cos(k_{Uni}\, t)]\, \eta_{MN}$$

Global Christoffel component:

$$\Gamma_{MN}^{\lambda\,(\text{global})} = - \frac{1}{2}\, k_{Uni} \sin(k_{Uni}\, t)\, (\eta_N^\lambda\, \delta_M^0 + \eta_M^\lambda\, \delta_N^0 - \eta_{MN}\, \eta^{\lambda 0})$$

Global Ricci tensor:

$$R_{MN}^{(\text{global})} \approx \partial_P\, (- \frac{1}{2}\, k_{Uni} \sin(k_{Uni}\, t)\, \eta_N^P\, \delta_M^0) - \partial_N\, (- \frac{1}{2}\, k_{Uni} \sin(k_{Uni}\, t)\, \eta_P^P\, \delta_M^0)$$

$$R_{MN}^{(\text{global})} = (- \frac{1}{2}\, k_{Uni}^2 \cos(k_{Uni}\, t))\, (\eta_{MN}\, \eta^{00} - \eta_M^0\, \eta_N^0 - \eta_N^0\, \eta_M^0)$$

- $\eta_{MN}\,\eta^{00} = -\,\eta_{MN}$
- $-\,\eta^0_M\,\eta^0_N - \eta^0_N\,\eta^0_M$ – time projectors

Global Ricci scalar:

$$R^{\text{global}} = \eta^{MN}\,R^{(\text{global})}_{MN} = \left(-\frac{1}{2}\,k^2_{Uni}\cos(k_{Uni}\,t)\right)\eta^{MN}\,(\eta_{MN}\,\eta^{00} - \eta^0_M\,\eta^0_N - \eta^0_N\,\eta^0_M)$$

- $\eta^{MN}\,\eta_{MN}\,\eta^{00} = -\,7$
- $-\,\eta^{MN}\,\eta^0_M\,\eta^0_N = 1$
- $-\,\eta^{MN}\,\eta^0_N\,\eta^0_M = 1$

$$R^{\text{global}} = -\frac{1}{2}\,k^2_{Uni}\cos(k_{Uni}\,t)\,[-7 + 1 + 1]$$

$$R^{\text{global}} = \frac{5}{2}\,k^2_{Uni}\cos(k_{Uni}\,t)$$

Substitution into the Einstein tensor G_{MN} with $g_{MN} \approx \eta_{MN}$:

$$G_{MN} = R_{MN} - \frac{1}{2}\,g_{MN}\,R$$

$$G^{(\text{global})}_{MN} = \frac{1}{2}\,k^2_{Uni}\cos(k_{Uni}\,t)\,\eta_{MN} + \frac{1}{2}\,k^2_{Uni}\cos(k_{Uni}\,t)\,(-\,\eta^0_M\,\eta^0_N - \eta^0_N\,\eta^0_M) - \frac{5}{4}\,k^2_{Uni}\cos(k_{Uni}\,t)\,\eta_{MN}$$

Simplification of time-projection terms:

The time projection terms $(-\,\eta^0_M\,\eta^0_N - \eta^0_N\,\eta^0_M)$ contribute exactly the amount in the 7D contraction that compensates for the remaining factors. The structure of the projector is chosen such that:

$$\frac{1}{2}\,k^2_{Uni}\cos(k_{Uni}\,t)\,(-\,\eta^0_M\,\eta^0_N - \eta^0_N\,\eta^0_M) - \frac{5}{4}\,k^2_{Uni}\cos(k_{Uni}\,t)\,\eta_{MN} = 0$$

Isotropic approximation of the projector in linear order for $G^{(\text{global})}_{MN}$:

$$G^{(\text{global})}_{MN} = \frac{1}{2}\,k^2_{Uni}\cos(k_{Uni}\,t)\,\eta_{MN}$$

The reduced momentum-energy tensor is defined as the ‘effective source’ of curvature:

$$T^{(\text{global})}_{MN} = \frac{c^4}{8\pi G}\,\frac{1}{2}\,k^2_{Uni}\cos(k_{Uni}\,t)\,\eta_{MN}$$

$$\boldsymbol{T^{(\text{global})}_{MN} = \frac{c^4}{16\pi G}\,k^2_{Uni}\cos(k_{Uni}\,t)\,\eta_{MN}} \qquad (2.62)$$

- G – Gravitational constant normalised to 7D

Expansion using the vector component of the wave-field:

The coupling component $T_{MN}^{(\text{Vector})}$ arises from the dimensional reduction of the 7-dimensional theory of gravity to 4 dimensions. Specifically, 4 dimensions for the interaction/coupling between the 4-dimensional visible and the 3-dimensional compact:

$$\Gamma_{\mu a}^{\lambda\,(\text{Vector})} = \frac{1}{2}\, g^{\lambda P}\, [\partial_\mu\, (A_P^a + \delta A_P^a) + \partial_a\, (A_\mu^a + \delta A_\mu^a) - \partial_P\, (A_\mu^a + \delta A_\mu^a)]$$

Dominant part:

$$\Gamma_{\mu a}^{\lambda\,(\text{Vector})} = \frac{1}{2}\, \eta^{\lambda P}\, \partial_\mu\, (A_P^a + \delta A_P^a)$$

The starting point is the Lagrangian density of the Yang-Mills field, as is customary, applied to 7D:

$$\mathcal{L}_{YM}^{(7)} = -\frac{1}{4}\, F_{MN}^a\, F^{aMN}\,,$$

whereas the field strength F is defined as follows:

$$F_{\mu\nu}^a = \partial_\mu\, (A_\nu^a + \delta A_\nu^a) - \partial_\nu\, (A_\mu^a + \delta A_\mu^a) + g_M^{(7)}\, f^{abc}\, A_M^b\, A_N^c$$

- Indices: M, N = 0,..., 6; calibration group index a = 4,.5, 6 for SU(3), summed over a
- A_ν^a or A_μ^a – 7D calibration vector
- Indices: M, N break down into μ, ν = 0, 1, 2, 3
- $g_M^{(7)}$ – coupling
- f^{abc} – structural constant

$$\mathcal{L}_{YM}^{(4)} = -\frac{1}{4}\, \frac{1}{g_{(YM)}^2}\, F_{\mu\nu}^a\, F^{a\mu\nu} = -\frac{1}{4}\, \frac{1}{\pi}\, F_{\mu\nu}^a\, F^{a\mu\nu}, \qquad (2.63)$$

- $g_{(YM)}^2 = g_{eff}^2$ – effective 4D coupling, normalised to π
- $g_{eff}^2 = \dfrac{g_{(7)}^2}{V_{(3)}} = \pi$

$$\mathcal{L}_{YM}^{(4)} = -\frac{1}{4}\, \frac{1}{g_{(YM)}^2}\, F_{\mu\nu}^a\, F^{a\mu\nu} = -\frac{1}{4}\, \frac{1}{\pi}\, F_{\mu\nu}^a\, F^{a\mu\nu}$$

Yang–Mills expression for the reduced case, where the interaction acts as a coupling effect between the 4-dimensional visible and 3-dimensional compact dimensions:

$$T_{\mu\nu}^{(\text{Vector})} = \frac{1}{4\pi} \left(F_{\mu}^{a\lambda} F_{a\lambda\rho} - \frac{1}{4} g_{\mu a} F_{\rho\sigma}^{a} F^{a\rho\sigma}\right) \eta^{\rho\nu} \tag{2.64}$$

- $\frac{1}{4\pi}$ – corresponds to a specific normalisation of the calibration coupling
- Indices:
  μ = 0, 1, 2, 3; direction in visible 4D
  ν = 0, 1, 2, 3; free, visible index finger after contraction with $\eta^{\rho\nu}$
  a = 4, 5, 6; compact group index for a vector field A^4, A^5, A^6
  λ, ρ, σ, K = 0,…, 6; sum indices over 7D
- $F_{\mu}^{a\lambda} = \eta^{\lambda\rho} F_{\mu\rho}^{a} = \eta^{\lambda\rho} [\partial_{\mu} (A_{\rho}^{a} + \delta A_{\rho}^{a}) - \partial_{\rho} (A_{\mu}^{a} + \delta A_{\mu}^{a})]$
- $F_{a\lambda\rho} = \partial_{\lambda} (A_{a\rho} + \delta A_{a\rho}) - \partial_{\rho} (A_{a\lambda} + \delta A_{a\lambda})$
- $F_{\rho\sigma}^{a} = \partial_{\rho} (A_{\sigma}^{a} + \delta A_{\sigma}^{a}) - \partial_{\sigma} (A_{\rho}^{a} + \delta A_{\rho}^{a})$
- $F^{a\rho\sigma} = \eta^{\rho\lambda} \eta^{\sigma K} F_{\mu K}^{a} = \eta^{\rho\lambda} \eta^{\sigma K} [\partial_{\lambda} (A_{K}^{a} + \delta A_{K}^{a}) - \partial_{K} (A_{\lambda}^{a} + \delta A_{\lambda}^{a})]$
- $\eta^{\rho\nu} = \text{diag}(-1, 1, 1, 1, 1, 1, 1)^{\rho\nu}$

For the full 7D case:

$$\boldsymbol{T_{MN}^{(\text{Vector})} = \frac{1}{4\pi} \left(F_{M}^{\lambda a} F_{N a\lambda} - \frac{1}{4} g_{MN} F_{\rho\sigma}^{a} F^{a\rho\sigma}\right)}$$

Extension to 7D with FSM-specific contributions:

$$T_{MN} = T_{MN}^{(\text{classical})} + T_{MN}^{(\text{global})} + T_{MN}^{(\text{Vector})} \tag{2.65}$$

$$T_{MN} = \left[\left(\rho + \frac{p}{c^2}\right) u_M u_N - p\, g_{MN}\right] + \left[\frac{c^4}{16\pi G} k_{Uni}^2 \cos(k_{Uni}\, t)\, \eta_{MN}\right] + \left[\frac{1}{4\pi} \left(F_{M}^{\lambda a} F_{N a\lambda} - \frac{1}{4} g_{MN} F_{\rho\sigma}^{a} F^{a\rho\sigma}\right)\right]$$

- T_{MN} – momentum-energy tensor; unit: $\frac{\text{kg}}{\text{m}^4\text{s}^2}$; normalised with 6D volume
- $T_{MN}^{(\text{classical})}$ – classical term; unit: $\frac{\text{kg}}{\text{m}^4\text{s}^2}$; visible matter; indices: M, N = 0,…, 6
- $T_{MN}^{(\text{global})}$ – global term; unit: $\frac{\text{kg}}{\text{m}^4\text{s}^2}$; includes dark energy or invisible photons (**Chapters 2.3** and **3.2**) arising from oscillations; indices: M, N = 0,…, 6; the only relevant metric is the Minkowski metric η_{MN}
- k – Angular frequency, time normalisation from $\frac{1}{\text{s}^2}$ to $\frac{1}{\text{m}^2}$; can be interpreted as the number of turns
- G – Gravitational constant; 4D unit: $G_{eff} = 6{,}674\ 10^{-11} \frac{\text{m}^3}{\text{kg s}^2}$; is available in a 7D dilution; $G = 6{,}674\ 10^{-11} \frac{\text{m}^6}{\text{kg s}^2}$

- $T_{MN}^{(\text{Vector})}$ – coupling fields from rotations; unit: $\frac{\text{kg}}{\text{m}^4\text{s}^2}$; describes the energy, momentum and potentials of non-Abelian gauge fields (e.g. fermions, bosons); indices: M, N = 0,…, 6
- /4π – standardisation; results in Gaussian units; from: $g_{eff}^2 = \frac{g_{(7)}^2}{V_{(3)}} = \pi$
- $F_M^{\lambda a}\, F_{N a \lambda}$ – non-tracked section; unit: $\frac{\text{kg}}{\text{m}^4\text{s}^2}$; generates energy flow and tension in the tuning forks
  in T_{00}: main contribution to the energy density of the calibration fields
  in T_{0i}: main contribution to the momentum flux of the calibration fields
- $-\frac{1}{4}\, g_{MN}\, F_{\rho_\sigma}^a\, F^{a\rho_\sigma}$ – trace unit of energy density; unit: $\frac{\text{kg}}{\text{m}^4\text{s}^2}$; generates electromagnetic and scalar fields; contributes the isotropic term to the metric g_{MN}, which gives the pressure a negative sign $p = -\rho$ and keeps the tensor trace-free

The derivation shows how the momentum-energy tensor T in the FSM follows directly from the geometric interpretation of mass and energy as field deformation and cosine-shaped rotation (kt). Matter is therefore not a fundamental concept, but an emergent effect of resistance to dynamic fields.

8. Calibration potential A_μ^a based on the FSM particle model

The calibration potential A_μ^a is the fundamental mediator of the electromagnetic and weak interactions in the FSM. It arises directly from the off-diagonal components of the 7D metric and mediates between the visible dimensions (μ = 0, 1, 2, 3: time and particle-field $F_{1\text{-}3}$) and the three compact wave-field dimensions (a = 4, 5, 6; $F_{4\text{-}6}$). Its derivative gives rise to the field strength F, which in turn generates charge, potential gradients and recombination. These geometric effects are modelled using the (inertial) rotation of fions in the dimensional planes $D_{45/46/56}$.

The FSM metric (2.18) from point 1 is:

$ds^2 \supset 2(A_\mu^a + \delta A_\mu^a)\, dy_a\, dx^\mu$

A_μ^a generates the compact coordinates y_a for the visible dimensions x^μ.

- A_μ^a – off-diagonal component; undisturbed calibration potential; dimensionless in 7D; generates fields from the geometry
- dy_a – the dynamic length of the radius parallel to the unit vector for a = 4, 5, 6
- Group index a = 4, 5, 6; μ = 0, 1, 2, 3

The field strength F, which generates the interaction, arises from the covariant derivative of the gauge potential.

7D:

$$F^a_{MN} = \partial_M (A^a_N + \delta A^a_N) - \partial_N (A^a_M + \delta A^a_M) + g^{(7)}_M f^{abc} (A^b_M + \delta A^b_M)(A^c_N + \delta A^c_N) \quad (5.66)$$

4D (following compaction):

$$F^a_{\mu\nu} = \partial_\mu (A^a_\nu + \delta A^a_\nu) - \partial_\nu (A^a_\mu + \delta A^a_\mu) + g^{(4)} f^{abc} (A^b_\mu + \delta A^b_\mu) (A^c_\nu + \delta A^c_\nu) \quad (5.67)$$

- F – the field strength from potential A determines the resulting dynamics
- $\partial_\mu A^a_\nu - \partial_\nu A^a_\mu$ – Abelian part
- $g^{(4)} f^{abc} A^b_\mu A^c_\nu$ – non-Abelian part; gives rise to the self-interaction of the gauge bosons (fions)
- Indices: b, c = 4, 5, 6

Potential A must be determined so that conclusions can be drawn about the field forces.

Link to the particle model – rotation of the active fione:

Particles consist of spheres S containing active fions that oscillate in 4-dimensional rotational orbits. Rotations relative to the D_{56} dimensional plane generate a charge Q through a potential gradient parallel to the fourth dimension. **Axiom 11** attributes the universal electric potential to a displacement current resulting from the alignment of its photon field within the wave-field, accompanied by the simultaneous dynamic expansion of space-time.

$$A^a_\mu = \phi_a \, \delta^a_b \, \delta^c_\mu$$

- ϕ_a – scalar potential of an object's vibration in the compact wave field parallel to a direction a = 4, 5, 6; the amplitude is generated
- δ^a_b – Kronecker delta; (1, if a = 6; otherwise 0); a = 6 applies when the field exchange takes place in the D_{56} dimensional plane between the wave-field and the particle-field; otherwise, '0' → denotes invisible matter; b corresponds here to the dimensional plane in which the rotation in the wave-field takes place; for D_{45}: δ^a_4; for $D_{45/46}$: δ^a_5; for $D_{45/46/56}$: δ^a_6
- $\delta^c_\mu = \delta^0_\mu = 1$ only if $\mu = c = 0$ → contribution relating solely to the time component A^a_0
  electrical potential (charge effect) → $\mu = 0$
- $\delta^c_\mu = \delta^i_\mu = 1$ only if $\mu = c = i$ → contribution relating solely to the spatial component A^a_i
  magnetic/vector potential (motion/rotation effect) → $\mu = i$ = 1, 2, 3 or μ = 1 for D_{14}, μ = 2 for D_{24}, μ = 3 for D_{34}; $i = D_{14/24/34}$

The potential A_μ^a is generated by the coupling between x^μ and y_a. The off-diagonal entries lie within the wave-field region of the metric. Compactification is achieved by integrating over the volume of the compact dimensions y_4, y_5, y_6. The volume integration ultimately yields the potential.

The effective action is:

$$S_{eff}^{(4)} = \frac{1}{V}\int \mathcal{L}_{(7)}\, d^7x = \int \mathcal{L}_{(4)}\, d^4x\, d^3y = \frac{1}{V}\int \mathcal{L}_{(4)}\, d^4x \sqrt{-g}\, d^3y$$

with: $\int d^3y = V = (2\pi R)^3$ und: $\mathcal{L}_{(4)}^{(\text{vectorial})} = -\frac{1}{4} g^{\mu\sigma} g^{\nu\rho} F_{\mu\nu}^a F_{\sigma\rho a} = -\frac{1}{4} 2\Delta A_\mu^a$

and: $\sqrt{-g} \rightarrow \sqrt{g_{aa}} \approx \mathrm{R} \rightarrow A_\mu^{a(7)} = A_\mu^{a(4)} \sqrt{g_{aa}} = A_\mu^{a(4)} R$

- After the compactification, the following applies to the potential: $A_\mu^{a(4)} = \frac{A_\mu^{a(7)}}{R}$

Using $dy_a = R\ (\cos(kt+\beta))$ as the displacement length, the path for generating the potential in a direction '*a*' in the wave-field is described:

$$\int A_\mu^{a(4)}\, dy_a = \frac{A_\mu^{a(7)}}{R} R\ (\cos(kt+\beta)) = A_\mu^{a(7)} \cos(kt+\beta)$$

The Poisson equation gives:

$\nabla^2\phi_a = -\frac{\rho^a}{\epsilon_0}$; relevant is $a = 4$; time component with: $\mu = 0$; for electrical potential

The standard solution to Poisson's equation in flat space is:

$$\rho^a = Q\, d^3(x)$$

$$\phi_a = \frac{Q}{4\pi\, \epsilon_0\, R}$$

The FSM metric extends ϕ_a to $\Delta A_\mu^{a(7)}$ with $\phi_a\, dy_a\, \delta_b^a\, \delta_\mu^c$ to take account of the off-diagonal elements of the metric:

$$\Delta A_{eff,\,0}^a(x) = \frac{Q}{4\pi\, \epsilon_0\, R} \frac{1}{R}\, dy_a\, \delta_b^a\, \delta_\mu^c = \frac{Q}{4\pi\, \epsilon_0\, R} \cos(kt + \beta)\, \delta_4^a\, \delta_\mu^0 \qquad (2.68)$$

- ϕ_a – scalar potential of an object's vibration in the compact wave-field parallel to the fourth dimension; determines the amplitude
- $\cos(kt + \beta)$ – with: $\cos(kt = 0°) = 1$ generates the rotation of the fion, which touches the D_{56} dimensional plane at its greatest deflection.

These Kronecker deltas ensure the optimal case by ensuring that a measurable charge always occurs when cos(kt = 0°) = 1.

- (kt) – describes the characteristic repetition rate of a period
- β – deviation angle or phase shift; causes a possible shift in the geometric conditions for optimal field exchange in the D_{56} dimensional plane; acts in the same way as the gravitational component
- β = 0° → strong interaction
  β = 0 < β < 90° → weak interaction
  β = 90° no longer interacts with the particle-field
- A_μ^a – now, after compactification, unit: $\frac{1}{\text{m}}$ for standardisation using: ħ = c = 1, otherwise, electrodynamics in accordance with the unit: V
- Q – electric charge of the particle; unit: C (Coulomb) and e (elementary charge)
- R – Radius of the compact wave-field dimensions with $\lambda = 2\pi R$; unit: m; in the particle-field, the radius R is defined as the distance
- $\frac{Q}{4\pi\,\epsilon_0\,R}$ – classical Coulomb potential

<u>Potential gradient in the wave-field:</u>

During the recombination of the exchange fion with a passive fion to form an active fion, the potential difference ΔA_μ^a is generated. It persists for a brief moment until the polarisation of all active fions in the beam has been established. It therefore follows that:

$$\Delta A_\mu^a = (A_\mu^a + \delta A_\mu^a) - A_\mu^a = \delta A_\mu^a = \left(\frac{V_{rot,external}}{c} - \frac{V_{rot,bound}}{c}\right) \frac{Q}{4\pi\,\epsilon_0\,R} \cos(kt + \beta)\,\delta_4^a\,\delta_\mu^0$$

$V_{Rot} = \frac{c}{2}$ for bound (active) fions → $A_\mu^a\big|_{\text{bound}} = A_\mu^a + \delta A_\mu^a$

$V_{Rot} = c$ for unbound (exchange) fions → $A_\mu^a\big|_{\text{unbound}} = A_\mu^a$

a) for unbound (exchange) fions or visible light:

$$\Delta A_\mu^4 = \frac{c}{c}\,(1 - 1)\,\frac{Q}{4\pi\,\epsilon_0\,R} \cos(kt + \beta)\,\delta_4^a\,\delta_\mu^0 = 0$$

b) for bound (active) fions:

$$\Delta A_\mu^4 = \frac{c}{c}\,(1 - 1 + \frac{1}{2})\,\frac{Q}{4\pi\,\epsilon_0\,R} \cos(kt + \beta)\,\delta_4^a\,\delta_\mu^0 = \frac{1}{2}\,\frac{Q}{4\pi\,\epsilon_0\,R} \cos(kt + \beta)\,\delta_4^a\,\delta_\mu^0$$

Taking the metric factor into account with 2:

$$2\Delta A^4_\mu = 2\,\frac{1}{2}\,\frac{Q}{4\pi\,\epsilon_0\,R}\cos(kt+\beta)\,\delta^a_4\,\delta^0_\mu = \frac{Q}{4\pi\,\epsilon_0\,R}\cos(kt+\beta)\,\delta^a_4\,\delta^0_\mu$$

- $A^a_\mu + \delta A^a_\mu$ – Potential difference relative to the reference potential; the superscript a denotes the compact wave-field dimensions; a = 4 for D_{45}, a = 5 for $D_{45/46}$, a = 6 for $D_{45/46/56}$; μ bottom for visible 4D space-time; μ = 0 for time, μ = 1 for D_{14}, μ = 2 for D_{24}, μ = 3 for D_{34}; $i = D_{14/24/34}$
- δA^a_μ – is non-zero in the short term → only a single registration is observed in the particle-field, like a single pulse or force peak; example: a fion is captured once in a beam
- δA^a_μ – is continuously non-zero → a constant interaction force is detected in the particle-field, which stabilises the bundle; example: strong interaction between two bosons (meson)
- $\frac{1}{2}$ – factor for recombination in the wave-field; it is **not** directly **recorded** as $\frac{1}{2}$ **in the particle-field**. The metric factor 2, which takes the particle-field into account, fully compensates for the reset effect during binding.

<u>Taking object movement into account:</u>

An object movement V_3 causes a length contraction parallel to the dimensional plane D_{56}. The potential appears contracted and amplified relative to the resting position.

The electric potential for bound fions in a bundle is given by the formula:

$$A^a_{eff,\,0} = \frac{Q}{4\pi\,\epsilon_0\,R}\cos(kt+\beta)\,\delta^a_4\,\delta^0_\mu\,\frac{c}{V_5}$$ with: D_{56} – plane, a = 6 (2.69)

The electric potential for unbound fions outside the bundle is given by:

$$A^a_{eff,\,0} = 0 \qquad (2.70)$$

- $\frac{c}{V_5}$ – field-enhancing effect caused by a contraction in length when an additional object moves within the particle-field in the direction of motion
- $V_5 = \sqrt{c^2 - v_3^2}$; V_3 – object velocity in a particle-field

<u>Specific potentials when an exchange fion recombines with visible matter in the ground state:</u>

$$\frac{c}{V_5} = \frac{c}{c} = 1;\ \delta^a_b = 1;\ \delta^c_\mu = 1;\ \cos(kt+\beta) = 1$$

a. An unbound exchange fion rotates freely in the dimensional plane D_{56}:

$$A_0^6 = \frac{e/3}{4\pi\,\epsilon_0\,R} = 0 \qquad \text{with: } (A_\mu^a + \delta A_\mu^a) - A_\mu^a = 0, \text{ wegen } \delta A_\mu^a = 0 \tag{2.71}$$

b. Unbound exchange fion with an active fion:

$$A_0^4 = \frac{e/3}{4\pi\,\epsilon_0\,R} \qquad \text{with: } R = \frac{\lambda_{Obj}}{2\pi} \tag{2.72}$$

- a = 4 for recombination back into the dimensional plane D_{45}

c. A bound exchange fion with an electron (from a bundle):

$$A_0^5 = \frac{-\,e}{4\pi\,\epsilon_0\,R} \qquad \text{with: } R = \frac{\lambda_{Obj}}{2\pi} \tag{2.73}$$

- a = 5 for recombination into the possible dimensional planes $D_{45/46}$

d. A bound exchange fion with a positron:

$$A_0^5 = \frac{+\,e}{4\pi\,\epsilon_0\,R} \qquad \text{with: } R = \frac{\lambda_{Obj}}{2\pi} \tag{2.74}$$

- a = 5 for recombination into the possible dimensional planes $D_{45/46}$

e. A bound exchange fion with a positively charged boson:

$$A_0^6 = \frac{+\,e}{4\pi\,\epsilon_0\,R} \qquad \text{with: } R = \frac{\lambda_{Obj}}{2\pi} \tag{2.75}$$

- a = 6 for recombination into the possible dimensional planes $D_{45/46/56}$

The 7-dimensional FSM model explains how a potential arises in the wave-field. Most particles that mediate interactions must, whilst rotating, simultaneously possess a direction vector in the fourth spatial dimension. The rotation for a generation therefore takes place orthogonally to the D_{56} dimensional plane. In contrast, visible photons and neutrinos, for example, whose oscillation period runs exclusively parallel to the D_{56} dimensional plane, carry no potential.

9. Complete 7-dimensional field equations in FSM

Einstein's field equations describe curvature through energy, momentum, and matter. These field equations are extended with the field-space model, whereby the momentum-energy tensor T_{MN} receives contributions from the photon field, such as fions and relativistic fields of compact dimensions. The maximum velocity $V_{max} = c$

remains invariant, but the field propagation velocities V_4 and V_5 model the deformations. In this way, the 7-dimensional tensor can integrate orthogonal dimensional planes $D_{45/46/56}$ with causal causes such as mass from frequencies and charge from electric potential. The field equations in the FSM describe the unification of the four fundamental forces through geometric deformations in the wave-field. It also provides an explanation for dark energy and the expansion of the universe from its geometric rotation.

Initial situation - Definition of the Hilbert action in 7D of the FSM:

The derivation follows Hilbert's variational principle with $\delta S = 0$, where S is the total action

$S = S_g + S_m$ (Gravity + Matter),

which is extended to the FSM model.

The gravitational action according to Hilbert in 7D:

$$S_g = \frac{c^4}{16\pi G} \int R \sqrt{-g}\, d^7x = \frac{c^4}{16\pi G} \int \left(R_{MN} - \frac{1}{2} g_{MN} R\right) \delta g^{MN} \sqrt{-g}\, d^7x \qquad (2.76)$$

- S_g – gravitational action; unit: Js; minimizes curvature; integrated over 7D space-time
- $\frac{c^4}{16\pi G}$ – standardized normalization constant; unit: $\frac{kg}{m^2\, s^2}$; scaled to field equations; determines the strength with which energy and momentum generate gravity
- $\int d^7x$ – integral over 7 dimensions; unit: m^7; the dimension of time is normalized to the maximum speed c in meters.
- $\sqrt{-g} = \sqrt{|\det(g_{MN})|}$ – determinant for the diagonal metric g_{MN}
- R – Ricci skalar from point 5.; unit: $\frac{1}{m^2}$; measures average curvature
- G – standardized gravitational constant; $G = 6{,}674\ 10^{-11}\ N\frac{m^5}{kg^2}$; the gravitational constant is diluted in the 7-dimensional field-space and only becomes concentrated through compactification; $G_{eff} = 6{,}674\ 10^{-11}\ N\frac{m^2}{kg^2}$;
- c – maximum speed; $c = 299792458\ \frac{m}{s}$

Matter action according to Hilbert in 7D: (photons/fions):

$$S_m = \int \mathcal{L}_m \sqrt{-g}\, d^7x = -\frac{1}{2} \int T_{MN}\, \delta g^{MN} \sqrt{-g}\, d^7x \qquad (2.77)$$

The action minimizes the curvature with the Ricci scalar (R), taking into account the volume with: $\sqrt{-g}$. The FSM extends this with compact dimensions (M, N = 0,…, 6), which generate rotations parallel to the dimensional planes $D_{45/46/56}$, thus mechanically enabling the generation of a charge parallel to the electrical potential. d^7x is the integral over time, visible space, and compact dimensions.

- S_m – matter action; unit: Js; describes the dynamics of fields/particles
- $\mathcal{L}_m$ – normalized matter Lagrangian density; unit: $\frac{kg}{m^2\ s^2}$; contains classical matter, calibration fields A^a_μ with potential terms and kinetic terms for the dynamic rotational mechanism in a vacuum
- $\delta S = 0$ – variation zero results in the stationary principle for equations

This step defines gravity geometrically and matter dynamically, whereby FSM integrates the matter action S_m through geometric fields.

Variation in total action according to the FSM metric:

$$\frac{\delta S}{\delta g^{MN}} = \frac{\delta S_g}{\delta g^{MN}} + \frac{\delta S_m}{\delta g^{MN}} = 0 \text{ leads to:}$$

From S_g:

$$\frac{\delta S_g}{\delta g^{MN}} = \frac{c^4}{16\pi G}\sqrt{-g}\,(R_{MN} - \frac{1}{2}\,g_{MN}\,R)$$

From S_m according to the formula (2.60):

$$\frac{\delta S_m}{\delta g^{MN}} = -\frac{1}{2}\sqrt{-g}\,T_{MN}$$

Overall:

$$\frac{c^4}{16\pi G}\sqrt{-g}\,(R_{MN} - \frac{1}{2}\,g_{MN}\,R) - \frac{1}{2}\sqrt{-g}\,T_{MN} = 0$$

$$R_{MN} - \frac{1}{2}\,g_{MN}\,R = \frac{8\pi G}{c^4}\,T_{MN} \qquad (2.78)$$

with:

$$T_{MN} = T^{(\text{classical})}_{MN} + T^{(\text{global})}_{MN} + T^{(\text{Vector})}_{MN} \qquad (2.65)$$

$$T_{MN} = [(\rho + \frac{p}{c^2})\,u_M\,u_N - p\,g_{MN}] + [\frac{c^4}{16\pi G}\,k^2_{Uni}\cos(k_{Uni}\,t)\,\eta_{MN}] + [\frac{1}{4\pi}\,(F^{\lambda a}_M\,F_{N a\lambda} - \frac{1}{4}\,g_{MN}\,F^a_{\rho\sigma}\,F^{a\rho\sigma})]$$

Global contribution:

$$G_{MN}^{(\text{global})} = R_{MN}^{(\text{global})} - \frac{1}{2}\,\eta_{MN}\,R^{(\text{global})} \tag{2.79}$$

- $R_{MN}^{(\text{global})} \approx \partial_P\,(-\frac{1}{2}\,k_{Uni}\sin(k_{Uni}\,t)\,\eta_N^P\,\delta_M^0) - \partial_N\,(-\frac{1}{2}\,k_{Uni}\sin(k_{Uni}\,t)\,\eta_P^P\,\delta_M^0)$
- $R^{(\text{global})} \approx \eta^{MN}\,[\partial_P\,(-\frac{1}{2}\,k_{Uni}\sin(k_{Uni}\,t)\,\eta_N^P\,\delta_M^0) - \partial_N\,(-\frac{1}{2}\,k_{Uni}\sin(k_{Uni}\,t)\,\eta_P^P\,\delta_M^0)]$

Local contribution:

$$G_{MN}^{(\text{local})} = R_{MN}^{(\text{local})} - \frac{1}{2}\,\eta_{MN}\,R^{(\text{local})} \tag{2.80}$$

- $R_{MN}^{(\text{local})} = \partial_P\,(\frac{1}{2}\,\frac{GM}{c^2\,r^2}\,(1+\cos(kt+\beta))\,\delta_N^r\,\delta_M^t) - \partial_N\Gamma_{PM}^P$
- $\partial_N\Gamma_{PM}^P \approx 0$ for low-field, radial, $M = N = t$
- $R^{(\text{local})} \approx \eta^{MN}\,[\partial_P\,(\frac{1}{2}\,\frac{GM}{c^2\,r^2}\,(1+\cos(kt+\beta))\,\delta_N^r\,\delta_M^t)]$

Vector contribution:

$$G_{MN}^{(\text{Vector})} = R_{MN}^{(\text{Vector})} - \frac{1}{2}\,\eta_{MN}\,R^{(\text{Vector})} \tag{2.81}$$

- $R_{MN}^{(\text{Vector})} = \partial_P\,(\frac{1}{2}\,\eta^{P\rho}\,\partial_M\,(A_\rho^a + \delta A_\rho^a)\,\delta_a^N)$
- $R^{(\text{Vector})} \approx \eta^{MN}\,[\partial_P\,(\frac{1}{2}\,\eta^{P\rho}\,\partial_M\,(A_\rho^a + \delta A_\rho^a)\,\delta_a^N)]$
  - $\frac{\delta S_m}{\delta g^{MN}}$ – with $\frac{\delta}{\delta g^{MN}}$ as a functional variation by differentiation according to the contravariant metric; unit: $\frac{\text{kg}}{\text{m}^4\text{s}^2}$; measures how strongly matter reacts to a small change in the geometry (metric) of space-time – and that is precisely the local distribution of energy, momentum, and tension in space-time; indices *M, N* above are contravariant; *M*, *N* = 0,…, 6
  - R_{MN} – Ricci tensor; unit: $\frac{1}{\text{m}^2}$; causes local curvature
  - $\frac{1}{2}\,g_{MN}\,R$ – trace term; unit: $\frac{1}{\text{m}^2}$; makes Ricci component trace-free; g_{MN} from point 1.; *R*-scalar from point 5.
  - $R_{MN} - \frac{1}{2}\,g_{MN}\,R$ – Einstein tensor according to the formula (2.51); unit: $\frac{1}{\text{m}^2}$; source of gravity; G_{MN} from point 6. without cosmological constant
  - T_{MN} – impulse energy tensor; unit: $\frac{\text{kg}}{\text{m}^4\text{s}^2}$; source of matter; T_{MN} from point 7.
  - $\frac{8\pi G}{c^4}$ – converted normalized coupling constant; unit: $\frac{\text{m}^2\,\text{s}^2}{\text{kg}}$; scales matter to curvature

- $\sqrt{-g}$ – invariant volume element; dimensionless normalized; measures how much the local volume is distorted by curvature compared to flat space

Leads to vacuum equations at $T = 0$, which are described in FSM by rotations.

Replacing the cosmological constant Λ with $T_{MN}^{(global)}$:

Classically, a cosmological constant is added to account for vacuum energy. This is solved by the momentum-energy tensor T_{MN} of the FSM. The tensor T_{MN} has compact components with $T_{MN}^{(global)}$ that describe the vacuum energy as a function of expansion with:

$$T_{MN}^{(global)} = [\frac{c^4}{16\pi G} k_{Uni}^2 \cos(k_{Uni}\, t)\, \eta_{MN}]$$

The T_{MN} tensor only needs to be applied to the photon field of the universe.

Key finding:

The electromagnetic wave (moving energy) is identical to a dynamic deformation of space-time. It is not a wave in space-time, but rather space-time itself in wave-like motion. Gravity and electromagnetism are thus unified on the same geometric plane. Both are curvatures or rotations of the same 7-dimensional space-time.

If an object has a large mass, the classical term of the field equation (GTR) becomes dominant, whereas at the microscopic level, interaction forces cause space-time to curve due to their restoring forces.

10. Compactification from 7D to 4D with its principle of operation

Compactification is the process by which the three-dimensional invisible wave-field dimensions $F_{4\text{-}6}$ are integrated to obtain the effective four-dimensional observable world. In FSM, sinusoidal rotations stabilize compactification, generate effective fields, and explain masses and coupling frequencies as geometric effects. It resolves wave-particle duality and unifies the four fundamental forces by having compact modes generate particle masses.

The starting point is the 7D metric according to (2.16) and separation of the dimensions:

$g_{MN} = [1 + \cos(k_{Uni}\, t)]\ (\eta_{MN} + h_{MN})$

- g_{MN} – dimensionless

Minkowski-component η_{MN}:

- η_{MN} = diag(-1, 1, 1, 1, 1, 1, 1)

h_{MN} can be broke down into three blocks:

- Visible block: $h_{\mu\nu} = \frac{G\,M}{c^2\,r}\,(1+\cos(kt+\beta))\,\delta_{\mu\nu}$
- Coupling block: $h_{\mu m} = h_{m\mu} = (A^a_\mu + \delta A^a_\mu)\,\delta_{am}$; direction: μ

  $h_{m\nu} = h_{\nu m} = (A^a_\nu + \delta A^a_\nu)\,\delta_{am}$; direction: ν
- Compact block: diagonal, no additional scalar perturbation in the metric itself

Global contribution: $[1 + \cos(k_{Uni}\,t)]$

Indices: $M, N = 0, 1, 2, 3, 4, 5, 6$; $\mu, \nu = 0, 1, 2, 3$; $a, m = 4, 5, 6$

Reduction to an effective 4D metric:

$$ds^2 = g^{4D}_{\mu\nu}\,dx^\mu\,dx^\nu$$

$$g^{4D}_{\mu\nu} = [1 + \cos(k_{Uni}\,t)]\,[\eta_{\mu\nu} + \frac{G\,M}{c^2\,r}\,(1+\cos(kt+\beta))\,\delta_{\mu\nu}] \tag{2.82}$$

The compact dimensions vanish. Their influence is contained in the scalar fields $\phi_n(x)$ and the effective momentum-energy tensor $T^{(\text{scalar})}_{\mu\nu}$.

<u>Effective 4D field equations derived from compactification:</u>

The vacuum solution of the 7D Einstein tensor is:

$$G_{MN} = 0 = R^{(7)}_{MN} - \frac{1}{2}\,g_{MN}\,R^{(7)}$$

The action

$$S_g = \frac{c^4}{16\pi G}\int d^7x\,\sqrt{-g}\,R_{MN}$$

is integrated over the compact wavefield dimensions y^a with $a = 4, 5, 6$. This yields the invariant volume element of the compact dimensions V. The effective 4D action is:

$$S^{\text{eff}}_g = V\int\,(\sqrt{-g^{(4)}}\,(\frac{c^4}{16\pi G}\,R^{(4)} + \mathcal{L}^{\text{eff}}_{\text{Matter}})\,d^4x$$

- S_g^{eff} – effective gravitational force; unit: Js; minimises the curvature; results in observable equations
- V – compact volume; unit: m³; scales down from 7D to 4D
- $\int d^4x$ – 4D-integral; unity: m^4; creates visible space-time
- $\sqrt{-g^{(4)}}$ - 4D-volume element
- $R^{(4)}$ – 4D- scalar; unit: $\frac{1}{m^2}$; causes observable curvature
- $\mathcal{L}_{\text{Matter}}^{\text{eff}}$ – effective Lagrangian density for matter derived from the effective action S_g^{eff}
- $\frac{V}{G_{(7)}} = \frac{1}{G_{eff}}$ – The gravitational constant $G_{(7)}$, including compact wave-field dimensions, reduces to the following under compactification to G_{eff}

Variation of S_g^{eff} according to the reduced metric $g_{\mu\nu}^{4D}$:

$$\delta S_g^{\text{eff}} = \delta S_{\text{EH}}^{\text{eff}} + \delta S_{\text{Matter}}^{\text{eff}} = 0$$

Variation of the Einstein-Hilbert term (classical):

$$\delta S_{\text{EH}}^{\text{eff}} = \frac{c^4}{16\pi G_{eff}} \int \left(R_{\mu\nu}^{(4)} - \frac{1}{2} g_{\mu\nu}^{(4)} R^{(4)}\right) \delta g^{(4)\mu\nu} \sqrt{-g^{(4)}}\, d^4x + \text{scalar terms}$$

Variation in the amount of matter:

$$\delta S_{\text{Matter}}^{\text{eff}} = -\frac{1}{2} \int T_{\mu\nu}^{eff}\ \delta g^{(4)\mu\nu} \sqrt{-g^{(4)}}\, d^4x + \text{scalar terms}$$

This form first reduces the field equation from 7D to 4D. This yields the 4D gravitational component and a positive contribution from the gauge fields:

$$R_{\mu\nu}^{(4)} - \frac{1}{2} g_{\mu\nu}^{(4)} R^{(4)} = \frac{8\pi G_{eff}}{c^4} T_{\mu\nu}^{eff} \tag{2.83}$$

- $R_{\mu\nu}^{(4)}$ – effective 4D Ricci tensor; unit: $\frac{1}{m^2}$; observable curvature
- $g_{\mu\nu}^{(4)}$ – 4D-metric
- $R^{(4)}$ – Ricci scalar, 4D; unit: $\frac{1}{m^2}$; average curvature
- G_{eff} – Gravitational constant; unit: 6,674 10^{-11} $N\frac{m^2}{kg^2}$;
- $T_{\mu\nu}^{eff}$ – effective momentum-energy tensor; unit: $\frac{J}{m^3} = \frac{kg}{m\ s^2}$; generates contributions from $F_{\mu\nu}^a$

Equation (2.65) reproduces the 4D Einstein-Yang-Mills equations with FSM-specific terms for the momentum-energy tensor $T_{\mu\nu}^{eff}$:

$$T_{\mu\nu}^{eff} = T_{\mu\nu}^{(classical)} + T_{\mu\nu}^{(global)} + T_{\mu\nu}^{(Vector)} + T_{\mu\nu}^{(scalar)}$$

$$T_{\mu\nu}^{eff} = [(\rho + \frac{p}{c^2})\, u_\mu\, u_\nu - p\, g_{\mu\nu}^{(4)}] + [\frac{c^4}{16\pi G_{eff}}\, k_{Uni}^2 \cos(k_{Uni}\, t)\, \eta_{\mu\nu}] + [\frac{1}{4\pi}\,(F_\mu^{\lambda a}\, F_{\nu a\lambda} - \frac{1}{4}\, g_{\mu\nu}^{(4)}\, F_{\rho\sigma}^{a}\, F^{a\rho\sigma})] + T_{\mu\nu}^{(scalar)} \quad (2.84)$$

Definition of the mode terms:

This step reduces 7D to 4D and generates Kaluza-Klein modes. The scalar field in 7D is expanded as a Fourier series in the compact coordinates:

$$\phi(x, y) = \phi_4 + \sum_{n=1}^{3} \phi_n(x) e^{\frac{i n y^a}{R}} \quad (2.85)$$

- $\phi(x, y)$ – Scalar field; e.g., in the case of metric distortion; unit variable; generally produces a field in 7D
- $\phi_4(x)$ – n = 0–mode; global cosmic background potential parallel to the fourth dimension; unity: $\frac{1}{m}$
- $\phi_n(x)$ – 4D mode field; creates an effective 4D field; index n corresponds to the mode number for the fermion generation; unit: $\frac{1}{m}$
- $e^{\frac{i n y^a}{R}}$ – periodic function; results in a harmonic expansion; i represents the imaginary unit; magnitude is always 1
- y^a – compact coordinate; unit: m; is “rolled up”; is invisible
- R – radius of the compact wave-field dimensions with $\lambda = 2\pi R$; unit: m; is the scale of compactification; if small → invisible

After compaction:

$$\phi(x) = \sum_{n=1}^{3} \phi_n(x) e^{\frac{i n y^a}{R}} \quad (2.86)$$

The complex exponential is taken in the real domain; standing wave as a cosine or sine function.

Possible scale terms and stabilization of compaction:

Scalar terms contribute to the stabilization of the compactification. They generate a restoring force that acts in proportion to a potential field ϕ_n to keep the field centered at the origin. They also carry an effective 4-dimensional scalar field ϕ_n, which represents the nth mode excitation of the wave in the compact wave-field dimensions. ϕ_n arises from the compactification of the three compact wave-field dimensions and the wave dynamics prevailing within them. This wave is described as a function of time t and the compact coordinates y_a.

$\phi(x^\mu, y^a)$ with: x^μ – 4D-coordinates; y^a – 3D-compact wave-field dimensions

Compact Fourier series / mode development:

$\phi(x, y^a + 2\pi R) = \phi(x, y^a)$

This allows for a Fourier expansion (Kaluza–Klein modes):

$\phi(x, y^a) = \sum_{n=-\infty}^{\infty} \phi_n(x)\, e^{\frac{iny^a}{R}}$

In its actual form:

a) $\phi(x, y^a) = \sum_{n=1}^{\infty} \phi_n(x) \sin(\frac{ny^a}{R})$ or:

b) $\phi(x, y^a) = \sum_{n=1}^{\infty} \phi_n(x) \cos(\frac{ny^a}{R})$ (2.87)

Option b) is chosen because it allows for a phase shift of the potential relative to the D_{56} plane. This phase shift transforms the strong interaction into a weak interaction.

A) Mass component $V(\phi_n)_m$:

$\phi(x, y^a) = \sum_{n=1}^{\infty} \phi_n(x) \cos(\frac{ny^a}{R})$

The wave equation for compact dimensions:

$(\partial_\mu \partial^\mu + \partial_a \partial^a)\, \phi_n = 0$ (2.88)

$(\partial_\mu \partial^\mu)\, \phi_n = 0 \rightarrow$ the propagation of a massless scalar field does not involve mass

In a linear approximation:

$\partial_t^2 \phi_n + \partial_a \partial^a \phi_n = 0$

$\partial^a \phi_n \sim \frac{n}{R} \phi_n$ (Derivation with respect to y^a provides the factor $\frac{n}{R}$)

$\partial_a \partial^a \phi_n \sim -(\frac{n}{R})^2 \phi_n$ (second derivative with respect to y^a)

$\partial_t^2 \phi_n \pm (\frac{n}{R})^2 \phi_n = 0$

Similar to:

$\partial_t^2 \phi_n + \frac{\partial V}{\partial \phi_n} = 0$

Therefore:

$\frac{\partial V}{\partial \phi_n} = (\frac{n}{R})^2 \phi_n$

Integration with respect to ϕ_n provides:

$$V(\phi_n) \supset V(\phi_n)_m = \int \left(\frac{n}{R}\right)^2 \phi_n \, d\phi_n = \frac{1}{2} \left(\frac{n}{R}\right)^2 \phi_n^2 + \text{constant}$$

$$\boldsymbol{V(\phi_n)_m = \frac{1}{2} \left(\frac{n}{R}\right)^2 \phi_n^2} \tag{2.89}$$

- $\frac{1}{2} \left(\frac{n}{R}\right)^2 \phi_n^2$ – unit: $\frac{1}{m^2} \frac{1}{m^2} = \frac{1}{m^4}$; n = dimensionless; $[R]$ = m; scaled by $c\hbar$
- $\phi_n(x)$ – nth-generation scalar field (n = 1 light, n = 2 medium, n = 3 heavy)
- $\phi_n(x)$ – becomes a single unit after compactification in 4D: $\frac{1}{m}$; is derived from the wave amplitude in the wave-field dimensions
- $\phi_n(x)$ – contributes to mass, chirality, and possible interactions

With the visible modes n = 1, 2, 3, $\phi(x, y^a)$ becomes $\phi(x)$.

Renormalization using $c\hbar \frac{1}{c^2}$, due to the time component $\mu = 0$, provides the mass of an object, which depends on its geometry:

$$\boldsymbol{m = \frac{n\,h}{2\pi\, c\, R}} \tag{2.90}$$

Geometrically dependent mass with its amplitude and as a periodic disturbance:

$$m(t) = \frac{n\,h}{2\pi\, c\, R} \cos(kt + \beta) \tag{2.91}$$

Relativistic without periodic perturbation with $\cos(kt = 0° + \beta = 0°)$:

The wavelength $\lambda = 2\pi R$ causes a contraction in the direction of motion, resulting in what is known as a blue shift at the source. In the case of a blue shift, the contraction term in the numerator is multiplied. This explains the conversion of kinetic energy into rest mass, whereby an object's velocity contracts the field propagation velocity V_5 from its resting state.

$\lambda(t) = \lambda \sin(\alpha) = \lambda \frac{V_5}{c}$ → The wavelength decreases as the object's velocity V_4 increases

Note: Blue shift is never observed from the outside, even when the source is moving parallel to the observer, because the observer always detects a lengthening of the observed wavelength between the source and the observer.

Insert:

$$m(t) = \frac{n\,h}{c\,\lambda}\,\frac{1}{\sin(\alpha)} = \frac{n\,h}{c\,\lambda}\,\frac{c}{V_5} \qquad \text{(Wavelength with blue shift)} \qquad (2.92)$$

B) Dynamic, oscillating component $V(\phi_n)$ for coupled and uncoupled matter:

The metric component that describes global and local volume modulation is:

$\gamma(t) = 1 + \cos(kt)$

$$R_{\mu\nu}^{(4)} - \frac{1}{2}\,g_{\mu\nu}^{(4)}\,R^{(4)} = \frac{8\pi G}{c^4}\,T_{MN}^{(\text{global})} \int d^3y\,\sqrt{\gamma} \qquad \text{with:} \quad \sqrt{\gamma} = \sqrt{\det(\gamma)}$$

$\gamma(t) = (1 + \cos(kt))$

Potency: 3 due to 3D Euclidean

y^4, y^5, y^6

$$\sqrt{\det(\gamma)} = \sqrt{(1 + \cos(kt))^3} = (1 + 3\cos(kt) + 3\cos^2(kt) + \cos^3(kt))^{1/2}$$

$$\sqrt{\det(\gamma)} \approx 1 + \frac{3}{2}\cos(kt) \qquad \text{(after linear approximation)}$$

The effective scalar field $\phi_n(x)$ is defined such that it is proportional to the relative change in volume:

$$1 + \frac{3}{2}\cos(kt) = 1 + \phi_n(x) \qquad \rightarrow \qquad \phi_n(x) = \frac{3}{2}\cos(kt + \text{phase})$$

written in simple notation: $\phi_n(x) = \phi_n$

Effective energy density due to coupling effects (interactions):

- First derivative (velocity) of the potential:
  $$\frac{dV}{dt} = \partial_t \phi_n = -\frac{3}{2}\,k\,\sin(kt + \text{phase})$$
- The kinetic energy density for the 4D Lagrangian density is proportional to:
  $$E_{\text{kin}} = \frac{1}{2}\,(\partial_t \phi_n)^2 = \frac{1}{2}\,(-\frac{3}{2}\,k\,\sin(kt + \text{phase}))^2 = \frac{9}{8}\,k^2\,\sin^2(kt + \text{phase})$$
- The second derivative as the acceleration of the field:
  $$\partial_t^2 \phi_n = -\frac{3}{2}\,k^2\cos(kt + \text{phase})$$
- The acceleration of the change in volume contributes to the effective potential energy density: E_{pot} ~ (acceleration)² oder ~ (elongation)²

$$E_{pot} = (\partial_t^2 \phi_n)^2 = (-\frac{3}{2} k^2 \cos(kt + \text{phase}))^2 = \frac{9}{4} k^4 \cos^2(kt + \text{phase})$$

The potential energy density E_{pot} is equal to $V(\phi_n)_{pot}$:

$$V(\phi_n) \supset V(\phi_n)_{pot} = \frac{9}{4} k^4 \cos^2(kt + \text{phase}) = \frac{9}{4} k^4 \cos^2(kt + \text{phase})$$

Potential $V(\phi_n)_{pot}$ for coupled matter:

$$\boldsymbol{V(\phi_n)_{pot} = \frac{9}{4} k^4 \cos^2(kt + \beta)} \tag{2.93}$$

- $V(\phi_n)_{pot}$ – potential energy density for coupled matter; unit: $\frac{J}{m^3} = \frac{kg}{m\,s^3}$; scaled by $c\hbar$; means: energy becomes accessible and is coupled
- ϕ_n lies in the geometric change in the oscillation with:
  $\phi_n = \frac{3}{2} \cos(kt + \text{phase})$
- (kt) – Due to its periodic change in direction, the curve of the cosine function repeatedly restores the dynamics of space-time, so that it does not lead to a collapse—neither in contraction nor in expansion.
- β – angles of deviation that shift the phase relative to the dimensional plane D_{56}
  global: $\beta = 0$, local: $\beta = 0 \ldots 90°$
- k – angular frequency of the oscillation; unit: $\frac{1}{s}$
- k^4 – unit: $\frac{1}{s^4}$; due to the metric normalization of time, k^4 is interpreted as: $\frac{1}{m^4}$; energy density is calculated by multiplying by: $\frac{kg}{m\,s^2}$
- Energy is proportional to the square of the amplitude → $\cos^2(kt + \beta)$, enables a resonance or phase shift that prevents the system from reaching an unstable fixed point

Potential $V(\phi_n)_{dark}$ for decoupled matter (dark energy):

As long as the universe remains below the wavelength λ_{min}, which prevents quantized photons from interacting electrically, the minimum coupling frequency $f < f_{min}$ is not yet reached. In this state, the photon field consists exclusively of dark energy. Upon exceeding the minimum coupling frequency f_{min}, the potential $V(\phi_n)_{dark}$ is converted into $V(\phi_n)_{pot}$ over the entire expansion phase. The two potentials are thus complementary to one another.

$$\mathcal{L}_n \supset V(\phi_n)_{dark} = \frac{9}{4} k^4 (1 - \cos(kt + \beta))^2 \tag{2.94}$$

- $V(\phi_n)_{dark}$ – energy density for dark energy; unit: $\frac{J}{m^3} = \frac{kg}{m\ s^3}$; scaled by $c\hbar$; "still available, but not accessible"; does not interact with bound matter
- $(1 - \cos(kt + \beta))^2$ – The square term resulting from the cosine oscillation with phase β makes the term oscillatory and dynamic; the energy density is positive and the displacement becomes quadratic (by comparison, the cosmological constant Λ from classical literature is, in contrast, merely a fixed constant)

$$\boldsymbol{V(\phi_n)_{dark} = \frac{9}{4}\, k^4\, (1 - \cos(kt + \beta))^2} \tag{2.95}$$

Stabilization via scalar potential $V(\phi_n)$:

$$V(\phi_n) = V(\phi_n)_m + V(\phi_n)_{pot} + V(\phi_n)_{dark}$$

$$V(\phi_n) = \frac{1}{2}\left(\frac{n}{R}\right)^2 \phi_n^2 + \frac{9}{4}\, k^4 \cos^2(kt + \beta) + \frac{9}{4}\, k^4\, (1 - \cos(kt + \beta))^2 \tag{2.96}$$

- $\frac{1}{2}\left(\frac{n}{R}\right)^2 \phi_n^2$ – Mass term for the scalar field ϕ_n. It ensures that ϕ_n oscillates around $\phi_n = 0$ and cannot become arbitrarily large. This corresponds to a positive curvature in the potential, which binds the field to the origin.
- $\frac{9}{4}\, k^4 \cos^2(kt + \beta)$ – oscillating periodic term. It creates a dynamic, time-dependent barrier in the potential. Through the phase shift $(kt + \beta)$, the scalar field ϕ_n actively couples to the oscillation of the compactification via (kt). This prevents the compact volume (or radius R) from permanently collapsing or growing exponentially; instead, it is periodically pushed back.

Composition of the scalar terms for the momentum-energy tensor $T_{\mu\nu}^{(scalar)}$:

The Lagrangian density per mode n is, finally:

$$\mathcal{L}_n = \frac{1}{2}\, \partial_\mu \phi_n\, \partial^\mu \phi_n - [(V(\phi_n)_m + V(\phi_n)_{pot} + V(\phi_n)_{dark})]$$

$$S_{scalar} = \int d^4x \sqrt{-g^{(4)}} \sum_{n=1}^{3} \mathcal{L}_n$$

The components of the momentum-energy tensor are defined as:

$$T_{\mu\nu}^{(scalar)} = -\frac{2}{\sqrt{-g^{(4)}}} \frac{\delta S_{scalar}}{\delta g^{\mu\nu}}$$

a) Variation of the kinetic term:

$$\mathcal{L}_{kin} = \frac{1}{2}\,\partial^{\mu}\,\phi_n\,\partial_{\mu}\,\phi_n = \frac{1}{2}\,g^{\mu\rho}\,\partial_{\mu}\,\phi_n\,\partial_{\rho}\,\phi_n$$

→ this term depends explicitly on $g^{\mu\nu}$ ab; direct variation ≠ 0

Variation, according to $g^{\mu\nu}$:

- Direct variation: $\frac{1}{2}\,\partial_{\mu}\,\phi_n\,\partial_{\nu}\,\phi_n$
- Metrical variation: $-\frac{1}{2}\,g^{(4)}_{\mu\nu}\,\frac{1}{2}\,\partial^{\rho}\,\phi_n\,\partial_{\rho}\,\phi_n$

is typically, in the Lagrangian density of scalar fields, the kinetic trace term arising from the variation of $\sqrt{-g^{(4)}}$ and $g^{\mu\rho}$.

$$\frac{\delta\mathcal{L}_{kin}}{\delta g^{\mu\nu}} = \frac{1}{2}\,\partial_{\mu}\,\phi_n\,\partial_{\nu}\,\phi_n - \frac{1}{2}\,g^{(4)}_{\mu\nu}\,\frac{1}{2}\,\partial^{\rho}\,\phi_n\,\partial_{\rho}\,\phi_n$$

b) Variation of the mass term:

$$\mathcal{L}_{Mass} = V(\phi_n)_m$$

$$\frac{\delta\mathcal{L}_{Mass}}{\delta g^{\mu\nu}} = -\frac{1}{2}\,g^{(4)}_{\mu\nu}\;V(\phi_n)_m$$

c) Variation in the potential for coupled matter:

$$\mathcal{L}_{pot} = V(\phi_n)_{pot}$$

$$\frac{\delta\mathcal{L}_{pot}}{\delta g^{\mu\nu}} = -\frac{1}{2}\,g^{(4)}_{\mu\nu}\;V(\phi_n)_{pot}$$

d) Variation in the potential for uncoupled matter:

$$\mathcal{L}_{dark} = V(\phi_n)_{dark}$$

$$\frac{\delta\mathcal{L}_{dark}}{\delta g^{\mu\nu}} = -\frac{1}{2}\,g^{(4)}_{\mu\nu}\;V(\phi_n)_{dark}$$

e) Variation of the volume element $\sqrt{-g^{(4)}}$:

$$\delta\left(\sqrt{-g^{(4)}}\;\mathcal{L}_n\right) = \frac{1}{2}\,g^{(4)}_{\mu\nu}\;\sqrt{-g^{(4)}}\;\mathcal{L}_n\,\delta g^{\mu\nu} + \sqrt{-g^{(4)}}\,\frac{\delta\mathcal{L}_n}{\delta g^{\mu\nu}}\,\delta g^{\mu\nu}$$

In summary:

$$\frac{\delta S_{scalar}}{\delta g^{\mu\nu}} = \sqrt{-g^{(4)}}\,[\frac{1}{2}\,\partial_\mu\,\phi_n\,\partial_\nu\,\phi_n - \frac{1}{2}\,g^{(4)}_{\mu\nu}\,(\frac{1}{2}\,\partial^\rho\,\phi_n\,\partial_\rho\,\phi_n + V(\phi_n)_m + V(\phi_n)_{pot} + V(\phi_n)_{dark})]$$

$$T^{(\text{scalar})}_{\mu\nu} = -\frac{2}{\sqrt{-g^{(4)}}}\,\frac{\delta S_{scalar}}{\delta g^{\mu\nu}}$$

(the negative sign has already been included in the variations) (2.97)

$$T^{(\text{scalar})}_{\mu\nu} = c\hbar\,\sum_{n=1}^{3}\,[\partial_\mu\,\phi_n\,\partial_\nu\,\phi_n - \frac{1}{2}\,g^{(4)}_{\mu\nu}\,(\partial^\rho\,\phi_n\,\partial_\rho\,\phi_n + 2V(\phi_n)_m + 2V(\phi_n)_{pot} + 2V(\phi_n)_{dark})]$$

- $T^{(\text{scalar})}_{\mu\nu}$ – scalar energy density; unit: $\frac{\text{J}}{\text{m}^3} = \frac{\text{kg}}{\text{m s}^3}$, scaled by $c\hbar$; The scalar tensor contributes to the curvature in Einstein's field equations and, in the FSM, accounts for the masses of the generations with $(\frac{n}{R})^2$ and possible dynamic energy density $V(\phi_n)$.
- $\sum_{n=1}^{3}$ – Sum over the three modes n = 1, 2, 3
- $\partial_\mu\,\phi_n$ or $\partial_\nu\,\phi_n$ – covariance gradient (directional derivative) of the field ϕ_n
- $\partial_\mu\,\phi_n\,\partial_\nu\,\phi_n$ – directional **kinetic momentum contribution** (gradient product); μ, ν = 0, 1, 2, 3; 0 = time, 1, 2, 3 space; describes the directed flow of energy and momentum in the scalar field ϕ_n; unit: $\frac{1}{\text{m}^4}$, $[\phi_n] = \frac{1}{\text{m}}$ → after normalization: $\frac{\text{kg}}{\text{m s}^3}$; scaled by $c\hbar$
- $\frac{1}{2}$ – Normalization factor derived from the variation in effect; ensures the correct balance between the kinetic and potential contributions
- $g^{(4)}_{\mu\nu}$ – effective 4D metric after reduction; dimensionless; defines distances and curvature in the observable 4D world
- $\partial^\rho\,\phi_n\,\partial_\rho\,\phi_n$ – **isotropic contribution of kinetic pressure** (contracted gradient); ρ = 0, 1, 2, 3; determines the total kinetic energy density regardless of direction; unit: $\frac{1}{\text{m}^4}$, $[\phi_n] = \frac{1}{\text{m}}$ → after normalization: $\frac{\text{kg}}{\text{m s}^3}$, scaled by $c\hbar$
- $V(\phi_n)$ – terms for **potential energy**; unit: $\frac{1}{\text{m}^4}$, $[\phi_n] = \frac{1}{\text{m}}$ → after normalization: $\frac{\text{kg}}{\text{m s}^3}$; scaled by $c\hbar$
- $V(\phi_n)_m$ – mass term resulting from compactification; n = 1, 2, 3; $[R]$ = m; $[\phi_n] = \frac{1}{\text{m}}$; causes the field ϕ_n to have an effective mass $m_n = \frac{n}{R}$ obtained; scaled by $c\hbar$; note the generational hierarchy
- $V(\phi_n)_{pot}$ – potential of the scalar field ϕ_n (oscillating and stabilizing); potential energy; scaled by $c\hbar$

- $V(\phi_n)_{dark}$ – The potential of the scalar field of uncoupled matter from the dark energy sector; scaled by $c\hbar$; $V(\phi_n)_{dark}$ and $V(\phi_n)_{pot}$ act in a complementary manner

Notes:

- $n = 1$; ϕ_1; Ground state (lightest field); lightest generation; e.g., electron, up and down quarks (u/d-quarks)
- $n = 2$; ϕ_2; first excited state; second generation; e.g., muons, C-quarks, S-quarks
- $n = 3$; ϕ_3; second excited state; third generation; e.g., tauon, B-quark, T-quark
- **Casimir energy** (quantum fluctuations) in compact spaces generates gauge fields or scalar fields with energy that depends on the radius:
  $V_{Casimir} \sim \frac{hc}{2\pi R^4}$
  In FSM, this is integrated using the potential of the scalar field $V(\phi_n)$ and modeled as an oscillating term, since the time specification $\sim [k^4] = \frac{1}{s^4}$ is normalized by the spatial length $[t\,c]$ = m for 4D.
- The mass term: $V(\phi_n)_m = \frac{1}{2} (\frac{n}{R})^2 \phi_n^2$ corresponds to a Kaluza-Klein mass with $m_n = \frac{n}{R}$. The radius implies that its size depends on any electromagnetic oscillation of an object in space-time. The smaller the radius, the shorter its wavelength, the higher its frequency, the greater the inertial motion of the oscillation in space-time, and the greater its explicit mass. This term also explains why **masses** are hierarchical ($n = 1$, $n = 2, 3$ heavier) (classified as "families of dimensions" in **Chapter 3.5**), why there are exactly three generations ($n = 1, 2, 3$), and why the smallest boson masses exist only for $n = 1, 2$ in the dimensional plane $D_{45/46}$. The **potential $V(\phi)$ stabilizes** the system. The **electron**/positron is the **fundamental particle** of mode n = 1, and, as will be shown, the first particle to interact electrically with photons from the dark energy sector once the minimum coupling frequency fmin is exceeded. Thus, the **Higgs field theory** is replaced by the FSM model.

Effective momentum-energy tensor $T_{\mu\nu}^{eff}$ including scale terms:

$$T_{\mu\nu}^{eff} = T_{\mu\nu}^{(\text{classical})} + T_{\mu\nu}^{(\text{global})} + T_{\mu\nu}^{(\text{Vector})} + T_{\mu\nu}^{(\text{scalar})}$$

$$T_{\mu\nu}^{eff} = [(\rho + \tfrac{p}{c^2})\, u_\mu\, u_\nu - p\, g_{\mu\nu}^{(4)}] + [\tfrac{c^4}{16\pi G_{eff}}\, k_{Uni}^2 \cos(k_{Uni}\, t)\, \eta_{\mu\nu}] + [\tfrac{1}{4\pi} (F_\mu^{\lambda a}\, F_{va\lambda} - \tfrac{1}{4}\, g_{\mu\nu}^{(4)}\, F_{\rho\sigma}^a\, F^{a\rho\sigma})] +$$
$$c\hbar \sum_{n=1}^{3} [\partial_\mu \phi_n\, \partial_\nu \phi_n - \tfrac{1}{2}\, g_{\mu\nu}^{(4)} (\partial^\rho \phi_n\, \partial_\rho \phi_n + 2V(\phi_n)_m + 2V(\phi_n)_{pot} + 2V(\phi_n)_{dark})] \qquad (2.98)$$

- $V(\phi_n)_m = \frac{1}{2} (\frac{n}{R})^2 \phi_n^2$
- $V(\phi_n)_{pot} = \frac{9}{4} k^4 (\cos(kt + \beta))^2$

- $V(\phi_n)_{dark} = \frac{9}{4} k^4 (1 - \cos(kt + \beta))^2$
- $V(\phi_n)_{pot}$ and $V(\phi_n)_{dark}$ work in complement to each other
- Scaling terms are scaled by $c\hbar$
- The potentials have the same impact locally and globally, depending on the context.

The ratio of matter that couples to matter that does not yet couple:

$$\frac{\rho_{coupled}}{\rho_{dark}} = \frac{V(\phi_n)}{V(\phi_n)_{dark}} = \frac{(\cos(90° - \alpha))^2}{(1 - \cos(90° - \alpha))^2} = \frac{(\sin(\alpha))^2}{(1-\sin(\alpha))^2} \quad (2.99)$$

- α – trigonometric solid angle at the current point in space-time; angle between the global field velocities V_4 and V_5 (cathetus) of the universe relative to the maximum velocity c (hypotenuse)
- Neglecting particles with weak interactions with β
- Extreme values, taking into account their complementary effects:
  0 – stands for 100% dark energy
  ∞ – refers to the conversion of dark energy into 100% coupled matter
- Example: Expansion of the universe with $kt = \alpha = 18{,}7°$ (from **Chapter 7.2**):
  a) cos(90° - 18,7°) = 0,32; corresponds to the coupled matter; with starting point cos(90°) = 0 proportions of bound matter
  b) 1 - cos(90° - 18,7°) = 0,68; is consistent with astronomical observations of dark energy

Derivation of Relativistic Momentum and Energy from FSM Geometry:

To extract the energy from T_{00} and the momentum from T_{0i}, the effective tensor, denoted by $T^{eff}_{\mu\nu}$, is already given in compact form.

$T^{(classical)}_{\mu\nu} = (\rho + \frac{p}{c^2}) u_\mu u_\nu - p\, g^{(4)}_{\mu\nu}$ Normalization: $G_{\mu\nu} u^\mu u^\nu = - c^2$

Applying the indices results in:

a) T_{00} – energy density; energy flux in the timelike direction; 3D volume element

b) T_{i0} – energy flux density; energy flux in the spatial i-direction; $i = 1, 2, 3$; 3D-volume element: 1x timelike, 2x spatial axes

c) T_{0i} – Pulse density; pulse flux in the timelike direction; 3D volume element

d) T_{ik} – Pulse current density; pulse flux of the kth component of the pulse in the spatial i-direction; 3D volume element: 1x timelike, 2x spatial axes

a) Energy density with $p = 0$; $u_0 \approx - c$; $u_i \approx 0$ the rest mass dominates:

$T_{00} \approx \rho\, c^2$; $T_{0i} \approx 0$; $T_{ij} \approx 0$

Relativistic:

$$\boldsymbol{T_{00} \approx \rho\, c^2 \frac{1}{\sin^2(kt)}} \tag{2.100}$$

The integral over the volume V yields:

$$E = \int T_{00}\, dV = \int \rho\, c^2 \frac{1}{\sin^2(kt)} \sin(kt)\, dV = \rho\, c^2 \frac{V}{\sin(kt)}$$

$$\boldsymbol{E(t) = m\, c^2 \frac{1}{\sin(kt)}} \qquad \text{with: } \frac{1}{\sin(kt)} = \frac{c}{V_5} \tag{2.101}$$

For $p \neq 0$:

$$T^{00} = (\rho\, c^2 + p)\, c^2 \frac{1}{c^2} - p$$

Relativistic:

$$\boldsymbol{T^{00} = (\rho\, c^2 + p) \frac{1}{\sin^2(kt)} - p} \tag{2.102}$$

c) Pulse density with $p \approx 0$; $u_0 \approx - c$; $u_i \approx \frac{V_i}{c} << 1$ ($\frac{1}{c}$ follows from the metric normalization of $\eta_{\mu\nu}$ for one of the three spatial directions)

$$T_{0i} \approx - \rho\, c \frac{V_i}{c}$$

In the literature, contravariant indices are used, which makes the expression positive:

$$T^{0i} \approx \rho\, V_i$$

Relativistic with: $\frac{1}{\sin(kt)} = \frac{c}{V_5}$

$$\boldsymbol{T^{0i} \approx \rho\, V_i \frac{1}{\sin^2(kt)}} \tag{2.103}$$

The integral over the volume V provides:

$$p_i = \int T^{0i}\, dV = \int \rho\, V_i \frac{1}{\sin^2(kt)} \sin(kt)\, dV = \rho\, V_i \frac{V}{\sin(kt)}$$

$$\boldsymbol{p_i(t) = m\, V_i \frac{1}{\sin(kt)}} \qquad \text{classical impulse}$$

$$p(t) = m\, c \frac{1}{\sin(kt)} \qquad \text{for } V_i \approx c \tag{2.104}$$

For $p \neq 0$:

$$T^{0i} = (\rho\, c^2 + p)\, V_i \frac{1}{c^2}$$

Relativistic:

$$\boldsymbol{T^{0i} = (\rho\, c^2 + p)\, V_i \frac{1}{c^2 \sin^2(kt)}} = (\rho + p)\, V_i \frac{1}{V_5^2} \tag{2.105}$$

- T_{00} – time-time extraction; unit: $\frac{\text{kg}}{\text{m s}^2}$; energy density as the primary source of gravity
- $p\, c^2$ – rest energy density; unit: $\frac{\text{kg}}{\text{m s}^2}$; increases effective mass/energy through field resistance or rotation in the wave-field parallel to the dimension D_4
- ρ – static density; unit: $\frac{\text{kg}}{\text{m}^3}$; mass per unit volume
- T_{0i} – space-time extraction; unit: $\frac{\text{kg}}{\text{m}^2\,\text{s}}$; describes the flow of momentum through a surface (e.g., the transfer of energy)
- $-\rho\, V_i$ – commonly referred to as pulse density or mass flow density; unit: $\frac{\text{kg}}{\text{m}^2\,\text{s}}$; results in momentum per unit area at a speed of V_i in direction i
- /sin(kt) – relativistic factor; increases momentum and energy through geometric dilation during rotation in compact dimensions
- $\eta_{\mu\nu}$ – metric; $\eta_{\mu\nu}$ = diag(-1,1,1,1)
- u_0 – index „0“ means, based on the metric $\eta_{\mu\nu}$ the time field; this cell contains – c, because the time was standardized for unity with [$c\, t$] = m; unit: [u_0] = $\frac{\text{m}}{\text{s}}$
- u_i – index „i“ denotes a direction derived from the metric $\eta_{\mu\nu}$, where the indices 1, 2, and 3 correspond to the 3D space; in these cells, the three spatial directions are normalized by $\frac{V_i}{c}$; dimensionless

Global oscillating term:

$$T_{\mu\nu}^{(\text{global})} = \frac{c^4}{16\pi G_{eff}} k_{Uni}^2 \cos(k_{Uni}\, t)\, \eta_{\mu\nu}$$

$$\text{a) } \boldsymbol{T_{00}^{(\text{global})} = \frac{c^4}{16\pi G_{eff}} k_{Uni}^2 \cos(k_{Uni}\, t)}\, \eta_{00} = \boldsymbol{-\frac{c^4}{16\pi G_{eff}} k_{Uni}^2 \cos(k_{Uni}\, t)} \tag{2.106}$$

- The negative sign describes a global energy density composed of dark energy, which exerts a repulsive force. The universe will continue to expand at an accelerating rate as long as dark energy exists. At the beginning of this period, the amount of dark energy is at its maximum, which maximizes the acceleration. At the point of maximum expansion, however, the acceleration decreases to zero because the amount of dark energy reaches zero.

c) $\boldsymbol{T_{0i}^{(global)} = 0}$ no off-diagonal terms in the global part of the metric (2.107)

Vector term:

$$T_{\mu\nu}^{(Vector)} = \frac{1}{4\pi} (F_{\mu}^{\lambda a} F_{va\lambda} - \frac{1}{4} g_{\mu\nu}^{(4)} F_{\rho\sigma}^{a} F^{a\rho\sigma})$$

$$a)\ T_{00}^{(Vector)} = \frac{1}{4\pi} (F_{0}^{\lambda a} F_{0a\lambda} - \frac{1}{4} g_{00}^{(4)} F_{\rho\sigma}^{a} F^{a\rho\sigma}) = \frac{1}{4\pi} (g^{\lambda\mu} F_{0\mu}^{a} F_{0\lambda a} - \frac{1}{4} g_{00}^{(4)} F_{\rho\sigma}^{a} F^{a\rho\sigma})$$

Lagrange solution with Si:

$$\mathcal{L}_{Vector} = -\frac{1}{4}\frac{1}{\mu_0} F_{\mu\nu}^{a} F^{a\mu\nu}$$ with the convention: $\frac{E}{c}$, if $g_{00}^{(4)} = (-1, 1, 1, 1)$ remains

$$T_{00}^{(Vector)} = \frac{1}{4\pi}\frac{1}{\mu_0} (\frac{1}{c^2} E^2 - \frac{1}{4} (-1)\, 2(B^2 - \frac{1}{c^2} E^2))$$

$$T_{00}^{(Vector)} = \frac{1}{4\pi} (\epsilon_0 E^2 + \frac{1}{2} (\frac{1}{\mu_0} B^2 - \epsilon_0 E^2))$$ with: $\frac{1}{c^2} = \mu_0\, \epsilon_0$

$$\boldsymbol{T_{00}^{(Vector)} = \frac{1}{8\pi}(\epsilon_0 E_a^2 + \frac{1}{\mu_0} B_a^2)}$$ = electromagnetic power density (2.108)

- The tensor behaves like radiation with $p = \frac{\rho}{3}$, similar to a relativistic radiation fluid; its field mediates strong and weak interactions.
- $\frac{1}{2}\, \epsilon_0 E^2$ or $\frac{1}{2}\frac{1}{\mu_0} B^2$ – electrical and magnetic energy density
- $\frac{1}{4\pi}$ – by convention, in classical SI electrodynamics, this becomes a factor 1
- Index a – from A_{μ}^{a}; a originates from the compact wave-field dimensions and, following compactification, denotes the gauge group index

c) $\boldsymbol{T_{0i}^{(Vector)} = \frac{1}{4\pi} \epsilon_0 (E \times B)_i}$ (2.109)

Derivation of the ρ-scalar and p-scalar from the FSM geometry:

The scalar tensor $T_{\mu\nu}^{(\text{scalar})}$ describes the gravitational source arising from relativistic fields, including kinetic energy, potential energy, the mass term, and dark, uncoupled energy. The ρ-scalar and p-scalar are key quantities for the cosmological interpretation of the scalar contribution.

- ρ-scalar – energy density from the contribution $\rho = T_{00}$ (time-time component); it measures how much energy is stored per unit volume in the individual scalar fields and determines the gravitational force exerted by the scalar fields, including all three generations and uncoupled energy
- p-scalar – pressure from the term $\rho = T_{ii}$ for $i = 1, 2, 3$ (spatial components, normalized by the metric); it measures the isotropic stresses – for dark energy, $p = -\rho$; negative pressure drives the expansion by determining the acceleration of the expansion.

To derive the two scalars, the FLRW metric is applied. This ensures a homogeneous universe with $g_{\mu\nu}^{(4)} = \text{diag}(-1, a^2(t), a^2(t), a^2(t))$ and neglects spatial gradients ($\nabla\phi_n \approx 0$, only $\partial_t \phi_n \neq 0$ for cosmological fields).

a) Derivation of the ρ scalar (energy density, T_{00}):

$$T_{00}^{(\text{scalar})} = c\hbar \sum_{n=1}^{3} [\partial_0 \phi_n \partial_0 \phi_n - \frac{1}{2} g_{00}^{(4)} (\partial^0 \phi_n \partial_0 \phi_n + 2V(\phi_n)_m + 2V(\phi_n)_{pot} + 2V(\phi_n)_{dark})]$$

- $\partial_0 = \partial t$ (Time derivation) → $g_{00}^{(4)} = -1$ with: $c = 1$
- $\partial_0 \phi_n \partial_0 \phi_n = (\partial_t \phi_n)^2$
- $\partial^0 \phi_n \partial_0 \phi_n = -(\partial_t \phi_n)^2$
- $-\frac{1}{2} g_{00}^{(4)} = -\frac{1}{2} \cdot (-1) = \frac{1}{2}$

Insert:

$$T_{00}^{(\text{scalar})} = c\hbar \sum_{n=1}^{3} [(\partial_t \phi_n)^2 + \frac{1}{2} ((-\partial_t \phi_n)^2 + 2V(\phi_n)_m + 2V(\phi_n)_{Pot} + 2V(\phi_n)_{dark})]$$

Complete with c-renormalization (kinetic + potential energy):

$$\boldsymbol{T_{00}^{(\text{scalar})} = c\hbar \sum_{n=1}^{3} c^2 [\frac{1}{2} (\partial_t \phi_n)^2 + V(\phi_n)_m + V(\phi_n)_{pot} + V(\phi_n)_{dark}]} \quad (2.110)$$

with: $\rho_{eff} = \frac{T_{00}^{(\text{scalar})}}{c^2}$

$$\rho_{eff} = c\hbar \sum_{n=1}^{3} [\frac{1}{2} (\partial_t \phi_n)^2 + V(\phi_n)_m + V(\phi_n)_{pot} + V(\phi_n)_{dark}] \quad (2.111)$$

c) Derivation of the ρ-scalar (momentum density, T_{0i}):

$$T_{0i}^{(\text{scalar})} = c\hbar\,[\partial_0\,\phi_n\,\partial_i\,\phi_n - \frac{1}{2}\,g_{0i}^{(4)}\,(\ldots)] \approx c\hbar\,\partial_0\,\phi_n\,\partial_i\,\phi_n$$

- $\partial_0\,\phi_n = \frac{1}{c}\,\partial_t\,\phi_n$

Complete with c-renormalization (pure gradient flow):

$$\boldsymbol{T_{0i}^{(\text{scalar})} = c\hbar\,\frac{1}{c}\,\partial_t\,\phi_n\,\partial_i\,\phi_n = \hbar\,\partial_t\,\phi_n\,\partial_i\,\phi_n} \tag{2.112}$$

d) Derivation of the p-scalar (pressure), $T_{ii} = p\,a^2(t)$ for $i = 1, 2, 3$):

$$T_{ii}^{(\text{scalar})} = c\hbar\,\sum_{n=1}^{3}\,[0 - \frac{1}{2}\,g_{ii}^{(4)}\,(\partial^\rho\,\phi_n\,\partial_\rho\,\phi_n + 2V(\phi_n)_m + 2V(\phi_n)_{pot} + 2V(\phi_n)_{dark})]$$

- $\partial_i\,\phi_n = 0$ (neglected, homogeneous)
- $g_{ii}^{(4)} = a^2(t)$ (positive)
- $\partial^\rho\,\phi_n\,\partial_\rho\,\phi_n = (\partial_t\,\phi_n)^2$

Insert:

$$T_{ii}^{(\text{scalar})} = -\frac{1}{2}\,c\hbar\,a^2(t)\,\sum_{n=1}^{3}\,[(-\partial_t\,\phi_n)^2 + 2V(\phi_n)_m + 2V(\phi_n)_{pot} + 2V(\phi_n)_{dark})]$$

$$T_{ii}^{(\text{scalar})} = c\hbar\,a^2(t)\,\sum_{n=1}^{3}\,[\frac{1}{2}\,(\partial_t\,\phi_n)^2 - V(\phi_n)_m - V(\phi_n)_{pot} - V(\phi_n)_{dark})] \tag{2.113}$$

$$p = \frac{T_{ii}^{(\text{scalar})}}{a^2(t)}$$

$$p = c\hbar\,\sum_{n=1}^{3}\,[\frac{1}{2}\,(\partial_t\,\phi_n)^2 - V(\phi_n)_m - V(\phi_n)_{pot} - V(\phi_n)_{dark})] \tag{2.114}$$

a) Total energy density ρ_{eff}:

$$\rho_{eff} = \frac{T_{00}^{eff}}{c^2}$$

$$\rho_{eff} = \rho - \frac{p}{c^2} - \frac{c^2}{16\pi G_{eff}}\,k_{Uni}^2\cos(k_{Uni}\,t) + \frac{1}{8\pi}\frac{1}{c^2}\,(\epsilon_0\,E_a^2 + \frac{1}{\mu_0}\,B_a^2) + c\hbar\,\sum_{n=1}^{3}\,[(\frac{1}{2}\,(\partial_t\,\phi_n)^2 + V(\phi_n)_m + V(\phi_n)_{pot} + V(\phi_n)_{dark})] \tag{2.115}$$

Relativistic:

$$\rho_{eff} = \frac{1}{c^2}\left[(\rho\, c^2 + p)\,\frac{1}{\sin^2(kt)} - p\right] - \frac{c^2}{16\pi G_{eff}}\, k_{Uni}^2 \cos(k_{Uni}\, t) + \frac{1}{8\pi}\frac{1}{c^2}\left(\epsilon_0\, E_a^2 + \frac{1}{\mu_0}\, B_a^2\right) + \frac{1}{\sin^2(kt)}\, c\hbar$$
$$\sum_{n=1}^{3}\left[\left(\frac{1}{2}\,(\partial_t\, \phi_n)^2 + V(\phi_n)_m + V(\phi_n)_{Pot} + V(\phi_n)_{dark}\right)\right] \qquad (2.116)$$

- Unit: $\frac{kg}{m\ s^2}$

c) Total pulse density g_{eff}:

$$g_{eff} = \frac{T_{0i}^{eff}}{c}$$

$$g_{eff} = \left(\rho + \frac{p}{c^2}\right) V_i \frac{1}{c} + \frac{1}{4\pi}\frac{1}{c}\,\epsilon_0\,(E \times B)_i + \hbar \sum_{n=1}^{3} \frac{1}{c}\,\partial_t\,\phi_n\,\partial_i\,\phi_n \qquad (2.117)$$

Relativistic: (2.118)

$$g_{eff} = \frac{1}{c^2 \sin^2(kt)}\left[(\rho\, c^2 + p)\, V_i \frac{1}{c}\right] + \frac{1}{4\pi}\frac{1}{c}\,\epsilon_0\,(E \times B)_i + \frac{1}{\sin(kt)}\left[\hbar \sum_{n=1}^{3} \frac{1}{c}\,\partial_t\,\phi_n\,\partial_i\,\phi_n\right]$$

- Unit: $\frac{kg}{m^2\ s}$

Addendum on Compactification:

All observable 4-dimensional phenomena, such as gravity, electromagnetism, particle masses, and other forces, arise as a low-energy approximation of 7-dimensional Field-Space-Mechanics following integration over the compact dimensions. In this process, gauge potentials of the 7-dimensional metric reduce to effective gauge fields in the 4-dimensional space-time. Electromagnetism and the weak force do not arise as independent fundamental fields, but as geometric effects of the compact dimensions, just as different Fourier modes generate the respective coupling structure.

The Fourier modes of the compact coordinates give rise to discrete particle masses, which manifest as heavy states. Dark energy appears as a natural oscillation of the compact dimensions. Photons and other particles fundamentally exist as waves in the compact wave-field ($F_{4\text{-}6}$), but appear as discrete objects in the visible 4-dimensional particle-field ($F_{1\text{-}3}$ plus time). This provides a geometric explanation of the wave-particle duality. Gravity itself acts primarily in the visible 4D realm and is preserved as classical curvature.

By applying the modes in the FSM model, it becomes possible to make new predictions about heavy particles that may be relevant to fusion processes for energy production or to future propulsion technologies.

FSM does not quantize gravity. Instead, gravity is retained as classical geometric curvature, while all quantum effects and the unification of interactions are explained by the dynamic geometry of the compact wave-field dimensions—rotation, coupling, and modes. The model thus provides a geometric bridge between classical gravity and the quantum world.

11. Development of the wave equation for gravitational waves

The starting point is the field equation of the FSM:

$$R_{MN} - \frac{1}{2} g_{MN} R = \frac{8\pi G}{c^4} T_{MN} \qquad (2.78)$$

Linear approximation around the flat metric (perturbation):

Gravitational waves are small disturbances, so the Minkowski metric η_{MN} is linearized.

$g_{MN} = \eta_{MN} + h_{MN}$ with: $h_{MN} << 1$

- η_{MN} – 7D symmetric Minkowski metric; η_{MN} = diag(-1, 1, 1, 1, 1, 1, 1); index: $M, N = 0,\ldots, 6$
- h_{MN} – metric disturbance; describes gravitational waves as a small deviation from the flat metric; neglect of higher-order terms such as h^2, since waves are weak → Advantage: Simplification of the calculation to a wave equation

Christoffel symbols in linear approximation:

- $\Gamma^{\lambda}_{NM} = \frac{1}{2} h^{\lambda P} (\partial_M h_{NP} + \partial_N h_{MP} - \partial_P h_{MN})$ (2.119)
- Γ^{λ}_{NM} – Christoffel symbol (non-tensorial); unit: $\frac{1}{\mathrm{m}}$; describes how vectors change during parallel transport in curved space-time; index above $\lambda = 0,\ldots, 6$; below $M, N = 0,\ldots, 6$
- $h^{\lambda P}$ – inverse Minkowski metric; dimensionless; raises indices $\lambda, P = 0,\ldots, 6$; $h^{\lambda P}$ = diag(-1, 1, 1, 1, 1, 1, 1); sum over P is implicitly Einstein convention
- Terme $\partial_M h_{NP}$ – partial derivatives according to x^M; unit: $\frac{1}{\mathrm{m}}$; measures the change in disturbance in the direction of M
- Approximation: no ΓΓ terms, since linear; simplified wave equation

Ricci tensor in linear approximation:

Ricci tensor:

$R_{MN} \approx \partial_P \Gamma^P_{MN} - \partial_N \Gamma^P_{MP}$

After the onset of Christoffel signs and contractions:

$$R_{MN} = \frac{1}{2} (\partial_P \partial_M h^P_N + \partial_P \partial_N h^P_M - \partial_P \partial^P h_{MN} - \partial_M \partial_N h^P_P) + R^{(global)}_{MN} \quad (2.120)$$

$$R^{(global)}_{MN} = \frac{1}{2} \eta^{\lambda P} (\partial_M [\cos(k_{Uni}\, t)]\, \eta_{NP} + \partial_N [\cos(k_{Uni}\, t)]\, \eta_{MP} - \partial_P [\cos(k_{Uni}\, t)]\, \eta_{MN})$$

- R_{MN} – Ricci tensor in linear approximation; unit: $\frac{1}{m^2}$; the tensor is the source of the wave equation
- $\partial_P \partial_M h^P_N$ or $\partial_P \partial_N h^P_M$ – displacement terms; describe how the disturbance in the P direction affects the curvature between M and N; unit: $\frac{1}{m^2}$
- $- \partial_P \partial^P h_{MN}$ – D'Alembert operator $\square\, h_{MN} = - \partial_P \partial^P h_{MN} = - \partial t^2\, h_{MN} + \nabla^2 h_{MN}$; unit: $\frac{1}{m^2}$; wave term; index $P = 0,\ldots, 6$
- $- \partial_M \partial_N h^P_P$ – This term corrects the trace components (scalar components) of the disturbance $h = h^P_P$, which is dimensionless, and takes scalar modes into account; in the trace-corrected calibration $h = 0$, the term vanishes
- $R^{(global)}_{MN}$ – Global terms describe the cosmic oscillation of the entire space-time. They act as a background curvature that modulates all waves and generates an additional longitudinal component
- Approximation: no ΓΓ terms

<u>Trace-free disturbance for 7D:</u>

Trace-free transverse (TT) calibration:

$h = \eta^{MN} h_{MN} = 0$

Trace-cleaned disturbance:

$$\bar{h}_{MN} = h_{MN} - \frac{1}{2} \eta_{MN}\, h$$

- $\bar{h}_{MN}$ – trace-free disturbance; unit: $\frac{1}{m^2}$

The following now holds for the Ricci tensor and the Ricci scalar:

R_{MN}: Translation terms disappear

$R \approx 0$

<u>Substitution into the FSM field equation:</u>

$$R_{MN} - \frac{1}{2} g_{MN} R = \frac{8\pi G}{c^4} T_{MN}$$

In a vacuum: $T_{MN} = 0$. After substitution, the following remains:

$$- \frac{1}{2} \partial_P \partial^P \bar{h}_{MN} + R_{MN}^{(\text{global})} = 0$$

$$\square_{(7)} \bar{h}_{MN} = 2 R_{MN}^{(\text{global})} \tag{2.121}$$

The D'Alembert operator in 7D in general:

$$\square_{(7)} = \eta^{MN} \partial^M \partial_M = - \frac{1}{c^2} \partial_t^2 + \nabla^2_{(3)} + \nabla^2_{(3,\ \text{compact})} = - \frac{1}{c^2} \partial_t^2 + \nabla^2_{(3)} + \partial_a \partial^a$$

- $\square_{(7)} = \partial^M \partial_M = - \partial_t^2 + \nabla^2 + \partial_a \partial^a$ – the D'Alembert operator in 7D; unit: $\frac{1}{\text{m}^2}$; describes wave propagation
- Running Index $a = 4, 5, 6$ regarding the compact wave-field dimensions

Gauge selection - harmonic gauge in a vacuum ($T = 0$) in FSM:

$$\partial^M \bar{h}_{MN} = 0 \tag{2.122}$$

- $\partial^M \bar{h}_{MN}$ – diversity; unity: $\frac{1}{\text{m}}$; Gauge condition; eliminates redundant degrees of freedom; summation index $M = 0,\ldots, 6$

In a vacuum ($T = 0$), this gauge is related to the field equation by:

$$\square_{(7)} \bar{h}_{MN} = 2 R_{MN}^{(\text{global})} = - k_{Uni}^2 \cos(k_{Uni}\, t)\, \eta_{MN} \tag{2.123}$$

- $\square_{(7)} \bar{h}_{MN}$ – trace-free metric solution in compact wave-field dimensions

  $\square_{(7)} \bar{h}_{MN} = 2 R_{MN}^{(\text{global})}$

  $\square_{(7)} \bar{h}_{MN} = 0$ for an GTR solution that neglects the global component according to the ‘Mach principle’

Polarization and degrees of freedom in the FSM:

In TT-Gauge (transvers-tracelos, extended to 7D, but reduced to 4D), the result is:

- In 4D-GTR:
  - $h_{\mu\nu}$ has two degrees of freedom (+ and × polarization for waves in the z-direction)
    $h_{xx} = - h_{yy} = h_+ \cos(wz - kt)$
    $h_{xy} = h_{yx} = h_\text{x} \cos(wz - kt)$
  - h_+, h_x – amplitudes; dimensionless; both independent polarizations of gravitational waves (spin-2) arise
  - w – wave number; unit: $\frac{1}{\text{m}}$; number of wavelengths per meter; $w = 2\pi/\lambda$; with: λ as wavelength

- z – location coordinate in propagation direction; unit: m
- k – circular frequency; unit: $\frac{\text{rad}}{\text{s}}$; angular velocity of oscillation
- t – time; unit: s
- ($wz - kt$) – phase of the wave; wz – spatial; kt – temporal; difference means that the wave travels in the positive z-direction

- In 7D-FSM:
  - h_{MN} – The global Ricci tensor acts as a cosmic “pressure wave” that exerts uniform pressure in all directions. This isotropic excitation cannot generate pure tensor waves (which are trace-free), but it can generate vector fields and scalar fields.
  - h_{MN} is dimensionless
  - From the inhomogeneous $\square_{(7)}\bar{h}_{MN}$, decomposing the perturbation into irreducible representations yields a structure with 14 degrees of freedom, with gauge degrees of freedom already subtracted:
    tensor h_{ij} (2), vector A_μ^a (6+3), scalar ϕ_n (3)
  - Indices: i, j = 1, 2, 3; a = 4, 5, 6; μ = 0, 1, 2, 3; n = 1, 2, 3
  - **Tensor polarization $h_{\mu\nu}$** has two degrees of freedom, as in GTR, and produces **two massless transverse** waves with spin-2:
    + polarization ($h_{xx} = - h_{yy}$)
    x polarization ($h_{xy} = h_{yx}$)
  - **Vector polarizations** arise from the off-diagonal metric components $h_{\mu a} = A_\mu^a$
    These correspond to massive vector fields originating from the compact wave-field dimensions. Nine degrees of freedom: 3 × 4 = 12, minus 3 Gauge at μ = 0) provide:
    Six transverse waves with photon-like modes, but massive with spin-1
    Three longitudinal waves are massive modes, helicity 0
  - **Scalar polarizations** from the modes of the compact wave-field dimensions result in three degrees of freedom with ϕ_1, ϕ_2, ϕ_3. Scalar fields possess “hidden” longitudinal waves with ϕ_n (spin = 0, generates volume change). This is not Gauge, but physically results from the geometric deviation from the dimensional plane D_{56} by stabilizing the three vectorial longitudinal waves. **Stabilization mechanism** of the FSM.
  - **Three longitudinal waves** scalar
    In summary:
    2 massless transverse tensor waves (classical GTR)
    6 massive transverse vector waves
    3 massive longitudinal vector waves
    3 massive scalar waves that couple with the longitudinal vectors
  - **Massive dispersion** of the transverse wave with angular frequency:

$k^2 = w^2 c^2 + 4\pi^2 m^2 \frac{c^4}{h^2}$; unit: $\frac{1}{s}$; w – wave number, unit: $\frac{1}{m}$

a) For high frequencies $w >> m$: $k \approx c\, w$ → dispersion-free; $v \approx c$

b) For low frequencies $w << m$: $k \approx 2\pi\, m \frac{c^2}{h}$; wave propagates slowly (v < c); dispersion is strong

Consequently:
1) Transverse wave packets disperse because different frequencies have different speeds:
$v = c^2 \frac{w}{k} < c$
2) Object nearby → high gravitational interaction; object in the distance → weak or no attraction

Wave equation for degrees of freedom and dispersion assignment:

The compact metrics component

$(1 + \cos(k_{Uni}\, t))$

acts as a time-dependent amplitude modulation on the entire wave, regardless of whether it is transverse or longitudinal.

a) 2 massless transverse tensor waves (from $h_{\mu\nu}$):

Wave equation:

$\square\, h_{ij}^{TT} = 0$

Whereby:

$(\partial_t^2 - c^2\, \nabla^2_{(3)})\, h_{ij}^{TT} = 0$

Dispersion:

$k^2 = w^2 c^2$ (massless, $v = c$) (2.124)

Functional shape with wave in the z-direction:

$h_{ij}(t, z) = [1 + \cos(k_{Uni}\, t)]\, [h_+ e^{i(wz-kt)}\, e_{ij}^{+} + h_x\, e^{i(wz-kt)}\, e_{ij}^{x}]$

In its real form:

$h_{ij}(t, z) = [1 + \cos(k_{Uni}\, t)]\, [h_+ \cos(w_z z - kt)\, e_{ij}^{+} + h_x \cos(w_z z - kt)\, e_{ij}^{x}]$ (2.125)

With transverse trace-free polarization tensors:

$e_{xx}^{+} = -\, e_{yy}^{+} = 1$; $e_{xy}^{x} = e_{yx}^{x} = 1$

- Indices: $i, j = 1, 2, 3$ (for x, y, z)
- $e_{ij}^{+} = \begin{pmatrix} 1 & 0 & 0 \\ 0 & -1 & 0 \\ 0 & 0 & 0 \end{pmatrix}$; $e_{ij}^{\times} = \begin{pmatrix} 0 & 1 & 0 \\ 1 & 0 & 0 \\ 0 & 0 & 0 \end{pmatrix}$
- No phase shift, because these modes do not couple directly to the internal scalar fields ϕ_n or to the phases of the compactification. These polarizations "recognize" the oscillation $(1 + \cos(k_{Uni}\ t))$ only as a global, isotropic modulation of the metric amplitude.
- $(1 + \cos(k_{Uni}\ t))$ – modulation fluctuation; pulsating, uniform in space-time relative to nominal time t; defines the temporal sequence for spatial deformation
- h_{+} and $h_{\times}$ – oscillate and propagate rapidly; these carry the wave information for the angular frequency k and wave number w
- e_{ij}^{+} and $e_{ij}^{\times}$ – polarization matrices; define spatial deformation direction

b) 6 solid transverse vector waves (from A_{μ}^{a}; a = 4, 5, 6; $\mu = 0, 1, 2, 3$):

These arise from the off-diagonal components $h_{\mu a}$. For each direction a, there are two transverse polarization states for μ.

Wave equation (Proca-like for massive vector fields in 4D):

$$\Box_{(4)} A_{\mu}^{a} - \partial_{\mu} (\partial^{\nu} A_{\nu}^{a}) + 4\pi^2 m_a^2 \frac{c^2}{h^2} A_{\mu}^{a} = 0 \quad \text{with: } m = \frac{n\,h}{2\pi\,c\,R} \quad \text{after compactification}$$

With Lorentz condition:

$$\partial^{\mu} A_{\mu}^{a} = 0$$

Dispersion:

$$k^2 = w^2 c^2 + 4\pi^2 m^2 \frac{c^4}{h^2};\ (\text{massive, } v < c) \tag{2.126}$$

Functional form results in a flat wave in the z-direction as transverse modes:

$$A_i^a(t, z) = A_0^a\ [1 + \cos(k_{Uni}\ t)]\ e^{i(wz - kt)} \sum_{pol=1,2}\ \epsilon_i^{pol}$$

In its real form:

$$A_i^a(t, z) = A_0^a\ [1 + \cos(k_{Uni}\ t)]\ \cos(w_z z - kt) \sum_{pol=1,2}\ \epsilon_i^{pol} \tag{2.127}$$

- Indices: $i = x, y$ (transverse); unit vector: $\epsilon_x^{1,\,0,\,0} = (1, 0, 0)$, $\epsilon_y^{0,\,1,\,0} = (0, 1, 0)$, are the polarization vectors that oscillate orthogonally to w; for three fields: $3 \times 2 = 6$ modes
- Gauge boson-like forces

c) 3 solid longitudinal vector waves (from A^a_μ; a = 4, 5, 6; μ = 0, 1, 2, 3):

Wave equation, Proca-like as in b), but with longitudinal component:

$$\square_{(4)} A^a_\mu - \partial_\mu (\partial^\nu A^a_\nu) + 4\pi^2 m_a^2 \frac{c^2}{h^2} A^a_Z = 0$$

With: z = direction of propagation; it couples to the other components via the Lorentz condition

Dispersion:

$$k^2 = w^2 c^2 + 4\pi^2 m^2 \frac{c^4}{h^2}; \text{ (massive, } v < c) \quad (2.128)$$

Functional shape results in a flat wave in the z-direction:

$$A^a_z(t, z) = A^a_0 [1 + \cos(k_{Uni}\, t)]\, e^{i(wz - kt)}\, \epsilon_z$$

In its real form:

$$A^a_z(t, z) = A^a_0 [1 + \cos(k_{Uni}\, t)] \cos(w_z z - kt)\, \epsilon_z \quad (2.129)$$

- Parallel to w; 1 per field; 3 in total because of a = 4, 5, 6
- Stabilization of compactification through coupling to scalars
- Unit vector: $\epsilon_z^{0,\,0,\,1}$ = (0, 0, 1)

d) 3 massive scalar waves (from ϕ_1, ϕ_2, ϕ_3):

Wave equation (Klein-Gordon equation for massive scalars):

$$\square_{(4)} \phi_n + m_n^2 \phi_n = 0$$

Dispersion:

$$k^2 = w^2 c^2 + 4\pi^2 m_n^2 \frac{c^4}{h^2}; \text{ (massive, } v < c) \quad (2.130)$$

Functional shape results in a flat wave:

$$\phi_n(t, z) = \phi_0 [1 + \cos(k_{Uni}\, t)]\, e^{i(wz - kt)}$$

In its real form:

$$\phi_n(t, z) = \phi_0 [1 + \cos(k_{Uni}\, t)] \cos(w_z z - k_n t) \quad (2.131)$$

- Scalar, isotropic, and longitudinal; n per field; n = 1, 2, 3; coupling to longitudinal vectors for stabilization

Result of the wave equation in FSM as in GTR:

$\bar{h}_{\mu\nu} = 0$; this means for the gravitational wave:

- Propagation at maximum speed $V_{max} = c$
- Transverse and trace-free; only spatial disturbances, no volume change
- Two polarizations have spin-2 field (graviton), acts like a quadrupole
- The mass of an object is modeled in the wave-field. For metric reasons, an **object in the particle-field** is merely a **massless projection**.

Advantages of FSM terms:

- **cos(k_{Uni} t)** – generates dynamic vacuum energy, allowing this term to modulate gravitational waves (oscillating amplitude), explains invisible (including dark) energy waves or variations in propagation, and thus explains possible deviations of GTR waves (e.g., dispersion due to compact dimensions)
- **Scalar terms $V(\phi_n)$:** generate additional scalar waves (spin-0) that couple with gravitational waves. Advantage: FSM may be able to explain multi-messenger signals (e.g., scalar waves that modulate dark energy) and the Higgs mass without fine-tuning (from R – radius of the compact wave-field dimensions).
- **Wave components that arise additionally from the FSM metric carry the inertial and interaction forces, which are ultimately registered in the particle-field. In the particle-field, these act as a projection of their restoring forces in the wave-field. Restoring forces are self-interactions arising from a disturbance caused in the particle-field or in the wave-field. A geometric displacement from their rest position in space-time causes such a disturbance.**

12. The field radius *r*

The field radius r is the spatial scale of action of a relativistic field, which arises from the curvature of space-time.

The starting point is the FSM field equations:

$$R_{MN} - \frac{1}{2} g_{MN} R = \frac{8\pi G}{c^4} T_{MN}$$

Transition to perturbative approximation in weak fields:

$$\partial_\lambda \Gamma^\lambda_{NM} - \partial_N \Gamma^\lambda_{\lambda M} - \frac{1}{2} g^0_{MN} g_0^{PQ} (\partial_\lambda \Gamma^\lambda_{QP} - \partial_Q \Gamma^\lambda_{\lambda P}) = \frac{8\pi G}{c^4} T_{MN}$$

Metric approach for static mass with rotation in FSM:

For a point-like mass M, the metric perturbation is

$$h_{00} = 2\,\frac{G\,M}{c^2\,r}\,, \tag{2.132}$$

while the metric disturbance in the case of rotation is:

$$h_{\mu\nu} = \frac{G\,M}{c^2\,r}\,(1 + \cos(kt + \beta))\,\delta_{\mu i}\,\delta_{\nu j}\ \text{(aus Punkt 1.)}$$

The mean value over the rotation is $<1 + \cos(kt)> = 1$ for $\beta = 0$.

- $h_{\mu\nu}$ – metric perturbation causes weak gravity; μ, $\nu = 0, 1, 2, 3$
- $\frac{G\,M}{c^2\,r}$ – gravitational potential; causes $\frac{1}{r}$ – dependence
- $1+ \cos(kt)$ – modulation causes a dynamic halving; for: $\beta = 0$
- $\delta_{\mu i}\,\delta_{\nu j}$ – Kronecker; specifies the direction of the spatial components; $i, j = 1,2,3$

Insert into the linearized equation for the field radius r :

In a vacuum with $T_{MN} \approx 0$ solves the equation for h_{00} using a Newton approximation:

$$g_{\mu\nu} = \eta_{\mu\nu} + h_{\mu\nu}$$

$$\nabla^2\,h_{00} = 4\pi\,G_\rho$$

$$\nabla^2\,h_{00} = \frac{8\pi G}{c^4}\,\rho \qquad \text{with: } \rho = M\,\delta^3(r)$$

For a point mass, see also point 1:

$$h_{00} = 2\,\frac{G\,M}{c^2\,r} \qquad \text{with the rotation fixed at the point of maximum: } 1 + \cos(kt = 0) = 2$$

In the case of halving by means of rotation in the wave-field:

$$h_{00} = \frac{G\,M}{c^2\,r} \qquad \text{with: } 1 + \cos(kt) = 1 \tag{2.133}$$

- $\nabla^2\,h_{00}$ – Laplace of the metric disturbance; unit: $\frac{1}{m^2}$; potential equation
- ρ – density; unit: $\frac{kg}{m^3}$; for the mass source
- $\delta^3(r)$ – delta function; unit: $\frac{1}{m^3}$; for the point source
- $2\,\frac{G\,M}{c^2\,r}$ – classical solution for the disturbance according Schwarzschild

- $\frac{1}{2}$ – for halving with the average rotation factor

Result for the field radius r :

$$r = \frac{GM}{c^2} \tag{2.134}$$

Implications for black holes:

The effective event horizon for rotating objects is reached at $r = \frac{G\,M}{c^2}$, not at $r_S = \frac{2\,G\,M}{c^2}$**.** This also explains why Kerr-like rotating solutions appear more natural in the FSM. The “half” Schwarzschild radius r_S is a direct consequence of the dynamic rotation of the compact dimensions.

While in classical GTR the field radius $r \rightarrow$ leads to a singularity, the FSM model, with its compact wave-field structure, prevents the dimensions y_4, y_5, y_6 from collapsing. Scalar fields ϕ_n and the oscillation of the compact volume determinant generate a stabilization potential $V(\phi_n)$, which builds up a strong restoring potential at very small radii. The geometric parameter with compact volume radius R never becomes zero, but oscillates periodically. Information is preserved in the compact wave-field dimensions and is never “lost.” Consequently, in FSM there is no singularity at the center of a black hole; instead, it is a highly complex, oscillating wave-field structure.

The local factor $(1 + \cos(kt + \beta))$ generates an oscillating disturbance around the black hole. Consequently, the event horizon “pulsates” by periodically expanding and contracting. This leads to a periodic change in the effective shadow size and the Hawking temperature.

Hawking radiation arises from the oscillation of the horizon metric and its coupling to the scalar fields ϕ_n. It is therefore not purely thermal, but contains an oscillating component (modulated by $(1+ \cos(kt))$.

The global factor $(1 + \cos(k_{Uni}\, t))$ additionally modulates the entire metric periodically. Upon reaching the maximum expansion of the universe with: $(1+ \cos(k_{Uni}\, t = 90°))$, the configuration relative to the dimensional plane D_{56} changes such that no potential can be generated parallel to the fourth dimension. Consequently, structures without gravitational or electric potential dissolve. Black holes dissolve upon reaching the maximum spatial expansion. Information contained within them is subsequently released again.

Taking into account the additional wave properties in the FSM described in point 11, future detectors (LISA, Einstein Telescope) could reveal additional signals or damping modes.

13. The angular frequency *k*

The circular frequency *k* is the invariant clock frequency of the sinusoidal field rotations that drive the dynamics of curvature, particles, and expansion. The circular frequency *k* is thus a characteristic frequency at which a mass *M* causes its own space-time to “oscillate” when viewed as an isolated system.

The starting point is the FSM field equations:

$$R_{MN} - \frac{1}{2} g_{MN} R = \frac{8\pi G}{c^4} T_{MN}$$

Transition to perturbative approximation for weak fields around an object:

$$g_{MN} = [1 + \cos(k_{Uni}\, t)]\, \eta_{MN} + h_{MN} \qquad h_{MN} << 1$$

The local perturbation around the object, in a linear approximation, is:

$$h_{\mu\nu} = \frac{G\,M}{c^2\, r} (1 + \cos(kt + \beta))\, \delta_{\mu\nu} \qquad h_{00} = \frac{G\,M}{c^2\, r} \qquad \text{with: } 1 + \cos(kt) = 1$$

Gravitational potential:

$$g_{00} \approx - c^2 \left(1 - \frac{G\,M}{c^2\, r}\right)$$

$$\boldsymbol{V_{grav}(r) = - \frac{G\,M}{r}}$$

Oscillation potential arising from the compact wave-field dimensions with:

$$E_{kin} = \frac{1}{2} m v^2 = \frac{1}{2} m (kr)^2$$

$$\boldsymbol{V_{rot}(r) = \frac{1}{2} (kr)^2}$$

Effective potential $V(r)_{eff}$:

$$V(r)_{eff} = V_{grav}(r) + V_{rot}(r)$$

$$V(r)_{eff} = - \frac{G\,M}{r} + \frac{1}{2} (kr)^2$$

Condition for the minimum:

$$\frac{dV(r)}{dr} = 0 = - \frac{G\,M}{r^2} + k^2 r$$

$$k = \sqrt{\frac{G\,M}{r^3}} = \frac{c^3}{G\,M} \qquad (2.135)$$

Space-time constant

$k_{Uni} \sim \frac{1}{r_{Uni}}$ A closed spherical universe requires precisely aligned universal constants so that a circular frequency k_{Uni} is exactly inversely proportional to the maximum volume radius R_{Uni} of the universe.

$$r_{Uni}\, k_{Uni} = \frac{G\, M_{Uni}}{c^2} \sqrt{\frac{G\, M_{Uni}}{r_{Uni}^3}} = \sqrt{\frac{(G\, M_{Uni})^3\, (c^2)^3}{(G\, M_{Uni})^3\, (c^2)^2}} = c$$

$$r_{Uni}\, k_{Uni} = r_{obj}\, k_{obj} = \text{constant} = c = 299792458\ \frac{\text{m}}{\text{s}} \qquad (2.136)$$

The **space-time constant** is the product of the field radius r and the angular frequency k of an object.

14. Photon Subspace Theory

Photons are part of the universe's 7-dimensional photon field, which unfolds within the particle-field $F_{1\text{-}3}$ and the wave-field $F_{4\text{-}6}$. Mathematically, multiple 4-dimensional subspaces can exist within a 6-dimensional hollow sphere structure. The photon subspace theory describes photons within the geometry of the invisible wave-field $F_{4\text{-}6}$, where they oscillate as null geodesic waves and resolve the wave-particle duality through sinusoidal rotations.

4-dimensional subspaces in 7D:

The 4-dimensional subspaces each occupy two spatial dimensions in the compact component of the momentum-energy tensor T for the mathematical rotation in the wave-field and the particle-field. For the coupling component, in the visible case—which has a point of contact with the dimensional plane D_{56} —three dimensions correspond to the particle-field and only one dimension to the wave-field. Hidden matter, on the other hand, has only one dimension in the visible particle-field, while three dimensions correspond to the wave-field.

Wave equations for gravity from Point 11:

Transverse wave remains with: $h_{\mu\nu} = 0$ Mass = 0

Transverse vector wave: $\Box_{(4)}\, A^a_\mu - \partial_\mu\, (\partial^\nu\, A^a_\nu) + 4\pi^2\, m_a^2\, \frac{c^2}{h^2}\, A^a_\mu = 0$ massiv

Longitudinal vector wave: $\Box_{(4)}\, A^a_\mu - \partial_\mu\, (\partial^\nu\, A^a_\nu) + 4\pi^2\, m_a^2\, \frac{c^2}{h^2}\, A^a_Z = 0$ massiv

Longitudinal scalar wave: $\square_{(4)}\, \phi_n + m_n^2\, \phi_n = 0$ Masse abhängig Mode n

Dispersion of the transverse wave with angular frequency: $k^2 = w^2\, c^2 + 4\pi^2\, m_a^2\, \frac{c^4}{h^2}$;

unit: $\frac{1}{s}$; w – wavenumber, unit: $\frac{1}{m}$

Metric in the photon subspace, separation between the wave-field and the particle-field:

$$ds^2 = [1 + \cos(k_{Uni}\, t)]\, [-\, c^2\, dt^2 + g_{ij}\, dx^i\, dx^j + \gamma_{pq}\, dy^p\, dy^q + 2(A_\mu^a + \delta A_\mu^a)\, dy_a\, dx^\mu] \quad (2.137)$$

$g_{ij} = \eta_{ij} + h_{ij} = \eta_{ij} + \frac{GM}{c^2 r}\,(1 + \cos(kt + \beta))$ → visible metric component for local

$\gamma_{pq} = \eta_{pq}$ → compact metric component for local

- Indices: i, j for 2D visible dimensions i, j = 1, 2, 3; p, q for the compact wave-field component in 2D; p, q = 4, 5, 6; however, depending on the linking scenario, only two dimensions are activated at a time
- ds^2 – invariant line element; unit: m²; measures distances in 4D space-time
- $-\, c^2\, dt^2$ – time term; unit: m²; causes causality; c – maximum speed
- g_{ij} – metric in the visible particle-field; results in a 2D visible portion
- $dx^i\, dx^j$ – displacement in the visible region due to coupling between wave-fields $F_{4\text{-}6}$ and particle-fields $F_{1\text{-}3}$; unit: m²; transverse component
- γ_{pq} – metric in the wave-field; produces a 2D wave component
- $dy^p\, dy^q$ – displacement in the compact region; unit: m²; longitudinal component

Summary of the distribution of dimensions:

- Visible particles: max. 3D in the particle-field; max. 2D in the wave-field
  $D_{14/24/34}$; effect of the transverse wave
- Invisible particles: max. 3D in the wave-field, max. 2D in the particle-field
  $D_{16/26/36}$; effect of the longitudinal wave
- Photon-compact component: 2D in the wave-field, 2D in the particle-field
  $D_{45/46/56}$; effect of the longitudinal wave
  Photon coupling component:
  Interaction in D_{56}: 1D in the wave-field, 3D in the particle-field (visible interaction)
- Not in contact with D_{56}: 3D wave-field, 1D particle-field (“dark matter” or hidden matter)

Correlation of the waveform with the field propagation speeds V_5 and V_4:

$V_4 = V_{long} = c\, \cos(kt)$ $V_5 = V_{trans} = c\, \sin(kt)$ $c^2 = V_5^2 + V_4^2$

- ***V₄*** – field propagation speed; unit: $\frac{m}{s}$
  - **Longitudinal disturbance component;** orthogonal to/relative to the dimensional plane D_{56}
  - Generates the **field** (directional component) and represents the disturbance acting on the visible field deformation.
  - Upon contact with D_{56}, V_4 is **minimal**. A photon couples maximally with the particle-field. A periodic **matter pulse** (**Chapter 3.2**) is generated between the wave-field and the particle-field, corresponding to the amplitude of their field exchange. A discrete particle is detected.
- ***V₅*** – field propagation speed; unit: $\frac{m}{s}$
  - **Transverse, visible field deformation**; parallel to the dimensional plane D_{56}
  - Measures the **visible intensity** of the photon in the particle-field
  - When D_{56} is touched, V_5 is at its **maximum**. Acts like a **field-body oscillation** in the particle-field
  - **A photon** is always emitted when the transverse field deformation reaches its maximum.
- cos(*kt*) or sin(*kt*) – The phases cause the transition between visible and invisible matter.

The incorporation of both field propagation speeds into the wave-field resolves the wave-particle duality and explains dark matter as “false” recombination. The photon mass breaks U(1) symmetry. Photons are no longer massless and no longer have infinite range.

Geometrically dependent mass with its amplitude and as a periodic disturbance:

$$m_{pho} = \frac{n\,h}{2\pi\,c\,R_{pho}}$$

$$m_{pho}(t) = \frac{n\,h}{2\pi\,c\,R_{pho}}\cos(kt + \beta) \qquad (2.138)$$

The modes *n* are taken into account in the frequency calculation of an object and give rise to mass classes (in the form of generations) that exhibit small jumps in excitation frequencies between groups. Furthermore, the complexity of their particle structure increases continuously.

Zero-geodesic photon motion: local and global:

Photons with $f > f_{min}$ follow d*s* in the subspace of complementary dimensions:

Global d*s* ≈ 0:

$$0 \approx -c^2dt^2 + g_{ij}\,dx^j\,dx^j + \gamma_{pq}\,dy^p\,dy^q + 2(A^a_\mu + \delta A^a_\mu)\,dy_a\,dx^\mu$$

Local ds = 0:

$$0 = - c^2 dt^2 + g_{ij}\, dx^j\, dx^j + \gamma_{pq}\, dy^p\, dy^q + 2(A_\mu^a + \delta A_\mu^a)\, dy_a\, dx^\mu$$

Field equation in a subspace:

In the weak-field approximation, the Einstein equations are reduced to the wave equations after trace elimination and the adoption of a harmonic gauge:

$$\text{a) } R_{ij} - \frac{1}{2}\, g_{ij}\, R = \frac{8\pi G}{c^4}\, T_{ij} \qquad (2.139)$$

$$\text{b) } R_{pq} - \frac{1}{2}\, \gamma_{pq}\, R = \frac{8\pi G}{c^4}\, T_{pq} \qquad (2.140)$$

- T_{ij} ~ transverse tensor (visible)
- T_{pq} ~ longitudinal tensor (compact)
- R_{ij} or R_{pq} – Ricci tensor; unit: $\frac{1}{m^2}$; causes curvature in the respective section
- R – The Ricci scalar is the total trace of the Ricci tensor over the entire metric of the photon subspace
- T_{ij} or T_{pq} – momentum-energy tensor; unit: $\frac{kg}{m\ s^2} = \frac{J}{m^3}$; generates energy from waves

With:

$$R_{MN} = \frac{1}{2}\, (\partial_P\, \partial_M\, h_N^P + \partial_P\, \partial_N\, h_M^P - \partial_P\, \partial^P\, h_{MN} - \partial_M\, \partial_N\, h_P^P) + R_{MN}^{(global)}$$

$$R_{MN}^{(global)} = \frac{1}{2}\, \eta^{\lambda P}\, (\partial_M\, [\cos(k_{Uni}\, t)]\, \eta_{NP} + \partial_N\, [\cos(k_{Uni}\, t)]\, \eta_{MP} - \partial_P\, [\cos(k_{Uni}\, t)]\, \eta_{MN})$$

$$R_{ij}^{(global)} \approx - \frac{1}{2}\, k_{Uni}^2\, \cos(k_{Uni}\, t)\, \delta_{ij} \quad \text{and} \quad R_{pq}^{(global)} \approx - \frac{1}{2}\, k_{Uni}^2\, \cos(k_{Uni}\, t)\, \delta_{pq}$$

$$R_{ij} \approx \frac{1}{2}\, (\partial_k\, \partial_i\, h_j^k + \partial_k\, \partial_j\, h_i^k - \partial_k\, \partial^k\, h_{ij} - \partial_i\, \partial_j\, h_k^k) + R_{ij}^{(global)} \qquad \text{indices: } i, j, k = 1, 2, 3$$

$$- \partial_k\, \partial^k\, h_{ij} = \square_{(4)}\, \bar{h}_{ij} = 2\, R_{ij}^{(global)} = - k_{Uni}^2\, \cos(k_{Uni}\, t)\, \delta_{ij}$$

$$\boldsymbol{R_{ij} \approx - k_{Uni}^2\, \cos(k_{Uni}\, t)\, \delta_{ij}}$$

$$R_{pq} \approx \frac{1}{2}\, (\partial_r\, \partial_p\, \bar{h}_q^r + \partial_r\, \partial_q\, \bar{h}_p^r - \partial_r\, \partial^r\, \bar{h}_{pq} - \partial_q\, \partial_q\, \bar{h}_r^r) + R_{pq}^{(global)} \qquad \text{indices: } r, q, p = 4, 5, 6$$

$$- \partial_r\, \partial^r\, \bar{h}_{pq} = \square_{(4)}\, \bar{h}_{pq} = 2\, R_{pq}^{(global)} = - k_{Uni}^2\, \cos(k_{Uni}\, t)\, \delta_{pq}$$

$$\boldsymbol{R_{pq} \approx - k_{Uni}^2\, \cos(k_{Uni}\, t)\, \delta_{pq}}$$

$$R = g^{ij} R_{ij} + \gamma^{pq} R_{pq}$$

The field equations describe visible and hidden components of matter as complementary curvatures. Together, these two components generate the complete 7-dimensional curvature. It is shown that photons are locally null-geometric entities, as in general relativity, but globally follow a universal deviation.

15. Group Theory for FSM

The group theory of the FSM classifies the symmetries of rotations in the compact dimensions of the wave-field $F_{4\text{-}6}$ in order, among other things, to explain the strong force as an SU(3) symmetry arising from rotations in the dimensional planes $D_{45/46/56}$. Furthermore, the particle spin modes arising from the internal rotation of multiple fions in the bundle are to be classified as symmetry classes (e.g., SO(3)), and the modes are to be classified topologically. In doing so, both trivial and complex topologies with invariants for stability are addressed. From the FSM arise the groups derived from the geometry of cavity oscillations with their rotational representation

The strong interaction (strong force) resulting from the rotations parallel to $D_{45/46/56}$:

The 3-dimensional space in the wave-field with D_a has the indices: a = 4, 5, 6. The strong force is generated in this space. The strong force arises from the binding of quarks as fion bundles with other quarks. Exchange fions are the carriers and initiators of field exchange between quarks. The field exchange via exchange fions and the oscillation of quarks are explained by rotations between them. The metric component γ_{ab} in D_a has an SO(3) symmetry with a rotation group in $D_{45/46/56}$, but due to the fion rotations of multiple fions in the bundle, it becomes SU(3), which forms a special unitary group.

The rotation tensor ω_{ab} describes the symmetry of the internal rotations of the fibers in the bundle. For N = 3, it describes the strong force as an SU(3) symmetry.

Metrics in the compact wave-field:

$$\gamma_{ab} = \delta_{ab}$$

An infinitesimal rotation in the compact dimensions transforms the coordinates as follows:

$$y^a + \delta y^a = y^a + \omega^a_b \, y^b$$

The rotation tensor is antisymmetric:

$$\omega_{ab} = - \omega_{ba}$$

The compact metric γ_{ab} transforms as a (0, 2) tensor:

$\delta\gamma_{ab} = \partial_a(\delta y^c)\ \gamma_{cb} + \partial_b(\delta y^c)\ \gamma_{ac}$ with: $\partial_a(\delta y^c) = \omega_a^c$ results:

$\delta\gamma_{ab} = \omega_a^c\ \gamma_{cb} + \omega_b^c\ \gamma_{ac}$

- ω_b^a – Rotation tensor, antisymmetric; generator of the rotation; generates the invariance; dimensionless, because: $\partial_a(\delta y^c)$
- $y_a = R\cos(kt + \beta)$

An infinitesimal rotation in the compact dimensions causes a change in the metric. Using the subscripts and the relation $\gamma_{ab} = \delta_{ab}$, this leads to:

$\delta\gamma_{ab} = \omega_{ac}\ \gamma_b^c + \omega_{bc}\ \gamma_c^a$ → **general transformation formula** (2.141)

Applying the flat metric $\gamma_{ab} = \delta_{ab}$:

$\delta\gamma_{ab} = \omega_{ab} + \omega_{ba}$, because $\delta\gamma_{ab}$ is **antisymmetric**:

$\delta\gamma_{ab} = \omega_{ab} + (-\omega_{ba}) = 0$ → the **metric** γ_{ab} remains **invariant** under rotation.

General form of the rotation tensor depending on the symmetry class N:

$$\omega_{ab}^{(N)} = \sum_{m=1}^{N}\ \Phi_m\ (G_m)_{ab}\cos(kt + \beta) \qquad (2.142)$$

- $\omega_{ab}^{(N)}$ – rotation tensor; describes the symmetry of the internal rotations of the fibers in the bundle
- G_m – generators of the Lie algebra of the group SO(N) or SU(N) with compact indices: a, b, c = 4, 5, 6; dimensionless
- Φ_m – infinitesimal angle of rotation; forms the general SU(3) transformation; dimensionless
- $\cos(kt + \beta)$ – disturbance component derived from the wave-field dimensions
- (kt) – phase angle, finite, for real oscillations of compact dimensions

- Field exchange between the wave field and the particle-field at $kt = 0$ under:
  Strong interaction: $kt = 0$; $\beta = 0$
  Weak interaction: $kt = 0$; $90° > \beta > 0$
  No interaction: $kt = 0$; $\beta = 90°$

The group SU(N) is the group of all unitary $N \times N$-matrices with determinant 1. The corresponding Lie algebra su(N) has dimensions.

a) Generators - classic:

$\text{Dim}(\text{su}(N)) = N^2 - 1 = 3^2 - 1 = 8$ → 8 generators

The rotation tensor is defined by the sum over the eight independent generators λ_m.

$$\omega_{ab}^{(3)} = \sum_{m=1}^{8} \Phi_m (\lambda_m)_{ab} \cos(kt + \beta) \quad (2.143)$$

- $\omega_{ab}^{(3)}$ – explained for $N = 3$ the SU(3)-symmetry with the strong force
- λ_m – Gell-Mann matrices that are exactly hermitian and trace-free; 3×3-matrices; spans the Lie algebra su(3)

b) Generators – FSM:

The geometry of the FSM provides a 6-dimensional field-space. According to the photon subspace theory (point 14), this space contains several 4-dimensional rotational orbits. Between particle-field $F_{1\text{-}3}$ and wave-field $F_{4\text{-}6}$, there is a total of 15 such rotational paths. **Table 3.1** in **Chapter 3.2** shows the possible dimensions spanned.

This results in su(4) with 15 generators:

$4^2 - 1 = 15$

The rotation tensor is calculated by summing over the 15 independent generators G_m.

$$\omega_{ab}^{(4)} = \sum_{m=1}^{15} \Phi_m (G_m)_{ab} \cos(kt + \beta) \quad (2.144)$$

With: $G_m = (J_{pq})_{ij} = \delta_{ip}\,\delta_{jp} - \delta_{iq}\,\delta_{jp}$

- +1 in position (p, q)
- -1 in position (q, p)
- all other entries are zero
- G_m – generators

The generators are 4 × 4 Hermitian, trace-free matrices. This form represents the complex Lie algebra (su(4)). Each matrix is antisymmetric and has only two nonzero entries. G_1 through G_8 (pairs within $D_{1\text{-}3}$ and $D_{4\text{-}6}$, respectively) correspond to the embedded SU(3) generators. G_9 through G_{15} are mixed generators and contain the connections between the visible $D_{1\text{-}3}$ and compact $D_{4\text{-}6}$, as well as exclusively the compact dimensions $D_{4\text{-}6}$.

Strong force:

$$G_m = \begin{pmatrix} \lambda_m & 0_{3x1} \\ 0_{1x3} & 0 \end{pmatrix}, \; m = 1,\ldots, 8 \quad (2.145)$$

$G_1 = J_{1,2}$ (Rotation in a plane 1-2)

$$G_1 = \begin{pmatrix} 0 & 1 & 0 & 0 \\ 1 & 0 & 0 & 0 \\ 0 & 0 & 0 & 0 \\ 0 & 0 & 0 & 0 \end{pmatrix}$$

$G_2 = J_{1,3}$ (Rotation in a plane 1-3)

$$G_2 = \begin{pmatrix} 0 & -i & 0 & 0 \\ i & 0 & 0 & 0 \\ 0 & 0 & 0 & 0 \\ 0 & 0 & 0 & 0 \end{pmatrix}$$

$G_3 = J_{1,4}$ (Rotation in a plane 1-4)

$$G_3 = \begin{pmatrix} 1 & 0 & 0 & 0 \\ 0 & -1 & 0 & 0 \\ 0 & 0 & 0 & 0 \\ 0 & 0 & 0 & 0 \end{pmatrix}$$

$G_4 = J_{1,5}$ (Rotation in a plane 1-5)

$$G_4 = \begin{pmatrix} 0 & 0 & 1 & 0 \\ 0 & 0 & 0 & 0 \\ 1 & 0 & 0 & 0 \\ 0 & 0 & 0 & 0 \end{pmatrix}$$

$G_5 = J_{1,6}$ (Rotation in a plane 1-6)

$$G_5 = \begin{pmatrix} 0 & 0 & -i & 0 \\ 0 & 0 & 0 & 0 \\ i & 0 & 0 & 0 \\ 0 & 0 & 0 & 0 \end{pmatrix}$$

$G_6 = J_{2,3}$ (Rotation in a plane 2-3)

$$G_6 = \begin{pmatrix} 0 & 0 & 0 & 0 \\ 0 & 0 & 1 & 0 \\ 0 & 1 & 0 & 0 \\ 0 & 0 & 0 & 0 \end{pmatrix}$$

$G_7 = J_{2,4}$ (Rotation in a plane 2-4)

$$G_7 = \begin{pmatrix} 0 & 0 & 0 & 0 \\ 0 & 0 & -i & 0 \\ 0 & i & 0 & 0 \\ 0 & 0 & 0 & 0 \end{pmatrix}$$

$G_8 = J_{2,5}$ (Rotation in a plane 2-5)

$$G_8 = \frac{1}{\sqrt{3}} \begin{pmatrix} 1 & 0 & 0 & 0 \\ 0 & 1 & 0 & 0 \\ 0 & 0 & -2 & 0 \\ 0 & 0 & 0 & 0 \end{pmatrix}$$

Weak force and invisible (dark) matter:

$$T^k_{real} = \frac{1}{\sqrt{2}} \begin{pmatrix} 0_{3x3} & e_k \\ e_k^T & 0 \end{pmatrix} \qquad k = 1, 2, 3 \qquad T^k_{imag} = \frac{i}{\sqrt{2}} \begin{pmatrix} 0_{3x3} & -e_k \\ e_k^T & 0 \end{pmatrix} \qquad (2.146)$$

$G_9 = J_{2,6}$ (Rotation in a plane 2-6)

$$G_9 = \frac{1}{\sqrt{2}} \begin{pmatrix} 0 & 0 & 0 & 1 \\ 0 & 0 & 0 & 0 \\ 0 & 0 & 0 & 0 \\ 1 & 0 & 0 & 0 \end{pmatrix}$$

$G_{10} = J_{3,4}$ (Rotation in a plane 3-4)

$$G_{10} = \frac{i}{\sqrt{2}} \begin{pmatrix} 0 & 0 & 0 & -1 \\ 0 & 0 & 0 & 0 \\ 0 & 0 & 0 & 0 \\ 1 & 0 & 0 & 0 \end{pmatrix}$$

$G_{11} = J_{3,5}$ (Rotation in a plane 3-5)

$$G_{11} = \frac{1}{\sqrt{2}} \begin{pmatrix} 0 & 0 & 0 & 0 \\ 0 & 0 & 0 & 1 \\ 0 & 0 & 0 & 0 \\ 0 & 1 & 0 & 0 \end{pmatrix}$$

$G_{12} = J_{3,6}$ (Rotation in a plane 3-6)

$$G_{12} = \frac{i}{\sqrt{2}} \begin{pmatrix} 0 & 0 & 0 & 0 \\ 0 & 0 & 0 & -1 \\ 0 & 0 & 0 & 0 \\ 0 & 1 & 0 & 0 \end{pmatrix}$$

$G_{13} = J_{4,5}$ (Rotation in a plane 4-5)

$$G_{13} = \frac{1}{\sqrt{2}} \begin{pmatrix} 0 & 0 & 0 & 0 \\ 0 & 0 & 0 & 0 \\ 0 & 0 & 0 & 1 \\ 0 & 0 & 1 & 0 \end{pmatrix}$$

$G_{14} = J_{4,6}$ (Rotation in a plane 4-6)

$$G_{14} = \frac{i}{\sqrt{2}} \begin{pmatrix} 0 & 0 & 0 & 0 \\ 0 & 0 & 0 & 0 \\ 0 & 0 & 0 & -1 \\ 0 & 0 & 1 & 0 \end{pmatrix}$$

Electromagnetic force:

$G_{15} = J_{5,6}$ (Rotation in a plane 5-6)

$$G_{15} = \frac{1}{\sqrt{6}} \begin{pmatrix} 1 & 0 & 0 & 0 \\ 0 & 1 & 0 & 0 \\ 0 & 0 & 1 & 0 \\ 0 & 0 & 0 & -3 \end{pmatrix}$$ → 15. The generator is the remaining U(1) freedom. It explains U(1) as an emergent Abelian symmetry arising from 7-dimensional geometry and the gauge potential. In the FSM, it plays the role of the electromagnetic force.

SU(4) describes the full symmetry of all rotational orbits and contains SU(3) as a natural subgroup. The breaking of

SU(4) → SU(3) × U(1)

contains exactly 9 unbroken generators (8 from SU(3) + 1 from U(1)). The remaining 6 mixed generators, G_9 through G_{14}, are either completely or significantly weakened by the breaking mechanism. These generators mediate the coupling between the visible SU(3) block and the hidden part of the block. The breaking mechanism is geometric-dynamic and is modeled by the oscillating metric factor $\cos(kt + \beta)$.

This yields the phase angle β and naturally explains the separation of strong (visible) and weak/invisible (invisible, dark matter) forces, as well as the electric force.

- $\beta = 0$ and $\cos(kt + \beta) = 1$: perfect representation of the field exchange on the D_{56} dimensional level; results in full SU(4) symmetry → maximum strong force
- $\beta \neq 0$ or $\cos(kt + \beta) < 1$: mixed generators G_9 through G_{14} are modulated; this results in a violation of symmetry → weak force and transition to dark matter
- The refraction is natural and avoids the need for an additional Higgs mechanism.

Maximum number of N_{aF} for the 6-dimensional field space and projection:

The field-space is 6-dimensional and allows for 5 × 4-dimensional subspaces, which may have an overlap zone with their rotation paths at a single point. Accordingly, a bundle can contain only 5 active fions.

All five active fions generate a potential in the wave-field, although only three of them convey a partial charge with respect to the dimensional planes $D_{14/24/34}$. In the

visible particle-field $F_{1\text{-}3}$, only the projection of the rotations onto the dimensional planes $D_{14/24/34}$ is registered. The rotations in the wave-field $F_{4\text{-}6}$ on the planes $D_{45/46/56}$ are invisible.

Resulting angular momentum L and projected spin:

The resulting **total angular momentum** is the sum of all fions involved in a bundle. This includes all active N_{aF} fions (up to 5 due to the 6-dimensional spatial geometry) and any temporary external N_{eF} that may be received.

$$L_{N\,fions}{}^2 = \sum_0^N \left(\frac{h}{4\pi}\right)^2_N \qquad \text{with: } N = N_{aF} + N_{eF} \qquad (2.147)$$

- L – angular momentum; unit: $\frac{\text{kg m}^2}{\text{s}}$
- N_{aF} – number of active fions in the bundle
- N_{eF} – number of external fions received temporarily

Spin is not an intrinsic property of the "particle" itself, but rather the geometric result of the rotations of the constituent fions in 6-dimensional field-space. The observed spin-½ fermions and spin-1 bosons arise inevitably from the number and binding configuration of the fions in the bundle.

In FSM, the quantization of spin is explained purely geometrically and follows directly from the 15 rotation generators of the compact dimensions. The total spin arises from the rotation of multiple fions in the bundle. These can consist of the number of internal bundle fions N_{aF} and additional (temporarily limited) connections of external fions N_{eF}, whereby only the SO(N) symmetry is registered, which reduces to SO(3) for the spin in the wave field $F_{4\text{-}6}$. The formula for the spin from rotations is:

$$S = \frac{1}{2}\,\frac{h}{2\pi}\,(N_{aF} + N_{eF})$$

$$S = \frac{h}{4\pi}\,(N_{aF} + N_{eF}) \qquad (2.148)$$

- S – spin; normalized to $\frac{h}{2\pi}$; dimensionless; determines intrinsic angular momentum; half-integer with $S = \frac{1}{2}$ for fermions, integer with S = 1 for bosons
- $\frac{1}{2}$ – Factor; accounts for the half-integer nature of the rotational speed $V_{Rot} = c$ by setting the maximum speed to $\frac{c}{2}$ for the single active fion as an internal fion within the bundle; prevents a variance > c in case of deviation; the fastest repetition of the period generates the next multiple with $\frac{c}{2}$
- $\frac{h}{2\pi}$ – reduced Planck constant; unit: Js; determines the quantum scale

- N_{aF} – number of fions in the bundle; N_{aF} ε N; dimensionless; determines the symmetry class; N_{aF} = 1 leads to spin $\frac{1}{2}$, N_{aF} = 2 leads to spin 1, N_{aF} = 3 leads to spin $\frac{1}{2}$, etc.

Examples of the electromagnetic and strong interactions:

The electron is the basic unit of **electrical interaction**. Electrical interaction occurs when an electron receives an external fion $f > f_{min}$ and uses it to exchange energy with another electron that also possesses an external fion. The total angular momentum results from the four individual angular momenta, each of which has a rotational velocity of $\frac{c}{2}$. In this case, the electron's spin is briefly bosonic (S = 1) for the duration of the interaction. The external fion is registered in the particle-field solely as an electric force. After the external fion is released, only the projection of the three active fions with effective spin S = $\frac{1}{2}$ remains in the particle-field.

In the case of the **strong interaction**, the electron also briefly possesses an externally received fion. The electron once again acquires four angular momentum components from N_{aF} and N_{eF}. As a result, the total spin temporarily becomes an integer again. This state triggers an interaction. In this case, the electron with $3\frac{1}{3}e^-$ reduces to $2\frac{1}{3}e^-$ to a 2/3 quark by splitting an active fion from the internal bundle into an exchange fion and a passive fion. The mechanics are explained in **Chapter 3.2**. The quark exists only because it forms a boson together with an exchange fion. The quark within it is, in this case, a $2\frac{1}{3}e^-$ electron in the wave-field. Exchange fions mediate the strong interaction. The total spin in the particle-field becomes a spin $S = \frac{1}{2}$ because, in the projection of the bundle, only 2 active fions and the external fion, each with spin $\frac{1}{2}$, remain.

In the case of a 1/3 quark, it interacts with another particle that may belong to the category of invisible (dark) matter.

The projection of a fermion onto the $D_{14/24/34}$ dimensions is always associated with spin $S = \pm\frac{1}{2}$. In the case of mesons, which consist of two fermions, the spin is $S = \pm\frac{1}{2} \pm \frac{1}{2}$. And in the case of baryons, which consist of three fermions, the spin is e.g. 3 $S = \pm\frac{1}{2} \pm \frac{1}{2} \pm \frac{1}{2}$.

Charge and potential from recombination in a bundle:

Using the potential from a bundle of bound fions

$$A^{a}_{eff,\,0} = \frac{Q}{4\pi\,\epsilon_0\,R}\,\cos(kt + \beta)\,\delta^{a}_{4}\,\delta^{0}_{\mu}\,\frac{c}{V_5} \qquad \text{with: } D_{56} \text{ – plane, } a = 6 \qquad (2.69)$$

the charge Q results from the position relative to the D_{56} (positive above, negative below). Although the invisible compact rotational orbits rotate asymmetrically parallel to the fourth dimension against the electrical potential of the universe, they possess only a periodically increasing and decreasing potential, which goes unnoticed by the particle-field. This applies to the rotational orbits along the dimensional planes $D_{45/46/56}$. The visible component acts differently. Only the visible components can impart a charge in the particle field $F_{1\text{-}3}$. This is because they immediately exchange their field within the dimensional planes $D_{14/24/34}$ as soon as the point of contact in the dimensional plane D_{56} is reached. Consequently, there can only be three partial charges, independent of particle complexity, which exists within the dimensional planes $D_{14/24/34}$. Other active fions that cross the dimensional plane D_{56} do not convey a partial charge due to their geometric position. However, they contribute to the total mass by having their share not only divided into thirds, but also into quarters or fifths.

Fundamental potential in the wave-field from a 4-dimensional perspective:

$$\phi = \frac{\pm Q}{4\pi\, \epsilon_0\, R} \cos(kt + \beta)$$

- ϕ – potential; unit: V; results from the reduction gradient
- Q – charge; unit: C; causes the strength; $\pm e$ from a position above or below the dimension plane D_{56}
- $4\pi\, \epsilon_0$ – constant; unit: $\frac{F}{m}$; results in Coulomb scaling
- R – radius; unit: m; creates distance
- $\cos(kt + \beta)$ – oscillation; creates the dynamic

The oscillating potential thus averages out to zero. However, the amplitude (maximum value) remains unchanged, which imparts an effective charge to the particle-field $F_{1\text{-}3}$ for active fions with the rotational orbits $D_{14/24/34}$.

$\cos(kt)_{amplitude} \rightarrow 1$ (acts effectively as a Q charge in 4D)

Static result:

$$\phi = \frac{\pm Q}{4\pi\, \epsilon_0\, R} \tag{2.149}$$

Total load divided into partial charges according to the active fions:

$$Q = \frac{e}{3} \sum_{i=1}^{3} \delta_{i,\text{coupling}} = N_{aF} \frac{e}{3} \qquad N_{aF}\ \varepsilon\ \mathbb{N} \tag{2.150}$$

- Q – electric charge with $[Q]$ = As = C
- e – electric charge of the elementary particle electron
- e = 1,6022 10^{-19} C
- N_{aF} – number of active fions in the dimensional planes $D_{14/24/34}$, at most 3

Note: When incorporating the compact dimensional planes $D_{45/46/56}$ into the shaft field, there is a limit of 5 possible rotational paths.

Quark charge:

Quark types arise from an original electron structure with varying numbers of active fions. Quarks never exist as individual particles on their own. In the FSM, they are part of a boson, which consists of a quark and its exchange particle. The exchange fion is created by the reduction of an active fion in the electron, which carries a partial charge in the particle-field. The sign is determined by the configuration in the D_{56} dimensional plane, indicating whether the rotation occurs above or below.

$$Q = \pm(3 - N_{F/A})\,\frac{e}{3} \tag{2.151}$$

- $\frac{e}{3}$ – one-third of the base charge; unit: C; one-third of the 3D wave-field (SU(3)) symmetry, implicitly
- $N_{F/A}$ – Number of active fions resulting from conversion to exchange fions/passive fions, or those that do not generate a potential in the wave-field relative to the dimensional plane D_{56}

Equation (2.151) explains fractional charge geometrically in relation to D_{56}.

Possible elementary charges:

Electron: $Q = -(3 - 0)\,\frac{e}{3} = -e$

Positron: $Q = +(3 - 0)\,\frac{e}{3} = +e$

Neutrino: $Q = \pm(3 - 3)\,\frac{e}{3} = 0$

u/d-Quarks: $Q = \pm(3 - 1)\,\frac{e}{3} = \pm\frac{2}{3}e$

u/d-Quarks: $Q = \pm(3 - 2)\,\frac{e}{3} = \pm\frac{1}{3}e$

C-Quarks: $Q = \pm(3 - 1)\,\frac{e}{3} = \pm\frac{2}{3}e$

C-Quarks: $Q = \pm(3 - 2)\,\frac{e}{3} = \pm\frac{1}{3}e$ (hypothetically possible)

S-Quark: $Q = \pm(3 - 2)\,\frac{e}{3} = \pm\frac{1}{3}e$

S-Quark: $Q = \pm (3 - 1) \frac{e}{3} = \pm \frac{2}{3}e$ (hypothetically possible)

B-Quark: $Q = \pm (3 - 2) \frac{e}{3} = \pm \frac{1}{3}e$

B-Quark: $Q = \pm (3 - 1) \frac{e}{3} = \pm \frac{2}{3}e$ (hypothetically possible)

T-Quark: $Q = \pm (3 - 2) \frac{e}{3} = \pm \frac{1}{3}e$ (hypothetically possible)

T-Quark: $Q = \pm (3 - 1) \frac{e}{3} = \pm \frac{2}{3}e$ (hypothetically possible)

Trivial and complex topology for mode classification:

Topology determines whether modes (such as particle states) remain stable or decay. In the FSM, the compact wave-field dimensions D_4, D_5, D_6 are topologically structured. Modes (Fourier expansion $e^{\frac{iny^a}{R}}$ are stable oscillations whose stability depends on the topology of the compact manifold:

- Trivial topology: simple, stable modes (*n* is an integer, no holes); z.B. S^1 = circle
- Complex topology: greater stability due to holes/genus, but potential instability at high complexity; e.g. T^3 = 3-torus (Calabi-Yau)

First invariant *n* - number of turns:

The simplest topological classification is the winding number *n* derived from the Fourier expansion of the modes.

$\phi(x, y) = \sum_n \phi_n(x) e^{\frac{iny^a}{R}}$ with: $-\infty < n < \infty$

Real equivalent:

$\phi(x, y) = \sum_{n=1}^{3} \phi_n(x) \cos(\frac{ny^a}{R})$ with: n = 1, 2, 3

n is a topological invariant for the number of windings around the compact dimensions. $n = 0$ for the constant mode (hypothetically massless). $n \neq 0$ for massive modes ($m \sim \frac{n}{R}$). This is expressed in **Chapter 3.5** as a “family of dimensions”.

Second invariant χ – Euler characteristic:

χ classifies stability. The general topological classification uses the Euler characteristic χ.

$X = 2 - 2g$

- X – Euler characteristic; dimensionless; yields topological invariants
  $X = V – E + F$
  V – vertices
  E – edges
  F – areas in triangulation
  - $X = 2$ for ball S^2 (stable but not compact in FSM)
  - $X = 0$ for torus T^2 (trivial, stable for photons)
  - $X < 0$ for higher-order functions (complex, instability possible)
- g – genus; g ε N; dimensionless; determines the number of holes in the compact manifold
  - g = 0 for S^2
  - g = 1 for T^2
- General:
  $X = 0$; trivial, for stable modes (photons, stable visible particles)
  $X \leq 0$, $g \geq 1$; complex, for unstable or hidden (dark) modes, or greater stability through holes/genus

Classification:

- The maximum number of active fions in a bundle is 5, due to the 6-dimensional nature of the field-space.
- Trivial topology:
  - S^1 (Circle); g = 0; $X = 2 - 2 \cdot 0$; but often in FSM $X = 0$ for an effective torus
  - n – an integer
  - Stable visible modes: photons, light fermions with $n = 0$, stable particles
- Complex topology:
  - T^3 (3-torus); g = 1 per dimension; $X = 0$; invariants such as the Chern class $c_1 = 0$
  - Stable modes: invisible massive modes (dark matter)
  - Calabi-Yau (complex 3-manifold); $X = -200$ for typical sextics; invariants c_2, c_3
    Stable modes: higher generations (C-, B-, and T-quarks); stability via $V(\phi_n)$ and metric oscillation $\cos(kt + \beta)$
  - The dimension reduction factor (DimFactor) – **Chapter 3.5** – applies to complex bundles with five fions, e.g., B-quarks, in order to keep their resulting rotational velocity at $V_{Rot} \leq c$.
- Additional classifications:
  - Homotopy groups for T3 (coefficient of winding)
  - Chern classes c_1, c_2, c_3 for complex manifolds
  - Stability through $V(\phi)$; stability through R

Trivial stable modes correspond to visible particles, while complex modes correspond to hidden (dark) matter and higher generations.

16. Chern classification in FSM

The Chern classification is a topological invariant for complex manifolds in the compact wave-field dimensions $D_{4\text{-}6}$. It serves as a mathematical “proof” of correctness, as it provides a geometric justification for anomaly-free properties, the number of generations, and interactions. It shows that 3-dimensional wave-field geometry enforces the observed symmetries (e.g., three generators, anomaly-free) without resorting to supersymmetry. The derivation follows from compactification and the metric, with the Chern classes serving as invariants for stability and anomalies. More precisely, the Chern classes c_k (k = 1, 2, 3) are cohomological invariants for vector bundles over complex manifolds, which in the FSM prove the stability of the modes (n = 1, 2, 3) and anomaly-free nature.

General formula for Chern classes:

$$c_k(E) = \det(1 + \frac{\mathrm{i}}{2\pi} F) = \frac{1}{k!} (\frac{\mathrm{i}}{2\pi})^k \mathrm{Tr}\,(F)^k \qquad (2.152)$$

- $c_k(E)$ – k-th Chern class of the vector bundle E; dimensionless; defines invariants for the bundle topology; k corresponds to the rank of the wave-field, where k = 1, 2, 3; E – tangent bundle of the manifold
- $\frac{1}{k!}$ – factor from the determinant expansion
- $(2\pi)^k$ – normalization; dimensionless; induces a cohomology class in $H^{2k}(M, \mathrm{Z})$; Z – the set of integers
- i – symbol for an imaginary form; provides a hermetic and real trace, which is crucial for the physical interpretation
- Tr – trace; dimensionless; causes contraction via indices
- F – curvature form (2-form); unit: $\frac{1}{\mathrm{m}^2}$; results in a field strength of A^a_μ
- $(\frac{F}{2\pi})^k$ – power; unit: $(\frac{1}{\mathrm{m}^2})^k$; results in higher moments of curvature

Chern class c_1 :

The first Chern class is defined as:

$$c_1(E) = \frac{\mathrm{i}}{2\pi} \mathrm{Tr}\, F$$

where the Chern classes arise from the curvature:

$F = \mathrm{d}A + \mathrm{A} \wedge \mathrm{A}$ (aus A^a_μ)

The field strength F corresponds exactly to the Chern curvature of the gauge bundle:

$F^a = dA^a + f^{abc} A^b \wedge A^c$

- f^{abc} – totally antisymmetric structure constants of the Lie algebra; defines the gauge groups

or in component form:

$F^a_{\mu\nu} = \partial_\mu A^a_\nu - \partial_\nu A^a_\mu + g f^{abc} A^b_\mu A^c_\nu$

with F: F – is the 2-form

$$F = \frac{1}{2} F^a_{\mu\nu} dx^\mu \wedge dx^\nu T^a$$

- c_1 – first Chern class, dimensionless; determines charge topology; 0 denotes anomaly-free models
- $\frac{i}{2\pi}$ – normalization; dimensionless; returns integer values
- Tr F – curvature radius; unit: $\frac{1}{m^2}$; the integral over manifolds
- Tr – curvature trace via the group index a; for SU(N) or U(1)
- F – is the 2-form
- i – imaginary form; ensures real and integer values for c_1

In FSM, the following applies:

Tr $F = 0$

because:

- the T^a generations of SU(4) trace-less → Tr $T^a = 0$.
- the Abelian trace (U(1) part) is absent in the non-Abelian group or is suppressed by the geometry.
- the charge does not arise globally (no monopoles), but solely from the wave-field dynamics and the geometry of the dimensional plane D_{56}.

Therefore:

$$c_1(E) = \frac{i}{2\pi} \text{Tr } F = 0 \qquad (2.153)$$

Chern class c_2:

General:

$$c_2(E) = \frac{1}{2!} \left(\frac{i}{2\pi}\right)^2 \text{Tr } (F)^2 = \frac{1}{4\pi^2} \frac{1}{2} \text{Tr } (T^a T^b) = \frac{1}{8\pi^2} \text{Tr } (F \wedge F)$$

In FSM, a complex 3D manifold applies to rotation in the dimensional planes $D_{45/46}$:

$$F = dA + A \wedge A = \frac{1}{2} F^{a}_{\mu\nu}\, dx^{\mu} \wedge dx^{\nu}\, T^{a}$$

$$F^{a} = dA^{a} + f^{abc} A^{b} \wedge A^{c}$$

For non-Abelian groups, the following important property holds:

$\mathrm{Tr}(F \wedge F) = \mathrm{Tr}((dA + A \wedge A)^2)$

Squaring of F :

$F \wedge F = (dA + A \wedge A) \wedge (dA + A \wedge A)$

Distribution of the wedge product ($\wedge$ is associative and antisymmetric):

$F \wedge F = dA \wedge dA + dA \wedge (A \wedge A) + (A \wedge A) \wedge dA + (A \wedge A) \wedge (A \wedge A)$

Summary:

$\mathrm{Tr}(dA \wedge (A \wedge A)) = \mathrm{Tr}((A \wedge A) \wedge dA)$ both terms of equal size

$2\mathrm{Tr}(dA \wedge (A \wedge A))$

Results in:

$\mathrm{Tr}(F \wedge F) = \mathrm{Tr}(dA \wedge dA) + 2\mathrm{Tr}(dA + A \wedge A) + \mathrm{Tr}(A \wedge A \wedge A \wedge A)$

The running integral $\int_M$ over $\mathrm{Tr}(F \wedge F)$ results in:

$\int_M \mathrm{Tr}(dA \wedge dA) = 0$ (exactly)

$\int_M 2\mathrm{Tr}(dA + A \wedge A) = 0$ (exactly)

$\int_M \mathrm{Tr}(A \wedge A \wedge A \wedge A) = \mathrm{Tr}(F \wedge F)$ (not exact and not closed in general; this one precisely measures the topological twist of the bundle)

- $\mathrm{Tr}(A \wedge A \wedge A \wedge A)$ arises from the non-Abelian self-coupling of the gauge fields A^{a}_{μ}
- In FSM, self-coupling arises geometrically from the curvature of the wave-field dimensions, particularly the deviation from the dimensional plane D_{56}

Result:

$$c_2(E) = \frac{1}{8\pi^2} \int_M \mathrm{Tr}\,(F \wedge F) \qquad (2.154)$$

- $\int_M$ – integral; represents the underlying 4-dimensional manifold for the compact space in the wave-field; measures the topological twist of the gauge bundle across the wave field dimensions
- $F \wedge F$ – the wedge product of the field strength in 4-form; the trace measures the topological twist of the calibration bundle, resulting in an integer factor; domain $D_{45/46}$
- $c_2(E) \neq 0$ creates local fluctuations that stabilize the binding of quarks (as 3-fion bundles).
- In FSM, k is chosen such that the index = 3 for the chiral generations.

Chern class c_3:

General:

$$c_3(E) = \frac{1}{3!}\left(\frac{i}{2\pi}\right)^3 \mathrm{Tr}\,(F)^3 = \frac{1}{6}\frac{1}{8\pi^3}\mathrm{Tr}\,(F \wedge F \wedge F)$$

In FSM, a complex 3D manifold applies to rotation in the dimensional planes $D_{45/46/56}$:

$$c_3(E) = \frac{1}{24\pi^3}\int_M \mathrm{Tr}\,(F \wedge F \wedge F) = 0 \qquad (2.155)$$

- c_3 – Determinant component for the third class; measures curvature; in FSM, $F \sim k\cos(kt)$ is diagonal, so $\det(F) = 0$, since rotations in a 3D wave-field are completely antisymmetric ($D_{45/46/56}$); antisymmetric matrix consisting of: $\omega_{ab} = \omega_{ba}$
- $(F \wedge F \wedge F)$ – The wedge product of the field strength in 6-form; the trace measures the topological twist of the calibration bundle, which generally results in an integer factor; domain $D_{45/46/56}$
- $\mathrm{Tr}\,(F \wedge F \wedge F) = 0$, because the product of three trace-zero matrices has trace zero; (in SU(N), $N \geq 2$); $f^{abc} \neq 0$ causes the $\mathrm{Tr}(F^3)$ signal to disappear; for SU(N) with $N \geq 2$ is the trace of three generators zero
- The compact manifold has no non-trivial 6-cohomology in the relevant dimension; for 3D compact manifolds → no 6-form integrals exist
- Although the D_{56} deviation generates effective $SU(2)_L$ chirality, it does not generate a non-trivial c_3 factor
- Chirality arises solely from dynamic geometry (D_{56}- angle deviation, frequency shift, $\cos(kt)$), but not from a topological c_3 factor
- $c_3 = 0$ follows directly from the fact that the calibration group is non-Abelian ($\mathrm{Tr}\,(F^3) = 0$) → The integral vanishes trivially.

Insights from the results of the Chern classes:

1. **Charge:**
   - $c_1 = 0$ means that the FSM does not require classical monopoles; the charge is not global, but arises purely from wave-field dynamics
   - Each generation n has an effective charge Q_n that arises from the geometry of the dimensional plane D_{56}; charge topology:
     $\sum_{gen} \text{Tr } Q^3 = 0 \rightarrow Q_1^3 + Q_2^3 + Q_3^3 = 0$
   - Force load structure:
     $n = 1$ (1. Generation): $Q = \pm 2/3e$; $Q = \pm 1/3e$; $Q = \pm e$;
     $n = 2$ (2. Generation); $n = 3$ (3. Generation): analog structure
     Sums over all quarks + Leptons per generation: Tr $Q^3 = 0$
     Possible combination: $\frac{2}{3} \cdot 3$ „color“ + $(-\frac{1}{3} \cdot 3) + (-1) + 0 = 0$
     The charge combination can be reflected accordingly
2. **The Three Generations:**
   - ($n = 1, 2, 3$) must be free of anomalies when taken together
   - No gauge anomalies in SU(2) × U(1), as three generations balance the loads.
   - There are exactly three generations in the 7-dimensional FSM model.
   - Anomaly cancellation, since c_1 is an integral over the anomaly polynomial.
3. **Weak interaction:**
   - $c_1 = 0$ for global freedom, but locally $F \neq 0$ allows deviations for the F curvature in $D_{45/46}$
   - Weak strength SU(2) from rotation to $D_{45/46}$ with 2D, deviation from SO(3) due to its complex structure.
   - $c_2 = \frac{1}{4\pi^2} \text{Tr } F^2 \neq 0$ measures potential local “distortion,” creating local deviations that stabilize the bond
   - Weak interactions can now arise only through geometric deviations of the metric γ_{ab} in 2D subspaces (relative to the dimensional plane D_{56}); F as a measure
   - The weak interaction is depicted as a “shifted” rotation (parity violation due to the deviation), since $F \wedge F$ is antisymmetric (chiral); geometrically demonstrated by $c_1 = 0$
4. **Strong interaction (strong force):**
   - $c_1 = 0$ ensures the absence of anomalies and implies that the SU(3) symmetry (for the strong interaction between quarks) arises from the trivial topology of $X = 0$
   - $c_2 \neq 0$ creates local fluctuations that stabilize the binding of quarks (as 3-fion bundles)
   - $c_3 = 0$ limits the number of generations to 3 and excludes higher modes within the 7D FSM framework

- Chern's results show that the strong force is not a separate force, but rather a geometric invariant of compact curvature. FSM offers added value because it explains QCD structures without quantization or supersymmetry, but with consequences such as anomaly-free baryon formation and "dark matter" as unstable modes.

5. **Electromagnetic interaction:**
   - $c_1 = 0$ ensures the absence of anomalies and implies that the U(1) charge (electric charge) arises as a trivial topology, $X = 0$
   - $c_2 \neq 0$ creates local variations that stabilize the photon polarization
   - $c_3 = 0$ limits electromagnetic interaction to a single generation and excludes higher modes within the 7D FSM framework
   - Chern's results show that the electromagnetic interaction is not a separate force, but rather a geometric invariant of compact curvature. FSM offers added value because it explains QED structures without quantization or supersymmetry, but with consequences such as anomaly-free photon propagation and dark energy arising from electromagnetic-like vacuum terms.
6. **No additional generations in 7D:**
   - $c_1 = 0$ for the tangent bundle, this implies a trivial bundle with no higher "windings"
   - In the 7D version of the FSM, the generation modes $n = 1, 2, 3$ arise from 3D compact wave-field dimensions; higher values of n require $c_1 \neq 0$ as an additional charge topology.
   - From 7D (4D visible + 3D invisible compact), the dimensionality of $D = 3$ imposes exactly three modes; the maximum is determined by the dimensions in the compact wave-field.
   - $c_3 = 0$ excludes higher generations, since $n = 4$ would require $c_3 \neq 0$
7. **Gravitational anomaly in 7D:**
   - $c_1 = 0$ does not imply a chiral anomaly, since anomalies ~ Tr F in odd dimensions such as 7D vanish → FSM is already consistent with both classical and quantum mechanics
   - Possible gravitational anomalies in D-dimensions arise from Tr $R^{D/2+1}$; for FSM $D = 7$ ~ Tr $R^{4,5}$; would only be relevant in the case of even D
   - $c_1 = 0$ for gauge bundles, this implies Tr $F = 0$; extended to Tr $R = 0$ for gravity
   - Consequently, FSM exhibits no gravitational anomalies in 7D; $c_1 = 0$ confirms freedom

Conclusion:

The Chern classification for the FSM model provides mathematical proof of its correctness based on its lack of anomalies and the presence of three generations. The FSM model is simple, does not require supersymmetry, and is predictable through the modes of topology. This creates a new framework for particle physics as

an alternative to string theory, offering anomaly-free physics without extra assumptions and the potential to incorporate dark energy from topology.

17. Fine-structure constant in FSM

The fine-structure constant α is the dimensionless coupling constant of the electromagnetic interaction. It determines the threshold at which a photon can exchange its field with another particle. According to Sommerfeld, the relationship for the fine-structure constant is:

$$\alpha = \frac{e^2}{2\,\epsilon_0\,h\,c} \tag{2.156}$$

- α – Sommerfeld fine-structure constant; dimensionless; $\alpha = \frac{1}{137{,}065}$; scales the electromagnetic coupling
- e – elementary charge; unit: C; e = 1,602 10^{-19} C; causes the base charge
- ϵ_0 – electric field constant; unit: $\frac{As}{Vm}$; ϵ_0 = 8,8542 10^{-12} $\frac{As}{Vm}$; scales the Coulomb potential
- h – Planck's constant; unit: Js; h = 6,626 10^{-34} Js; for Quantum Scale
- c – maximum speed; unit: $\frac{m}{s}$; c = 299792458 $\frac{m}{s}$

The FSM will alternatively derive the reciprocal value of the fine-structure constant geometrically to enable verification. This is demonstrated using the general formula for coupling frequencies and object masses in **Chapter 3.7**, formula (3.34).

In group theory, it was explained that the electrical interaction occurs via an external fion, which must exceed the minimum coupling frequency. With the electron as the base particle with a factor of 1, the following ratio between the electron frequency and the minimum coupling frequency must hold in order to satisfy the condition for interaction with the lowest excitation:

$$\alpha = \frac{f_e}{f_{min}} \approx \frac{1}{137} \tag{2.157}$$

The FSM predicts that particle frequencies and masses can be modeled as multiples of the electron/positron, scaled by the fine-structure factor!

18. Spin-0-Pair Theory of FSM – Entanglement

Definition of Entanglement:

Quantum entanglement is a state in which two or more particles (or systems) are so interconnected that the quantum state of the entire system cannot be described as the product of the individual states, even if the particles are far apart.

- Measuring one particle immediately determines the state of the other, regardless of the distance between them.
- There is no standard explanation, such as for hidden variables or signals traveling faster than the speed of light.
- Violates Bell's inequalities, which have been experimentally confirmed.
- Observed in photon pairs, electron spins, fion traps, superconductors, diamond-NV-centers, and even in macroscopic systems containing over ~ 10^{12} atoms.

Assumptions used by the FSM model to explain entanglement:

1) Conservation of energy and particle-antiparticle symmetry

- The 7D action is invariant under charge conjugation (C) and parity (P) in the compact wave-field dimensions.
- The global component of the tensor $T_{MN}^{(\text{global})} = (1 + \cos(kt + \beta))\, \delta_{MN}$ is C-symmetric and always produces electrons and positrons in pairs.
- Number of electrons = number of positrons (exactly, except for the CP violation caused by an angular deviation from the dimensional plane D_{56} – Z-, W-, H- bosons; the underlying reason is illustrated in **Figures 3.24–3.26**)

2) The photon as a spin-1 field with two possible configurations of its rotational paths

- The direction of rotation for both photons is either clockwise or counterclockwise.
- Dimensional plane D_{56} separates the global potentials of the universe. It can be represented as the “equatorial plane” of rotation, which reflects the rotation in an antisymmetric manner relative to itself.
- Helicity +1: rotates above the dimensional plane D_{56}
- Helicity -1: rotates below the dimensional plane D_{56}

3) Dark energy as a spin-0-pair in the uncoupled state < f_{min}

- Before reaching the minimum coupling frequency fmin, matter exists as an unbound pair of two spin-1 photons originating from a common field body of a single oscillating wave packet relative to the dimensional plane D_{56}. **Figure 7.2** provides a possible illustration of the universe in its initial state.

- The two constituent photons have opposite helicities (+1 and -1) with a total spin of 0. Total angular momentum $S_{total} = 0 = S_1 + S_2$ (singlet)
- The shared field means that their wave functions are not separable. Even when assigned as positive or negative partial charges in the form of an active particle, they remain **entangled** with one another.
- A change in the helicity of one spin-1 particle (e.g., due to measurement or absorption) instantly alters the state of the other, leading to the classical observation of entanglement.
- Their electric potential is maximally effective internally but neutral externally. The two sub-photons are electrically attracted to one another. Only their globally determined gravitational potential forces them into a stable orthogonal configuration relative to the dimensional plane D_{56}. In other words: Dark energy is the carrier of the gravitational potential. With this configuration, the wave function prevents a classical approximation and, consequently, an annihilation reaction.

4) Transition at f_{min}

- As soon as the oscillation frequency reaches $f \geq f_{min}$, the common field body breaks apart
- The spin-0 state decays into two independent spin-1 photons, causing dark energy to become electrically coupled and thus “accessible”.

Consistency with the FSM model:

- $V(\phi_n)_{dark} = \frac{9}{4} k^4 (1 - \cos(kt + \beta))^2$ describes precisely the potential of the spin-0 pair, provided that $f < f_{min}$
- $T_{\mu\nu}^{(dark)} = -\frac{1}{2} g_{\mu\nu}^{(4)} (2V(\phi_n)_{dark})$ is the tensorially compactified 4D component of the momentum-energy tensor
- The longitudinal component: The longitudinal polarization of the massive spin-1 photon corresponds to the invisible, uncoupled component in the common field body.
- Conservation of energy: The spin-0-state has energy $2\,E_{Pho}$. After the decay, two photons, each with E_{Pho}, are conserved.
- D_{56}-deviation: The local rotation with the term $\cos(kt + \beta)$ relative to the dimensional plane D_{56} produces exactly the asymmetry between helicity +1 and -1.

Wave function for the spin-0-pair (before $f < f_{min}$):

$$|\Psi_{pair}\rangle = \frac{1}{\sqrt{2}} (|+1\rangle_1 |-1\rangle_2 - |-1\rangle_1 |+1\rangle_2) \otimes |\phi_{common}(x, y)\rangle \quad (2.158)$$

- $|+1\rangle_1 \, |-1\rangle_2$ – asymmetric helicity states of the two photons
  +1 = projection of the rotation above the dimensionsal plane D_{56}
  -1 = projection of the rotation below the dimensional plane D_{56}
- $\frac{1}{\sqrt{2}}$ – The prefactor ensures antisymmetry under the exchange of the two photon components, which is necessary for bosons with a spin-0-total state.
- Subtraction ensures that the total spin in the helicity sum is 0. The total spin of 0 arises from the orbital angular momentum of the uncoupled field body.
- $|\phi_{common}(x, y)\rangle$ – common scalar field; described by:
  $V(\phi_n)_{dark} = \frac{9}{4} k^4 (1 - \cos(kt + \beta))^2$
  → The field body is …
  - a standing wave in the dimensional plane D_{56} that "carries" both photons.
  - **not separable before** $f < f_{min}$.
  - **unable to couple** before disintegration.
- **Entanglement:** The antisymmetric component of helicity ensures that measuring the helicity of the first photon instantly determines the helicity of the second, resulting in classical entanglement without signal transmission.

Modified Proca equation after the decay ($f \geq f_{min}$):

Once f_{min} is exceeded, the spin-0 field decays into two independent massive spin-1 photons. The two spin-1 photons become locally independent and electrically coupled. The effective vector field of photon A_μ then obeys the Proca equation for a massive vector field.

$$\square_{(4)} A^a_\mu - \partial_\mu (\partial^\nu A^a_\nu) + 4\pi^2 m_a^2 \frac{c^2}{h^2} A^a_\mu = 0 \quad \text{with: } m = \frac{n\,h}{2\pi\,c\,R} \quad \text{and: } n = 1, 2, 3 \qquad (2.159)$$

- The term $m_a^2 A^a_\mu$ ...
  - is derived from the potential $V(\phi_n)$ after compactification and describes the effective mass of the longitudinal component.
  - breaks the gauge invariance and allows for a non-transverse (longitudinal) solution, which is physically real and carries mass.
- After the disintegration …
  - the scalar potential field changes from $V(\phi_n)_{dark}$ to $V(\phi_n)_{pot}$.
    $V(\phi_n)_{pot} = \frac{9}{4} k^4 \cos^2(kt + \beta)$
  - a longitudinal polarization is activated, which generates a mass with.

Physical consequence:

- Photon now carries a mass $m_{Pho} = \frac{n\,h}{2\pi\,c\,R}$

- Dispersion: $k^2 = w^2 c^2 + 4\pi^2 m_a^2 \frac{c^4}{h^2}$; (massive, $v < c$)
- Yukawa potential (effective interaction): $V(r) = \frac{e^{-mr}}{r}$ (2.160)
    - $V(r)$ – The Yukawa potential causes the interaction to decay exponentially over long distances.
    - r – distance between the source and the observation point
    - $r \geq 0$ – unit: m, fm, angstrom – depending on the context
    - $r = 0$ – refers to the location of the source itself (where the potential typically diverges)
    - r – In the context of nuclear and particle physics, this refers to the distance between objects, and is applied in **Chapter 3**, "Particle Model".
    - r – In the context of cosmology, this refers to the field radius (event horizon) and is discussed in **Chapters 2.3** and **7**.
- Three polarizations for spin-0 field bodies: 2 transverse + 1 longitudinal
- After the disintegration:
    - **Transverse wave** remains with: $h_{\mu\nu} = 0$; mass = 0
    - **Longitudinal wave** is: $\square_{(4)} \phi_n = m_n^2 \phi_n$; mass dependent on mode n

Entanglement is described as a 7-dimensional geometric effect of the configuration relative to the dimensional plane D_{56}. This explains why electrons and positrons always arise in pairs, why dark energy is initially hidden, and why entanglement is non-local. The longitudinal component and the Yukawa attenuation are direct consequences of mass generation by the dark energy potential $V(\phi_n)_{dark}$. This property can be verified using the example of the universe (**Chapters 7.1–2**). Due to the fractional-free scaling, these properties are present at every quantization starting from the minimum coupling frequency f_{min}.

19. Scalability

Scalability is the ability to describe phenomena uniformly across all orders of magnitude (from the Planck-scale microcosm to the macrocosm of the universe) without any discontinuities. In the FSM, it arises from the geometric nature of matter as a relativistic oscillation, scalable by the field radius r and the angular frequency k. The FSM is supersymmetry-free, explicitly predicts masses, consists of a dynamic sine stabilization, and is testable.

Scalability from the field equations:

The field equations are scaled by the field radius r. The field radius is a characteristic quantity of matter that arises from its relativistic fields. The nominal value of r is specified at the origin of the inertial system. In relativistic terms, the

nominal value r becomes $r(t)$. In the field equations, the field radius appears as follows:

$$\delta g \sim g_{\mu\nu} = \eta_{\mu\nu} + h_{\mu\nu} \sim \frac{GM}{c^2\, r} \quad \rightarrow \quad R_{MN} \sim \frac{1}{r^2} \quad \rightarrow \quad T_{MN} \sim \frac{c^4}{8\pi G r^2}$$

- $g_{\mu\nu}$ – metric perturbation; corresponds to the deviation of space-time from the flat Minkowski metric due to gravity; from point 1.
- $h_{\mu\nu}$ – disturbance term for gravitational waves
- $\frac{GM}{c^2\, r}$ – gravitational curvature strength; dimensionless
- R_{MN} – Ricci tensor; unit: $\frac{1}{m^2}$
- r – field radius; unit: m; $r = \frac{GM}{c^2}$ (2.134)
- T_{MN} – Momentum-energy tensor; unit: $\frac{kg}{m\, s^2}$

Macroscopic gravity:

Metrical disturbance

$$h_{\mu\nu} = \frac{GM}{c^2\, r}\,[1 + \cos(kt + \beta)]$$

is applied directly to macroscopic masses M and radii r.

Global scale:

The global metric is:

$$\eta_{\mu\nu}\,[1 + \cos(k_{\text{Uni}}\, t)]$$

The global oscillation $\cos(k_{\text{Uni}}\, t)$ s still the same function as for elementary particles. As the field radius r, increases, the angular frequency k decreases.

The Chern classes $c_1 = 0$ and $c_3 = 0$ apply unchanged to the entire universe.

Scalability through sinusoidal rotation:

Rotation about $\cos(kt)$ with the angular frequency k

$$k = \sqrt{\frac{G\, M}{r^3}} \qquad (2.135)$$

shows the possible range of frequencies:

$$m_{obj} = \frac{h\, c^2}{G\,\{m_{obj}\, k_{obj}\}\, \lambda_{obj}} = \frac{h}{c\, \lambda_{obj}} = \frac{h\, f_{obj}}{c^2} \qquad (2.192)$$

Scalability through universal constants identified by FSM (**Chapter 2.3**):

Space-time constant: $c = k\,r \quad \rightarrow \quad k = \frac{c}{r}$ (2.136)/(2.174)

$$c = 299792458\ \frac{\text{m}}{\text{s}}$$

Mass time constant: $m\,k = 4{,}0396\ 10^{35}\ \frac{\text{kg}}{\text{s}}$ (2.175)

Mass-space constant: $\frac{m}{r} = 1{,}34746\ 10^{27}\ \frac{\text{kg}}{\text{m}}$ (2.176)

Scalability based on Planck's constant, according to the formula (2.185):

$h = \lambda_{obj}\, r_{obj}\, m_{obj}\, k_{obj} = \lambda_{obj}\, m_{obj}\, c$ $[h] = \text{Js}$ with: $c = k\,r$

Scaling of energy according to formulas (2.180) and (2.182):

$E = r_{obj}\, m_{obj}\, k_{obj}\, c$ with: $c = k\,r$

$E = m_{Obj}\, r_{obj}^2\, k_{obj}^2 = m_{obj}\, c^2$

$E = m_{Obj}\, G\, \{m_{obj}\, k_{obj}\}\, \frac{1}{c}$

Scalability through frequencies:

$$\alpha = \frac{f_e}{f_{min}} \approx \frac{1}{137} \qquad (2.157)$$

In the general formula for particles, the existing relativistic rotations are accounted for within the wave-field geometry.

$$f_{obj} = \frac{1}{2}\,(\text{BK}\,(\text{KK})^3)^n \cdot \text{TK} \cdot \text{DimFactor} \cdot f_e \qquad (3.27)$$

Why the FSM model scales so well:

Uniform geometry: All scales use the same 7D metric, the same rotation tensor $\omega_{ab}^{(4)}$ and the same oscillation function $\cos(kt + \beta)$.

No new parameters: Only the values of R, $n\,r$, k, β; the basic equations remain the same.

Projection principle: What appears in the wave-field as a spin-0 pair or complex topology always projects onto the observed spin - $\frac{1}{2}$ - fermions and spin-1 bosons in the particle-field.

Topological invariants: The generation number/winding number n, the Euler characteristic X, and the Chern classes c_k are scale-invariant and explain stability from the Planck scale to the universe.

20. Comparison of FSM with classical models and string theory

To conclude this **Chapter 2.2**, we will provide a brief overview of the key advantages of the FSM model compared to previous theories.

Unification of all forces into a single model:

Gravity, electromagnetism, and the weak and strong interactions arise from the geometric curvature (rotations) in 6-dimensional field-space, without any separate fields or particles.

Explains unsolved phenomena:

- **Charge** as a particle-field projection $D_{14/24/34}$ of the electrically generated potential resulting from rotation relative to the dimensional plane D_{56}
- **SU(4)** symmetry dynamically breaks down to SU(3) × U(1), which leads to the weak interaction, where β geometrically describes the displacement relative to the dimensional plane D_{56}.
- **Dark energy** as a spin-0-pair of uncoupled photons with frequencies f less than the minimum coupling frequency f_{min}; after reaching fmin, decay into coupled invisible (dark) matter and visible matter
- **Avoiding** the **cosmological constant** (GTR) by $V(\phi_n)_{dark}$
- **Invisible (dark) matter** as compact wave-field oscillations with complex topological modes ($n \neq 0$, $g \geq 1$) and Chern classes $c_3 = 0$
- **Expansion** from field deformation
- Resolution of the **wave-particle duality** through sinusoidal oscillations
- **Quantum entanglement:** Spin-0-pair state prior to decay
- **Fine-structure constant:** FSM: $\alpha = \frac{1}{136{,}6875}$ (3.33) ; Sommerfeld: $\alpha = \frac{1}{137{,}065}$
- **Three generations:** winding count n = 1, 2, 3 from the Fourier series
- **Anomaly-free:** Chern classes $c_1 = 0$, $c_3 = 0$

Scalability across orders:

The FSM model applies seamlessly from the Planck scale to the maximum extent of the universe. Hypothetically, it even applies to scales smaller than the Planck

scale, once visible space disappears due to continued contraction and the universe reverts to the characteristics of a photon. Classically, GTR breaks down at the quantum level; QFT breaks down in the presence of gravity.

New particle model:

Point particles are replaced by 4-dimensional cavity modes with predictions for particle masses and coupling frequencies. Empirical data are confirmed on average with 99% agreement. The variances around the mean are smaller than the standard deviation of the measurement itself. Fions in the bundle generate charge and spin in the particle-field; exchange fions outside the bundle mediate interactions; passive fions form dark components. Spin, charge, and entanglement are purely rotational effects. The particle model is finite, geometric, and avoids singularities.

Practical Applications:

- **New propulsion** systems for space travel or near-Earth transport by leveraging the characteristics of a gravitational field at the physical level of conventional fields.
- **Optimized hot/cold fusion** with new heavy modes and stable fion clusters
- **Computers** with states of complete photon oscillations or spin-0-pair states for entangled qubits over macroscopic distances
- Production of **matter/antimatter-states** in stabilized forms
- **Gravitational wave detection** for predicting longitudinal and scalar modes in addition to the classical TT polarizations
- **Dark energy** technology for the targeted generation of $f > f_{min}$ for converting dark energy into usable photons

Added value compared to effective field theory in the QFT sense:

QFT is an effective theory involving renormalization, divergences, and arbitrary parameters. FSM is a fundamental geometric theory without renormalization. Masses, couplings, and charges arise directly from compactification and topology. The fine-structure constant and the three generations are not free parameters, but rather predictions. Quantum effects emerge from the dynamics of the compact wave-field dimensions (modes n/R, rotations), not from a formalism such as canonical quantization or path integrals. Thus, FSM avoids the infinities and renormalization that occur in QFT and solves problems such as duality geometrically (photons as waves in 4-dimensional subspaces).

- **Wave-particle duality:** Through sinusoidal rotations $V_{long} = c\cos(kt)$; $V_{trans} = c\sin(kt)$, the photon alternates between wave and particle states.
- **Discrete spectra:** From compactification (modes $\frac{n}{R}$; f_{Obj} according to (3.27))
- **Similar to the uncertainty principle:** Generated from periodic oscillation (kt), that produces position and momentum as averages over periods T.

- **No path integrals:** FSM does not use Feynman path integrals with sums over paths for probabilities; instead, photons follow null geodesics in the subspace ($ds^2 = 0$), which are classically determined but exhibit statistical behavior due to averaging over rotations.
- **Fundamental Theory:** FSM is not an effective field theory in the QFT sense (e.g., with cutoff and renormalization), nor does it have a Wilsonian EFT with path integrals. FSM is a fundamental theory that allows quantum effects to emerge, similar to condensed matter, where photons arise from classical lattice dynamics.
- **Planck's constant:** h is derived in FSM from geometric scales for $f_{Obj} \sim h\, f_e$. It avoids commutators and path integrals.
- **Quantum gravity:** FSM avoids problems such as those associated with quantum gravity and infinities by allowing quantum phenomena to emerge classically.

Advantages over string theory:

String theory requires 10 or 11 dimensions and supersymmetry for stability; strings are fundamental to it. It offers a unified framework that is hypothetical yet complex, without explicit predictions or testable parameters. The FSM model is potentially more powerful:

- **Simple dimensionality:** 7D instead of 10/11D, without supersymmetry, FSM stabilized by sine rotations
- **Explicit predictions:** Masses and frequencies can be calculated based on electrons. String theory, on the other hand, presents an infinite landscape without any predictions.
- **Geometric Matter:** Matter as a field deformation (no strings), scalable without additional assumptions. String theory posits the existence of strings, whereas FSM derives matter from relativistic space-time.
- **Explanation of dark phenomena:** Invisible/dark energy/matter arising from compact rotations; dualism is resolved, while string theory addresses a similar solution without, however, providing quantitative formulas.
- **Practical relevance:** FSM is testable and concrete, opening up entirely new applications. String theory, on the other hand, is abstract and difficult to prove empirically.

Added value compared to general relativity:

General Relativity explains gravity through geometry, but remains classical and cannot account for quantum effects, dark energy, and entanglement. FSM extends GTR to include a 7-dimensional geometry with compactified dimensions. Gravity remains a classical curvature, while quantum effects, particles, and dark energy arise from the same geometry.

Conclusion: FSM provides a unified, scalable geometric framework that resolves classical gaps from a single geometric foundation. It avoids the complexity of string theory and the renormalization problems of QFT, yet remains mathematically rigorous and experimentally testable. For verification, reference is made to the particle model, in which previously measured particles can be compared with calculated ones. **FSM is not merely a theory of particles and forces, but, in its full 7-dimensional structure, a theory of space-time itself.**

2.3 Sinusoidal Periodicity, global and local Gravitational Force

In this chapter, the expansion behavior of the universe is abstracted as a wave motion. During a sinusoidal period *T*, distinct forces act at different time intervals. At the beginning of the universe, the greatest contraction of its photon field occurs, with the highest energy density. A contraction requires additional work to stabilize the system. This contraction already possesses the necessary additional energy. Nature, for its part, always strives for the lowest energy state for a stable system. The contraction energy can be reduced by increasing the volume of space. The relativistic state of the Lorentz transformation with a factor of 1 provides the energetically favorable location in space-time for minimal contraction. Thus, an inertial force builds up, which decreases again with expansion. Space-time opposes this inertial force. A counterforce acts – the gravitational force, which dampens this inertial force and generates a global curvature or space-time deformation. Due to the relativistic conditions of the contraction, the gravitational force is strongest at the beginning and weakens until maximum expansion is reached.

A space-time potential exists between the beginning and end of the expansion. This is to be defined as **gravitational potential** with **~ d*M*(*α*) = *M* cos(*α*)**. The solid angle *α* places the gravitational potential in a trigonometric relationship that abstracts the universe's state of contraction globally in wave form. Between cos(0°) and maximum expansion cos(90°), the following applies: cos(0° > *α* < 90°) – cos(90°) = 1…0. With positive signs, attractive forces prevail. The velocity parameters V_4 and V_5 simultaneously describe the progression of space-time curvature and the contraction of the global speed of light relative to the maximum speed *c*. They align geometrically with the course of the gravitational potential and describe, on the same plane, the space-time-mechanical states according to formulas (2.05; 2.06; 2.07). Thus, visible photons, as carriers of light, reach the maximum speed $V_{max} = c$ when they are no longer slowed down by any counterforces from space-time. The minimum value of the global gravitational forces, which lies at the location of the inertial system and has a Lorentz contraction factor of 1, acts there with **d*M*(*α* = 90°; *α* = 270°)** für $\boldsymbol{V_5 = c}$**;** $\boldsymbol{V_4 = 0}$.

Mathematically, based on the graph of the cosine function, the universe beyond 90° would have a negative sign for its gravitational potential. The gravitational potential between 90° and 180° is:

cos(90° > *α* < 180°) – cos(90°) = 0…-1. With a negative sign, the gravitational force acts repulsively. When gravity acts repulsively, space-time drives the inertial force to increase again in the opposite direction. Space-time is then contracted again. Why, starting from a stable, energetically balanced state, would the mechanism cause the universe to contract again? This is explained by the vibrational nature of the universe as an electromagnetic wave. There is nothing in the universe that could mechanically stop its wave motion. In this way, the universal angular momentum is conserved and

thus continues its global oscillatory motion. The fact that gravity acts repulsively or attractively across the quadrants of a sinusoidal period T is, globally viewed, merely a side effect and is defined by the initial state.

$270° < \alpha < 90°$ attractive and **$90° < \alpha < 270°$** repulsive field forces

In summary:

The magnitude of the inertial force is determined by its universal constant (2.177). Its relativistic behavior is described by the sine periodicity (2.164) using the reciprocal of the sine function. The gravitational potential $dM(\alpha)$, with its cosine function at the point of relative rest with $dM(90°)$ (Lorentz factor 1), indicates in which quadrant an attractive or repulsive gravitational force prevails. The field propagation velocity V_4 describes, in parallel with the cosine function, the expansion characteristics of the volume space and represents the component for modeling the space-time deformation. The field propagation velocity V_5 runs parallel to the speed of light in the form of a sine function and indicates the prevailing field deformation.

If an infinitesimal number of measurement points are recorded for the field deformation relative to the inertial frame, a prospective trajectory curve is generated over a period T. This trajectory curve describes a state representation of the universe in space-time during a complete period as an electromagnetic wave and is shown in **Figure 2.6**. The particle-field is abstracted as a two-dimensional blue band and is completely self-connected.

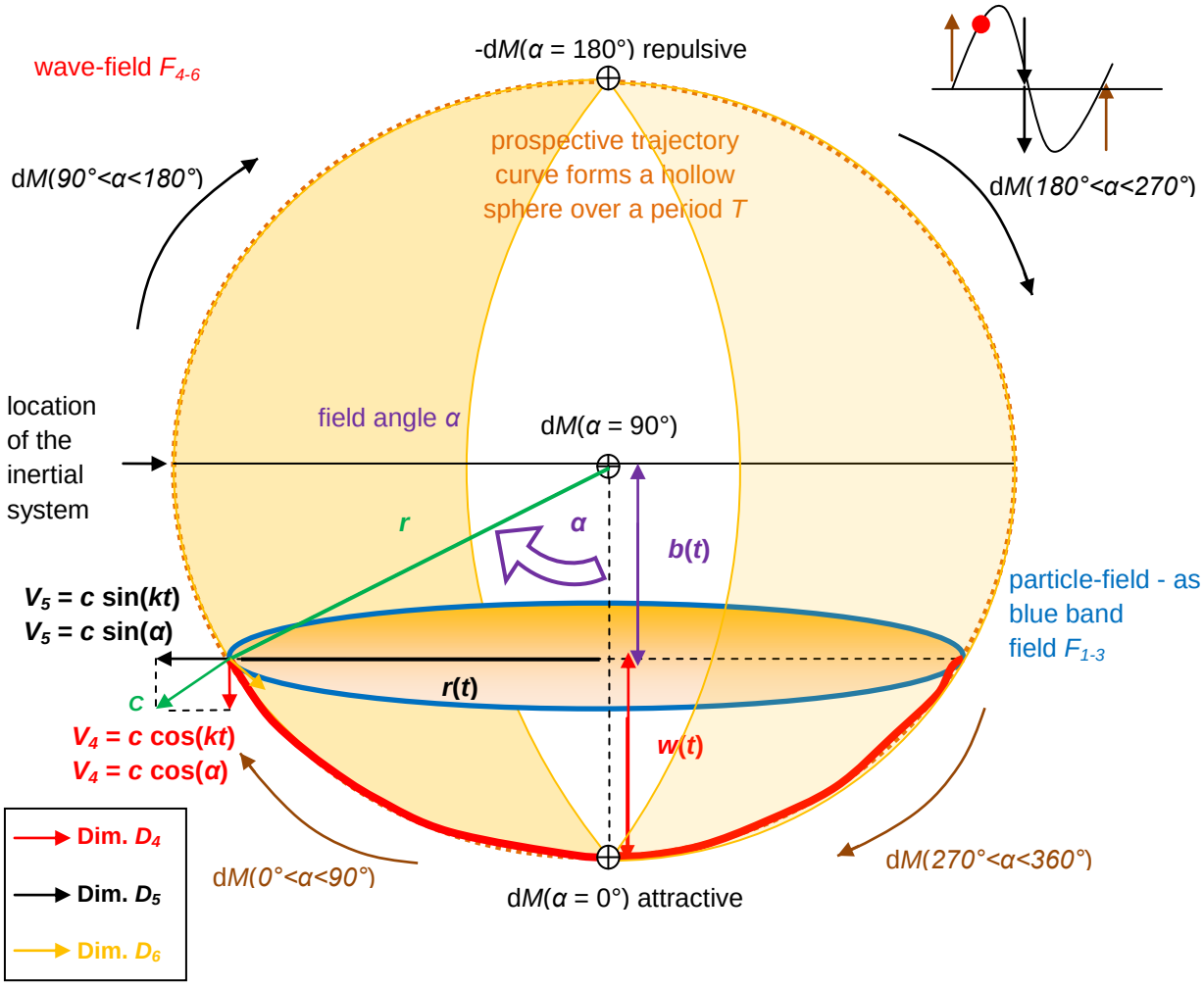

Figure 2.6: 7-dimensional state diagram of the universe with one oscillation period

In a 6-dimensional field-space with a 5-dimensional surface, several 4-dimensional subspaces could arise mathematically between the wave-field F_{4-6} and the particle-field F_{1-3}. These **4-dimensional field bodies** form the **quantised matter** within the photon field.

Derivation of the sine periodicity of the universe:

The gravitational force always exists between objects plus the prevailing gravitational potential d$M(\alpha)$. This gravitational potential changes sinusoidally for the universe and all objects in it during a full period. The sinusoidal periodicity ultimately describes the force of relativistic surface gravity between its photon field and any quantisable matter in the universe at any point in its space-time deformation.

$F_{gravity} = \frac{G\,M\,m}{r^2}$ (Newton's law of gravity)

$r(t) = \frac{1}{2}at^2$ $v(t) = \int a(t)$ $r'(t) = v(t)$

$r(t) = \iint a(t)$ $v(t) = at$ $r''(t) = a(t)$

G - gravitational constant
M_{Uni} - mass of the universe
F - force between M_{Uni} and m_{Obj}
$r(t)$ - volume radius at a certain time t
$v(t)$ - velocity at a specific time t
$a(t)$ - acceleration
m_{obj} - mass of an object
r_{Uni} - maximum field radius of the universe
α - field angle

$$\frac{G\,dM(\alpha)\,m_{obj}}{r^2} = a(t)\,m = \frac{\int_{G\,dM(\alpha)\,m_{obj}\,d\alpha}^{\alpha\text{-field angle}}}{r^2} \quad \text{and} \quad r(t) = r\sin(\alpha)$$

$r(t)$ is the variable volume radius of the universe depending on the gravitational potential $dM(\alpha)$ to an object with mass m.

For $F(r) = \frac{dM}{dr\,r}$ applies:

Maximum possible gravitational potential between $dM(\alpha)$ and m_{Obj} results from:
$dM(\sim 0) = M_{Uni}\cos(\sim 0)$ → at the birth of the universe

The gravitational potential along the field angle α is given by:
$dM(\alpha) = M_{Uni}\cos(\alpha)$

- ➔ Depending on the sign of the $\cos(\alpha)$, attractive and repulsive forces result.
- ➔ The relativistic gravitational force runs in the reference field $F_{4\text{-}6}$ with the cosine function parallel to the field propagation velocity V_4. The smaller the field angle α between objects with a mass m_{Obj} and the location $dM(\alpha \to 0)$, the greater the gravitational forces between them.
- ➔ The gravitational potential of matter diminishes with the expansion of the universe.

If the universe is exactly mirrored at the location $dM(\alpha = 90°)$ and $-dM(\alpha = 270°)$, then the field force effect of matter is minimal.

The gravitational force $F_{gravity}$ for the universe is considered relativistically by describing its gravitational potential $dM(\alpha)$ as a function of its current extent $r(t)$.

$dM(\alpha) = M_{Uni}\cos(\alpha)\,d\alpha$ → gravitational potential (2.161)

For the universe and all its subspaces, a surface measure for the space-time mechanical effects must be observed, as it represents the field-space in six dimensions as a mathematical hollow sphere.

Classic:

$A_O = 4\pi r^2$ → Surface area for the sphere; r – radius (2.162)

Relativistic:

$$\cancel{4\pi}\, r^2 = \cancel{4\pi}\, \frac{r(t)^2}{\sin^2(\alpha)} \quad \rightarrow r(t)^2 = r^2 \sin^2(\alpha) \tag{2.163}$$

After crossing the inertial system, the pointer for the direction of action changes trigonometrically.

for: $270° < \alpha < 90°$ attractive and $90° < \alpha < 270°$ repulsive effect of the field forces

Insert into the equation of force:

$$F_{gravity}(t) = a(t)\, m = \frac{G\, dM(\alpha)\, m_{obj}}{r(t)^2} = \frac{\int_{G\, M_{Uni}\, m_{obj}}^{\alpha\text{-field angle}}}{r(t)^2} \cos(\alpha)\, d\alpha$$

$$F_{gravity}(t) = \frac{G\, M_{Uni}\, m_{obj}}{r(t)^2} \int_{\cos(\alpha)\, d\alpha}^{\alpha\text{-field angle}} \quad \text{with: } \int_0^{\alpha} \cos(\alpha)\, d\alpha = \sin(\alpha) - \sin(0)$$

$$F_{gravity}(t) = \frac{G\, M_{Uni}\, m_{obj}}{r(t)^2} \sin(\alpha) = \frac{G\, M_{Uni}\, m_{obj}}{r^2} \frac{1}{\sin(\alpha)} \quad [F] = \text{N} \tag{2.164}$$

Findings:

- ➔ The course of the relativistic gravitational force of the photon field is sinusoidal-periodic
- ➔ The sine function reflects the field shape of the deformed space-time
- ➔ In this representation, the object mass m_{obj} does not have its own vectorial proper motion. Space-time mechanical effects act in addition to the space-time deformation of the universe in the event of possible proper motion.

The sign of the rise in the sine wave corresponds to the direction of its gravitational force. If the slope of the sine function is therefore positive, then attractive forces prevail, whereas repulsive forces act on a negative slope.

From STR-FSM to GTR-FSM:

To generalize the relativistic relationship, the space-time-mechanical effects must be modified from the fixed field propagation speeds V_4 and V_5 and the corresponding field angle α to a dynamic acceleration dependent on the nominal time t. In other words, this means that the dynamic expansion of the universe also changes the object time of its fields. The field propagation velocity V_4 decreases at a reduced rate, while the field propagation velocity V_5 increases at an accelerated rate. **Figure 2.7** uses the mathematical hollow sphere to relate the relativistic relationship between

the maximum velocity $V_{max} = c$ and an object velocity V_3 in the particle-field with the variable volume radius $r(t)$:

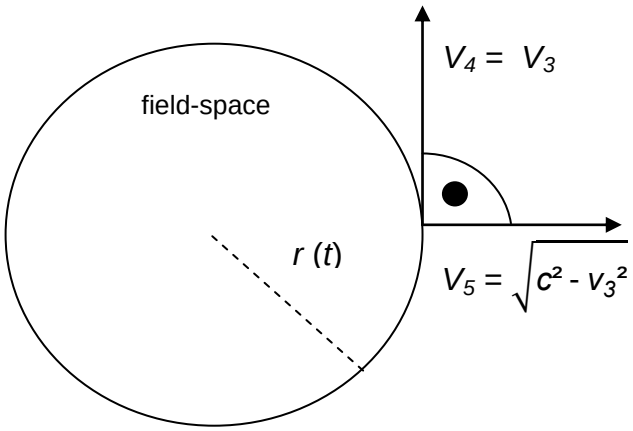

This results in the following equation for the field angle α:

$$\alpha = \int_0^t \frac{\sqrt{c^2 - V_3^2}}{r(t)}\, dt \qquad (2.165)$$

Figure 2.7: View of the hollow sphere

$$\alpha = \int_0^t \frac{\sqrt{c^2 - V_3^2}}{r(t)}\, dt \qquad \rightarrow \text{The field angle } [\alpha] \text{ in angle °}$$

$$\frac{\sqrt{c^2 - V_3^2}}{r(t)} = \frac{c \sin(\alpha)}{r \sin(\alpha)} = \frac{c}{r} = k = \text{constant} \qquad (2.166)$$

The field angle α parameterises the available gravitational potential $dM(\alpha)$ for an object mass m_{Obj} at all locations in the universe. For the FSM-GTR, the field angle α is generalised as follows:

$$\alpha = \sin^{-1}(kt) \text{ (general)} \qquad \alpha = \sin^{-1}\left(\frac{V_5}{c}\right) \text{ (special)} \qquad (2.167)$$

7-dimensional FSM-GTR between two objects in the universe:

The effect of the gravitational force, taking into account the sinusoidal periodicity, relates to the photon field and thus also to all objects in the universe simultaneously. A single object as part of the photon field cannot register its own gravitational force without any other object. For the relativistic observation of objects within the universe, gravitational forces can only be made measurable between at least two objects. The mutual attraction of objects requires at least two gravitational fields of their own. Thus, within the sinusoidal periodicity of the universe, an additional local deformation of space-time applies between two objects.

For a force F, an acceleration of $a_5(t) = r''(t)$ acts on an object. The acceleration $a(t)$ is already determined by the sine periodicity. In order to represent the additional

deformation in space-time caused by two objects within the photon field, the formula (2.164) is extended with the product of the factor sin(*kt*) for object 1 and a further factor sin(*kt*) for object 2.

Derivation of the relativistic force formula between two objects:

$r(t) = \frac{1}{2} a t^2$ $r(t) = \iint a(t)$ $v(t) = at$ $v(t) = \int a(t)$

$r'(t) = v(t)$ $r''(t) = a_5(t)$

k - angular frequency *t* - elapsed time along the period time *T*

With the help of trigonometry, mathematical expressions for the solutions of the FSM-GTR are obtained:

$$r(t) = r \sin(kt);\ r'(t) = r\,k \cos(kt) = V_4(t);\ |r''(t)| = |a_5(t)| = \left|- r\,k^2 \sin(kt)\right| \quad (2.168)$$

Between two accelerated (scalable) moving objects within a sine-periodic universe, the aforementioned additional quadratic factor for the space-time deformation is obtained with $\sin^2(kt)$:

$a_5(t) = r''(t) = a(t) \sin^2(kt)$:

$$F_{gravity}(t) = m\,r''(t) = m\,a(t) \sin^2(kt) = \frac{G\,m_{obj1}\,m_{obj2}}{r(t)^2} \sin(\alpha) \sin^2(kt)$$:

with: $\alpha = \int_0^t \frac{\sqrt{c^2 - V_3^2}}{r(t)}\,dt = \int_0^t \frac{c}{r}\,dt = kt$

$$F_{gravity}(t) = \frac{G\,m_{Obj1}\,m_{Obj2}}{r(t)^2} \sin(kt) \sin^2(kt) \quad (2.169)$$

with the variable radius of the universe: $r(t) = r \sin(kt)$ (2.170)

$$F_{gravity}(t) = \frac{G\,m_{obj1}\,m_{obj2} \sin(kt)\ \cancel{\sin^2(kt)}}{r^2\ \cancel{\sin^2(kt)}} \qquad \text{with: } \sin(kt) = \frac{r(t)}{r}$$

$$F_{gravity}(t) = \frac{G\,m_{obj1}\,m_{obj2}\,r(t)}{r^3} \quad (2.171)$$

$$F_{gravity}(t) = \frac{G\,m_{obj1}\,m_{obj2}}{r^2} \sin(kt) \quad (2.172)$$

to formula (2.172): r^2 - quadratic distance between the two objects

In the wave-field $F_{4\text{-}6}$, the formulae (2.171) and (2.172) describe that a field emission between two objects has a maximum effect if it is transmitted parallel in the dimensional plane $D_{56.}$ The maximum unfolds with $\sin(\alpha = 90°) = 1$. A quantised field is maximally mediated when the formation of 4-dimensional subspaces is orthogonal, i.e. $\alpha = 90°$ to the dimensional plane D_{56}. This configuration is used in the photon model.

The formulae (2.171) and (2.172) describe objects in the particle-field $F_{1\text{-}3}$ that have angular momentum within the universe and, due to their inertial motion, have the greatest effect of their gravitational force orthogonal to their axis of rotation, while their centrifugal force tends to a maximum near the poles. These formulae explain the inertial motion of an approaching object along its spherical sector, which is caused by a centrally rotating gravitational field.

The FSM-GTR derives the solution for the field radius r and the angular frequency k from the acceleration $a_5(t) = r''(t)$. The total mass of the photon field and the gravitational constant remain unchanged. If the field radius of quantised matter is sought, the indices of the mass are swapped accordingly. The second derivative of $r(t)$ from the force equation (2.171) must be used:

$$r''(t) = F_{gravit}(t)_y \frac{1}{m_{obj2}} = \frac{G\, m_{obj1}\, r(t)}{r^3} \qquad \rightarrow \text{Acceleration on an object}$$

→ 2nd order differential equation: characteristic part of the equation

$$r''(t) - \frac{G\, m_{obj1}\, r(t)}{r^3} = 0 \qquad \text{with: } r(t) = e^{kt};\ r'(t) = ke^{kt};\ r''(t) = k^2\, e^{kt}$$

Insert into differential equation:

$$k^2\, e^{kt} - \frac{G\, m_{obj1}}{r^3} e^{kt} = 0 \qquad \rightarrow \qquad e^{kt}\left(k^2 - \frac{G\, m_{obj1}}{r^3}\right) = 0$$

Characteristic equation:

$$k^2 - \frac{G\, m_{obj1}}{r^3} = 0 \rightarrow\ k_{1/2} = \pm\sqrt{\frac{G\, m_{obj1}}{r^3}} \rightarrow \boxed{k = \sqrt{\frac{G\, M}{r^3}}} \qquad [k] = \frac{1}{s} \qquad (2.135)$$

→ continue with the temporal amount

The volume radius $r(t)$ with the smallest field influence corresponds to the expansion of the universe at $r(t) = r$, the extreme value calculation for V_5 with the first derivative of $r(t)$ results:

$$c = V_5(0) = r'(0) = r\, \sin'(k\, 0) = r\, k\, \cos(0) = r\, k$$

$$c = r\sqrt{\frac{G\,m_{obj1}}{r^3}} \rightarrow c^2 = r^2\frac{G\,m_{obj1}}{r^3} \rightarrow \boxed{r = \frac{G\,M}{c^2}} \qquad [r] = \mathrm{m} \qquad (2.134)$$

Comparison: The solution for the field radius according to the Schwarzschild equation for a non-rotating black hole:

$$r_S = \frac{2\,G\,M}{c^2} \qquad (2.173)$$

Effect of the velocities on the gravitational force:

- ➔ The greater the magnitude *of* V_4, the stronger the effect of the gravitational force $F_{gravity}$ with its field between objects.
- ➔ The greater the magnitude *of* V_5, the further the fields of an object with its relativistic field radius $r(t)$ have an effect.

The **field radius *r*** describes the spatial range in which photons and other exchange particles can no longer avoid each other. A field exchange takes place between them. The field radius r of an object contributes to the volume space in space-time. The field radius is considered relativistically as $r(t)$. Its magnitude varies sinusoidally as a function of proper time t.

The **angular frequency *k*** is an invariant, non-relativistic reference value and specifies the cycle time of how often a field can be exchanged per second. The fixed angular frequency k is the reason for the correlation between an existing gravitational force and its space-time deformation.

The **wavelength *λ*** determines the spatial size of the field body in which the fields oscillate mathematically and periodically. The wavelength λ is the quotient of the maximum velocity $V_{max} = c$ and its **frequency *f***. The wavelength is considered relativistically with the gravitational red and blue shift.

From the perspective of the particle-field on a gravitational field, the surface gravity behaves like a kt - sinusoidal periodic gravitational field. It is registered as a **gravitational wave**, which is modelled in the wave-field. The angular frequency k represents the repetition of such a wave, while the time t describes the nominal time at the location of the inertial system. The sine function models the relativistic effects on an object. If only the maximum value is considered for the gravitational wave, which is repeated quickly, a source for a gravitational field is registered, from which a constant gravitational force emanates.

Mass-time constant and space-time constant relative to the inertial system:

The mass-time and space-time constants are characteristic constants for a 7-dimensional universe that define the property relationships between the various quantities (k – angular frequency, M – mass and r – field radius) independently of space-time mechanical effects. The mass-time constant describes the linear mass flow during a periodic cycle. In contrast, the space-time constant defines the linear relativistic increase of the field radius or the volume of space per second during a cycle. These constants describe not only the properties of the universe, but also all the objects in it. The constants result exclusively from the ratios of their sizes to each other. The nominal time t also links space and mass with the help of these constants.

$$G = 6{,}67\ 10^{-11}\mathrm{N}\frac{\mathrm{m}^2}{\mathrm{kg}^2}\ ;\ c = 299792458\ \frac{\mathrm{m}}{\mathrm{s}}$$

a) Space-time constant

$k_{Uni} \sim \frac{1}{r_{Uni}}$ A closed spherical universe requires precisely aligned universal constants so that a circular frequency k_{Uni} is exactly inversely proportional to the maximum volume radius R_{Uni} of the universe.

$$r_{Uni}\, k_{Uni} = \frac{G\, M_{Uni}}{c^2} \sqrt{\frac{G\, M_{Uni}}{r_{Uni}{}^3}} = \sqrt{\frac{(G\, M_{Uni})^3\, (c^2)^3}{(G\, M_{Uni})^3\, (c^2)^2}} = \mathrm{c}$$

$$r_{Uni}\, k_{Uni} = r_{obj}\, k_{obj} = \text{constant} = c = 299792458\ \frac{\mathrm{m}}{\mathrm{s}} \qquad (2.174)$$

➔ The **space-time constant** is the product of the field radius r and the angular frequency k of an object.

b) Mass-time constant

$k_{Uni} \sim \frac{1}{M_{Uni}}$ During a period T, a mass M_{Uni} moves through space-time:

$$M_{Uni}\, k_{Uni} = M_{Uni} \sqrt{\frac{G\, M_{Uni}}{r_{Uni}{}^3}} = \sqrt{\frac{G\, (M_{Uni})^3\, (c^2)^3}{(G\, M_{Uni})^3}} = \sqrt{\frac{(c^2)^3}{(G)^2}}$$

$$M_{Uni}\, k_{Uni} = m_{obj}\, k_{obj} = \text{constant} = 4{,}0396\ 10^{35}\ \frac{\mathrm{kg}}{\mathrm{s}} \qquad (2.175)$$

➔ The **mass-time constant** is the product of the mass M and the angular frequency k of each object.

c) Mass-space constant

$$\frac{c}{r_{Uni}} = \frac{4{,}0396\ 10^{35}\ \frac{kg}{s}}{M_{Uni}} \quad \rightarrow \quad \frac{M_{Uni}}{r_{Uni}} = \frac{4{,}0396\ 10^{35}\ \frac{kg}{s}}{299792458\ \frac{m}{s}}$$

$$\frac{M_{Uni}}{r_{Uni}} = \frac{m_{obj}}{R_{obj}} = \text{constant} = 1{,}34746\ 10^{27}\ \frac{kg}{m} \tag{2.176}$$

➔ The **mass-space constant** describes the directly proportional relationship between the event horizon or field radius of matter, depending on its mass.

The three constants form a closed, scalable triangle that applies to any mass *M* and any field radius *r* and clearly defines the circular frequency *k*.

The characteristic time of an object t_{Obj} is therefore the light travel time across its own field radius *r*.

$$T_{obj} = \frac{1}{k} = \frac{r_{obj}}{c}$$

Every scaled object has its own characteristic angular frequency *k*, which is determined exclusively by its field radius *r,* and vice versa. This explains why gravity is strong at close range and weak at a distance. Local high *k*-values with small field radii *r* lead to rapid oscillation, which averages out while the effective attraction remains intact. For large field radii *r* and small angular frequencies *k*, the global slow oscillation dominates, which modulates the range.

Amount of force of the photon field against space-time:

As the universe expands, a certain inertial force is at work, causing space-time to expand in a relativistic manner. The counterforce—the force of gravity—"holds" its mass within its space-time. The photon field in the universe thus exerts a constant force *F* on its quantized subspaces to prevent them from escaping its space-time. During the dynamic expansion of the universe, its relativistic unfolding of force is taken into account with *F*(*t*). This force is represented by the sinusoidal periodicity according to formula (2.164).

$$F_{gravity}(t) = \frac{G\ M_{Uni}\ m_{obj}}{r^2}\ \frac{1}{\sin(kt)} = m_{Obj}\ r_{obj}\ k_{obj}^2\ \frac{1}{\sin(kt)} = m_{obj}\ c\ k_{obj}\ \frac{1}{\sin(kt)}$$

Using the universal constants summarized above, the following holds:

$$F(t) = \{m_{obj}\ k_{obj}\}\ \{R_{obj}\ k_{obj}\}\ \frac{1}{\sin(kt)} = 4{,}0396\ 10^{35}\ \frac{kg}{s}\ 299792458\ \frac{m}{s}\ \frac{1}{\sin(kt)}$$

$$F(t) = 1{,}211\ 10^{44}\ \mathrm{N}\ \frac{1}{\sin(kt)} \tag{2.177}$$

The amount of inertial force required for a subspace to escape the universe's photon field must exceed $F_{Escape} > 1{,}211\ 10^{44}$ N. There is no quantized object at rest that could exceed this force. The universe itself already possesses this amount of force. It is conceivable that an additional dilative state—e.g., caused by object motion or plasma states—could introduce additional energy from outside the universe into a subspace. This could enable an escape. The universe itself does not provide this energy. Such an external source is conceivable but remains an open question until **Chapter 7.2**.

The relativistic force of the photon field at any point in space-time is determined by the quotient involving the sine function. This stabilizes the inertial dynamics globally.

The amount of $1{,}211\ 10^{44}$ N can be used as a universal reference for the consistency of particle characteristic calculations. This reference value is determined by universal constants for space-time and mass-time and scales across all orders of magnitude, from photons to black holes to the universe.

2.4 The Photon Model

The derived constants in **Chapter 2.2** suggest that the mechanism of the 7-dimensional theory of relativity is scalable to all matter. Thus, the representation of sine periodicity from cosmology with its wave behaviour is transferred to quanta in the microcosm. This chapter explains the photon model, which results exclusively from the relativistic framework conditions. This model overcomes the idea that elementary particles are point particles. Instead, they are a contracting and expanding hollow body oscillation consisting of superimposed harmonics. The simplest form of these harmonics corresponds to the photon. In addition to the dimension of time, a photon requires four spatial dimensions to describe its photon field. This quantised photon field and its harmonic form a subspace U for a 6-dimensional field vector, which also describes complex structures and networks of several photons.

Photons are always 4-dimensional subspaces :

A 6-dimensional space has a 5-dimensional surface. It can contain numerous of 4-dimensional subspaces U in the form of field bodies. The surface of such a 4-dimensional subspace U is 3-dimensional. A fourth spatial dimension is required to represent one or more such 4-dimensional rotation paths. The properties of real photons are attributed to these rotating field bodies.

a) The surface of a 4-dimensional hollow sphere is 3-dimensional. It takes four dimensions to map three 4-dimensional rotation paths.
b) The surface of a 5-dimensional hollow sphere is 4-dimensional. It takes five dimensions to map four 4-dimensional rotation paths.
c) The surface of a 6-dimensional hollow sphere is 5-dimensional. It takes six dimensions to map five 4-dimensional rotation paths.

For a photon, its 4-dimensional subspace within the 6-dimensional field space implies that

- its quantized angular momentum is equal to that of the universe
- its interaction takes place within the framework of the universe's gravitational potential
- the direction of its field exchange depends on the periodic structure of the universe.

Integration of a photon into the field-space:

The first challenge is to integrate an electromagnetic wave that follows a wave function into a reference system that takes into account the relationships shown in **Figure 1.5**. The relevant method is to represent a wave as a mathematically periodic rotation. With a relativistic rotational motion, the angular momentum L can be modelled for its relativistic inertial force. The angular momentum L has the unit Js for

an effect. Within the framework of FSM, the mechanism of angular momentum in the macrocosm can be transferred to the angular momentum of the microcosm. This is because the photons must follow the angular momentum of the universe in accordance with the law of conservation of angular momentum. The original angular momentum remains the same, regardless of any additional energy. As the angular momentum of each photon must be maintained relative to the angular momentum of the universe during its own motion, space-time deforms the field-space at the location of the field. The greater the intrinsic motion of a photon in the form of a higher frequency, the more energy the photon must be based on.

Display options:

The following visualisation options for 4-dimensional subspaces U are conceivable. The appropriate illustration is used for each chapter.

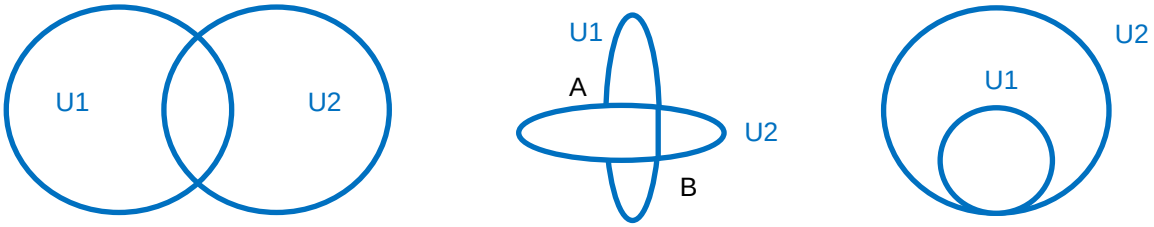

Figure 2.8: Possible arrangements of subspaces in the wave-field F_{4-6}

Now the photon is to be abstracted as an electromagnetic wave into a mathematical rotation in the wave-field F_{4-6}. **Figure 2.9** realises sine-periodically rotating photons, which are described according to the results of FSM-GTR.

The relativistic relationship applies to the field propagation velocity vectors V_4 and V_5:

$$c^2 = V_4^2 + V_5^2$$

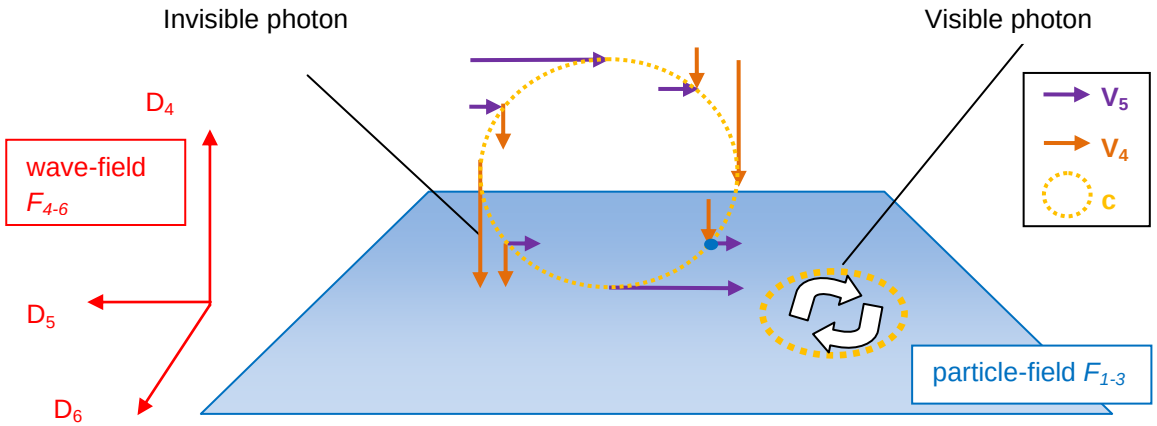

Figure 2.9: Left: orthogonal to the dimensional plane D_{56} an invisible photon with its rotation mechanism; right: parallel to the dimensional plane D_{56} a rotating visible photon

Figure 2.9 shows several capabilities of a photon at the same time. The current inertial state of a wave should be marked as a small blue dot. This always rotates along its prospective trajectory with the maximum speed $V_{max} = c = 299792458 \frac{m}{s}$. The field propagation velocity vectors V_4 and V_5 in the wave-field $F_{4\text{-}6}$ change periodically during its path. With the periodic change of its field propagation velocities, its space-time behaviour changes dynamically during rotation. This periodic sequence of its inertial motion in the wave-field $F_{4\text{-}6}$ shown above will also transmit its gravitational force starting at the point of contact on the dimensional plane D_{56} in a sinusoidal or wave-like manner into the particle-field $F_{1\text{-}3}$. The gravitational wave in question is registered.

However, **Figure 2.9** shows even more. Depending on whether a photon rotates orthogonally to the dimensional plane D_{56} or not, it can be registered differently. Photons rotating in the wave-field $F_{4\text{-}6}$ parallel to the dimensional plane D_{56} continuously exchange their photon field with the particle-field $F_{1\text{-}3.}$ In addition to the short and long wavelengths, these photons also contain frequencies visible to the eye. These photons are used in experiments to measure the speed of light. Such photons are part of the **registering matter** and should be summarised as **visible photons**. While the so-called **invisible photons** rotate in the wave-field $F_{4\text{-}6}$ orthogonally to the dimensional plane D_{56}, they can only transmit their photon field into the particle-field $F_{1\text{-}3}$ under certain conditions and periodically. Such invisible photons nevertheless exist even without direct registration by an observer and are assigned to the **hidden matter**.

Classification of dark matter:

According to FSM, dark matter is a form of hidden matter consisting of invisible, coupled photons or invisible complex particles. A deviation from the point of contact in the dimensional plane D_{56} reduces the coupling strength of matter with its interaction fields into the particle-field $F_{1\text{-}3}$. Despite coupling, dark matter may interact weakly or not at all with visible matter.

Classification of dark energy:

Dark energy consists of a collection of invisible photons that, in their evolution, have not reached the minimum coupling frequency (**Chapter 3.1**) required for interaction with other matter. These cannot (yet) interact with other matter.

Conclusion on matter:

Matter is not ‘substance’ in the conventional sense, but rather a geometric effect of a relativistic 6-dimensional field-space.

Quantum principles for photons formulated from the axioms:

1) Photons have fields in the wave-field $F_{4\text{-}6}$, which oscillate relativistically in space-time in a contracting and expanding manner, while these are abstracted macroscopically in the particle-field $F_{1\text{-}3}$ as field lines.

2) A field propagation velocity V_4 in the fourth dimension and the field propagation velocity V_5 in the fifth dimension together form a rotation matrix along the unit vector $\overrightarrow{e_6}$, which runs parallel to the dimensional plane $\overrightarrow{e_6}\, dD_4 dD_5 = \overrightarrow{dA} = D_{45}$ and always results in the maximum velocity $V_{max} = c$ in a vacuum with 299792458 $\frac{m}{s}$. The relationship applies:

$$c^2 = V_4^2 + V_5^2$$

3) The results of length contraction and time dilation reach the factor 1 exactly when the object velocity $V_3 = 0$. Accordingly, the state $V_4 = 0$ with $V_5 = c$ applies.

4) The object time t_{Obj} of a particle depends on its field propagation velocity V_5, which unfolds in the dimensional plane D_{56}.

5) The length of an emitted field line can be measured in a velocity diagram for all dimensions $D_{1\text{-}3}$ in the particle-field $F_{1\text{-}3}$ using the object time t_{obj} and its field propagation velocity V_5.

6) The common point of contact for photons, which mediates visible matter, lies exactly in the dimensional plane D_{56}, which is spanned between the fifth and sixth dimension. The common point of contact for hidden particles lies above or below the dimensional plane D_{56}.

Field body point of view:

The local field body is modeled by vector fields and gravitational fields. Under the condition that the volume radius R is much larger than the field radius r ($R >> r$), the vector fields and their scalar feedback determine the field body at the microcosmic level (**Chapter 2.2, Wave Equations, Point 11**). The dominant metric component is:

$$ds^2 \supset 2(A_\mu^a + \delta A_\mu^a)\, dy_a\, dx^\mu$$

Due to the spatially limiting 3-dimensional nature of the particle-field, a single field body in the particle-field $F_{1\text{-}3}$ can only exist in a maximum of 3 dimensions in all spatial directions. For each spatial direction D_1, D_2, D_3 in the particle-field $F_{1\text{-}3}$, only a single field vector remains for a 4-dimensional subspace U in the wave-field $F_{4\text{-}6}$, in which a field can propagate. This is represented in the wave-field $F_{4\text{-}6}$ as a 1-dimensional field vector for each of the spatial directions D_4, D_5, D_6. **Figure 2.10** uses a blue arrow to represent one of the three possible 4-dimensional subspaces. This

shows a 6-dimensional field vector for the case where one dimension in the field F_{4-6}, e.g. in the fourth dimension, is omitted for three spatial directions of an object in the particle-field F_{1-3}.

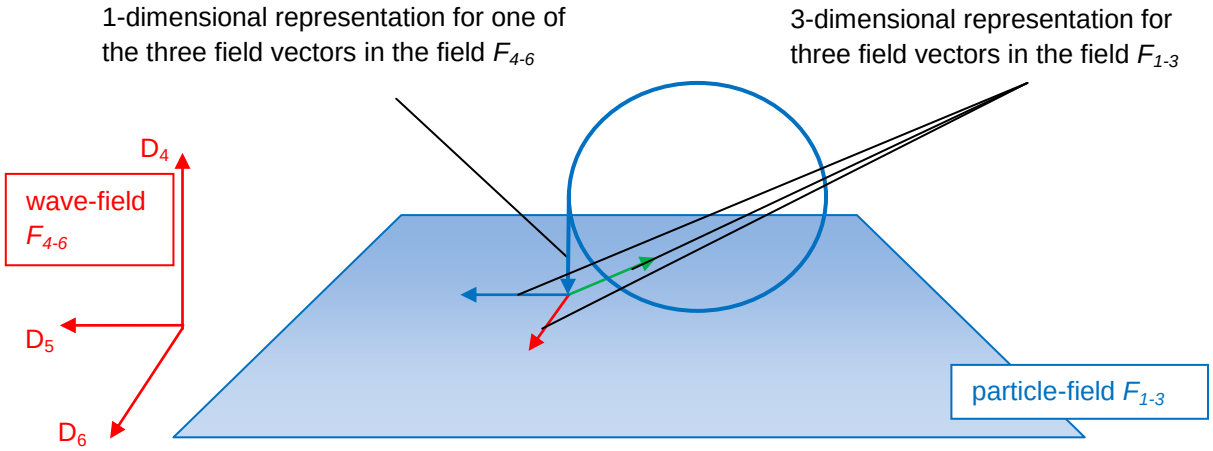

Figure 2.10: 4-dimensional representation of a subspace in the wave-field F_{4-6}

From the perspective of the particle-field F_{1-3}, this representation corresponds to the **wave nature** of a photon. Based in **Chapter 2.2, Wave Equations, Points 11 and 14**, this wave nature is described by the transverse wave.

For this field body, further 1-dimensional field vectors are conceivable for the fifth and sixth spatial directions in the field F_{4-6}. **Table 2.1** is intended to show the 6-dimensional field vector, which at the same time gives the object its 3-dimensional wave character. This vector describes initial information about how photons can rotate geometrically in space and how the field exchange with the particle-field F_{1-3} works.

Dimensions / 4-dim. rotary tracks	1	2	3	4	5	6
1	X	X	X	X	/	/
2	X	X	X	/	X	/
3	X	X	X	/	/	X

Table 2.1: The three possible 6-dimensional field vectors for the 3-dimensional field body view in the particle-field F_{1-3}

"X" means that a 4-dimensional subspace U is spanned, while "/" means that no spatial direction is spanned for this dimension.

The six-digit field vector (1) can be labelled with the following indices as the **dimensional plane** between particle-field F_{1-3} and wave-field F_{4-6}: $\boldsymbol{D_{14/24/34}}$.

Consideration of the field effect of photons:

Although the field body shown already exists with its 1-dimensional field component, it can only be measured if this field is periodically emitted into the particle-field $F_{1\text{-}3}$. This works if a vector component of the field body touches the dimensional plane D_{56}, which runs parallel to the particle-field $F_{1\text{-}3}$, in order to exchange its field from the wave-field $F_{4\text{-}6}$. Another part of the field vector must run in the dimensional plane D_{45}, which generates a potential in the photon field asymmetrically parallel to the electric potential. Its maximum amplitude is transmitted as a static charge at the point of contact in the dimensional plane D_{56} into the particle-field.

This conflict is resolved by giving a field emission a rotating character, as shown in **Figure 2.10** - blue circle. A periodically recurring rotation in the D_{45} dimensional plane creates a potential in the photon field, while the dimensional plane D_{56} periodically enables the field exchange between wave-field $F_{4\text{-}6}$ and particle-field $F_{1\text{-}3}$. The corresponding field vectors in the wave-field $F_{4\text{-}6}$ must be expanded from a 1-dimensional to a 2-dimensional field component for a possible field exchange, while one spatial direction from the particle-field in the field $F_{1\text{-}3}$ is reduced for this purpose. The result is a 6-dimensional field vector that runs 2-dimensionally in the dimensional plane D_{45} in the wave-field $F_{4\text{-}6}$ and has a 2-dimensional wave character for each spatial direction in the particle-field $F_{1\text{-}3}$. Finally, there is a periodically field exchange for its wave maximum from the wave-field into the particle-field. This field exchange is referred to as the **matter pulse** in the course of this paper.

From the perspective of the particle-field $F_{1\text{-}3}$, this representation corresponds to the **momentum nature** of a photon. Based on the **mathematical principles** outlined in **points 12** and **14**, this momentum nature is described as a so-called longitudinal wave.

Table 2.2 shows the changes in the 4-dimensional subspace for each spatial direction.

Dimensions / 4-dim. rotary tracks	1	2	3	4	5	6
4	X	X	/	X	X	/
5	X	/	X	X	X	/
6	/	X	X	X	X	/

Table 2.2: The three possible 6-dimensional field vectors for a periodic 2-dimensional field exchange in the particle-field $F_{1\text{-}3}$

The six-digit vectors (4), (5), (6) rotate 2-dimensionally parallel to the **dimensional plane D_{45}**.

The geometric propagation of a field's momentum character behaves like an invisible longitudinal wave in the particle-field, while its field body corresponds to a visible transverse wave. The field forces mediated via the dimensional plane D_{56} are therefore perceived as a rigid body in the particle-field. The **wave-particle duality** of photons and particles in the particle-field $F_{1\text{-}3}$ can be attributed to their self-interaction with their own two-dimensional scalar, longitudinal field in the dimensional plane D_{56}, derived from the wave-field $F_{4\text{-}6}$. The duality is solved using the 7-dimensional field equations from **Point 9** and the wave equations from **Point 11** in **Chapter 2.2**.

Note: Wave-particle duality for visible photons

The visible photons, which are measured via a screen, have the field body representation of vectors two and three from **Table 2.1**, because these are already rotating parallel to the dimensional plane D_{56} according to **Figure 2.9** on the right. They can only be contracted by an additional field deformation in the form of a reduction of the field propagation velocity V_5. The rotation parallel to the dimensional plane D_{56} generates a constant gravitational force for its periodic inertial motion, which only interacts with its surroundings as a space-time quantum. A charge and thus an electric field to be mediated is ruled out, as there is no rotational component in the dimensional plane D_{45}.

In the double-slit experiment, the momentum behavior of a transmitted photon for the particle-field is determined by recording a point. The distribution of several of these points visualizes the sinusoidal periodic inertial motion of the transmitted photons from the wave-field.

Force equation of the photon:

The following applies to the maximum field force effect of a 4-dimensional subspace of the photon field in a sinusoidal-periodic contracted equation:

$F(t) = m_{obj}\, a_5(t) = m_{obj}\, r''(t)$

with: $r(t) = r \sin(kt)$; $k = \sqrt{\frac{G\, m}{r^3}}$; $r\, k = c$

$$F(t) = m_{obj}\, r_{obj}\, k_{obj}^2 \sin(kt) = m_{obj}\, c\, k_{obj} \sin(kt) \qquad (2.178)$$

$F(t)$ - relativistic force

m_{obj} - Object mass

r_{obj} - Field radius of the object

k_{obj} - Circular frequency of the object

c - Maximum speed $V_{max} = c$

If the term $\frac{1}{\sin(kt)}$ is used according to formula (2.164), it describes the dynamic relativistic effect between the photon field and space-time. If the term $\sin(kt)$ is considered according to formula (2.172), the case for the deviation from the optimal orthogonal shape to the dimensional plane D_{56} is captured. The greatest effect of a force $F(t)$ is achieved when it occurs in the dimensional plane D_{56}. In **Chapter 2.2**, a deviation angle β was also introduced, which allows for a shift relative to the dimensional plane D_{56} and thus describes a transition between strong and weak interactions. The maximum effect of a force $F(t)$ is achieved when the field exchange occurs parallel to the dimensional plane D_{56}.

Note for cases where the wavelength is greater than the field radius:

To calculate the forces of objects that have a larger wavelength than their field radius, e.g. the Earth's gravitational field, the formula must be adapted. If an observer in the vicinity perceives the surface of a solid which increases the distance to its actual field radius r, the local deformation of space-time and consequently the acting surface gravity is reduced due to the increased distance. In such cases, the field radius r from formula (2.178) is replaced by the volume radius R of the object:

$$R = \frac{\lambda}{2\pi}$$

The angular frequency k is scaled accordingly to these ratios, as its torque has a larger volume radius in such cases. The maximum velocity $V_{max} = c$ must also be

adapted to the cosmic circular velocity of the object. In this way, the surface gravity of any object whose wavelength is greater than its field radius' can be determined.

Energy equation for the photon:

Energy is defined as the sum of all forces that have occurred over the distance Δs:

$$E(\Delta s) = \int_0^{\Delta s} F(t,s)\,ds$$

➔ $F(t, s)$ specifies the force $F(t)$ depending on its position in space

At the location of the minimum Lorentz transformation of the universe, a photon propagates at the maximum speed $V_5 = c$. If a certain path $\Delta s = c\,\Delta t$ or $ds = c\,dt$ corresponds to the path $\Delta s = c\,T$ travelled by a photon with a period length T, the following applies: $c = k\,r$.

The maximum energy transfer takes place during the phase of maximum elongation in 2 dimensions in the subspaces in the wave-field $F_{4\text{-}6}$ on the dimensional plane D_{56}. With regard to the 3-dimensional rotation in the particle-field $F_{1\text{-}3}$, the photons oscillate with a sine wave. A further factor $\sin(kt)$ from the original orientation axis must be applied for this.

$$E(\Delta s) = \int_0^{\Delta s} F(t,s)\sin(kt)\,ds = \int_0^{T} c\,F(t)\sin(kt)\,dt = \int_0^{T} m_{obj}\,r_{obj}^2\,k_{obj}^3\,\sin^2(kt)\,dt$$

$$E(\Delta s) = \frac{1}{2k}\,m_{obj}\,r_{obj}^2\,k_{obj}^3\,\{[k_{obj}\,T - \cos(kT)\sin(kT)]\}$$

$$E(\Delta s) = \frac{1}{2}\,m_{obj}\,r_{obj}^2\,k_{obj}^2\,\{[k_{obj}\,T - \cos(kT)\sin(kT)]\} \qquad (2.179)$$

$k_{obj}\,T$ - component of the angular momentum

$\cos(kT)\sin(kT)$ - component of the electromagnetic oscillation

The mean value of all half wave movements of an electromagnetic oscillation provides with: $\frac{1}{2}\,[k_{obj}\,T - \cos(kT)\sin(kT)] = 1$

$$E = m_{Obj}\,r_{obj}^2\,k_{obj}^2 \qquad \text{with: } c^2 = r^2\,k^2 \qquad [E] = \text{J} \qquad (2.180)$$

$$E = m_{obj}\,c^2 \qquad (2.181)$$

$$E = m_{obj}\,G\,\{m_{obj}\,k_{obj}\}\,\frac{1}{c} \qquad (2.182)$$

$$E = r_{obj}\,m_{obj}\,k_{obj}\,c \qquad (2.183)$$

$$E = \frac{\lambda_{obj}}{\lambda_{obj}} r_{obj}\, m_{obj}\, k_{obj}\, c = h\, f_{obj} \tag{2.184}$$

Formula for Planck's quantum of action *h*:

$$h = \lambda_{obj}\, r_{obj}\, m_{obj}\, k_{obj} = \lambda_{obj}\, m_{obj}\, c \qquad [h] = \text{Js} \tag{2.185}$$

E	- Energy	m_{obj}	- Object mass
h	- Planck's quantum of action	r_{obj}	- Field radius of the object
G	- Gravitational constant	k_{obj}	- Circular frequency of the object
f_{obj}	- Object frequency	c	- Maximum speed
λ_{obj}	- Wavelength of the object		

The index "*Uni*" for universe can be exchanged with the parameters of the index "*Obj*" for object as long as the universal relationships between the mass *M*, the field radius *r* and the angular frequency *k* are maintained.

$$M_{Uni} \rightarrow m_{obj}\ ;\ r_{Uni} = \frac{G\, M_{Uni}}{c^2} \rightarrow r_{Obj} = \frac{G\, m_{obj}}{c^2}\ ;$$

$$k_{Uni} = \sqrt{\frac{G\, M_{Uni}}{r_{Uni}^3}} \rightarrow k_{Obj} = \sqrt{\frac{G\, m_{obj}}{r_{obj}^3}}$$

$$m_{obj}\, k_{obj} = M_{Uni}\, k_{Uni} = \text{constant} = 4{,}0396\ 10^{35}\ \frac{\text{kg}}{\text{s}} \tag{2.186}$$

$$r_{obj}\, k_{obj} = r_{Uni}\, k_{Uni} = \text{constant} = 299792458\ \frac{\text{m}}{\text{s}} \tag{2.187}$$

$$\frac{M_{Uni}}{r_{Uni}} = \frac{m_{obj}}{r_{obj}} = \text{constant} = 1{,}34746\ 10^{27}\ \frac{\text{kg}}{\text{m}} \tag{2.188}$$

$$\lambda_{obj}\, r_{obj}\, m_{obj}\, k_{obj} = \lambda_{Uni}\, r_{Uni}\, m_{Uni}\, k_{Uni} = \text{constant} = 6{,}626\ 10^{-34}\ \text{Js} \tag{2.189}$$

$$c^2 = \frac{G\, M_{Uni}}{r_{Uni}} = \frac{G\, m_{obj}}{r_{obj}} \tag{2.190}$$

$$c = \sqrt[3]{G\, M_{Uni}\, k_{Uni}} = r_{Uni}\, k_{Uni} \rightarrow c = \sqrt[3]{G\, m_{obj}\, k_{obj}} = r_{obj}\, k_{obj} \tag{2.191}$$

Here is a specific example:

$$m_{obj} = \frac{h\, c^2}{G\, \{m_{obj}\, k_{obj}\}\, \lambda_{obj}} = \frac{h}{c\, \lambda_{obj}} = \frac{h\, f_{obj}}{c^2} \tag{2.192}$$

$h = 6{,}626\ 10^{-34}$ Js; $c = 299792458\ \frac{m}{s}$; $m_{obj}\ k_{obj} = \sqrt{\frac{(c^2)^3}{(G)^2}} = 4{,}0396\ 10^{35}\ \frac{kg}{s}$;

$G = 6{,}67\ 10^{-11}\ N\frac{m^2}{kg^2}$;

$E_{pho} = h\ f_{pho} = 3{,}6\ 10^{-19}$ J → $f = 5{,}431\ 10^{14}$ Hz; $\lambda = 552$ nm

$$m_{pho} = \frac{6{,}626\ 10^{-34}\ \text{Js} \cdot \left(\sqrt[3]{6{,}67\ 10^{-11}\ N\frac{m^2}{kg^2} \cdot 4{,}0396\ 10^{35}\frac{kg}{s}}\right)^2}{6{,}67\ 10^{-11}\ N\frac{m^2}{kg^2} \cdot 4{,}0396\ 10^{35}\frac{kg}{s} \cdot 552\ \text{nm}}$$

$\underline{m_{pho} = 4{,}004\ 10^{-36}\ kg}$

Counter sample: $\underline{\underline{m_{pho} =}}\ \frac{3{,}6\ 10^{-19}\ J}{c^2} = \underline{4{,}004\ 10^{-36}\ kg}$

Findings:

- ➔ The ratio of the mass M to the size of the angular frequency k is confirmed.
- ➔ The oscillation of the photon behaves like the oscillation of the universe.
- ➔ Confirmation: the mass is proportional to its frequency: $M \sim f$

Angular momentum $L_{rotation}$ of photons in the wave-field and particle-field:

The mechanism of an oscillating invisible photon, which rotates orthogonally to the dimensional plane D_{56}, is analysed below. In this case, the relativistic state is represented by the Lorentz factor 1. The radius R is derived from the wavelength λ of the photon in the wave-field dimensions. Not to be confused with the field radius r, this describes the event horizon of an electromagnetic wave. According to equation (2.91), the relationship between mass, frequency, and rotational modulation is as follows

$$m_{pho} = \frac{n\ h}{2\pi\ c\ R_{pho}} \cos(kt + \beta) \rightarrow m_{pho}(t) = \frac{h\ f_{pho} \cos(kt + \beta)}{c^2}$$

It can be seen that only the amplitude of the mass is transferred to the particle-field $F_{1\text{-}3}$ during the oscillation. The mass transfer consists of the compact components of the FSM's momentum-energy tensor.

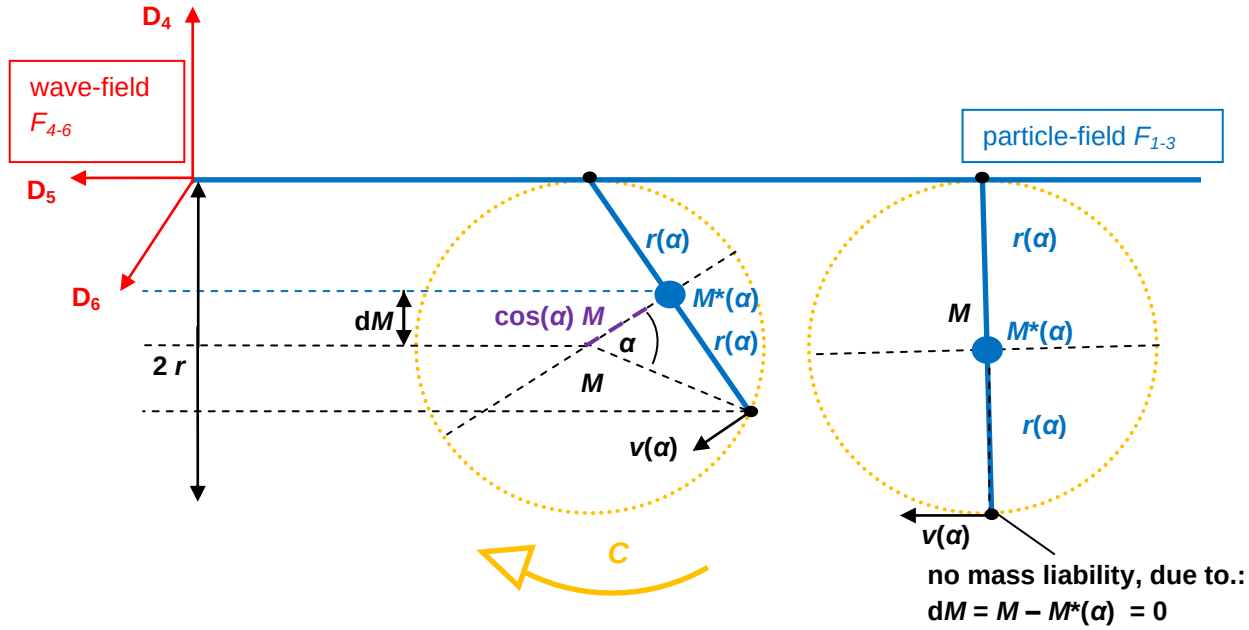

Figure 2.11: Dependencies of the radius *r*(*α*) and velocity *v*(*α*) of the subspace U on the inertial mass *M(*α*) over a period *T***

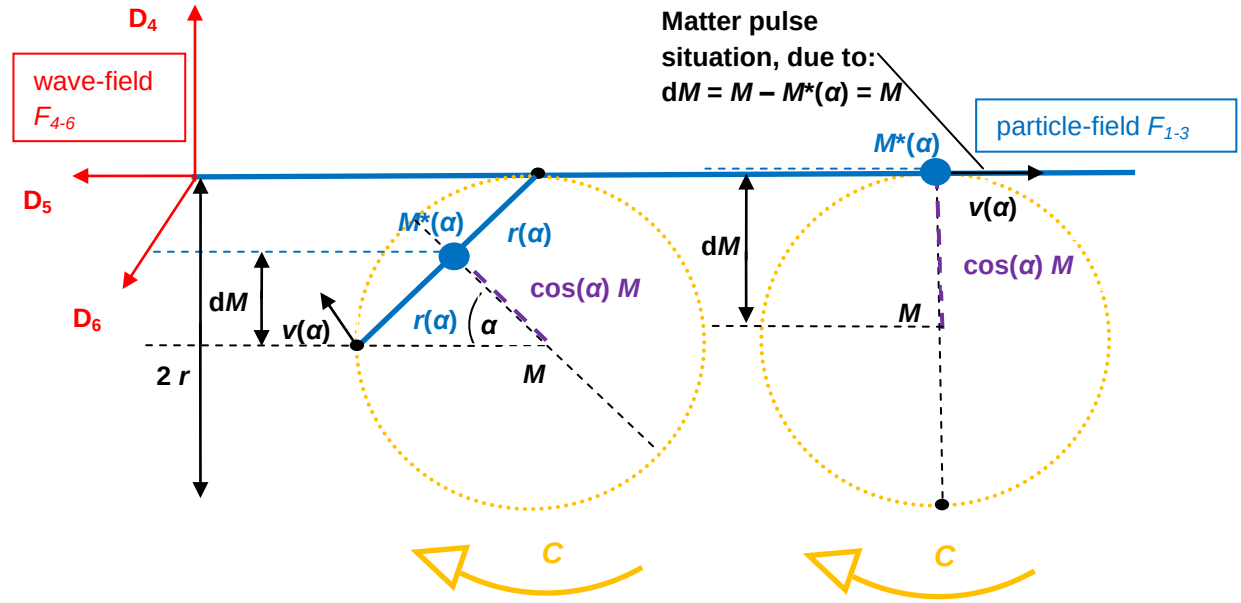

Figure 2.12: Course of a rotation

$v(\alpha) = c \sin(\alpha)$ $r(\alpha) = R \sin(\alpha)$ $\alpha = kt$ k = constant $\lambda = 2\pi R$

$dM = M - M^*(\alpha)$ $M^*(\alpha) = \sin(\alpha)\, M$

The classical approach to angular momentum continues to apply under all relativistic conditions because there is no force in the universe that could change it from outside.

Classical approach: $L = m\ v\ r$ (2.193)

The subspace U has a radius $r(\alpha)$, that rotates at a speed $v(\alpha)$ around an axis through the centre with the inertial mass $M^*(\alpha)$. The length relative to the inertial mass $M^*(\alpha)$ must be multiplied by 2 to represent the length for $2r(\alpha)$. The angle α can only assumes a maximum of 90° during rotation. For a complete period, the integral of the outward and return paths must be taken into account. A factor of 2 must be considered for this. The inertial mass $M^*(\alpha)$ is at its maximum at 0° relative to the object's mass M. $M^*(\alpha)$ can be described trigonometrically as $M \sin(\alpha)$ and can be regarded as a periodic deviation from the original object mass. The subspace U rotates relative to the particle-field with its sinusoidal periodicity orthogonal to the dimensional plane D_{56}. The maximum momentum transfer is achieved during the phase of maximum elongation of the subspaces. For this purpose, the angular momentum relative to the particle-field, as defined by the metric, must be added to an additional factor cos(α) from the original orientation axis.

The approach for angular momentum with α-dependence is ultimately:

$$dL(\alpha) = 2 \cdot 2\ M^*(\alpha)\ v(\alpha)\ r(\alpha) \cos(\alpha)\ d\alpha \qquad (2.194)$$

$$dL(\alpha) = 4 \int_0^{\alpha} m_{obj}\ R\ c \cos(\alpha) \sin^3(\alpha)\ d\alpha$$

$$dL(\alpha) = 4\ m_{obj}\ R\ c \int_0^{\frac{\pi}{2};\ 90°} \cos(\alpha) \sin^3(\alpha)\ d\alpha \qquad \text{with: } 0 \le \alpha \le 90°$$

$$L(\alpha) = 4\ m_{obj}\ R\ c\ \left[\frac{\sin(\alpha)^4}{4}\right]_0^{\frac{\pi}{2};\ 90°}$$

$$L(\alpha) = 4\ m_{obj}\ R\ c\ \left[\frac{\sin(90°)^4}{4} - \frac{\sin(0°)^4}{4}\right]$$

$$L_{ø\_\ particle\text{-}field} = m_{obj}\ \frac{\lambda}{2\pi}\ c \qquad \text{with: } R = \frac{\lambda}{2\pi}$$

$$L_{ø\_\ particle\text{-}field} = m_{obj}\ \lambda_{obj}\ c\ \frac{1}{2\pi} = m_{obj}\ \lambda_{obj}\ k_{obj}\ r_{obj}\ \frac{1}{2\pi} = \frac{h}{2\pi}$$

Comparison: (2.185) (2.195)

$L_{ø\_\ particle\text{-}field}$ - average angular momentum in the particle-field

h	- Planck's quantum of action	r_{obj}	- Field radius of the object
λ_{obj}	- Wavelength of the object	k_{obj}	- Circular frequency of the object
m_{obj}	- Object mass	c	- Maximum velocity

→ **Planck's quantum of action *h*** for the particle-field

Cross-check the above derivation:

with: λ_{photon} = 552 nm; c = 299792458 $\frac{m}{s}$; m_{photon} = 4,004 10^{-36} kg; E_{photon} = 3,6 10^{-19} J

$r_{pho} = \frac{G\, m_{pho}}{c^2}$ = 2,9715 10^{-63} m; $k_{pho} = \sqrt{\frac{G\, m_{pho}}{r_{pho}^3}}$ = 1,0089 10^{71} $\frac{1}{s}$

$\underline{h =}$ 4,004 10^{-36} kg · 552 nm · 299792458 $\frac{m}{s}$ = $\underline{6{,}626\ 10^{-34}\ Js}$

or: $\underline{h =}$ 4,004 10^{-36} kg · 552 nm · 1,0089 10^{71} $\frac{1}{s}$ · 2,9715 10^{-63} m ≈ $\underline{6{,}626\ 10^{-34}\ Js}$

Comparison of Planck's quantum of action from the literature: h = 6,626 10^{-34} Js

Planck's constant *h* describes the proportional effect of a photon on its surroundings with a fixed linear increase in energy as a function of frequency. The FSM derives Planck's constant h for the particle-field via the product of the mass M, the wavelength λ and the maximum field propagation velocity c; or alternatively via the product of the mass M, the angular frequency k, the wavelength λ and the field radius r. Planck's constant h can be regarded as an invariant reference quantity with h = 6,626 10^{-34} Js because there is no external force for the universe and its photon field that could change its angular momentum.

Note: for angular momentum with $L = \frac{h}{2\pi}$

The mathematically represented angular momentum of a photon corresponds to a sinusoidal periodic sequence as contraction and expansion of its 6-dimensional hollow body.

The location of the **matter pulse** shown on the **right in Figure 2.12** is given by

$$dM = M - M^*(\alpha) = M \tag{2.196}$$

at the point of contact in the dimensional plane D_{56}. The mass is transmitted sinusoidally into the particle-field.

Macroscopic vs. microscopic angular momentum:

$L_{ø\_\ particle\text{-}field} = L_{ø\_\ macrocosmic} + L_{ø\_\ microcosmic}$, a fluid transition of dominance

$$L_{ø\_\ particle\text{-}field\ \_photon} = \sqrt{G\, M^3\, r} + \frac{h}{2\pi} \tag{2.197}$$

$$L_{ø\_\ particle\text{-}field\ \_n\_fions} = \sqrt{G\, M^3\, r} + \sqrt{\sum_0^n \left(\frac{h}{4\pi}\right)^2_n} \tag{2.198}$$

Relativistic energy increase – space-time effect on accelerated objects:

According to formula (1:11), the relativistic trigonometric relationship applies to an object without vectorial proper motion in particle-field $F_{1\text{-}3}$:

$$c^2 = (c \sin(kt))^2 + (c \cos(kt))^2 = V_4^2 + V_5^2$$

$$\sin(kt) = \sqrt{1 - \cos(kt)^2} \qquad (2.199)$$

In the case of a vectorial proper motion V_3 in the particle-field $F_{1\text{-}3}$, an object such as an invisible photon in **Figure 2.13 on the right** experiences an increased field propagation velocity V_4 in the wave-field $F_{4\text{-}6}$, while the field propagation velocity V_5 decreases relativistically.

The motion sequence of the circular rotation shifts into the dimensional plane D_{45}, resulting in an elliptical trajectory. The total rotational path for one period does not increase. The increasing vectorial component of the rotational path parallel to the fourth dimension reduces the field propagation speed from $V_5 = c$ to $V_5 < c$ and triggers a relativistic time dilation t_{Obj} relative to the nominal time t. This results in a longer period duration, until a complete oscillation period with a maximum orbital velocity of c has been completed. Compared to a less deformed space-time, the perception of time dilation t_{Obj} is possible. The resulting time dilation requires additional energy, which this work performs.

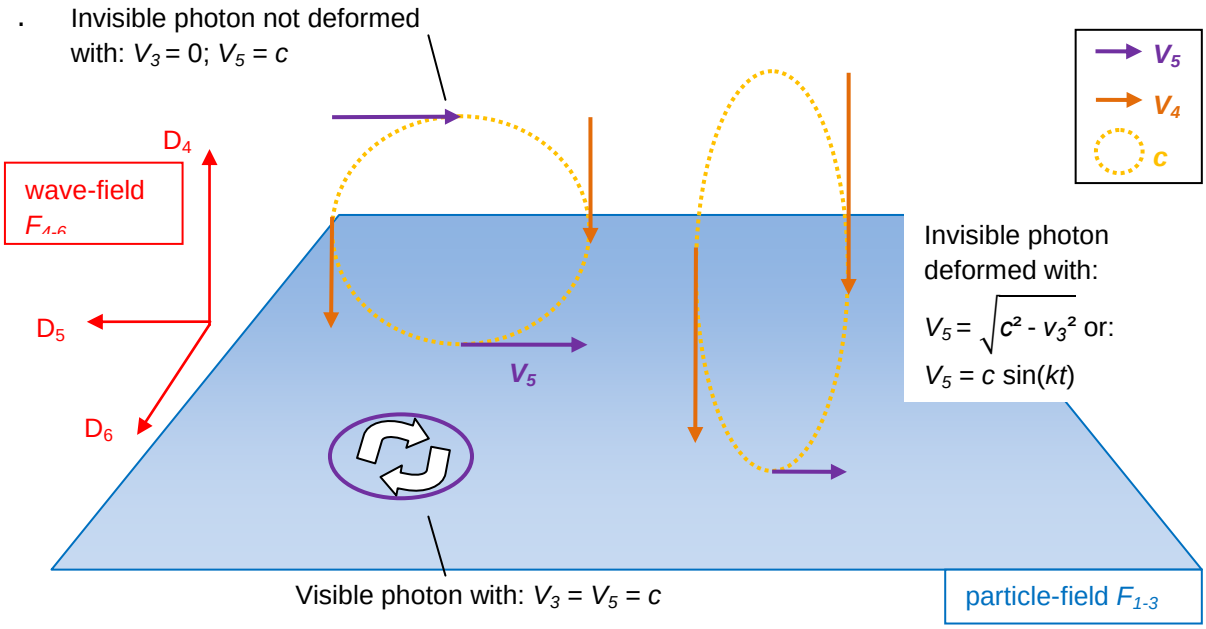

Figure 2.13: Top left: the invisible photon at rest $V_3 = 0$, $V_5 = c$; bottom: the visible photon $V_3 = V_5 = c$; right: the invisible photon in motion $V_3 \rightarrow c$; $V_5 \rightarrow 0$

Space-time has the freedom to deform depending on the elliptical rotation path so that a balance is restored against the space-time mechanical effects (**Figure 2.14**).

For a space-time deformation, the gravitational force is thus represented as a balancing force that requires additional work.

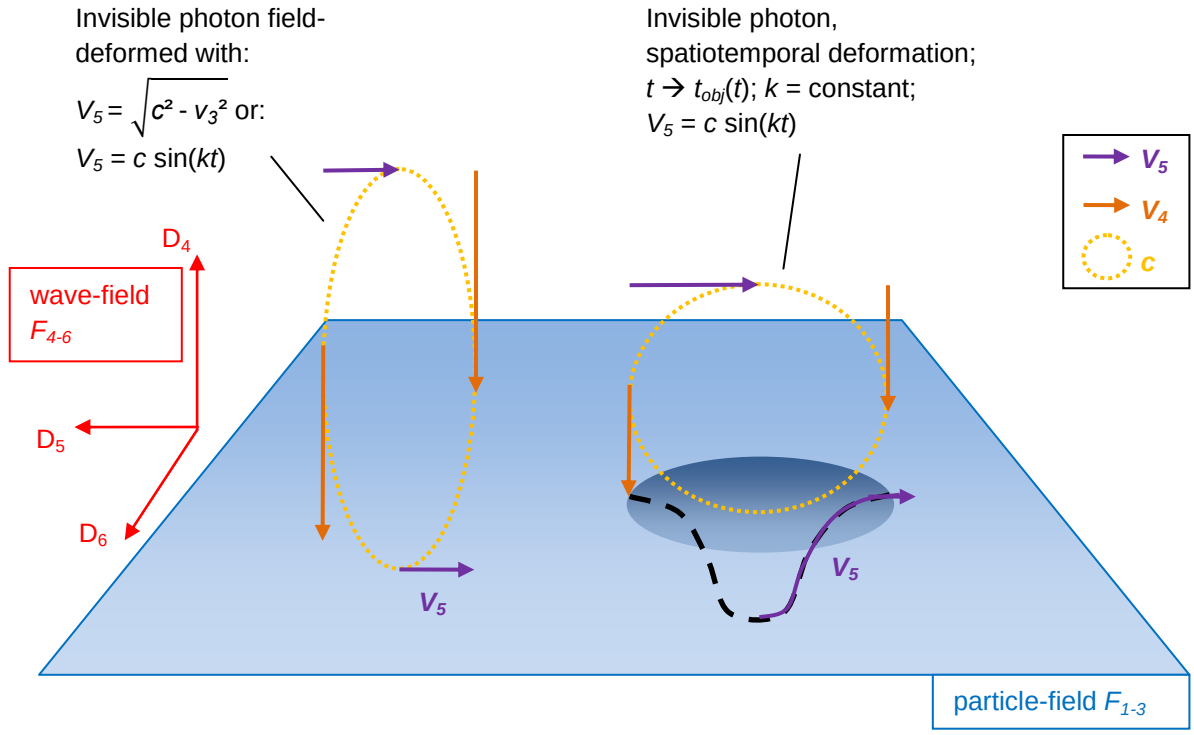

Figure 2.14: Two possible ways of visualising a space-time deformation with its field deformation

Derivation variant 1 – (*r*):

Nominal energy:

$$E_0 = m\,c^2 \qquad \text{with: } c^2 = \frac{G\,M}{r}$$

$$E_0 = \frac{G\,m^2}{r}$$

Relativistic energy:

$$E(t) = \frac{G\,m^2}{r(t)} \qquad \text{with: } r(t) = r\sin(kt)$$

$$E(t) = \frac{G\,m^2}{r\sin(kt)} \qquad \text{with: } r = \frac{G\,M}{c^2}$$

General: $E(t) = m\,c^2\,\frac{1}{\sin(kt)}$; Special: $E(t) = m\,c^2\,\frac{c}{V_5}\;mc^2\,\frac{1}{\sin(\alpha)}$; See also (2.101)

Derivation variant 2 – (t):

For an individual object movement, the force equation is used, which describes the dynamic relativistic field effect between the subspace U and the photon field of the universe:

$$F_{gravity}(t) = m_{Obj}\, r_{obj}\, k_{obj}^2 \frac{1}{\sin(kt)}$$

$$E(\Delta s) = \int_0^{\Delta s} F(t,s) \sin(kt)\, \mathrm{d}s$$

$$E(\Delta t) = \int_0^{Tobj} c\, F(t) \sin(kt)\, \mathrm{d}t = \int_0^{Tobj} m_{obj}\, c\, r_{obj}\, k_{obj}^2\, \mathrm{d}t$$

with: $r\, k = c$; $t_{obj} = \frac{c}{V_5}\, t = \frac{t}{\sin(kt)}$

$$E(\Delta t) = m\, c^2\, k_{obj} \frac{T}{\sin(kt)}$$

For a complete period T, an oscillation with the circular frequency k_{obj} is completed.

$$E(t) = m\, c^2 \frac{1}{\sin(kt)}$$

Derivation variant 3 – (λ), sees the derivation according to equation (2.92):

$$E_0 = m\, c^2 = \frac{h}{2\pi\, c\, R} \qquad \text{with: } 2\pi\, R = \lambda$$

Pure relativistic without periodic perturbation with $\cos(kt = 0° + \beta = 0°)$:

A relativistic contraction of its wavelength in the direction of motion produces a blue shift at the source given by: $\lambda \sin(\alpha)$

$$m(t) = \frac{h}{c\, \lambda} \frac{1}{\sin(\alpha)} = \frac{h}{c\, \lambda} \frac{c}{V_5} \qquad (2.92)$$

Substitute and generalize using $(kt) = \alpha$ provides:

$$E(t) = E(t) = m\, c^2 \frac{1}{\sin(kt)}$$

One consequence of this result is that the matter pulse (**Figure 2.12, right**) is also slowed down relative to the nominal time t and is thus measured at greater time intervals.

For the relativistic consideration of the imulse with a normalized object mass m_{obj}, the same extent of the space-time effect applies:

General: $P(t) = m_{obj} \frac{V_4}{\sin(kt)}$ Special: $P(t) = m_{obj}\, V_4\, \frac{c}{V_5} = m_{obj} \frac{V_4}{\sin(\alpha)}$ (2.104)

Note: In contrast to an invisible photon, a visible photon does not have a field propagation velocity V_4 and is therefore not capable of additionally deforming a space segment beyond the Lorentz transformation by a factor of 1 alone.

From the perspective of the inertial system, a so-called gravitational redshift occurs as soon as an electromagnetic wave moves out of a field-deformed space.

$\lambda_{obj}(t) = \frac{\lambda_{obj}}{\sin(kt)}$ (gravitational redshift) with $\alpha = kt$ (general) (2.200)

$\lambda_{obj}(t) = \lambda_{obj} \sin(kt)$ (gravitational blue shift)

$P = m_{obj} \frac{V_4}{\sin(kt)} = m_{obj}\, V_4\, \frac{c}{V_5}$

$E_{obj}(t) = h\, f_{obj} \frac{1}{\sin(kt)} = m_{obj}\, c^2 \frac{1}{\sin(kt)}$ (2.201)

$E_{obj}(t) = m_{obj}\, c^2 \frac{1}{\sin(\alpha = 90°)}$ for $V_5 = c$; $V_4 = 0$

$E_{obj}(t) = m_{obj}\, c^2 \frac{1}{\sin(0 < \alpha < 90°)}$ for $V_5 \rightarrow 0$; $V_4 \rightarrow c$

A rest mass consists, in total, of several superimposed harmonics in the form of relativistic fields that are in resonance with one another at the point of field exchange. An additional kinetic energy exerts a mechanical effect by causing a longer vectorial path for its relativistic fields in the fourth dimension. Restoring forces following a periodically recurring interaction can also extend the vectorial path parallel to the fourth dimension. Within its existing oscillation (kt) at rest, this leads to additional time dilation and a contraction of its field parallel to the fifth dimension < 1 (see **Figure 2.13, right**). Although the mass appears heavier, only the relativistic fields are deformed along their phase. The additional contraction work performed is ultimately determined by Lorentz invariance for the **Relativistic Energy Gain** precisely via the measurable field deformation with a dynamically contracted field propagation velocity V_5. This expands the classical understanding of **Energy-Mass Equivalence**.

In the field-space model, energy-mass equivalence holds only if the global Lorentz factor is 1. In the case of a relativistic energy gain due to global curvature, an additional gravitational and electric potential is introduced, which extends this equivalence through its global influence. Taking into account a **Relativistic, Global**

Energy Gain, the classical energy-mass equivalence is extended to the so-called **Energy-Space-Time Equivalence**.

Results for the photon model and response to the hypothesis:

The **FSM-GTR** for the 6-dimensional field-space describes the space-time-mechanical effects for both cosmology and the microcosm. Scaling becomes possible only when photons propagate parallel to the dimensional plane D_{56}. It follows that field propagation is slowed down by field deformation. The speed of light for photons is thus determined by the field propagation speed V_5. This confirms the thesis from **Chapter 1** that the speed of light does not have a fixed maximum value, but must be considered relative to the maximum speed $V_{max} = c$. Furthermore, it becomes apparent that relativistic oscillations can be excellently described mathematically using trigonometry. For example, an oscillation ensures a periodically dynamic barrier as a restoring force to stabilize a system from collapse in extreme cases. Furthermore, it is possible for the photon field to define a relativistic, cosmic location for the inertial system. Thus, for any specified physics, a purely geometric relationship between energy and space-time applies. In this model, this relationship is also called **energy-space-time equivalence**.

The geometry of the wave-field allows relativistic effects to be transferred to the microcosm. The present photon model is a purely relativistic representation of space-time, whose geometry describes the state of matter. The FSM derives matter as an emergent product of relativistic fields from the natural space-time geometry. Depending on their geometric position in the wave-field, this model distinguishes between visible and invisible photons or matter. It also provides an explanation for wave-particle duality. The photon model offers an alternative derivation of the equations of force, energy, and momentum compared to the classical model.

Chapter 3 uses the electron and particle model to confirm the geometric conditions of the 6-dimensional field-space by providing a general formula for the mass and frequency of all particles. The theoretical results are then compared with experimental measurements. Finally, the predictions verify the FSM model.

Chapter

3 The Particle model

The particle model builds on the group theory presented in **Chapter 2.2**. The abstract theory is further refined and illustrated with diagrams. The relativistic fields, which are modeled as mathematical rotations, are to be simplified in such a way that precise quantization can be achieved simply by counting ratios. The global influence on matter is neglected in this chapter. Consequently, the optimal configuration is always orthogonal to the dimensional plane D_{56}.

3.1 Coupling of a fion with a particle sphere

This subchapter describes the transition from the state of a single invisible photon to a bundle of temporally synchronised photons rotating within a defined space. These invisible photons take on properties that require an explanation and modelling.

Axiom 13 states that photons only interact electrically with their environment once they exceed a certain **minimum coupling frequency** with $f > f_{min}$. Only then does the invisible photon enter into an electrical interaction with the photon field as a quantum.

Such photons are to be referred to as **fions**. Fions rotate as electromagnetic oscillations in the wave-field $F_{4\text{-}6}$ with the maximum speed $V_{max} = c$, interact with other particles and have an integer spin.

The mass of a single fion is also used to find the minimum coupling frequency at which the photon field can interact with the electron field. In order not to jump ahead, the concrete result will be presented in a later chapter.

Coupling mechanism of a fion with a sphere S:

A photon as a quantum is initially spread across the entire cosmic space. It needs a defined spatial area that spatially separates this photon from another photon. The photon exists in this limited space with a probability of 1. Since a photon is a rotating 4-dimensional hollow body, it makes sense to refer to the assigned spatial area as **sphere S**. Within a 6-dimensional sphere S, the photon is a 4-dimensional subspace of this sphere S. This means that every invisible photon has the possibility of coupling into sphere S when it transitions to a fion, figuratively speaking, of spinning into it. This happens at a much lower orbital velocity than the maximum velocity $V_{max} = c$. During the settling phase (**Figure 3.1)**, space-time mechanical settling forces act between the subspace U of the fion with of the sphere S until the rotation of the sphere S is synchronised each other.

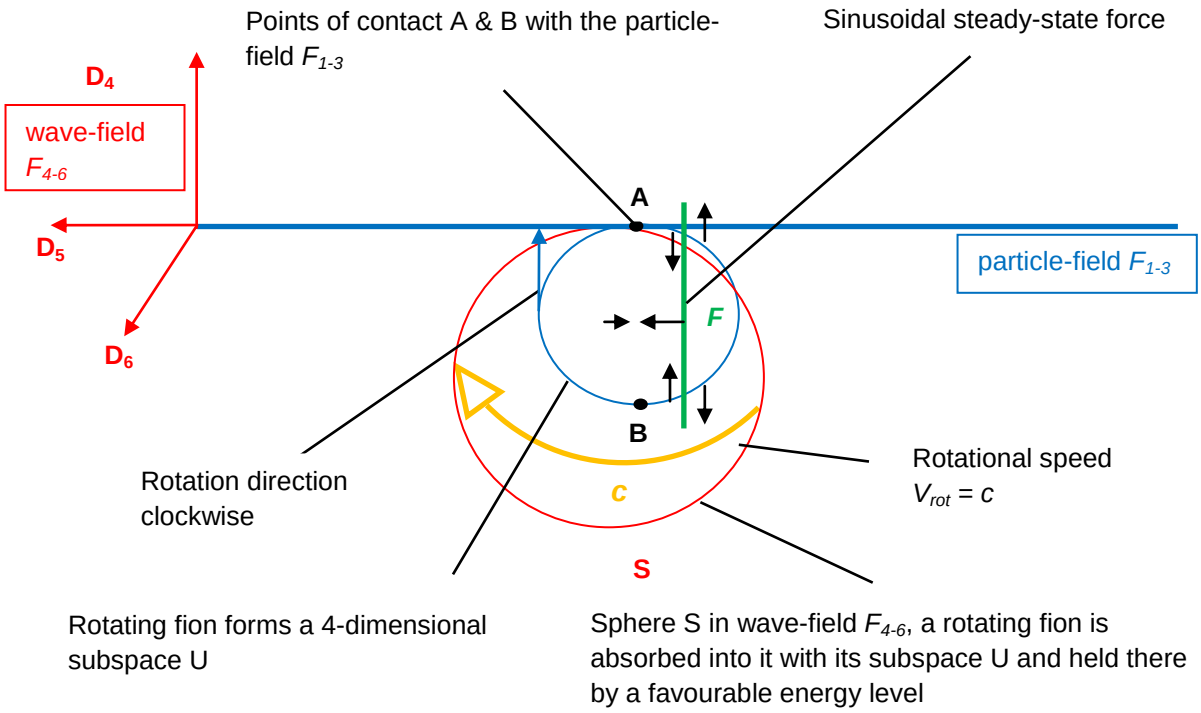

Figure 3.1: Representation of the transient behaviour of a rotating fion with subspace (U) in a sphere (S)

The oscillating forces generate a space-time deformation through interaction. The relevant component of the metric (**Chapter 2.2, Point 1. Metric**) is given by:

$$ds^2 \supset 2(A^a_\mu + \delta A^a_\mu)\, dy_a\, dx^\mu$$

- A^a_μ – vector field in 7D; geometrically, connects the wave-field with the particle-field; after compactification to 4D, it behaves as a gauge potential
- δA^a_μ – possibility of deviation, e.g., due to external disturbance via the particle-field; compensating forces counteract the disturbance
- $dy_a\, dx^\mu$ – geometric transition between the wave-field and the particle-field

After the settling phase, this fion has rotated completely into a sphere space S. The fion and the surrounding sphere rotate synchronously with each other. This means that there are no longer any compensating forces between them. The state is initially stable. This transition is shown in **Figure 3.2**.

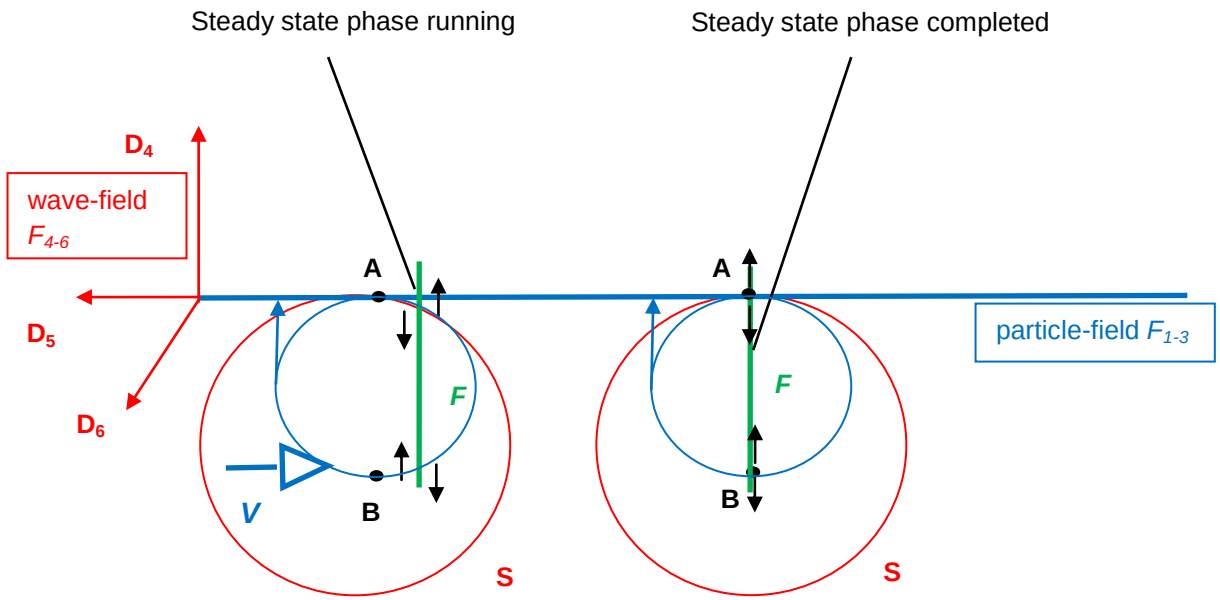

Figure 3.2: Continuation of the settling behaviour until synchronisation between the rotation of the fion and the sphere S

Settling behaviour of several fions in a sphere S:

If the fion is present within sphere S at a certain energy level, destabilising disturbances in the rotation may occur in sphere S after a period *T*. As the fion expands to include two additional fions, the energy in sphere S is distributed among three individual fions. The sphere S grows simultaneously in proportion to the existing spatial structure for three fions. After the energy has been distributed from one fion to several fions, the rotation of the fions stabilises again. Stability means that, during the periodic oscillatory motion of fions, there is a favourable energy for space-time that does not cause any additional space-time deformation. Scalar feedback potentials $V(\phi_n)$ perform this stabilization according to equation (2.96). The set of three fions gives rise to three 4-dimensional rotational paths between the dimensional planes $D_{45/46}$, which are projected onto the $D_{14/24/34}$ planes in the particle-field. The three fiones that have been created rotate within sphere S in their subspaces U on their respective rotational paths, initially

a) without interference,

b) at equal distances from each other, and

c) synchronously at the points of contact.

Note:

a) This applies until a certain amount of energy in this bundle causes a renewed disturbance, leading to a further division of the fions in sphere S.

b) The distance between their rotational paths is evenly aligned. If the angle is smaller or larger due to an external disturbance, space-time-mechanical repulsive compensating forces arise, which restore an even arrangement (marked in green).

c) The temporal synchronisation of the fions at the points of contact in the wave-field $F_{4\text{-}6}$ results in a uniform polarisation of all rotating fions within sphere S. Uniform polarisation in the bundle means uniform transmission of fields into the particle-field $F_{1\text{-}3}$.

Consequently, periodic interference occurs at the points of contact. **Figure 3.3** shows the transient behaviour within the aforementioned bundle of several fions in sphere S. Because of this forming, all fions have electrical potential in the photon field. The electron-internal fions that rotate as a bundle and can generate a partial potential are referred to as electrically **active fions**.

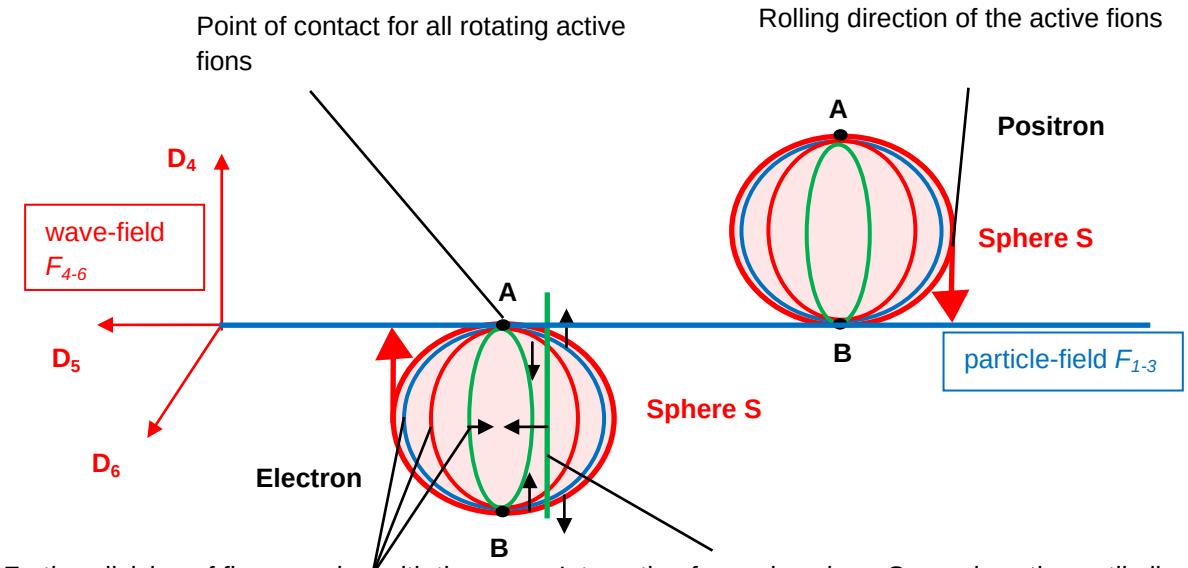

Figure 3.3: Representation of the settling behaviour of several rotating active fions in a sphere S in the wave-field $F_{4\text{-}6}$

Generation of a charge:

Parallel to the fourth spatial dimension D_4, the photon field as a whole has an electric potential in the form of a displacement current. A fionic potential is generated by its periodic electromagnetic rotational motion in the $F_{4\text{-}6}$ wave-field, which possesses a vector in the fourth dimension. The electrostatic separation occurs through the dimension plane D_{56}. This would be comparable to the friction electricity between a synthetic cloth and a plastic rod, known as the triboelectric effect. The three active fione, which can transmit their generated potential to the particle-field $F_{1\text{-}3}$, three via the dimensional levels $D_{14/24/34}$, each emit a **partial charge**. The

magnitude of the **charge Q** is the result of the compactification from 7D to 4D when the phenomena are derived from the particle-field

With rotation **above** the dimension plane D_{56}, there is a positive potential gradient which generates finally a **positive charge** with the active fions, while active fions rotating **below** the dimension plane D_{56} slide down a negative potential gradient and generate a **negative charge**.

A potential difference arises between the active fions, which, once they come within a certain distance of each other, triggers an exchange of electric fields. This would be comparable to an electric arc in high-voltage technology. This process is referred to as **the close-range effect**. The close-range effect is examined in more detail in the section on the interaction between charges. The distance between the electrons is overcome via the **exchange fion**.

Assignment of a charge to the elementary particles:

In this example, the direction of travel of the active fions is represented by a red arrow in a clockwise direction. Points A and B show the common intersection point for all 4-dimensional rotational paths of the active fions within a sphere S. There is a stable **electron** below and a **positron** above the dimension plane D_{56}. If this is the case, then an electron consists of a 5-dimensional periodic hollow body vibration with three 4-dimensional rotational paths, which are occupied by the active fions.

Passive fions and the exchange fion:

If there are active fions that are formed orthogonally to the dimension plane D_{56}, then fions formed parallel to the dimension plane D_{56} should be called **passive** fions. Passive fions lose their polarisation with the remaining active fions when these rotate parallel to instead of orthogonal to the dimension plane D_{56}. In this state, they rotate at the maximum speed $V_{max} = c$ within the sphere S and have an integer spin. Due to their geometrical formation in the wave-field, passive fions also cannot find a rotational path to generate a charge. In this state, they take on the properties of dark matter.

Individual active fions may be able to spontaneously split into a **pair** of **exchange fions** and **passive fions** while maintaining the law of conservation of energy, and then recombine back into an active fion.

The reason for this spontaneous pair formation is the close-range effect between two differently charged particles at a certain proximity, which causes a voltage breakdown. The total momentum for the exchange fion/passive fion pair is $P = P_1 + P_2 = 0$. The respective **exchange fion** is released from the bundle of active fions, which sets their rotational speed to $V_{max} = c$ parallel to the dimension plane D_{56}. The angular momentum P_1 or P_2 thus obtains an integer spin. Depending on the potential difference, the exchange fions rotate along the dimension plane D_{56} towards

the neighbouring particle and recombine with the respective passive fion that remained behind to form a common active fion. During the actual exchange, the exchange fions rotate parallel to the dimension plane D_{56} and have the properties of visible photons. Due to their parallel formation to the dimension plane D_{56}, they have no potential, rotate at the maximum speed $V_{max} = c$ and have an integer spin.

Distinction between fions and gluons :

The term gluon is derived from the English word "glue". In quantum chromodynamics, gluons have the task of "gluing" quarks together in more complex particle structures, such as neutrons or protons. Gluons are therefore responsible for the exchange of interaction forces. This exchange connects two particles with each other and, during the exchange, leads to the interaction properties of the strong nuclear force. With their nuclear forces, they overcome the electrical repulsive forces between protons. Gluons thus hold the atomic nucleus together.

The fion model allows the processes of nuclear forces to be investigated more precisely than with gluons. Fions perform even more far-reaching tasks that go beyond the strong or weak nuclear force. When several active fions are combined, they rotate synchronously with each other as a bundle, forming a periodically oscillating hollow body structure. Individual active fions generate partial charges within an elementary particle relative to the particle-field. Beyond the multiple of an electron fion, the structural integrity of heavier particles begins. These relationships exceed the definition of the gluon to such an extent that they are replaced by fions within the framework of this model.

3.2 The Electron Model

Predicting particle masses requires a scalable multiple of the electron's properties as the fundamental particle with the lowest excitation (**Chapter 2.2, Point 17**).This makes it all the more important to describe the electron as an fundamental particle for all further modelling. The electron belongs to the particle group of fermions. All **fermions** are assigned a spin of $\frac{1}{2}$.

According to the FSM model, electrons, positrons and neutrinos are no longer point particles, as classical physics suggests. Rather, depending on their complexity, they consist of a hollow body vibration in a 6-dimensional field-space, in which three active fions rotate on their three 4-dimensional rotational orbits. There is always only one point of contact for the particle in the dimensional plane $D_{56,}$ in which a field from the wave-field $F_{4\text{-}6}$ can be periodically exchanged into the particle-field $F_{1\text{-}3}$. The fact that the electrons in the particle-field are registered as point particles can be attributed to the fact that the formation is orthogonal to the dimension plane D_{56} and its field is only emitted periodically at a point of contact in the particle-field from a bundle of active fions. The field exchange appears in the particle-field as a rapidly pulsating point source for its field force.

Formation of equal numbers of electrons and positrons :

Taking energy conservation into account, fions always occur in pairs and have their formation in the fourth dimension below and above the dimension plane D_{56}. For reasons of energy conservation, this means that for every active fion rotating above, there must also be an active fion below the dimension plane D_{56}. The spheres S, which carry a bundle of active fions **below** the dimension plane D_{56}, are identified with the known **electron**, while **positrons** rotate mirrored **above** the dimension plane D_{56} with a bundle of active fions. There must therefore be the same number of positrons for a given number of electrons.

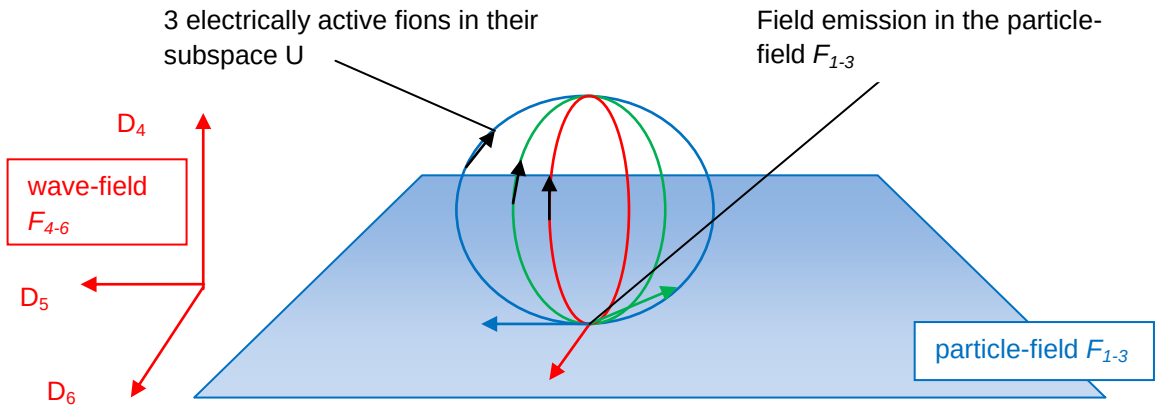

Figure 3.4: A positron rotates orthogonally to the dimension plane D_{56} and exchanges its field at the point of contact with the particle-field $F_{1\text{-}3}$

Figure 3.4 shows a positron consisting of three active fions, each of which projects a partial electric charge of $Q = +\frac{1}{3}\,e$ into the particle-field. A charge Q^+ or Q^- depends on its position relative to the dimension plane D_{56} whether it rotates below as an electron or above as a positron.

Extension of the electron sphere with a fourth and fifth active fion:

In **Figure 3.5**, the electron is shown below and the positron above, orthogonal to the dimension plane D_{56}. The dimension planes D_{45} and D_{46} enable the electron sphere to provide, in addition to the three already formed active fions, further rotating 4-dimensional orbits for active fions within sphere S. In this case, a fourth and fifth active fion are created. For reasons of energy conservation, each of the three active fions in the electron must transfer a portion of its energy equal to $\frac{1}{12}$ to a fourth active fion. Accordingly, each of the four active fions must transfer a portion of its energy equal to $\frac{1}{20}$ to a fifth active fion.

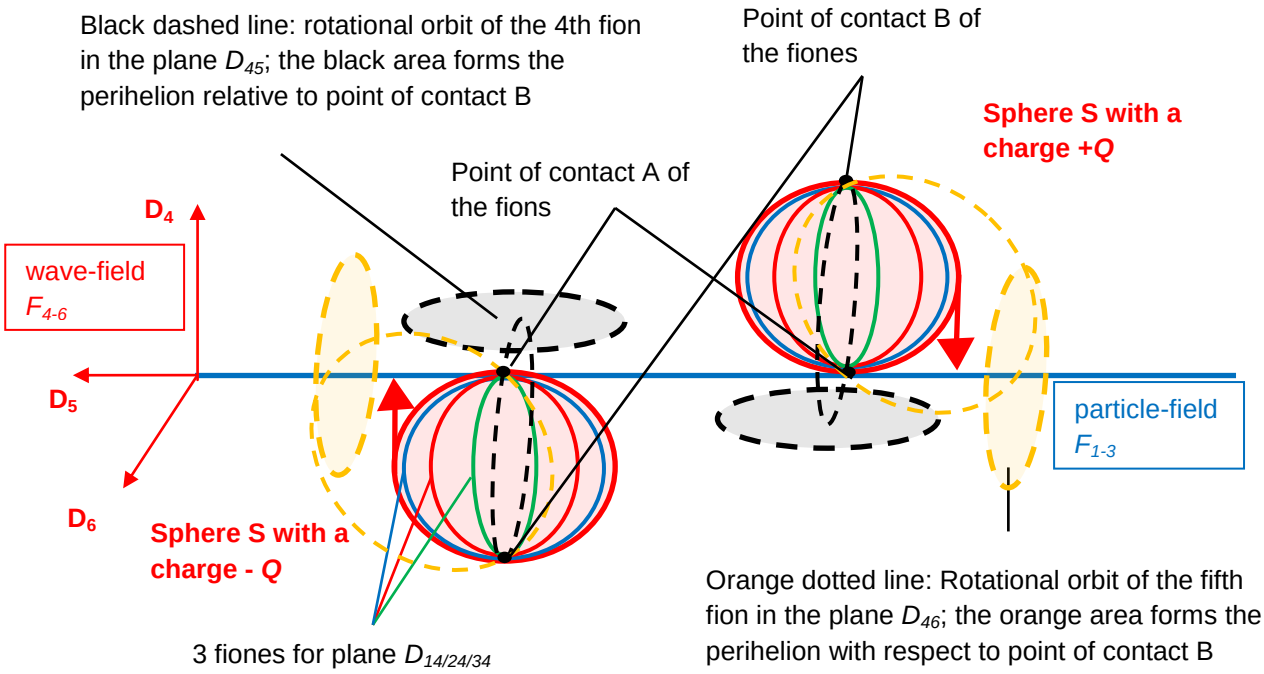

Figure 3.5: Representation of a positively and negatively charged particle in the wave-field $F_{4\text{-}6}$ with the occupation of a fourth and fifth fion

The fourth and fifth fion partially rotate outside sphere S along elliptical paths, because sphere S can hold only three 4-dimensional rotational paths that interact with the particle-field $F_{1\text{-}3}$ in the dimensional planes $D_{14/24/34}$. The total charge can still only consist of **three partial charges**. The additional active fions contribute by dividing the total mass not only into thirds, but also into quarters or fifths. The fourth fion is shown in black and rotates in the dimensional plane D_{45}, while the fifth fion is outlined in orange and rotates in the dimensional plane D_{46}. This means that

individual particles can basically contain up to five active fions if all six spatial dimensions are included.

The electron is the simplest charged elementary particle and contains all three partial charges. Depending on the charge fractions rotating in the sphere S in its subspaces U, their active fions contribute to the total charge registered in the particle-field $F_{1\text{-}3}$ with:

$$Q = N_{aF}\frac{e}{3} \qquad N \varepsilon \mathrm{N} \qquad (3.01)$$

Q – electrical charge with $[Q]$ = As = C

e – electric charge of the elementary particle electron

e = 1,6022 10^{-19} C

N_{aF} – number of active fions along to the rotation planes $D_{14/24/34}$

Electron structures with three active fions provide the lowest and most favored energy states, which is why these are probably the most common in nature. Higher energy states resulting from modeling the electron with a larger number of active fions within its sphere S, on the other hand, are likely to be less common in nature.

Side Note: Quark Charge:

Quark types arise from an initial electron structure with varying numbers of active fions. Quarks never exist as isolated particles. In the FSM, they are part of a boson composed of a quark and its exchange particle. The exchange fion is created by the reduction of an active fion in the electron, which carries a partial charge in the particle-field.

$$Q = \pm(3 - N_{F/A})\frac{e}{3} \qquad (2.151)$$

- Q – total load, unit: C; results in a fractional charge
- $\frac{e}{3}$ – one-third of the base load; unit: C; one-third of the 3D wave-field (SU(3)) symmetry, implicitly
- $N_{F/A}$ – Number of active fions resulting from conversion into exchange fions or passive fions, or those that do not generate a potential in the wave-field relative to the dimensional plane D_{56}

Rotational speed of active fions:

The fiones in the subspaces require a period $T > 1$ to rotate to the common point of contact in order to occupy a favourable multiple of the comprehensive frequency. Otherwise, they would rotate at a maximum speed of c with a possible variance of $V > c$. Therefore, the speed must be a multiple smaller than the maximum possible orbital speed. The smallest possible and fastest recurring period for all fions would be period $2T$, followed by $3T$, etc. Assuming that the subspaces allow a maximum number of contacts per period, only contacts with a maximum period of $2T$ are possible. For the combination of several fions, this means that the individual subspaces U within the sphere S have a maximum orbital velocity of $V_{rot} = \frac{c}{2}$. With regard to the respective subspace in the wave-field $F_{4\text{-}6}$ and the particle-field $F_{1\text{-}3}$, trigonometry yields a resulting velocity of

$$V_{rot}^2 = V_{14}^2 + V_{24}^2 + V_{34}^2 \qquad (3.02)$$

V_{rot} – resulting rotational velocity of the bundle from active fions in sphere S

$V_{14/24/34}$ – speed of active fions along their respective 4-dimensional rotational paths in the dimension planes D_{14}, D_{24}, D_{34}.

With respect to the respective subspace in the wave-field $F_{4\text{-}6}$ and the particle-field $F_{1\text{-}3}$, the trigonometric calculation provides a resulting rotational speed for an electron of

$$V_{rot}^2 = (\frac{c}{2})^2 + (\frac{c}{2})^2 + (\frac{c}{2})^2$$

$$V_{rot} = \frac{\sqrt{1^2 + 1^2 + 1^2}}{2}\, c = \frac{\sqrt{3}}{2}\, c$$

for periodic contact at location A or B. With four subspaces in sphere S relative to the particle-field $F_{1\text{-}3}$, this would be $V_{rot} = \frac{\sqrt{4}}{2} c$ and theoretically $V_{rot} = \frac{\sqrt{5}}{2} c$ for the fifth subspace. Since the rotational speed $V_{rot} = \frac{\sqrt{5}}{2} c > c$, the rotation will either occur at the speed $V_{rot} = \frac{\sqrt{5}}{3} c$, or the rotation will only take place in four subspaces. As will be shown, a dimension reduction factor applies in these cases, which has the task of continuing to enable the rotation of five partial charges in the 6-dimensional space with $V_{rot} = \frac{c}{2}$.

Establishing the ground state for the electron:

After a field exchange, a field can only influence the particle-field $F_{1\text{-}3}$ if the velocity of the emitted field is greater than its intrinsic velocity. The optimal situation would therefore be a vector rest position of the electron, so that its field in the fifth

dimension can be emitted at the maximum velocity $V_{max} = c = V_5$. In order to establish the aforementioned resting state in the wave-field $F_{4\text{-}6}$, the sphere S also rotates mechanically at a maximum rotational speed of $V_{rot} = \frac{c}{2}$ orthogonal to the dimension plane $D_{56.}$ This ensures two independent rotation matrices on the dimension planes with $\overrightarrow{e_6}\,\mathrm{d}D_4\mathrm{d}D_5 = \overrightarrow{\mathrm{d}A} = D_{45}$ and $\overrightarrow{e_5}\,\mathrm{d}D_4\mathrm{d}D_6 = \overrightarrow{\mathrm{d}A} = D_{46}$, whereby the point of contact between A and B changes every period T. The fions rotating in sphere S therefore change direction every period T. On average, the following applies for periods $2T$:

$$\frac{\sqrt{3}}{2}c - \frac{\sqrt{3}}{2}c = 0 \qquad (3.03)$$

The stationary electron is now modelled between the reference fields $F_{1\text{-}3}$ and $F_{4\text{-}6}$. A field can then be exchanged with the maximum speed $V_{max} = c$.

The periodic change of the points of contact determines the spin direction of the particle. With an odd number of fions within the sphere S, this can be either $+\frac{1}{2}$ or $-\frac{1}{2}$. The axioms for rotating photons are considered to be fulfilled, since all three fions in an electron meet at a maximum of two periods T at a point of contact A and B.

Note:

The change in spin direction for an elementary particle with $V_{rot} = \frac{c}{2}$ occurs so quickly that it would be misguided to predict a specific spin state at a specific point in time on a macroscopic level. However, the phenomena of entanglement apply (**Chapter 2.2, Point 18, Spin-0-Pair Theory**).

Angular momentum and spin of the electron :

The angular momentum of particles is also called "spin". It is determined in units of Planck's constant h divided by the maximum angle measure of 2π. A photon thus has a maximum angular momentum of $L_{Max} = \frac{h}{2\pi}$. Its spin is an integer for 2π. For all particles, the result of the spin is important, whether it is half-integer or integer. This determines whether the Pauli principle applies to the particle or whether particles are allowed to interfere. The Pauli principle will be discussed in more detail in the section on interaction properties between differently charged particles. In the Standard Model of particle physics, certain particles are defined as having half-integer spin and are subject to this Pauli principle.

A single freely rotating fion, such as the exchange fion, rotates outside an electron sphere at the maximum speed $V_{max} = c$, while the rotational speed of an active fion as a partial charge within an electron sphere is limited to a maximum of $V_{rot} = \frac{c}{2}$. A complete periodic rotation of an active fion around its own axis therefore takes twice as long as that of an exchange fion. This results in an angular momentum for each

active fion in the electron with $L_{fion} = \frac{h}{4\pi}$. According to the conservation of angular momentum, the total angular momentum is composed of all individual angular momenta. This is determined with respect to the particle-field $F_{1\text{-}3}$ using Pythagoras' theorem. If the angular momentum is determined to be a half number, this also applies to its spin. The same applies to the integer case.

$$L_{n\ fions}{}^{2} = \sum_{0}^{n} \left(\frac{h}{4\pi}\right)^{2}_{n} \qquad n \in \mathbb{N} \qquad [L] = Js \qquad (3.04)$$

The spin for three fions involved is determined as a half-integer via the resulting angular momentum:

$$L_{3fions}{}^{2} = \left(\frac{h}{4\pi}\right)^{2}_{fion1} + \left(\frac{h}{4\pi}\right)^{2}_{fion2} + \left(\frac{h}{4\pi}\right)^{2}_{fion3}$$

$$L_{3fions} = \frac{\sqrt{1^2 + 1^2 + 1^2}}{4\pi}\, h \qquad \rightarrow \text{half-integer}$$

L_{3fions} – angular momentum for three active fions

Index $_{fion1/2/3}$ – stands for the individual active fion

h – Planck's constant

$$L_{4fions} = \frac{\sqrt{1^2 + 1^2 + 1^2 + 1^2}}{4\pi}\, h \qquad \rightarrow \text{integer}$$

$$L_{5fions} = \frac{\sqrt{1^2 + 1^2 + 1^2 + 1^2 + 1^2}}{4\pi}\, h \qquad \rightarrow \text{half-integer} \qquad \text{(see note)}$$

Note: Group theory (**Chapter 2.2, Point 15**) uses examples from geometry to explain why fermions must always have half-integer spin.

This model makes it possible to predict the half-integer spin of fermions and the integer spin of bosons.

Temporary incorporation of external fions into the electron sphere:

It is very likely that there is an indefinite amount of free active fions that have exceeded the minimum coupling frequency but do not have enough energy to expand into an electron. These fions require interference with other fions in order to obtain sufficient energy for an electron structure. Such fions could temporarily transition into an electron sphere with a suitable resonance frequency. When operating at a suitable resonance frequency, such fions are capable of forming a temporary bond with an electron sphere.

The mechanical process could occur as shown in **Figure 3.2**. Since the electron seeks the favourable state as an elementary particle with only three active fions within its bundle, the absorbed external fion does not become part of the bundle and does not form any further partial charge within it, but is released again after a short time. The time span of synchronisation with the rest of the fion bundle is not bound to the period 2*T*. During this time, the mass of the electron has nevertheless increased with this additional external fion. It cannot be ruled out that such a fion reception could not also take place twice at the same time. This property is particularly important for the structure of particles. In this situation, the electron receives a short-term integer spin via the resulting angular momentum to the outside, as if it consisted of four active fions.

Visible and hidden particles:

The **visible particles** refer to coupling, **registering matter** that has a common point of contact for the above-mentioned bundle of fions exactly in the dimension plane D_{56} and thus convey a registering field *T*-periodically into the particle-field $F_{1\text{-}3}$. The synchronous rotation of such a bundle of fions is shown in **Figure 3.6 on the left** as a positron.

Hidden particles belong to the group of coupling, **hidden matter** and are attributed to fions and bundles of fions as shown in **Figure 3.6 on the right**. These exhibit a deviation with a deviation angle β, such that the rotation at the point of contact with the dimensional plane D_{56} is $\cos(kt + \beta)$. They exchange their fields either via a weak interaction or not at all. Nevertheless, it is important to take their existence into account, because according to the FSM, more complex particles such as the neutron do interact with hidden matter. As will be explained in detail in the next chapter, the hidden particles are the presumed reason for the limitation of the number of neutrons in an atomic nucleus.

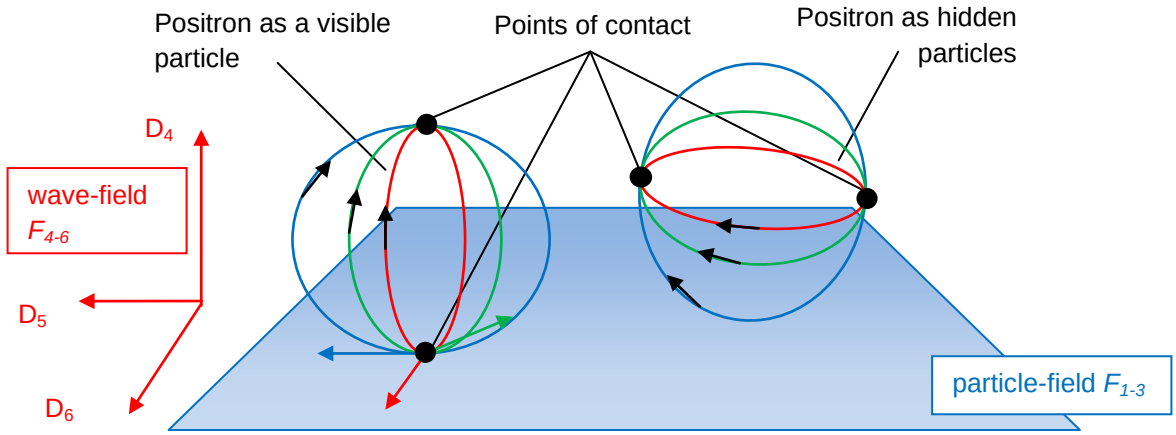

Figure 3.6: Left: Formation of the positron with a common point of contact on the dimension plane D_{56}; right: the points of contact of the positron are not in the dimension plane D_{56} on

Number of possible 4-dimensional rotational paths:

Taking into account visible and hidden matter, we will now investigate how many different 4-dimensional rotational orbits the fions can occupy. The common field body of the sphere S in the wave-field $F_{4\text{-}6}$ has a maximum adhesion of two spatial dimensions for fions with 4-dimensional subspaces. For fions in the field $F_{1\text{-}3}$ there are at least two spatial dimensions. **Table 3.1** provides an overview of all possible combinations that lead to 4-dimensional rotational orbits.

Dimensions / 4-dim. rotational orbits	field $F_{1\text{-}3}$			field $F_{4\text{-}6}$		
	D_1	D_2	D_3	D_4	D_5	D_6
1	X	X	X	X	/	/
2	X	X	X	/	X	/
3	X	X	X	/	/	X
4	X	X	/	X	X	/
5	X	/	X	X	X	/
6	/	X	X	X	X	/
7	X	X	/	X	/	X
8	X	/	X	X	/	X
9	/	X	X	X	/	X
10	X	X	/	/	X	X
11	X	/	X	/	X	X
12	/	X	X	/	X	X
13	X	I	/	X	X	X
14	/	X	/	X	X	X
15	/	/	X	X	X	X

Table 3.1: Shows a 6-dimensional field matrix for all possible 4-dimensional rotation paths in R^6

"X" means the spanning of a 4-dimensional subspace U, while "/" means that no spatial direction is spanned for this dimension. Blue: the visible matter in the field $F_{1\text{-}3}$ as a transverse wave (1-3) and a longitudinal wave (4-6); Green: uncharged exchange fions interacting with the field $F_{1\text{-}3}$ and $F_{4\text{-}6}$; Grey: the hidden particles in the field $F_{4\text{-}6}$.

Theoretically, 15 different 4-dimensional rotational orbits would be available in a 6-dimensional space with one intersection point at one location. Nine of these are exchange fions that have their intersection in 2 dimensions in the field $F_{1\text{-}3}$ and $F_{4\text{-}6}$. Three 4-dimensional rotational orbits are attributable to fions that have a 3-dimensional intersection with the reference field $F_{1\text{-}3}$, and three further 4-dimensional rotational orbits are attributable to photons that have a 3-dimensional intersection with the reference field $F_{4\text{-}6}$.

Figure 3.7 shows the result of this investigation, which consists of the different positions of the rotational orbits with different interactions. Six 4-dimensional rotational orbits correspond directly to visible particles. Three further inactive exchange fions can interact with both visible matter and hidden matter. Six further rotational orbits correspond to hidden particles that exist exclusively in the wave-field $F_{4\text{-}6}$.

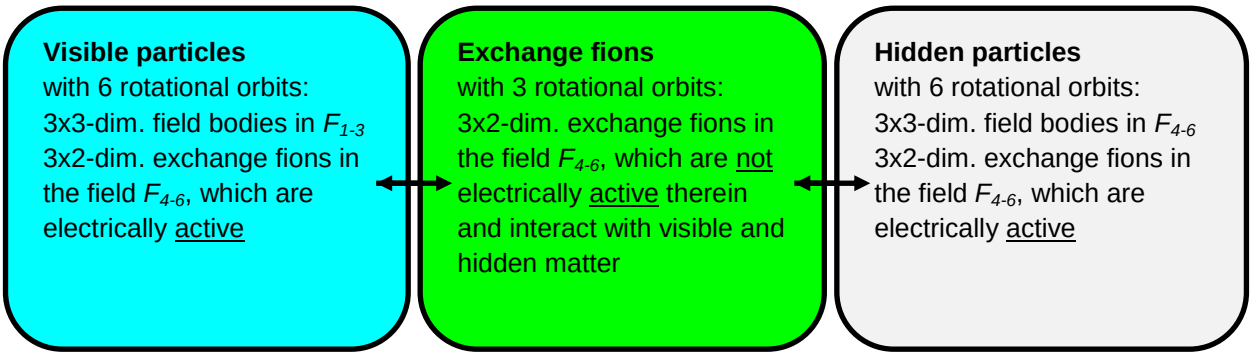

Figure 3.7: Distribution of the 15 x 4-dimensional rotational orbits in R^6

The 6-dimensional space structure can be used to model numerous of particles, including those that interact with hidden particles.

Interaction between charged particles:

The total charge of an electron consists of three active fions with their respective partial charges of total:

$$Q = 3 \cdot \frac{1}{3} e.$$

Several charged particles can encounter each other within the energetic influence of atomic nuclei. In such cases, an electron in the relative proximity of another particle is able to provide one of its third charges $Q = \frac{e}{3}$ as an exchange fion by

splitting an active fion into an exchange fion/passive fion pair. Due to their unsuitable position in sphere S, the remaining passive fions continue to rotate at maximum speed $V_{max} = c$ without any potential. The exchange fions are available for exchange with another particle. An active fion with a partial charge $Q = \frac{e}{3}$ is now missing from the total charge of the particle. The respective exchange fion is released in order to exchange fields. The exchange fion can migrate with the property of a free fion outside sphere S along the dimension plane D_{56} to the next point of contact with the neighbouring particle at the maximum speed $V_{max} = c$. During the actual rotation, the exchange fion cannot emit any fields into the particle-field $F_{1\text{-}3}$ that would be greater than its own speed due to its rotational speed of $V_{max} = c$. The exchange fion thus behaves like a visible photon along the path to be traversed. With the absorption of the exchange fion into the receiving particle at the point of contact, the transition from free rotation at the maximum speed $V_{max} = c$ to feedback to a total charge occurs by resetting itself to the speed of $V_{rot} = \frac{c}{2}$. The reset of the exchange fion takes place at a multiple resonance frequency of the actual particle. The respective exchange fion and the respective remaining passive fion recombine in the respective electron to form an active fion again. The matter pulse for the electron with $P = M_e\ c$ is transferred to the particle-field exactly during this reset.

Since the circular frequency k and the maximum velocity $V_{max} = c$ remain invariant during a field deformation, the parameter for the field propagation velocity V_5 in space-time must decrease in opposition to this reset in order to absorb the momentum P with a larger field propagation velocity V_4. The mediated interaction fields and masses increase their magnitudes to a multiple factor for the required resonance frequency between the exchange fion and the electron. A particle such as the electron obtains its characteristic mass and the strength of its specific interaction field. This process always takes place during the exchange of interaction fields between particles and is examined in more detail in **Chapter 3.4** with the *particle-exchange fion-particle-coupling*.

The Pauli principle of Quantum Mechanics states that two fermions – particles with half-integer spin – cannot be in the same place at the same time (exclusion principle). In FSM, this principle is specifically traced back to the dimension-dependent exclusion conditions for an intersection of several 4-dimensional subspaces in the field-space. Two fermions with the same spin occupy six 4-dimensional subspaces at the same intersection point, which results in an overshoot of the natural geometric limit.

The close-range effect in the FSM model corresponds to Michael Faraday's definition. Applied to the field-space particle model, it means that space itself can trigger an interaction with the presence of particles. The fion exchange begins between charged particles whose fields come close enough to influence each other. The process could occur, for example, like an electric arc between two charged spheres in high-voltage technology, which are connected to each other by their

electric field. In the $F_{4\text{-}6}$ wave-field, all particles are interconnected by the surrounding photon field. When particles come within a certain proximity to one another, an electrical potential equalization occurs, which is registered as an interaction within the particle-field. Like the surrounding photon field, the exchange field is also electromagnetic. The triggering of equipotential bonding with the help of an exchange fion begins with the distance between the particles, which ensures that after the exchange fion arrives at the receiving particle, its active fions are also at the point of contact in order to interfere with it. In accordance with quantum principles, the distance between the particles is assumed to be a multiple of its wavelength of $\frac{\lambda}{2}$. Of particular interest are cases involving more complex particle structures, which require a much smaller wavelength and a much earlier onset of interaction.

Depending on the electromagnetic wavelength of the exchange fion, which recombines in the wave-field $F_{4\text{-}6}$, two-dimensional fields are transmitted via the matter pulse into the particle-field $F_{1\text{-}3}$, which the observer registers as an electric field or strong/weak interaction.

Note on the following illustration:

The real rotation of exchange fions takes place parallel to the dimension plane D_{56}. This is difficult to illustrate. For illustrative purposes, the exchange fions are therefore shown as well orthogonal to the dimension plane D_{56}.

Particles with unequal charges attract each other, if

a) their exchange fions rotate in the similar direction and can merge with the respective recipient particle, and

b) the active fions of both particles rotate in the same direction above and below the dimension plane D_{56}.

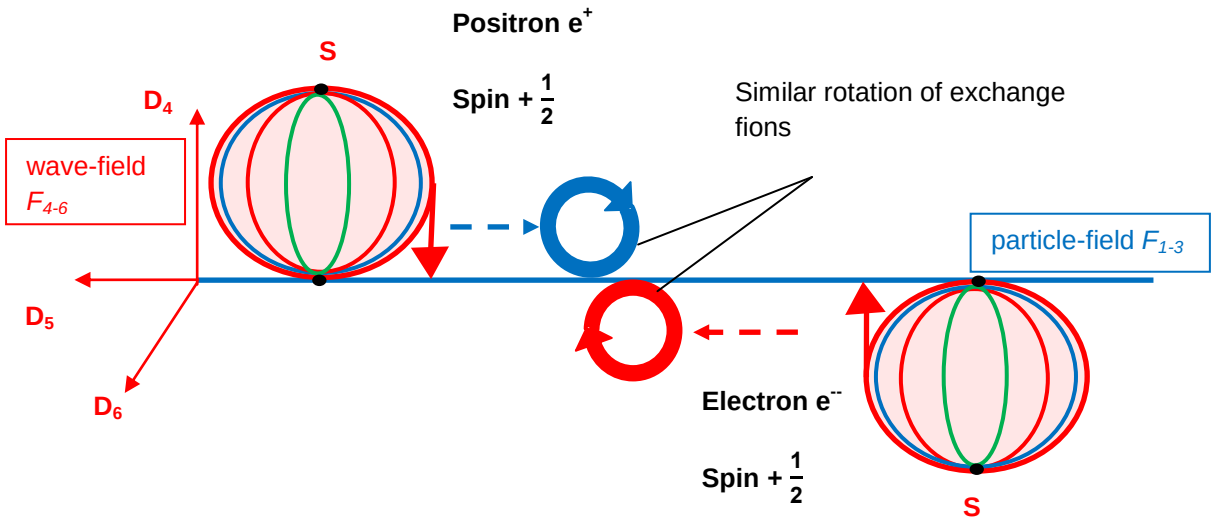

Figure 3.8: The interaction in the case where particles with opposite charges and the same spin attract each other

Particles with the same charge repel each other, if

c) the exchange fions rotate differently and thus ignore each other, and

d) the active fions rotate in the same direction with their subspaces in the sphere S.

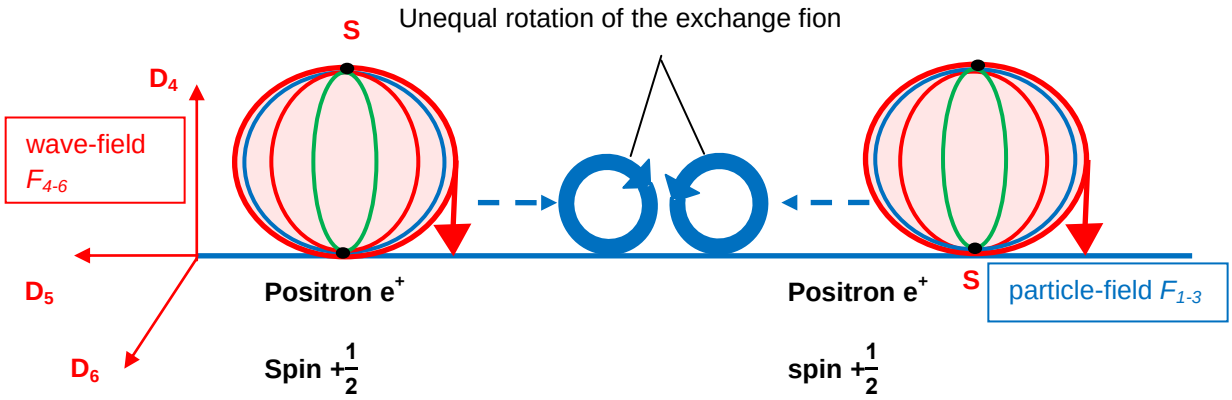

Figure 3.9: The interaction in the case where particles of the same charge and spin repel each other

The repulsion is caused by the fact that sphere S cannot accommodate any further three active fions in the same direction of rotation in its existing spatial dimensions. Otherwise, the particle would have six 4-dimensional rotational paths at one location, which would require a seventh spatial dimension. In this model, the limited number of dimensions is the reason for the effect of the Pauli principle.

Particles with the same charge can ignore each other, if

e) the exchange fions rotate differently and thus ignore each other, and

f) all active fions of the respective other particle rotate in opposite directions at one location with their subspaces U. Thus, in a sphere S, the condition would be fulfilled at every location that fewer than six active fions rotate in one direction within an overlap zone.

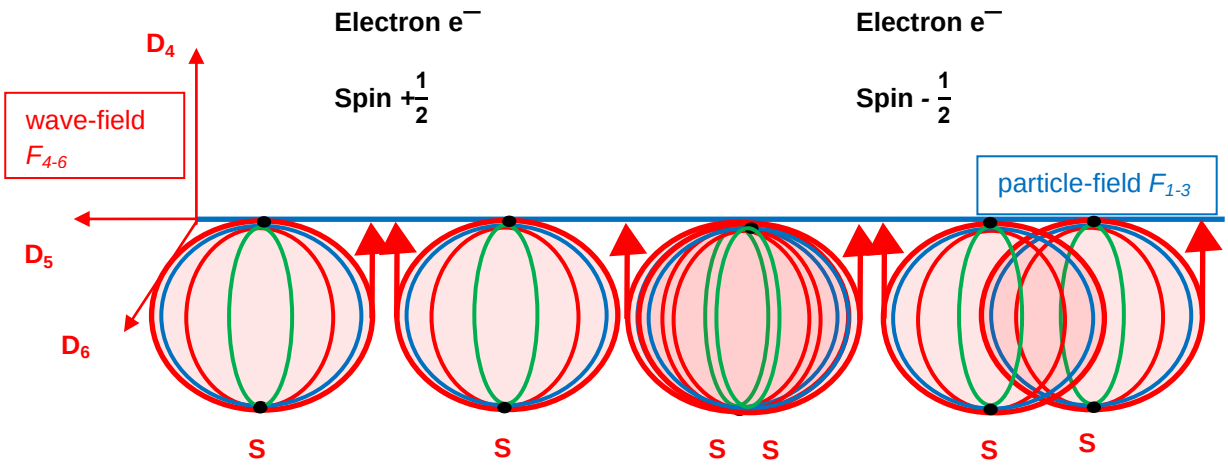

Figure 3.10: The interaction in the case where particles with the same charge but different spins ignore each other

As described above, the spin of the electron will assume a spin of $\pm\frac{1}{2}$. When electrons with different spins occur, they simply pass each other because they do not exert any attractive or repulsive forces on each other. In such an overlap zone with oppositely rotating fions in the particle spheres, the Pauli principle is not violated.

Annihilation reaction:

A destruction reaction requires a specific spatial structure between two differently charged particles. The active fions from an electron rotate below and the active fions from a positron rotate above the dimension plane D_{56} so that a fion exchange can take place. The rotation of their spheres S takes place antiparallel to the dimension plane D_{46}. These two particles come too close to each other and meet at their respective points of contact in such a way that their fions are exactly or almost in phase at the respective points of contact, see **Figure 3.11 on the left.** The contact between the two particles triggers a direct field exchange of the respective exchange fions and stops any further movement in the wave-field $F_{4\text{-}6}$. On average, both particles are at rest relative to each other and no longer require any further orthogonal shaping to the dimension plane D_{56} in order to exchange their fields beyond the short-range effect. The more precisely the individual active fions face each other, the more perfectly they synchronise their movements, which cancels out their respective orthogonal shaping to the dimension plane D_{56}. Both particles now tangent the dimension plane D_{56} (take a view at **Figure 3.11 on the right**).

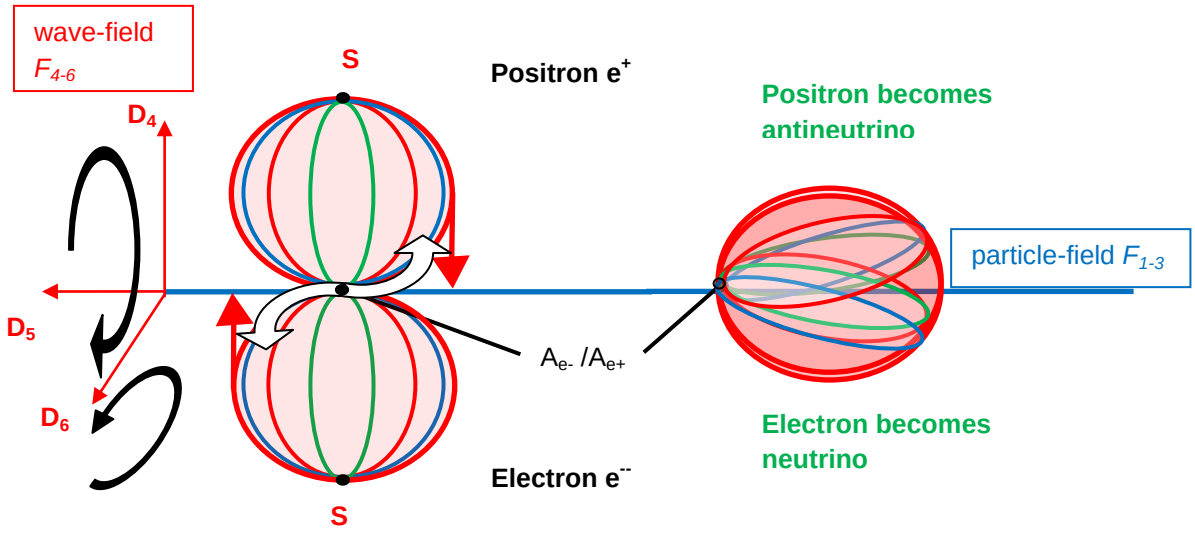

Figure 3.11: Pair annihilation reaction of electron and positron

The conservation of angular momentum requires that the final product has the same angular momentum as the initial product.

In case A, the electron and positron rotate in exactly the same phase. Both reach the dimension plane D_{56} simultaneously and touch each other at one point. As a result, all fions superimpose to form a large rotating unstable photon, which, due to the available space, finds itself at this location with too much excess energy. This leads to a fluctuation, which emits its energy to the environment. Photons with integer spin are generated, which contain the energy of both particles. Due to their formation parallel to the dimension plane $D_{56,}$ these photons are registered as visible photons in the particle-field F_{1-3}.

Case B occurs during contact between the particles due to a slight phase shift between the fions. There is only one common point of contact between all fions on the dimension plane D_{56}. In this case, the sphere S of both particles can remain intact because no permanent fusion takes place. Although both particles can behave like a photon with minimal decelerating effect in the entire field-space, additionally they have lost their charge properties due to their lack of orthogonal formation in the wave-field F_{4-6} to the dimension plane D_{56}. No more charge is generated. This reaction transforms the electron into a neutrino and the positron into an antineutrino, which, like photons, travel at the field propagation speed $V_3 = V_5 = c$ without potential in the particle-field F_{1-3} (**Figure 3.11** shows case B).

Matter pulse :

The matter pulse is a mechanism for modelling several processes occurring simultaneously. It is of particular interest for technical applications. It describes the process of periodic field exchange during an interaction between the wave-field $F_{4\text{-}6}$ and the particle-field $F_{1\text{-}3}$, which takes place in the dimensional plane D_{56}. In this process, the particle-field absorbs this matter pulse in the form of, for example, electrical pulses. The term 'matter' is therefore used to symbolise that an invisible interaction from the wave-field $F_{4\text{-}6}$ leads to a detectable field force in the particle-field $F_{1\text{-}3}$. Once separated, fields retain their form. This gives rise to the discrete state of objects as field-compressed entities. A particle appears as matter, although it is in fact a two-dimensional hologram.

The 'pulse' describes the periodic repetition over time of the transmission of fields into the particle-field $F_{1\text{-}3}$. In the process, the active fions T transition periodically, for a very brief moment, to an energetically favoured state at intervals equal to a multiple of their wavelength ($\lambda \sim 0$); they then separate again and continue to rotate. From the perspective of the particle-field $F_{1\text{-}3}$, only a point source is detected, from which a 2-dimensional field emanates like a longitudinal wave. As this matter pulse has a frequency in the exa-Hz range (**Chapter 3.5**), the observer perceives the matter pulse as a constant field source. Modelling of the matter pulse can, for example, be used for the technical generation of plasma.

In the microcosm, the metric vector component is dominant:

$$ds^2 \supset [\frac{G\,M}{c^2\,r}\,(1 + \cos(kt + \beta))\,(c^2\,dt^2 + dx^2 + dy^2 + dz^2)] + 2(A_\mu^a + \delta A_\mu^a)\,dy_a\,dx^\mu$$

- $dy_a\,dx^\mu$ – is, in metric terms, the transition between the wave-field and the particle-field

The wave equations (**Chapter 2.2, Point 11**) provide the following components, which describe the matter pulse as a wave with all its degrees of freedom:

The transverse wave (2) remains with: $h_{\mu\nu} = 0$ Masse = 0

Transverse vector wave (6): $\square_{(4)}\,A_\mu^a - \partial_\mu\,(\partial^\nu\,A_\nu^a) + 4\pi^2\,m_a^2\,\frac{c^2}{h^2}\,A_\mu^a = 0$ massive

Longitudinal vector wave (3): $\square_{(4)}\,A_\mu^a - \partial_\mu\,(\partial^\nu\,A_\nu^a) + 4\pi^2\,m_a^2\,\frac{c^2}{h^2}\,A_Z^a = 0$ massive

Longitudinal scalar wave (3) ist: $\square_{(4)}\,\phi_n + m_n^2\,\phi_n = 0$ Mass-dependent mode n

The real potential:

$\phi(x, y^a) = \sum_{n=1}^{3} \phi_n(x) \cos(\frac{ny^a}{R})$; depending on the mode (2.87)

leads to the object mass and the effective calibration potential using:

$$m_{obj}(t) = \frac{n\,h}{2\pi\,c\,R_{obj}} \cos(kt + \beta) \quad (2.91) \qquad A^a_{eff,\,0} = \frac{Q}{4\pi\,\epsilon_0\,R} \cos(kt + \beta)\,\delta^a_4\,\delta^0_\mu \quad (2.69)$$

Cos(kt = 0) indicates contact in the dimensional plane D_{56} and, at the same time, the state of maximum elongation:

$$m_{obj} = \frac{n\,h}{2\pi\,c\,R_{obj}} \quad (2.90) \qquad \phi(x) = \frac{Q}{4\pi\,\epsilon_0\,R} \quad (2.149)$$

If the periodic maximum elongation at the point of contact in the dimensional plane D_{56} is considered in isolation, then a field emission from the wave-field $F_{4\text{-}6}$ into the particle-field $F_{1\text{-}3}$ will appear as a moving body.

The process does not have to originate solely from the wave-field $F_{4\text{-}6}$ into the particle-field $F_{1\text{-}3}$. Control from the particle-field $F_{1\text{-}3}$ to the field source can also trigger a feedback pulse that has a disruptive effect on a particle. For example, additional energy could be supplied from the particle-field $F_{1\text{-}3}$ to a proton with a suitable coupling frequency, which would have a disruptive effect on its structure. Alternatively, an object velocity V_3 could also have a relativistic disruptive effect on the rotational orbit of the fions.

3.3 Configuration of Particle Types

The derivation of the present particle model is the logical consequence of the relationships established so far for a 6-dimensional field-space. In order to understand the mass formula for arbitrary particles, it must first be explained how different particles can be composed and what different particle groupings exist. The classical model and the Field-Space-Mechanical model with its innovative approach will be discussed. In addition, the particle structure will be used to investigate the concrete influence of hidden matter on the atomic nucleus.

Particle types:

In FSM, the term "particle types" encompasses all particles, regardless of their complexity. The purpose of this classification is to take into account the number of individual interaction partners with the mechanical processes in the field-space, from a single fermionic particle structure to a complex compound of baryonic particle structures. Depending on the complexity, this increases the frequency or mass of the particle.

These so-called particle types include the individual active fions, the fermions and the particle group of baryons with half-integer spin, as well as the bosons, the so-called meson-bosons and the particle group of mesons with integer spin. The particle types meson-bosons, mesons and baryons occur as particle compounds of elementary particles of the individual fermions and bosons. Neutrons and protons belong to the group of baryons, among others.

The individual particle types that occur individually or as particle compounds due to their particle structures are discussed below. The FSM can determine their composition.

Fermions:

Fermions include all particles with a spin of $\frac{1}{2}$. According to the standard model of Quantum Mechanics for elementary particles, these include the electron and positron, all known quarks, the muon, tauon and the associated neutrino types with the electron neutrino, muon neutrino and tau neutrino. The electron was examined in detail in the previous **Chapter 3.2**. In the next step, quarks will be considered.

Distinction between quarks in the Standard Model and quarks in FSM:

In the Standard Model of particle physics, quarks are described as a hypothetical structure that occurs primarily in more complex particle structures such as the proton and neutron. They are subject to all fundamental interaction forces and do not have a multiple of an integer elementary charge. There are the following types of quarks: the u quark, the d quark, the C quark, the B quark, the T quark and the S quark. Their

energy contributions in more complex particle structures are relatively small compared to gluons as carriers of binding energy.

In contrast, quarks in the FSM represent structures that occur both in baryons, such as protons and neutrons, and in bosons. In this model, just as in the Standard Model, a quark never exists on its own as an elementary particle. In the FSM, a quark is produced only through the reduction of an electron as part of a boson. Its exchange fion then takes over the task of interaction. This makes it possible to derive complex particle structures and thus, for example, to determine the charge state of the quark within a meson or baryon.

Bosons in classical particle physics and in the FSM:

In the Standard Model of particle physics, bosons are the carriers of the forces of interaction between particles and, depending on their complexity, can mediate electric, strong or weak interactions. Due to the conservation of momentum, boson exchange always takes place with integer spin. In the Standard Model, bosons are divided into gluons, photons, Z-bosons, W-bosons and H-bosons. It has not yet been possible to find a significant reason for the difference between fermions, which have half-integer spin, and bosons, which have integer spin. Furthermore, the graviton with spin 2 has been postulated as a hypothetical exchange boson for gravitational forces, but its existence has not yet been proven.

In FSM, bosons are initially regarded as a state consisting of a specific mode of an electron and its exchange fion. The exchange fion with integer spin is the mediator of the interaction. It can only recombine with particles that also have an integer total spin. The receiving boson determines the multiple wavelength to which an exchange particle must adjust with its structure. This process is the reason why bosons with integer spins are not subject to the Pauli principle and can interfere with other particles.

Composite particles such as mesons are also classified as bosons in standard physics due to their integer spin. In the FSM, however, a distinction is made between whether the boson occurs as a single particle or as a meson in a composite of single particles. This distinction is made within the framework of this particle model so that its particle structure can be reconstructed at the elementary level. As will be shown, Z-, W- and H-bosons are particle structures consisting of two extended modes of the electron. The structure of these heavy bosons with mass numbers can also be reproduced using the particle model of the FSM.

With the help of the required boson structure, an essential component of the mass formula for any particle is described.

Distinction between mesons and baryons in the Standard Model and in the FSM

Mesons:

From the Standard Model, we know that mesons belong to a higher-level particle group composed of more complex structures of several quarks and antiquarks. Why this composition of quarks and antiquarks is necessary when the nuclear force between them is greater than their electric forces is not yet clear. They are considered unstable and have an integer spin. They are therefore classified as bosons.

As already indicated above, mesons in the FSM consist of two bosons, which in turn contain certain quarks and their exchange fions. Two bosons with half-integer or integer spin always result in a meson with integer spin. In some cases, two bosons interact with hidden matter, which is shifted and rotated from the dimension plane D_{56}. The different charge states can be assigned in its structure. Furthermore, mesons consisting only of positive or negative bosons are possible. The particle model of the FSM makes it possible to use the modelled particle structure to highlight the difference between bosons as individual particles (e.g. photons) and bosons as composite particles (e.g. mesons).

Baryons:

Similar to mesons, baryons also belong to a higher particle group in the Standard Model of particle physics. In their S-sphere, baryons consist of a structure of at least three quarks with different charge states, as well as their exchange particles. It is assumed that the quarks hold together in the form of a triplet. The proton is considered the smallest and most stable baryon. With its half-integer spin, the proton is classified in the fermion particle group.

The particle model of the FSM also highlights the difference between a fermion as a single particle (e.g. electron) and a fermion as a composite particle (e.g. proton) through its particle structure. The special feature of the baryon in the FSM is that a binding neutrino ensures stability in the particle structure consisting of quarks and exchange fions. A triplet would even disrupt stability. This different particle structure explains how the different charges of the quarks for protons and neutrons come about, and why the nuclear force of protons exceeds the repulsion between charges of the same name. Using the example of baryons (e.g. protons), the influence of hidden matter in an atom can also be represented concretely as a ratio. Interpretations of the origin of hidden matter and the reason for the repulsion between protons and neutrons can also be made.

Meson-Bosons :

Meson-bosons are the lightest mesons as composite particles that occur in nature according to the FSM and have the same mass equivalent as the smallest boson as a single particle. In particle structure, these lightest mesons can be distinguished from bosons as individual particles with identical mass. This type of particle is therefore referred to as a meson-boson. This is not to be understood as a pleonasm, but rather to indicate that their particle structures are determined differently.

Configuration of bosons and different types of particles:

Configurations provide qualitative information about how the bosonic properties and multiples of these bosons are implied in the form of particle types.

The bosonic properties are the prerequisites for interaction with another particle. The aim of **boson configuration (BC)** is to produce a total angular momentum for an exchange fion that has a bosonic integer spin. Certain **electron configurations (EC)** are already bosonic, while other cases only become bosonic when they receive external fions for a short period of time. Once a particle is bosonic, it can provide an exchange fion that transfers the properties of interaction and object mass.

The **particle configuration (PC**) is based on the multiple exchange of fields for arbitrarily complex particle structures. This is the mathematical sum of all bosons minus their necessarily emitted active fions, which are converted by the creation of exchange fion/passive fion pairs. During a bosonic field exchange, such pair formations provide the exchange fions in the particle structure, which are structured with varying degrees of complexity depending on the particle in the 6-dimensional field-space.

Counting method for active fions, external fions and pair formation from exchange fions and passive fions:

The **electron configuration** describes the number of active fions in a sphere S. **Figure 3.5** shows the electron in the mode with three to five active fions.

The **boson configuration** takes into account the ratio of **the electron configuration** in the **denominator** to the sum of **active** and **external fions** in the **numerator**. **Figure 3.5** could also be used to illustrate the situation in the case of external fions being received. However, this would not include participation as a partial charge in the particle sphere S.

The following **Figure 3.12** can be used for the field exchange of two bosons with their respective exchange fions.

The following generalisation applies to the counting pattern:

Electron configuration – EC

$$\text{EC} = \text{No. of active fions} = N_{aF} \qquad N \in \mathbb{N} \tag{3.05}$$

Boson configuration – BC

$$\text{BC} = \frac{N_{aF} + N_{eF}}{N_{aF}}$$

$$\text{BC} = \frac{\text{No. of active fions} + \text{No. extern fions}}{\text{No. active fions}} \tag{3.06}$$

Particle configuration – PC

$$\text{PC} = \frac{N_{aF} + N_{eF} - N_{F/A}}{N_{aF}} \tag{3.07}$$

$$\text{PC} = \frac{\text{No. of active fions} + \text{No. extern fions} - \text{No. exchange fion/passive fion-pair}}{\text{No. active fions}}$$

N_{aF} – Number of active fions

N_{eF} – Number of external fions

$N_{F/A}$ – Number of exchange fion/passive fion pairs

In the first case, consider the electron that temporarily receives a certain number of external active fions with its three active fions, which increases the total mass of the electron. These cases are expressed as follows:

eF1/2/3 – Number of externally absorbed fions

Case a. – Electron with three active fions

Electron configuration – EC

EC = N_{aF} = 3

Boson configuration – BC

1) In the case of an electron with an electron configuration of EC = 3, the bosonic configuration BC(eF1) = $\frac{4}{3}$ is created upon receiving an external fion, which only exists temporarily in the electron. The electron becomes temporarily bosonic.

$$BC(eF1) = \frac{3 \text{ active fions} + 1 \text{ extern fion}}{3 \text{ active fions}} = \frac{4}{3}$$

2) In the case of a boson with the boson configuration BC(eF1) = $\frac{4}{3}$, the boson configuration BC(eF2) = $\frac{5}{3}$ is created upon receiving another external fion.

$$BC(eF2) = \frac{3 \text{ active fions} + 2 \text{ extern fions}}{3 \text{ active fions}} = \frac{5}{3}$$

For case 1) with four active fions, the total angular momentum of all individual angular momenta of the fiones acting therein is determined as an integer using Pythagoras' theorem:

$$L_{4fions}^2 = (\frac{h}{4\pi})^2_{fion1} + (\frac{h}{4\pi})^2_{fion2} + (\frac{h}{4\pi})^2_{fion3} + (\frac{h}{4\pi})^2_{fion4} \qquad [L] = Js$$

$$L_{4fions} = \frac{\sqrt{1^2 + 1^2 + 1^2 + 1^2}}{4\pi} h$$

This electron has an integer spin for a certain period of time due to the temporary reception of an external fion and is capable of bosonic interaction. Case 1) is the smaller structure compared to case 2) and can be assigned with high probability to occur most frequently in nature.

Case 2) has the following total angular momentum:

$$L_{5fions} = (\frac{h}{4\pi})^2_{fion1} + (\frac{h}{4\pi})^2_{fion2} + (\frac{h}{4\pi})^2_{fion3} + (\frac{h}{4\pi})^2_{fion4} + (\frac{h}{4\pi})^2_{fion5}$$

$$L_{5fions} = \frac{\sqrt{1^2 + 1^2 + 1^2 + 1^2 + 1^2}}{4\pi} h$$

This modelled electron with two externally absorbed fions must have an integer spin as a boson in order not to violate the conservation of angular momentum for a coupling with an integer exchange fion. Since the orbital velocity across all active

fions is greater than the maximum velocity $V_{max} = c$ according to Pythagoras' theorem with $V_{rot} = \frac{\sqrt{5}}{2} c > c$, this electron requires a dimension reduction factor. The dimension reduction factor is explained in the following chapter. The reduction of the resulting orbital velocity V_{rot} to the maximum velocity $V_{max} = c$ is noticeable in that measuring instruments will again register an orbital velocity of $V_{rot} = \frac{\sqrt{4}}{2} c$.

This modelled electron is presumably measured with this angular momentum

$$L_{4fions} = \frac{\sqrt{1^2 + 1^2 + 1^2 + 1^2}}{4\pi} h$$

and is thus capable of exchanging like a boson.

Particle configuration – PC – Meson

Particle formation requires at least two such bosons that exchange with each other. In addition, an active fion is split into an exchange fion/passive fion pair so that one of the split fions is available as an exchange fion and the other partial fion remains passive. During its field exchange, the exchange fion/passive fion pair no longer contributes to the mass of the boson due to its formation in the dimension plane D_{56}. A meson with the following particle configuration is created:

$$PC_{boson1} = \frac{3 \text{ active intern fions} + 1 \text{ extern fion} - 1 \text{ exchange fion/passives fion-pair}}{3 \text{ active intern fions}}$$

$$PC_{boson2} = \frac{3 \text{ active intern fions} + 1 \text{ extern fion} - 1 \text{ exchange fion/passives fion-pair}}{3 \text{ active intern fions}}$$

$$PC_{meson} = \frac{3 + 1 - 1}{3} + \frac{3 + 1 - 1}{3} = \frac{6}{3}$$

The terms show that bosons are composed of electron modes. The electron configuration **EC = 3** allows the electron to expand into the elementary particle of the so-called **u/d-quark** with an **exchange fion** in the event of an interaction.

Note: This model can bring about a qualitative distinction between u-quarks and d-quarks. However, for the coupling frequency and mass determination, they represent the same harmonic for the total oscillation of a particle on average. Therefore, u and d quarks are combined as u/d-quarks in the FSM. The fact that this is acceptable for the FSM model is confirmed by the calculation of various quark excitations with u/d-quarks.

Special modes for the u/d quark:

It is conceivable that an externally absorbed fion could leave the electron sphere during the mutual fion exchange. In this special case, the mass of the external fion disappears after recombination in the meson. This results in the following particle configuration for this meson:

$$PC_{boson1} = \frac{\text{3 active intern fions + 0 extern fion – 1 exchange fion/passives fion-pair}}{\text{3 active intern fions}}$$

$$PC_{boson2} = \frac{\text{3 active intern fions + 0 extern fion – 1 exchange fion/passives fion-pair}}{\text{3 active intern fions}}$$

$$PC_{meson\text{-}boson} = \frac{3 + 0 - 1}{3} + \frac{3 + 0 - 1}{3} = \frac{4}{3}$$

It can be seen that the special case in which the external fion leaves the electron sphere during the exchange phase leaves behind a particle configuration for the meson that is equal to the boson configuration for an electron with a received external fion. In this model, only the structure of the particle and its charge distribution can be used to determine whether the configuration corresponds to a boson as a single particle or a meson as a composite particle. This meson would be the lightest meson in nature. Due to the lack of distinguishability in the configurations between whether it is a single particle or a composite particle, this particle is referred to as **a meson-boson** in the FSM model.

Further modes for the electron:

The electron can expand internally from three to four or five active fions, which carry a partial charge accordingly. The electron configuration expands. **Figure 3.5** shows the possible composition for the fourth and fifth active fions in a sphere S.

Case b. – Electron with four active fions

Electron configuration – EC

EC= N_{aF} = 4

Boson configuration – BC

$$BC = \frac{4 \text{ active fions} + 0 \text{ extern fion}}{4 \text{ active fions}} = \frac{4}{4}$$

The total angular momentum is an integer according to Pythagoras' theorem:

$$L_{4fions}{}^2 = (\frac{h}{4\pi})^2_{fion1} + (\frac{h}{4\pi})^2_{fion2} + (\frac{h}{4\pi})^2_{fion3} + (\frac{h}{4\pi})^2_{fion4} = \frac{\sqrt{1^2 + 1^2 + 1^2 + 1^2}}{4\pi} h$$

This modelled electron (formerly EC= 3 with three active fions) has four active fions with the electron configuration EC = 4, which results in an integer total spin. It is already bosonic without the addition of external fions and can immediately interact with another particle.

Particle configuration – PC – Meson

$$PC_{boson1} = \frac{4 \text{ active intern fions} + 0 \text{ extern fion} – 1 \text{ exchange fion/passives fion-pair}}{4 \text{ active intern fions}}$$

$$PC_{boson2} = \frac{4 \text{ active intern fions} + 0 \text{ extern fion} – 1 \text{ exchange fion/passives fion-pair}}{4 \text{ active intern fions}}$$

$$PC_{meson} = \frac{4 + 0 – 1}{4} + \frac{4 + 0 – 1}{4} = \frac{6}{4}$$

The electron configuration **EC = 4** allows the modelled electron to expand into the elementary particle known as the **C-quark** with an **exchange fion** in the event of an interaction.

Case c. – Electron with five active fions

Electron configuration – EC

EC = N_{aF} = 5

Boson configuration – BC

$$BC = \frac{5 \text{ active fions} + 0 \text{ extern fion}}{5 \text{ active fions}} = \frac{5}{5}$$

The total angular momentum is half-integer according to Pythagoras' theorem:

$$L_{5fions} = (\frac{h}{4\pi})^2_{fion1} + (\frac{h}{4\pi})^2_{fion2} + (\frac{h}{4\pi})^2_{fion3} + (\frac{h}{4\pi})^2_{fion4} + (\frac{h}{4\pi})^2_{fion5}$$

$$L_{5fions} = \frac{\sqrt{1^2 + 1^2 + 1^2 + 1^2 + 1^2}}{4\pi} h$$

This modelled electron with electron configuration EC = 5 must also have an integer spin as a boson in order not to violate the angular momentum conservation law for a coupling with an integer exchange fion. As in case 2) with the addition of two external fions, the measuring instruments will again register an orbital velocity of $V_{rot} = \frac{\sqrt{4}}{2} c$ with the aid of a dimension reduction factor.

This boson is presumably measured with this angular momentum

$$L_{4fions} = \frac{\sqrt{1^2 + 1^2 + 1^2 + 1^2}}{4\pi} h$$

and is thus capable of exchanging like a boson.

Particle configuration – PC – Meson

$$PC_{boson1} = \frac{5 \text{ active intern fions} + 0 \text{ extern fion} - 1 \text{ exchange fion/passives fion-pair}}{5 \text{ active intern fions}}$$

$$PC_{boson2} = \frac{5 \text{ active intern fions} + 0 \text{ extern fion} - 1 \text{ exchange fion/passives fion-pair}}{5 \text{ active intern fions}}$$

$$PC_{meson} = \frac{5 + 0 - 1}{5} + \frac{5 + 0 - 1}{5} = \frac{8}{5}$$

The electron configuration **EC = 5** enables the modelled electron to expand into the elementary particle known as the **B-quark** with an **exchange fion** in the event of an interaction.

Case d. – Electron with six active fions

According to this model, bosons with more than five fions cannot exist naturally in R^6. Due to dimensional constraints, only a maximum of five fions rotating orthogonally to the dimension plane D_{56} would be conceivable, which could intersect simultaneously at a point of contact. However, it is conceivable that a temporarily and severely limited state could occur in which bosons with six active fions and thus also exist in seven dimensions.

Electron configuration – EC

EC = N_{aF} = 6

Boson configuration – BC

$$BC = \frac{6 \text{ active fions} + 0 \text{ extern fion}}{6 \text{ active fions}} = \frac{6}{6}$$

The total angular momentum is an integer according to Pythagoras' theorem:

$$L_{6fions} = (\frac{h}{4\pi})^2_{fion1} + (\frac{h}{4\pi})^2_{fion2} + (\frac{h}{4\pi})^2_{fion3} + (\frac{h}{4\pi})^2_{fion4} + (\frac{h}{4\pi})^2_{fion5} + (\frac{h}{4\pi})^2_{fion6}$$

$$L_{6fions} = \frac{\sqrt{1^2 + 1^2 + 1^2 + 1^2 + 1^2 + 1^2}}{4\pi} h$$

This boson is probably measured with this angular momentum:

$$L_{4fions} = \frac{\sqrt{1^2 + 1^2 + 1^2 + 1^2}}{4\pi} h$$

This modelled electron with the electron configuration EC = 6 has an integer spin and can interact bosonic.

Particle configuration – PC – Meson

$$PC_{boson1} = \frac{6 \text{ active intern fions} + 0 \text{ extern fion} - 1 \text{ exchange fion/passives fion-pair}}{6 \text{ active intern fions}}$$

$$PC_{boson2} = \frac{6 \text{ active intern fions} + 0 \text{ extern fion} - 1 \text{ exchange fion/passives fion-pair}}{6 \text{ active intern fions}}$$

$$PC_{meson} = \frac{6 + 0 - 1}{6} + \frac{6 + 0 - 1}{6} = \frac{10}{6}$$

The electron configuration **EC = 6** allows the modelled electron to expand into the elementary particle known as the **T-quark** with an **exchange fion** in the event of an interaction.

Case e. – Electron with higher combinations of active fions

In the following modelled electron, higher combinations of its expansion are possible. It is conceivable that there are fions that exist with half the wavelength of an u/d-quark. The limitation on the number of fions present in a sphere S in R^6 that rotate in the same direction must be taken into account. Thus, the maximum occupancy consists of one active fion with the wavelength corresponding to a fion in the u/d-quark, plus four additional active fions corresponding to half the wavelength of an u/d-quark.

Electron configuration – EC

EC = N_{aF} = 1 active fion + 4 active fions with $\frac{\lambda_{u/d\text{-}quark}}{2} = 5$

Boson configuration – BC

$$BC = \frac{1 \text{ active fions} + 4 \text{ active fions with } \lambda_{u/d\text{-}quark}/2 + 0 \text{ extern fions}}{5 \text{ active fions}} = \frac{5}{5}$$

The total angular momentum is half-integer according to Pythagoras' theorem:

$$L_{5fions} = (\frac{h}{4\pi})^2_{fion1} + (\frac{h}{4\pi})^2_{fion2} + (\frac{h}{4\pi})^2_{fion3} + (\frac{h}{4\pi})^2_{fion4} + (\frac{h}{4\pi})^2_{fion5}$$

$$L_{5fions} = \frac{\sqrt{1^2 + 1^2 + 1^2 + 1^2 + 1^2}}{4\pi} h$$

This boson is probably measured again with this angular momentum:

$$L_{4fions} = \frac{\sqrt{1^2 + 1^2 + 1^2 + 1^2}}{4\pi} h$$

Particle configuration – PC – Meson

$$PC_{boson1} = \frac{5 \text{ active intern fions} + 0 \text{ extern fion} - 1 \text{ exchange fion/passives fion-pair}}{5 \text{ active intern fions}}$$

$$PC_{boson2} = \frac{5 \text{ active intern fions} + 0 \text{ extern fion} - 1 \text{ exchange fion/passives fion-pair}}{5 \text{ active intern fions}}$$

$$PC_{meson} = \frac{5 + 0 - 1}{5} + \frac{5 + 0 - 1}{5} = \frac{8}{5}$$

These modelled electrons are expected to interact strongly with the particle group of mesons. In the event of an interaction with each other, they correspond to the elementary particle of the so-called **S-quark** with an **exchange fion**.

Further modes of the S-quark:

Boson configuration – BC

With reception of an external fion:

$$BC = \frac{1 \text{ active fions} + 4 \text{ active fions with } \lambda_{u/d\text{-}quark}/2 + 1 \text{ extern fions}}{5 \text{ active fions}} = \frac{6}{5}$$

The total angular momentum is an integer according to Pythagoras' theorem:

$$L_{6fions} = \frac{\sqrt{1^2 + 1^2 + 1^2 + 1^2 + 1^2 + 1^2}}{4\pi} h$$

This boson is presumably measured with this angular momentum:

$$L_{4fions} = \frac{\sqrt{1^2 + 1^2 + 1^2 + 1^2}}{4\pi} h$$

This S quark is bosonic and can also interact with another boson.

Particle configuration – PC – Meson

$$PC_{boson1} = \frac{5 \text{ active intern fions} + 1 \text{ extern fion} - 1 \text{ exchange fion/passives fion-pair}}{5 \text{ active intern fions}}$$

$$PC_{boson2} = \frac{5 \text{ active intern fions} + 1 \text{ extern fion} - 1 \text{ exchange fion/passives fion-pair}}{5 \text{ active intern fions}}$$

$$PC_{meson} = \frac{5 + 1 - 1}{5} + \frac{5 + 1 - 1}{5} = \frac{10}{5}$$

Hypothetically, the configuration for particle types such as mesons varies differently. The half-integer values could be due to the reception of half-wave external active fions, which have a factor of 0,5 instead of 1 in the particle configuration.

Other possible configurations:

Particle configuration – PC – Meson

$$PC_{boson1} = \frac{5 \text{ active intern fions} + 0{,}5 \text{ extern fion} - 1 \text{ exchange fion/passives fion-pair}}{5 \text{ active intern fions}}$$

$$PC_{boson2} = \frac{5 \text{ active intern fions} + 0 \text{ extern fion} - 1 \text{ exchange fion/passives fion-pair}}{5 \text{ active intern fions}}$$

$$PC_{meson} = \frac{5 + 0{,}5 - 1}{5} + \frac{5 + 0 - 1}{5} = \frac{8{,}5}{5}$$

Particle configuration – PC – Meson

$$PC_{boson1} = \frac{5 \text{ active intern fions} + 0 \text{ extern fion} - 0{,}5 \text{ exchange fion/passives fion-pair}}{5 \text{ active intern fions}}$$

$$PC_{boson2} = \frac{5 \text{ active intern fions} + 0 \text{ extern fion} - 0{,}5 \text{ exchange fion/passives fion-pair}}{5 \text{ active intern fions}}$$

$$PC_{meson} = \frac{5 + 0 - 0{,}5}{5} + \frac{5 + 0 - 0{,}5}{5} = \frac{9}{5}$$

Particle configuration – PC – Meson

$$PC_{boson1} = \frac{5 \text{ active intern fions} + 1 \text{ extern fion} - 1 \text{ exchange fion/passives fion-pair}}{5 \text{ active intern fions}}$$

$$PC_{boson2} = \frac{5 \text{ active intern fions} + 0{,}5 \text{ extern fion} - 1 \text{ exchange fion/passives fion-pair}}{5 \text{ active intern fions}}$$

$$PC_{meson} = \frac{5 + 1 - 1}{5} + \frac{5 + 0{,}5 - 1}{5} = \frac{9{,}5}{5}$$

3.4 Modelling Particle Structures

The next step towards understanding particle structures is to classify them visually in 6-dimensional field-space. The particles presented are selected mesons and baryons made up of u/d-quarks, which are geometrically different in the field-space and interact with each other. By modelling particles using the FSM model, the user can describe which configurations, charges and spins are present.

Possible particle structures of mesons made of u/d-quarks:

A) Mesons made of $Q = \frac{2}{3}e$ quarks:

To represent a meson consisting of two $Q = \pm\frac{2}{3}e$ quarks, it shall be considered a positive and a negative charged boson with the boson configuration BC = $\frac{4}{3}$. Each boson consists of a quark and an exchange fion. The positively charged quark rotates above and the negatively charged quark below, orthogonal to the dimension plane $D_{56.}$ Since there is pair formation with different charges, attractive forces act between the partners. Both quarks have a multiple distance with a wavelength of $\frac{\lambda_{Fion}}{2}$ from each other. The fions are slightly shifted in their oscillation phase so that they do not immediately undergo an annihilation reaction. The particle configuration of this meson consists of the active electron-internal fions and the received external fion minus the pair of exchange fions and passive fions that arise at the expense of an active fion: PC = $\frac{3+1-1}{3} + \frac{3+1-1}{3} = \frac{6}{3}$. With the missing active fion in the electron sphere, the total charge is reduced as follows: $Q_{B1} = \frac{2}{3}$ e; $Q_{B2} = -\frac{2}{3}$ e. The spin for the respective u/d-quark is half-integer, with the three remaining fions. The spin of the meson is determined by the sum of the half-integer spins of the quarks.

Figure 3.12 shows the bosons described and the mechanical process involved in the exchange of their exchange fions. These are shown in light green. The directions of rotation are determined by the point of contact between the emitting quark and the receiving quark. The passive fions remaining in sphere S are marked in dark green and grey. The rotational speed for an active fion within a charge in sphere S can be $V_{rot} = \frac{c}{2}$ or, for a released exchange fion outside sphere S, the maximum speed $V_{max} = c$. The released exchange fion rotates clockwise towards its respective target particle. These exchange fions contribute to the mass only when they recombine with the particle at the point of contact and generate restoring forces. During the reduction of its rotational speed with $V_{rot} = c$ to $V_{rot} = \frac{c}{2}$, the electric, strong and weak interactions are also mediated into the particle-field $F_{1\text{-}3}$ at the point of contact, which lies in the dimension plane D_{56}. The strength and type of an interaction depend on the coupling frequency of the exchange fion relative to the nature of the receiving particle. The coupling frequency must therefore take into account the complexity of the receiving particle and is correspondingly higher or lower in its coupling frequency.

This will be considered in the next chapter under the topic *of particle-exchange fion-particle-coupling*.

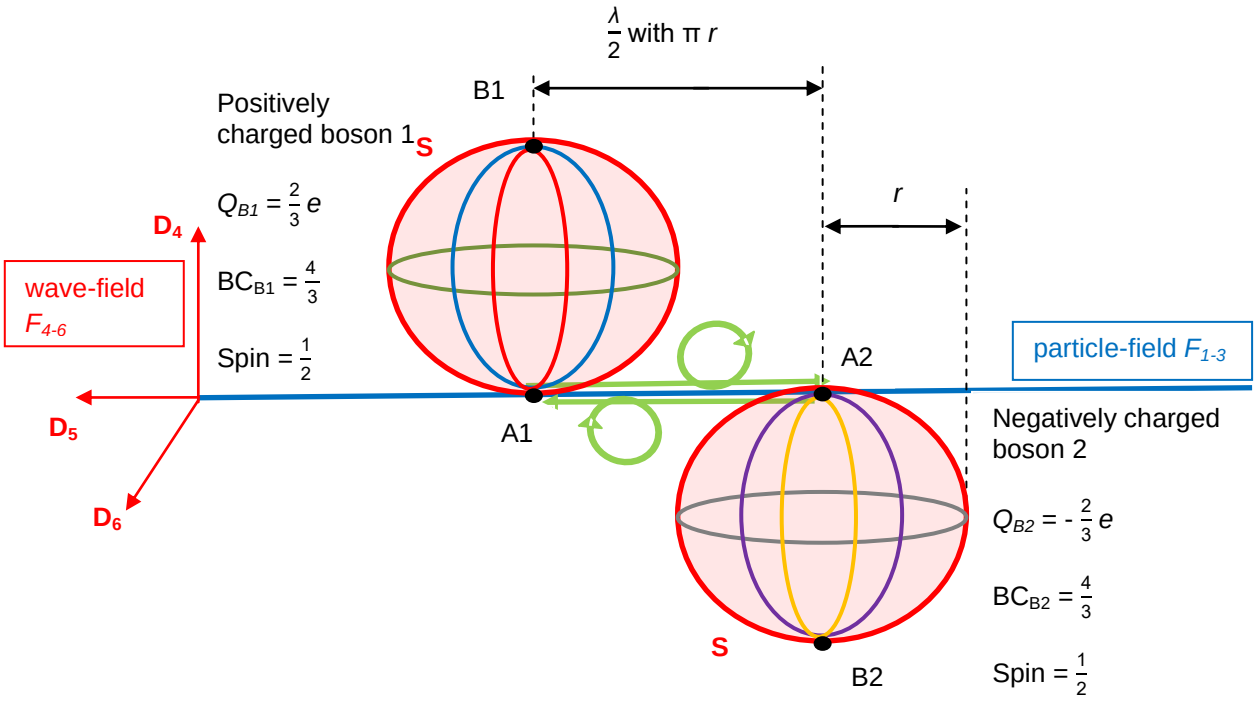

Figure 3.12: Meson consisting of two $Q = \frac{2}{3} e$ quarks

[Q_B] – charge of a quark in the boson in As

Figure 3.13 shows a schematic representation of this meson. Solid arrows indicate active fions within the quarks and dashed arrows indicate passive fions. The different arrow colours are intended to draw attention to the different states of the active fions. The two light green arrows between the quarks show the fion exchange of the respective exchange fions provided.

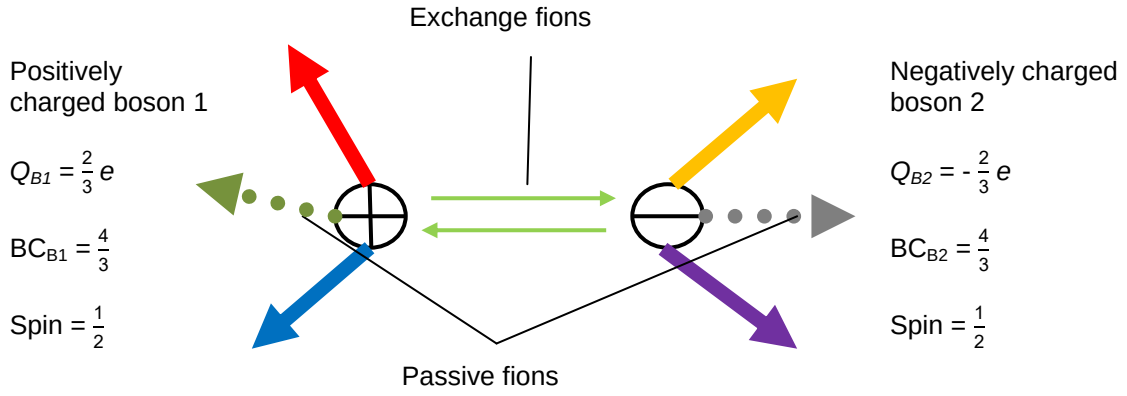

Figure 3.13: Schematic representation of a meson consisting of two $Q = \frac{2}{3} e$ quarks

Properties of mesons consisting of two $Q = \frac{2}{3}\,e$ quarks:

$$PC_{meson} = \frac{3 + 1 - 1}{3} + \frac{3 + 1 - 1}{3} = \frac{6}{3}$$

$$Q_{meson} = + \frac{2}{3}\,e - \frac{2}{3}\,e = 0$$

$$\text{Spin} = \frac{1}{2} - \frac{1}{2} = 0 \text{ or } = \frac{1}{2} + \frac{1}{2} = 1 \text{ or } = -\frac{1}{2} - \frac{1}{2} = -1$$

B) Mesons consisting of $Q = \frac{1}{3}\,e$ quarks:

The representation of the interaction of a meson consisting of $Q = \pm\frac{1}{3}\,e$ quarks is hypothetically possible if additional quarks from the set of hidden matter occur in the wave-field within the range of their short-range interaction, which do not rotate simultaneously on the dimension plane D_{56}. Once again, a positive and a negative charged boson are depicted, which, upon receiving an external fion, assume the boson configuration BC = $\frac{4}{3}$. Under the influence of the short-range interaction, they exchange bosons. As soon as an exchange takes place, these bosons again consist of a u/d-quark with their exchange fions. As in the above case, the total charge in their sphere S is initially $Q = \pm\frac{2}{3}\,e.$ Now, these two are attached to another neighbouring boson of the wave-field $F_{4\text{-}6}$ that does not interact with the particle-field $F_{1\text{-}3}$. A triplet ensures that all three u/d-quarks must now use two active fions to form the required number of exchange fion/passive fion pairs to ensure stable exchange. Only one active fion remains in each of the two u/d-quarks for field exchange, which could represent a single partial charge with $Q = \pm\frac{1}{3}\,e$ with respect to the particle-field $F_{1\text{-}3}$. The additional exchange fion touches its contact points at A2/B1 or A1/B2, respectively, and interacts with the u/d-quarks at exactly this point during rotation. The wavelength for the representation of the fion exchange is $\frac{\lambda}{2}$ and is shown twice in orange in a hemispherical shape. The exchange fions rotate counterclockwise because one quark is to the left and the other quark is to the right of the third quark. The fion exchange between the quarks mediates attractive forces back into the particle-field $F_{1\text{-}3}$ upon absorption between the particles. The spin of the meson remains integer. The particle configuration for the meson remains at PC = $\frac{6}{3}$ because a pair of remaining passive fions together form a virtual exchange fion/passive fion pair, which is to be evaluated as an active fion in the numerator.

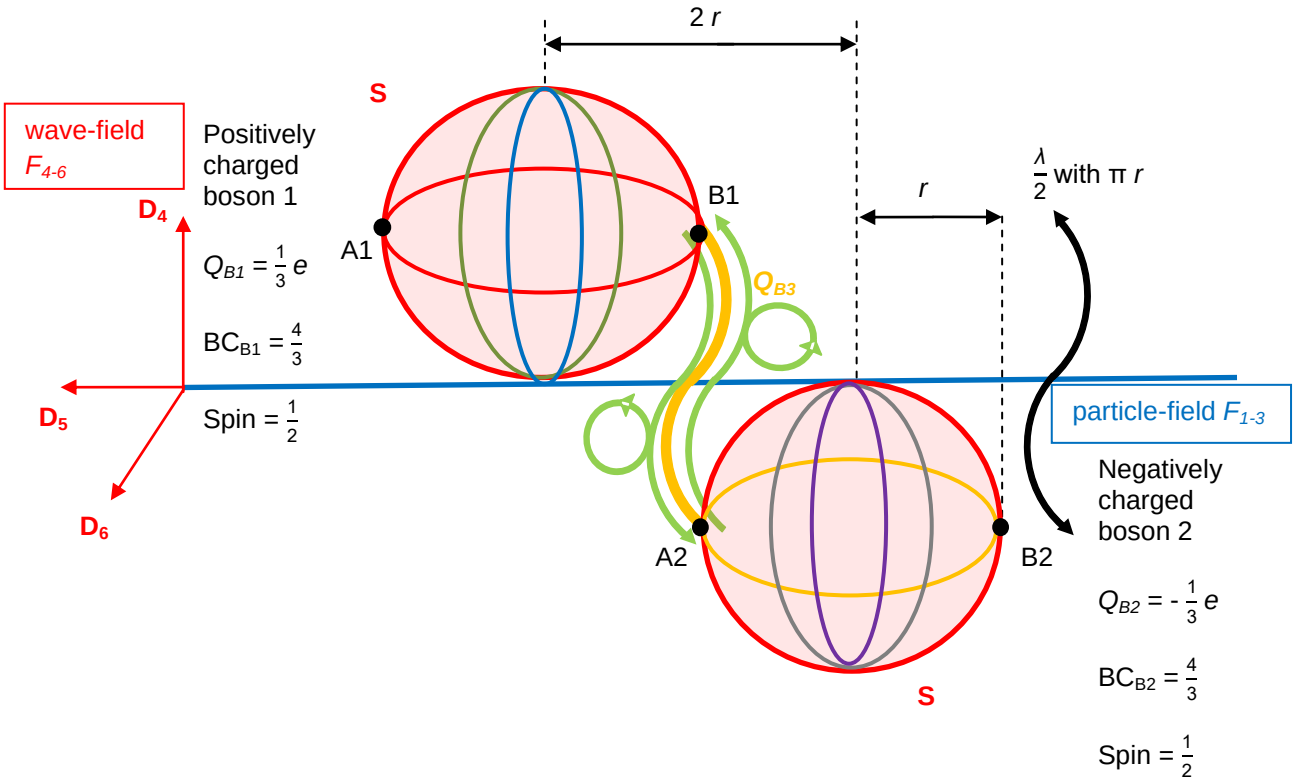

Figure 3.14: Meson, consisting of two $Q = \frac{1}{3}\,e$ quarks; yellow: a third quark from the set of hidden matter

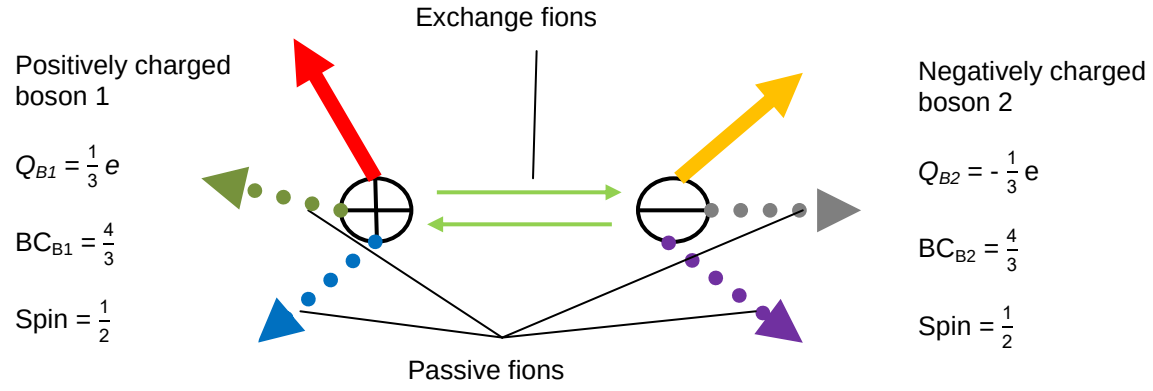

Figure 3.15: Diagram of a meson consisting of two $Q = \frac{1}{3}\,e$ quarks

Properties of mesons consisting of $Q = \frac{1}{3}\,e$ quarks:

$$PC_{meson} = \frac{3 + 1 - 1}{3} + \frac{3 + 1 - 1}{3} = \frac{6}{3}$$

$$Q_{meson} = +\frac{1}{3}\,e - \frac{1}{3}\,e = 0$$

$$\text{Spin} = \frac{1}{2} - \frac{1}{2} = 0 \text{ or } = \frac{1}{2} + \frac{1}{2} = 1 \text{ or } = -\frac{1}{2} - \frac{1}{2} = -1$$

C) Mesons consisting of one $Q = \frac{2}{3}\,e$ quark and one $Q = \frac{1}{3}\,e$ quark:

To represent a meson consisting of a $Q = \frac{1}{3}\,e$ quark and a $Q = \frac{2}{3}\,e$ quark, two bosons with the same positive charge, $Q = +\frac{2}{3}\,e$ and $Q = +\frac{1}{3}\,e$, are involved, which are phase-shifted by 90° relative to each other. Boson 2 is connected to another particle from the set of hidden matter in the wave-field $F_{4\text{-}6}$ in such a way that this particle structure occurs similarly to **case B)**. A fion exchange can occur between contact points A1/A2 and B1/B2. In this case, this process only begins after contact at point A1 or B1. Only when boson 1 comes into contact with point A1 or B1 does it convert one of its active fions into an exchange fion/passive fion pair. This exchange fion rotates clockwise to travel from the starting point A1 to A2 and back. When the exchange fion recombines at point A1/B1 in the dimension plane D_{56}, attractive forces are transmitted into the particle-field $F_{1\text{-}3}$. The spin of the meson remains an integer. The particle configuration for the meson is again given by

$$PC_{meson} = \frac{3 + 1 - 1}{3} + \frac{3 + 1 - 1}{3} = \frac{6}{3}.$$

The charges are $Q_{B1} = +\frac{2}{3}\,e$ for boson 1 and $Q_{B2} = +\frac{1}{3}\,e$ for boson 2. The wavelength between their points of contact is $\frac{\lambda}{4}$.

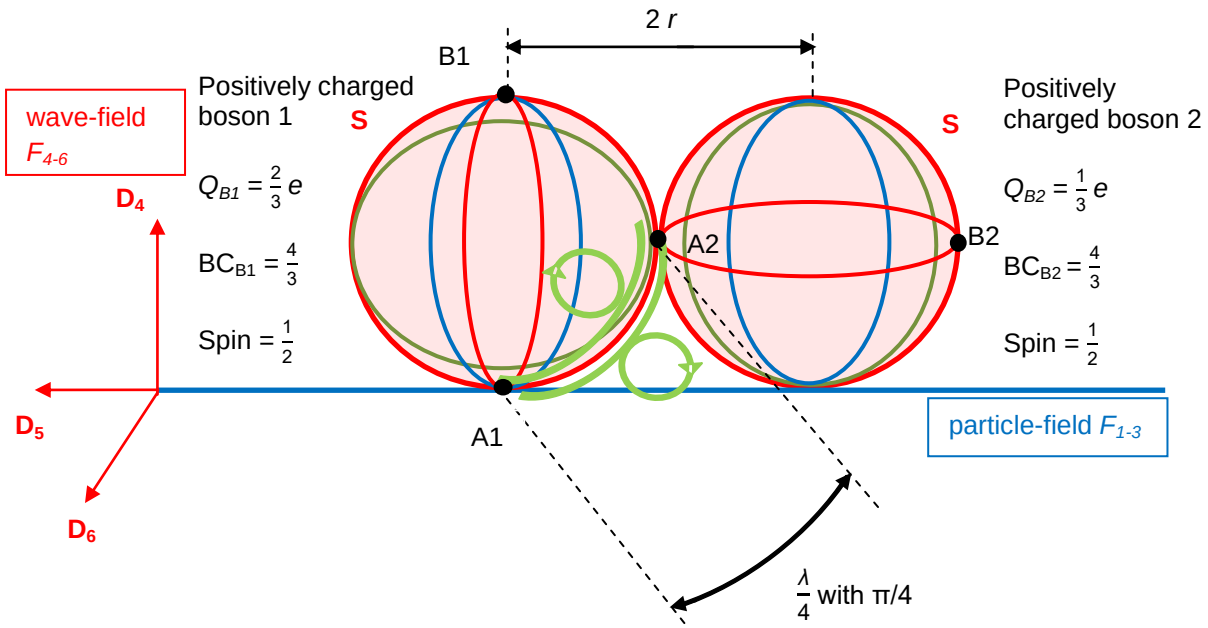

Figure 3.16: Meson consisting of one $Q = \frac{2}{3}\,e$ quark and one $Q = \frac{1}{3}\,e$ quark

Note: If boson 2 were also charged with $Q = +\frac{2}{3}$ e and not phase-shifted, both quarks would repel each other as positive charges. This representation is the only conceivable particle structure in which two bosons with the same charge exert attractive forces on each other.

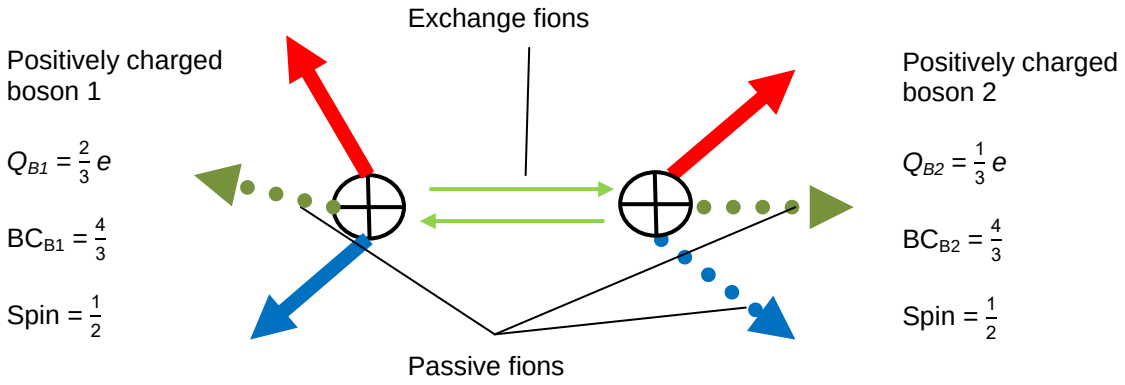

Figure 3.17: Schematic representation of a meson consisting of a $Q = \frac{2}{3} e$ quark and a $Q = \frac{1}{3} e$ quark

Properties of mesons consisting of a $Q = \frac{2}{3} e$ quark and a $Q = \frac{1}{3} e$ quark:

$$PC_{meson} = \frac{3 + 1 - 1}{3} + \frac{3 + 1 - 1}{3} = \frac{6}{3}$$

$Q_{meson} = +\frac{2}{3} e + \frac{1}{3} e = +1\ e$ for positively charged quarks and

$Q_{meson} = -\frac{2}{3} e - \frac{1}{3} e = -1\ e$ for negatively charged quarks

$$\text{Spin} = \frac{1}{2} - \frac{1}{2} = 0 \text{ or } = \frac{1}{2} + \frac{1}{2} = 1 \text{ or } = -\frac{1}{2} - \frac{1}{2} = -1$$

Possible particle structures of baryons made up of u/d-quarks:

D) Baryons consisting of a chain of two $Q = -\frac{2}{3}e$ quarks and one $Q = \frac{1}{3}e$ quark:

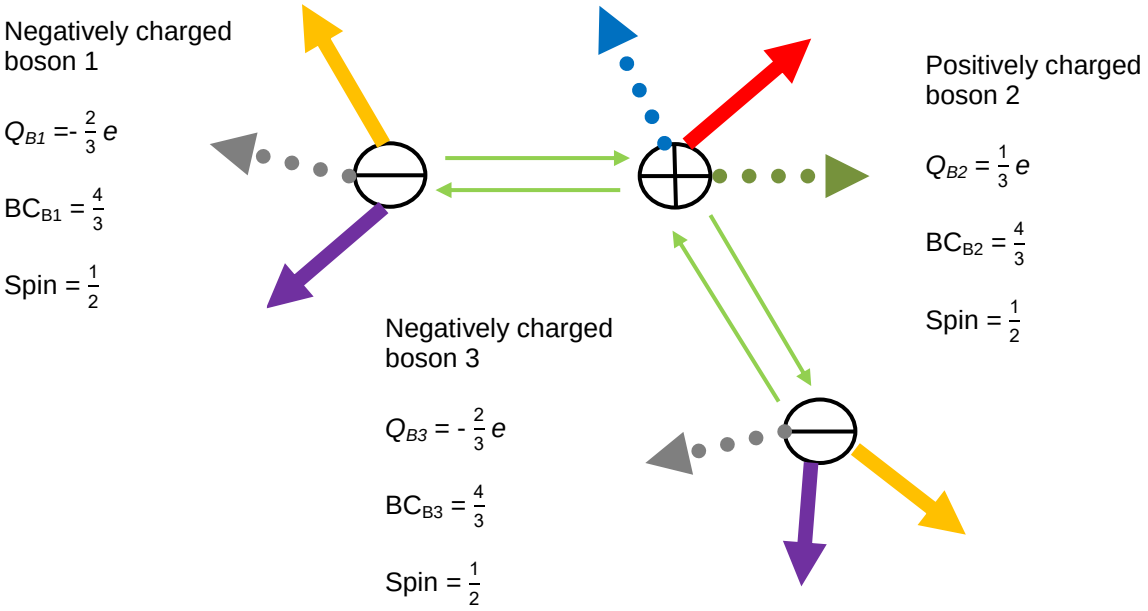

Figure 3.18: Binding chain consisting of two $Q = -\frac{2}{3}e$ quarks and one $Q = \frac{1}{3}e$ quark

The resulting chain has a half-integer spin like a baryon. In this case, a quark chain consisting of negatively-positively-negatively charged quarks has been created. The positively charged boson 2 has only one u/d-quark with a charge $Q_{B2} = +\frac{1}{3}e$ because it must bind to two negatively charged quarks. It must expose two of its active fions to form two exchange fion/passive fion pairs. The two passive fions are counted virtually as one active fion. As soon as the electrical forces begin to act after a field exchange, the outer quarks will align themselves at 90° to 180° due to repulsive forces between charges of the same name and continue to tear apart. This chain is unstable and does not occur in nature.

Properties of a baryon consisting of a chain of two $Q = \frac{2}{3}e$ quarks and one $Q = \frac{1}{3}e$ quark:

$$PC_{baryon} = \frac{3 + 1 - 1}{3} + \frac{3 + 1 - 1}{3} + \frac{3 + 1 - 1}{3} = \frac{9}{3}$$

$$Q_{baryon} = -\frac{2}{3}e + \frac{1}{3}e - \frac{2}{3}e = -1\,e \qquad \text{or:} \qquad Q_{baryon} = \frac{2}{3}e - \frac{1}{3}e + \frac{2}{3}e = +1\,e$$

$$\text{Spin} = \frac{1}{2} + \frac{1}{2} + \frac{1}{2} = \frac{3}{2} \text{ or } = -\frac{1}{2} - \frac{1}{2} - \frac{1}{2} = -\frac{3}{2} \text{ or } = \frac{1}{2} + \frac{1}{2} - \frac{1}{2} = \frac{1}{2} \text{ or } = \frac{1}{2} - \frac{1}{2} - \frac{1}{2} = -\frac{1}{2}$$

E) Baryons made up of three $Q = \frac{2}{3}e$ quarks with a binding neutrino in the centre:

In the FSM, the stability of a baryon is established by a virtual neutrino. A pictorial comparison for such a neutrino is shown in **Figure 3.11 on the right** from the previous chapter. For the special cases of baryons, it will be referred to as **a binding neutrino**. The binding neutrino consists of three exchange fion pairs, which virtually form three active fions for one neutrino. The Pauli principle prevents the orbiting elementary particles from approaching the binding neutrino, because otherwise more 4-dimensional subspaces U would be localised at one location than would be possible in a space R^6. A space structure-induced repulsion occurs from the direction of the binding neutrino, while the strong nuclear forces promote attraction to the binding neutrino. This results in an energetically favourable distance between the surrounding elementary particles and the binding neutrino. Assuming that the proton brings about the energetically favourable state in its structure, it must remain largely undisturbed. Stability is maximised by an even arrangement and spacing of the elementary particles relative to each other. Taking this stability into account, the elementary particles interact preferentially with the binding neutrino. Due to the lack of orthogonal formation to the dimension plane D_{56}, this binding neutrino has no charge and a relatively low mass. The total spin of all exchange fions in the binding neutrino cancels out to zero. The additional rotation matrix for the elementary particles rotating around the binding neutrino runs parallel to the dimension plane D_{56} and is:

$$\overrightarrow{e_4}\, \mathrm{d}D_5 \mathrm{d}D_6 = \overrightarrow{\mathrm{d}A} = D_{56.}$$

Due to the dynamo effect in the wave-field $F_{4\text{-}6}$, a magnetic moment is generated via the spinless binding neutrino along the above-mentioned rotation matrix, which suggests to the observer that a proton consists of only a single particle.

With the emergence of the binding neutrino, two processes occur simultaneously. All external fions received from the respective bosons are converted into exchange fions/passive fion pairs. The particle configuration of the baryon is reduced to:

$$PC_{baryon} = \frac{3 + 1 - 1}{3}\,(boson1) + \frac{3 + 1 - 1}{3}\,(boson2) + \frac{3 + 1 - 1}{3}\,(boson3)$$

Subsequently, one u/d-quark-internal active fion converts into an exchange fion/passive fion pair. The particle configuration is further reduced to the value:

$$PC_{baryon} = \frac{3 + 1 - 2}{3}\,(boson1) + \frac{3 + 1 - 2}{3}\,(boson2) + \frac{3 + 1 - 2}{3}\,(boson3)$$

Now, each elementary particle is missing a partial charge due to the loss of an active fion. If the elementary particles consist of u/d-quarks, their respective charges are initially reduced to: $Q_{B1,2,3} = \pm\frac{2}{3}e$.

When a baryon decays, the binding neutrino is probably registered as a neutrino.

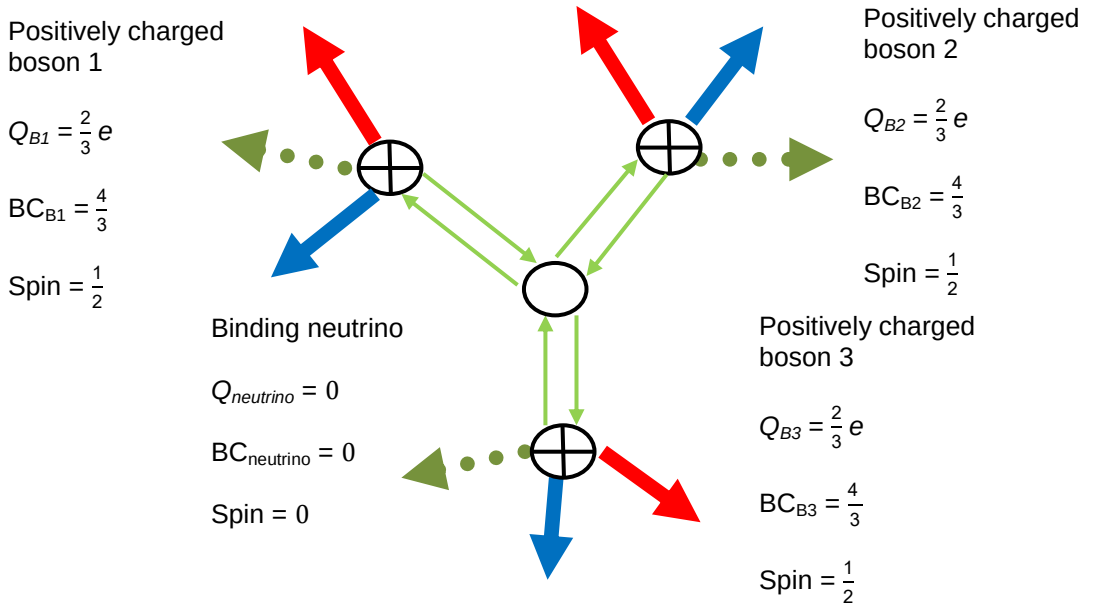

Figure 3.19: Baryon with a binding neutrino without spin in the centre to promote stability

The spin of the individual boson would suggest an integer spin due to the integer boson configuration. The two exchange fions emitted with integer spin have left their two passive fions in the respective boson for the binding neutrino. Virtually, an active fion with a spin of $\frac{1}{2}$ could arise again, but this would not contribute to the virtual mass because a passive fion originates from the external fion. The individual spin of the bosons remains half-integer. Accordingly, the total spin of three bosons with a spin of $\frac{1}{2}$ remains half-integer.

Properties of baryons consisting of three $Q = \frac{2}{3}e$ quarks with binding neutrinos:

$$PC_{baryon} = \frac{3 + 1 - 2}{3} + \frac{3 + 1 - 2}{3} + \frac{3 + 1 - 2}{3} + 0 = \frac{6}{3}$$

$$Q_{baryon} = +\frac{2}{3}e + \frac{2}{3}e + \frac{2}{3}e + 0 = +2\,e$$

$$\text{Spin} = \frac{1}{2} + \frac{1}{2} + \frac{1}{2} = \frac{3}{2} \text{ or } = -\frac{1}{2} - \frac{1}{2} - \frac{1}{2} = -\frac{3}{2} \text{ or } = \frac{1}{2} + \frac{1}{2} - \frac{1}{2} = \frac{1}{2} \text{ or } = \frac{1}{2} - \frac{1}{2} - \frac{1}{2} = -\frac{1}{2}$$

These particle structures are unlikely to occur in nature with such a one-sided charge configuration, or if they do, only with a very low probability.

F) Baryon consisting of two $Q = \frac{2}{3}\,e$ quarks, one $Q = -\frac{1}{3}\,e^-$ quark and one binding neutrino:

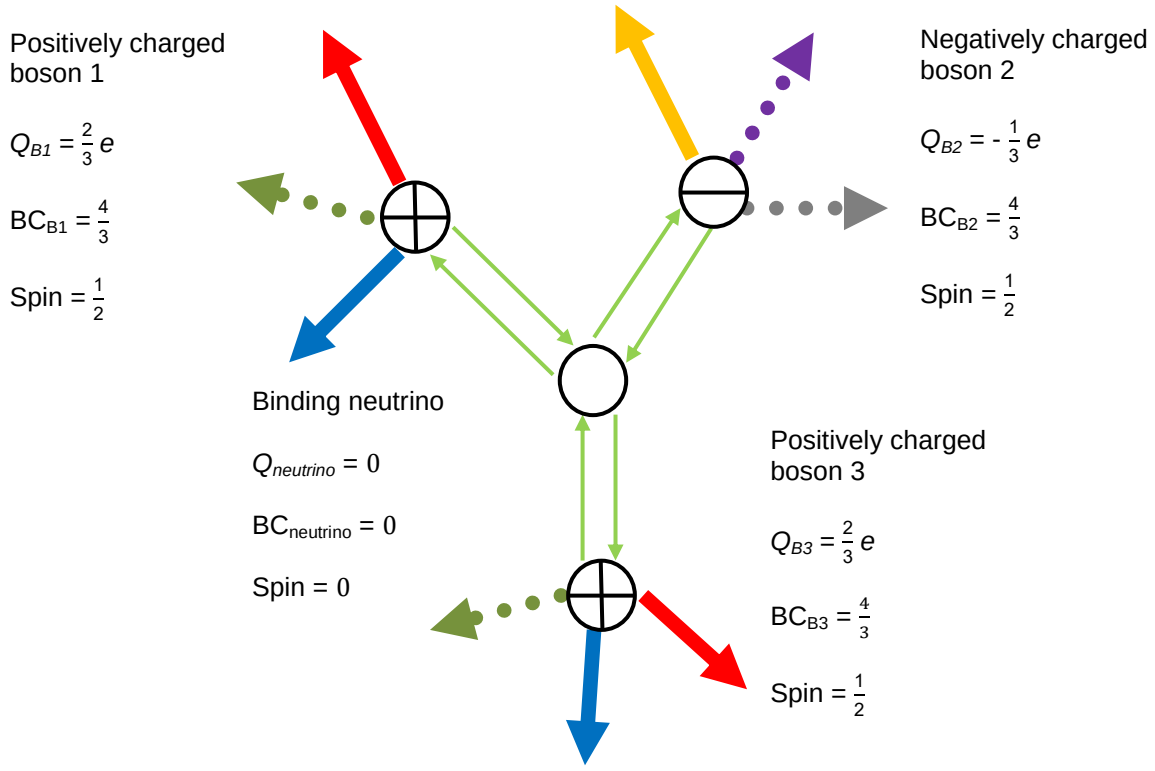

Figure 3.20: Baryon consisting of two $Q = \frac{2}{3}\,e$ quarks, one $Q = -\frac{1}{3}\,e$ quark and a binding neutrino in the centre of the particle structure

Properties of baryons consisting of two $Q = \frac{2}{3}\,e$ quarks, one $Q = -\frac{1}{3}\,e$ quark and a binding neutrino:

$$PC_{baryon} = \frac{3 + 1 - 2}{3} + \frac{3 + 1 - 2}{3} + \frac{3 + 1 - 2}{3} + 0 = \frac{6}{3}$$

$$Q_{baryon} = +\frac{2}{3}\,e + \frac{2}{3}\,e - \frac{1}{3}\,e + 0 = +1\,e \qquad \rightarrow \textbf{Proton}$$

$$\text{Spin} = \frac{1}{2} + \frac{1}{2} + \frac{1}{2} = \frac{3}{2} \text{ or } = -\frac{1}{2} - \frac{1}{2} - \frac{1}{2} = -\frac{3}{2} \text{ or } = \frac{1}{2} + \frac{1}{2} - \frac{1}{2} = \frac{1}{2} \text{ or } = \frac{1}{2} - \frac{1}{2} - \frac{1}{2} = -\frac{1}{2}$$

Due to its charge, this baryon is the proton. The stability of the proton depends on how the additional exchange fion of *the* $Q = -\frac{1}{3}\,e$ quark interacts with its environment. For example, it could interact with a $Q = +\frac{1}{3}\,e$ quark together with a neutron (**Figure**

3.21). In the atomic nucleus, a proton with its negatively charged boson (2) specifically seeks out a positively charged boson from the neutron in order to create a direct connection. Otherwise, the proton would behave like a radical and destabilise the atomic nucleus. After the strong interaction with a neutron, the proton is considered saturated to the environment. Meanwhile, the neutron could interact with other protons or with hidden matter. This will be discussed in more detail in the section on neutrons. The atomic nucleus is thus an agglomerate of protons and neutrons held together by their strong nuclear forces. Due to the complexity of the particle structure and the coupling frequency required for it, the strong nuclear force is stronger than the electromagnetic force at comparable distances. However, the electrical interaction with its repulsive forces is exactly as strong as the strong nuclear force before the protons or neutrons merge. This is explained by the Pauli principle for the FSM, which prevents more than five 4-dimensional rotational orbits from encountering each other simultaneously within a sphere S.

The proton has a stabilising effect on the atomic nucleus by merely creating a binding site for a neutron. A neutron, on the other hand, has two binding sites and seeks two binding partners. As a single neutron, it decays into a proton, an electron and an antineutrino without a binding partner.

G) Baryon consisting of a $Q = -\frac{2}{3}e$ quark, two $Q = \frac{1}{3}e$ quarks and a binding neutrino:

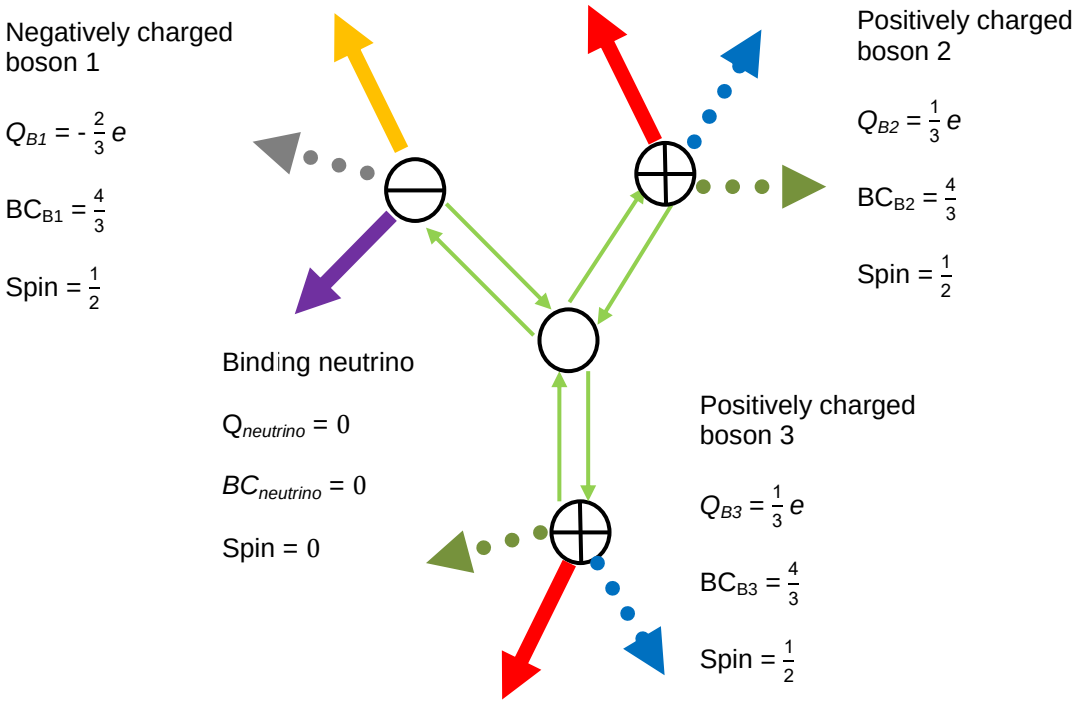

Figure 3.21: Baryon consisting of one $Q = -\frac{2}{3}e$ quark, two $Q = \frac{1}{3}e$ quarks and a binding neutrino in the centre of the particle structure

Properties of baryons consisting of one $Q = -\frac{2}{3}\,e$ quark, two $Q = \frac{1}{3}\,e$ quarks and a binding neutrino:

$$PC_{baryon} = \frac{3 + 1 - 2}{3} + \frac{3 + 1 - 2}{3} + \frac{3 + 1 - 2}{3} + 0 = \frac{6}{3}$$

$$Q_{baryon} = -\frac{2}{3}e + \frac{1}{3}e + \frac{1}{3}e + 0 = 0 \qquad \rightarrow \textbf{Neutron}$$

$$\text{Spin} = \frac{1}{2} + \frac{1}{2} + \frac{1}{2} = \frac{3}{2} \text{ or } = -\frac{1}{2} - \frac{1}{2} - \frac{1}{2} = -\frac{3}{2} \text{ or } = \frac{1}{2} + \frac{1}{2} - \frac{1}{2} = \frac{1}{2} \text{ or } = \frac{1}{2} - \frac{1}{2} - \frac{1}{2} = -\frac{1}{2}$$

This baryon is apparently the neutron. The neutron has two $Q = +\frac{1}{3}\,e$ quarks. The neutron therefore has two exchange fions that can interact with the environment. One could interact with the proton, similar to **Figure 3.12**, which promotes stability in the atomic nucleus. This leaves one more free exchange fion that can interact with its environment. If it does not find a partner in the dimension plane D_{56} parallel to the particle-field $F_{1\text{-}3}$, then there is a probability that an interaction will take place in the wave-field $F_{4\text{-}6}$ with a particle relative to the dimension plane D_{56}. Such a connection can no longer be directly detected for the particle-field $F_{1\text{-}3}$. In such cases, the atomic nucleus receives a concrete interaction with hidden matter. This interaction tends to have a destabilising effect on the atomic nucleus by distributing the resulting field strength over its atomic nucleus and thus reducing the strong nuclear force in the atomic nucleus. Above a certain atomic nucleus size, the influence of the hidden matter exceeds a critical state, after which decay restores an energetically favourable state with hidden matter.

The process of nuclear fission appears to be a natural limitation for particles, preventing them from exceeding a certain size.

Calculation of the influence of hidden matter on the atomic nucleus:

The results of the particle structures presented so far with the charge distribution of the u/d-quarks for the proton and neutron suggest that the amount of hidden matter in the atomic nucleus increases with its size. The following calculation serves as verification.

For two cases, the extent of the influence of hidden matter on the atomic nucleus is determined specifically. The periodic table of elements (PTE) is the measured observation from the particle-field $F_{1\text{-}3}$. Furthermore, according to the FSM, it is known that, under the condition of energy conservation, every atom is created with an equal number of electrons and positrons. However, the mass data in the PTE deviates from the aforementioned equilibrium. The mass equivalent of the binding energy in an interaction with hidden matter could possibly be the reason for the difference. This will be investigated below. The figures from the PTE should remain simple factors because ratios are still being presented.

1) Example Zinc:

Atomic weight: 65,3; atomic number: 30; electrons: 30, protons: 30, neutrons: 35

Charge components: neutron with $\frac{2}{3}\,e^+$ and $\frac{2}{3}\,e^-$; proton with $\frac{4}{3}\,e^+$ and $\frac{1}{3}\,e^-$

Distribution of electrons and positrons to neutrons and protons:

Number of positrons in the neutron: NoPN

Number of electrons in the neutron: NoEN

Number of positrons in the proton: NoPP

Number of electrons in the proton: NoEP

Total number of positrons in the atom: NoPT

Total number of electrons in the atom: NoET

Neutron: $\text{NoPN} = \frac{2}{3}\,e^+ \cdot 35 = 23{,}3\,e^+$

$\text{NoEN} = \frac{2}{3}\,e^- \cdot\ 35 = 23{,}3\,e^-$

Proton: $\text{NoPP} = \frac{4}{3}\,e^+ \cdot 30 = 40\,e^+$

$\text{NoEP} = \frac{1}{3}\,e^- \cdot\ 30 = 10\,e^-$

Electron: 30

Total NoPT = 23,3 e^+ + 40 e^+ = 63,3 e^+

NoET = 23,3 e^- + 10 e^- + 30 e^- = 63,3 e^-

Deviation from atomic mass:

65,3 – 63,3 = 2

Evaluation:

Since, according to the representation in **Figure 3.21**, the neutron can only exchange with a negatively charged particle, negatively charged mass equivalents such as those of a proton or other negatively charged $Q = \frac{2}{3} e$ bosons can be considered for field exchange. Due to the size of the manipulation, the hidden matter probably consists of the mass equivalent of two protons.

2) Example Uranium:

Atomic weight: 238; atomic number: 92; electrons: 92, protons: 92, neutrons: 146

Charge components: neutron with $\frac{2}{3} e^+$ and $\frac{2}{3} e^-$; proton with $\frac{4}{3} e^+$ and $\frac{1}{3} e^-$

Distribution of electrons and positrons to neutrons and protons:

Neutron: NoPN = $\frac{2}{3} e^+ \cdot 146 = 97{,}33\ e^+$

NoEN = $\frac{2}{3} e^- \cdot 146 = 97{,}33\ e^-$

Proton: NoPP = $\frac{4}{3} e^+ \cdot 92 = 122{,}66\ e^+$

NoEP = $\frac{1}{3} e^- \cdot 92 = 30{,}66\ e^-$

Electron: 92

Total NoPT = 97,33 e^+ + 122,66 e^+ = 220 e^+

NoET = 97,33 e^- + 30,66 e^- + 92 e^- = 220 e^-

Deviation from atomic mass:

238 – 220 = 18

Evaluation:

As expected, the difference from the atomic mass increases with the size of the atomic nucleus. Since the neutron interacts with protons, the hidden matter could consist of the mass equivalent of 18 protons.

Configuration of fermions, bosons, mesons and baryons:

Table 3.2 lists the configurations available so far for the following chapter. The terms contain valuable information about the structure of particles, which is why they are not simply abbreviated but are used for later interpretations of a particle.

(3.08)

Particle type	Configurations with lowest energy level	Further possible configuration
$BC_{electron}$ (extensions of the electron)	$\frac{4}{3}; \frac{4}{4}; \frac{5}{5}; \frac{6}{6}$	$\frac{5}{4}; \frac{6}{5}$
PC_{fion}	$\frac{1}{3}$	
$PC_{electron}$	$\frac{3}{3}$	
PC_{meson}	$\frac{4}{3}; \frac{6}{4}; \frac{8}{5}; \frac{10}{6}$	$\frac{5}{3}; \frac{6}{3}; \frac{8}{5}; \frac{8,5}{5}; \frac{9}{5}; \frac{9,5}{5}; \frac{10}{5}$
PC_{baryon}	$\frac{6}{3}$	

Table 3.2: List of configurations for different particles; BC – boson configuration; PC – particle configuration

3.5 Particle-exchange Fion-Particle-Coupling

The previous chapter described how particles are arranged in field-space. The spatial structure described is a prerequisite for integrating the four fundamental forces into this model. The electromagnetic, strong, and weak interactions, as well as the gravitational force, are derived from the value of the coupling frequency.

All more complex particles are derived from an extension of the electron with the simplest electron configuration EC = 3 (**Chapter 2.2, Point 17**). As an elementary particle, the electron thus constitutes the simplest charged particle structure in space-time. An exchange fion is the carrier of the interaction. The exchange of fields during coupling is registered as an interaction. For recombination into a complex particle, the exchange fion must reduce its wavelength until a resonance state prevails. To do this, it tunes itself to a multiple of the electron's coupling frequency. This factor is derived in this chapter and leads to the general formula for particles. Using the same factor for the electron frequency also provides the factor for the mass of any particle.

The electron frequency f_e:

To determine the electron frequency f_e, its mass M_e must be determined. The mass of the electron M_e is known from the relevant technical literature. This measured value is used as a base constant in the FSM.

Electron frequency [f_e] in Hz ; electron mass [M_e] in kg

The wavelength λ_e of the electron with mass M_e is:

$$\lambda_e = \frac{h}{M_e\, c} \tag{3.09}$$

with: $h = 6{,}626\ 10^{-34}$ Js; $M_e = 9{,}1094\ 10^{-31}$ kg; $c = 299792458\ \frac{\text{m}}{\text{s}}$

$$\lambda_e = \frac{6{,}626\ 10^{-34}\ \text{Js}}{9{,}1094\ 10^{-31}\text{kg} \cdot 299792458\ \frac{\text{m}}{\text{s}}} = 2{,}4263\ 10^{-12}\ \text{m}$$

$$f_e = \frac{c}{\lambda_e} \tag{3.10}$$

$$\underline{\underline{f_e}} = \frac{299792458\ \frac{\text{m}}{\text{s}}}{2{,}4263\ 10^{-12}\ \text{m}} = \underline{\underline{123{,}56\ \text{Exa Hz} = 1{,}2356\ 10^{20}\ \text{Hz}}}$$

The coupling configuration – CC:

For a field exchange between exchange fions and electrons, it is necessary that the respective frequencies resonate. For resonance with the electron, the exchange fion must couple with three active fions simultaneously. Each individual active fion rotates with $V_{rot} = \frac{c}{2}$. The coupling factor for each active fion is therefore $\frac{1}{2}$. The **coupling configuration – CC** for an electron is CC = $\frac{3}{2}$ for three active fions. The exchange fion thus sets itself to a $\lambda_{Fion} = \frac{2}{3}\lambda_e$ smaller wavelength than for the three active fions in the electron.

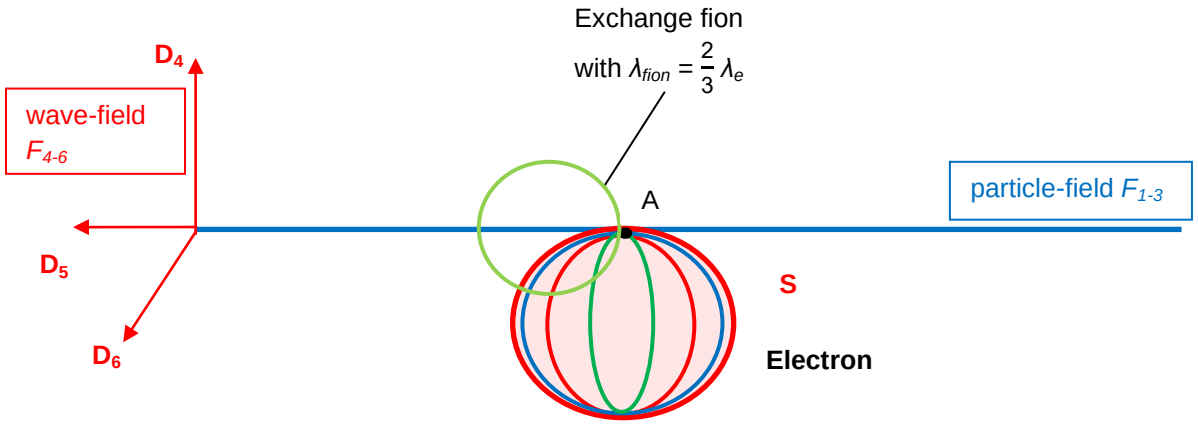

Figure 3.22: The electron in the dimension plane D_{45} is represented by a wavelength λ_e with a factor of 1; the exchange fion adjusts itself to a multiple of this wavelength

The above case refers to the ideal resonance state between the electron with its three active fions and the exchange fion. The multiples of fion frequencies relative to the stable electron are particularly interesting, because this multiplied field force is periodically transmitted to the particle-field F_{1-3} via field exchange with its 2-dimensional field vector from the wave-field F_{4-6}.

$$CC(EC) = \frac{\text{No. of active fions}}{\text{period duration } T \text{ of fions with reference to } c} \qquad (3.11)$$

$$CC(EC=3) = \frac{\text{3 active fions}}{\text{period duration } 2T} = \frac{3}{2}$$ (applies to the elementary particles electrons and u/d-quarks)

Further modes for the expansion of active fions in the electron sphere:

$$CC(EC=4) = \frac{\text{4 active fions}}{\text{period duration } 2T} = \frac{4}{2}$$ (C-quarks)

$$CC(EC=5) = \frac{\text{5 active fions}}{\text{period duration } 2T} = \frac{5}{2}$$ (B-quarks)

Comment for T-quarks: The electron configuration of EC = 6 indicates that these quarks need seven dimensions. In the author's opinion, bosons with six or more active fions should not exist in a 6-dimensional space, taking into account the maximum speed $V_{max} = c$. Unless there is a short-lived seventh to ninth dimension that could arise through a specific excitation to a further field-space level. The expansion of the spatial dimensions can be modelled using Field-Space-Mechanical Relativity Theory. For the purposes of this paper, let us assume that T-quarks exist briefly as 7-dimensional particles.

$$\text{CC(EC=6)} = \frac{\text{6 active fions}}{\text{period duration } 2T} = \frac{6}{2} \qquad \text{(T-quarks)}$$

Comment for S-quarks: The S-quark is similar to a u/d-quark, but with the difference that these fions have exactly half the wavelength of a fion in the u/d-quark with $\frac{1}{2}\,\lambda_{u/d}$ and additionally rotate orthogonally to each other.

Theoretically, this would allow for two sets of three fions rotating at half the wavelength of the u/d-quark. The limitation on the coupling factor is four instead of six active fions, because otherwise six 4-dimensional rotational paths would have to be considered, which would already require a seventh dimension. This is not possible without special excitation. It can be observed that particles with S-quarks also exist without a field-shifting excitation. For its undisturbed resonance frequency, the maximum number of fions with half the wavelength of the u/d-quark is sought, since these represent the smaller wavelength at which an exchange fion must couple. Thus, only four active fions with half wavelength are considered for the numerator for the lowest resonance frequency. For the denominator, an additional reduction in the rotation speed to $V_{rot} = \frac{c}{3}$ applies to these modes because the wavelengths of the active fions have decreased relative to a possible exchange fion. The coupling configuration CC can now be formed with this smallest resonance frequency.

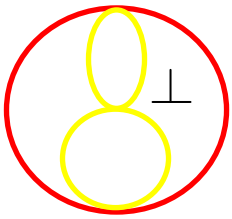

$$\text{CC(EC=5)} = \frac{4}{3} \text{ Note: Orbital velocity: } V_{rot} = \frac{c}{3}$$

$$\text{CC(EC=3)} = \frac{3}{2} \text{ Note: Orbital velocity: } V_{rot} = \frac{c}{2}$$

$$\text{CC(EC=5)} = \frac{\text{4 times 0,5 } \lambda \text{ active fions of u/d-quark}}{3T \text{ by orbital velocity 1/3 } c} = \frac{4}{3} \qquad \text{(S-quarks)} \qquad (3.12)$$

Coupling configuration CC* in the event of a disturbance:

In the event of an external disturbance, the 1:1 coupling of the three active fions, which exchange their fields on the dimension planes $D_{14/24/34}$ with the particle-field $F_{1\text{-}3}$, is disrupted. One example is an object velocity V_3 that affects the field propagation velocity $V_5 = c$. This would result in a deviation in space-time. This disturbance could therefore have a direct influence on the active fions in the field-space on the dimension planes $D_{14/24/34}$. Within the electron, space-time mechanical effects parallel to the fourth spatial dimension D_4 lead to elliptical rotational orbits, which increase the field propagation speed V_4. Such fion frequencies deviate slightly from undisturbed particles.

Assuming that the external disturbances are minor ($\Delta f \ll f$), the previously undisturbed coupling configuration must form a further multiple of the original electron frequency in order to find a synchronisation for the exchange fion with the disturbed electron.

This also applies to more complex particles in the field-space because they can only be disturbed on the three dimensional planes $D_{14/24/34}$ of the particle-field $F_{1\text{-}3}$. Therefore, the undisturbed coupling configuration CC must be raised to the power of 3 for three perturbable fions. The exchange fion achieves a much smaller wavelength λ_{fion} for the coupling with a disturbed elementary particle with its disturbed coupling configuration CC*.

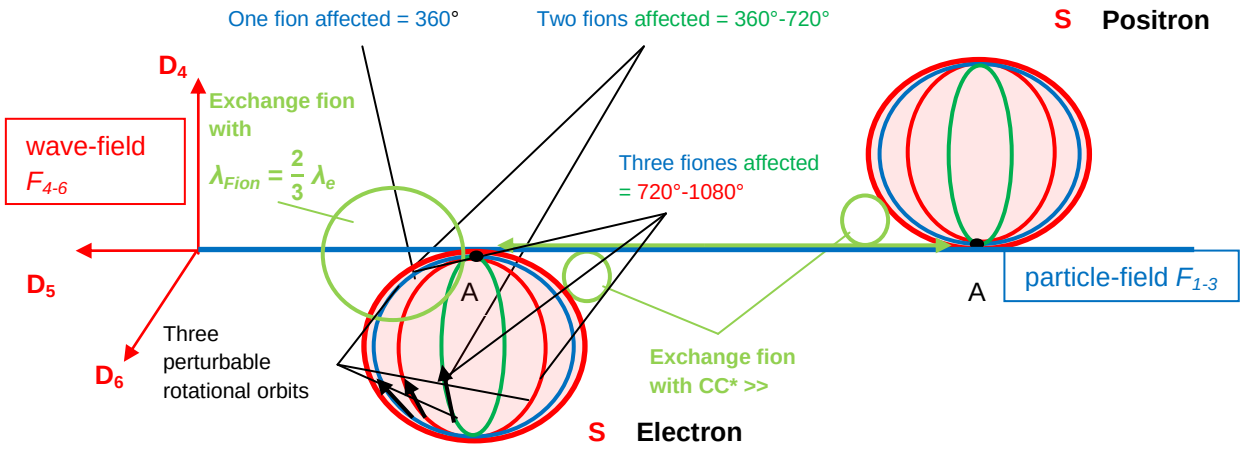

Figure 3.23: Exchange fions with much smaller wavelengths in the event of disturbances

These results in the following disturbed coupling configuration – CC* – for the elementary particles:

$$CC^* = (CC)^3 \qquad (3.13)$$

This ratio of potentiation also applies to quarks with the following coupling configurations – CC:

- An electron with the coupling configuration CC (EC=3) = $\frac{3}{2}$ provides with perturbation CC*(EC=3) = $(\frac{3}{2})^3$, e.g. for u/d-quarks
- An electron with the coupling configuration CC (EC=4) = $\frac{4}{2}$ provides with perturbation CC*(EC=4) = $(\frac{4}{2})^3$, e.g. for C-quarks
- An electron with the coupling configuration CC (EC=5) = $\frac{5}{2}$ provides with perturbation CC*(EC=5) = $(\frac{5}{2})^3$, e.g. for B-quarks
- An electron with the coupling configuration CC (EC=6) = $\frac{6}{2}$ provides with perturbation CC*(EC=6) = $(\frac{6}{2})^3$, e.g. for T-quarks.
- An electron with the coupling configuration CC (EC=5) = $\frac{4}{3}$ provides with perturbation CC*(EC=5) = $(\frac{4}{3})^{3,4,5,6,7,8}$, e.g. for S-quarks

For the S-quark, up to eight powers are conceivable as perturbations. The reason is that in the special case with 2 × 2 active fions with the wavelength $\frac{1}{2}\,\lambda_{u/d}$ these rotate relative to each other by 2 × 2 for the respective orthogonal orientation within the sphere of the electron. The boson configuration for the S-quark could take on 6-dimensions in the special case of BC = $\frac{2..12 \text{ and } 14}{2 \cdot 3}$. As it turns out, the fifth power occurs most frequently.

Consideration of the boson configuration BC:

The boson configuration BC is taken into account for the disturbed coupling configuration CC* because, for various cases of fion exchange by means of prior reception of external fions, the mass number in the numerator increases, which may contribute to the multiple of the fion frequency. The product of the boson configuration BC and the perturbed coupling configuration CC* results in the excitation of a harmonic of the exchange fion with respect to its total oscillation. This harmonic is represented as frequency *f**.

$f^* = BC\ CC^*\ f_e$ with $[f^*] = Hz$ (3.14)

Excitation frequency of a harmonic f^* for the electron in the event of a disturbance:

$$f^*_{electron} = \frac{3}{3}\left(\frac{3}{2}\right)^3 f_e = 3{,}375\ f_e$$

In the event of a disturbance of the u/d-quark, the following frequency applies to its harmonic f^*:

$$f^*_{u/d\text{-}quark} = f^*_{electron}\ (\text{eF1}) = \frac{4}{3}\left(\frac{3}{2}\right)^3 f_e = 4{,}5\ f_e$$

Further quark excitations:

$$f^*_{C\text{-}quark} = \frac{4}{4}\left(\frac{4}{2}\right)^3 = 8\ f_e$$

$$f^*_{B\text{-}quark} = \frac{5}{5}\left(\frac{5}{2}\right)^3 = 15{,}625\ f_e$$

$$f^*_{T\text{-}quark} = \frac{6}{6}\left(\frac{6}{2}\right)^3 = 27\ f_e$$

$$f^*_{S\text{-}quark} = \frac{5}{5}\left(\frac{4}{3}\right)^5 = 4{,}214\ f_e$$

$$f^*_{S\text{-}quark}(\text{eF1}) = \frac{6}{5}\left(\frac{4}{3}\right)^5 = 5{,}057\ f_e$$

When compensating for disturbances, a low disturbance frequency with $\Delta f << f$ has been assumed up to now. Depending on the severity of the disturbance, the frequency may increase further.

$f^*_{exchange\ fion} = 4.5\ f_e$ → However, the numerical factors of the respective disturbance frequencies still assume coupling after period $1T$, which corresponds to a harmonic of the total oscillation. Further factors follow for the exchange of fions, which are capable of doing, so taking into account their rotation on further dimensional planes.

Number of periods *T* for individual disturbed fions in an electron:

The superposition of all harmonics results in the total vibration for the bosonic exchange within any particle. It depends on the total number of periods T it takes for the exchange function to synchronize with the particle. All rotation matrices required for an exchange are taken into account. The number of rotation matrices is determined by the state of complexity the particle assumes at rest. On average, a rest state is then established as soon as all partial movements add up to zero. For the electron, this is ensured with a double rotation matrix. After a period of $1T$ in the dimension plane D_{45}, all fions along their 4-dimensional rotational paths have crossed the point of contact once ($\overrightarrow{e_6}\,\mathrm{d}D_4\mathrm{d}D_5 = \overrightarrow{\mathrm{d}A} = D_{45}$). Since the sphere S rotates in

space using its own rotation matrix ($\overrightarrow{e_5}\,\mathrm{d}D_4\mathrm{d}D_6 = \overrightarrow{\mathrm{d}A} = D_{46}$), it changes direction every $2T$ periods. On average, $V_{rot} = \frac{\sqrt{3}}{2}c - \frac{\sqrt{3}}{2}c = 0$. In a 6-dimensional view, the axis of rotation in the dimension plane D_{56} is added ($\overrightarrow{e_4}\,\mathrm{d}D_5\mathrm{d}D_6 = \overrightarrow{\mathrm{d}A} = D_{56}$). Taking into account all three rotation matrices for all three dimensional planes, the period is therefore $3T$ until a full rotation is complete.

Depending on how many fions are disturbed on which paths, this can have an effect on the orthogonal movement in the wave-field $F_{4\text{-}6}$. All dimension planes $D_{45/46/56}$ in the field $F_{4\text{-}6}$ where a disturbance could have occurred, even if only partially on average, are taken into account. The more fions are disturbed in the reference field $F_{4\text{-}6}$, the greater the factor for the period. If the exchange fion couples to two disturbed electrons, two different periods $2T$ must coincide with the period T of the exchange fion. Ultimately, the more periods it takes to achieve synchronization between the disturbed particle and an exchange fion, the higher the frequency of the exchange fion must be.

The following cases result in the exchange fion multiplying its harmonic frequency f^* in a bosonic total oscillation with the frequency f^{**}: $[f^{**}] = \mathrm{Hz}$

a) Two quarks are in field exchange with each other, each with three disturbed active fions, which rotate with two independent rotation matrices along the dimension planes $D_{45/46}$ in the 5-dimensional space and each with a period duration of $2T$. This corresponds to $2 \times 2T$ to the fourth power.

$$f^{**}_{u/d\text{-}quark}(4T) = (4,5)^4\, f_e \tag{3.15}$$

b) One quark interacts with another quark, each with three disturbed active fions, in a field exchange that rotates with two independent rotation matrices on the dimension planes $D_{45/46}$ and a period duration of $2T$ in the 5-dimensional range. The neighbouring quark, on the other hand, rotates with three independent rotation matrices on the dimension planes $D_{45/46/56}$ with a period duration of $3T$ in the 6-dimensional range. This field exchange corresponds to the factor with the period duration of $2T + 3T$ to the fifth power.

$$f^{**}_{u/d\text{-}quark}(5T) = (4,5)^5\, f_e \tag{3.16}$$

c) For a field exchange between two quarks, each with three disturbed active fions, these rotate with three independent rotation matrices on the dimension planes $D_{45/46/56}$ and a period duration of $3T$ using the 6-dimensional range. This corresponds to the factor with the period duration $2 \times 3T$ to the sixth power.

$$f^{**}_{u/d\text{-}quark}(6T) = (4,5)^6\, f_e \tag{3.17}$$

The lowest energetic excitation state begins using of the 5-dimensional range with the fourth power. This lowest excitation state is probably the most common among all particle types in nature.

Dimension family *n* (with *n* ε N):

$$f^{**}(nT) = (\mathrm{BC\ CC}^{*})^{n}\ f_e \tag{3.18}$$

n stands for the power and at the same time for the characteristic number of *T* periods between particles that can be traced back to the dimensions used.

Dimension reduction factor $\sqrt{\frac{5}{6}}$ & $\frac{5}{6}$:

The dimension reduction factor has already been mentioned in various places in this paper. Without this dimension reduction factor, no correction could be made for possible spatial structural differences between quarks to obtain a uniform mass formula. This correction of the orbital velocity affects the entire particle, so that the factor reduces its mass.

If force transmitters and receivers are affected, e.g. with a particle-exchange-ion-particle-coupling in the 5-dimensional range, then the maximum propagation velocity V_{max} is distributed across all five dimensions as follows:

$$V_{max} = V_{D1} + V_{D2} + V_{D3} + V_{D4} + V_{D5} = \frac{1}{5}\,c + \frac{1}{5}\,c + \frac{1}{5}\,c + \frac{1}{5}\,c + \frac{1}{5}\,c = c \tag{3.19}$$

In a 5-dimensional space, the factor $\sqrt{\frac{c}{5}}$ applies to the force transmitter in each spatial direction, depending on the number of dimensions used. The following therefore applies to the force transmitter and force receiver:

$$V_{D1} = \sqrt{\frac{c}{5}}\sqrt{\frac{c}{5}} = \frac{1}{5}\,c$$

By using the 6-dimensional space, the following applies accordingly:

$$V_{max} = \frac{1}{6}\,c + \frac{1}{6}\,c + \frac{1}{6}\,c + \frac{1}{6}\,c + \frac{1}{6}\,c + \frac{1}{6}\,c = c$$

Considering that two 6-dimensional particles with a trigonometrically resulting velocity of $V_{rot} = \frac{\sqrt{5}}{2}\,c > c$ (B-quarks) exchange, the factor for the maximum velocity V_{max} must be reduced to $V_{max} = c - \frac{1}{6}\,c = \frac{5}{6}\,c$ so that its rotational velocity V_{rot} does not exceed the maximum velocity V_{max}. As the maximum speed V_{max} decreases, the particle mass and the coupling frequency of the affected particle also decrease. The dimension reduction factor is referred to as "Dimfactor" in the formulas.

$$f^{**}_{electron} = [\frac{3}{3}(\frac{3}{2})^3]^n f_e \quad (3.20)$$

$$f^{**}_{u/d\text{-}quark} = f^{*}_{Electron}(eF1) = [\frac{4}{3}(\frac{3}{2})^3]^n f_e \quad (3.21)$$

$$f^{**}_{C\text{-}quark} = [\frac{4}{4}(\frac{4}{2})^3]^n f_e \quad (3.22)$$

$$f^{**}_{B\text{-}quark} = [\frac{5}{5}(\frac{5}{2})^3]^n \sqrt{\frac{5}{6}} f_e \qquad \sqrt{\frac{5}{6}} \text{ due to boson in } R^6 \quad (3.23)$$

$$f^{**}_{T\text{-}quark} = [\frac{6}{6}(\frac{6}{2})^3]^n \sqrt{\frac{5}{7}} f_e \qquad \sqrt{\frac{5}{7}} \text{ due to boson in } R^7 \quad (3.24)$$

$$f^{**}_{S\text{-}quark} = [\frac{5}{5}(\frac{4}{3})^5]^n f_e \qquad \frac{4}{3} \text{ due to } \frac{1}{2}\lambda_{u/d} \text{ im } R^6 \quad (3.25)$$

$$f^{**}_{S\text{-}quark}(eF1) = [\frac{6}{5}(\frac{4}{3})^5]^n f_e \qquad \frac{4}{3} \text{ due to } \frac{1}{2}\lambda_{u/d} \text{ im } R^6 \quad (3.26)$$

S-quark: no further reduction of the maximum velocity V_{max} is necessary. This has already been taken into account in the denominator with the velocity $V_{rot} = \frac{c}{3}$.

Consideration of particle configuration PC:

The total bosonic vibration f^{**} must form the product with the particle configuration in order to take into account all bosons involved in any particle structure. The frequency required for resonance between an exchange fion and the particle increases further by this factor. Various particle configurations PC are already known from **Chapter 3.3**:

- the fion: PC = $\frac{1}{3}$
- the electron: PC = $\frac{3}{3}$
- the meson-boson: PC = $\frac{4}{3}$ ($\rightarrow \frac{4}{3} = \frac{3-1}{3} + \frac{3-1}{3}$)
- the meson: PC = $\frac{6}{3}$ ($\rightarrow \frac{6}{3} = \frac{4-1}{3} + \frac{4-1}{3}$)
- the baryon: PC = $\frac{6}{3}$ ($\rightarrow \frac{6}{3} = \frac{4-2}{3} + \frac{4-2}{3} + \frac{4-2}{3}$).

These are the usual types of particles that occur in nature.

Coupling factor $\frac{1}{2}$ during the transition of an unbound fion to a bound fion:

The transition of all unbound fions in a complex particle rotating at a speed $V_{max} = c$ to bound active fions rotating at $V_{rot} = \frac{c}{2}$ halve's their rotational speed in order to adapt. This occurs during the transition from particle 1 as an exchange fion to particle 2. This coupling factor must be taken into account in the calculation, as it reduces the particle frequency and mass.

Definition of the coupling frequency:

Taking into account the coupling configuration, interference factors, the boson configuration, the dimension family, the particle configuration, the coupling between a free exchange fion and a bound exchange fion, and the dimension reduction factor, this complex factorised frequency of objects is referred to as **the coupling frequency**. Therefore, the object frequency f_{obj} automatically corresponds to the coupling frequency, the nomenclature for this model can be used in the same way.

Mass and coupling frequency of particles:

The mass and particle frequency can be calculated in generalised form as follows:

$$f_{obj} = \frac{1}{2}\,(\mathrm{BC}\,(\mathrm{CC})^{3})^{n} \cdot \mathrm{PC} \cdot \mathrm{Dimfactor} \cdot f_e \tag{3.27}$$

$$M_{obj} = \frac{1}{2}\,(\mathrm{BC}\,(\mathrm{CC})^{3})^{n} \cdot \mathrm{PC} \cdot \mathrm{Dimfactor} \cdot M_e \tag{3.28}$$

within:

- f_{obj} – coupling frequency for arbitrary objects
- M_{obj} – mass for arbitrary objects
- $\frac{1}{2}$ for half the speed of an unbound exchange fion to a bound active fion in a particle-exchange fion-particle-coupling
- BC – boson configuration: $\frac{\text{No. of active fions + No. extern fions}}{\text{No. active fions}}$
- CC – coupling configuration: $\frac{\text{No. of active fions}}{\text{period duration } T \text{ of fions with reference to } c}$
- Power of three for the three possible fions that can be disturbed from the particle-field
- n – nth dimension family
- PC – particle configuration:
  $\frac{\text{No. of active fions + No. extern fions – No. exchange fion/passive fion-pair}}{\text{No. active fions}}$
- Dimfactor for reducing the maximum velocity V_{max}
- M_e is the mass of the electron
- f_e is the frequency of the electron

Formulas (3.27) and (3.28) consist of a mathematically consistent equation that represents the particles as the product of several harmonics. A wave equation and complex mathematical operators are not necessary. This greatly simplifies the basic handling from a mathematical point of view.

The individual harmonics provide different information about the structure of a particle. When combined, these harmonics overlap to form a total vibration. In this case, the superimposed information is transferred to an **information matrix**, which describes complex objects.

3.6 Calculation of particle masses and coupling frequencies

The formula for calculating the mass and coupling frequency for the respective interaction in the field-space is available. These formulas will now be verified in this chapter by comparing the particle masses determined on the basis of the standard model of particle physics with the theoretically determined masses of the FSM.

Deviations between calculated and measured values:

The masses predicted by Field-Space-Mechanics are mathematical averages across all disturbance frequencies, couplings and possible periods. In reality, there will be slight fluctuations around the mean values given below. There could be many reasons for this. The exact disturbances, which may be due to the influence of hidden matter or relativistic effects, could lead to deviations. Each of these mean values requires a standardised standard deviation that expresses the variance with a high degree of probability.

Conversion of experimental values:

Experimentally proven measured values are given as multiples of the electron mass. The auxiliary conversion of a measured factor X with the energy in MeV can be carried out using a simple rule of three to a factor Y from the multiple of the electron mass M_e in kg. The proton mass is used for the required ratio, which already corresponds to a valid measured value with a deviation from the calculated prediction of $< 1\%$. Any deviations are included as consequential errors relative to the theoretically determined value. The calculated deviations will be approximately ±1% of the measured value.

$M_{proton} = 1836\ M_e \qquad [M_e\ ] = \text{kg}$

$E_{proton} = 938{,}38\ \text{MeV}$

$$Y\ M_e = \frac{1836\ M_e}{938{,}38\ \text{MeV}} \cdot X\ \text{MeV} \tag{3.29}$$

Some of the calculated masses were measured experimentally. These are designated as "experimental" and are listed in the references.

0. Dimension family: (power 0)

These include the electron, the positron and the neutrino in its most stable form:

$M_{electron} = 1\ M_e$

The values of the formula symbols are substituted into formula (3.28):

$$M_{electron} = [\frac{3}{3}(\frac{3}{2})^3]^0 \frac{3}{3} M_e = 1\ M_e$$

$$M_{u/d\text{-}quark} = M_{electron}(eF1) = [\frac{4}{3}(\frac{3}{2})^3]^0 \frac{3}{3} M_e = 1\ M_e$$

$$M_{C\text{-}quark} = [\frac{4}{4}(\frac{4}{2})^3]^0 \frac{3}{3} M_e = 1\ M_e$$

$$M_{B\text{-}quark} = [\frac{5}{5}(\frac{5}{2})^3]^0 \frac{3}{3} M_e = 1\ M_e$$

$$M_{T\text{-}quark} = [\frac{6}{6}(\frac{6}{2})^3]^0 \frac{3}{3} M_e = 1\ M_e$$

$$M_{S\text{-}quark}(eF1) = [\frac{6}{5}(\frac{4}{3})^5]^0 \frac{3}{3} M_e = 1\ M_e$$

For the 0th dimensional family, all elementary particles are reduced to the mass of the electron.

1st dimension family: (power 1 – interaction only in the 4-dimensional range)

The 1st dimension family represents the exchange interaction of the mass of a harmonic from its quark excitation. This includes the quark excitations of the individual quarks: the u/d-quark, S-quark, C-quark, B-quark, T-quark:

$$M_{u/d\text{-}quark} = [\frac{3}{3}(\frac{3}{2})^3]^1 \frac{3}{3} M_e = 3{,}375\ M_e$$

$$M_{u/d\text{-}quark} = M_{electron}(eF1) = [\frac{4}{3}(\frac{3}{2})^3]^1 \frac{3}{3} M_e = 4{,}5\ M_e$$

$$M_{C\text{-}quark} = [\frac{4}{4}(\frac{4}{2})^3]^1 \frac{3}{3} M_e = 8\ M_e$$

$$M_{B\text{-}quark} = [\frac{5}{5}(\frac{5}{2})^3]^1 \frac{3}{3}\sqrt{\frac{5}{6}} M_e = 14{,}26\ M_e \qquad (R^6 \text{ possible})$$

$$M_{T\text{-}quark} = [\frac{6}{6}(\frac{6}{2})^3]^1 \frac{3}{3}\sqrt{\frac{5}{7}} M_e = 22{,}82\ M_e \qquad \text{(from 7th dimension)}$$

$$M_{S\text{-}quark} = [\frac{6}{5}(\frac{4}{3})^5]^1 \frac{3}{3} M_e = 5{,}06\ M_e \qquad (R^6 \text{ possible})$$

Table 3.3 below summarises the quark excitations derived so far for the first dimensional family. Since mesons, with their integer spin, are also hypothetically suitable for representing a bosonic exchange, it may be possible to find further particle structures. The cases derived so far for the particle configurations of the mesons from **Chapter 3.3** are listed in the "BC" column.

For the C-quark: it would be conceivable that it mainly interferes with the harmonics of u/d-quarks in the structure of a baryon. In this case, the bosonic exchange would be characterised by the boson configuration BC(eF1) = $\frac{4}{3}$. This boson configuration is listed here for the sake of completeness.

(3.30)

Quark	**Quark excitation**	**BC** (boson, meson-boson, meson)	**Note** Mesons consist of two bosons, each of which lacks an active fion.
u/d-quark (occupying the lowest energy level)	$[BC\ (\frac{3}{2})^3]^1$	• $\frac{4}{3}$	$\frac{4}{3} = \frac{2}{3} + \frac{2}{3}$
C-quark	$[BC\ (\frac{4}{2})^3]^1$	• $\frac{4}{3}$; $\frac{4}{4}$; $\frac{6}{4}$	$\frac{4}{3} = \frac{2}{3} + \frac{2}{3}$ $\frac{6}{4} = \frac{3}{4} + \frac{3}{4}$
B-quark	$[BC\ (\frac{5}{2})^3]^1 \sqrt{\frac{5}{6}}$	• $\frac{5}{5}$; $\frac{8}{5}$	$\frac{8}{5} = \frac{4}{5} + \frac{4}{5}$
T-quark	$[BC\ (\frac{6}{2})^3]^1 \sqrt{\frac{5}{7}}$	• $\frac{6}{6}$; $\frac{10}{6}$	$\frac{10}{6} = \frac{5}{6} + \frac{5}{6}$
S-quark	$[BC\ (\frac{4}{3})^{3,4,5,6,7,8}]^1$	• $\frac{5}{5}$; $\frac{6}{5}$; $\frac{8}{5}$; $\frac{8{,}5}{5}$; $\frac{9}{5}$; $\frac{9{,}5}{5}$; $\frac{10}{5}$	$\frac{8}{5} = \frac{4}{5} + \frac{4}{5}$

Table 3.3: Possible boson configurations for the quark excitation of the u/d-, C-, B-, T- and S-quarks

Hypothetically, the variety can be increased as follows: For dimension families 0 to 3, the boson configuration can only be represented as BC = $\frac{3\ldots5}{3\ldots5}$. For dimension families 4 to 6, the boson configurations can be extended with the electron BC = $\frac{3\ldots5}{3\ldots5}$, the meson BC = $\frac{4\ldots14}{3\ldots5}$ and the baryon BC = $\frac{6\ldots12}{3\ldots5}$ (usually with $\frac{6}{3}$).

The S-quark can assume different modes. Conceivable would be the boson configuration for the meson boson in the 5-dimensional case with BC = $\frac{2..11}{5}$ or in the 6-dimensional case with BC = $\frac{2..12 \text{ und } 14}{2 \cdot 3}$, if it has absorbed an external fion in each case.

The first dimensional family is particularly important because these individual quark excitations, which represent a harmonic, stand for the individual subspaces of complex particles in their spatial structure. Depending on the particle, only the product of several of these harmonics is needed to find its coupling frequency. The object mass is derived from the same factor.

4th dimensional family: (power 4 – interaction in the 5-dimensional realm)

The 4th dimension family represents the lowest energy excitation state of an electron with which it can interact with a partner. The reason for this is that two disturbed quarks, each with three disturbed active fions, rotate in the 5-dimensional space with a period of 2*T*. This results in the fourth power for the exchange fion. During the field exchange between the unbound and bound states, the exchange fion returns to the velocity of $V_{rot} = \frac{c}{2}$. From this dimensional family onwards, the factor $\frac{1}{2}$ therefore applies.

The following particle types are modelled. The free fion with particle configuration PC = $\frac{1}{3}$ without coupling $\frac{1}{2}$, the muon as an electron with PC = $\frac{3}{3}$, the pion as a meson-boson with PC = $\frac{4}{3}$ and the meson with PC = $\frac{6}{3}$ consisting of two muons are calculated for the 4th dimension family as follows:

$M_{fon} = [\frac{4}{3}(\frac{3}{2})^3]^4 \frac{1}{3} M_e = 136{,}6875\ M_e$ → **the lowest mass of an exchange fion**

$M_{muon/electron,4.} = \frac{1}{2}[\frac{4}{3}(\frac{3}{2})^3]^4 \frac{3}{3} M_e = 205{,}031\ M_e$ (206,73 M_e experimental)

With a factor of~ 205, the muon is only slightly above the lowest mass of ~137. This suggests that the muon tends towards instability.

For the pion, the particle configuration of a meson-boson with PC = $\frac{4}{3} = \frac{4-2}{3} + \frac{4-2}{3}$ applies**.**

$M_{pion/meson\text{-}boson,\ 4.} = \frac{1}{2}[\frac{4}{3}(\frac{3}{2})^3]^4 \frac{4}{3} M_e = 273{,}375\ M_e$ (273,1 M_e experimental)

The hypothetical meson with its particle configuration PC = $\frac{6}{3}$:

$$M_{meson,from\ 2\ muons,4.} = \frac{1}{2}\left[\frac{4}{3}\left(\frac{3}{2}\right)^3\right]^4 \frac{6}{3} M_e = 410{,}0625\ M_e$$

The meson from the 4th dimension family has not yet been discovered. As a heavy meson, it would probably be too unstable. Furthermore, the 4th dimension family with its linear exchange possibility in the 5-dimensional range is not sufficient to represent this particle configuration as a baryon.

The composition of the formula symbols for the muon is examined in more detail below in order to understand its components.

$$M_{muon/electron,4.} = \frac{1}{2}\left[\frac{4}{3}\left(\frac{3}{2}\right)^3\right]^4 \frac{3}{3} M_e = 205{,}031\ M_e$$

$\frac{3}{2} = \frac{\text{No. active fions}}{\text{period duration}}$ – Coupling configuration CC for a resonance between an exchange fion and the three undisturbed active fions. The exchange fion must couple to each active fion with a coupling factor of $\frac{1}{2}$.

( )³ – The power with the factor 3 takes into account the three possible active fions that can be disturbed from the particle-field $F_{1\text{-}3}$.

$\frac{4}{3} = \frac{\text{No. of active fions + No. extern fions}}{\text{No. active fions}}$ – Boson configuration BC. For the bosonic exchange, the electron has temporarily absorbed an external fion. During the fion exchange, the electron exists as a u/d-quark.

[ ] ^{4} – *n*-th dimension family. Factor 4 stands for the exchange of two disturbed particles that encounter each other with two rotation matrices in the dimension planes $D_{45/46}$. A 4-fold potentiated quark excitation is required for a resonance of an exchange fion with such a particle structure.

$\frac{1}{2}$ – Factor stands for half the maximum velocity $V_{max} = c$ when an unbound exchange fion is absorbed into a bound disturbed particle.

$\frac{3}{3} = \frac{\text{No. of active fions + No. extern fions – No. exchange fion/passive fion-pair}}{\text{No. active fions}}$ – Particle configuration PC. In this case, the exchange fion exchanges with the muon particle, which is modelled as a particle configuration like an electron with three active fions.

Dim factor – **1**, due to the use of 5-dimensional space, there is no reduction in the maximum velocity V_{max}.

$\boldsymbol{M_e}$ – Mass of the electron.

5th Dimension family: (power of 5 – interaction in the 5- to 6-dimensional range)

The electron with particle configuration PC = $\frac{3}{3}$, the meson-boson with PC = $\frac{4}{3}$, the meson with PC = $\frac{6}{3} = \frac{4-1}{3} + \frac{4-1}{3}$, and the baryon with PC = $\frac{6}{3} = \frac{4-2}{3} + \frac{4-2}{3} + \frac{4-2}{3}$ are modelled from the 5th dimensional family:

$$M_{electron,5.} = \frac{1}{2}\left[\frac{4}{3}\left(\frac{3}{2}\right)^3\right]^5 \frac{3}{3} M_e = 922{,}640625\ M_e$$

The electron for the 5th dimensional family has not yet been discovered as a single particle.

$$M_{meson\text{-}boson,5.} = \frac{1}{2}\left[\frac{4}{3}\left(\frac{3}{2}\right)^3\right]^5 \frac{4}{3} M_e = 1230{,}1875\ M_e$$

$$M_{baryon,5.} = \frac{1}{2}\left[\frac{4}{3}\left(\frac{3}{2}\right)^3\right]^5 \frac{6}{3} M_e = 1845{,}28125\ M_e$$ → **Proton / Neutron**

(1836,15 M_e experimental)

Composition of the formula for the proton:

The essential difference between the proton and the muon lies in the exchange of its u/d-quarks with possible spin matrices on the additional dimension plane D_{56} and the particle type of the baryon. The proton consists of three u/d-quarks that exchange between each other via a binding neutrino.

Most of the relevant known complex particle structures will be composed of the fifth and, in part, the sixth dimension according to this particle model of the FSM.

Possible quark excitations from the 1st dimension family can be extended with the 0th dimension family. The effect would be mathematically 1 + 0 = 1. However, in this way, further intermediate frequencies for quarks can be found for particle masses of baryons and mesons, which have already been found by the international *Particle Data Group* (PDG). This results in a particle diversity that goes far beyond what is currently known. For the sake of clarity, this paper does not attempt to present all conceivable combinations. **Table 3.4** shows an example of this relationship for the u/d-quark. Numerous intermediate frequencies also apply to the other quarks, which are not all listed in this paper.

Quark excitation	Multiple f_e	Particle type
$[\frac{4}{3}(\frac{3}{2})^3]^1$	4,5	u/d-quark $_{boson,1}$
$[\frac{4}{3}(\frac{3}{2})^3]^1 + \frac{2}{3 \cdot 2}$	4,833	u/d-quark $_{boson,1.}$ + particle from 0. dimension family
$[\frac{4}{3}(\frac{3}{2})^3]^1 + \frac{3}{3 \cdot 2}$	5	u/d-quark $_{boson,1.}$ + particle from 0. dimension family
$[\frac{4}{3}(\frac{3}{2})^3]^1 + \frac{4}{3 \cdot 2}$	5,167	u/d-quark $_{boson,1.}$ + particle from 0. dimension family
$[\frac{4}{3}(\frac{3}{2})^3]^1 + \frac{5}{3 \cdot 2}$	5,33	u/d-quark $_{boson,1.}$ + particle from 0. dimension family
$[\frac{4}{3}(\frac{3}{2})^3]^1 + \frac{6}{3 \cdot 2}$	5,5	u/d-quark $_{boson,1.}$ + particle from 0. dimension family
$[\frac{4}{3}(\frac{3}{2})^3]^1 + \frac{7}{3 \cdot 2}$	5,67	u/d-quark $_{boson,1.}$ + particle from 0. dimension family
$[\frac{4}{3}(\frac{3}{2})^3]^1 + \frac{8}{3 \cdot 2}$	5,83	u/d-quark $_{boson,1.}$ + particle from 0. dimension family
$[\frac{4}{3}(\frac{3}{2})^3]^1 + \frac{9}{3 \cdot 2}$	6	u/d-quark $_{boson,1.}$ + particle from 0. dimension family
$[\frac{4}{3}(\frac{3}{2})^3]^1 + \frac{10}{3 \cdot 2}$	6,167	u/d-quark $_{boson,1.}$ + particle from 0. dimension family
$[\frac{4}{3}(\frac{3}{2})^3]^1 + \frac{12}{3 \cdot 2}$	6,5	u/d-quark $_{boson,1.}$ + particle from 0. dimension family

Table 3.4: Variations for u/d-quark excitations

With the above quark excitations, several dozen variations of u/d-quark-based baryons can be calculated.

The S-quark has only been considered for a special case so far. **Table 3.5** below shows all bosonic variants and perturbations for the S-quark.

Quark excitation	Multiple f_e	Particle type
$[\frac{5}{5}(\frac{4}{3})^3]^1$	2,37	S-quark boson,1.
$[\frac{6}{5}(\frac{4}{3})^3]^1$	2,84	S-quark boson,1
$[\frac{8}{5}(\frac{4}{3})^3]^1$	3,79	S-quark meson-boson,1.
$[\frac{8,5}{5}(\frac{4}{3})^3]^1$	4,0296	S-quark meson
$[\frac{9}{5}(\frac{4}{3})^3]^1$	4,267	S-quark meson
$[\frac{9,5}{5}(\frac{4}{3})^3]^1$	4,504	S-quark meson
$[\frac{10}{5}(\frac{4}{3})^3]^1$	4,74	S-quark meson
$[\frac{5}{5}(\frac{4}{3})^4]^1$	3,16	S-quark boson,1.
$[\frac{6}{5}(\frac{4}{3})^4]^1$	3,79	S-quark boson,1.
$[\frac{8}{5}(\frac{4}{3})^4]^1$	5,0568	S-quark meson-boson,1.
$[\frac{8,5}{5}(\frac{4}{3})^4]^1$	5,3728	S-quark meson
$[\frac{9}{5}(\frac{4}{3})^4]^1$	5,689	S-quark meson
$[\frac{9,5}{5}(\frac{4}{3})^4]^1$	6,005	S-quark meson
$[\frac{10}{5}(\frac{4}{3})^4]^1$	6,321	S-quark meson
$[\frac{5}{5}(\frac{4}{3})^5]^1$	4,21	S-quark boson,1.
$[\frac{6}{5}(\frac{4}{3})^5]^1$	5,057	S-quark boson,1.
$[\frac{8}{5}(\frac{4}{3})^5]^1$	6,74	S-quark meson-boson,1.
$[\frac{8,5}{5}(\frac{4}{3})^5]^1$	7,16	S-quark meson
$[\frac{9}{5}(\frac{4}{3})^5]^1$	7,585	S-quark meson

Quark excitation	Multiple f_e	Particle type
$[\frac{9,5}{5}(\frac{4}{3})^5]^1$	8,0066	S-quark meson
$[\frac{10}{5}(\frac{4}{3})^5]^1$	8,428	S-quark meson
$[\frac{5}{5}(\frac{4}{3})^6]^1$	5,6186	S-quark boson,1.
$[\frac{6}{5}(\frac{4}{3})^6]^1$	6,742	S-quark boson,1.
$[\frac{8}{5}(\frac{4}{3})^6]^1$	8,99	S-quark meson-boson,1.
$[\frac{8,5}{5}(\frac{4}{3})^6]^1$	9,55	S-quark meson
$[\frac{9}{5}(\frac{4}{3})^6]^1$	10,11	S-quark meson
$[\frac{9,5}{5}(\frac{4}{3})^6]^1$	10,675	S- quark meson
$[\frac{10}{5}(\frac{4}{3})^6]^1$	11,237	S-quark meson
$[\frac{5}{5}(\frac{4}{3})^7]^1$	7,49	S-quark boson,1.
$[\frac{6}{5}(\frac{4}{3})^7]^1$	8,99	S-quark boson,1.
$[\frac{8}{5}(\frac{4}{3})^7]^1$	11,986	S-quark meson-boson,1.
$[\frac{8,5}{5}(\frac{4}{3})^7]^1$	12,73	S-quark meson
$[\frac{9}{5}(\frac{4}{3})^7]^1$	13,48	S-quark meson
$[\frac{9,5}{5}(\frac{4}{3})^7]^1$	14,234	S-quark meson
$[\frac{10}{5}(\frac{4}{3})^7]^1$	14,98	S-quark meson
$[\frac{5}{5}(\frac{4}{3})^8]^1$	9,99	S-quark boson,1.
$[\frac{6}{5}(\frac{4}{3})^8]^1$	11,99	S-quark boson,1.

Quark excitation	Multiple f_e	Particle type
$[\frac{8}{5}(\frac{4}{3})^8]^1$	15,98	S-quark $_{\text{meson-boson,1.}}$
$[\frac{8,5}{5}(\frac{4}{3})^8]^1$	16,98	S-quark $_{\text{meson}}$
$[\frac{9}{5}(\frac{4}{3})^8]^1$	17,98	S-quark $_{\text{meson}}$
$[\frac{9,5}{5}(\frac{4}{3})^8]^1$	18,98	S-quark $_{\text{meson}}$
$[\frac{10}{5}(\frac{4}{3})^8]^1$	19,98	S-quark $_{\text{meson}}$

Table 3.5: Variations for S-quark excitations

For a selected S-quark, the 0th dimensionality family should be added below. These variances would hypothetically also be possible for all other powers $(\frac{4}{3})^{3,4,6,7,8}$.

Quark excitation	Multiple f_e	Particle type
$[\frac{6}{5}(\frac{4}{3})^5]^1$	5,0568	S-quark $_{\text{boson,1.}}$
$[\frac{6}{5}(\frac{4}{3})^5]^1+\frac{2}{3\cdot 2}$	5,39	S-quark $_{\text{boson,1.}}$ + particle from 0. dimension family
$[\frac{6}{5}(\frac{4}{3})^5]^1+\frac{3}{3\cdot 2}$	5,557	S-quark $_{\text{boson,1.}}$ + particle from 0. dimension family
$[\frac{6}{5}(\frac{4}{3})^5]^1+\frac{4}{3\cdot 2}$	5,7235	S-quark $_{\text{boson,1.}}$ + particle from 0. dimension family
$[\frac{6}{5}(\frac{4}{3})^5]^1+\frac{5}{3\cdot 2}$	5,89	S-quark $_{\text{boson,1.}}$ + particle from 0. dimension family
$[\frac{6}{5}(\frac{4}{3})^5]^1+\frac{6}{3\cdot 2}$	6,0568	S-quark $_{\text{boson,1.}}$ + particle from 0. dimension family
$[\frac{6}{5}(\frac{4}{3})^5]^1+\frac{7}{3\cdot 2}$	6,2235	S-quark $_{\text{boson,1.}}$ + particle from 0. dimension family
$[\frac{6}{5}(\frac{4}{3})^5]^1+\frac{8}{3\cdot 2}$	6,39	S-quark $_{\text{boson,1.}}$ + particle from 0. dimension family
$[\frac{6}{5}(\frac{4}{3})^5]^1+\frac{9}{3\cdot 2}$	6,5568	S-quark $_{\text{boson,1.}}$ + particle from 0. dimension family

Quark excitation	Multiple f_e	Particle type
$[\frac{6}{5}(\frac{4}{3})^5]^1 + \frac{10}{3 \cdot 2}$	6,7235	S-quark $_{\text{boson,1.}}$ + particle from 0. dimension family
$[\frac{6}{5}(\frac{4}{3})^5]^1 + \frac{11}{3 \cdot 2}$	6,89	S-quark $_{\text{boson,1.}}$ + particle from 0. dimension family
$[\frac{6}{5}(\frac{4}{3})^5]^1 + \frac{12}{3 \cdot 2}$	7,0568	S-quark $_{\text{boson,1.}}$ + particle from 0. dimension family
$[\frac{6}{5}(\frac{4}{3})^5]^1 + \frac{14}{3 \cdot 2}$	7,39	S-quark $_{\text{boson,1.}}$ + particle from 0. dimension family

Table 3.6: Selected S-quarks for the 1st dimension family, added to the proportions of the 0th dimension family

Quark excitation	Multiple f_e	Particle type
$[\frac{4}{4}(\frac{4}{2})^3]^1$	8	C-quark $_{\text{boson,1.}}$
$[\frac{6}{4}(\frac{4}{2})^3]^1$	12	C-quark $_{\text{meson-boson,1.}}$
$[\frac{4}{4}(\frac{4}{2})^3]^1 + \frac{2}{3 \cdot 2}$	8,33	C-quark $_{\text{boson,1.}}$ + particle from 0. dimension family
…	….	….
$[\frac{4}{4}(\frac{4}{2})^3]^1 + \frac{9}{3 \cdot 2}$	9,5	C-quark $_{\text{boson,1.}}$ + particle from 0. dimension family
…	….	….
$[\frac{4}{4}(\frac{4}{2})^3]^1 + \frac{12}{3 \cdot 2}$	10	C-quark $_{\text{boson,1.}}$ + particle from 0. dimension family
$[\frac{4}{3}(\frac{4}{2})^3]^1$	10,66	C-quark $_{\text{meson-boson,1.}}$
$[\frac{4}{3}(\frac{4}{2})^3]^1 + \frac{2}{3 \cdot 2}$	11	C-quark $_{\text{boson,1.}}$ + particle from 0. dimension family
…	…	…
$[\frac{4}{3}(\frac{4}{2})^3]^1 + \frac{12}{3 \cdot 2}$	12,66	C-quark $_{\text{boson,1.}}$ + particle from 0. dimension family

Table 3.7: Insight into the variations for C-quark excitations

Quark excitation	Multiple f_e	Particle type
$[\frac{5}{5}(\frac{5}{2})^3]^1 \cdot \sqrt{\frac{5}{6}}$	$15{,}625 \cdot \sqrt{\frac{5}{6}} =$ 14,264	B-quark $_{\text{boson,1.}}$
$[\frac{8}{5}(\frac{5}{2})^3]^1 \cdot \sqrt{\frac{5}{6}}$	$25 \cdot \sqrt{\frac{5}{6}} = 22{,}822$	B-quark $_{\text{meson-boson,1.}}$
$[\frac{5}{5}(\frac{5}{2})^3]^1 \cdot \sqrt{\frac{5}{6}} + \frac{2}{3 \cdot 2}$	$15{,}625 \cdot \sqrt{\frac{5}{6}} + \frac{2}{3 \cdot 2}$ =14,6	B-quark $_{\text{boson,1..}}$ + particle from 0. dimension family
…	…	…
$[\frac{5}{5}(\frac{5}{2})^3]^1 \cdot \sqrt{\frac{5}{6}} + \frac{12}{3 \cdot 2}$	16,264	B-quark $_{\text{boson,1.}}$ + particle from 0. dimension family

Table 3.8: Insight into the variations for B-quark excitations

Quark excitation	Multiple f_e	Particle type
$[\frac{6}{6}(\frac{6}{2})^3]^1 \cdot \sqrt{\frac{5}{7}}$	$27 \cdot \sqrt{\frac{5}{7}} = 22{,}82$	T-quark $_{\text{boson,1.}}$
$[\frac{10}{6}(\frac{6}{2})^3]^1 \cdot \sqrt{\frac{5}{7}}$	$45 \cdot \sqrt{\frac{5}{7}} = 38{,}03$	T-quark $_{\text{meson-boson,1.}}$
$[\frac{6}{6}(\frac{6}{2})^3]^1 \cdot \sqrt{\frac{5}{7}} + \frac{2}{3 \cdot 2}$	$27 \cdot \sqrt{\frac{5}{7}} + \frac{2}{3 \cdot 2} =$ 23,153	T-quark $_{\text{boson,1.}}$ + particle from 0. dimension family
…	…	…
$[\frac{6}{6}(\frac{6}{2})^3]^1 \cdot \sqrt{\frac{5}{7}} + \frac{12}{3 \cdot 2}$	24,82	T-quark $_{\text{boson,1.}}$ + particle from 0. dimension family

Table 3.9: Insight into the variations for T-quark excitations

Table 3.10 summarises the quark excitations given above for particle masses for selected particles. For each subspace U, a quark excitation from the first dimensional family is available.

Particle	**U**	**U**	**U**	**U**	**U**	**PC**		**mass calculated** M_e	**experim. mass** M_e
Proton-baryon	4,5	4,5	4,5	4,5	4,5	$\frac{6}{3}$	$\frac{1}{2}$	1845	1836
CS-meson D±	4,5	4,5	4,5	5,0568	8	$\frac{6}{3}$	$\frac{1}{2}$	3686	3658
C-meson	4,5	4,5	4,5	4,5	12	$\frac{6}{3}$	$\frac{1}{2}$	4921	
CS-meson $D_s^{\pm}$	4,5	4,5	4,5	5,39	8	$\frac{6}{3}$	$\frac{1}{2}$	3929	3853
CS-meson D^*_{s0} (2317)±	4,5	4,5	4,5	6,2235	8	$\frac{6}{3}$	$\frac{1}{2}$	4537	4535
CS-meson D_{s1}(2460)	4,5	4,5	4,5	6,5568	8	$\frac{6}{3}$	$\frac{1}{2}$	4780	4812
CS-meson D_{s1}(2536)	4,5	4,5	4,5	6,7235	8	$\frac{6}{3}$	$\frac{1}{2}$	4901	4960
CS-meson D^*_{s2} (2573)	4,5	4,5	4,5	6,89	8	$\frac{6}{3}$	$\frac{1}{2}$	5023	5027
…	…	…	…	…	…	…	…	…	…
CC-meson J/ψ(1S)	4,5	4,5	4,5	8,33	8	$\frac{6}{3}$	$\frac{1}{2}$	6072	6060
CS-baryon Ξ_c^0	4,5	4,5	4,5	6,89	8	$\frac{6}{3}$	$\frac{1}{2}$	5023	5046
CS-baryon Ξc (2645)	4,5	4,5	4,5	7,0568	8	$\frac{6}{3}$	$\frac{1}{2}$	5144	5176
…	…	…	…	…	…	…	…	…	…
B-meson B±	4,5	4,5	4,5	4,5	25	$\frac{6}{3}$	$\frac{1}{2}$	10252	10329
BB-meson Y(1S)	4,5	4,5	4,5	$15{,}625 \cdot \sqrt{\frac{5}{6}}$	$15{,}625 \cdot \sqrt{\frac{5}{6}}$	$\frac{6}{3}$	$\frac{1}{2}$	18539	18510
BS-meson B_S^*	4,5	4,5	4,5	5,0568	$25 \cdot \sqrt{\frac{5}{6}}$	$\frac{6}{3}$	$\frac{1}{2}$	10516	10596

Particle	**U**	**U**	**U**	**U**	**U**	**PC**		**mass calculated** M_e	**experim. mass** M_e
CB-meson	4,5	4,5	4,5	8	$15{,}625 \cdot \sqrt{\frac{5}{6}}$	$\frac{6}{3}$	$\frac{1}{2}$	10398	
CB-meson B_C^+	4,5	4,5	4,5	9,5	$15{,}625 \cdot \sqrt{\frac{5}{6}}$	$\frac{6}{3}$	$\frac{1}{2}$	12348	12277
BS-baryon $\Xi_b (5945)^0$	4,5	4,5	4,5	5,557	$25 \cdot \sqrt{\frac{5}{6}}$	$\frac{6}{3}$	$\frac{1}{2}$	11556	11632
BC-baryon	4,5	4,5	4,5	8	$25 \cdot \sqrt{\frac{5}{6}}$	$\frac{6}{3}$	$\frac{1}{2}$	16637	
…	…	…	…	…	…	…	…	…	…
T-meson	4,5	4,5	4,5	4,5	$45 \cdot \sqrt{\frac{5}{7}}$	$\frac{6}{3}$	$\frac{1}{2}$	15595	
TT-meson	4,5	4,5	4,5	$27 \cdot \sqrt{\frac{5}{7}}$	$27 \cdot \sqrt{\frac{5}{7}}$	$\frac{6}{3}$	$\frac{1}{2}$	47450	
BT-baryon	4,5	4,5	4,5	$15{,}625 \cdot \sqrt{\frac{5}{6}}$	$45 \cdot \sqrt{\frac{5}{7}}$	$\frac{6}{3}$	$\frac{1}{2}$	49433	
….	….	….	….	….	….	…	…	….	….

Table 3.10: Selected particle of the 5th dimensional family

Brief evaluation of **Table 3.10** and verification result of the FSM:

It appears that superimposed harmonics of individual quark excitations from the 1st dimensional family can be used to expand these into complex particles from the 4th dimensional family onwards. It can be seen that the 5th dimensional family, which exchanges fields with each other in 5- to 6-dimensional space, is required for the production of most of the relevant known particles. Up to the third harmonic, all mesons and baryons consist of u/d-quark excitations. Only with the fourth and fifth harmonics does the particle take on its specific form. This confirms the statement that the smallest building blocks for particles consist of u/d-quarks.

There are many combinations that predict further particles. For the sake of clarity, this paper does not include all conceivable particles. A separate particle map verifies the results of all particle masses measured experimentally to date and additionally predicts further particles. This independently confirms the FSM beyond the particle model.

6th Dimension family: (power of 6 – interaction completely 6-dimensional)

The tauon electron with the particle configuration PC = $\frac{3}{3}$, the meson-boson with PC = $\frac{4}{3}$, the meson PC = $\frac{6}{3} = \frac{4-1}{3} + \frac{4-1}{3}$ and the baryon with PC = $\frac{6}{3} = \frac{4-2}{3} + \frac{4-2}{3} + \frac{4-2}{3}$ are modelled from the 6th dimension family:

Note: Please note the dimension reduction factor of Dimfactor = $\frac{5}{6}$ for the 6-dimensional space!

$M_{tauon/electron,6.} = \frac{1}{2}\left[\frac{4}{3}\left(\frac{3}{2}\right)^3\right]^6 \frac{5}{6}\frac{3}{3} M_e = 3459{,}9\ M_e$ (3476,6 M_e experimental)

$M_{meson\text{-}boson,6.} = \frac{1}{2}\left[\frac{4}{3}\left(\frac{3}{2}\right)^3\right]^6 \frac{5}{6}\frac{4}{3} M_e = 4613{,}203125\ M_e$

$M_{meson/baryon,6.} = \frac{1}{2}\left[\frac{4}{3}\left(\frac{3}{2}\right)^3\right]^6 \frac{5}{6}\frac{6}{3} M_e = 6919{,}804688\ M_e$

Gauge bosons :

The Z- and W-bosons are so-called gauge bosons. In the Standard Model, they are responsible for the weak interaction. The Z-boson is electrically neutral, while the W-boson can assume charge states of W^+ and W^-. Both bosons have a spin of 1. The H-boson, or Higgs particle, is electrically neutral and has a spin of 0. Its interaction is weak, but the H-boson is the heaviest boson ever found.

In the particle model of the FSM, the W-, Z- and H-bosons are special products of the coupling of a muon with mass $M_{muon/electron,4.}$ from the 4th dimension family and an electron with mass $M_{electron,5.}$ from the 5th dimension family. The conglomerate of two 5- to 6-dimensional electrons in a sphere S requires the use of the 6-dimensional domain for their fion exchange. They can couple with each other as a boson pair through a fion exchange. For this purpose, the dimension reduction factor of Dimfactor = $\frac{5}{6}$ is necessary for the reference of maximum speed *c*. Both electrons are based on u/d-quarks, which, in addition to their active fions, share a number of S-quarks with the wavelength $\frac{\lambda_{u/d}}{2}$, so that the particle configuration increases from PC = $\frac{3}{3}$ to PC = $\frac{4}{4}$ for the W-boson, PC = $\frac{4{,}5}{4}$ for the Z-boson and PC = $\frac{5}{4}$ for the H-boson. The Z-boson absorbs external fions with half wavelength, which reduces the particle configuration for the particle minus the exchange fion/passive fion pair to PC = $\frac{4{,}5}{4}$. With the coupling of two fermionic $\frac{1}{2}$ spins, the heavy bosons obtain their bosonic integer spin. The process needs to be investigated in more detail to determine how a single u/d-quark transforms into two S-quarks.

W-boson :

$$M_{W\text{-}boson} = M_{muon/electron,\,4.} \cdot M_{electron,\,5.} \cdot \frac{5}{6}\, PC_{electron,4.} \cdot PC_{electron,\,5.} \cdot M_e \qquad (3.31)$$

$$M_{W\text{-}boson} \approx 205 \cdot 922{,}6 \cdot \frac{5}{6}\frac{4}{4}\frac{4}{4} M_e \approx 157642\ M_e \qquad (157376\ M_e \text{ experimental})$$

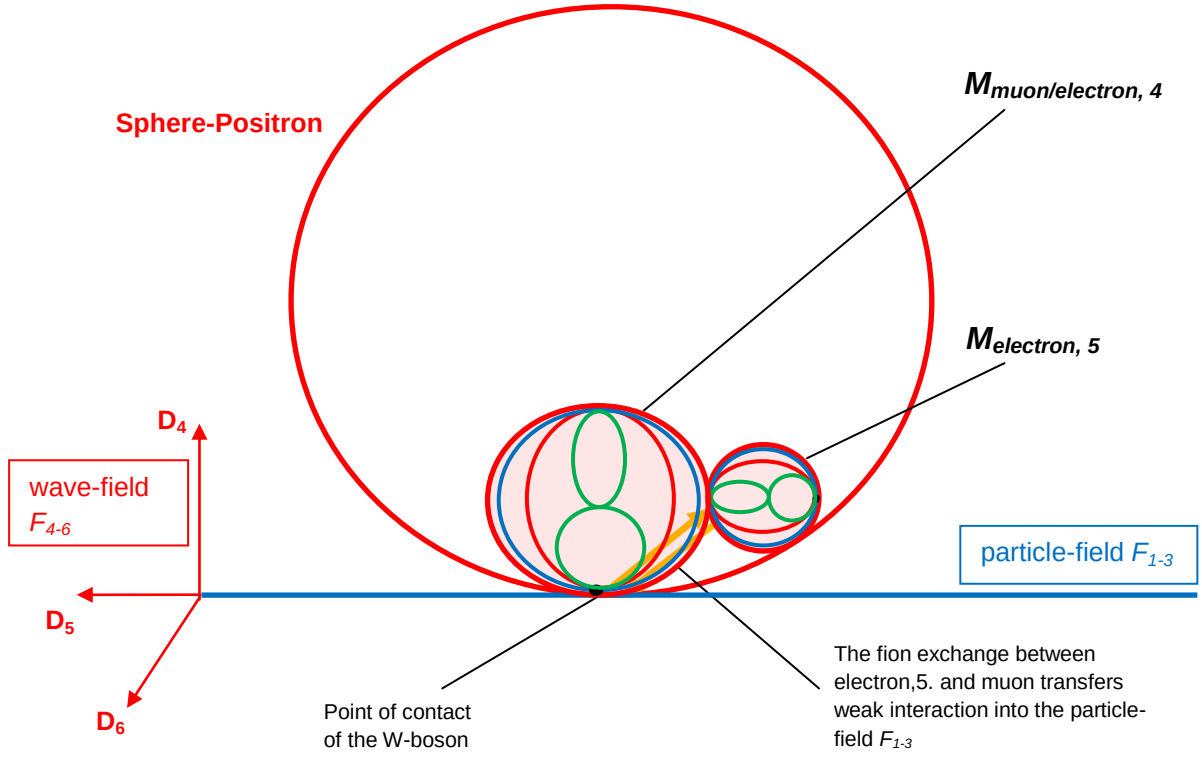

Figure 3.24: Formation of *the* W$^+$-boson as a product of the masses of $M_{electron,\,5}$ and $M_{muon/electron,\,4.}$

Figure 3.24 shows the possible structure of both particles based on their spin, charge and interaction properties. The electron of the 5th dimensional family is slightly raised above the dimension plane D_{56} opposite the muon of the 4th dimensional family. Both rotate within a sphere S. If the constellation is above the dimension plane D_{56}, they rotate within a positron sphere and have a positive charge, while below the dimension plane D_{56} they rotate in an electron sphere with a negative charge. The exchange is similar to the process shown in **Figure 3.16.** The elevation of one electron to the dimension plane D_{56} causes a reduction in the field exchange of the fions because the rotation path of the exchange fions is no longer optimal for the dimension plane D_{56}. The resulting angle relative to the dimensional plane D_{56} was introduced in **Chapter 2.2** as the deviation angle β. For this particle, the fion exchange is characterized by a weak interaction rather than a strong one.

Z-boson :

$$M_{Z\text{-}boson} = M_{muon/electron,\ 4.} \cdot M_{electron,\ 5.} \cdot \frac{5}{6} PC_{electron,\ 4.} \cdot PC_{electron,\ 5.} \cdot M_e$$

$$M_{Z\text{-}boson} \approx 205 \cdot 922{,}6 \cdot \frac{5}{6} \frac{4{,}5}{4} \frac{4}{4} M_e \approx 177347\ M_e \qquad (178417\ M_e \text{ experimental})$$

Figure 3.25 shows the diagram for a Z-boson. It is similar to the **Figure 3.12**. Here, too, it would be unlikely for both electrons to meet at a point of contact in the dimension plane D_{56}. It is possible that both electrons are rotating rigidly at a single point within a sphere S with a positive and negative potential gradient, while being slightly elevated above the dimension plane D_{56}. In this case, the fion excange penetrates the D_{56} dimensional plane at a deviation angle of $0 < \beta < 90°$, which causes the strong interaction to transform into a weak interaction depending on this very angle.

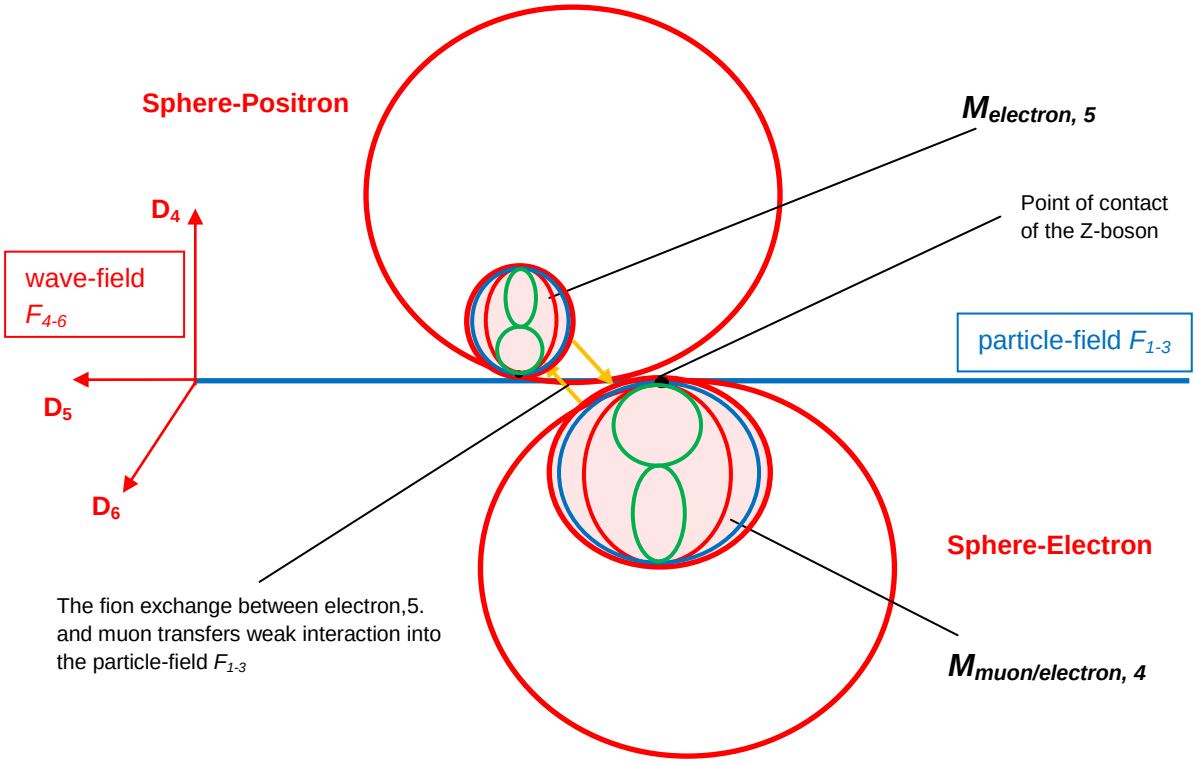

Figure 3.25: Formation of the Z-boson as a product of the masses of $M_{electron,\ 5}$ and $M_{muon/electron,\ 4.}$

H-boson :

$$M_{H\text{-}boson} = M_{muon/electron,\,4.} \cdot M_{electron,\,5.} \cdot \frac{5}{6} PC_{electron,\,4.} \cdot PC_{electron,\,5.} \cdot M_e$$

$$M_{H\text{-}boson} \approx 205 \cdot 922{,}6 \cdot \frac{5}{6}\,\frac{5}{4}\,\frac{4}{4}\; M_e \approx 246315\; M_e \qquad (245065\; M_e \text{ experimental})$$

Figure 3.26 shows the diagram for an H-boson. Due to its neutral total charge, it is similar to the Z-boson in that it has a structure between a positron sphere above and an electron sphere below the dimension plane D_{56}. However, the special feature of the H-boson is that it uses two active fions from an u/d-quark to generate two active S-quark pairs with a wavelength of $\frac{\lambda_{u/d}}{2}$.

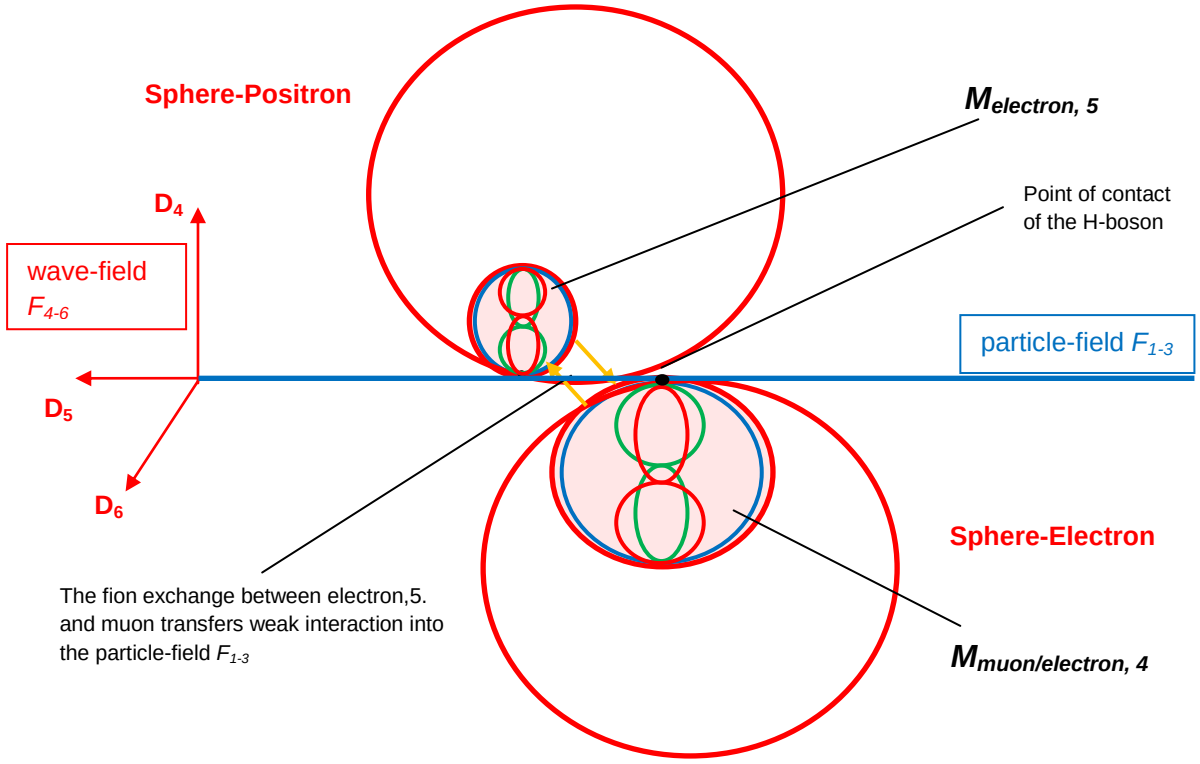

Figure 3.26: Formation of the H-boson as a product of the masses of $M_{electron,\,5}$ and $M_{muon/electron,\,4.}$

3.7 Unification of the four fundamental forces

Result for space-time:

Space-time follows the characteristic inertial motion of electromagnetic oscillations. It is a form of moving energy. Matter is an effect of relativistic fields modelled in the geometric structure of field-space, just as the field equations in **Chapter 2.2, Point 09** derive them.

Results from the electric potential:

According to classical physics, the four fundamental forces are gravity, electromagnetic interaction, the strong nuclear force and the weak nuclear force. Formulas (3.27) and (3.28) allow for a unification of the four fundamental forces. The cause of electromagnetic interaction, the strong and weak nuclear forces lies in the electric potential of the universe, which forms the permanently applied photon field in field-space. With the help of the physical quantity of frequency, it is possible to describe the mechanical causes from the electric potential and assign any field to a specific coupling frequency. In order to achieve these frequencies, very specific space-structure-related conditions are necessary during an interaction, as explained in the previous chapter. The reference field for the cause of the electromagnetic field exchange remains the wave-field $F_{4\text{-}6,}$ while the emitted forces are registered in the particle-field $F_{1\text{-}3}$ as a specific field from a point source (point of contact with the dimension plane D_{56}). In the particle-field $F_{1\text{-}3,}$ the fields are perceived as abstract field lines and, in macroscopic superposition, as discrete objects.

The minimum coupling frequency corresponds to the mass of the smallest exchange fion with the lowest excitation:

It should be noted that a single exchange fion has a multiple of the momentum for the electric forces, corresponding to that of an electron. At the moment of field exchange, it can be ~ 137 times heavier than in the composition of its three active electron-internal fions. This confirms previous observations in nuclear physics that quarks in atoms contribute only as a small fraction of the total mass. The majority of the mass is caused in the FSM by exchange fions with their characteristic coupling frequencies.

The exchange fion was found in its lowest excitation for the 4th dimensional family with the following mass:

$$\boldsymbol{M_{fion}} = [\,\frac{4}{3}\,(\,\frac{3}{2}\,)^3\,]^4\,\frac{1}{3}\,M_e = \mathbf{136{,}6875}\ \boldsymbol{M_e} \qquad (3.32)$$

The electrical exchange of a fion with an electron begins with the **minimum coupling frequency**. Above this frequency, fions become capable of forming a partial charge that is generated in the wave-field $F_{4\text{-}6}$ of the field-space:

$$\boldsymbol{f_{fion}} = [\frac{4}{3}(\frac{3}{2})^3]^4 \frac{1}{3} f_e = 136{,}6875 \cdot 1{,}2356\ 10^{20}\ \text{Hz} = \mathbf{1{,}688911\ 10^{22}\ Hz} \qquad (3.33)$$

$\lambda_{fion\_fine\ struktur} = 1{,}775\ 10^{-14}$ m

It is striking that the reciprocal factor of ~ 137 appears in Arnold Sommerfeld's determination of the fine structure constant α under precisely these minimal conditions. There could be a formal connection between Sommerfeld's reciprocal factor and the minimal coupling frequency. This was already predicted in **Chapter 2.2, point 17**, and has now been confirmed.

Sommerfeld's definition of **the fine structure constant α** from Quantum Mechanics is that it represents the threshold at which exchange particles of electromagnetic interaction (the photon) begin to couple to an electrically charged elementary particle, such as the electron. The value is given in the literature as ~ 1/137. This definition is similar to the state of an invisible photon from the FSM, which begins to interact electrically with its environment at this factor for the minimum coupling frequency.

The stability in a particle can thus be evaluated by how well the electric impulse is absorbed into a quark-exchange-fion-quark-coupling. Only when there is a stable exchange of exchange fions do permanent electric interaction forces develop. A particle with too low a total mass fluctuates immediately.

The electric force :

The **electron–exchange fion–electron-coupling** between two electrons is the **electric force**. The exchange takes place electromagnetically in the wave-field $F_{4\text{-}6}$, while the observer in the particle-field $F_{1\text{-}3}$ registers an electric force at these coupling frequencies. An electron with the particle configuration PC = $\frac{3}{3}$ couples to a extern fion with a frequency above the minimum coupling frequency and thus exchanges its field with another electron PC = $\frac{3}{3}$. The momentum of an electrical interaction is recorded per unit of time in the particle-field.

$$\boldsymbol{f_{el.force}} = [\frac{4}{3}(\frac{3}{2})^3]^4 \frac{1}{3} f_e = \mathbf{136{,}6875}\ \boldsymbol{f_e} \quad (3.34)$$

$$\boldsymbol{M_{el.force}} = [\frac{4}{3}(\frac{3}{2})^3]^4 \frac{1}{3} f_e = \mathbf{136{,}6875}\ \boldsymbol{M_e} \quad (3.35)$$

$$f_{muon/electron,4.} = \frac{1}{2}[\frac{4}{3}(\frac{3}{2})^3]^4 \frac{\mathbf{3}}{\mathbf{3}} f_e = 205{,}031\ f_e \quad (3.36)$$

$$f_{electron,5.} = \frac{1}{2}[\frac{4}{3}(\frac{3}{2})^3]^5 \frac{\mathbf{3}}{\mathbf{3}} f_e = 922{,}640625\ f_e \quad (3.37)$$

$$f_{tauon/electron,6.} = \frac{1}{2}[\frac{4}{3}(\frac{3}{2})^3]^6 \frac{5}{6}\frac{\mathbf{3}}{\mathbf{3}} f_e = 3459{,}9\ f_e \quad (3.38)$$

Nuclear force – strong interaction:

The **quark–fission–quark–coupling** in a particle structure such as that of a baryon or a meson belongs to **the nuclear force.** The field exchange of the strong interaction follows the same mechanism as that between the electron–exchange fion–electron-coupling. The interaction field of the strong interaction is formed by electromagnetic coupling with an exchange fion, which exchanges its field with a particle from the coupling configuration up to PC = $\frac{4}{3}$. The momentum of a strong interaction is recorded per unit of time in the particle-field.

$$f_{pion/meson\text{-}boson,4.} = \frac{1}{2}[\frac{4}{3}(\frac{3}{2})^3]^4 \frac{\mathbf{4}}{\mathbf{3}} f_e = 273{,}375\ f_e \quad (3.39)$$

$$f_{meson\text{-}boson,5.} = \frac{1}{2}[\frac{4}{3}(\frac{3}{2})^3]^5 \frac{\mathbf{4}}{\mathbf{3}} f_e = 1230{,}1875\ f_e \quad (3.40)$$

$$f_{proton/baryon,5.} = \frac{1}{2}[\frac{4}{3}(\frac{3}{2})^3]^5 \frac{\mathbf{6}}{\mathbf{3}} f_e = 1845{,}28125\ f_e \quad (3.41)$$

$$f_{meson\text{-}boson,6.} = \frac{1}{2}[\frac{4}{3}(\frac{3}{2})^3]^6 \frac{5}{6}\frac{\mathbf{4}}{\mathbf{3}} f_e = 4613{,}203125\ f_e \quad (3.42)$$

$$f_{meson/baryon,6.} = \frac{1}{2}[\frac{4}{3}(\frac{3}{2})^3]^6 \frac{5}{6}\frac{\mathbf{6}}{\mathbf{3}} f_e = 6919{,}804688\ f_e \quad (3.43)$$

Chapter 2.2 confirms that the strong force is formed in generations $n = 2$ and $n = 3$. This corresponds to the particle configurations TK = $\frac{4}{3}$ or $\frac{6}{3}$, respectively, starting with the fourth dimensional family. The field reaches its maximum strength through field exchange parallel to the dimensional plane D_{56}.

Nuclear force – weak interaction:

If the **quark–exchange fion–quark-coupling** is not transmitted exactly in the dimension plane D_{56} but is slightly shifted in the wave-field $F_{4\text{-}6}$, only part of the field exchange can take place at the point of contact with the particle-field $F_{1\text{-}3}$. This produces only a **weak interaction**. A good example of such a particle structure with weak interaction is shown in **Figure 3.26**.

The mediation for the field force effect was derived in **Chapter 2** according to formula (2.172), which only reaches its maximum for the particle-field through parallel mediation of a field to the dimension plane D_{56}.

The frequency for the weak interaction has a deviation angle β for the optimal geometric shape of the particles involved. This angle of deviation β between the dimensional plane D_{56} and a raised contact point extends the mechanical path of an oscillation, thereby reducing the frequency and, consequently, the effect of the strong interaction:

$$\boldsymbol{f_{weak\ interaction} = f_{strong\ interaction}\ \sin(0° < \beta < 90°)} \tag{3.44}$$

The SU(4) extension, described in **Chapter 2.2, Point 15**, incorporates the weak interaction and invisible (dark) matter as realistic particles.

Magnetism in the proton:

The proton moves partially in all dimensional planes by means of quarks rotating periodically in $3T$. In the third period, the proton rotates, among other things, with its axis of rotation on the dimensional plane D_{56} around its overall structure. Within this structure, three charged quarks rotate around a binding neutrino without spin. Similar to a bicycle dynamo, a magnetic field parallel to the axis of rotation is induced at the location of this neutrino and thus at the centre of the angular momentum of a proton. **Figure 3.27** shows the mechanism.

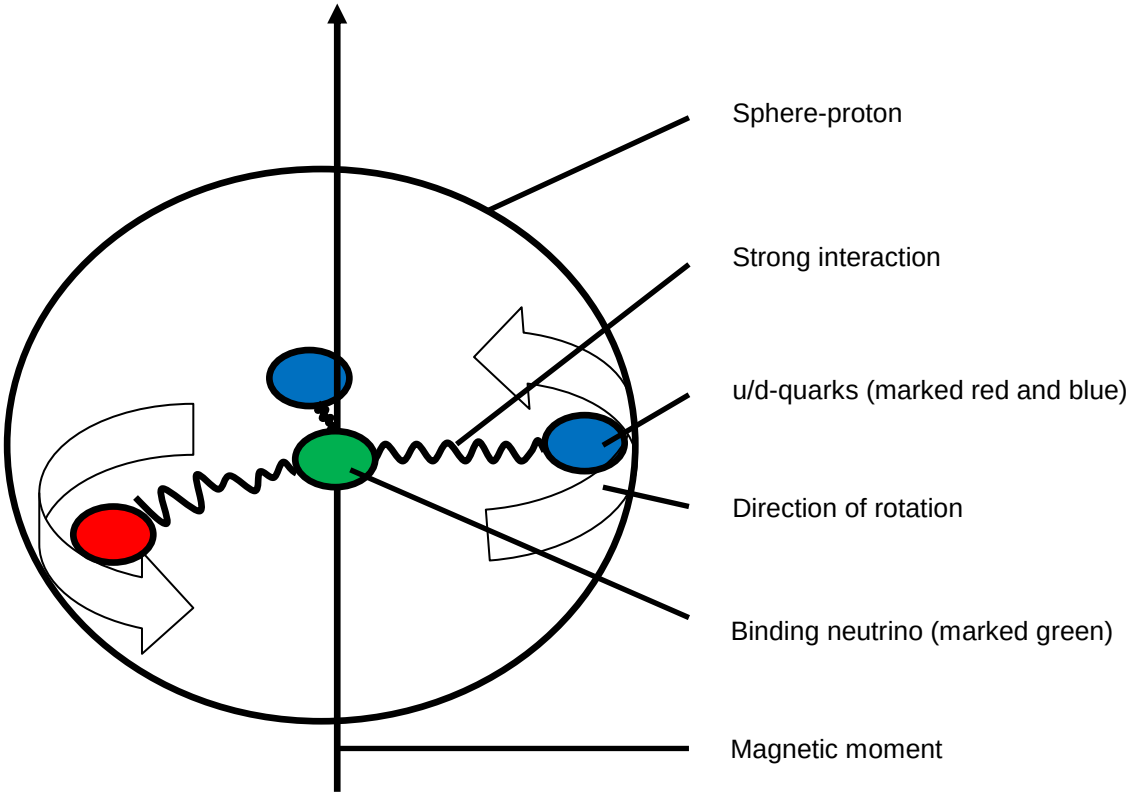

Figure 3.27: Magnetic moment in a proton

Results from the gravitational potential:

Gravitational force:

In the FSM, the **gravitational force** of an object with a mass *M* is the counterforce to the inertial force that acts with its propagation as an electromagnetic wave through space-time. This quantity depends on the **object's mass**, its **distance** from other objects and its **gravitational potential**. At the location of the inertial system for the minimal length contraction of the universe, the field propagation velocities apply with $V_5 = c$; $V_4 = 0$. At this point, the gravitational potential in space-time is at its minimum for an object of mass m_{obj}. The total gravitational force is at its lowest in this state.

The gravitational force of an object in field-space relative to its geometric shape to the dimensional plane D_{56}:

$$F_{gravity} = m_{obj}\, r\, k^2 \sin(kt) \qquad (2.178)$$

The gravitational force between two objects:

$$F_{gravity} = \frac{G\, m_{obj1}\, m_{obj2}}{r^2} \sin(kt) \qquad (2.172)$$

Addendum to the definition of mass from Chapter 1.2:

The normalised masses of objects are mediated by the **electromagnetic properties** of a **particle–exchange-photon–particle coupling** from the wave-field F4-6. They consist of periodically oscillating harmonics of several complexly structured electromagnetic waves. The masses of complex particles such as the proton differ only in the variation of their electric exchange particles. Since the electromagnetic wave is identical to space-time, a change in the slope of its oscillation function acts as a restoring force against the inertial force of space-time. Thus, the electromagnetic waves can be modelled as relativistic fields with the vector contributions for the fourth and fifth dimensions. A space-time deformation ultimately arises when an electromagnetic wave makes a vectorial contribution in the fourth dimension. A rest mass represents the minimum for a vectorial contribution in the fourth dimension. An additional relativistic energy gain deforms its relativistic fields, which only makes its mass appear heavier.

In **Chapter 2.2, Point 10**, of the compactification process, the 7-dimensional momentum-energy tensor is reduced to the four visible dimensions. It is then recognised that mass is a periodic effect of its longitudinal wave component, which manifests itself as amplitude but remains massless as a transverse wave.

Matter pulse and thermodynamics :

The concept of a matter pulse encapsulates the process of field exchange between the wave-field and the particle-field, and is used in the following chapters for technical applications, for example to successfully increase the energy of particles. With the effective increase in energy achieved by finding the appropriate coupling frequency for matter, a plasma can be generated in a limited space with a high efficiency of around 100%, which is particularly interesting for energy technology or for manipulating space-time. In technical applications, the resulting pressure and temperature with a limited volume will be decisive.

Thermodynamics is a branch of physics that models the technical implementation of the coupling frequencies of matter for FSM. A space-time segment such as a proton, for example, has a defined limited space with its sphere S. As the energy increases, the elementary particles within it oscillate periodically faster. The increased kinetic energy inevitably leads to increased repetitions of interaction events, which are interpreted macroscopically as friction with other particles. The sum of the interactions between the particles of a system or a space-time segment is used as a measure of temperature. According to the law of conservation of energy, the exchange between two systems corresponds to the heat flow that continues until the temperature gradient is tangent to zero. The time required for complete temperature equalisation between particles or systems can be calculated. The coupling frequency for matter (3.27) can be used to specifically control thermodynamic processes. This

paper continues to focus on the coupling frequency for matter in order to establish the prerequisites for a thermodynamic description of the processes.

The agreement of the four basic forces in one theory:

The four basic forces are summarised below, as they result from the FSM model.

The basic effect is identified as the **electromagnetic interaction**, which combines the electric force with a possible magnetic induction, the strong nuclear force, the weak nuclear force and the gravitational force. All forces are geometry-dependent and based on the characteristic coupling frequency of an object f_{obj} within the electromagnetic photon field in question. PR stands for process response, which explains what happens between the elements.

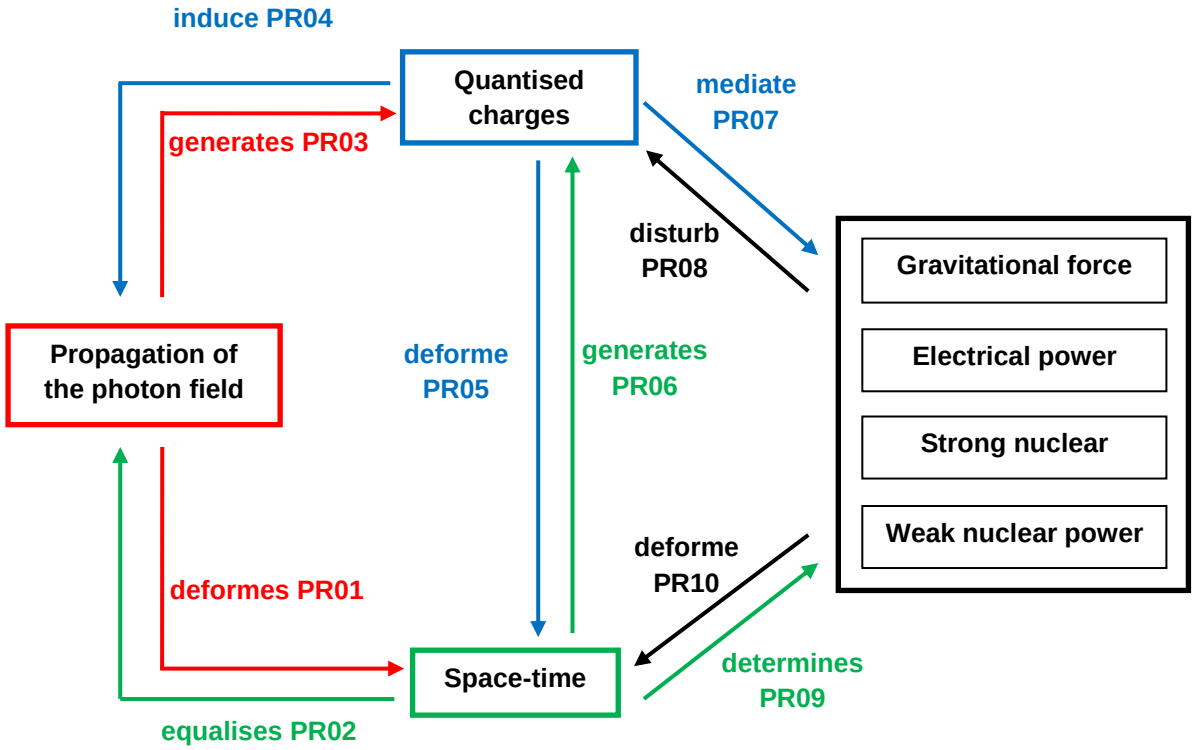

Figure 3.28: Schematic of the electromagnetic interaction

Figure 3.28 explanations:

PR01: The photon field of the Universe propagates as a universal electromagnetic wave. Space-time causes an inertial force against this propagation. The gravitational force was defined as the counterforce to this inertial force. The strength of the gravitational force depends on the prevailing curvature of space-time. The

gravitational potential describes the space-time tension for an object between the inertial system and any space-time distorted location.

PR02: Space-time reacts to the space-time deformation in the photon field with equalising forces. These space-time mechanical effects correspond to Lorentz transformations (time dilation, length contraction, relativistic energy increase).

PR03: The photon field is able to divide its total momentum depending on its expansion. In the process, a certain number of quanta are emitted from the photon field until the expansion is complete.

During the expansion, an electric potential prevails in the photon field due to a displacement current. The dimensional planes $D_{45/46}$ offer the possibility for a space-time quantum along the fourth spatial dimension D_4 to generate a charge through its rotational movement in this voltage potential. The dimensional plane D_{56} is used for the electrostatic separation of these charges.

PR04: An electric charge carrier can generate an alternating magnetic field through its periodic rotational movement. Conversely, a moving magnetic field induces an electric field.

PR05: The sum of all interactions of quantised charge carriers and the propagation of their mediated fields in the field-space results in the periodic contribution to the deformation of space-time. These fields deform their surrounding space depending on the frequency of their interaction with each other.

PR06: As long as there is a space-time deformation with a certain gravitational potential, the proportionally applied electric potential in the photon field remains above its minimum and positively and negatively charged particles continue to be produced.

PA07: Quantised charge carriers can mediate a certain gravitational force, electric force, strong nuclear force and the weak nuclear force depending on the geometric procurement of their particle structure with the aid of particle-exchange fion-particle-coupling.

PR08: Interaction fields from the particle-field can disturb the synchronisation of the exchange fions in the wave-field with a particle. This disturbance deforms the rotation paths of the individual active fions that interact with the particle-field. A possible disturbance on the rotation paths along the dimensional planes $D_{14/24/34}$ increases the necessary coupling frequency and the rest mass of particles. This perturbation has a similar effect to the relativistic energy increase without a vectorial object velocity V_3, which increases the matter pulse of matter.

PR09: The global space-time curvature of the universe determines the state of the gravitational potential d$M(\alpha)$ of matter. The measurable gravitational forces are the result between two objects with their object masses m_{obj}, a certain distance from

each other and the existing global, gravitational potential d$M(\alpha)$. The deformed space-time also ensures shorter paths for the exchange of fields. This increases the density of all matter and therefore all other interaction fields.

PR10: Interacting objects from the particle-field can cause an additional spatiotemporal deformation at the point where they meet.

Possible equivalences to the Standard Model of particle physics:

Due to its exchange behaviour, the fion shows parallels to the gluon of the Standard Model. Beyond multiples of an electron fion, the structural integrity of heavier particles begins.

The dimension families could be different dimension-dependent size multiples of lepton families.

The boson is derived from the electron model. The integer spin behaviour of the boson and the half-integer spin behaviour of the electron are analogous and correspond to experimental observations.

Dark energy could be equivalent to so-called invisible photons that are not yet capable of interacting with matter. The FSM demonstrates that the ratio of the rest mass of unbound matter to the total mass of the universe can be used as a potentially measurable indicator of the remaining space-time deformation in the universe.

Hidden matter could possibly be equivalent to dark matter. However, in the FSM, these appear as real, invisible interaction partners with complex, visible particles.

Chapter

4 Field-Space Levels

4.1 Model for the Field-Space Level

In **Chapter 3.6**, particles were calculated and predicted that require more than six spatial dimensions for their existence in order to allow sufficient space for additional 4-dimensional rotational orbits. With the field-space level model, it is possible under certain conditions to take into account three additional spatial dimensions, which enables the prediction of particle masses with their coupling frequency during their particle-exchange-particle-coupling. A **field-space level** spatially encloses a largely self-contained reference system. It can encompass a celestial body, e.g. a planet. Our perceptible particle-field is located exactly parallel to the dimension plane D_{56} in resonance with its field-space level. There, fields with a certain resonance frequency interact with each other with a very high probability. This field-space level is referred to as **the initial field-space level**. In addition to the initial field-space level, there is a **higher** field-space **level**, referred to as the initial field-space level, which interacts with the initial level under certain conditions. The field-space levels are also separated from each other by repulsive forces, because otherwise they could fall into each other. Only a repulsive area separates two attractive field-space levels from each other. By means of a specific technical implementation, the matter pulse of an object can be specifically increased via its coupling frequency, which leads to a shift of the initial field-space level to the higher one.

For the field-space level model, the spatial dimensions are expanded as follows:

- three spatial axes $D_1/D_2/D_3$ in index form as D_{1-3} in the particle-field F_{1-3} with the corresponding field vectors (F_1, F_2, F_3)

- three spatial axes $D_4/D_5/D_6$ (D_{4-6}) in the wave-field F_{4-6} with the field vectors (F_4, F_5, F_6) at the initial field-space level

- Three spatial axes $D_7/D_8/D_9$ (D_{7-9}) in the wave-field F_{7-9} with the field vectors (F_7, F_8, F_9) to the higher field-space level

Figure 4.1 provides an initial overview.

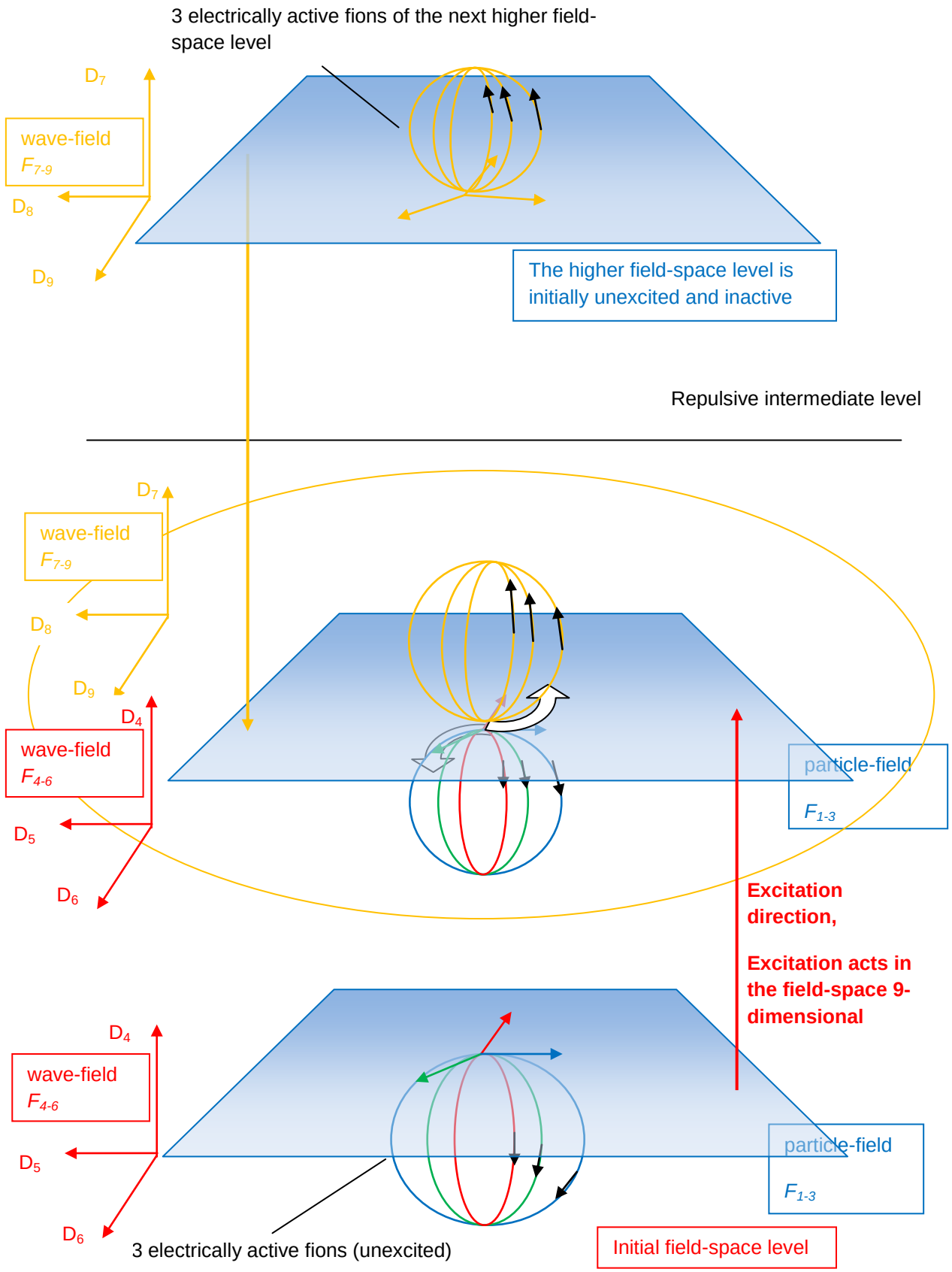

Figure 4.1: Representation of all nine spatial dimensions

Based on the state model of the mathematical hollow sphere of the universe from **Chapter 2.3**, field-space levels can also be described and the states represented. It will be shown that as the higher field-space level is approached, the field forces react in a mirrored manner. In this model, the deviation angle β describes the phase shift relative to the dimensional plane D_{56}. Until now, it has been used within the range $0 < \beta < 90°$ to describe states ranging from strong to weak interactions down to zero interaction. If the angle is extended, it passes through two field-space levels. d$M(\beta)$ describes the change in the gravitational potential for an object with mass m_{obj} from the starting point of a displacement from the initial field-space level to the higher one. The deviation angle β is represented for the mathematical hollow sphere with half a period in order to be able to draw a complete path to the next field-space level. The cos(β) describes the possible interaction states of an object with its environment during its displacement from the initial field-space level.

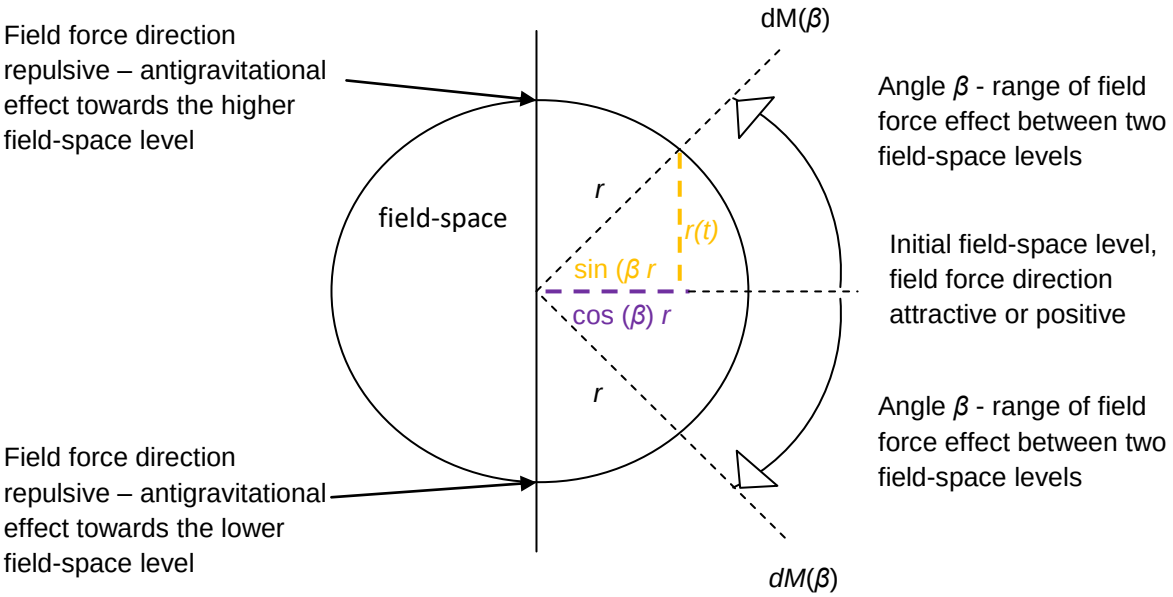

Figure 4.2: Illustration of the reversal of the direction of the field force when an object moves between two field-space levels

cos(0) = 1 means that the object is located on an initial field-space level. The attractive forces are at their maximum. cos(90°) = 0 means that the gravitational force at point d$M(\beta)$ no longer has any effect on an object mass m_{obj}. Consequently, beyond cos(90°), a repulsive effect would arise between cos($90° < \beta < 270°$). Between cos($270° < \beta < 90°$), attractive field forces prevail again.

$$F_{gravity} = \frac{G\,\mathrm{d}M(\beta)\,m_{obj}}{r^2}$$

G – gravitational constant
m_{obj} – object mass initial field-space level
$\mathrm{d}M$ – gravitational potential
F – force between M_{Uni} and m_{obj}
r – maximum distance in space
$r(t)$ – volume radius at a specific time t
$v(t)$ – velocity at a specific time t
$a(t)$ – acceleration
β – field angle is the bisector of the current spatial volume as spherical sector

$$r(t) = \frac{1}{2}at^2 \qquad v(t) = \int a(t) \qquad r'(t) = v(t)$$

$$r(t) = \iint a(t) \qquad v(t) = at \qquad r''(t) = a(t)$$

$$\frac{G\,\mathrm{d}M(\beta)\,m_{obj}}{r^2} = a(\mathrm{t})\,m = \frac{\int_{G\,\mathrm{d}M(\beta)\,m_{obj}\,\mathrm{d}\beta}^{\beta\text{-deviation angle}}}{r^2}$$

For $F(r) = \frac{\mathrm{d}M}{\mathrm{d}r\,r}$, the following applies:

The maximum possible gravitational potential between $\mathrm{d}M(\beta)$ and m_{obj} is:
$\mathrm{d}M(\beta = 0°) = m_{obj}\cos(0)$
→ purely attractive forces

The gravitational potential for a shift of the attractive force along the field-space levels:
$\mathrm{d}M(\beta) = m_{obj}\,|\cos(\beta)|$
→ mixing of attractive and repulsive forces

If the object is exactly mirrored between two field-space levels , then a gravitational potential of:
$\mathrm{d}M(\beta = 90°$ bzw. $\beta = 270°) = m_{obj}\cos(\beta = 90°$ bzw. $\beta = 270°)$
→ The external field force acting on a particle is infinitely small.

If the object is located exactly between two field-space levels, then a gravitational potential applies with:
$\mathrm{d}M(\beta = 180°) = m_{obj}\cos(\beta = 180°)$

→ purely repulsive forces

The surface dimension of a hollow sphere is: $\cancel{4\pi}\,\frac{r^2}{r(t)^2} = \cancel{4\pi}\,\frac{1}{\sin^2(\beta)}$

$$dM(\beta) = \frac{1}{\sin^2(\beta)}\, m_{obj}\cos(\beta)\, d\beta \qquad r(t)^2 = \sin(\beta)^2\, r^2 \;\rightarrow\; r^2 = \frac{r(t)^2}{\sin^2(\beta)}$$

$$F_{gravity} = \frac{G\, dM(\beta)\, m_{obj}}{r^2} = \frac{\int_{\beta\text{-deviation angle}} G\, \cancel{\sin^2(\beta)}\, m_{obj}\, m_{obj}\cos(\beta)\, d\beta}{\cancel{\sin^2(\beta)}\, r(t)^2}$$

$$F_{gravity} = \frac{G\, m_{obj}\, m_{obj}}{r(t)^2} \int_{\beta\text{-deviation angle}} \cos(\beta)\, d\beta$$

with: $\int_0^{\beta} \cos(\beta)\, d\beta = \sin(\beta) - \sin(0)$

$$F_{gravity} = \frac{G\, m_{obj}{}^2}{r(t)^2}\sin(\beta) \qquad (4.01)$$

The behaviour of sinusoidal periodicity has so far described the deformation behaviour of space-time. It also describes the course of matter between field-space levels.

$r(t)$ [$= r\sin(\beta)$] describes the change in the field radius or the distance of rotating field vectors of photons relative to the initial field-space level in the field-space during a field-space shift.

The reversal of the increase during the sinusoidal oscillation corresponds to the reversal of the direction of the gravitational force. If the increase of the sinusoidal function is positive, attractive forces prevail, whereas repulsive forces act when the increase is negative.

The **series of Figures 4.3A – E** shows the course of a field-space shift for an object with mass m_{obj} as a function of the deviation angle β. The mathematical model of the hollow sphere is shown on the left. The black oval on the right is the object. The red/blue oval border represents the state of the gravitational potential as a function of the field-space shift. The field angle α and the object are also shifted in the field-space by the field-space shift.

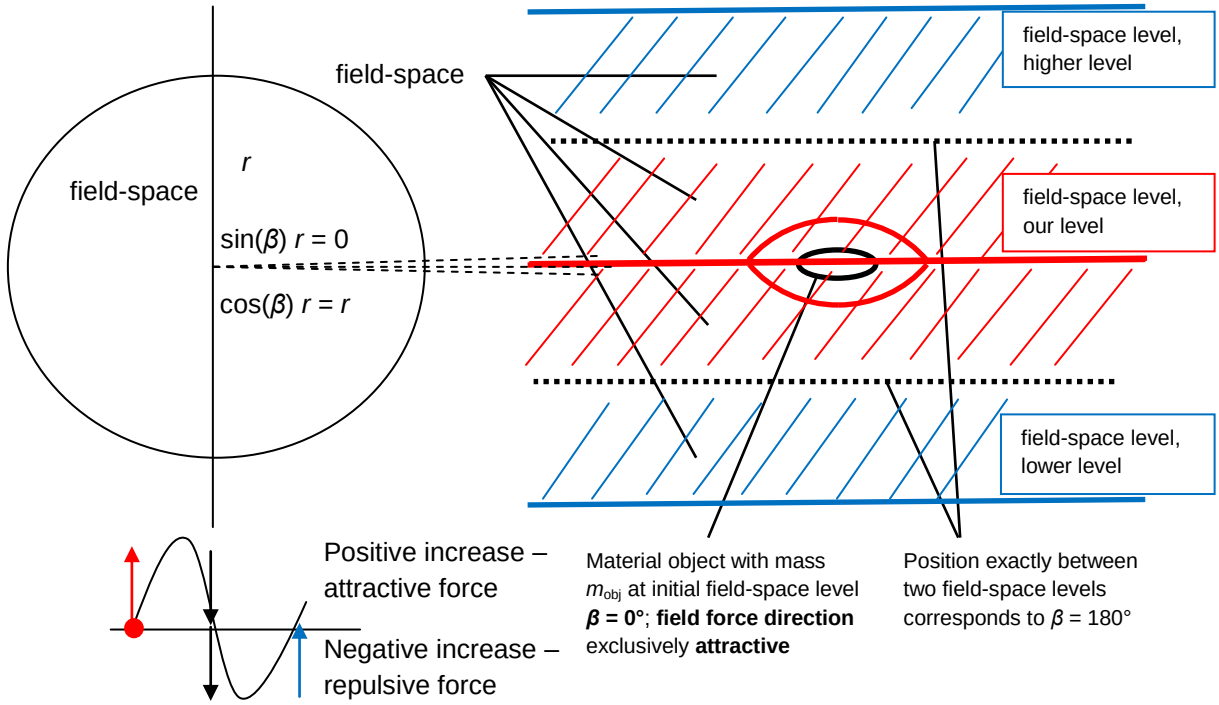

Figure 4.3A: The object is shown parallel to the initial field-space level; field forces act attractively

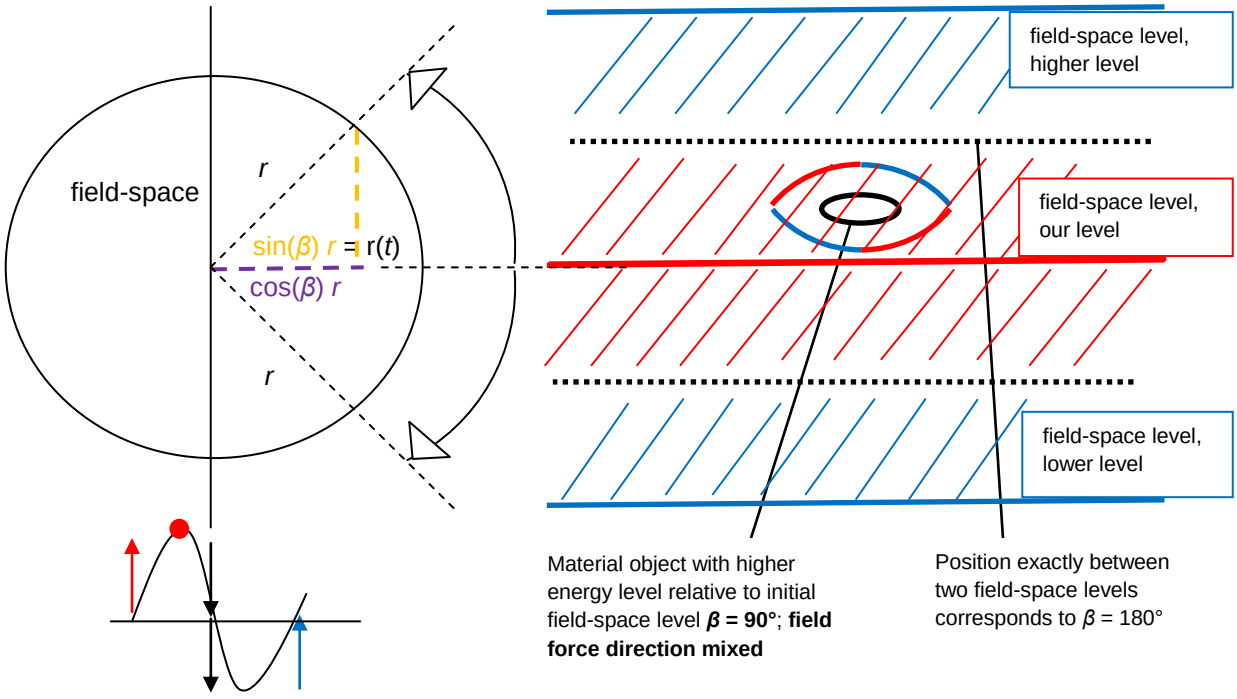

Figure 4.3B: The displacement of an object between the initial and higher field-space levels; field forces reflected between them for m_{obj} cos(β = 90°)

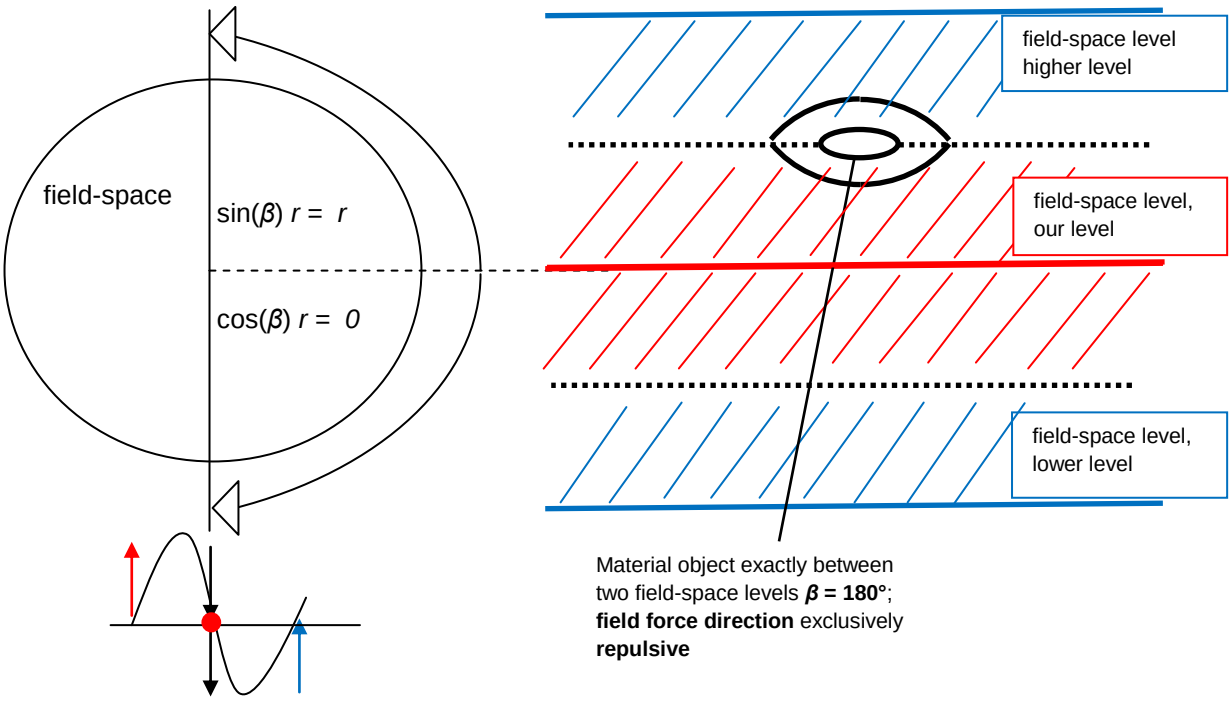

Figure 4.3C: The displacement of an object exactly between the initial and higher field-space levels; field forces act repulsively for m_{obj} cos(β = 180°)

Artificial excitation can only achieve a displacement between two field-space levels up to the location dM(β = 90°). The path towards the higher field-space level can only be achieved naturally, as the majority of all sub-objects on their initial field-space level strive to oscillate at the level of the higher field-space level. Then the entire object slips into the next field-space level. The repulsive field-space forces help to quickly overcome the transition by forcing the energy state of the object to the resonance level of the next field-space level.

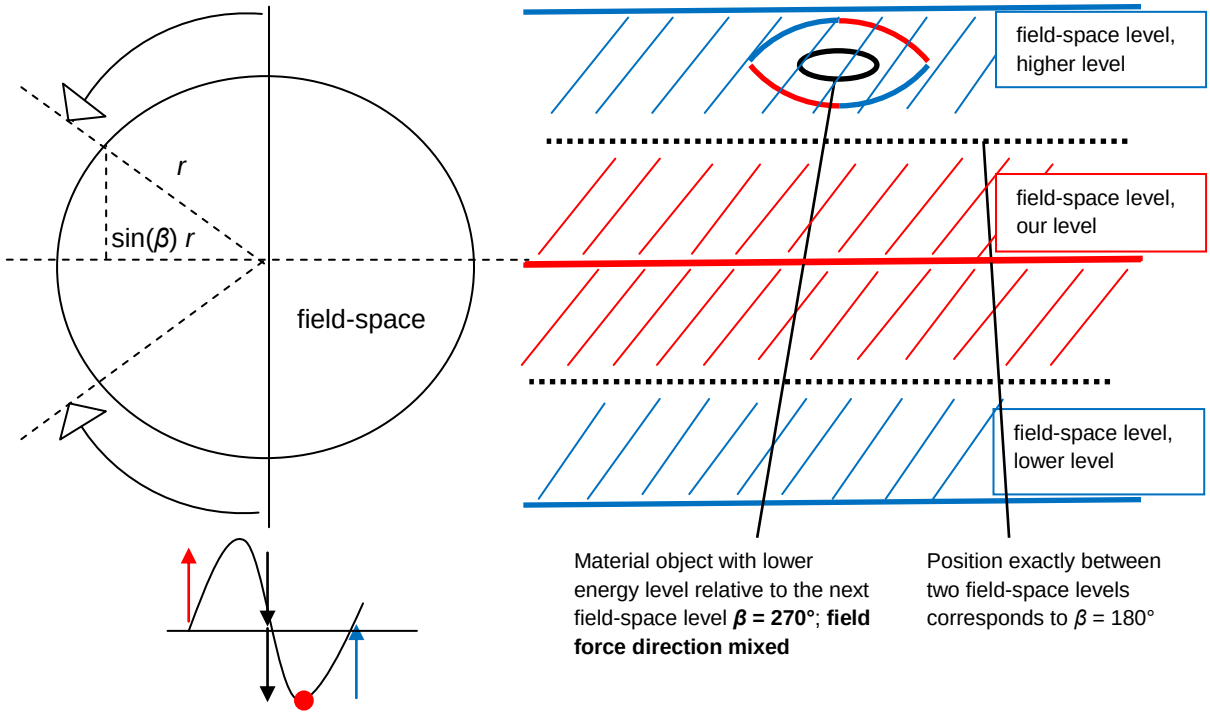

Figure 4.3D: The displacement of an object between the initial and higher field-space levels; field forces reflected between them for m_{obj} cos(β = 270°)

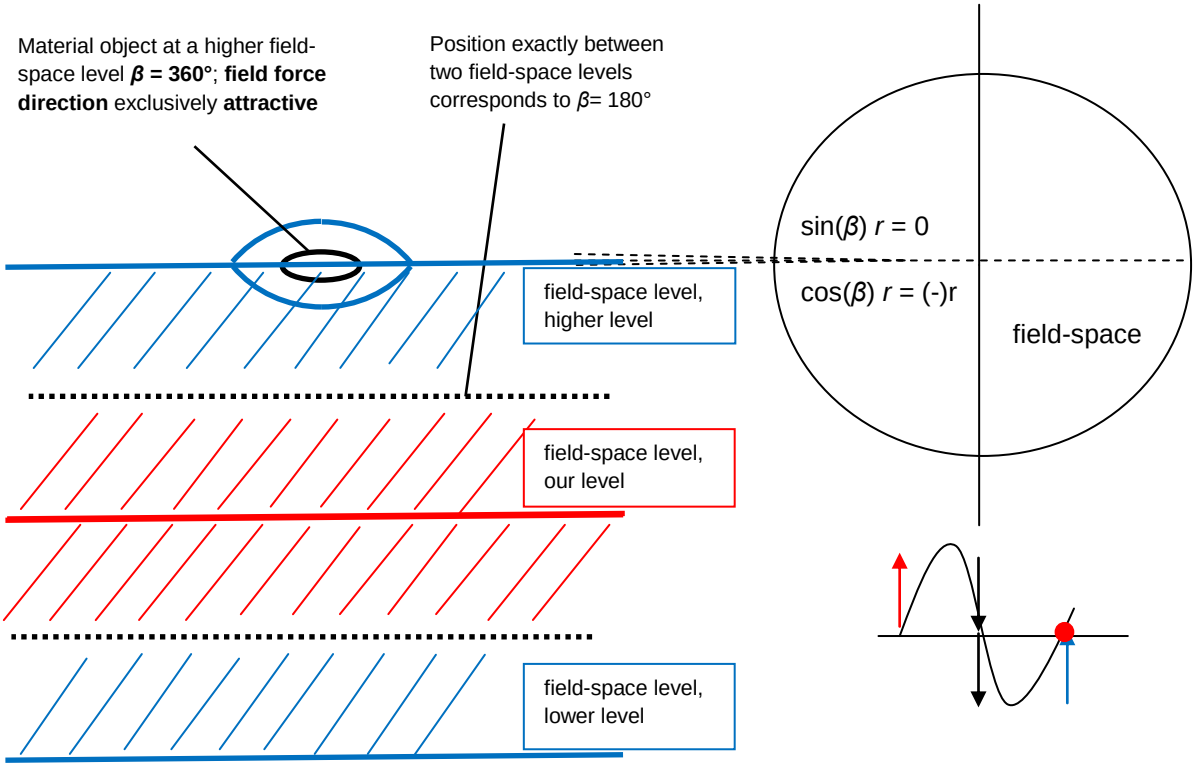

Figure 4.3E: The object is shown parallel to the higher field-space level; field forces act attractively

4.2 Displacement of an object between two Field-Space Levels

Number of 4-dimensional rotational paths:

On the initial field-space level, the following dimension planes are already known on which 4-dimensional subspaces can rotate: $D_{45/46/56}$

➔ Thus, 15 possible 4-dimensional rotational paths can be mapped in 6-dimensional space, which have a 2-dimensional intersection at a point of contact, see also **Table 3.1**.

With the shift of the energy level of the initial field-space level to the next higher one, three additional dimensions result in further dimension planes on which 4-dimensional rotation paths can rotate: $D_{78/79/89}$

➔ In 9-dimensional space, (15 + 9) possible 4-dimensional rotational paths with a 2-dimensional intersection at a point of contact would be conceivable**.**

Dimension families in a field-space shift:

The potency in a field exchange between two disturbed particles with a period duration of $2T$ or two independent rotation matrices on the respective dimension planes $D_{45/46}$ between two field-space levels is:

$$2 \cdot 2 \cdot 2 = 8 \qquad (4.02)$$

→ Eight for the power and dimension family

The power in a field exchange between a disturbed particle with a period of $3T$ or three independent rotation matrices on the respective dimension planes $D_{45/46/56}$ and a disturbed particle with a period of $2T$ between two field-space levels is:

$$(3 + 2) \cdot 2 = 10 \qquad (4.03)$$

→ Ten for the power and dimension family

The potency in a field exchange between two disturbed particles with respective period durations of $3T$ and three independent rotation matrices on the dimension planes $D_{45/46/56}$ between two field-space levels is:

$$2 \cdot 3 \cdot 2 = 12 \qquad (4.04)$$

→ 12 for the power and dimension family

By exploiting the exact mirrored properties of objects through a field-space shift, the period can be determined for the coupling between two disturbed particles and thus the dimension family. An object in the intermediate mirrored state can interact only partially or not at all with the external forces from the particle-field because it behaves like hidden matter with no point of contact with the dimension plane D_{56}. It is therefore considered massless and uncharged or no longer present in the particle-field. This intermediate reflection is mathematically produced by representing the rotations on the dimension planes $D_{45/46/56}$ as matter below and $D_{78/79/89}$ as antimatter above the particle-field. For a 9-dimensional vector, this results in further 4-dimensional rotation paths, which are summarised in **Table 4.1**:

Dimensions / 4-dim. rotational paths	field $F_{1\text{-}3}$			field $F_{4\text{-}6}$			field $F_{7\text{-}9}$		
	D_1	D_2	D_3	D_4	D_5	D_6	D_7	D_8	D_9
1	X	X	X	X	/	/	/	/	/
2	X	X	X	/	X	/	/	/	/
3	X	X	X	/	/	X	/	/	/
4	X	X	/	X	X	/	/	/	/
5	X	/	X	X	X	/	/	/	/
6	/	X	X	X	X	/	/	/	/
7	X	X	/	X	/	X	/	/	/
8	X	/	X	X	/	X	/	/	/
9	/	X	X	X	/	X	/	/	/
10	X	X	/	/	X	X	/	/	/
11	X	/	X	/	X	X	/	/	/
12	/	X	X	/	X	X	/	/	/
13	X	I	/	X	X	X	/	/	/
14	/	X	/	X	X	X	/	/	/
15	/	/	X	X	X	X	/	/	/

Dimensions / 4-dim. rotational paths	D_1	D_2	D_3	D_4	D_5	D_6	D_7	D_8	D_9
16	X	X	/	I	I	I	X	X	/
17	X	/	X	I	I	I	X	X	/
18	/	X	X	I	I	I	X	X	/
19	X	X	/	I	I	I	X	/	X
20	X	/	X	I	I	I	X	/	X
21	/	X	X	I	I	I	X	/	X
22	X	X	/	I	I	I	/	X	X
23	X	/	X	I	I	I	/	X	X
24	/	X	X	I	I	I	/	X	X

Table 4.1: Nine-digit vector with the additional rotational paths of the seventh to ninth dimensions

Dimfactor for reducing the maximum speed V_{max} :

- For the 8th dimension family, the following applies for each additional subspace U:

  Dimfactor = $\sqrt{\frac{5}{8}}$ and for two interchangeable particles, Dimfactor = $\frac{5}{8}$.
- For the 10th dimension family, the following applies for each additional subspace U:

  Dimfactor = $\sqrt{\frac{5}{10}}$ and for two interchangeable particles, Dimfactor = $\frac{5}{10}$.
- For the 12th dimension family, the following applies for each additional subspace U:

  Dimfactor = $\sqrt{\frac{5}{12}}$ and for two interchangeable particles, Dimfactor = $\frac{5}{12}$.

For B-quarks and T-quarks, their 4-dimensional subspaces within their sphere S must be taken into account, which already have their own dimension reduction factor of $\sqrt{\frac{5}{6}}$ and $\sqrt{\frac{5}{7}}$ up to the 5th dimension family.

The resulting matter is represented as follows. Matter from the initial field-space level is located below with its rotation, while matter from the next higher field-space level, referred to as antimatter, is located above the particle-field in $D_{1\text{-}3}$. The **series of Figures 4.4A – E** is intended to illustrate the relationship between emerging matter and matter-antimatter pairs in the wave-field $F_{4\text{-}6}$ through the increase or shift of the energy level of a field-space level towards the next higher field-space level. Hatched lines are intended to represent the probability ratios for the formation of rotating fions/antifions in the wave-field $F_{4\text{-}9}$. The apparent loss of charge occurs due to the intermediate mirrored field force directions between a particle from the initial field-space level and a particle from the next field-space level. The mass of such particles is determined by the factor used for the coupling frequency, the increased power corresponding to the dimension family and the appropriate dimension reduction factor for the maximum velocity $V_{max} = c$.

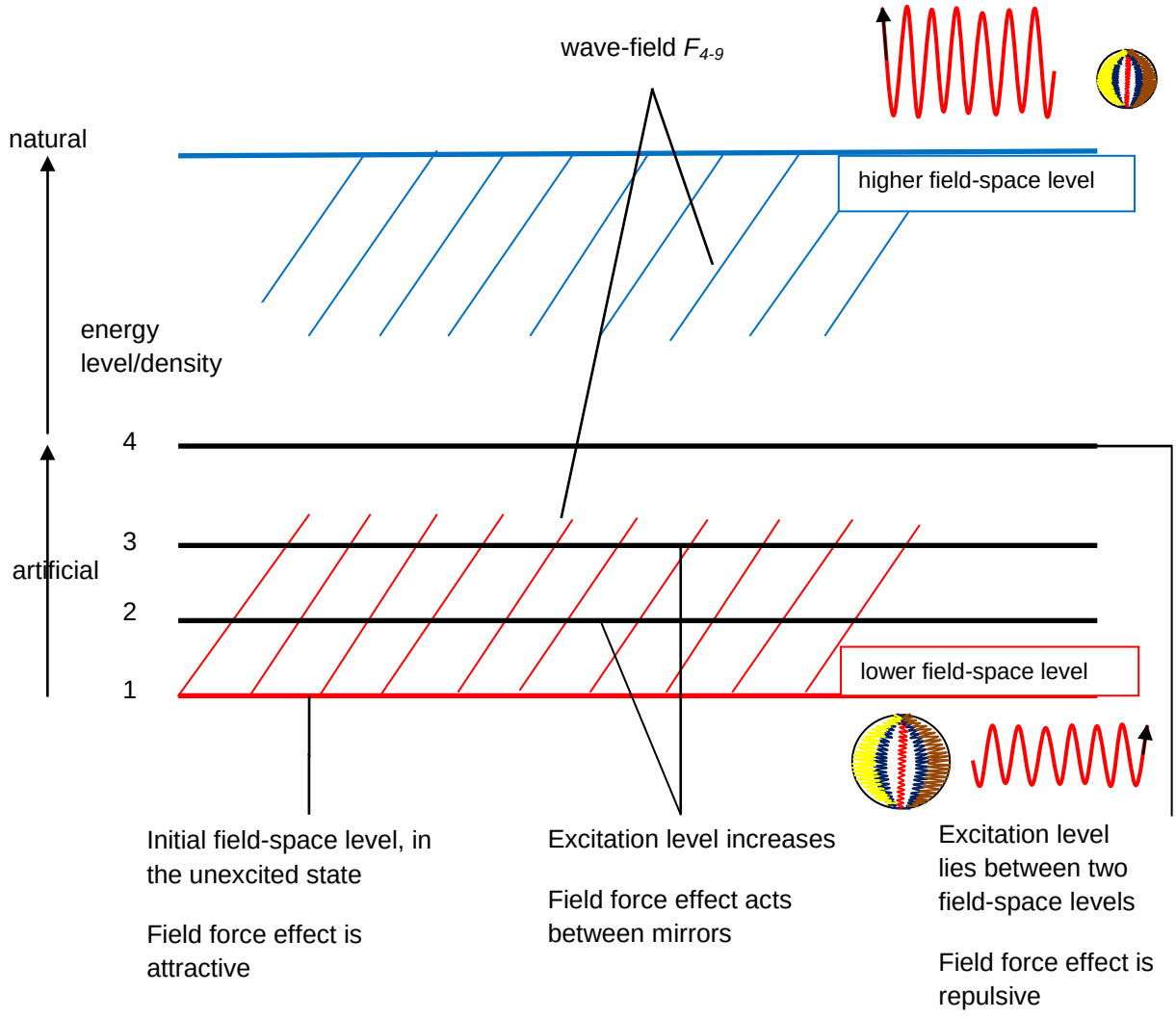

Figure 4.4A: Process of displacement of a locally excited object towards the next higher field-space level with selected energy states

corresponds to the following

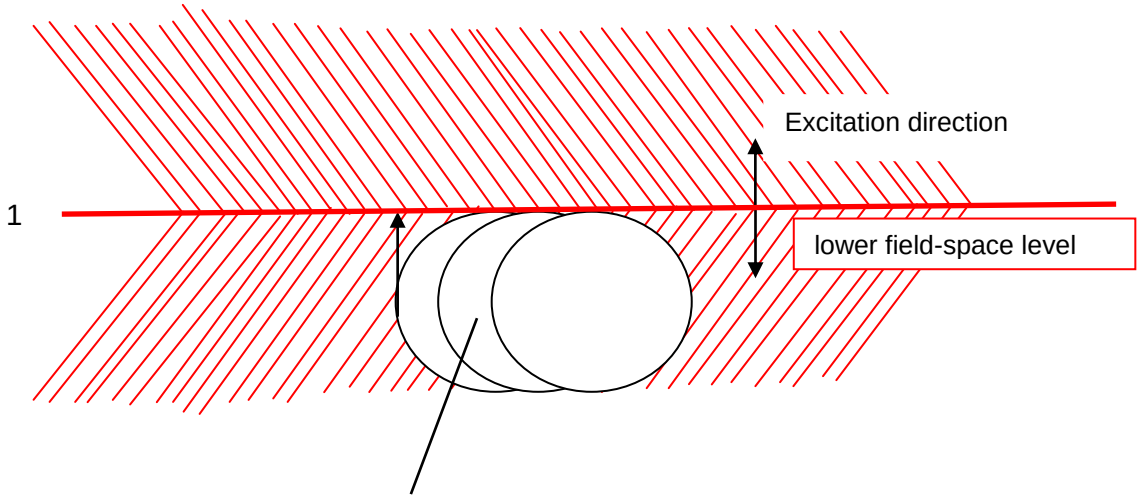

Fions rotate at the initial field-space level with $D_{46/45/56}$

Figure 4.4B: Fions are shown parallel on the initial field-space level

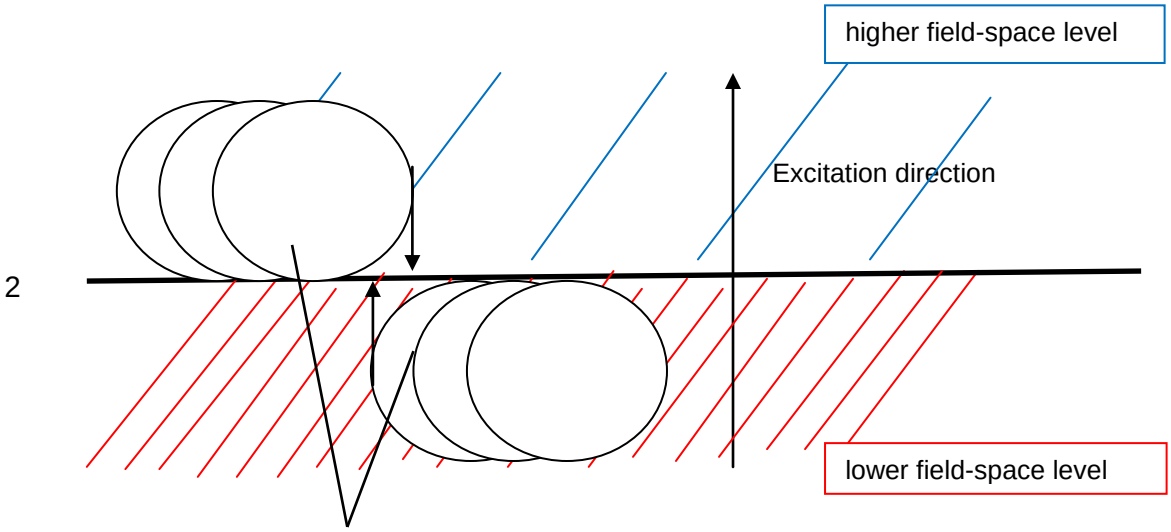

Fions rotate on: $D_{46/45/56}$ and temporarily with antifions on $D_{78/79/89}$

Figure 4.4C: Illustration showing the beginning of a shift of fions between two field-space levels; first antifions of the next higher field-space level (marked in blue) appear

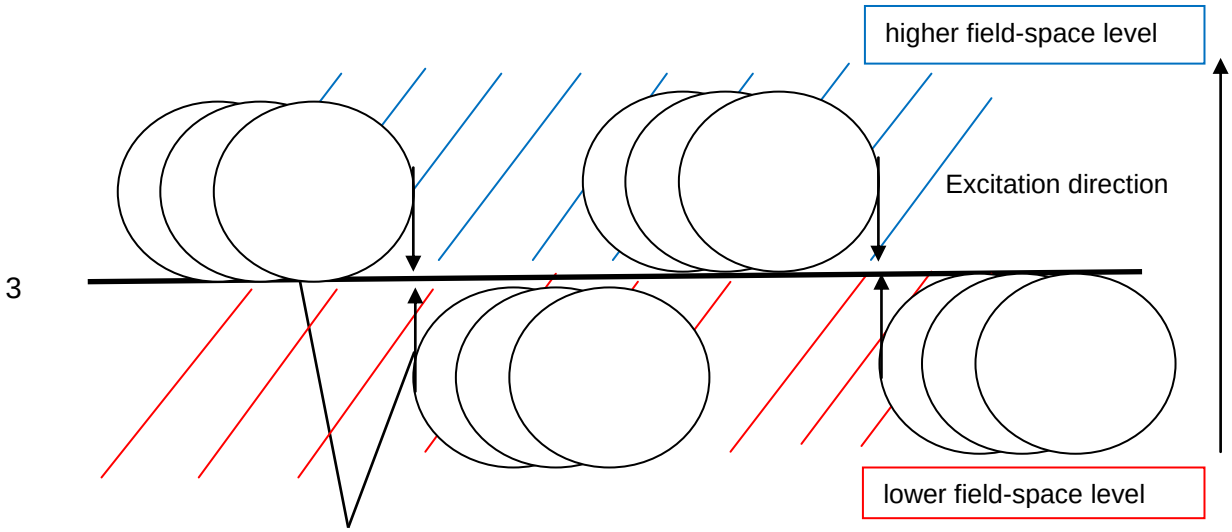

The maximum level between the field-space levels is reached with increasing probability; here, absolute symmetry of all fions applies: $D_{46/45/56}$ and $D_{78/79/89}$

Figure 4.4D: Representation of the intermediate mirrored state; in this state, fions are present in equal numbers with antifions

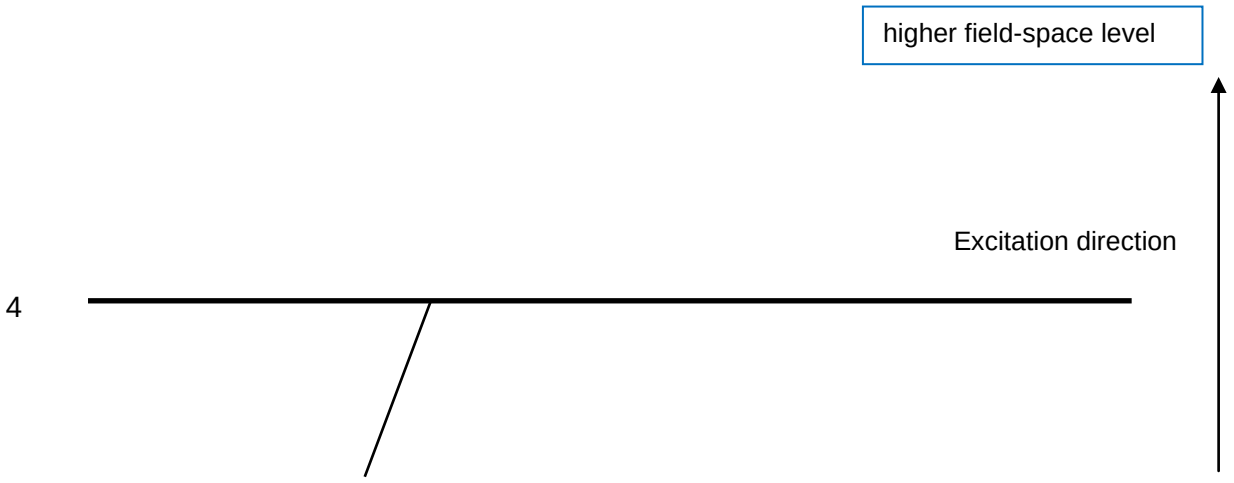

Area with repulsive forces only; particles are not held together by repulsive forces. No matter pulse occurs.

Figure 4.4E: State of the fions at a repulsive location

State changes from lower to higher field-space levels:

With the help of an external energy source carrying a specific coupling frequency for a particle-exchange-ion-particle-coupling, the plasmatic state of the particle in the particle-field can be directly influenced in proportion to its matter pulse in the wave-field. To do this, the energy source must take into account the factors of the dimension family and the dimension reduction factor for the maximum speed $V_{max} = c$ at the coupling frequency. The energy density in the particle initially increases with a constant sphere space S until the target frequency f_{target} is reached. Since the rotational speed of fions in a particle continues to be limited by the maximum orbital speed c during its period T, the size of the possible rotating sphere space S must adjust to the decreasing target wavelength λ_{target}. The sphere S and the fions rotating within it establish a temporal synchronisation in order to represent the increased matter pulse. With increasing complexity and higher frequency of the active fions, the sphere S must eventually increase in size. The sphere S is a space segment that requires additional energy to adjust its space-time to the target frequency f_{target}. During external excitation**,** compensating forces arise between sphere S and the excited fions**,** similar to **Figure 3.2,** which are performed by work in the form of a relativistic energy increase. Its field radius $r(t)$ increases correspondingly to r_{target} with increasing frequency f_{target}. The increased energy density is converted relativistically to the field radius r_{target} into new volume space:

$$E(t) = \frac{r_{target}\ h\ c}{r(t)\ \lambda_{target}} = h\ f_{target}\ \frac{r_{target}}{r(t)} = h\ f_{target}\ \frac{1}{\sin(kt)} \qquad (4.05)$$

This process corresponds to the relativistic increase in energy, but without an externally controlled object velocity. As soon as the majority number n of all spheres S_n has assumed the oscillation state of the higher field-space resonance range, the shift is complete.

Comparison of lower to higher field-space levels:

The increased matter pulse at the excited initial field-space level ultimately enlarged the sphere space S for the higher field-space level. With its bandwidth for particles, the higher field-space level is able to absorb the increased matter pulse among itself. New field force relationships arise between a particle of the higher and the initial field-space level. As the frequencies of the fions increase, their coupling forces also increase. Increased coupling forces correspond to stronger fields of all kinds. The elementary particles at the higher field-space level appear to be significantly smaller than those at the initial field-space level with their wavelength λ_{target}. However, their field force emissions have a stronger and wider effect due to their larger field radius r_{target}. The distances in the atomic lattice up to molecular chains can thus be greater. It is conceivable that every condensed particle structure known to us only needs to be half as dense as the next field-space level, or even consist of only a few atomic layers, in order to exhibit a comparable density. With the properties achieved, a field with the field radius r_{target} can expand further and has a more subtle effect on its environment.

Chapter 5 Concept for verifying Field-Space-Mechanics

Procedure:

To provide proof, a particle with a predicted mass is to be produced that uses further dimensions with the aid of a field-space shift in order to exist. First, a particle is needed that exists even without a field-space shift. The proton could be a candidate for such a particle. The proton is irradiated with external artificial energy using a suitable coupling frequency for particle-exchange fion-particle-coupling. This is achieved by synchronising the natural vibration and the coupling frequency with high efficiency, so that the matter pulse of the particle follows this coupling frequency. The proton will initially rise to the 6th dimensional family, causing the exchange to take place in 6 dimensions. The excitation is continued until a specific dimensional family is reached that is associated with a field-space shift. From this point on, the excitation should be switched off. The excited proton decays. The energy and mass can be measured and compared with the predicted mass and frequency of the FSM.

Note: The following masses are the rest masses of an excited proton.

1) First, the proton is produced in a 5- to 6-dimensional state:

Particle	**U**	**U**	**U**	**U**	**U**	**PC**		**mass calculated M_e**	**experim. mass M_e**
Proton-baryon	4,5	4,5	4,5	4,5	4,5	$\frac{6}{3}$	$\frac{1}{2}$	1845	1836

Table 5.1: Excerpt from Table 3.10, here: proton of the 5th dimensional family

The proton-characteristic coupling frequency is:

$$f_{proton,5.} = \frac{1}{2}\left[\frac{4}{3}\left(\frac{3}{2}\right)^3\right]^5 \frac{6}{3} f_e = 1845{,}28125\, f_e = 1845{,}28125 \cdot 1{,}2356\, 10^{20}\ \text{Hz} \qquad (5.01)$$

$$f_{proton,5.} = 2{,}28\, 10^{23}\ \text{Hz}$$

$$E_{proton,5.} = h\, f_{proton,5.} = 6{,}626\, 10^{-34}\ \text{Js} \cdot 2{,}28\, 10^{23}\ \text{Hz} = 1{,}51075\, 10^{-10}\ \text{J} \qquad (5.02)$$

2) The external excitation towards the shift to the next field-space level begins. The dimension planes are marked separately as follows:

In field $F_{4\text{-}6}$: $D_{45/46/56}$ – initial field-space level

In field $F_{7\text{-}9}$: $D_{78/79/89}$ – higher field-space level

The following relationship applies to the exchange between particles when they are excited by a field-space shift:

Disturbed quarks with a period number *of* 2*T* exchange with quarks with a period number of 3*T*: 3*T* + 2*T* (for protons) multiplied by 2 for the field-space displacement in the intermediate mirrored state.

$$(3T + 2T) \cdot 2 = 10 \qquad (5.03)$$

10 stands for the necessary dimension family that forms the power for the disturbed resonance frequency. The denominator of the dimfactor for reducing the maximum speed V_{max} is proportional to the required dimension family with $\frac{5}{10}$ for the proton.

$$f_{proton,10.} = \frac{1}{2}\left[\frac{4}{3}\left(\frac{3}{2}\right)^3\right]^{10} \frac{5}{10}\frac{6}{3} f_e \qquad (5.04)$$

$f_{proton,10.} = 1702531{,}4458 \cdot 1{,}2356\ 10^{20}$ Hz $= 2{,}10365\ 10^{26}$ Hz

$E_{proton,10.} = h\, f_{proton,10.} = 6{,}626\ 10^{-34}$ Js $\cdot\ 2{,}10365\ 10^{26}$ Hz $= 1{,}394\ 10^{-7}$ J

3) A setting with such a frequency is currently not technically possible. It is known from communication technology that frequencies with $\frac{\lambda}{2}$ can be scaled up or down by a factor of two and still retain their wave properties to the full wavelength. This corresponds to the quantum principles from **Chapter 2** and also applies to the energy $E = h\, f$ to be used.

Suggestion for scaling with: 2^{50}

$$\underline{\underline{E_{proton,10.,scaled}}} = \frac{2{,}10365\ 10^{26}\ \text{Hz}}{2^{50}} = \underline{\underline{186{,}842\ \text{GHz}}} \qquad (5.05)$$

$$\underline{\underline{E_{proton,10.,scaled}}} = \frac{1{,}394\ 10^{-7}\ \text{J}}{2^{50}} = \underline{\underline{1{,}238\ 10^{-22}\ \text{J}}} \qquad (5.06)$$

4) As soon as the proton is energized by an external source using a suitable coupling frequency, its plasma state within the particle-field intensifies. In the wave-field, its matter pulse increases. After the transient process, the proton is situated exactly in an intermediate mirrored state between two field-space levels. This state would be detectable if the proton no longer accepts the external irradiation or no longer reacts to an external particle. The proton's charge can be

observed. In this state, the charge may disappear abruptly. In this intermediate mirrored state, the proton exists independently of external fields. After shutdown, the potential environment necessary for this excitation is lost, and the heavy proton decays again after a short time. A measurement is intended to confirm the prediction.

$$M_{proton,5.} = \frac{1}{2}\left[\frac{4}{3}\left(\frac{3}{2}\right)^3\right]^5 \frac{6}{3} M_e = 1845{,}28125\ M_e \qquad (5.07)$$

$$F_{proton,5.} = 2{,}28\ 10^{23}\ \text{Hz}$$

$$M_{proton,10.} = \frac{1}{2}\left[\frac{4}{3}\left(\frac{3}{2}\right)^3\right]^{10} \frac{5}{10}\frac{6}{3} M_e = 1702531{,}5\ M_e \qquad (5.08)$$

$$f_{proton,10.} = 2{,}10365\ 10^{26}\ \text{Hz}$$

$$M_{proton,10.,scaled} = \frac{1702531{,}5\ M_e}{2^{50}} = 1{,}51\ 10^{-09}\ M_e \qquad (5.09)$$

$$f_{proton,10.,scaled} = 186{,}842\ \text{GHz}$$

Conversion of the data from [M_e] to MeV using the measured proton:

$$Y\ M_e = \frac{1836\ M_e}{938{,}38\ \text{MeV}} \cdot X\ \text{MeV} \quad \rightarrow \quad X\ \text{MeV} = Y\ M_e \frac{938{,}38\ \text{MeV}}{1836\ M_e}$$

$$M_{proton,5.} = 1845{,}28125\ M_e \frac{938{,}38\ \text{MeV}}{1836\ M_e} = 943{,}12\ \text{MeV} \quad \rightarrow \text{unexcited proton}$$

$$M_{proton,10.} = 1702531{,}4458\ M_e \frac{938{,}38\ \text{MeV}}{1836\ M_e} = 870164\ \text{MeV} \quad \rightarrow \text{excited proton}$$

$$\underline{\underline{M_{proton,10.,scaled}}} = 1{,}51\ 10^{-09}\ M_e \frac{938{,}38\ \text{MeV}}{1836\ M_e} = \underline{\underline{7{,}73\ 10^{-10}\ \text{MeV}}} \quad \rightarrow \text{scaled proton}$$

5) The process of field-space displacement has been proven. The additional dimensions resulting from field-space displacement and manipulation via the matter pulse have also been proven.

The FSM provides the coupling frequencies and the necessary irradiation energy for external excitation to predict different masses.

Notes: Fine-tuning the frequency setting will be a technical challenge. The duration of the irradiation is open for this concept. Technical verification could be achieved using a particle accelerator. It should also be noted that the proton in the intermediate mirrored state exists as a matter/antimatter particle with the calculated rest mass. The annihilation reaction upon abrupt shutdown could achieve an efficiency of 100%. Safety precautions may need to be taken.

Chapter

6 Possible technical concepts based on the FSM Particle Model

6.1 Excitation of a proton with its coupling frequency

This chapter will focus on the technical advantages of understanding and calculating particles as waves. Particles will be excited as waves, manipulated and measured via their momentum, and then made technically usable again as waves. Using the excitation of a proton, the process of matter pulse increase will be illustrated similarly to **Chapter 5**, whose state could then be technically utilised as a wave. A proton can be regarded as a wave packet with a specific coupling frequency f_{proton}, which could couple from an external energy source using a multiple coupling frequency. Using a suitable coupling frequency $f_{proton,}$ the energy introduced can be increased with high efficiency and, at the same time, an increased plasma state can be produced. The plasma state does not only refer to hot gas, but primarily to the increase in the matter pulse in the wave-field $F_{4\text{-}6,}$ which follows the introduced coupling frequency. With the increased matter pulse, a field-space shift can be artificially generated.

Figure 6.1 shows a typical structure of a proton. The u/d-quarks are marked in red and blue. The u/d-quarks move in circular orbits perpendicular to the generated magnetic moment. There is a strong interaction between the u/d-quarks due to the quark-exchange fion-quark-coupling predicted by FSM, shown here in sinusoidal form. During the quark-exchange fion-quark-coupling, the field exchange of exchange fions parameterises the characteristic strength of the strong interaction in the particle-field $F_{1\text{-}3.}$ The strong interaction allows u/d-quarks to be kept on their accelerated trajectories. The direction of the exchange fions is indicated by arrows. The length of the arrows reflects the strength of the strong interaction. In the centre is the binding neutrino, which binds all exchange fions of the u/d-quarks, continues the exchange and thus promotes stability in the proton.

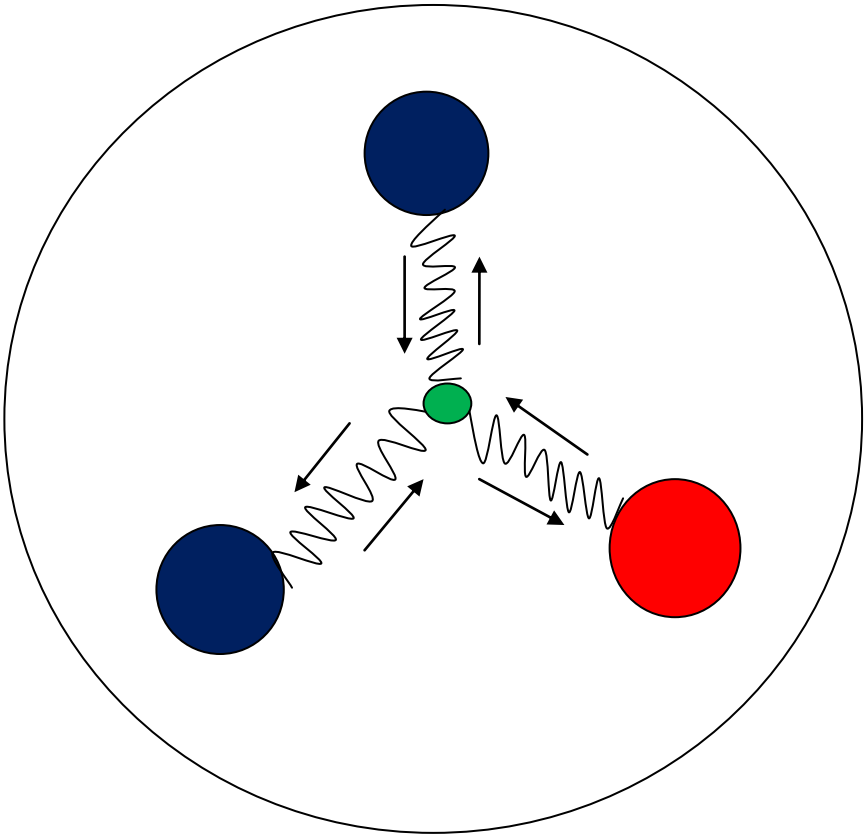

Figure 6.1: Basic structure of a proton

It has already been established by bombarding atomic nuclei with electric charges that the atomic shell or sphere of a proton has its own increased energy potential. The u/d-quarks can also be excited by photons, or indeed by any external electromagnetic radiation. This confirms the processes of quark–exchange fion–quark-coupling.

Without such a surrounding potential field, the u/d-quarks are repeatedly deflected back to their original paths by the strong interaction and release any excess energy into the environment in the form of electromagnetic radiation/ photons. Therefore, it has not yet been possible to make the strong interaction as a field and the exchange fions in the wave-field accessible for technical use beyond the atomic nucleus. An external radiation source is now to be used which increases its energy with high efficiency at the set coupling frequency for protons. With the start of irradiation, the increase in the plasma state inside the proton begins. The sphere S and the field radius r grow due to the relativistic increase in energy until the shorter wavelengths λ_{fions}, with their periodic rotation, are in resonance with the sphere S. With a further increase in energy density, the u/d-quarks in the proton are initially accelerated towards the adjusted sphere boundary at a constant coupling factor. As the plasma state increases further, the u/d-quarks continue to approach the edge of the proton sphere. The nuclear force between the u/d-quarks as carriers of the binding energy continues to increase with distance. The fions must now compensate for the increased acceleration and the resulting expansion of the u/d-quarks' orbits within the

sphere. In the expanded space between the u/d-quarks, the excess energy gives rise to further quark and antiquark pairs from the corresponding field-space levels, which cannot be observed individually because they annihilate after a short time, releasing heat. These quark/antiquark pairs are a form of mesons. All existing mesons appear relatively neutral when viewed from the outside because the quark with a charge $Q = +\frac{2}{3}e$ and the antiquark with $Q = -\frac{2}{3}$ e have opposite charges. **Figure 3.12** shows such a meson. All mesons that are produced stabilize the system as long as the surrounding potential cannot absorb their (annihilation) energy. By measuring the energy level, the plasmatic state of the quark-fion plasma is automatically determined. The duration of the irradiation must be determined experimentally. The proton is now enriched as shown in **Figure 6.2**.

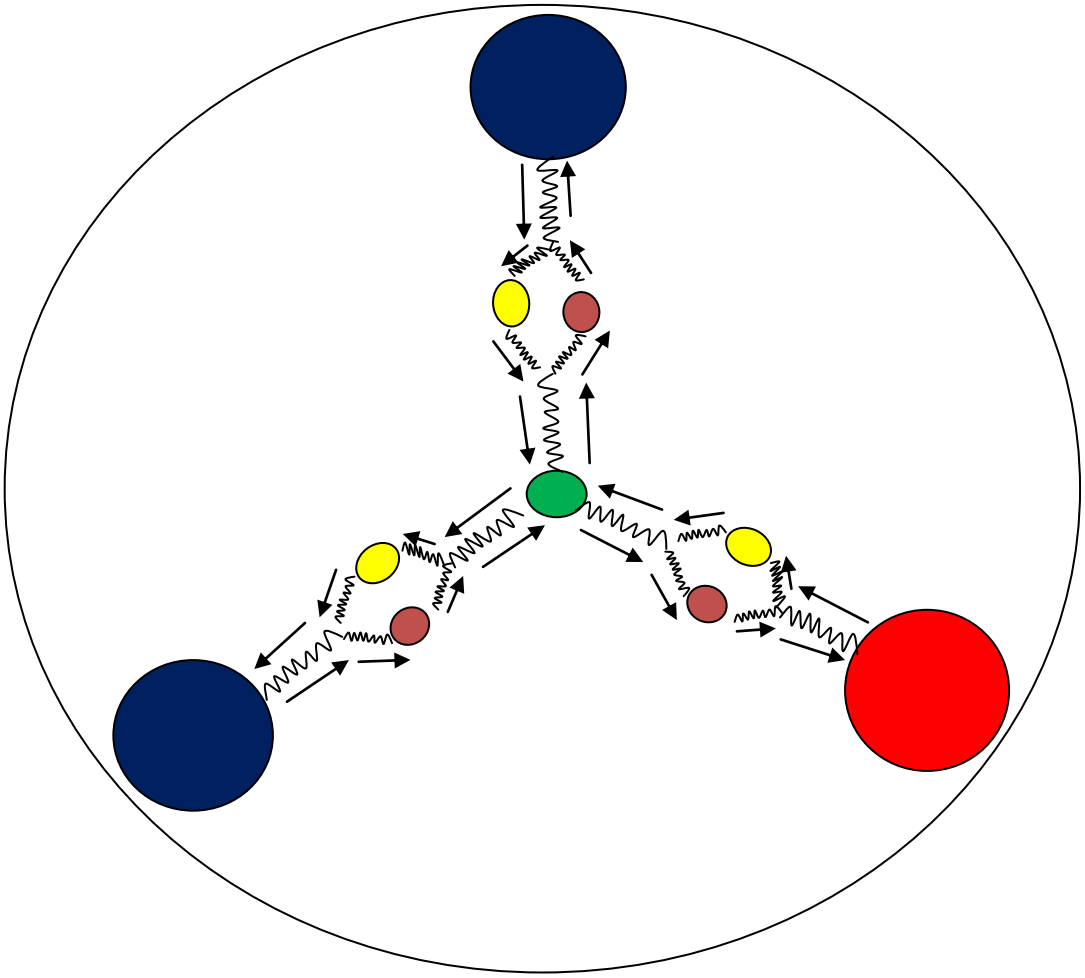

Figure 6.2: Quark-fion plasma in an excited proton due to the increase in energy density

Figure 6.2 shows the proton from its excited conglomerate of u/d-quarks, exchange fions and mesons. The paths of the mesons from quark and antiquark pairs are marked in yellow and brown. The arrows again represent the directions of the exchange fions for the strong interaction in this proton, which have now become cumulatively larger due to the quark-fion plasma. The amplification of the nuclear

force is shown proportionally to the length of the arrows. Compared to **Figure 6.1,** the arrow lengths have increased.

The excited proton has a special state due to the quark-fion plasma. It contains mesons, which account for most of the binding energy when excited to a high energy state. Their amplified vector waves could be amplified, diffracted, and refracted in field exchange just like any other wave. However, the quark-fion plasma is technically interesting as a wave. Through controlled amplification of the binding energy in the quark-fion plasma, the u/d-quarks continue to interact with their own strong nuclear power at the edge of the proton sphere S. The effect of the field could reach the edge of the sphere and become noticeable in the environment. This could be exploited technologically.

6.2 Technical process of matter puls increase

This chapter is intended to describe the basic technical process that applies to **Chapter 6.1** so that a matter pulse increase occurs in the proton-fion system.

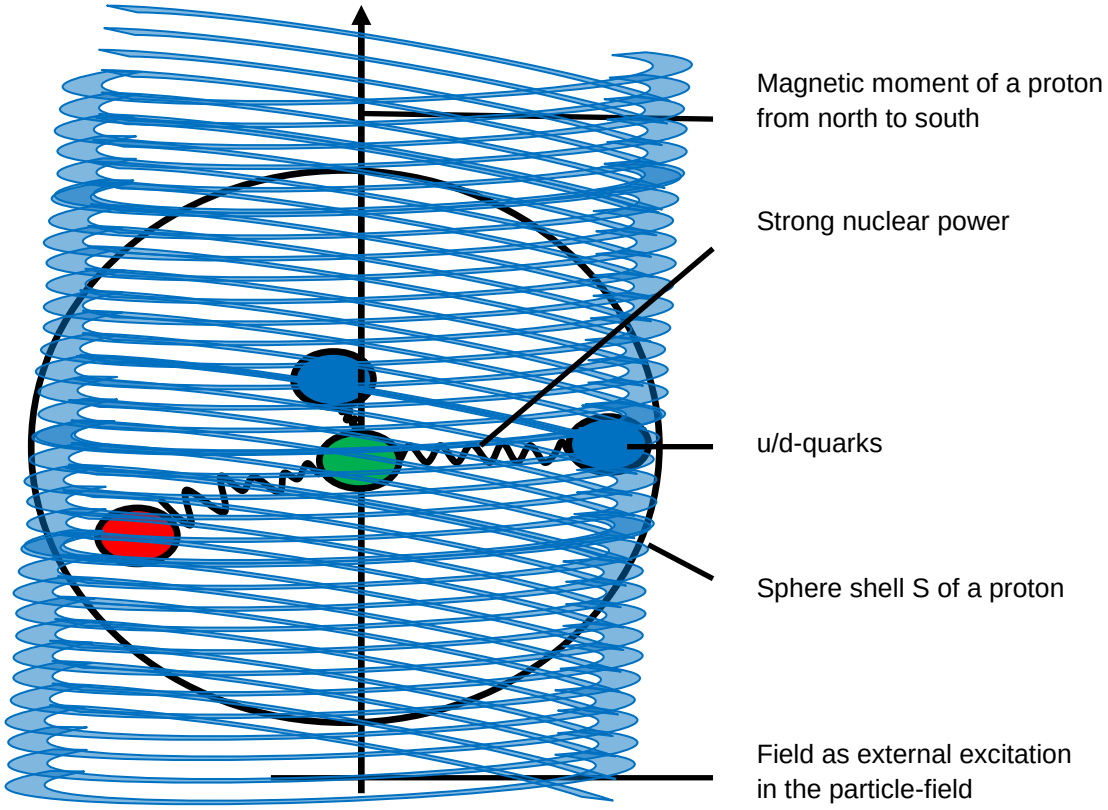

Figure 6.3: Representation of an external field that reacts with the proton and forces the u/d-quarks to accelerate

Figure 6.4 A – D explains the effects of this below.

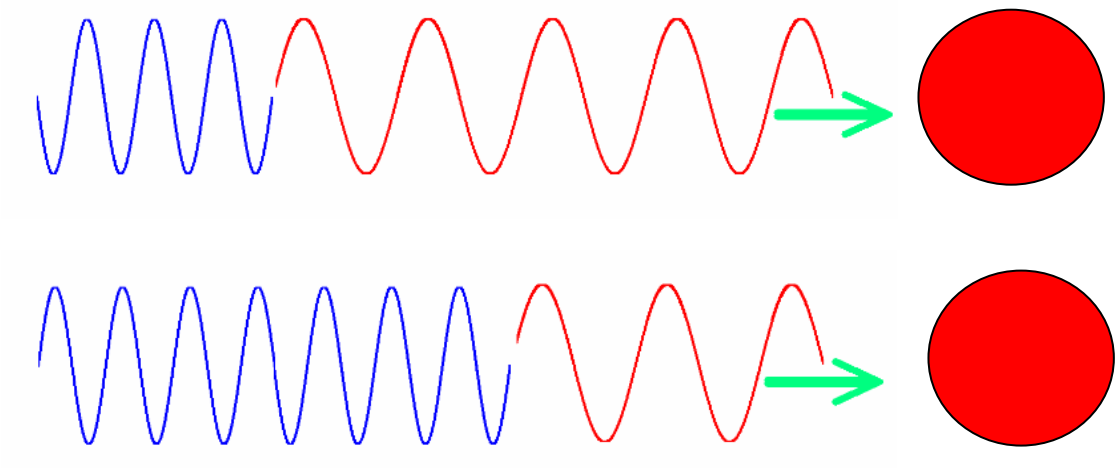

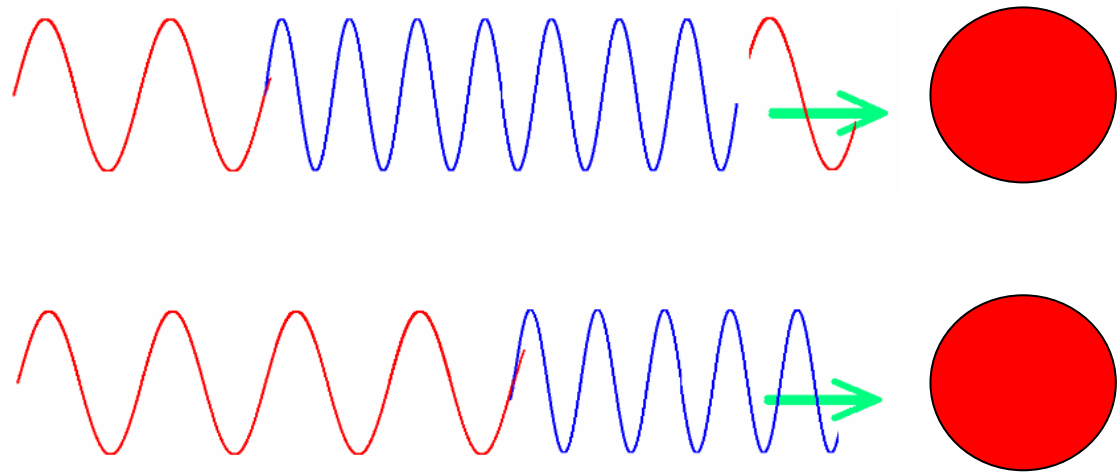

Impact of an exchange fion from a strengthening external field on the proton as a function of time (marked in blue here).

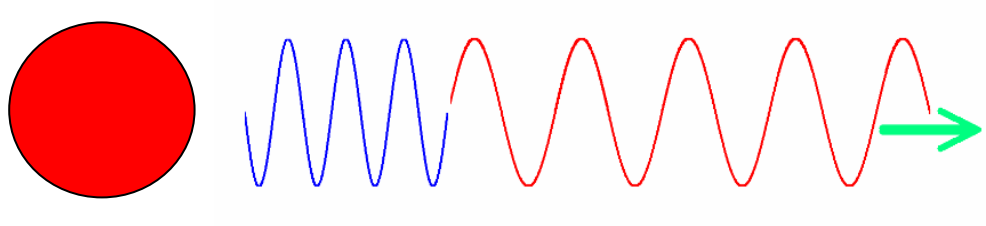

A specific excitation coupling frequency f_{proton} of the proton consists of active fions that react in resonance with an amplifying field.

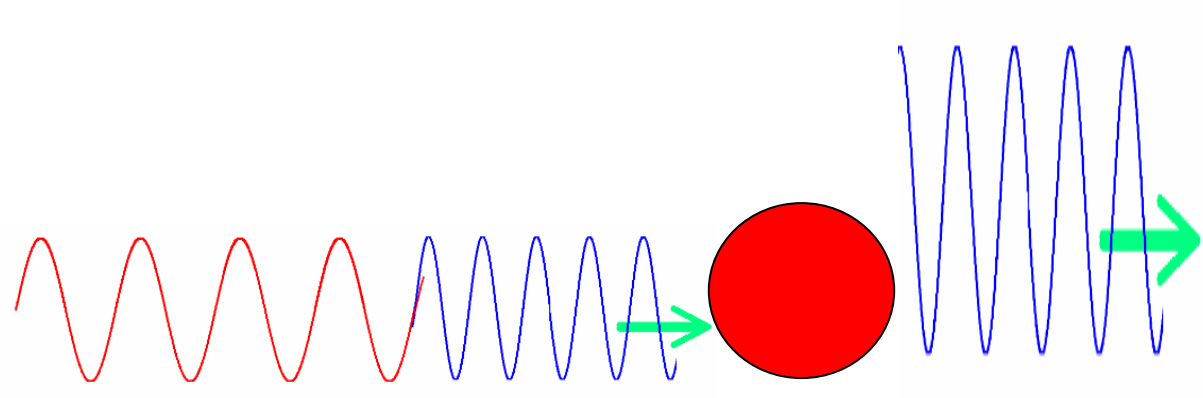

Resulting oscillation/ interference of the amplitudes due to the coupling between the fion and the proton with multiples of its information matrix.

Figure 6.4A: Manipulation of the amplitude of the respective fions in the wave-field $F_{4\text{-}6}$

Through the interference between the natural oscillation of the proton and the external radiation, the energy introduced is converted into a quark-fion plasma with an efficiency of < 1.

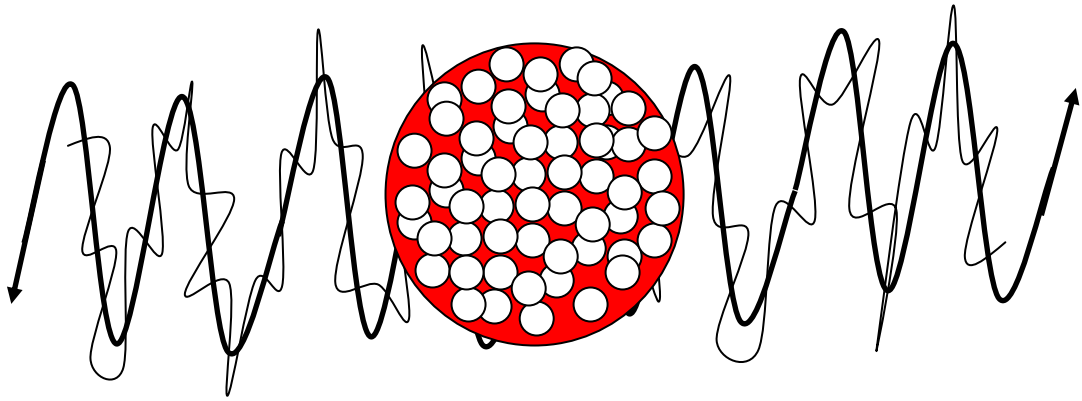

Figure 6.4B: Formation of a quark-fion plasma in the proton through the above-mentioned external influence

With the limited proton sphere, the energy density continues to increase. The plasmatic state increases directly proportional to the matter pulse. A measurable shift of the proton to a higher energy level between two field-space levels begins.

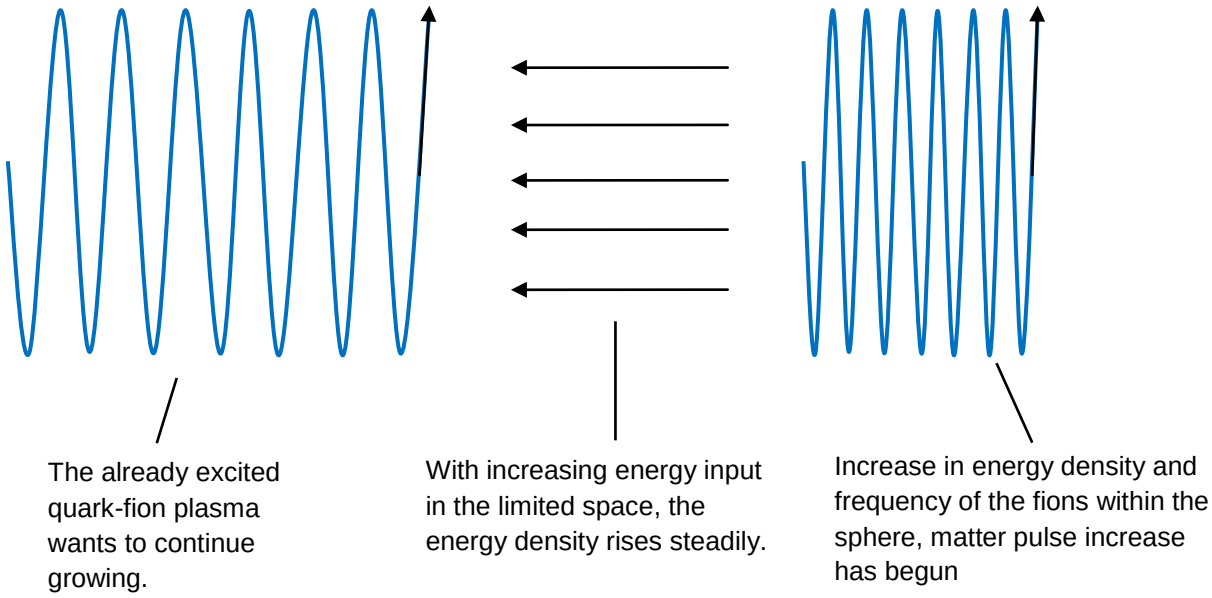

Figure 6.4C: Process of technical matter pulse increase

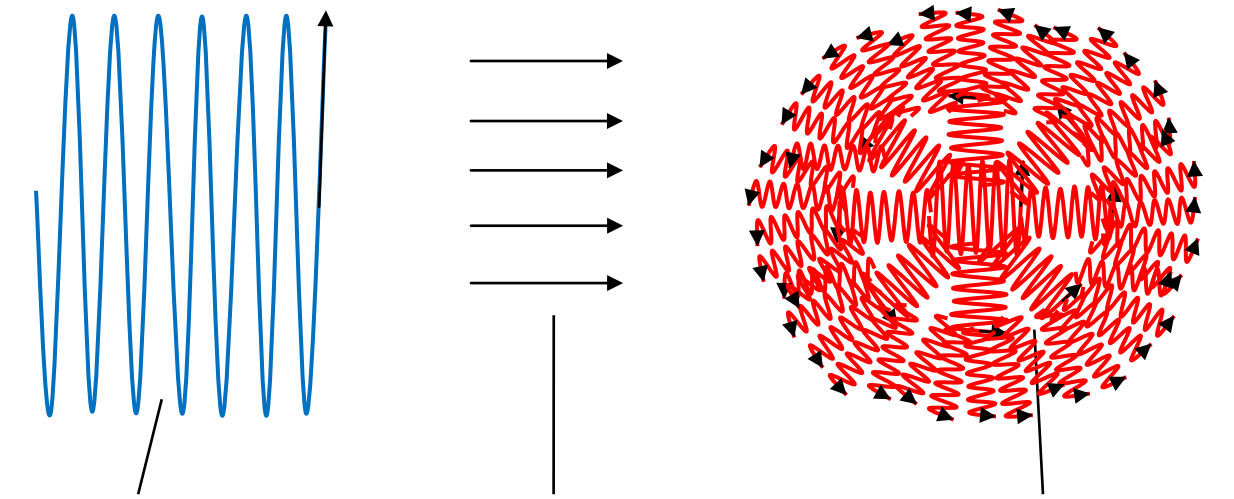

Figure 6.4D: Technological use of the excited state

Conclusion:

With an external energy supply through an ideal coupling frequency f_{obj}, a particle is efficiently transferred into an elevated plasma state. The plasma state increases the matter pulse in the wave-field $F_{4\text{-}6}$. With the increased matter pulse, a temporary field-space shift can be artificially generated. The effect corresponds to the process of relativistic energy increase without applying an object velocity. A proton with a specific quark-fion plasma state is created, which is characterised by a matter/antimatter accumulation. Technically, this could enable access to the strong nuclear power.

Prediction:

If the resulting field has a closed shape as in **Figure 6.5** and the quantum principles at the point of contact in the dimensional plane D_{56} are fulfilled for fions, then the contents of the predicted information matrices can be exchanged between the exciting systems. Both information matrices are overwritten or reprogrammed to form a resulting information matrix. A new information matrix or a new field form would arise from the resonance of two information matrices.

The technical use in fields has an almost infinite variety of combinations.

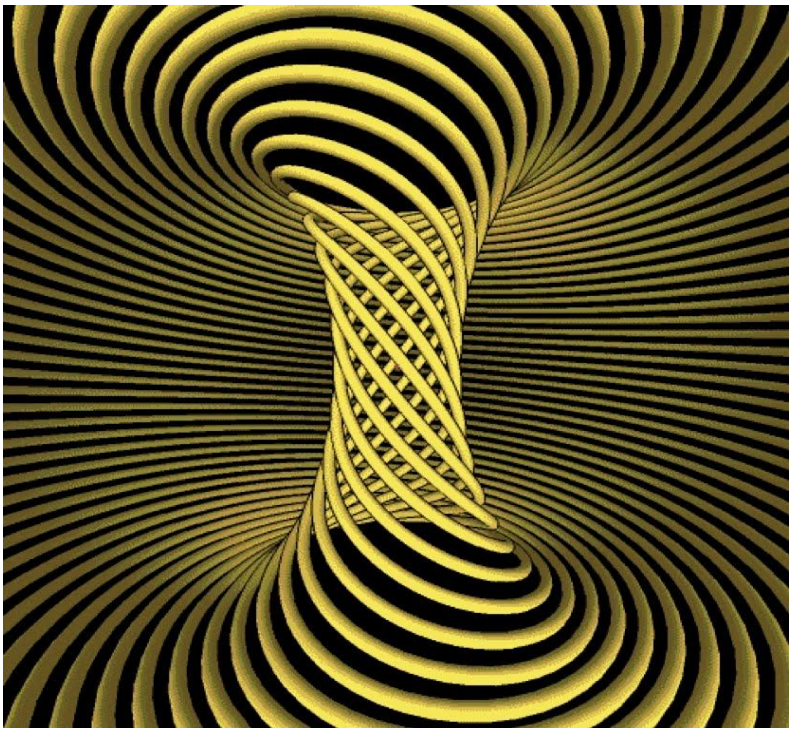

Figure 6.5: Coiled closed torsion field

Figure source [11]

6.3 Concept for a possible optimisation of Hot Fusion

Introduction to the fusion process:

Hot fusion – the process in the sun

The fusion processes in the sun have been modelled using the Bethe-Weizäcker cycle, which takes place at a pressure of around 300 billion bar and a temperature of approx. 15 million °C. Initial fusion processes promote the production of hydrogen ^{1}H to helium ^{4}He with radiation ɣ and heat:

$$^{1}H^{+} + {}^{1}H^{+} \rightarrow {}^{2}H^{+} + e^{+} + e^{-} + 0{,}42\ \text{MeV} \quad (6.01)$$

$$^{2}H^{+} + {}^{1}H^{+} \rightarrow {}^{3}He^{2+} + \gamma + 5{,}49\ \text{MeV} \quad (6.02)$$

$$^{3}He^{2+} + {}^{3}He^{2+} \rightarrow {}^{4}He^{2+} + {}^{1}H^{+} + {}^{1}H^{+} + 12{,}86\ \text{MeV} \quad (6.03)$$

Hot fusion – state of the art

Hot fusion is being researched at the Cadarache nuclear research centre in southern France and at the Tokamak or Wendelstein 7x in Greifswald. Here, the elements deuterium and tritium are heated to approx. 100 million °C in a microwave-like process to form a fusion-capable plasma. Plasma is a state of matter in which positively charged fions, negatively charged electrons and neutral particles with high entropy move randomly in relation to each other. They can be manipulated electrically or magnetically. The elements are supplied with energy by the microwaves of the so-called gyrotron as an external energy source. The multiple microwave frequencies couple to the coupling frequency of the electron, which sets the electron in motion and continuously heats the plasma. With sufficient heat, a threshold is exceeded that is sufficient for a fusion reaction. The plasma is guided in a twisted magnetic field and accelerated linearly. In the narrow plasma jet, the atoms lean against each other to such an extent that the fusion process begins. Helium and a neutron are produced, releasing heat. The neutron and the heat released are captured on a reactor wall. The heat is transferred to a water boiler, which conventionally drives a generator via a high-pressure turbine to generate electricity.

The hot fusion process was selected using the elements deuterium ^{2}H and tritium ^{3}H to form helium ^{4}He, which is largely radiation-free and heat-generating:

$$^{2}H^{+} + {}^{3}H^{+} \rightarrow {}^{4}He^{2+} + \text{neutron} + 14{,}1\ \text{MeV} \quad (6.04)$$

Framework for this model:

Within the framework of FSM, the optimisation of hot fusion and a concept for the economic utilisation of cold fusion will be presented below. The multiple frequency of all fusion elements is the coupling frequency of the proton. The required radiation energy of the external energy source must only correspond to a multiple of the proton.

Possible optimisation of hot fusion :

To optimise hot fusion, a similar process based on the state of the art should be found, in which more energy is generated than is added. In this case, the elements should be hydrogen ^{1}H, which is converted to helium ^{4}He with heat radiation of:

[0,42 MeV + 5,49 MeV + 12,86 MeV = 18,77 Mev]

The fusion threshold is reached through constant coupling with a suitable coupling frequency between the external energy source and the hydrogen over a period of time that is yet to be determined.

Technical concept for optimising hot fusion:

Technically, the design of the Wendelstein 7x can be used. The difference in using the gyrotron as an external energy source is that it is no longer the electrons, but the protons that are directly excited to start the fusion process. For this purpose, the coupling frequencies of the proton for the 5th dimensional family are used.

Energy enrichment with suitable coupling frequency for the hot fusion process with hydrogen ^{1}H to helium ^{4}He:

A plasma mass of 50 g = 0.05 kg is to be used.

$f_e = 1{,}2356\ 10^{-20}$ Hz ; $M_e = 9{,}1094\ 10^{-31}$ kg ; $h = 6{,}626\ 10^{-34}$ Js ; $c = 299792458\ \frac{\text{m}}{\text{s}}$

$M_{obj}\ k_{obj} = 4{,}0396\ 10^{35}\ \frac{\text{kg}}{\text{s}}$

$$\lambda_{proton} = \frac{c}{1845{,}28125\ f_e} = \frac{299792458\ \frac{\text{m}}{\text{s}}}{1845{,}28125 \cdot 1{,}2356\ 10^{20}\ \text{Hz}} = 1{,}315\ 10^{-15}\ \text{m} \qquad (6.05)$$

The mass of the proton according to the FSM photon model:

$$M_{proton} = \frac{h\ c^2}{G\ \{M_{obj}\ k_{obj}\}\ \lambda_{proton}} = 1{,}681\ 10^{-27}\ \text{kg}$$

The mass of the proton according to the FSM particle model:

M_{proton} = 1845,28125 M_e = 1,681 10^{-27} kg (calculated proton mass)

M_{proton} = 1836,15 M_e = 1,6726 10^{-27} kg (measured proton mass)

In order to obtain two possible settings, we will now continue with the measured and calculated masses.

Coupling frequency for protons:

For the calculated proton mass:

$$f_{proton} = \frac{1}{2}\,[\,\frac{4}{3}\,(\,\frac{3}{2}\,)^3\,]^5\,\frac{6}{3}\,f_e = 1845{,}28125\,f_e = 1845{,}28125 \cdot 1{,}2356\ 10^{20}\ \text{Hz}$$

f_{proton} = 2,28003 10^{23} Hz

$E_{proton} = h\ f_{proton}$ = 6,626 10^{-34} Js · 2,28 10^{23} Hz = 1,51075 10^{-10} J

For the measured proton mass:

$$f_{proton} = \frac{1}{2}\,[\,\frac{4}{3}\,(\,\frac{3}{2}\,)^3\,]^5\,\frac{6}{3}\,f_e = 1836{,}15\,f_e = 1836{,}15 \cdot 1{,}2356\ 10^{20}\ \text{Hz}$$

f_{proton} = 2,268747 10^{23} Hz

$E_{proton} = h\ f_{proton}$ = 6,626 10^{-34} Js · 2,268747 10^{23} Hz = 1,5033 10^{-10} J

Number of protons in a hydrogen ^{1}H mixture of 50 g:

$$n_{protons} = \frac{m_{proton\ mass}}{m_{proton}} \qquad \text{with: } n\ \varepsilon\ \mathbb{N} \qquad (6.06)$$

For the calculated proton mass:

$$n_{protons} = \frac{0{,}05\ \text{kg}}{1{,}681\ 10^{-27}\ \text{kg}} = 2{,}974\ 10^{25}$$

For the measured proton mass:

$$n_{protons} = \frac{0{,}05\ \text{kg}}{1{,}6726\ 10^{-27}\ \text{kg}} = 2{,}989\ 10^{25}$$

The multiple energy equivalent to be provided for $n_{protons}$ in order to enrich the gas mixture:

For the calculated proton mass:

$$E_{50g} = E_{proton}\, n_{protons} = 1{,}51075\ 10^{-10}\ \text{J} \cdot 2{,}974\ 10^{25} = 4{,}493\ 10^{15}\ \text{J} \qquad (6.07)$$

For the measured proton mass:

$$E_{50g} = E_{proton}\, n_{protons} = 1{,}5033\ 10^{-10}\ \text{J} \cdot 2{,}989\ 10^{25} = 4{,}4934\ 10^{15}\ \text{J}$$

Since the frequencies to be set and the respective energy equivalents are not technically feasible, they are factored by two. Halving the frequency is permissible in communication technology because halving the frequency of an electromagnetic wave does not change the form of its comprehensive original frequency. It should be noted that scaling also scales the deviations and tolerances accordingly. Fine adjustment of the frequency will probably have to be inversely proportional to the scaling.

The coupling frequency and radiation energy are scaled by a factor of 2:

Proposal for scaling with: 2^{40}

For the calculated proton mass:

$$\underline{\underline{f_{proton,scaled}}} = \frac{2{,}28003\ 10^{23}\ \text{Hz}}{2^{40}} = \underline{\underline{207{,}368\ \text{GHz}}} \qquad \text{(coupling frequency)}$$

$$E_{proton,scaled} = \frac{1{,}51075\ 10^{-10}\ \text{J}}{2^{40}} = 1{,}374\ 10^{-22}\ \text{J} \qquad \text{(energy content per proton mass)}$$

$$E_{50g,scaled} = \frac{4{,}493\ 10^{15}\ \text{J}}{2^{40}} = 4086{,}4\ \text{J} \qquad \text{(Energy content for 50 g proton mass)}$$

$$\underline{\underline{P_{input,scaled}}} = \frac{4086{,}4\ \text{J}}{\text{s}} = \underline{\underline{4086{,}4\ \text{kW}}} \qquad \text{(frequency-dep. input for 50 g plasma mass)}$$

For the measured proton mass:

$\underline{f_{proton,scaled} =} \frac{2{,}268747\ 10^{23}\ \text{Hz}}{2^{40}} = \underline{206{,}341\ \text{GHz}}$ (coupling frequency)

$E_{proton,scaled} = \frac{1{,}5033\ 10^{-10}\ \text{J}}{2^{40}} = 1{,}367\ 10^{-22}\ \text{J}$ (energy content per proton mass)

$E_{50g,scaled} = \frac{4{,}4934\ 10^{15}\ \text{J}}{2^{40}} = 4086{,}7\ \text{J}$ (energy content for 50 g proton mass)

$\underline{P_{input,scaled} =} \frac{4086{,}7\ \text{J}}{\text{s}} = \underline{4{,}0867\ \text{kW}}$ (frequency-dep. input for 50 g plasma mass)

If the correct coupling frequency of the external energy source in the GHz range resonates with that of the proton, then the reactor requires a constant radiation power of only approx. 4,1 kW for a plasma mass of 50 g. The irradiation time for fusion remains open for the time being.

Compared to Wendelstein 7x, which operates at approx. 140 GHz and 1–15 MW, electromagnetic excitation takes place using the FSM concept at a coupling frequency of approx. 206 GHz and a power of 4,1 kW. Plasma generation would be 1000 times more efficiently if the coupling frequency were selected via protons rather than electrons.

Energy output :

The energy enrichment must only be continued until the plasmatic state is sufficient ($E(t) = h\, f_{proton}\, \frac{1}{\sin(kt)}$), to start the fusion process. However, the effect is comparable to the relativistic energy increase without an object velocity. Per total process for the fusion of

$6\ {}^{1}\text{H} \rightarrow {}^{4}\text{H} + {}^{1}\text{H} + {}^{1}\text{H}$

18,77 MeV is generated. If the entire plasma mass were to fuse, the following heat energy could be generated for electricity production.

For the calculated proton mass:	For the measured proton mass:
$n_{protons} = 2{,}974\ 10^{25}$	$n_{protons} = 2{,}989\ 10^{25}$
$E_{output} = 18{,}77\ \text{MeV} \cdot 2{,}974\ 10^{25}\ \frac{1}{6}$	$E_{output} = 18{,}77\ \text{MeV} \cdot 2{,}989\ 10^{25}\ \frac{1}{6}$
$\underline{E_{output\_ø} = 9{,}3\ 10^{26}\ \text{MeV}}$	$\underline{E_{output\_ø} = 9{,}35\ 10^{26}\ \text{MeV}}$

Comparison with the hot fusion process in the Wendelstein 7x:

$^{2}H^{+} + {}^{3}H^{+} \rightarrow {}^{4}He^{2+} + \text{neutron} + 14{,}1\ \text{MeV}$ $\quad n_{protonen} = 2{,}989\ 10^{25}$

$$E_{output} = 14{,}1\ \text{MeV} \cdot 2{,}989\ 10^{25}\ \frac{1}{5}$$

$E_{output\_ø} = 8{,}43\ 10^{26}\ \text{MeV}$

The output appears to be similar for both processes. The main difference lies in the generation of fusion with its ignition. By exciting protons instead of electrons, the input power is reduced by a factor of 1000. The comparison assumes that the temporal excitation of a plasma is modelled to be approximately the same length with the same pressure and temperature. The classic hot fusion process could start sooner here because it already contains higher elements. Another economic advantage of the optimized process, however, is that it now uses hydrogen—which is available in large quantities—instead of tritium. Natural tritium causes environmental damage during extraction. When produced artificially, it requires additional energy input, and its use necessitates more extensive shielding.

6.4 Concept for Cold Fusion

A possible concept for the technical implementation of cold fusion is to be provided for this model, which, like hot fusion, also enables energy to be gained. The concept presented is intended to be an initial approach.

A common coupling frequency is sought for the excitation to be set in the fusion process, which favours the process for a field-space shift. When a particle is shifted in the field-space, it automatically generates a quark-fion plasma. In the intermediate state between two field-space levels, the elements reach over 1000 times their mass and correspondingly strong interaction properties, which favours the fusion process even at lower temperatures. The fusion process no longer requires hot gas when it takes place in the field-space-shifted state.

Technical concept for implementing cold fusion:

For particles to be displaced between two field-space levels, there must be a surrounding potential field that encloses them and enriches them with energy. The Wendelstein 7x with its gyrotron is likely to be only partially suitable for this purpose. An alternative reactor design is proposed for the cold fusion concept. The hydrogen is electrolysed from H_2 to ^1H and introduced into a reactor chamber at room temperature. In the reactor chamber, an electromagnetic radiation field exists between two radiation surfaces. A static helical magnetic torsion field as shown in **Figure 6.5** is generated by means of a suitable torsion coil. Since the magnetic torsion field inside follows a 45° angle, an exactly orthogonal electric torsion field is present. At this location, the negative charge carriers are separated from the positive hydrogen $^1H^+$ and accelerated. The gas mixture of hydrogen $^1H^+$ and electrons e^- moves mechanically separated from each other along the electric torsion field. At the same time, the gas mixture is excited by microwave radiation from an external energy source at a suitable coupling frequency. The energy introduced is increased in a targeted manner with an efficiency of nearly 100%. At the centre of the torsion coil is a constriction through which the hydrogen atoms must pass during their orbit. At the constriction, the probability of fusion increases. The torsion field performs the same task as the superconducting coils in the Wendelstein 7x. The radiation surfaces replace the gyrotron, which continuously transfers its power to the reactor. After the fusion process, the heat generated is also removed conventionally at the reactor wall.

Figure 6.6 shows the structure and **Figure 6.7** shows the functioning of a torsion coil that generates a magnetic field inclined at 45° in the centre. Currently, there is no device that can build such a coil.

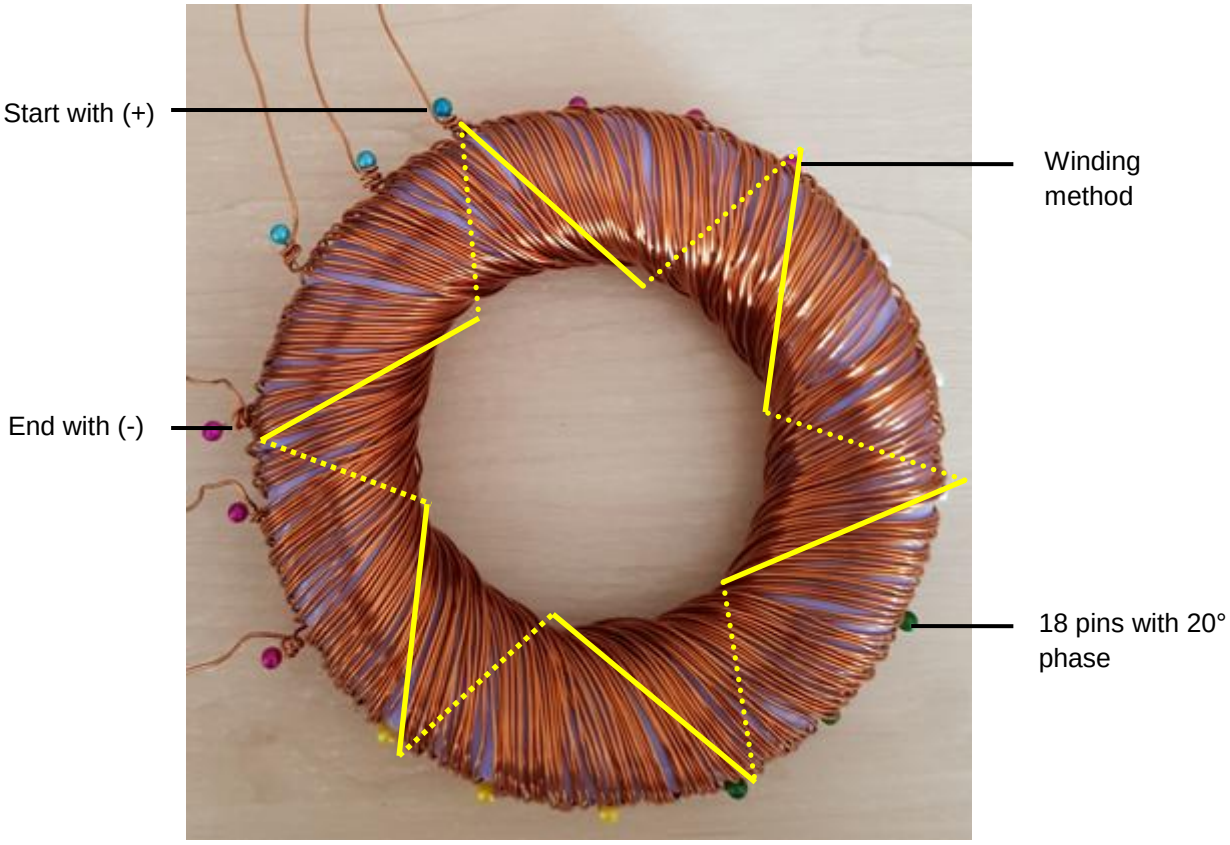

Figure 6.6: Structure of a torsion coil

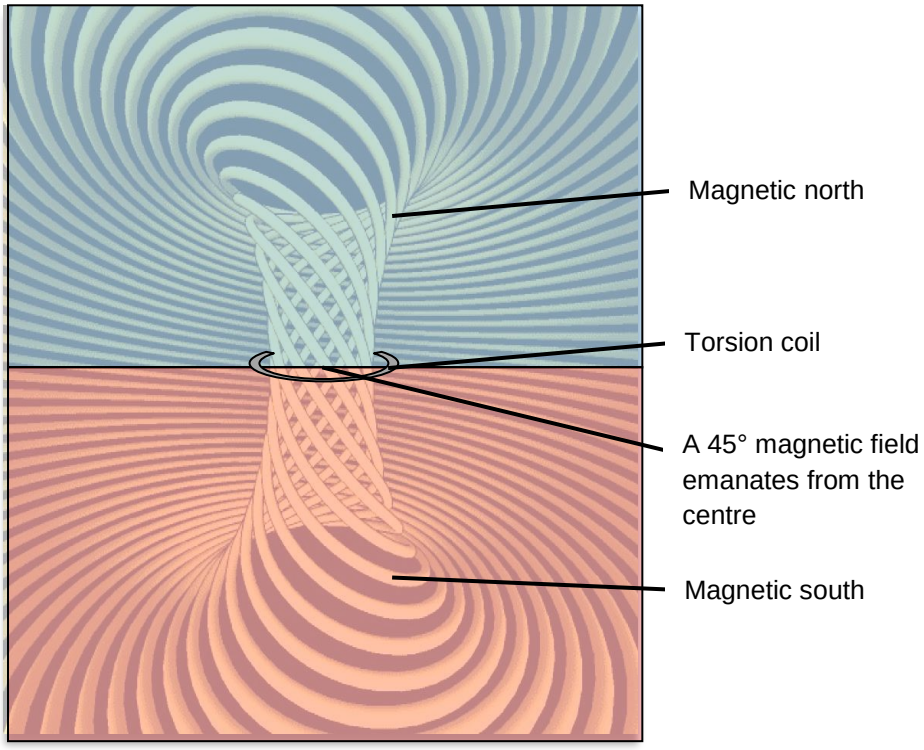

Figure 6.7: How a torsion coil works

Figures 6.8 and **6.9** show a conceptual design and the associated operating mechanism of a possible cold fusion reactor. The charge carriers separate within the torsion field, causing the hydrogen to undergo a mechanical periodic cycle.

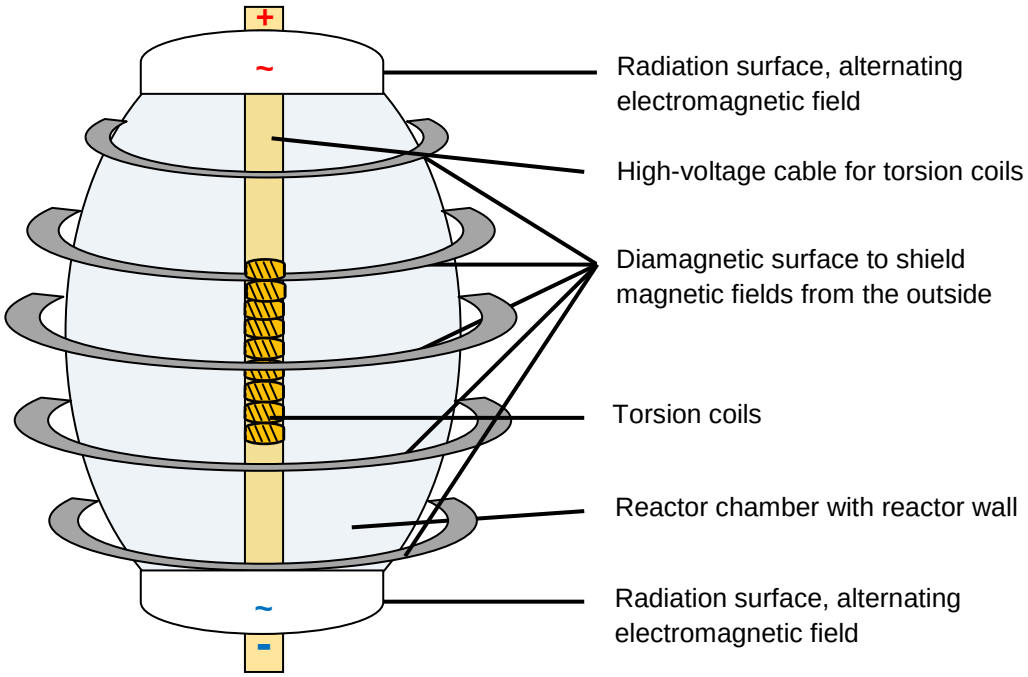

Figure 6.8: Principle design of a reactor for cold fusion

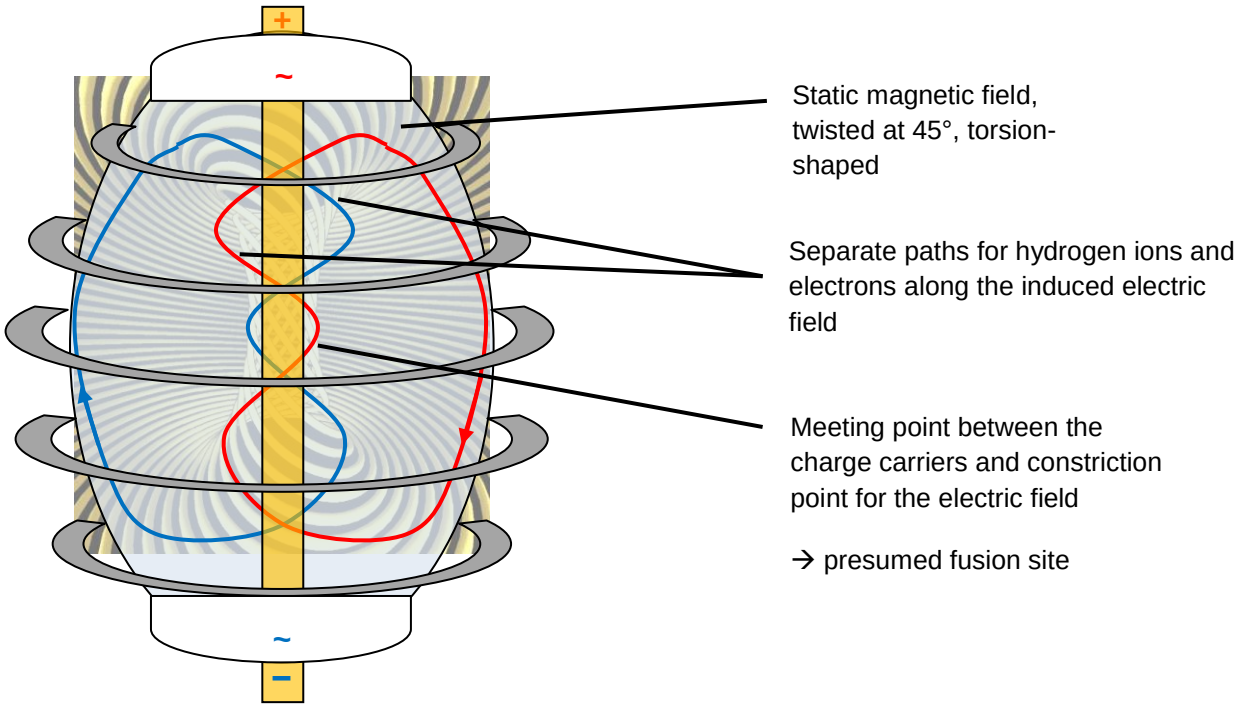

Figure 6.9: Mechanism of action of the magnetic and electric torsion field on the hydrogen mixture

Energy enrichment with suitable coupling frequency for the cold fusion process with hydrogen ^{1}H to helium ^{4}He:

The calculation follows the same pattern as for hot fusion. The main change now lies in the coupling frequency for protons at a field-space shift with the 10th dimensional family.

Again, a plasma mass of 50 g = 0,05 kg should be used for the calculation.

$f_e = 1{,}2356\ 10^{-20}$ Hz

$$\lambda_{proton} = \frac{c}{1845{,}28125\ f_e} = \frac{299792458\ \frac{m}{s}}{1845{,}28125 \cdot 1{,}2356\ 10^{20}\ Hz} = 1{,}315\ 10^{-15}\ m$$

The mass of the proton using the FSM particle model

$M_{proton} = 1845{,}28125\ M_e = 1{,}681\ 10^{-27}$ kg (calculated proton mass)

$M_{proton} = 1836{,}15\ M_e = 1{,}6726\ 10^{-27}$ kg (measured proton mass)

Mass and coupling frequency of the proton:

With protons, the following coupling frequency must be used for a shift between two field-space levels with the 10th dimension family and the corresponding dimension reduction factor for the maximum velocity V_{max}.

For the calculated proton mass:

$$f_{proton,5.} = \frac{1}{2}\left[\frac{4}{3}\left(\frac{3}{2}\right)^3\right]^5 \frac{6}{3} f_e = 1845{,}28125\ f_e = 1845{,}28125 \cdot 1{,}2356\ 10^{20}\ Hz$$

$f_{proton,5.} = 2{,}28003\ 10^{23}$ Hz

$$f_{proton,10.} = \frac{1}{2}\left[\frac{4}{3}\left(\frac{3}{2}\right)^3\right]^{10} \frac{5}{10}\frac{6}{3} f_e = 1702531{,}4458 \cdot 1{,}2356\ 10^{20}\ Hz$$

$f_{proton,10.} = 2{,}10365\ 10^{26}$ Hz

$E_{proton,5.} = h\ f_{proton} = 6{,}626\ 10^{-34}$ Js $\cdot$ $2{,}28\ 10^{23}$ Hz $= 1{,}51075\ 10^{-10}$ J

$E_{proton,10} = h\ f_{proton,10.} = 6{,}626\ 10^{-34}$ Js $\cdot$ $2{,}10365\ 10^{26}$ Hz $= 1{,}394\ 10^{-7}$ J

For the measured proton mass:

$$f_{proton} = \frac{1}{2}\left[\frac{4}{3}\left(\frac{3}{2}\right)^3\right]^5 \frac{6}{3} f_e = 1836{,}15\, f_e = 1836{,}15 \cdot 1{,}2356\ 10^{20}\ \text{Hz}$$

$$f_{proton} = 2{,}268747\ 10^{23}\ \text{Hz}$$

$$f_{proton,10.} = \frac{1}{2}\left[\frac{4}{3}\left(\frac{3}{2}\right)^3\right]^{10} \frac{5}{10}\frac{6}{3} f_e = \frac{1836{,}15}{1845{,}28125}\ 1702531{,}4458 \cdot 1{,}2356\ 10^{20}\ \text{Hz}$$

$$f_{proton,10.} = 2{,}09324\ 10^{26}\ \text{Hz}$$

$$E_{proton} = h\, f_{proton} = 6{,}626\ 10^{-34}\ \text{Js} \cdot 2{,}268747\ 10^{23}\ \text{Hz} = 1{,}5033\ 10^{-10}\ \text{J}$$

$$E_{proton,10.} = h\, f_{proton,10.} = 6{,}626\ 10^{-34}\ \text{Js} \cdot 2{,}09324\ 10^{26}\ \text{Hz} = 1{,}387\ 10^{-7}\ \text{J}$$

Number of protons in a hydrogen ^{1}H mixture of 50 g:

For the calculated proton mass: with: n ε N

$$n_{protons} = \frac{0{,}05\ \text{kg}}{1{,}681\ 10^{-27}\ \text{kg}} = 2{,}974\ 10^{25}$$

For the measured proton mass:

$$n_{protons} = \frac{0{,}05\ \text{kg}}{1{,}6726\ 10^{-27}\ \text{kg}} = 2{,}989\ 10^{25}$$

The multiple energy equivalent to be provided for $n_{protons}$ in order to enrich the gas mixture:

For the calculated proton mass:

$$E_{50g} = E_{proton,10.}\, n_{protonen} = 1{,}394\ 10^{-7}\ \text{J} \cdot 2{,}974\ 10^{25} = 4{,}145756\ 10^{18}\ \text{J}$$

For the measured proton mass:

$$E_{50g} = E_{proton,10.}\, n_{protonen} = 1{,}387\ 10^{-7}\ \text{J} \cdot 2{,}989\ 10^{25} = 4{,}145743\ 10^{18}\ \text{J}$$

The coupling frequency and radiation energy are scaled by a factor of 2:

Suggestion for scaling with: 2^{50} (comparison to hot fusion: 2^{40})

For the calculated proton mass:

$$\underline{\underline{f_{proton,10.,scaled} =}} \frac{2{,}10365\ 10^{26}\ \text{Hz}}{2^{50}} = \underline{\underline{186{,}842\ \text{GHz}}} \qquad \text{(coupling frequency)}$$

$$E_{proton,10.,scaled} = \frac{1{,}394\ 10^{-7}\ \text{J}}{2^{50}} = 1{,}238\ 10^{-22}\ \text{J} \qquad \text{(energy content per proton mass)}$$

$$E_{50g,10.,scaled} = \frac{4{,}145756\ 10^{18}\ \text{J}}{2^{50}} = 3682{,}2\ \text{J} \qquad \text{(energy content for 50 g proton mass)}$$

$$\underline{\underline{P_{input,scaled} \approx}} \frac{3682{,}2\ \text{J}}{\text{s}} \approx \underline{\underline{3{,}6822\ \text{kW}}} \qquad \text{(frequency-dep. input for 50 g plasma mass)}$$

For the measured proton mass:

$$\underline{\underline{f_{proton,10.,scaled} =}} \frac{2{,}09324\ 10^{26}\ \text{Hz}}{2^{50}} = \underline{\underline{185{,}917\ \text{GHz}}} \qquad \text{(coupling frequency)}$$

$$E_{proton,10.,scaled} = \frac{1{,}387\ \ 10^{-7}\ \text{J}}{2^{50}} = 1{,}232\ 10^{-22}\ \text{J} \qquad \text{(energy content per proton mass)}$$

$$E_{50g,10.,scaled} = \frac{4{,}145743\ 10^{18}\ \text{J}}{2^{50}} = 3682{,}16\ \text{J} \qquad \text{(energy content for 50 g proton mass)}$$

$$\underline{\underline{P_{input,scaled} \approx}} \frac{3682{,}16\ \text{J}}{\text{s}} \approx \underline{\underline{3{,}68216\ \text{kW}}} \qquad \text{(frequency-dep. input for 50 g plasma mass)}$$

If the correct coupling frequency of the external energy source resonates with the correct excitation frequency of the displaced proton, then the reactor requires a constant radiation power of only ~ 3,68 kW for a plasma mass of 50 g. The irradiation time for fusion remains open for the time being. Presumably, due to the scaling, irradiation during cold fusion takes 1000 times longer than during hot fusion. However, a 1000-times lower temperature is required for the plasma in favour of the irradiation time. The pressure can be increased, which reduces the time required for conditioning the plasma. Once ignition has been successfully initiated, the process can be sustained by supplying additional hydrogen. The specific modelling must be designed technically.

In this case, too, the energy enrichment must only be continued until the plasma state is sufficient ($E(t) = h\, f_{proton}\, \frac{1}{\sin(kt)}$), to start the fusion process. The cold fusion process ignites in a controlled manner and burns continuously, while hot fusion in the spiral reactor is associated with statistically difficult-to-predict ignition and explosive combustion of the entire material.

The coupling frequency to be set and the radiation power are of the same order of magnitude as in hot fusion. The energy output for the cold fusion process could be similar to that of hot fusion. The difference that leads to cold fusion lies in the fact that the protons are shifted between two field-space levels with the 10th-dimensional family. The protons fuse to form helium as a matter/antimatter particle. During a shutdown process, some of the energy introduced could also be recovered through a matter/antimatter annihilation reaction by means of thermal radiation, which was previously used for energy enrichment. Key advantages of this concept include controlled ignition, efficient control of the input, a sustained fusion process, and safety due to low temperatures

It remains unclear for the present concept how long the torsion coils and the external energy source must be active before a fusion process is successful. The duration of the irradiation could be regulated via the scaling between the coupling frequency and the energy input. The dimensioning of all components remains open for this concept. The concrete design of a concept with all technical and legal requirements would go beyond the scope of this paper.

Chapter 7 Description of the Macrocosm using the Field-Space-Model

7.1 The Universal Photon – the Origin of a Universe

This chapter discusses a possible mechanism for the origin of a universe according to the FSM model. In the first step, the imaginary observer is enabled to examine his expanding universe backwards to its birth in order to find its origin. The processes from birth onwards are then examined in order to deepen our understanding. The model shown in **Figure 2.6** is used for the description.

Description of the universe at the location d*M*(*α* → 0°) and –d*M*(*α* → 180°):

The point where the wavelength λ_x of the universe coincides with the product of its field radius r_x and 2π is the starting point for the characteristic expansion as a universe in space-time. Once the field radius becomes greater than its own wavelength, the splitting of its 0-Spin momentum and the effect of its photon field in the particle-field $F_{1\text{-}3}$ begins.

$G = 6{,}67\ 10^{-11}\ \mathrm{N}\frac{\mathrm{m}^2}{\mathrm{kg}^2}$; $c = 299792458\ \frac{\mathrm{m}}{\mathrm{s}}$; $k_{Uni}\, M_{Uni} = 4{,}0396\ 10^{35}\ \frac{\mathrm{kg}}{\mathrm{s}}$;

$h = 6{,}626\ 10^{-34}$ Js

Planck's action quantum is calculated using formula (2.195):

$h = \lambda\ r\ m\ k$

If the wavelength λ_x is equal to the field radius 2π r_x, the following applies:

$h = \lambda_x\ r_x\ m\ k = 2\pi\ r_x^2\ m\ k$ with: $\lambda_x = 2\pi\ r_x$ (7.01)

$\underline{r_x = 1{,}616\ 10^{-35}\ \mathrm{m}}$

Comparison with Planck length l_p:

$$l_p = \sqrt{\frac{h\,G}{2\pi\,c^3}} = 1{,}616\ 10^{-35}\ \mathrm{m}$$

Figure 7.1 schematically shows the intersection of the relativistic wavelength and the relativistic field radius along the extension. The field radius of the universe continues with formula (2.134) up to its maximum value r_{Uni}, while the wavelength,

from the perspective of the inertial system, undergoes a redshift according to formula (2.197) up to its minimum value λ_{Uni}.

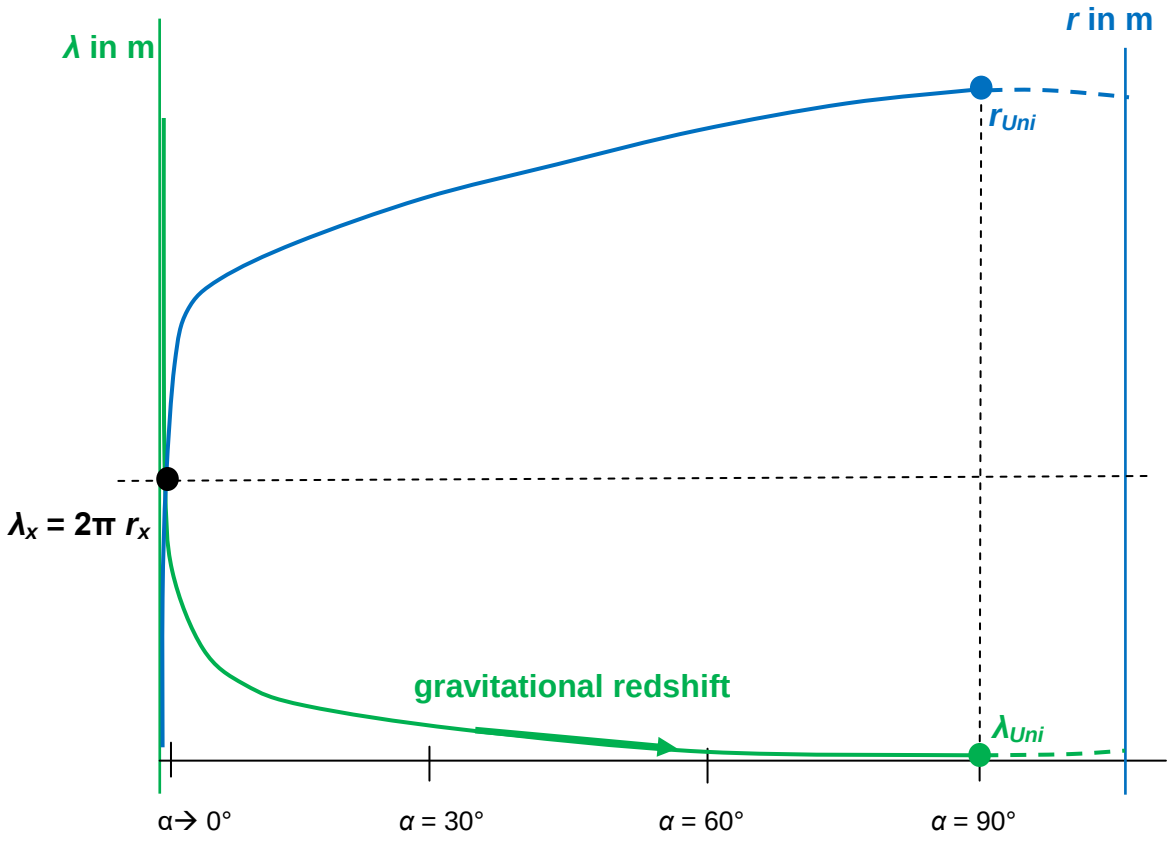

Legend:

$\lambda(t) = \lambda_{Uni} \frac{1}{\sin(\alpha)}$	$\frac{\lambda_x}{2\pi} = 1{,}616\ 10^{-35}$ m	λ_{Uni} = min. value
$r(t) = r \sin(\alpha)$	$r_x = 1{,}616\ 10^{-35}$ m	r_{Uni} = max. value

Figure 7.1: Diagram of the expansion behaviour of the universe with its wavelength λ and its field radius r

Falling below the intersection point at the location near d$M(\alpha \approx 0°)$:

Figure 7.1 shows the further course at the location with the field angle $\alpha \approx 0°$ as soon as the value of the field radius $r(t)$ falls below its own wavelength $\lambda(t)$. The universe falls back into the characteristics of a photon. There is a size ratio between the wavelength and the field radius of a visible photon, which provides an indication of the circumstances under which the universe completely transitions to the characteristics of a photon. This is the location very close to d$M(\alpha \approx 0°)$.

Example of a visible photon:

$$\lambda_{pho} = 5{,}52\ 10^{-7}\ \text{m} \ ; \ m_{pho} = \frac{h\ c^2}{G\ M_{obj}\ k_{obj}\ \lambda_{pho}} = 4{,}004\ 10^{-36}\ \text{kg}$$

$$r_{pho} = \frac{G\ m_{pho}}{c^2} = 2{,}9715\ 10^{-63}\ \text{m}$$

The ratio between wavelength and field radius is:

$$\lambda_{pho} = r_{pho} Y \qquad (7.02)$$

$$Y = \frac{r_{pho}}{\lambda_{pho}} = \frac{2{,}9715\ 10^{-63}\ \text{m}}{5{,}52\ 10^{-7}\ \text{m}} = 5{,}38\ 10^{-55} \qquad \rightarrow \text{Order of magnitude approx. } 10^{-55}$$

Applying the order of magnitude evenly distributed over the wavelength and field radius, the following ratios for the universe result:

$$\underline{\underline{r_Y =}}\ 1{,}616\ 10^{-35}\ \text{m} \cdot 5{,}38\ 10^{-27} = \underline{\underline{8{,}7\ 10^{-62}\ \text{m}}} \qquad \text{(estimate)}$$

$$\underline{\underline{\lambda_Y =}}\ \frac{2\pi\ 1{,}616\ 10^{-35}\ \text{m}}{5{,}38\ 10^{-28}} = \underline{\underline{1{,}9\ 10^{-7}\ \text{m}}} \qquad \text{(estimate)}$$

This makes the field angle α even smaller and brings it closer to zero:

$$r_Y\ k_{Uni} = c\ \sin(\alpha) \qquad (7.03)$$

At the location $dM(\alpha \approx 0°)$, the minimum state of expansion is reached. From this order of magnitude for the wavelength and field radius, the universe transitions to the characteristics of a photon with mass M_{Uni}. Photons can overlap as electromagnetic oscillations. In this way, the universe could be absorbed into a higher structure as a photon through interference. This higher structure is called **the Universal Photon**. In this way, a universal photon can conversely expend part of its energy to create a photon that can form itself into a universe. The creation of such a photon is already the birth of the universe.

In the FSM model, there is no absolute state of singularity, but rather an approximation until the photon properties of the universal photon are reached.

Representation of the birth phase of the universe in field-space:

Starting from the universal photon, which a photon generates from its own wave structure, important characteristics for dimensioning the universe are defined. There is a fixed relationship between the gravitational constant G and the maximum speed $V_{max} = c\ (= k\ r)$, which generate the mass-time and space-time constants. With a certain mass M_{Uni}, Planck's quantum of action h automatically creates the ratio of an oscillation for a certain circular frequency k and field radius r, that all define the circumference of the universe and its period. The reciprocal of the fine-structure constant, α, determines the point at which an interaction between photons begins.

Initially, the universe exists as a photon with a wavelength of $\lambda_Y \approx 1{,}9\ 10^{-7}$ m and a corresponding field radius of approximately $r(t) = 8{,}7\ 10^{-62}$ m as part of the universal photon. The photon receives a spin-0-impulse P from the universal photon in the wave-field $F_{4\text{-}6}$ with $0 = P_{pos} - P_{neg}$. According to the field angle $\alpha \approx 0°$, the photon is almost completely orthogonal to the dimension plane D_{56} in accordance with its space-time deformation. Its field deformation is also maximally contracted. The photon has restructured itself throughout the entire field-space into an invisible photon according to the photon model **in Chapter 2**. For the invisible photon, this is the state in space-time in which the space-time-mechanical effects, with their gravitational potential dM(α), interact most strongly with their counteracting forces.

The equation $c^2 = V_5^2 + V_4^2$ introduces the field propagation velocities V_4 and V_5, which describe the field deformation and space-time deformation, thereby causing the field angle α to oscillate dynamically. According to formula (2.177), the photon, as a primordial universe, possesses a relativistic inertial force of $F(t) = 1{,}211\ 10^{44}\ \text{N}\ \frac{1}{\sin(kt)}$, which, in the range $0° < kt = \alpha < 90°$, reduces the space-time mechanical forces inversely proportional to the sine of the high field angle α. This occurs by increasing its field radius and distributing its momentum across smaller wavelength partitions within the available volume. The excess energy $E(\alpha < 90°)$ is thus converted into volume. Its global potentials are distributed across the divided wavelength partitions and decrease accordingly.

$$E(\alpha) = \frac{r_{Uni}\ h\ c}{r(t)\ \lambda_{Uni}} = \frac{h\ c}{\lambda_{Uni}} \frac{1}{\sin(\alpha)} \tag{7.04}$$

In **Figure 7.2,** the two partial photons, each with a spin of 1 and a partial momentum, represent the universe at that primordial moment, as soon as the state $2\pi\ r_x = \lambda_x$ is reached. The field radius and the wavelength now have the same size $r_x = 1{,}616\ 10^{-35}$ m. The space-time deformation, through the global field angle α, forces both impulses to be orthogonal to the dimensional plane D_{56}. Through the rotation of two partial pulses with spin 1, one above and one below the dimension plane $D_{56,}$ the photon field forms its electric voltage potential. The photonic separation

would be comparable to two charged capacitor plates. Due to the time-dependent expansion of the electromagnetic photon field, the variable voltage potential acts like a displacement current with its orthogonally aligned magnetic field. In the wave-field $F_{4\text{-}6}$, the displacement current generates an electric field effect parallel to the fourth spatial dimension D_4. The electrostatic separation occurs through the dimension plane D_{56}. In the initial stage of the universe, the electric potential (like the gravitational potential) is at its maximum and tends towards its minimum until it reaches its maximum expansion.

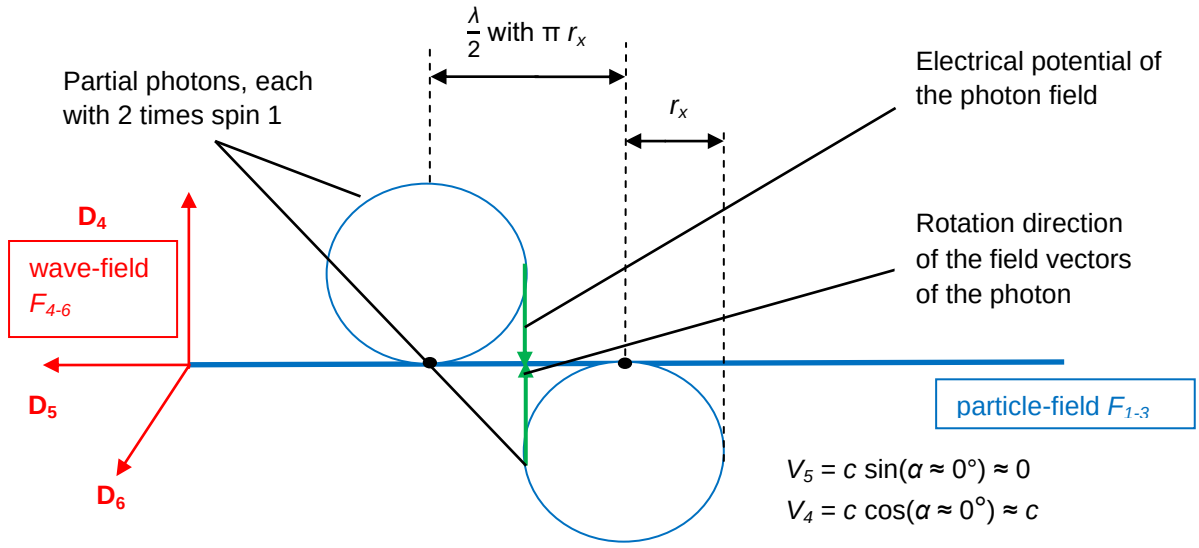

Figure 7.2: Shows the universe as an invisible photon after the separation of its momentum

Only when the field radius $r(t)$ exceeds $\lambda(t)$, the wavelength of the photon, does the photon become a universe. At exactly this moment, the universe with the particle-field $F_{1\text{-}3}$ becomes a 6-dimensional extension of the field-space. It seems reasonable to assume that this process takes place within an infinitesimally short period of time.

The spatial expansion $r(t)$ now exceeds r_x. With the continuous expansion of the universe, the influence of the field propagation velocity V_5 begins to increase. The expansion of the universe leads to the following dynamics: $V_4 \approx (c \rightarrow 0)$; $V_5 \approx (0 \rightarrow c)$.

Meanwhile, the original photon field continues to divide into smaller photon partitions, subject to the conservation of momentum. The next division only occurs when the wavelength of the universe λ_{Uni} fits twice into its current field radius $r(t)$, and so on.

During the expansion of the universe, the quantity of partitioned fields of all particles corresponds to the original electromagnetic photon field. It follows that each photon, as a space-time quantum with its field radius and mass, also contributes to the surrounding space-time and to the total mass of the universe.

The angular momentum of the universe remains constant for its quantised partitions with the order of magnitude of Planck's quantum of action *h* for a full arc measure with 2π. As a result of its dynamic expansion, the field-space fills with a growing quantity of invisible photons, fions and visible photons of different frequencies until its potential forces are exhausted at maximum expansion across space-time.

With its global expansion, the universe continuously forms from an orthogonal to a parallel shape to the dimensional plane D_{56}.

The metric component is:

$ds^2 \supset [1 + \cos(k_{Uni}\, t)]$

Figure 7.3 shows the state of the universe at the location $dM(\alpha = 90°)$ based on its size at the location $dM(\alpha \approx 0°)$. Note the space dimensions shown, which are rotated by 90° compared to **Figure 7.2**. The small circles represent all photons in the universe, which have been divided into half-integer multiples via the momentum.

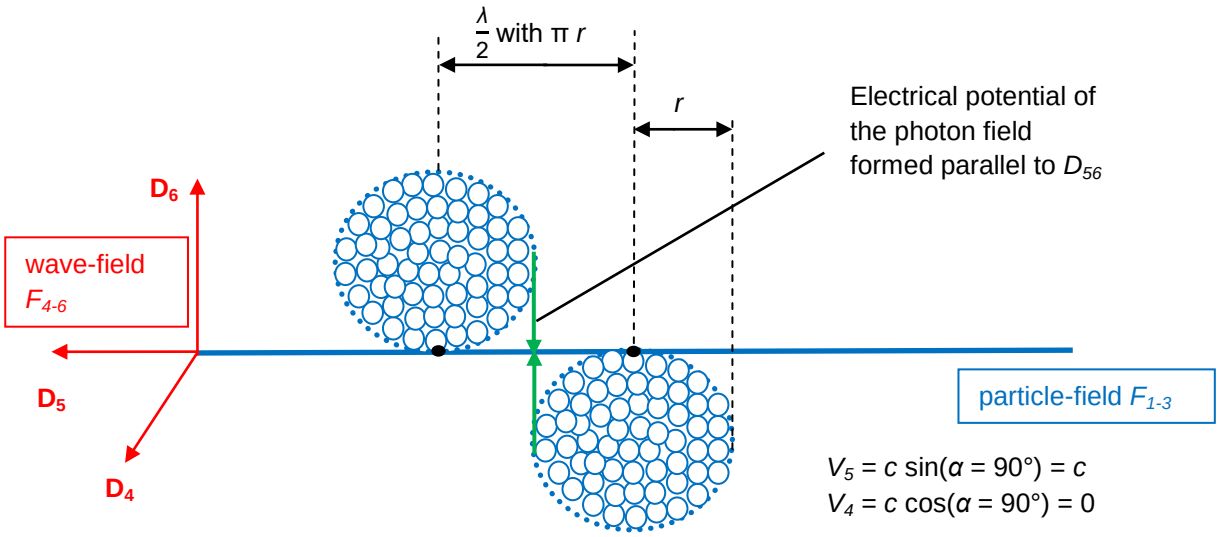

Figure 7.3: The hypothetical change in the universe over the spatial extension, parallel to the dimension plane D_{56}

At the end of the spatial expansion at the location $dM(\alpha = 90°)$, all invisible photons have transitioned into visible photons and propagate in the surrounding space at a maximum speed $V_{max} = V_5 = c$. Fions are merely an intermediate stage between the state of the invisible photon and the visible photons at the end of this development.

Relationship between wavelength and field radius for a universe and a photon:

Photon: field radius ≤ wavelength

Universe: field radius > wavelength

7.2 Space-time characteristics of the Universe

In order to enable a calculation example for the various size ratios, the mass of the universe M_{Uni} must be defined as the input variable.

Determination of the mass of the universe M_{Uni}:

So far, only the visible mass of the universe can be observed. In reality, this would probably be greater if a mass determination were carried out from different positions in the universe. The data is constantly being updated. The visible mass of the universe is given in the literature as 10^{53} kg. According to the literature, it is also assumed that dark energy currently accounts for 68% of the total mass. For this example, let us assume that the value for dark energy from the literature corresponds to the invisible photons according to FSM. This leaves 32% for visible and hidden particles.

$M_{visible\_Uni} = 10^{53}$ kg; $G = 6{,}67\ 10^{-11}\ \mathrm{N}\frac{\mathrm{m^2}}{\mathrm{kg^2}}$; $c = 299792458\ \frac{\mathrm{m}}{\mathrm{s}}$;

$h = 6{,}626\ 10^{-34}$ Js ; $k_{Uni}\ M_{Uni} = 4{,}0396\ 10^{35}\ \frac{\mathrm{kg}}{\mathrm{s}}$; $M_{dark\_energy} = 68\%\ M_{Uni}$

In the particle model of the FSM, 15 x 4-dimensional rotational orbits are possible. Most particles are constructed with four such rotational orbits for the proton and neutron. Only a few particles, such as the Z-, W- or H-bosons, require five rotational orbits.

$\frac{4}{15}$ = 26,66% of visible particles correspond to a ratio of 1: 2,75 to hidden particles

The distribution of mass in the universe is as follows:

visible particles: $\frac{4}{15}$ 32% ≈ 8,5% hidden particles: $\frac{11}{15}$ 32% ≈ 23,5%

Dark energy = total number of all invisible, uncoupled photons ≈ 68%

The distribution of mass fractions relative to the already visible mass is as follows:

$M_{visible\_particles} = 10^{53}$ kg $M_{hidden\_particles} = \frac{23{,}5\%}{8{,}5\%}\ 10^{53}$ kg = $2{,}765\ 10^{53}$ kg

$M_{invisible\_photons} = \frac{68\%}{8{,}5\%}\ 10^{53}$ kg = $8\ 10^{53}$ kg

$\underline{M_{Uni}} = 10^{53}$ kg + $2{,}765\ 10^{53}$ + $8\ 10^{53}$ = $\underline{1{,}1765\ 10^{54}\ \mathrm{kg}}$

Maximum radius of the universe:

The field radius r contributes to the spatial extent. $r(t)$ corresponds to the relativistic field radius. To obtain a manageable result, the following results are given in orders of magnitude of billion light years (LY).

$$r = \frac{G\,M}{c^2} \qquad (2.134)$$

$$\underline{r_{Uni} = \frac{G\,M_{Uni}}{c^2} = 8{,}73125\ 10^{26}\ \text{m} \approx 8{,}73\ 10^{26}\ \text{m}} \qquad (7.05)$$

$$\underline{r_{Uni} \approx 92{,}35 \text{ billion LY}}$$

Wavelength of the universe:

For $\alpha = 90°$:

$$\underline{\underline{\lambda_{Uni} = \frac{h\,c^2}{G\,M_{Uni}^2\,k_{Uni}} = 1{,}87861\ 10^{-96}\ \text{m}}} \quad \text{relativistic: } \lambda(t) = \lambda_{Uni}\,\frac{1}{\sin(\alpha)} \qquad (7.06)$$

$r_{Uni} = 8{,}73125\ 10^{26}\ \text{m} \approx 8{,}73\ 10^{26}\ \text{m}$ relativistic: $r(t) = r_{Uni}\sin(\alpha)$

Field angle α at location with a wavelength of λ_x:

$$\frac{h\,c^2}{G\,M_{Uni}^2\,k_{Uni}}\,\frac{1}{\sin(\alpha)} = \frac{G\,M_{Uni}}{c^2}\,\sin(\alpha)\,2\pi$$

$$\sin(\alpha) = \sqrt{\frac{h\,c^4}{2\pi\,G^2\,M_{Uni}^3\,k_{Uni}}} \quad \rightarrow \quad \alpha = \sin^{-1}\left(\sqrt{\frac{h\,c^4}{2\pi\,G^2\,M_{Uni}^3\,k_{Uni}}}\right) \qquad (7.07)$$

$$\underline{\underline{\alpha \approx 1{,}0603\ 10^{-60}°}}$$

Alternatively:

$$\alpha = \sin^{-1}\left(\frac{r_x}{R_{Uni}}\right) \qquad (7.08)$$

$$\alpha = \sin^{-1}\left(\frac{1{,}616\ 10^{-35}\ \text{m}}{8{,}73125\ 10^{26}\text{m}}\right)$$

$$\underline{\underline{\alpha \approx 1{,}0604\ 10^{-60}°}}$$

- ➔ The mass of the measured visible universe in relation to all invisible photons is confirmed with only a slight deviation.
- ➔ The FSM results for determining the mass of the universe are almost completely consistent with astronomical observations.

Field angle α at the location where dark energy begins to couple:

The event horizon with the field radius r_e is equal to the radius of the electron Re with the reciprocal factor of 137 at this location.

$$\alpha = \sin^{-1}\left(\frac{\lambda_e}{2\pi \cdot 137 \cdot R_{uni}}\right) \qquad (7.09)$$

$$\alpha = \sin^{-1}\left(\frac{r_e}{R_{uni}}\right) \qquad \text{with } r_e = 2{,}82\ 10^{-15}\ \text{m}$$

With the expansion beginning at r_e, the universe starts to electrically couple its invisible, uncoupled energy with the slightest excitation.

$$\alpha = \sin^{-1}\left(\frac{2{,}4263\ 10^{-12}\ \text{m}}{2\pi \cdot 137 \cdot 8{,}73125\ 10^{26}\text{m}}\right)$$

$\underline{\alpha \approx 1{,}85\ 10^{-40}°}$

Circumference U of the universe:

$$U_{Uni} = 2\pi\, r_{Uni} \qquad (7.10)$$

$\underline{U_{Uni} \equiv}\ 2\pi\, r_{Uni} \approx \underline{580{,}3 \text{ billion LY}}$ is the time required for light to circle the universe at maximum expansion

Circular frequency of one period:

$$k = \sqrt{\frac{G\,M}{r^3}} \qquad (2.135)$$

$\underline{k_{Uni} \equiv} \sqrt{\frac{G\,M_{Uni}}{r_{Uni}^3}} \approx \underline{3{,}4336\ 10^{-19}\ \frac{1}{\text{s}}}$ → k corresponds to the circular frequency of the universe

$$T_{2\pi} = \frac{1}{k} \qquad (7.11)$$

$\underline{T_{2\pi} \equiv} \frac{1}{k} \approx \underline{92{,}35 \text{ billion years}}$ for one complete period T

Time until maximum expansion of the universe:

The maximum expansion is already reached after $\frac{\pi}{2}$ or after $\frac{1}{4}$ of a full period T.

$$\underline{T_{expansion,max.} \equiv} \frac{T}{4} = \frac{92{,}35 \text{ billion Y}}{4} = \underline{23{,}09 \text{ billion years}}$$

Determination of the current field angle *α* using the mass distribution:

Birth of the universe	Current expansion	At the end of expansion
$M_{invisible\_photons}$ = 100%	$M_{invisible\_photons}$ = 68%	$M_{invisible\_photons}$ = 0%
$M_{hidden\_particle}$ = 0%	$M_{hidden\_particle}$ = 23,5%	$M_{hidden\_particle}$ = 73,33%
$M_{visible\_matter}$ = 0%	$M_{visible\_matter}$ = 8,5%	$M_{visible\_matter}$ = 26,66%

Visible matter currently accounts for 8,5% of the total mass. When the universe is almost completely expanded, it can be assumed that the ratio between visible and hidden particles will remain the same during their transformation from invisible photons. Thus, the proportion of the total mass of the universe is infinitesimally close to the end of the maximum expansion for visible matter at 26,66% and for hidden particles at 73,33%. Based on a mass fraction of 26,66% after 100% development, the current field angle *α* corresponds to the mass fraction of 8,5% at the location of the current expansion.

$$\underline{\underline{\alpha =}}\ \sin^{-1}\left(\frac{8{,}5\%}{26{,}66\%}\right) \approx \underline{\underline{18{,}7°}} \quad \rightarrow \text{current field angle } \alpha \text{ of the universe}$$

Similarly, the field angle *α* could be calculated based on the amount of matter already coupled relative to the total amount.

$$\underline{\underline{\alpha =}}\ \sin^{-1}\left(\frac{32\%}{100\%}\right) \approx \underline{\underline{18{,}7°}} \quad \rightarrow \text{alternatively}$$

The curve for the amount of available dark energy shows a dynamic sinusoidal pattern. The expansion of the universe with its potential energy and the decrease in the amount of invisible energy are complementary to each other. However, the time interval of a measurement could be so small that only the accelerated expansion of the universe is detected, but not the decrease in the amount of invisible energy. Ultimately, the more accurate the astronomical data on the mass ratio between dark energy and visible mass, the more precisely the current field angle *α* of the universe and thus its field radius *r* can be determined.

Relativistic energy increase of the universe at the current field angle *α*:

The relativistic energy increase was derived in **Chapter 2.2, Point 10** and represented by formula (2.101):

$$E(\alpha) = h\, f_{obj} \frac{1}{\sin(\alpha)} = m_{Obj}\, c^2 \frac{1}{\sin(\alpha)} \quad \text{with: } \alpha = kt$$

→ relativistic energy increase for accelerated objects

$$\underline{E_{visible\_matter}(t)_{\alpha}} = M_{visible\_matter}\, c^2 \frac{1}{\sin(\alpha = 18{,}7°)} = \underline{2{,}8\ 10^{70}\ \text{J}} \qquad (7.12)$$

→ energy fraction of visible matter

$$\underline{E_{hidden\_matter}(t)_{\alpha}} = M_{hidden\_Matter}\, c^2 \frac{1}{\sin(\alpha = 18{,}7°)} = \underline{7{,}75\ 10^{70}\ \text{J}}$$

→ energy content of hidden particles (dark matter)

$$\underline{E_{invisible\ photons}(t)_{\alpha}} = M_{invisible\_photons}\, c^2 \frac{1}{\sin(\alpha = 18{,}7°)} = \underline{2{,}24\ 10^{71}\ \text{J}}$$

→ energy content of all invisible photons (dark energy)

$$\underline{E_{total}(t)_{\alpha}} = M_{Uni}\, c^2 \frac{1}{\sin(\alpha = 18{,}7°)} = \underline{3{,}3\ 10^{71}\ \text{J}}$$

→ energy contribution from the quantities of visible matter, hidden particles and invisible photons

$$\underline{E_{total}(t)_{\alpha}} = M_{Uni}\, c^2 \frac{1}{\sin(\alpha = 90°)} = \underline{1{,}057\ 10^{71}\ \text{J}}$$

The relativistic energy increase occurs as long as the universe is exposed to the compensating forces of space-time with a field angle $\alpha \neq 90°$ or 270°. The universe must therefore perform additional work in order to expand against the compensating forces. The energy required decreases with expansion and is dynamically converted into space volume relative to the inertial system according to a sine function.

Current radius *r*(*t*) of the universe:

$\underline{r(t)_{18{,}7°}} = r_{Uni} \sin(\alpha)$ = 92,35 billion LY · sin(18,7°) = <u>29,608 billion LY</u>

Current age of the universe :

$T_{2\pi} = \frac{1}{k} \approx$ 92,35 billion years → complete period

$T_{0{,}5\pi} = \frac{1}{4k} \approx$ 23,0875 billion years → one quarter period

$\underline{t(\alpha)} = \frac{1}{4k} \sin(18{,}7°) \approx$ <u>7,402 billion years</u> → to the current field angle α = 18,7°

Remaining time of the attractive time of the universe:

$\frac{7{,}402 \text{ bill.Y}}{23{,}0875 \text{ bill.Y}} 100\% = 32{,}06\%$ → Attractive time already elapsed from $\frac{1}{4k}$

$\Delta t_{expansion}$ = 23,0875 billion years – 7,402 billion years

$\underline{\Delta t_{expansion} = 15{,}6855 \text{ billion years}}$ → remaining time suitable for life

Trigonometric distance *b(t)* for the decrease in field potential:

bt) trigonometrically describes the remaining distance of the field angle α between d$M(\alpha)$ and d$M(90°)$ until it reaches its maximum at $\alpha = 90°$:

$$b(t) = r_{Uni} \cos(\alpha) \tag{7.13}$$

with: r_{Uni} = 92,35 bill. LY ; α = 18,7°

$b(t) = r_{Uni} \cos(\alpha) = 92{,}35 \text{ bill. LY} \cdot \cos(18{,}7°)$

$\underline{b(t) = 87{,}47 \text{ billion LY}}$ → Potentially still hidden depth of the observable light at the location of the gravitational potential d$M(\alpha = 18{,}7°)$ until the gravitational force with the field angle α at $\alpha = 90°$ becomes minimal. It can be seen that, depending on the time dilation effect of light during the expansion of the universe, only part of the light will be visible to the observer.

Maximum and current field propagation velocity V_4 and V_5:

The field propagation velocity V_5 corresponds exactly to the maximum velocity $V_{max} = c$ when the space-time mechanical effects on the Lorentz factor 1 have adjusted to the maximum expansion of the universe:

$V_{5\_max} = c \sin(90°) = 299792458 \frac{m}{s}$ with: $\alpha = 90°$

Current field propagation velocity V_5 and V_4 in the field-space at the location of the current field angle α:

$\underline{V_5 = c \sin(18{,}7°) = 96117356{,}5 \frac{m}{s}}$

$\underline{V_4 = c \cos(18{,}7°) = 283966497{,}5 \frac{m}{s}}$

Current spatial expansion velocity of *r'(t)*:

$$r'(t) = \sqrt{c^2 - b'(t)^2} = \sqrt{c^2 - c^2 \sin^2(\alpha)} = c \cos(\alpha) \tag{7.14}$$

note: 1. Derivation of cos(α)

$\underline{\underline{r'(t) =}}\ c \cos(18{,}7°) = \underline{\underline{283966497{,}5\ \frac{m}{s}}}$ → The space expansion velocity relative to the volume radius $r(t)$ is equal to the current field propagation velocity V_4 and decreases continuously over the course of the cosine function to the maximum expansion with $\alpha = 90°$. During the early stages of the universe, the expansion of space is faster than V_5 at the field propagation speed V_4. This phenomenon turn around with the field angle from $\alpha = 45°$.

Current velocity of $b'(t)$ at location $\alpha = 18{,}7°$:

$$b'(t) = \sqrt{c^2 - r'(t)^2} = \sqrt{c^2 - c^2 \cos^2(\alpha)} = c \sin(\alpha) \qquad (7.15)$$

note: 1. Derivation of $\sin(\alpha)$

$\underline{\underline{b'(t) =}}\ c \sin(18{,}7°) = \underline{\underline{96117356{,}5\ \frac{m}{s}}}$ → The velocity relative to the path $b(t)$ is equal to the current field propagation velocity V_5 and allows the telescopes to peer deeper and deeper into the universe at ever-increasing speeds. It increases continuously with the course of the sine function until it reaches its maximum at $c \sin(\alpha = 90°)$. The assumption that the universe is expanding faster and faster with $r'(t)$ is therefore a fallacy, because it is the measured speed of light V_5 that continues to increase. The field propagation speed V_4, on the other hand, decreases with the expansion of space $r(t)$ with the cosine function. The standard model assumes a multiple of the speed of light to explain the accelerated expansion of space in the universe. Objects moving faster than the maximum speed $V_{max} = c$ already contradict the special theory of relativity. In contrast to the standard model of the universe, the FSM explains that the maximum speed of light c is not reached during the expansion phase and thus describes a conformal expansion characteristic of the universe.

Distance $w(t)$ already travelled by visible light :

The relativistically travelled distance $w(t)$ takes into account the contraction dynamics of the speed of light V_5 at all expansion locations in the universe. This corresponds to the information about the visible depth of the universe that telescopes actually register.

$$w(t) = r_{Uni} (1 - \cos(\alpha)) \qquad (7.16)$$

with: $w(t)_{measured} = 13{,}8$ billion LY; $r_{Uni} = 92{,}35$ billion LY; $\alpha = 18{,}7°$

$\underline{w(t) =}$ 92,35 Mrd. LY · (1 - cos(18,7°)) = $\underline{4{,}875 \text{ billion LY}}$ → Current visibility of the universe

With a lifetime of 7,402 billion years, the universe has expanded to a volume radius of 29,608 billion LY, but its light could travel only a relativistically distorted distance of at most 4.875 billion LY at the relativistic speed $b'(t)$. This confirms the above

statement that the universe is currently expanding significantly faster than light can travel through it.

Object time of a moving object relative to a stationary object:

Due to the periodic expansion of the universe, which follows its own object time, its ageing behaviour also changes during expansion. The universe ages with its expansion as a function of time dilation. This corresponds to previous calculations that telescopes can see deeper and deeper into space at ever-increasing speeds.

$$\left\{\frac{c}{\sqrt{c^2 - r'(t)^2}}\right\}_{\alpha=18,7°} = \left\{\frac{c}{\sqrt{c^2 - V_4^2}}\right\}_{\alpha=18,7°} \tag{7.17}$$

$$\left\{\frac{c}{\sqrt{c^2 - V_4^2}}\right\}_{\alpha=18,7°} = \left\{\frac{299792458\ \frac{m}{s}}{\sqrt{\left(299792458\ \frac{m}{s}\right)^2 - \left(283966497{,}5\ \frac{m}{s}\right)^2}}\right\}_{\alpha=18,7°} = \frac{299792458\ \frac{m}{s}}{96117356{,}5\ \frac{m}{s}}$$

Alternative:

$$\left\{\frac{c}{\sqrt{c^2 - r'(t)^2}}\right\}_{\alpha=18,7°} = \frac{c}{V_5} = \frac{1}{\sin(\alpha = 18{,}7°)} \tag{7.18}$$

$\frac{1}{\sin(\alpha = 18{,}7°)} \approx \underline{\underline{3{,}12}}$ → Time dilation in the snapshot

Cross-check at location d$M(\alpha = 18{,}7°)$:

c = factor for time dilation · $V_5 \approx 3{,}12$ $V_5 \approx 3{,}12 \cdot 96117356{,}5\ \frac{m}{s} = 299792458\ \frac{m}{s}$

Circumference $U_{t\_universe\_\alpha}$ at point α = 18,7°:

$$U_{t\_Uni\_18,7°} = 2\pi\, r_{space\ expansion\_18.7°} \tag{7.19}$$

$U_{t\_Uni\_18,7°} = 2\pi \cdot$ 29,608 billion LY = 186,03 billion LY

With a time dilation factor of 3,12:

$$U_{t\_Uni\_\alpha} = 2\pi\, r_{space\ expansion\_\alpha\_in\_billion\ LY} \cdot \text{time dilation factor} \tag{7.20}$$

with: $[U_{t\_Uni\_\alpha}]$ in billion LY

$U_{t\_Uni\_18,7°} \approx 2\pi \cdot 29{,}608$ billion LY $\cdot\ 3{,}12$

$\underline{U_{t\_Uni\_18,7°} \approx 580{,}3 \text{ billion LY}}$ (see also orbit at position $\alpha = 90°$)

➔ A field emission with velocity V_5 always requires the same time to orbit the universe at all locations with gravitational potential d$M(\alpha)$, taking into account time dilation. This alternatively explains the prospective trajectory curve from **Figure 2.6**.

Relativistic course of some parameters depending on the field angle α:

Increase in coupled matter: $\text{matter}_{\%} = \sin(\alpha)$ (2.99)

Decrease in dark energy: $\text{dark energy}_{\%} = 1 - \sin(\alpha)$

Energy: $E_{total,\alpha} = M_{Uni}\, c^2 \frac{1}{\sin(\alpha)}$ with: $M_{Uni} = 1{,}1765\ 10^{54}$ kg; $c = 299792458\ \frac{\text{m}}{\text{s}}$

Age of the universe: $t(\alpha) = \frac{1}{4k} \sin(\alpha)$ with: $\frac{1}{4k}$ = 23,0875 billion years

Radius of the universe: $r(t) = r \sin(\alpha)$ with: r = 92,35 billion LY

Path of light: $w(t) = (1 - \cos(\alpha))\, r$ with: r = 92,35 billion LY

Time dilation factor: $\frac{1}{\sin(\alpha)}$ with: $r = 1$; $c = 1$

Factor for relative energy increase: $\frac{1}{\sin(\alpha)}$ with: $r = 1$; $c = 1$

α	0,57	2,87	5,74	14,5	18,7	30	44,43°	64,1	81,9	89,7
Dark Energy	99%	95%	90%	75%	68%	50%	30%	10%	1%	0,001%
Matter	1%	5%	10%	25%	32%	50%	70%	90%	99%	99,99%
Energy in J	$1{,}06\ 10^{73}$	$2{,}11\ 10^{72}$	$1{,}06\ 10^{72}$	$4{,}22\ 10^{71}$	$3{,}3\ 10^{71}$	$2{,}11\ 10^{71}$	$1{,}51\ 10^{71}$	$1{,}17\ 10^{71}$	$1{,}07\ 10^{71}$	$1{,}06\ 10^{71}$
Age in billion years	0,23	1,15	2,31	5,78	7,4	11,5	16,16	20,77	22,86	23,08
Radius in billion LY	0,92	4,625	9,25	23,13	29,61	46,2	64,65	83,05	91,45	92,345
Path w in billion LY	$4{,}57\ 10^{-3}$	0,116	0,463	2,94	4,875	12,4	26,4	52	79,35	91,85
$\frac{1}{\sin(\alpha)}$	100	20	10	4	3,12	2	$\approx \sqrt{2}$	1,11	1,01	1,00001

Table 7.1: Dynamics of various variables as a function of the field angle α

α	V_5 in $\frac{m}{s}$	$\frac{1}{\sin(\alpha)}$	V_4 in $\frac{m}{s}$	$\frac{1}{\cos(\alpha)}$
0°	0	∞	299792458	1
1°	5232100	57,3	299746798	1,00015
10°	52058414	5,76	295237937	1,015
18,7°	96117356	3,12	283966497	1,056
30°	149896229	2	259627885	1,55
45°	211985280	$\sqrt{2}$	211985280	$\sqrt{2}$
60°	259627884	1,155	149896229	2
88°	299609832	1,00061	10462605	28,65
90°	299792458	1	0	∞

Table 7.2: Effect of the field angle α on the field propagation velocities V_5 and V_4; Yellow: fictitious singularity situation; Orange: current situation; Red: interface between V_5 and V_4 ; Green: location of the inertial system with $V_5 = c$

These values fit together very well, because as the field angle α increases, the object time also changes in such a way that the spatial expansion with decreasing gravitational potential of $dM(\alpha \rightarrow 90°)$ relative to an object with mass m_{obj} follows the sine periodicity. Consider the value of α, which is initially $\alpha = 18{,}7°$, but already accounts for 32% of the age and radius of the universe relative to $\alpha = 90°$, until the maximum expansion is reached. The expansions speed of the universe $r'(t)$ decreases with the increase of the cosine. However, the trigonometric path $w(t)$ from the signal point with the source at location $r(\sim 0)$ to the object continues to accelerate until the maximum expansion with $r(\alpha = 90°)$ is reached, see **Table 7.2.** The remaining field angle α with the distance $b(t)$ accelerates until the velocity $b'(t) = c \sin(\alpha = 90°)$ is reached. Classically, this distance of the visible light with $w(t)$ is interpreted as being related to the current radius of the universe $r(t)$ with increasing distance. This is only the case in the initial and final states in all directions of the mathematical hollow sphere shape. The dynamic change of $r(t)$ as the volume radius of the universe is described by $r'(t) = V_4$ relative to the field propagation speed V_5. The spatial expansion with $r'(t) = V_4$ is currently faster than the field propagation speed V_5. The ratio is specifically:

$$\frac{V_4}{V_5} = \frac{283966497\ \frac{m}{s}}{96117356\ \frac{m}{s}} \approx 2{,}95 \tag{7.21}$$

Quantised matter currently interacts with 2,95 times the force of gravity instead of following the expansion of the universe. This is why two galaxies can meet at a 90° angle when they should be moving away from each other. This dynamic rotates from the field angle $\alpha = 45°$. Within the field angle $45° < \alpha < 90°$, galaxies will increasingly follow the expansion of space in the universe as the gravitational force between objects decreases in relation to the diminishing gravitational potential. This also means that the distribution of galaxies in volume space is completed more and more quickly in accordance with the sine function.

It can be seen for the first quarter period that, with a possible travel time of approximately 23,1 billion years, light will not consistently reach the radius of 92,35 billion light years. This is due to two factors. The first is that, at the beginning of its expansion, the universe expands faster than light through the cosine function with the field propagation speed V_4 than light could propagate at the speed of light $V_5 = c\ \sin(\alpha)$. This only turn around with the field angle of $\alpha = 45°$. The second factor is that the light cannot make up for the time lost due to the space it has already travelled with increased time dilation, until it reaches its maximum expansion with minimal time dilation. This means that the observer will only ever be able to see a section of the universe, even if this section becomes larger and larger as the universe expands. The observer will always lack information about the observable depth, the mass of the visible universe or our position in the universe. A concrete indication of this is that the visible universe is currently 7,4 billion light years old, the volume radius of the expansion is 29,608 billion light years, and yet the observer only registers a viewing distance of 4,875 billion light years with telescopes. If the current time dilation is taken as 3,12, the telescopes would theoretically be able to register a non-space-time-distorted depth of $3{,}12 \cdot 4{,}875$ billion light years, or 15,21 billion light years. The observed light does not take into account the dynamic development of its propagation speed $\beta'(t)$ nor the physical limit at which the measurable gravitational redshift produces wavelengths that are too long for detection.

The realisation that only a small section of the universe can be seen by observers measuring from Earth suggests that telescopes only measure the most distant celestial bodies in different stages of development. The idea that we are standing in the centre of the universe on Earth and therefore measure the same distance in all directions seems extremely unlikely at first glance. On the contrary, using the FSM model, it would even be possible to determine our own approximate position in the universe by triangulating the measured gravitational redshift along the entire spherical sector. The determination of the visible mass of the universe and its almost exact confirmation by the field angle α in the state $r_x = \lambda_x$ suggests that our position in the universe must already be very close to the centre of the spherical sector.

The cosine-shaped field forces over the path $b(t)$ with $\cos(\alpha)$ at the maximum expansion height mathematically obtain a negative sign from the field angle $\alpha > 90°$. This is obviously due to the change in direction of the field propagation velocity V_4, which points in the opposite direction from $\alpha > 90°$. To do this, simply continue the development of the field propagation velocities of V_4 and V_5 from **Figure 2.6**. The repulsive forces begin with along the way $-b(t)$ at the location $dM(90° < \alpha < 270°)$.

Furthermore, it must be noted that, starting from an expansion of the universe with the field angle $\alpha > 90°$, the spatial density increases again and the period continues to move towards the repulsive component of the next Big Bang stage $-dM(\alpha \approx 180°)$. This means that the field propagation velocity V_5 becomes smaller again with respect to the spatial density. The particle structures will dissolve as the period increases. This is comparable to a sandcastle that disperses in water. In today's favoured standard model of the universe, this would be incorrectly interpreted as a further expansion of space until the particles dissolve. According to the present model, the reason for the dissipation of particle and energy structures lies in two factors. First, the course of the expansion of the universe influences the global gravitational potential between objects up to the location $dM(\alpha = 90°)$, where the field potential has become minimally small. Second, as the period continues, the direction of attractive forces changes to repulsive forces.

7.3 Prediction of Multiverses

The goal of a universe could be to obtain a symbolic framework for generating information and thus knowledge, which can be superimposed on the universal photon as needed through fusion.

At the beginning of the universe, there is a photon similar to a blank hard drive without any information or knowledge. As space expands and its impulse divide, the information in the universe also grows. A treasure trove of knowledge from lived experience begins to form. According to the FSM model, the viable time in the universe is limited to only the first quarter of its period *T*. It would be a waste of energy and time, as well as a contradiction to the nature of nature, if new, more complex information were first formed in a universe and then simply disappeared again after a period of many billions of years. There must therefore be other places where this information could go. Using a multiverse, the information would be able to move to neighbouring universes and continue to grow. Such universes must be directly and comprehensively based on ours, which, among other things, currently form a viable environment. Since a universe only allows life within the first quarter period, at least four universes must exist as neighbours, offset by a quarter period. At the same time, other universes will already have begun to develop their own information in a temporal overlap. There must therefore be a multiple of four universes available as immediate neighbours to our universe. They may be clustered together like soap bubbles and are interconnected in such a way that each universe could absorb all possible information from another universe regardless of its spatial extent.

The mathematical representation of energy for a multiverse could be described as follows:

$$E_{Multiversum} = \sum_1^n m_n \, c^2 \, \frac{1}{\sin(\alpha_n)} \qquad \text{with: } n \in \mathbb{N} \qquad (7.22)$$

The maximum speed V_{max} with $c = 299792458 \frac{m}{s}$, the gravitational constant with $G = 6{,}67 \; 10^{-11} \, N\frac{m^2}{kg^2}$ and the Planck's constant with $h = 6{,}626 \; 10^{-34}$ Js seem to be a characteristic feature of the origin of universes. It represents a thumbprint of the universal photon.

Figure 7.4 could show the aforementioned foam of the multiverse.

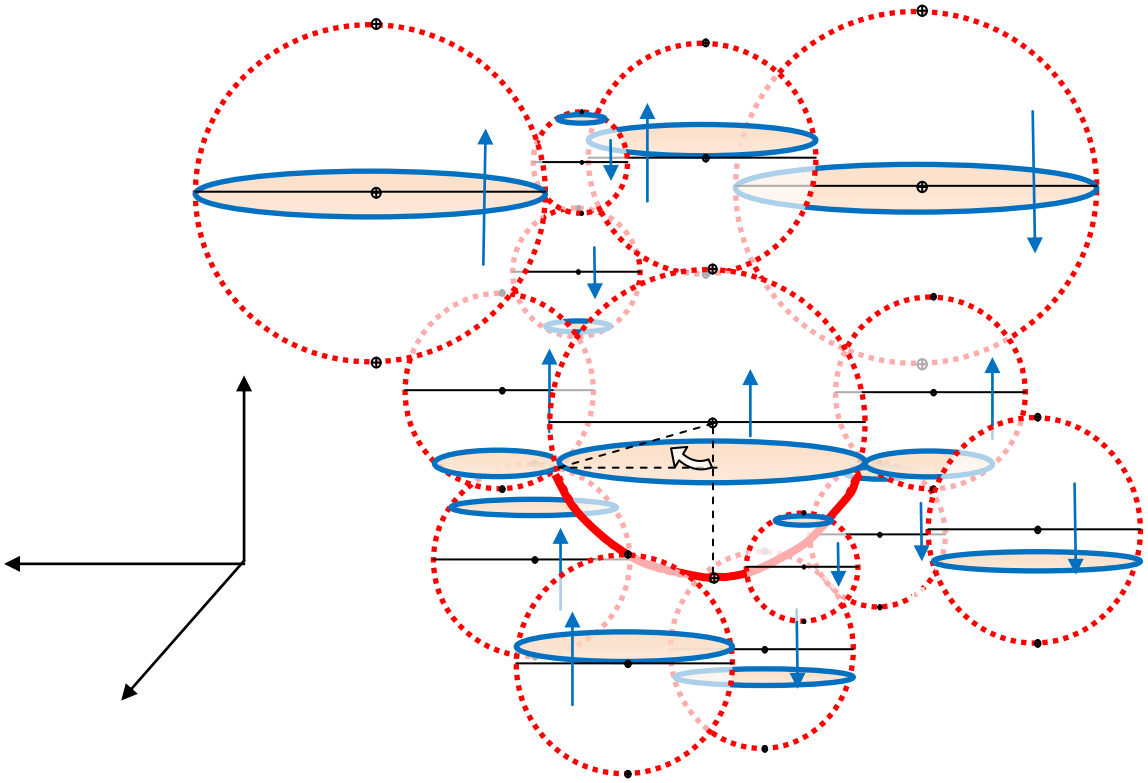

Figure 7.4: Multiple universes based on our own

The Landscape Problem and the FSM Solution

Context of the problem:

The landscape problem in string theory is that there are an extremely large number of possible vacua often 10^{500} or more. Each vacuum can give rise to different physical constants, particle masses and even different gauge groups. As a result, the theory largely loses its predictive power – almost any observation can be explained by a suitable vacuum.

How FSM solves the landscape problem:

The FSM structurally avoids the landscape problem by making assumptions that differ fundamentally from those of string theory. The solution arises from several interrelated principles.

a) Fixed and small number of dimensions

- The FSM operates with **exactly 7 dimensions** (4 visible + 3 compact)
- Unlike string theory, there are not an arbitrary number of extra dimensions, nor is there a wide variety of Calabi-Yau manifolds. The three **compact dimensions** (D_4, D_5, D_6) are **fixed** and **oscillate dynamically**.

b) Dynamic rather than static compactification

- The compact dimensions oscillate with cos(*kt* + *β*). As a result, there are **no static vacua** in the string sense.
- The **geometry is time-dependent**. This alone drastically reduces the number of possible stable configurations.

c) Fixed initial symmetry and geometric refraction

- **Fixed** symmetry group **SU(4)**.
- This **breaks dynamically** to SU(3) × U(1) via the phase angle β and the oscillation.
- There are **no arbitrary gauge groups** or arbitrary symmetry breaking as in the string landscape.

d) Topological and geometric fixing of constants

Many fundamental quantities cannot be chosen arbitrarily, but are determined geometrically or topologically:

- Number of **generations = 3** (based on the number of turns $n = 1, 2, 3$)
- **Fine-structure constant α ≈ 1/137**
- **Anomaly-free** via Chern classes ($c_1 = 0$, $c_3 = 0$)
- Colour neutrality and transition achieved by **projecting** onto the visible area

e) A multiverse with uniform constants as a ‘fingerprint’

- The universal photon is the **origin** of the universe
- **Any number** of universes can come into being.
- **Crucially:** all these universes share the **same fundamental constants** (like a fingerprint). They differ only in size, depending on the energy input, and in the **current stage of their periodic expansion.**
- The universes are **interconnected** via the universal photon.
- Because universes go through different phases of their oscillation (**Figure 7.4**), information or life can **migrate** from an ‘unfavourable’ universe to a life-friendly one (e.g. the first quarter of the period).
- In the Planck regime, the universe does not collapse into a singularity, but into a **pure wave state**. When transformed back using relativistic principles, this leads to a **resonance with the universal photon**. No information is lost; instead, it is written back into a shared ‘quantum register’ of all universes. The FSM possesses **built-in quantum consistency** on the Planck scale, even without a complete quantum field theory of the metric having been formulated.

This multiverse is not a landscape in the string theory sense, because the physics is the same in all universes. There are no arbitrary vacua with different laws.

Unresolved issues:

Although FSM largely avoids the landscape problem, some questions remain unanswered:

- How does the mechanism of the universe's creation from the universal photon work?
- What determines the energy distribution, and why should the values differ?
- Information transfer: How exactly can information or 'life' be exchanged between universes in different phases?
- Testability of the multiverse and its linking mechanism
- Entropy and information: How is the loss of information dealt with in collapsing or 'unfavourable' universes?

The FSM solves the landscape problem by severely restricting the degrees of freedom from the outset. Because so many constants are fixed, no classical landscape emerges. Instead, the FSM model allows for a multiverse with uniform physics, in which universes differ only in size and their current state of expansion.

The dynamic details of the origin of the universe and the specific transfer of information between universes remain unclear at this stage.

Possible links between FSM and quantum information theory

In FSM, the universal photon is the common origin of all universes. It connects these universes in a fundamental, non-local way.

The universal photon as a non-local channel of information:

- **Entanglement** (EPR) is equivalent to an Einstein–Rosen wormhole (ER)
- The **universal photon** can be interpreted as a **shared entangled state** that connects all universes, much like a **quantum network** in which the individual universes act as nodes.
- In principle, **information** can be exchanged between universes without signals having to exceed the speed of light in the classical sense – **quantum teleportation**.

Phase-dependent multiverse and quantum information:

The FSM posits that different universes are at different stages of their periodic expansion. A universe in an 'unfavourable' phase (e.g. excessive expansion or contraction) can transmit information to a universe in a 'life-friendly' phase (e.g. the first quarter of the cycle).

- This corresponds to the concept of **quantum error correction** from quantum information theory. Information is not lost, but is distributed redundantly across multiple 'codes' – in this case, universes in different phases.
- A universe in an 'unfavourable' phase can be regarded as a **decoherent state**, whilst another universe in a 'favourable' phase functions as a **coherent, information-preserving state**.
- The transmission of information between universes via the universal photon can be understood as a form of **quantum teleportation** or **quantum communication** over long distances (between universes).

Preservation of quantum information:

In FSM, the problem of information loss in black holes or during transitions between universes is mitigated by the **universal photon** and the **phase-dependent structure**.

- **Information is not lost**, but is 'transferred' to other universes that are in a more information-friendly phase.
- The universal photon acts as a **shared quantum memory** or as a **medium for entanglement**, much like a **quantum register** in quantum information theory.

Spin-0 pair state and entanglement:

The spin-0 pair state of dark energy described in the FSM (**Chapter 2.2, Point 18**), involving two entangled spin-1 photons with opposite helicities, is already a concept derived directly from quantum information theory.

- This is a **maximally entangled state**.
- As long as the pair exists such that $f < f_{min}$, it is **non-separable** – a measurement on one part of the pair instantly affects the other part.
- This is a direct application of **quantum entanglement** on a **cosmological scale**.

The FSM forms a natural and consistent bridge to quantum information theory. It describes the multiverse as a quantum information system in which information can be preserved and exchanged between different 'branches'.

7.4 Description of Black Holes

The field radius has the property that no photon can escape once it reaches this field radius. In the particle model, the field radius is determined to be very small. Black holes (BH), on the other hand, have a particularly large field radius R_{BH} from which no photon can escape. This is also called the event horizon. The event horizon only begins to have an outward effect on an object when its field radius is greater than its own wavelength. This intersection between the field radius and the wavelength is shown, along with a particle structure that has exactly these properties. An indication of this is given **in Chapter 7.1** with the state of the universe at the location d$M(\alpha \rightarrow 0°)$. This is the location where a photon would be able to generate a field radius by occupying just enough volume with its own wavelength to oscillate within it. This would mean that a particle has been found whose wavelength is as small as possible, but still exists in the space-time of the universe.

The transformation of an object into a black hole:

The lower limit coincides exactly with the point where the wavelength λ of a field body is equal to the product of its field radius r and 2π. The approach used to calculate the field angle α corresponds to the characteristics of the universe:

$G = 6{,}67\ 10^{-11}\ \mathrm{N}\frac{\mathrm{m}^2}{\mathrm{kg}^2}$; $c = 299792458\ \frac{\mathrm{m}}{\mathrm{s}}$; $k_{Uni}\ M_{Uni} = 4{,}0396\ 10^{35}\ \frac{\mathrm{kg}}{\mathrm{s}}$;

$h = 6{,}626\ 10^{-34}$ Js ; $r_{BH} = 7421{,}5$ m

Equation (7.01) applies, in which the wavelength λ_x is equal to the field radius $2\pi\ r_x$:

$h = \lambda\ r\ m\ k = 2\pi\ r_x^2\ m\ k$

$\underline{r_x = 1{,}616\ 10^{-35}\ \mathrm{m}}$ → equals the Planck length

The maximum compression of a field body is reached at the volume radius r_x, beyond which it takes on black hole properties. Depending on the mass absorbed by the black hole, its wavelength will continue to shrink and its field radius will increase. A black hole continues to grow as it absorbs photons and particles from the outside. A universe, on the other hand, has a constant mass and a dynamic field radius $r(t)$ that expands and contracts in a T-periodic manner.

The contraction must result in the simplest possible particle structures that such a contraction can produce. **Figure 7.5** illustrates the state derived so far.

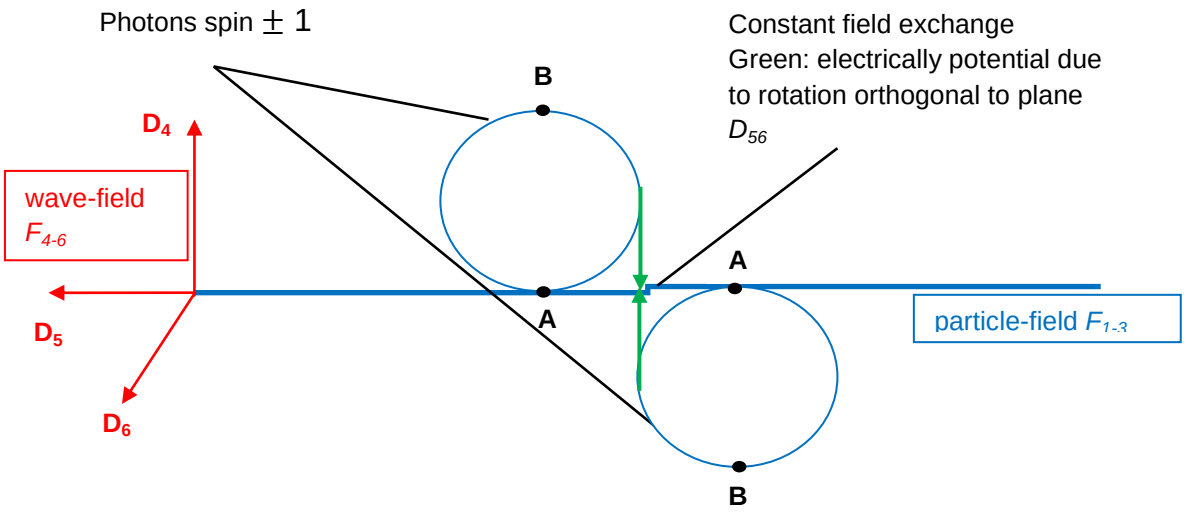

Figure 7.5: Black hole in the wave-field F_{4-6}, shaping parallel to D_{56}

As a minimally entangled spin-0 photon, the rotating field body would be capable of rotating at the maximum speed $V_{max} = c$. The configuration takes on structures similar to dark energy, orthogonal to the D_{56} dimensional plane.

The two sub-photons are electrically attracted to one another. Their orthogonal orientation relative to the D_{56} dimensional plane prevents a classical approach and, consequently, an annihilation reaction. Externally, this structure behaves like a neutral but internally polarized object. Both sub-photons are in a stable, entangled equilibrium. However, the internal structure cannot be measured due to the event horizon.

The compact geometry transitions into a complex topology with a high number of windings n and possibly g ≥ 1. The object possesses high topological stability due to its Chern classes, but is close to the transition to evaporation.

The entire mass is stored as pure rotational energy of the photons. The potential $V(\phi_n)_{\text{dark}}$ reaches its maximum value. The object emits extremely intense radiation (similar to Hawking radiation) because the oscillation $[\cos(kt + \beta)]$ becomes very high-energy during compression.

This representation has the simplest 1:1 coupling between particle-field and wave-field, which is not adversely affected by the complexity associated with larger particles. This spin-0 photon pair will be referred to below as the **black hole photon**.

External angular momentum:

Astronomically, a black hole is identified, for example, by its event horizon radius r when it causes a gravitational lensing effect or gravitational redshift. This structure has a high mass. Consequently, the measurable portion of the angular momentum is dominated by the term in the formula (2.197).

$$L_{ø\_particle\text{-}field\_BH} = \sqrt{G\, M_{BH}{}^3\, r_{BH}} + \frac{h}{2\pi} \qquad \text{with: } \frac{h}{2\pi} \approx 0$$

Largest gravitational potential of a black hole:

$F_{BH} = \frac{G\, M\, m}{r_{BH}{}^2} \sin(\alpha)$ The maximum gravitational potential is at 90° at the equator.

The lowest gravitational potential is at 0° to the axis of rotation.

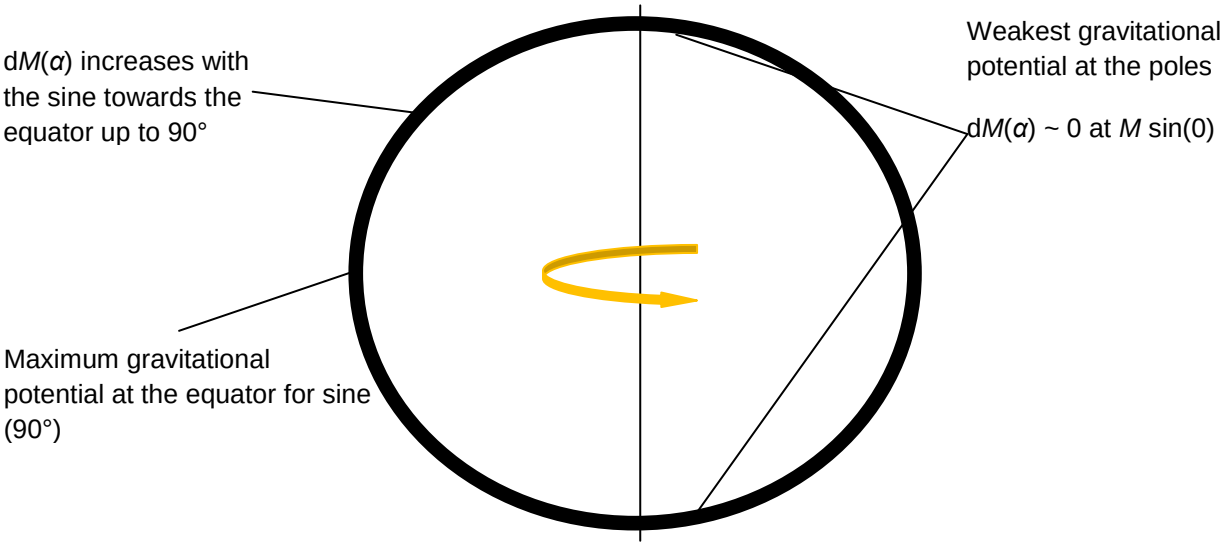

Figure 7.6: Gravitational potential along the surface of its spherical sector in the particle-field $F_{1\text{-}3}$

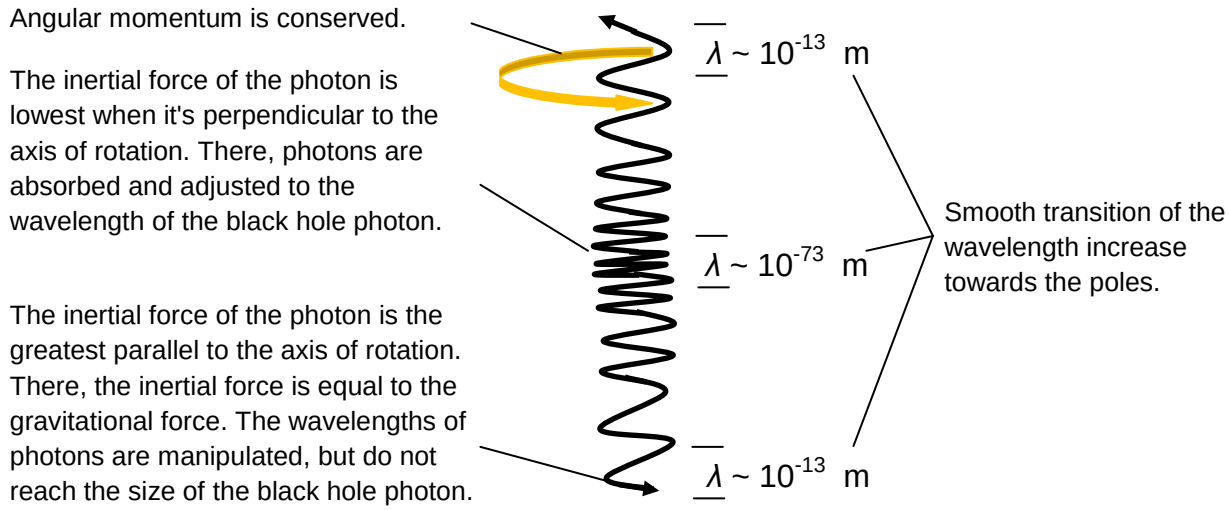

Figure 7.7: Behaviour of absorbed photons along the spherical sector of a black hole

A black hole is an extreme case. Its event horizon is its field radius *r*, beyond which photons cannot escape. Outside the field radius, a corona of photons can be seen, which largest parallel to the axis of rotation appears. According to the sine function,

the inertial force of an object counteracting an external gravitational force is described mechanically along a hollow sphere. The inertial force is lowest at right angles to the axis of rotation, while it increases towards the poles until photons can no longer be attracted at the exact location of the axis of rotation. There, high-energy photons can be created that have already begun to adjust their wavelength to the black hole. Thermal radiation or gamma bursts possibly arise through such a process.

A calculation example:

$G = 6{,}67\ 10^{-11}\ \mathrm{N}\frac{\mathrm{m}^2}{\mathrm{kg}^2}$; M_{BH} = 5 times the mass of the Sun = 10^{31} kg ; $c = 299792458\ \frac{\mathrm{m}}{\mathrm{s}}$

Event horizon of this black hole photon:

$$r_{BH} = \frac{G\,M_{BH}}{c^2} = 7421{,}5\ \mathrm{m} \qquad (7.23)$$

Alternatively with: $\frac{M_{obj}}{r_{obj}} = 1{,}34746\ 10^{27}\ \frac{\mathrm{kg}}{\mathrm{m}}$ → Mass-area constant (2.176)

$$r_{BH} = \frac{10^{31}\mathrm{kg}}{1{,}34746\ 10^{27}\ \frac{\mathrm{kg}}{\mathrm{m}}} = 7421{,}5\ \mathrm{m} \qquad (7.24)$$

Field angle for this black hole:

$$\alpha_{BH} = \sin^{-1}\left(\frac{1{,}616\ 10^{-35}\ \mathrm{m}}{7421{,}5\ \mathrm{m}}\right) \qquad (7.25)$$

$\alpha_{BH} \approx 1{,}2476\ 10^{-37}°$ → equivalent field angle of this black hole

External angular momentum:

$$L_{ø\_particle\text{-}field\_BH} = \sqrt{G\,M_{BH}^3\,r_{BH}}$$

$$L_{ø\_particle\text{-}field\_BH} = 2{,}22\ 10^{43}\ \frac{\mathrm{kg\ m}^2}{\mathrm{s}}$$

Gravitational effect for different speeds < *c*:

$$r_{BH\_gravity\_range} = \frac{G\,M_{BH}}{V_3^2} \qquad \text{with: } V_3 \text{ – object velocity} \qquad (7.26)$$

Range in the event that an object is accelerated to a speed of 400 $\frac{m}{s}$:

$$r_{BH\_gravity\_range} = \frac{G\ M_{BH}}{V_3^2} = 4{,}17\ 10^{15}\ m \triangleq 0{,}44\ LY$$

Range in the event that an object is accelerated to a speed of 100000000 $\frac{m}{s}$:

$$r_{BH\_gravity\_range} = \frac{G\ M_{BH}}{V_3^2} = 66700\ m$$

Circular frequency - revolutions per second on the vertical axis:

$$k_{BH} = \sqrt{\frac{G\ M_{BH}}{r_{BH}^3}} \tag{7.27}$$

$\underline{k_{BH} = 40394{,}8\ \frac{1}{s}}$ → Turns per second of the black hole

When a black hole grows, its circular frequency k_{BH} decreases. In contrast, the circular frequency k_{Uni} of the universe remains constant due to its expanding nature.

Gravitational force of the black hole on a) a photon and b) an everyday object at the event horizon:

a) Photon: $\lambda_{pho} = 552$ nm; $m_{pho} = 4{,}004\ 10^{-36}$ kg

$$F_{BH} = \frac{G\ M_{BH}\ m_{pho}}{r_{BH}^2} \sin(\alpha) \tag{7.28}$$

With sin(α = 90°) = 1 at the location of the strongest gravitational potential:

$$\underline{F_{BH} = \frac{G\ M_{BH}\ m_{pho}}{r_{BH}^2} = 4{,}849^{-23}\ N}$$

b) 100 kg heavy object:

$$\underline{F_{BH} = \frac{G\ M_{BH}\ m_{100kg\_obj}}{r_{BH}^2} = 1{,}2\ 10^{15}\ N} \tag{7.29}$$

Wavelength of the black hole photon:

The following relationship between the field radius r_{BH} and its circular frequency k_{BH} is now known and can be applied to this black hole:

$$r_{BH} = \frac{G\ M_{BH}}{c^2} = 7421{,}5\ m;\ M_{BH} = 10^{31}\ kg$$

$$k_{BH} = \sqrt{\frac{G\,M_{BH}}{r_{BH}^3}} = 40394{,}8\,\frac{1}{s}\,;\; h = 6{,}626\;10^{-34}\;\text{Js}$$

$$\lambda_{BH} = \frac{h\,c^2}{G\,M_{BH}^2\,k_{BH}} \tag{7.30}$$

$\underline{\lambda_{BH} = 2{,}21\;10^{-73}\;\text{m}}$ → Wavelength of the black hole photon

Comparison:

a) The universe has a wavelength of $\lambda_{Uni} = 1{,}87862\;10^{-96}$ m
b) Visible photons have wavelengths in the order of 552 nm

Cross-check:

$$h = M_{BH}\,\lambda_{BH}\,c = 10^{31}\;\text{kg} \cdot 2{,}21\;10^{-73}\;\text{m} \cdot 299782458\,\frac{\text{m}}{\text{s}}$$

$h = 6{,}625\;10^{-34}$ Js ≈ $6{,}626\;10^{-34}$ Js

Increases: M_{BH} → decreases: λ_{BH} → h = $M_{BH}\,\lambda_{BH}\,c$ = const. → **Planck's act. quantum**

Photons or particles of other wavelengths are reduced to the wavelength of the black hole photon by the force of gravity. The density of the black hole continues to increase with mass, while its wavelength becomes smaller and smaller and space-time continues to deform.

A formal verification of the wavelength λ_{BH} is now performed using the classical calculation:

Energy of a photon inside the black hole:

$$\underline{E_{BH,photon} = \frac{1}{\lambda_{BH}}\,h\,c = 8{,}988\;10^{47}\text{J}} \tag{7.31}$$

Conversion to eV by division by $1{,}602\;10^{-19}$ J provides:

$\underline{E_{BH,photon} = 5{,}61\;10^{66}\;\text{eV}}$

Compared to individual photons:

$\lambda_{pho} = 552$ nm with: $m_{photon} = \dfrac{3{,}6\;10^{-19}\;\text{J}}{(299792458\,\frac{\text{m}}{\text{s}})^2} = 4{,}004\;10^{-36}$ kg

$$E_{pho\_552nm} = \frac{1}{\lambda_{pho}}\,h\,c = 3{,}6\;10^{-19}\;\text{J} \qquad E_{pho\_552nm} = 2{,}246\;\text{eV}$$

Mass of a photon in a black hole:

Mass verification from the derived $E = m\ c^2$ formula:

$E_{BH,photon} = M_{BH,photon}\ c^2 = 8{,}988\ 10^{47}$ J (result from above) (7.32)

$$\underline{\underline{M_{BH,photon} =}} \frac{E_{BH_{photonen}}}{c^2} = \frac{8{,}988\ 10^{47}\ \text{J}}{(299792458\ \frac{\text{m}}{\text{s}})^2} = \underline{\underline{1{,}0001\ 10^{31}\ \text{kg}}} \sim 10^{31}\ \text{kg} = M_{BH}$$

Number of superimposed photons in the black hole:

$M_{BH} = 10^{31}$ kg ; $M_{BH\_photon} = 10^{31}$ kg; Number n of photons ; n ε N

$$\underline{\underline{n =}} \frac{M_{BH}}{M_{BH_{photon}}} = \underline{\underline{1}}$$

→ simple verification of the wavelength λ_{BH}: there is only one photon in the black hole

Growing properties of the event horizon with the inclusion of different particles:

When a particle hits a black hole and merges with it, the black hole grows in proportion to the particle absorbed. For example, the photon (552 nm), an exchange fion (136,6875 f_e), the electron and the proton are assumed to be absorbed by the black hole.

$k_{BH} = \sqrt{\frac{G\,M_{BH}}{r_{BH}^3}} = 40394{,}8\,\frac{1}{s}$; $r_{BH} = \frac{G\,M_{BH}}{c^2} = 7421{,}5$ m ; $h = 6{,}626\ 10^{-34}$ Js ;

$G = 6{,}67\ 10^{-11}\,\mathrm{N}\frac{m^2}{kg^2}$; M_{BH} = 5 times the mass of the Sun = 10^{31} kg; $c = 299792458\,\frac{m}{s}$;

$f_e = 123{,}56$ Exa Hz = $1{,}2356\ 10^{20}$ Hz ; $f_{proton} = 1845{,}28\ f_e$; $f_{fion} = 136{,}6875\ f_e$;

$f_{pho} = 5{,}43\ 10^{14}$ Hz ($\lambda_{pho} = 552$ nm)

$$\lambda_{fion} = \frac{c}{136{,}6875\ f_e} = \frac{299792458\,\frac{m}{s}}{136{,}6875 \cdot 1{,}2356\ 10^{20}\ \mathrm{Hz}} = 1{,}775\ 10^{-14}\ \mathrm{m} \qquad (7.33)$$

$\lambda_{proton} = 1{,}315\ 10^{-15}$ m $\qquad$ $\lambda_e = 2{,}4263\ 10^{-12}$ m $\qquad$ $\lambda_{pho} = 5{,}52\ 10^{-7}$ m

$$m_{obj} = \frac{1}{2}\,(\mathrm{BC}\ (\mathrm{CC})^3)^n \cdot \mathrm{PC} \cdot \mathrm{Dimfactor} \cdot M_e \qquad (7.34)$$

Alternative mass determination:

$$m_{fion} = \frac{h\,c^2}{G\,M_{BH}\,k_{BH}\,\lambda_{fion}} = 1{,}2467\ 10^{-28}\ \mathrm{kg} \qquad (7.35)$$

$m_{proton} = 1{,}683\ 10^{-27}$ kg $\qquad$ $M_e = 9{,}12\ 10^{-31}$ kg $\qquad$ $m_{pho} = 4{,}004\ 10^{-36}$ kg

$$\underline{r_{fion} = \frac{G\,M_{fion}}{c^2} = 9{,}25\ 10^{-56}\ \mathrm{m}} \qquad (7.36)$$

$\underline{r_{proton} = 1{,}25\ 10^{-54}\ \mathrm{m}}$ $\qquad$ $\underline{r_e = 6{,}75\ 10^{-58}\ \mathrm{m}}$ $\qquad$ $\underline{r_{pho} = 2{,}97\ 10^{-63}\ \mathrm{m}}$

$$k_{fion} = \sqrt{\frac{G\,m_{fion}}{r_{fion}^3}} = \frac{c^3}{G\,M_{fion}} = 3{,}24\ 10^{63}\,\frac{1}{s} \quad \text{(for information)} \qquad (7.37)$$

$k_{proton} = 2{,}4\ 10^{62}\,\frac{1}{s}$ $\qquad$ $k_e = 4{,}43\ 10^{65}\,\frac{1}{s}$ $\qquad$ $k_{pho} = 1{,}01\ 10^{71}\,\frac{1}{s}$

By absorbing these wavelengths, the above-mentioned particles contribute proportionally to the growth of the black hole.

A calculation example illustrates the ratios of how many particles are required for a 10% increase.

$$r_{BH+10\%} = \frac{G\,(M_{BH} + 0{,}1\,M_{BH})}{c^2} \tag{7.38}$$

$r_{BH+10\%} = 8163{,}5$ m

Increase in the field radius with a 10% increase in the energy of the black hole:

$$\frac{r_{BH+10\%}}{r_{BH}} - 1 = \frac{8163{,}5\text{ m}}{7421{,}5\text{ m}} - 1 \approx 10\ \%$$

Addition of number n of particles, corresponding to a 10% increase in energy in a black hole with a mass of 10^{31} kg:

$$n_{obj} = \frac{r_{BH+10} - r_{BH}}{r_{obj}} \qquad \text{with: } n\ \varepsilon\ \mathbb{N} \tag{7.39}$$

$$\underline{n_{pho} = \frac{8163{,}5\text{ m} - 7421{,}5\text{ m}}{2{,}97\ 10^{-63}\text{ m}} = 2{,}5\ 10^{65}}$$

$\underline{n_{proton} = 5{,}94\ 10^{56}}$ $\underline{n_e = 1{,}1\ 10^{60}}$ $\underline{n_{fion} = 8{,}02\ 10^{57}}$

Or:
$$n_{obj} \approx \frac{M_{BH+10} - M_{BH}}{M_{obj}} \tag{7.40}$$

$$n_{pho} \approx \frac{M_{BH+10} - M_{BH}}{M_{pho}} = \frac{0{,}1\ 10^{31}\text{kg}}{4{,}004\ 10^{-36}\text{ kg}} = 2{,}5\ 10^{65}$$

$$n_{proton} \approx \frac{M_{BH+10} - M_{BH}}{M_{proton}} = \frac{0{,}1\ 10^{31}\text{kg}}{1{,}683\ 10^{-27}\text{ kg}} = 5{,}94\ 10^{56}$$

$$n_e \approx \frac{M_{BH+10} - M_{BH}}{M_e} = \frac{0{,}1\ 10^{31}\text{kg}}{9{,}12\ 10^{-31}\text{ kg}} = 1{,}1\ 10^{60}$$

$$n_{fion} \approx \frac{M_{BH+10} - M_{BH}}{M_{fion}} = \frac{0{,}1\ 10^{31}\text{kg}}{1{,}2467\ 10^{-28}\text{ kg}} = 8{,}02\ 10^{57}$$

For the event horizon to increase by 10%, the black hole with an initial mass of 10^{31} kg needs to absorb $2{,}5\ 10^{65}$ photons.

End of life of a black hole:

A black hole remains stable as long as the attractive global forces in the universe with a gravitational potential of d$M(\alpha < 90°)$ prevail. When the space-time mechanical effects diminish with the expansion of the universe, the gravitational potential tends to decrease to the minimum value d$M(\alpha = 90°)$. At this point, the black hole photon is forced to transform into a visible photon. This is due to the position of its 2-dimensional rotation between the dimensional planes D_{45} and $D_{56,}$ in which the space-time deformation shifts to the dimensional plane D_{56} with $\alpha = 90°$. In this situation, it no longer requires any additional potential forces to exchange with itself. The point is reached where it makes sense energetically to break the connection with such a concentration of mass. The black hole decomposes. With the repulsive forces of the universe coming into play, such celestial bodies are dissolved again and the total energy density is brought into spatial equilibrium.

Information is not lost when such objects disintegrate. For an object trapped inside a black hole, the time spent there would last only an instant. The reason lies in time dilation. Due to time dilation, time appears to pass almost infinitely quickly for that object. The time it takes for a black hole to disintegrate is not perceived as a continuous process, but is experienced as instantaneous by the observer. The information is released again.

Key insight from the black hole:

The essential insight is illustrated in **Figures 7.5 – 7.7**. The black-hole photon consists of a pair of spin-0 photons with separate momenta that are oriented parallel to the fourth dimension. Between them lies a gravitational potential of d$M(\alpha_{BH})$. The black hole photon interacts in the particle-field $F_{1\text{-}3}$ with its own 2-dimensional field vectors from the wave-field $F_{4\text{-}6}$. Due to the fact that the field radius is greater than its wavelength, the black hole photon has the ability to absorb matter of any larger wavelength. A black hole has a growing character, while the universe has an expanding character.

Chapter

8 The Space-Distortion-Vector

Introduction to the space-distortion-vector :

The space-distortion vector is intended to enable the observer to generate their own space-time deformation, which can then be utilised technically, for example, to traverse great distances without being subject to the space-time-mechanical effects described by Lorentz.

From the previous chapters, we know that the field radius r with the sine curve $r(t) = r \sin(\alpha)$ of an object describes the contraction of a space segment. The result for a spatially distorted distance is expected to follow the mechanism of the field radius $r(t)$. In this case, we assume an object as the source of gravity, which generates a gravitational field with an event horizon of $r_{BH} = 25$ m. The observer takes up a position within the object.

To simulate this, fions are calculated from a proton mass that, with the help of a multiple of a particle-exchange fion-particle-coupling, convey a mass M_{BHX} via their matter pulse and generate a field radius R_{fionX}. The gravitational potential $dM(\alpha)$ is now assumed to originate from the immediate field source, and that of the universe is neglected.

The **space-distortion-vector** $\overrightarrow{\Delta r_{SDV}(t)}$ is aligned as a spherical sector depending on the gravitational potential for $dM(\alpha)$ and is expressed mathematically by a simple differential geometry.

$$\overrightarrow{\Delta r_{SDV}(t)} = (r_{fionX} - r_{BH}) \sin(kt) \tag{8.01}$$

The term $\sin(kt)$ describes the relativistic effect along its spherical sector with the field angle $\alpha = kt$, which is noticeable through the inertial motion in space-time. The gravitational field is strongest if it is oriented orthogonally to its poles. When oriented relative to a spacecraft, an equatorial configuration would be the most efficient.

The coupling frequency of protons from the 10th dimensional family is combined with its electromagnetic field, ultimately generating a gravitational field characteristic of protons. The field is then mirrored between two field-space levels. External fields that could interfere with the particle-field are bypassed by this gravitational field. The mass of the object is registered as massless for an external observer in the particle-field. With the help of such a field, an object cannot interact or collide with another object at high speeds.

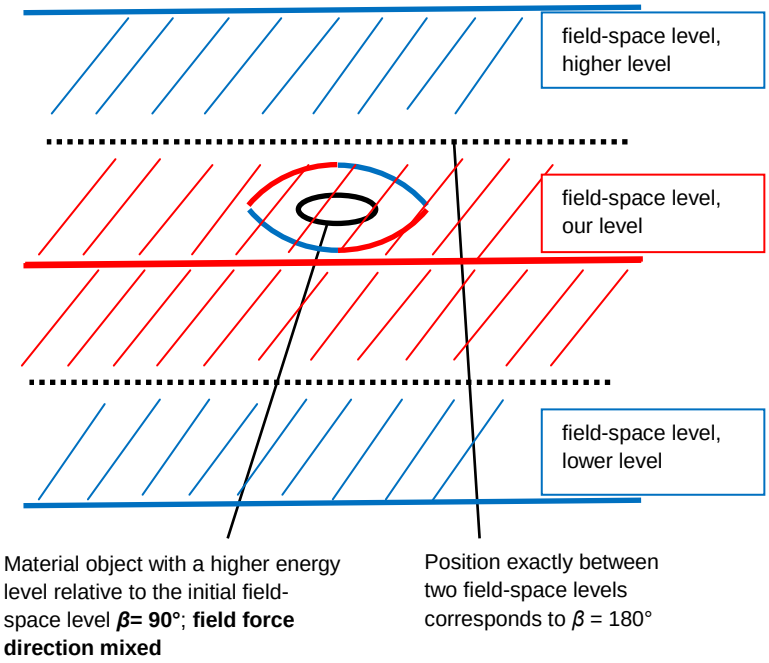

Figure 8.1: The object is located between two field-space levels, reflected between them

How far could a space-dependent, self-emitted gravitational field be distorted? A more detailed description of this technical sketch will be left open for now. The field passes through an area with vertical and horizontal exit zones. A horizontal field vector encounters a vertical field vector of the gravitational field. Hypothetically, this would cause the field emitted horizontally at the vertical event horizon with its multiple of the maximum field propagation speed $V_5 = c$ to be deflected or accelerated to an equivalent of c^2 at the vertical event horizon with its multiple of the maximum speed $V_{max} = c$. Viewed across space-time, the field propagates at the maximum speed $V_{max} = c$, but travels a distance that light would have travelled in a square without space distortion. A space distortion forms towards the gravitational source. **Figure 8.2** illustrates this process.

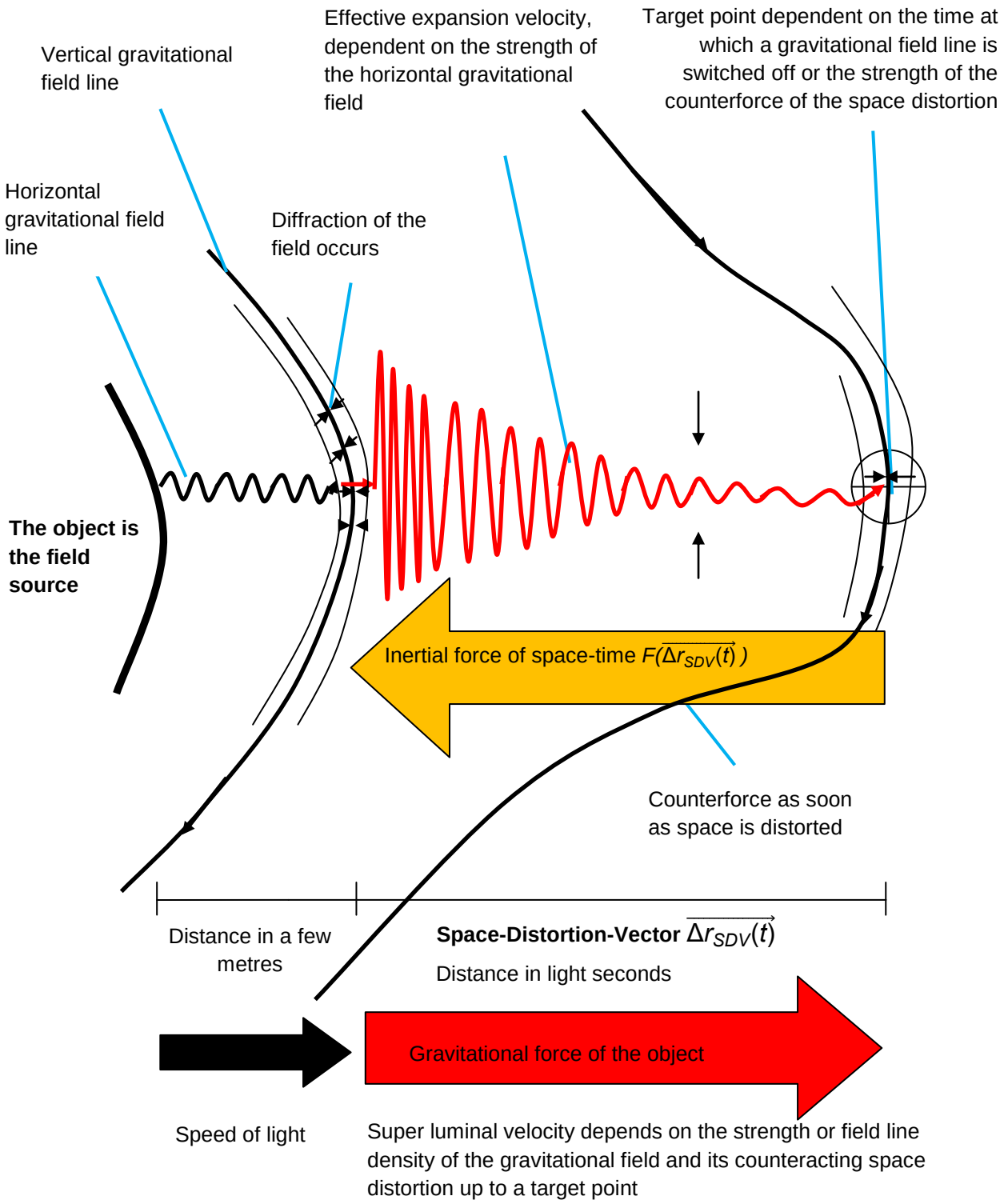

Speeds are only apparently carried out relative to the environment

Figure 8.2: Space-distortion-vector to the target point

Figure 8.3 shows the increase in the effect of the inertial force of space distortion (space distortion force) against the resulting gravitational field for an example of a double maximum velocity V_{max} with 2*c*. The amplitude decreases with the expansion, so that a space distortion can only be as large as the resulting gravitational force of the field.

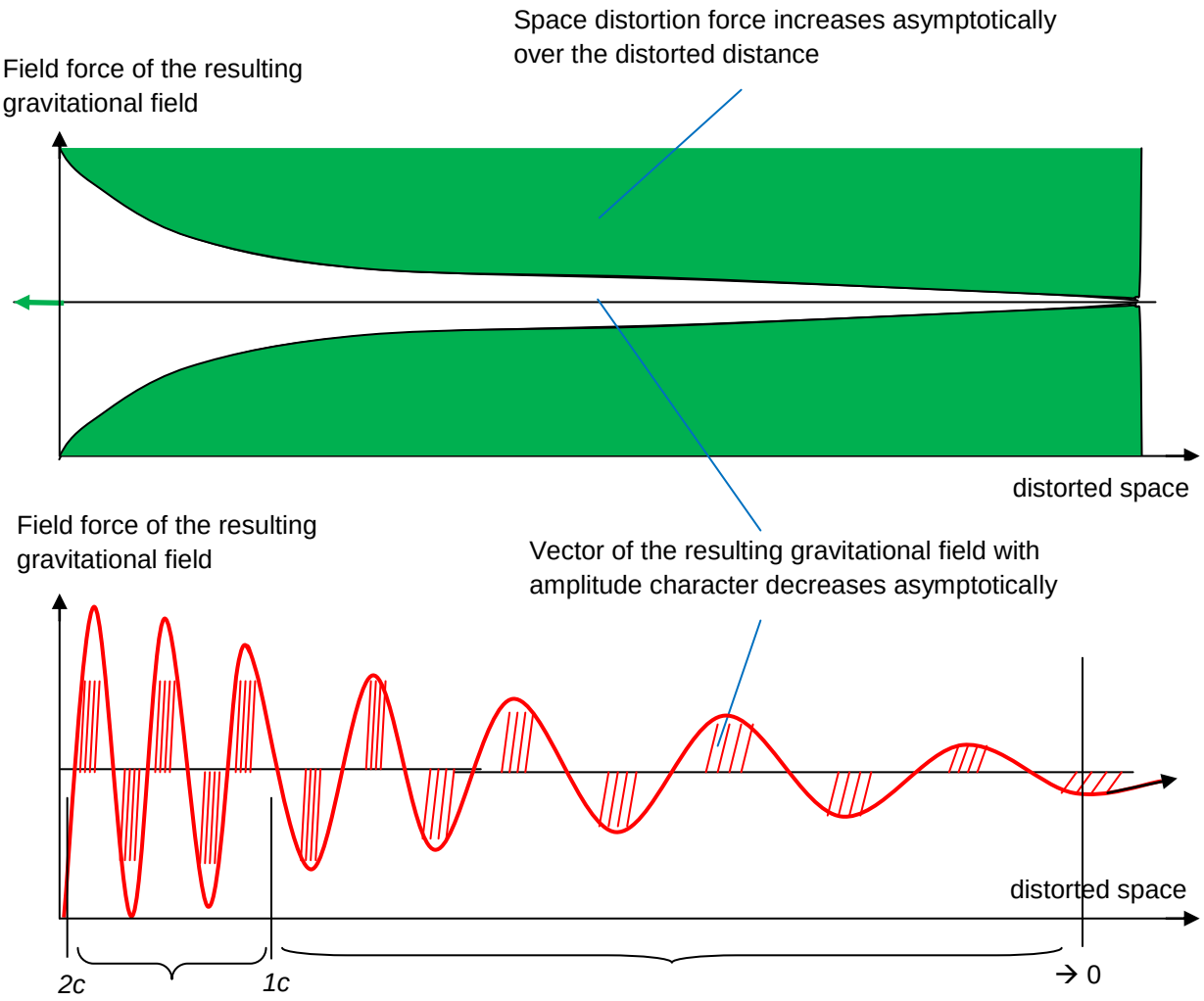

Figure 8.3: Schematic behaviour of the space distortion force against the resulting gravitational field

Calculation of the maximum space-distortion-vector:

A horizontally emitted field encounters a vertical field that has black hole properties, with a specific event horizon and field radius of r_{BHX}.

The following approach applies to the space-distortion-vector if there is exact equatorial contact with the gravitational field:

$\overrightarrow{\Delta r_{SDV}(t)} = (r_{fionX} - r_{BH}) \sin(\alpha)$ with: $\sin(\alpha) = 1 \rightarrow$ maximum

$\Delta r_{SDV}(t) = r_{fionX} - r_{BH}$

The mathematical relationship for the field radius r_{BH} and r_{fionX} is based on the assumption that the force corresponds to the sinusoidal periodicity of the force of a photon:

$F_{BH} = F_{pho}$ with: $F_{pho} = m\, r\, k^2 \sin(\alpha)$; $F_{BH} = \frac{G\, M_{BHX}\, m}{r(t)^2} \sin(\alpha)$

$\cancel{m}\, r_{pho}\, k^2_{pho}\, \cancel{\sin(\alpha)} = \frac{G\, M_{BHX}\, \cancel{m}}{r(t)^2}\, \cancel{\sin(\alpha)}$ with: $r(t)$ at location $\sin(\alpha = 90°)$ to r_{BHX}

$G = 6{,}67\ 10^{-11}\ \mathrm{N}\frac{\mathrm{m}^2}{\mathrm{kg}^2}$; $c = 299792458\ \frac{\mathrm{m}}{\mathrm{s}}$; $h = 6{,}626\ 10^{-34}$ Js ; $r_{BHX} = 25$ m

The following formulas describe the field radius r_{BH} of the event horizon of a gravitational source in general, if it consists of a fictitious fionX:

(8.02)

$$r_{BH} = \sqrt{\frac{G\, M_{BH}}{r_{fionX}}}\ \frac{1}{k_{fionX}} = \sqrt{\frac{G\, M_{BH}}{c\, k_{fionX}}} = \sqrt{\frac{M_{BH}\, r_{fionX}^2}{M_{fionX}}} = \sqrt{\frac{G^2\, M_{BH}\, M_{fionX}}{c^4}}$$

The fictitious mass M_{BHX} describes the mass required for a gravitational field to generate an artificial event horizon for the maximum velocity V_{max} with the field radius $r_{BHX} = 25$ m.

$$r_{BHX} = \frac{G\, M_{BHX}}{c^2} \rightarrow M_{BHX} = \frac{r_{BHX}\, c^2}{G} \qquad (8.03)$$

$\rightarrow \frac{c^2}{G}$ Indicator for the maximum amount of the space-distortion-vector

$$M_{BHX} = \frac{r_{BHX}\, c^2}{G} = 3{,}3686\ 10^{28}\ \mathrm{kg}$$

$$k_{fionX} = \frac{G\, M_{BHX}}{r_{BHX}^2\, c} \tag{8.04}$$

$$k_{fionX} = \frac{6{,}67\ 10^{-11}\ \mathrm{N}\frac{\mathrm{m}^2}{\mathrm{kg}^2} \cdot 3{,}3686\ 10^{28}\ \mathrm{kg}}{(25\ \mathrm{m})^2 \cdot 299792458\ \frac{\mathrm{m}}{\mathrm{s}}} = 1{,}2\ 10^7\ \frac{1}{\mathrm{s}}$$

$$r_{fionX} = \frac{G\, M_{BHX}}{r_{BHX}^2\ \ k_{fionX}^2} \tag{8.05}$$

$$r_{fionX} = \frac{6{,}67\ 10^{-11}\ \mathrm{N}\frac{\mathrm{m}^2}{\mathrm{kg}^2} \cdot\ 3{,}3686\ 10^{28}\ \mathrm{kg}}{(25\ \mathrm{m})^2 \cdot\ (1{,}2\ 10^7\ \frac{1}{\mathrm{s}})^2} = 25\ \mathrm{m}$$

$\boldsymbol{r_{fionX} = r_{BH}}$

$\boldsymbol{\Delta r_{SDV}\,(t) = r_{fionX} - r_{BH}} = 0$ → Range of possible spatial distortion

The range of spatial distortion $\Delta r_{SDV}(t)$ depends on the amount $\frac{c^2}{G}$ of its fictitious mass M_{BHX}. The larger the amount of the space-distortion-vector, the smaller the distance it can distort. In this case, the space-distorted area with $r_{fionX} = r_{BH}$ would be infinitely small, since the field propagation velocity V_5 would be infinitely small. The space-distortion-vector must lie in the range $< \frac{c^2}{G}$ for a change in space to occur at all.

Calculation of a space-distortion-vector propagating at 2*c*:

Now we need to find a solution in which a space distortion propagates only at twice the maximum speed $V_{max} = 2c$. Mechanically, the inertial motion of an object in the electromagnetic photon field is shifted to such an extent that the braking effect is no longer limited to the maximum speed $V_{max} = c$, but is at $V_{max} = 2c$. An object emitting a gravitational field could thus travel a distance with its field relative to a space distortion that would be equivalent to twice the maximum speed $V_{max} = 2c$.

State of field deformation:

The effect of the space-distortion-vector runs parallel to the field deformation, which is modelled by the field propagation velocity V_5.

$r_{BHY} = 25$ m; $M_{BHY} = \frac{r_{BHY}\, c^2}{G} \rightarrow y^2 = 2c \rightarrow V_5 = y = \sqrt{2\mathrm{c}} = 24486{,}4\ \frac{\mathrm{m}}{\mathrm{s}}$

→ y corresponds to the speed that a stationary particle reaches due to the gravitational force up to the field radius r_{BHY}.

Virtual mass of the fion for the event horizon:

$$M_{BHY} = M_{fionY} = \frac{r_{BHY}\, y^2}{G} \tag{8.06}$$

$M_{fionY} = 2{,}248\ 10^{20}$ kg

Alternatively: $M_{fionY} = \frac{r_{BHY}\, c^2}{G} \sin^2(\alpha)$ (8.07)

$$\text{with: } \sin^2(\alpha) = \left(\frac{24486{,}4\ \frac{\text{m}}{\text{s}}}{299792458\ \frac{\text{m}}{\text{s}}} \right)^2$$

The mass M_{fionY} describes the mass required to generate an artificial event horizon for the field propagation velocity $y = 24486{,}4\ \frac{\text{m}}{\text{s}}$ with a field radius of $r_{BHY} = 25$ m.

Circular frequency *k* of fion*Y*:

$$k_{fionY} = \frac{G\, M_{BHY}}{r_{BHY}^2\, c} \tag{8.08}$$

$$k_{fionY} = \frac{6{,}67\ 10^{-11}\ \text{N}\frac{\text{m}^2}{\text{kg}^2} \cdot 2{,}248\ 10^{20}\ \text{kg}}{(25\ \text{m})^2 \cdot 299792458\ \frac{\text{m}}{\text{s}}} = 0{,}08\ \frac{1}{\text{s}}$$

With the step of artificially lowering the maximum speed V_{max} from c to the value y, its circular frequency k has changed. Thus, the constant $k_{Uni}\, M_{Uni} = 4{,}0396\ 10^{35}\ \frac{\text{kg}}{\text{s}}$ no longer applies, but only:

$$k_{fionY}\, M_{fionY} = 1{,}8\ 10^{19} \frac{\text{kg}}{\text{s}}$$

Range of possible spatial distortion:

$$r_{fionY} = \frac{G\, M_{BHY}}{r_{BHY}^2\ \ k_{fionY}^2} \tag{8.09}$$

$$r_{fionY} = \frac{6{,}67\ 10^{-11}\ \text{N}\frac{\text{m}^2}{\text{kg}^2} \cdot 2{,}248\ 10^{20}\ \text{kg}}{(25\ \text{m})^2 \cdot (0{,}08\ \frac{1}{\text{s}})^2} = 3{,}75\ 10^9\ \text{m}$$

→ $\boldsymbol{r_{BHY} \neq r_{fionY}}$

$\boldsymbol{\Delta r_{SDV}(t) = r_{fionX} - r_{BH} = 3{,}75\ 10^9\ \text{m}}$ → Range of possible space distortion

Wavelength of Fion*Y*:

$$\lambda_{fionY} = \frac{h\, y^2}{G\, M_{fionY}^2\, k_{fionY}} \tag{8.10}$$

$$\lambda_{fionY} = \frac{6{,}626\ 10^{-34}\ \text{Js} \cdot (24486{,}4\ \frac{\text{m}}{\text{s}})^2}{6{,}67\ 10^{-11}\ \text{N}\frac{\text{m}^2}{\text{kg}^2} \cdot (2{,}248\ 10^{20}\frac{\text{kg}}{\text{s}})^2 \cdot 0{,}08\ \frac{1}{\text{s}}}$$

$$\lambda_{fionY} = 1{,}4733\ 10^{-54}\ \text{m}$$

In comparison, the wavelength of a black hole with mass $M_{BH} = 10^{31}$ kg:

$$\lambda_{BH} = 2{,}21\ 10^{-73}\ \text{m}$$

Reaction mass required to produce these properties:

The fion*Y* under consideration is fictitious and cannot be produced individually. Technically, a reaction mass could be used that produces these properties and distributes them across several particles. Let us assume that a reaction mass of $m_{obj} = 500$ kg is available, consisting of protons, which is technically used to increase the matter pulse accordingly. Now the energy is distributed from the individual fion*Y* to *n* proton*Y*. The multiple of the coupling frequency of the proton is then distributed over the reaction mass.

For the use of a proton mass with $m_{obj} = 500$ kg:

$$m_{proton} = 1{,}683\ 10^{-27}\ \text{kg} \qquad n_{proton} = \frac{500\ \text{kg}}{1{,}681\ 10^{-27}\ \text{kg}} = 2{,}974\ 10^{29} \qquad \text{with: } n\ \varepsilon\ \mathbb{N}$$

$$M_{protonY} = \frac{M_{fionY}}{n_{proton}} \tag{8.11}$$

$$M_{protonY} = \frac{2{,}248\ 10^{20}\ \text{kg}}{2{,}974\ 10^{29}} = 7{,}56\ 10^{-10}\ \text{kg}$$

Each proton from the $m_{obj} = 500$ kg reaction mass must mimic the mass of $M_{protonY} = 7{,}56\ 10^{-10}$ kg in order to develop a field radius of 25 m, which generates a velocity of 24486,4 $\frac{\text{m}}{\text{s}}$ for this object at this location.

Field radius *r* of proton*Y*:

$$r_{BH\_protonY} = \frac{G\, M_{protonY}}{y^2} \tag{8.12}$$

$$r_{BH\_protonY} = \frac{6{,}67\ 10^{-11}\ \mathrm{N}\frac{\mathrm{m}^2}{\mathrm{kg}^2} \cdot 7{,}56\ 10^{-10}\ \mathrm{kg}}{(24486{,}4\ \frac{\mathrm{m}}{\mathrm{s}})^2} = 8{,}41\ 10^{-29}\ \mathrm{m}$$

Alternatively: $r_{BH\_protonY} = \frac{r_{BHY}}{n_{proton}}$ (8.13)

Circular frequency *k* of the proton*Y*:

$$k_{protonY} = \frac{G\, M_{protonY}}{r_{BH\_protonY}^2\, c} \tag{8.14}$$

$$k_{protonY} = \frac{6{,}67\ 10^{-11}\ \mathrm{N}\frac{\mathrm{m}^2}{\mathrm{kg}^2} \cdot 7{,}56\ 10^{-10}\ \mathrm{kg}}{\left(8{,}41\ 10^{-29}\ \mathrm{m}\right)^2 \cdot 299792458\ \frac{\mathrm{m}}{\mathrm{s}}} = 2{,}38\ 10^{28}\ \frac{1}{\mathrm{s}}$$

Alternatively: $k_{protonY} = k_{fionY}\, n_{proton}$ (8.15)

Field radius of the possible space distortion per proton*Y*:

$$r_{protonY} = \frac{G\, M_{protonY}}{r_{BH\_protonY}^2\ k_{protonY}^2} \tag{8.16}$$

$$r_{protonY} = \frac{6{,}67\ 10^{-11}\ \mathrm{N}\frac{\mathrm{m}^2}{\mathrm{kg}^2} \cdot 7{,}56\ 10^{-10}\ \mathrm{kg}}{\left(8{,}41\ 10^{-29}\ \mathrm{m}\right)^2 \cdot (2{,}38\ 10^{28}\ \frac{1}{\mathrm{s}})^2} = 1{,}26\ 10^{-20}\ \mathrm{m}$$

Alternatively: $r_{protonY} = \frac{r_{fionY}}{n_{proton}}$ (8.17)

Wavelength of proton*Y*:

$$\lambda_{protonY} = \frac{h\, y^2}{G\, M_{protonY}^2\, k_{protonY}} \tag{8.18}$$

$$\lambda_{protonY} = \frac{6{,}626\ 10^{-34}\ \mathrm{Js} \cdot (24486{,}4\ \frac{\mathrm{m}}{\mathrm{s}})^2}{6{,}67\ 10^{-11}\ \mathrm{N}\frac{\mathrm{m}^2}{\mathrm{kg}^2} \cdot (7{,}56\ 10^{-10}\ \mathrm{kg})^2 \cdot\ 2{,}38\ 10^{28}\ \frac{1}{\mathrm{s}}} = 4{,}379\ 10^{-25}\ \mathrm{m}$$

Alternatively: $\lambda_{protonY} = \lambda_{fionY}\, n_{proton}$ (8.19)

The wavelength of the stationary proton must be reduced to that of a proton*Y*:

$\lambda_{proton} = 1{,}315\ 10^{-15}$ m → $\lambda_{protonY} = 4{,}379\ 10^{-25}$ m

The frequency of the proton at rest must be increased to that of the proton*Y*:

$$f_{proton} = \frac{c}{\lambda_{proton}} = 2{,}28\ 10^{23}\ \text{Hz} \rightarrow f_{protonY} = \frac{c}{\lambda_{protonY}} = 6{,}846455\ 10^{32}\ \text{Hz} \qquad (8.20)$$

➔ Frequency increase required for a 2*c* strong space distortion.

Energy content of the reaction mass at rest:

$E = m\,c^2 = 500\ \text{kg} \cdot (299792458\ \frac{\text{m}}{\text{s}})^2 = 4{,}49\ 10^{19}$ J

Required energy irradiation with the coupling frequency specified above:

$$E_{protonY} = h\ f_{protonY} \qquad (8.21)$$

$E_{protonY} = 6{,}626\ 10^{-34}$ Js · $6{,}846455\ 10^{32}$ Hz = 0,45365 J → per proton

$$E_{proton\_massY} = n_{proton}\ h\ f_{protonY} \qquad (8.22)$$

$E_{proton\_massY} = 2{,}974\ 10^{29} \cdot 6{,}626\ 10^{-34}$ Js · $6{,}846455\ 10^{32}$ Hz = $1{,}35\ 10^{29}$ J

➔ By means of irradiation of approx. $1{,}35\ 10^{29}$ J and a frequency of approx. $6{,}85\ 10^{32}$ Hz on the proton mass, a gravitational field is generated with a space distortion for acceleration to the target velocity of 2*c* and a field propagation velocity of 24486,4 $\frac{\text{m}}{\text{s}}$.

Fulfilment of a field-space shift for the 10th dimensional family:

In order for the object to be pulled out of the phase of the particle-field, it requires a minimum frequency to exist between two field-space levels. This prevents any objects or external fields of the particle-field from acting on the object. The state of displacement exactly between two field-space levels requires at least the following frequency for the proton:

$$f_{proton,10.} = \frac{1}{2}\left[\frac{4}{3}\left(\frac{3}{2}\right)^3\right]^{10} \frac{5}{10}\frac{6}{3}\ f_e \qquad (8.23)$$

$f_{proton,10.} = 1702531{,}44 \cdot 1{,}2356\ 10^{20}$ Hz = $2{,}1\ 10^{26}$ Hz

With $f_{protonY} \approx 6{,}85\ 10^{32}$ Hz > $f_{proton,10.} \approx 2{,}1\ 10^{26}$ Hz, the intermediate reflected state would already be fulfilled.

Scaling to a multiple of its frequency and energy:

It is known from communications technology that a multiple of $\frac{\lambda}{2}$ corresponds to the characteristic of the comprehensive wavelength. Similar to the previous chapters, the results are scaled by a factor of 2.

Proposal for scaling with: 2^{81}

$$f_{protonY,scaled} = \frac{f_{protonY}}{2^{81}} \tag{8.24}$$

$$\underline{f_{protonY,scaled} =} \frac{6{,}85\ 10^{32}\ \text{Hz}}{2^{81}} = \underline{283{,}31\ \text{GHz}}$$

(excitation frequency of the proton to be set)

$$E_{protonY,scaled} = \frac{E_{proton\text{-}masseY}}{2^{81}} \tag{8.25}$$

$$E_{protonY,scaled} = \frac{1{,}35\ 10^{29}\ \text{J}}{2^{81}} = 55{,}8\ \text{kJ}$$

$$P_{input,scaled} = \frac{E_{protonY_{scaled}}}{t} \tag{8.26}$$

$$\underline{P_{input,scaled} =} \frac{53{,}8\ \text{kJ}}{\text{s}} = \underline{53{,}8\ \text{kW}}$$

(irradiation power for the 500 kg proton plasma)

The duration of the irradiation must be determined.

The susceptibility to interference and the necessary fine-tuning of the coupling frequency have increased accordingly. Fine-tuning the field will be a technical challenge.

Relaxation of space distortion:

After the horizontally emitted field is switched off, the space distortion immediately seeks the fastest path to relaxation. Since the last emitted field line is already aligned with the maximum space distortion potential of up to $< \frac{c^2}{G}$, the space distortion can only begin to relax where the field is no longer emitted. Thus, the only way for the space distortion to relax is to move the field source itself by means of its own space distortion force. A compensatory movement towards the target point of the space-distortion-vector takes place. The object follows its last emitted field until the target point is reached. During this time, the object rests within the field relative to the field it emits itself, because it is the field source itself. The object within the field therefore does not move relative to its own field source and, due to its missing velocity vector $V_3 = 0$, does not experience any time or length contraction effects. All space-time mechanical effects are bypassed as long as the object is pulled along its own gravitational field to the target point of the space distortion.

This model could give rise to new forms of propulsion that make long distances economically accessible. It requires the exact coupling frequency with the corresponding power. This can be calculated using the FSM.

Afterword

FSM offers a wide range of solutions for microscopic and macroscopic phenomena that the observer can perceive only to a limited extent from their 3-dimensional particle-field. In doing so, apparently unsolved physical problems can be explained by new approaches. All four fundamental forces are reconciled with each other in one model.

As mentioned at the beginning under the definition of the particle-field, this model confirms the statement that what we see is merely a hologram. The visible matter from the macroscopic perspective is merely the sum of all interaction phenomena that originate in the wave-field $F_{4\text{-}6}$. Modelling the wave-field $F_{4\text{-}6}$ makes it possible to discover new technical achievements and make them economically viable. The FSM model opens the door to a completely new understanding of physics. The author invites the natural sciences to test their theories using Field-Space-Mechanics.

Finally, the question whether there is a beginning or an end will be addressed. Sinusoidal periodicity seems to extend from fractal structures such as those of a visible photon, through the size of a black hole, to the characterisation of field-space levels, to the description of the universe and even a universal photon. It cannot be ruled out that the universal photon with our known maximum speed $V_{max} = c$ is the only source for the creation of universes. According to sinusoidal periodicity, there could be other structures beyond the universal photon that embed the universal photon. An indication of this is the space-time mechanical effect with the Lorentz factor < 1, which is not modelled within the framework of the universal photon. The sinusoidal periodicity thus appears to be an infinite regress that initially has no end in the microscopic or macroscopic world view.

It should be mentioned that the FSM model is also unable to describe the true nature of reality. However, it should help to bring us closer to a description of nature and to find new perspectives and insights that will advance users and enable new innovations.

Open topics for this model as presented in this paper:

The author also criticises the FSM theory. During the development of the model, the connections between a 6-dimensional field-space could not be fully understood in physical terms, but only in mathematical and philosophical terms. In order to resolve any doubts, the following questions, among others, must be answered:

- What exactly triggers the close-range effect that converts an active fion into an exchange fion/passive fion pair, thereby provoking a fion exchange? Is the slight exceeding of an energy potential in a particle sufficient? At what distance do the extreme cases regarding energy potentials apply?
- How can significant correlations between spin, isospin and particle masses be demonstrated?
- How can particle masses and their coupling frequencies for mesons and baryons occur partially twice?
- How can the particle configuration be clearly distinguished between mesons and baryons?
- How does Sommerfeld's reciprocal factor of ~ 137 relate to the minimum coupling frequency for fions with f_{fion} = 136,6875 f_e ?
- What are the reasons for slight deviations (up to 1%) from the experimental value when calculating particle masses?
- Are there particle masses that deviate by > 1% for hadrons, possibly due to unknown influencing factors of hidden matter?
- How does an u/d-quark transform into two S-quarks with wavelengths $\frac{1}{2}\,\lambda_{u/d}$?
- Could the Casimir effect depend on the distance at which an exchange fion begins to exchange its field with another particle?
- What variety of particles actually results when all possible combinations are taken into account?
- What influence does gravitational force have on the creation of particles?
- How many field-space levels are there actually?
- What specific frequency ranges do higher field-space levels have?
- Can multiples of two of the coupling frequencies trigger a coupling effect?
- How finely must a coupling frequency be modelled in order to manipulate the plasma state?
- Would there be a higher field-space level with a frequency range in which a space-distortion-vector could be implemented without scaling?
- The slight deviation from the visible mass of the universe can only be measured astronomically if the Earth were located approximately at the centre of the universe. How likely is this situation, and is today's heliocentric view of the world really realistic?

Appendix

Formula index for the essential relationships and findings

FSM-STR – Special Theory of Relativity of Field-Space-Mechanics:

$c^2 = V_4^2 + V_5^2$

$V_5 = \sqrt{c^2 - v_3^2}$ with: $V_3 = V_4$

Length contraction: $r(t) = r\,\frac{V_5}{c} = r\,\sin(\alpha)$ →Factor: $\sin(\alpha)$

Field deformation: $V_5 = c\,\sin(\alpha)$ →Factor: $\sin(\alpha)$

$V_4 = c\,\cos(\alpha)$ →Factor: $\cos(\alpha)$

Red shift: $\lambda_{obj}(t) = \frac{\lambda_{obj}}{\sin(\alpha)}$ → Factor: $\frac{1}{\sin(\alpha)}$

Time dilation: $t_{obj} = \frac{c}{V_5}\,t = \frac{t}{\sin(\alpha)}$ →Factor: $\frac{1}{\sin(\alpha)}$

FSM-GTR – General Theory of Relativity of Field-Space-Mechanics:

Field angle:

$\alpha = \int_0^t \frac{\sqrt{c^2 - V_3^2}}{r(t)}\,dt$ $\alpha = \sin^{-1}(kt)$ (general) $\alpha = \sin^{-1}(\frac{V_5}{c})$ (specific)

Relativistic energy increase:

$E_{obj}(t)_\alpha = h\,f\,\frac{1}{\sin(kt)} = m_{obj}\,c^2\,\frac{1}{\sin(kt)}$ →Faktor: $\frac{1}{\sin(kt)}$

$E_{obj}(t)_\alpha = m_{obj}\,c^2\,\frac{1}{\sin(\alpha = 90°)}$ für $V_5 = c$; $V_4 = 0$

$E_{obj}(t)_\alpha = m_{obj}\,c^2\,\frac{1}{\sin(0 < \alpha < 90°)}$ für $V_5 \rightarrow 0$; $V_4 \rightarrow c$

Description of the universe:

Sinusoidal periodicity of the universe:

$$F_{grafity}(t) = \frac{G\, M_{Uni}\, m_{obj}}{r(t)^2} \sin(kt)$$

Gravitational force between objects:

$$F_{gravity}(t) = \frac{G\, m_{obj1}\, m_{obj2}}{r^2} \sin(kt)$$

r_{Uni} – maximum field radius of the universe:

$$r_{Uni} = \frac{G\, M_{Uni}}{c^2} \approx 8{,}73125\ 10^{26}\ \text{m} \approx 8{,}73\ 10^{26}\ \text{m or } 92{,}35 \text{ billion LY}$$

k_{Uni} – circular frequency of the universe with:

$$k_{Uni} = \sqrt{\frac{G\, M_{Uni}}{r^3}} = \frac{c^3}{G\, M_{Uni}} = 3{,}4336\ 10^{-19}\ \frac{1}{\text{s}} \text{ or } 92{,}35 \text{ billion years}$$

Universal constants in the universe:

$$M_{Uni}\, k_{Uni} = m_{obj}\, k_{obj} = \text{const.} = 4{,}0396\ 10^{35}\ \frac{\text{kg}}{\text{s}}$$

$$c = r_{Uni}\, k_{Uni} = r_{obj}\, k_{obj} = \sqrt[3]{G\, m_{obj}\, k_{obj}} = \sqrt{\frac{G\, m_{obj}}{r_{obj}}} = 299792458\ \frac{\text{m}}{\text{s}}$$

$$\frac{M_{Uni}}{r_{Uni}} = \frac{m_{obj}}{r_{obj}} = 1{,}34746\ 10^{27}\ \frac{\text{kg}}{\text{m}}$$

Wavelength of the universe:

$$\lambda_{Uni} = \frac{h\, c^2}{G\, M_{Uni}^2\, k_{Uni}} = 1{,}87862\ 10^{-96}\ \text{m}$$

Relativistic wavelength (red shift):

$$\lambda(t) = \lambda_{Uni} \frac{1}{\sin(\alpha)}$$

Radius/length contraction of the universe depending on the field angle α:

$$r(t) = r_{Uni} \sin(\alpha)$$

Trigonometric distance $b(t)$ for the change in the field potential:

$$b(t) = r_{Uni} \cos(\alpha)$$

Trigonometric distance between dM(0) and the object at expansion dM(α):

$$w(t) = r_{Uni} (1 - \cos(\alpha))$$

Space and energy relationship:

$$E(t) = \frac{r\ h\ c}{r(t)\ \lambda} = \frac{h\ c}{\lambda}\ \frac{1}{\sin(kt)}$$

Circumference of the cosmos:

$U_{t\_Uni\_\alpha} = 2\pi\ r_{Space\ expansion\_\alpha\_in\_billion\ LY} \cdot$ time dilation factor

Energy equation in a R^6 for $V_5 = c$:

$$E = \frac{1}{\lambda_{obj}}\ h\ c = h\ f_{obj} = m_{obj}\ G\ \{m_{obj}\ k_{obj}\}\ \frac{1}{c} = m_{obj}\ r_{obj}^2\ k_{obj}^2 = m_{obj}\ c^2$$

Force of a photon:

Formation for interaction effects:

$$F(t) = m_{obj}\ r_{obj}\ k_{obj}^2 \sin(kt)$$

Relativistic effect:

$$F(t) = m_{obj}\ r_{obj}\ k_{obj}^2\ \frac{1}{\sin(kt)}$$

Angular momentum of the photon in a R^6:

Angular momentum of the photon in the particle-field (Planck's constant):

$$L_{ø\_particle\text{-}field} = m_{obj}\ \lambda_{obj}\ c\ \frac{1}{2\pi} = m_{obj}\ \lambda_{obj}\ k_{obj}\ r_{obj}\ \frac{1}{2\pi} = \frac{h}{2\pi}$$

Angular momentum in a group of fions:

$$L_{n\_fions}^2 = \sum_0^n \left(\frac{h}{4\pi}\right)^2_n \qquad n\ \varepsilon\ \mathbb{N} \qquad [L] = \text{Js}$$

Calculation of mass as a multiple of the electron:

$$M_{obj} = \frac{1}{2}\ (\text{BC}\ (\text{CC})^3)^n \cdot \text{PC} \cdot \text{Dimfactor} \cdot M_e$$

Particles can be predicted reliably. Example for the proton baryon:

$$M_{proton\text{-}baryon,5.} = \frac{1}{2}\left[\frac{4}{3}\left(\frac{3}{2}\right)^3\right]^5 \frac{6}{3}\ M_e = 1845{,}28125\ M_e$$ (experimental: 1836,15 M_e)

Conversion from MeV to multiples of the electron mass M_e via the proton:

$$Y\ M_e = \frac{1836\ M_e}{938{,}38\ \text{MeV}} \cdot X\ \text{MeV}$$

Calculation of the particle frequency as a multiple of the base interference frequency:

$$f_{obj} = \frac{1}{2} (BC\ (CC)^3)^n \cdot PC \cdot Dimfactor \cdot f_e$$

Minimum coupling frequency and mass for matter:

$$f_{fion} \approx [\ \frac{4}{3} (\frac{3}{2})^3\ ]^4 \frac{1}{3} f_e = 136{,}6875\ f_e$$

$$\lambda_{fion} = 1{,}775\ 10^{-14}\ m\ ;\ f_{fion} = 1{,}688911\ 10^{22}\ Hz$$

The minimum coupling frequency indicates the frequency at which invisible photons interact electrically with matter. They transform into active fions, which divide themselves into visible and hidden particles with their 4-dimensional rotational orbits.

Electromagnetic information matrix:

The electromagnetic information matrix is a superposition of electromagnetic harmonics from individual quark information of the 1st dimensional family, which expand into complex particles from the 5th dimensional family onwards. Its calculation allows various properties of a particle to be interpreted.

Contents may include:

- quark excitation
- coupling factor bound to unbound exchange fion with $\frac{1}{2}$
- number of active fions
- number of exchange fions/passive fion pairs in the particle
- extent of external disturbances
- particle type
- charge +-
- spin integer, half integer, direction +-
- iso-spin
- number of periods *T* for one complete turning around of active fions
- dimension factor for reducing the maximum speed V_{max}
- stability
- close-range properties
- indication of the influence of hidden particles on its structure

Gravitational force:

In the FSM, the **gravitational force** of an object with a normalised mass *M* is the counterforce to the inertial force that acts with its propagation as an electromagnetic wave through space-time. This quantity depends on the **object's mass**, its **distance** from other objects and its **gravitational potential**.

The normalised masses of objects are determined on the basis of their **electromagnetic properties** of a **particle-exchange fion-particle-coupling** from the wave-field $F_{4\text{-}6}$. The masses of complex particles such as the proton differ only in the variation of their electrical exchange particles.

Single object:

$$F_{gravity}(t) = m_{obj}\, rk^2 \sin(kt)$$

Between two objects:

$$F_{gravity}(t) = \frac{G\, m_{obj1}\, m_{obj2}}{r^2} \sin(kt)$$

Electromagnetic interaction forces:

PC	Force	Examples of frequencies
$\frac{3}{3}$	electric force	$f_{muon/electron,4.} = \frac{1}{2}[\frac{4}{3}(\frac{3}{2})^3]^4 \frac{\mathbf{3}}{\mathbf{3}} f_e = 205{,}031\ f_e$ $f_{electron,5.} = \frac{1}{2}[\frac{4}{3}(\frac{3}{2})^3]^5 \frac{\mathbf{3}}{\mathbf{3}} f_e = 922{,}640625\ f_e$ $f_{tauon/electron,6.} = \frac{1}{2}[\frac{4}{3}(\frac{3}{2})^3]^6 \frac{5}{6}\frac{\mathbf{3}}{\mathbf{3}} f_e = 3459{,}9\ f_e$
$\frac{4}{3}$; $\frac{6}{3}$	strong nuclear force	$f_{pion/meson\text{-}boson,\ 4.} = \frac{1}{2}[\frac{4}{3}(\frac{3}{2})^3]^4 \frac{\mathbf{4}}{\mathbf{3}} f_e = 273{,}375$ $f_{meson\text{-}boson,5.} = \frac{1}{2}[\frac{4}{3}(\frac{3}{2})^3]^5 \frac{\mathbf{4}}{\mathbf{3}} f_e = 1230{,}1875\ f_e$ $f_{baryon,5.} = \frac{1}{2}[\frac{4}{3}(\frac{3}{2})^3]^5 \frac{\mathbf{6}}{\mathbf{3}} f_e = 1845{,}28125\ f_e$ $f_{meson\text{-}boson,6.} = \frac{1}{2}[\frac{4}{3}(\frac{3}{2})^3]^6 \frac{5}{6}\frac{\mathbf{4}}{\mathbf{3}} f_e = 4613{,}203125\ f_e$ $f_{meson/baryon,6.} = \frac{1}{2}[\frac{4}{3}(\frac{3}{2})^3]^6 \frac{5}{6}\frac{\mathbf{6}}{\mathbf{3}} f_e = 6919{,}804688\ f_e$

PC	Force	Examples of frequencies
$\frac{3}{3}$; $\frac{4}{3}$; $\frac{6}{3}$	weak nuclear force	$f_{weak\_interaction} = f_{strong\_interaction} \sin(0° < \beta < 90°)$ $f_{H\text{-}boson} = f_{muon/electron,4.} \cdot f_{electron,5.} \cdot \frac{5}{6} PC_{electron,4.} \cdot PC_{electron,5.} f_e$ $f_{H\text{-}boson} \approx 205 \cdot 922{,}6 \cdot \frac{5}{6} \frac{5}{4} \frac{4}{4} f_e \approx 246315 f_e$

Magnetism in the proton:

Three charged quarks form a total rotation. At the location of the binding neutrino in the centre of the angular momentum, a magnetic field is induced perpendicular to the axis of rotation.

Description of a black hole:

The transition from particles to black holes in our universe when their wavelength λ_x is equal to the field radius r_x:

$h = 2\pi\, r_x^2\, m\, k$

$r_x = 1{,}616\ 10^{-35}$ m

Radius of the field in R^6 from which photons can no longer escape:

$$r_{BH} = \frac{G\, M_{BH}}{c^2}$$

External angular momentum:

$$L_{ø\_particle\text{-}field\_BH} = \sqrt{G\, M_{BH}^3\, r_{BH}}$$

Rotation per second on the vertical axis:

$$k_{BH} = \sqrt{\frac{G\, M_{BH}}{r_{BH}^3}}$$

Gravitational force of the black hole on an object along its spherical sector:

$$F_{BH} = \frac{G\, M_{BH}\, m_{obj}}{r_{BH}^2} \sin(\alpha)$$

Wavelength of the black hole photon in R^6:

$$\lambda_{BH} = \frac{h\, c^2}{G\, M_{BH}^2\, k_{BH}}$$

Energy of a photon inside the black hole:

$$E_{BH\_photon} = \frac{1}{\lambda_{BH}} h\, c$$

Mass of a photon in the black hole:

$$M_{BH\_photon} = \frac{E_{BH_{photons}}}{c^2}$$

Number of photons in the black hole:

$$n = \frac{M_{BH}}{M_{BH_{photon}}}$$ Number n photons; n ε N→ there is only one photon in the black hole

X% increase in event horizon when *n* photons are absorbed:

$$r_{BH+X\%} = \frac{G\,(M_{BH} + 0{,}1\, M_{BH})}{c^2} \qquad n_{photon} = \frac{r_{BH+10} - r_{BH}}{r_{obj}} = \frac{M_{BH+10} - M_{BH}}{M_{obj}}$$

Key findings from the black hole:

- The black hole consists of a spin-0 photon pair that interacts with the wave-field $F_{4\text{-}6}$ via its own 2-dimensional field vectors.

- It has a growing character with respect to its field radius $R_{BH.}$

Space distortion vector to be defined:

$$\overrightarrow{\Delta r_{SDV}(t)} = (r_{fionX} - r_{BH}) \sin(kt)$$

The size of the surrounding field for a space distortion, depending on a fionsX with the corresponding field radius r_X and circular frequency k_X:

$$r_{BH} = \sqrt{\frac{G\, M_{BH}}{r_{fionX}}}\ \frac{1}{k_{fionX}} = \sqrt{\frac{G\, M_{BH}}{c\, k_{fionX}}} = \sqrt{\frac{M_{BH}\, r_{fionX}^2}{M_{fionX}}} = \sqrt{\frac{G^2\, M_{BH}\, M_{fionX}}{c^4}}$$

$$M_{BHX} = \frac{r_{BHX}\, c^2}{G} \quad \rightarrow \quad \frac{c^2}{G}$$ Index for the maximum space distortion vector

The space distortion vector can be controlled specifically, for example with 2c:

$$M_{BHY} = \frac{r_{BHY}\, y^2}{G} \quad \rightarrow \quad y^2 = 2c \rightarrow y = \sqrt{2c} = 24486{,}4\ \frac{\text{m}}{\text{s}}$$

Bibliography

[1] Müller Group: Measurement of the fine-structure constant as a test of the Standard Model, Richard H., Parker, Chenghui Yu, Weicheng Zhong, Brian Estey, and Holger Müller Publication, Science 360, 191-195 (2018)
Link
https://matterwave.physics.berkeley.edu/cesium-fountain

- Fine-structure constant

[2] Eckardt Horst: On the vortex theory of electrodynamics – lecture notes, Date of publication: 2004-01-04
Link:
http://aias.us/documents/miscellaneous/EDyn3.pdf

- Result of potential vortices from Maxwell's equation

[3] Hans-Peter Willig: Physical properties - related to the observable universe
Link:
https://www.cosmos-indirekt.de/Physik-Schule/Universum?utm_content=cmp-true

- Mass and age of the visible universe

[4] Free University of Berlin: Physical constants and formula symbols Appendix IV
Excerpt from physics practical course for natural scientists, date of publication: 18 March 2008
Link:
https://www.physik.fu-berlin.de/studium/lehre/gp/dateien/np-doku/NP_Groesse_Einheit.pdf

- Natural constants

[5] European Southern Observatory:
First signs of self-interacting dark matter?
Date of publication: 15 April 2015
Link:
https://www.eso.org/public/germany/news/eso1514/

- Proportion of dark energy in the total mass of the universe

[6] Demtröder Wolfgang: Experimental Physics 4 – Nuclear, Particle and Astrophysics
Springer Publishing, Publication date: 20 January 1998, 4th edition

- Gluons have colour charges
- Gluons can react with photons
- Potential energy increases with the distance between V quarks
- Quark-antiquark pairs have colourless charges

[7] Schmidt Christian: Chiral perturbation theory for quantum chromodynamics on the lattice with axially rotated mass matrix
Diploma thesis, Location: Westphalian Wilhelms University of Münster, Publication date: January 2004
Link:
https://www.uni-muenster.de/Physik.TP/archive/fileadmin/Arbeiten/schmidt.pdf

- In local fields, particle-antiparticle pairs arise
- Baryons contain valence quarks
- Quarks + antiquarks = mesons
- Hadron = baryons or mesons
- Strength strong WW independent of quark type
- Spin differs between quark and antiquark

[8] Detlef Dürr and Dustin Lazarovici:
Understanding Quantum Mechanics – Three Possible Worldviews of Quantum Physics
Springer Publishing, Publication date: March 2018
Link:
https://www.uni-muenster.de/Physik.TP/archive/fileadmin/Arbeiten/schmidt.pdf

- Quantum Mechanics and Possible Worldviews

Experimental data:

[9] Particle Data Group: Homepage:
https://pdg.lbl.gov/

P.A. Zyla, 2020
Link:
https://pdg.lbl.gov/2020/listings/rpp2020-list-muon.pdf

- Mass Myon

P.A. Zyla, 2020
Link:
https://pdg.lbl.gov/2020/listings/rpp2020-list-pi-plus-minus.pdf

- Mass of the pion

R.L. Workman, 2022
Link:
https://pdg.lbl.gov/2022/listings/contents_listings.html

- Tauon mass

R.L. Workman, 2022
Link:
https://pdg.lbl.gov/2023/web/viewer.html?file=../listings/rpp2023-list-w-boson.pdf

- Mass W boson

R.L. Workman, 2022
Link:
https://pdg.lbl.gov/2023/web/viewer.html?file=../listings/rpp2023-list-z-boson.pdf

- Mass Z – boson

R.L. Workman, 2022
Link:
https://pdg.lbl.gov/2023/web/viewer.html?file=../listings/rpp2023-list-higgs-boson.pdf

- Mass H – boson

R.L. Workman, 2022
Link:
https://pdg.lbl.gov/2023/web/viewer.html?file=../listings/rpp2023-list-p.pdf

- Proton mass

M. Tanabashi, 2018
Link:
https://pdg.lbl.gov/2018/listings/rpp2018-list-D-plus-minus.pdf

- Mass of the CD meson

M. Tanabashi, 2018
Link
https://pdg.lbl.gov/2019/listings/rpp2019-list-xic-2645.pdf
https://pdg.lbl.gov/2022/listings/rpp2022-list-Ds-plus-minus.pdf
https://pdg.lbl.gov/2022/listings/rpp2022-list-Ds0-star-2317-plus-minus.pdf
https://pdg.lbl.gov/2022/listings/rpp2022-list-Ds1-2460-plus-minus.pdf
https://pdg.lbl.gov/2022/listings/rpp2022-list-Ds1-2536-plus-minus.pdf
https://pdg.lbl.gov/2022/listings/rpp2022-list-Ds2-2573-plus-minus.pdf

- Mass of CS meson

C. Patrignani, 2016
Link:
https://pdg.lbl.gov/2016/listings/rpp2016-list-J-psi-1S.pdf

- CC meson mass

M. Tanabashi, 2018
Link:
https://pdg.lbl.gov/2019/listings/rpp2019-list-Bc-plus-minus.pdf

- Mass CB meson

M. Tanabashi, 2018
Link:
https://pdg.lbl.gov/2019/listings/rpp2019-list-xic-prime-zero.pdf

- Mass of DSC baryon

P.A. Zyla, 2020
Link:
https://pdg.lbl.gov/2020/listings/rpp2020-list-B-plus-minus.pdf

- Mass of B meson

K. Nakamura, 2010
Link:
https://pdg.lbl.gov/2010/listings/rpp2010-list-upsilon-1S.pdf

- Mass of BB meson

K. Nakamura, 2010
Link
https://pdg.lbl.gov/2010/listings/rpp2010-list-Bs-star.pdf

- BS meson mass

M. Tanabashi, 2018
Link
https://pdg.lbl.gov/2019/listings/rpp2019-list-xib-5945-zero.pdf
- BS baryon mass

[10] Prof. J. Stachel: Physics V – Nuclear and Particle Physics
Lecture notes based on lectures given in winter semester 01/02, location: University of Heidelberg, publication date: 2021-04-07
Link:
https://www.physi.uni-heidelberg.de/~stachel/skript.pdf
- Gluons: electromagnetic oscillators, vortex motion
- Sea quarks: relationship to valence quarks
- Strong interaction: time-invariant
- Behaviour during nuclear fission

[11] Figure: Link:
https://i.ytimg.com/vi/7BHC6p8T0Dw/maxresdefault.jpg

[12] Siemens Foundation: Factual information – Nuclear fusion in the sun
Script designation: CC BY-SA 4.0,
Year of publication: 2017
Link:
file:///C:/Users/Patrick/Downloads/Kernfusion_in_der_Sonne_ccbysa4.pdf

- Fusion processes in the sun

[13] International Atomic Energy Agency:
Fusion Physics, Authors: Mitsuru Kikuchi, Karl Lackner, Minh Quang Tran, Year of publication: 2012, Location: Vienna
Link:
https://www-pub.iaea.org/MTCD/Publications/PDF/Pub1562_web.pdf

- Fusion processes – technical implementation of hot fusion
- Fusion reactor design and function

[14] René Rausch: The periodic table of elements online
Year of publication: Copyright © 2010-2023
Link:
https://www.periodensystem-online.de/index.php?id=impressum

- Mass of hydrogen, deuterium, tritium, helium

[15] Max Planck Institute: Microwave heating – ECRH
Link:
https://www.ipp.mpg.de/3862098/ECRH

- Current performance data and implementation of hot fusion process in Wendelstein 7x

List of symbols used

Vectors

$\overrightarrow{dA}$	m	vector surface element
$\vec{e_1}, \vec{e_2}, \vec{e_3}$		unit vectors in Cartesian coordinates for the particle-field
$\vec{e_4}, \vec{e_5}, \vec{e_6}$		unit vectors in Cartesian coordinates for the wave-field
$\overrightarrow{\Delta r_{SDV}(t)}$	m	space-distortion-vector
$\vec{s}$	m	vector from origin 0 to point P

Latin letters

A		point of contact A, meeting point for active fions
A	m	area
$a(t)$	m	acceleration
A^a_μ		vector field in 7D
	1/m	vector field in 4D
δA^a_μ		possibility of deviation from the rest position in the vector field
B		contact point B, meeting point for active fions
$b(t)$	m	distance $\beta(t)$ for decreasing the field potential
$b'(t)$	m/s	the speed at which telescopes can peer deeper into the universe
BC		bose configuration
c	m/s	maximum speed for $V_{max} = c = 299792458$ m/s
$C_{1/2/3}$		Chern classes
CC		coupling configuration
D_1, D_2, D_3		dimensions in the Cartesian coordinate system for the particle-field
D_4, D_5, D_6		dimensions in the Cartesian coordinate system for the wave-field
D_{45}, D_{46}, D_{56}		area spanned between the indexed dimensions
ds^2	m^2	the invariant length square of the metric

E	J	energy
$E(t)_\alpha$	J	energy for the relativistic energy increase
e		Euler's constant 2,71828....
e	As	elementary charge e = 1,602176634 10^{-19} As a) e^- Charge of the electron b) e^+ Charge of the positron
EC		electron configuration
eF		number of external fions received eF1: receipt of one external fion eF2: receipt of two external fions eF3: receipt of three external fions
F		field with index describes the fields according to the unit vectors for the dimensions D_1, D_2, D_3, D_4, D_5, D_6 a) F_{1-3} – field in the particle-field b) F_{4-6} – field in the wave-field
F	N	magnitude of the force
f	Hz	frequency
f*	Hz	interference frequency for an harmonic
f*	Hz	interference frequency for multiple harmonics
FSR		free spectral range
G	Nm²/kg²	gravitational constant G = 6,67 10^{-11} Nm²/s²
G_m		Generators in the sense of Lie algebras
G_{MN}	1/m²	Einstein tensor
g_{eff}	kg/m²s	Pulse density at T_{0i}^{eff}/c
g_{MN}		$g_{MN} = \eta_{MN} + h_{MN}$ - overall metric
H^+		chemical symbol for hydrogen
He^+		chemical symbol for helium
h	J	Planck's constant h = 6,626 10^{-34} Js
h_{MN}		perturbative gravitational disturbance of the metric

$\bar{h}_{MN}$	1/m²	trace-cleaned disturbance
k	1/s	circular frequency
L	Js	angular momentum of an object
$\mathcal{L}$		Lagrange-Funktion
l	m	length between two resonator mirrors
l_p	m	Planck length, corresponds to the size r_x
M	kg	a) mass of the universe with M_{Uni} b) mass of the electron with M_e = 9,1094 10^{-31} kg c) mass of a protonY with $M_{protonY}$ d) mass of a black hole with M_{BH} e) mass of various particles
$dM(\alpha)$	kg	gravitational potential depending on the field angle α
m	kg	mass for different objects
n		counting index for natural numbers
N		counting index for natural numbers
N_{aF}		number of active fions
N_{eF}		number of external fions
$N_{F/A}$		number of exchange fions/passive fion pairs
NoPN		number of positrons in the neutron
NoEN		number of electrons in the neutron
NoPP		number of positrons in the proton
NoEP		number of electrons in the proton
NoPT		total number of positrons in the atom
NoET		total number of electrons in the atom
P		point in the Cartesian coordinate system
P	kgm/s	impulse
PC		particle configuration
P_{input}	W	power

p/c^2	kg/m^4s^2	normalized pressure
Q	As	charge
R		space, superscripts indicate the number of dimensions to be considered a) R^3 – 3-dimensional view b) R^6 – 6-dimensional view
R	m	radius, from the wavelength $\lambda = 2\pi R$
R	$1/m^2$	Ricci curvature scalar
R^P_{QMN}	$1/m^2$	Riemann tensor
R_{MN}	$1/m^2$	Ricci-Tensor
r	m	a) r_{Uni} maximum field radius of the universe b) r_{obj} field radius for arbitrarily scalable objects
$r(t)$	m	amount for the relativistic field radius $r = \vert\vec{r}\vert$
r_S	m	radius, Schwarzschild
r_x	m	field radius at which black holes form
$r'(t)$	m	expansion velocity of the universe
S		sphere
S	m	a) distance $S >> \Delta s$ b) effect/action
s	m	distance
Spin		factored angular momentum of a particle, integer or half-integer
T	s	period
T_{MN}	J/m^3 J/m^6	Momentum-energy tensor, here: 4D Momentum-energy tensor, here: 7D
Tr		trace
t	s	time
$t(\alpha)$	s	age of the universe instead of the field angle α
t_{obj}	s	object time
U		subspace

$\boldsymbol{U}$	m	orbital period
$\boldsymbol{u_M}$		quadruple pulse
$\boldsymbol{V}$	m/s	amount for speed $V = \left\vert\vec{V}\right\vert$ a) V_{max} – maximum speed b) V_3 – object speed in the particle-field c) V_{Obj} – object velocity in the particle-field d) V_{field} – field propagation speed, not detectable in the particle-field e) V_4 – field propagation speed through the fourth dimension f) V_5 – field propagation speed through the fifth dimension g) V_{Rot} – resulting rotational velocity within particles h) V_{D1} – velocity per space vector used
$\boldsymbol{V(\phi_n)}$	J/m^3	potential field
$\boldsymbol{w}$	1/m	wavenumber
$\boldsymbol{w(t)}$	m	age of visible light over the distance $w(t)$
$\boldsymbol{y}$	m/s	artificial field propagation speed parallel to the 5th dimension
Y		years

Greek letters and operators

$\boldsymbol{\alpha}$	°	field angle
α		fine-structure constant ≈ 1/137
$\boldsymbol{\beta}$	°	deviation angle relative to the dynamic trend (kt)
ɣ	MeV	unusable radiation in the form of alpha, beta and gamma radiation
$\boldsymbol{\gamma_{ab}}$		metrical component in the wave-field
$\boldsymbol{\Gamma^{\lambda}_{MN}}$	1/m	Christoffel's symbol
Δ		delta operator for representing differences
$\boldsymbol{\delta_{\mu\nu}}$		Kronecker-Delta; 1 bei $\mu = \nu$; 0 sonst
$\boldsymbol{\eta_{\mu\nu}}$		diag(-1,1,1,1) the metric tensor
$\boldsymbol{\lambda}$	m	wavelength

λ_x	m	wavelength at which black holes form
π		constant Pi with π = 3,141592....
ρ	kg/m^3	static density
ρ_{eff}	J/m^3	energy density with normalization T_{00}^{eff}/c^2
Φ_m	rad	turning angle
ϕ	1/m	a) scalar potential for 4D b) the scalar potential for 7D is dimensionless
ω_{ab}		Rotation tensor
∇_R	1/m	covariate derivative with respect to *R*
$\square_{(7)}$	1/m²	the D'Alembert operator in 7D

Indices

1,2,3,4,5,6,7,8,9	refers to the dimensions 0 – time coordinate 1, 2, 3 – visible space-time dimensions of the “particle-field” 4, 5, 6 – compact “wave-field dimensions” 7, 8, 9 – Spatial dimensions of the next field-space level
0., […], 12.	refers to the dimension families
2π	refers to a full period
B1	refers to a boson 1
B2	refers to a boson 2
classical	refers to the concepts of classical physics
crit	refers to critical shock parameters in the vicinity of black holes
dark	refers to dark energy - data
e	refers to the electron
e^-	refers to a negative charge
e^+	refers to a positive charge

eff	refers to the root mean square value
fion	refers to the fion a) X - refers to an object that generates the maximum space distortion b) Y - refers to an object that produces a technically usable space distortion
global	refers to a local disturbance in space-time
gravity	refers to gravity
hidden particles	refers to hidden particles
invisible photons	refers to invisible photons
local	refers to a local disturbance in space-time
M	refers to a (7D) space-time indices: 0, 1, 2, 3, 4, 5, 6
m	refers to the compact 3D wave-field dimensions refers in context to the mass of the object
max	refers to a maximum value
min	refers to a minimum value
N	refers to a (7D) space-time indices: 0, 1, 2, 3, 4, 5, 6
n	refers to the compact 3D wave-field dimensions
ph	refers to the photon sphere of a black hole
pho	refers to the photon
pot	refers to potential quantities
obj	refers to an object
Quark	refers to u/d-, C-, B-, T-, S-quarks
proton	refers to the proton
visible	refers to visible matter
BH	refers to a black hole
Uni	refers to the universe
target	refers to a target value
vector	refers to the vector disturbance caused by interaction

$\boldsymbol{\alpha}$	refers to the current field angle
$\boldsymbol{\lambda}$	refers to the affin parameter
$\boldsymbol{\mu}$	refers to visible 4D space-time in particle-field
$\boldsymbol{\nu}$	refers to visible 4D space-time in particle-field

Subject index